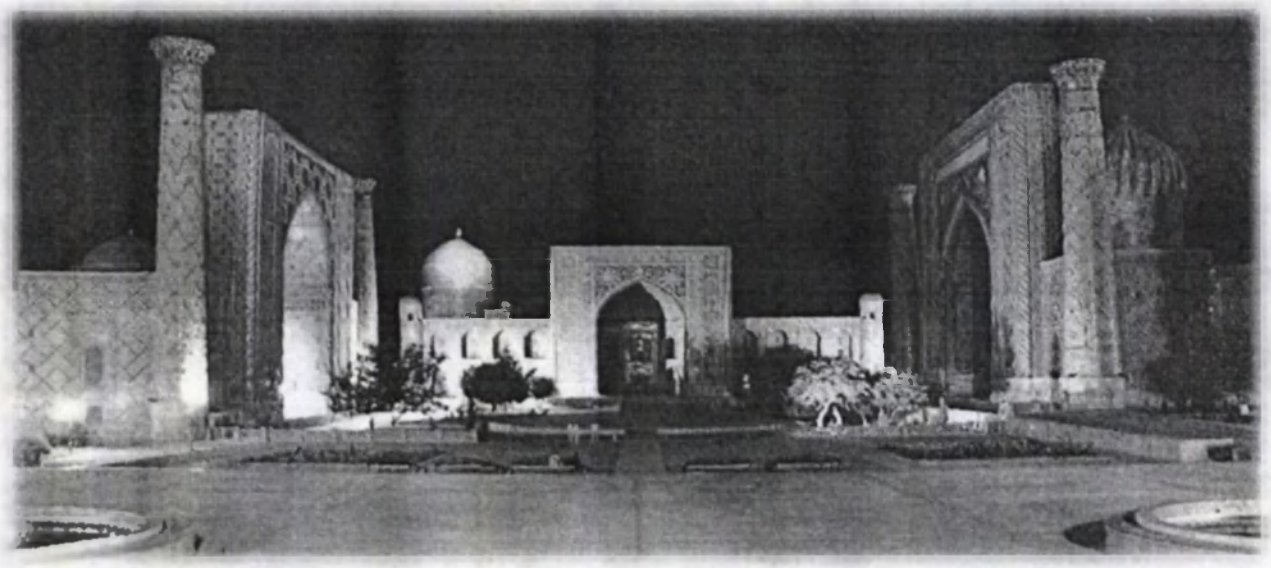


A Z Khasanov, Z A Khasanov

Editors



Samarkand 21–23 September 2012

Proceedings of the

IVth Central Asian Geotechnical Symposium (IVth CAGS)

Geo-Engineering for Construction and Conservation of Cultural Heritage and Historical Sites

- Challenges and Solutions -

– *Organized by* –

GEOFUNDAMENTPROJECT Co. Ltd.

– *Organizing Committee* –

Symposium Chair	A Z Khasanov
Symposium Co-Chair	I I Usmonkhodjaev
Secretary	Z A Khasanov

– *Symposium Advisory Committee* –

Prof. Jean-Louis Briaud, President of ISSMGE, USA
Prof. Askar Zhussupbekov, VP of ISSMGE for Asia, Kazakhstan
Prof. Yoshinori Iwasaki, Chair, ATC 19, Conservation of Heritage and Historical Sites, JGS, ISSMGE
Prof. Neil Taylor, General Secretary of ISSMGE, UK
Prof. Calro Viggianni, Chair, TC301, Preservation of Historic Sites, ISSMGE
Prof. Vyacheslav Ilichev, President of Russian Geotechnical Society, Moscow, Russia
Prof. Ikuo Towhata, Chair,ATC3: Geotechnolgies for Natural Hazards, Appointed Board member of ISSMGE, University of Tokyo, Japan
Prof. Mamoru Mimura, Chair, ATC 10: Urban Geo-Informatics,Kyoto University, Japan
Prof. Vladimir Ulitsky, Chair, TC 207, PGUPS, Saint –Petersburg, Russia
Dr. Michael Lisyuk, Co-Chair, TC 207, Corporate Associates Presidential Group (CAPG) ISSMGE, Saint–Petersburg, Russia
Prof. V.P. Petrukhin, Director of NIIOSP, Moscow, Russia
Prof. Tuncer B.Edil, Chair, Department of Civil and Environmental Engineering, The University Wisconsin, Madison, USA
Prof. R.A.Mangushev, Head of Department of Geotechnical Engineering, SPBGASU, Sain – Petersburg, Russia
Dr. Abbas Sorush, Chair, Iranian Geotechnical Society, Tehran, Iran
Eng. Saeed Heidari, Secretary, Iranian Geotechnical Society, Tehran, Iran
Dr. Yoshiyuki Mohri, Manager National Institute of Rural Engineering, Ministry of Agriculture, Forestry and Fisheries, Tsukuba, Japan
Prof. Chikaosa Tanimoto, International Institute for Advanced Studies, Kyoto, Japan
Prof. Toshinori Kawabata, Faculty of Agriculture, Kobe University, Japan
Prof. T.I. Mirsajapov, Head of Dep. of Geotechnical Engineering, Kazan State Architectural and Civil Engineering University, Tatarstan, Russia
Prof. Tadatsugu Tanaka, JARUS, Tokyo, Japan
Prof. Susumu Yasuda, Tokyo Denki University, Japan
Prof. Kunio Watanabe, Geosphere Research Institute of Saitama University, Japan
Prof. Eun Chul Shin, University of Incheon, Incheon, Korea
Prof. Hoe Ling, Columbia University, New York, USA

Alisher Navoiy nomidagi O'zbekiston MK 201__

2013/15 1173 Alisher Navoiy nomidagi O'zbekiston MK

PVIII 42842

Contents

Key note Lectures

Earthen Heritages should be passed on to the Future 8
K. Watanabe & R . Vatandoust

The measurements of Temperature and Humidity in Ancient Tomb in Dahshur, Egypt 20
Y. Iwasaki

Preservation and Reconstruction of historical monuments with provisions for soil-structure interaction analyses 27
V.M. Ulitsky, A.G. Shashkin, K.G. Shashkin, M.B. Lisyuk

Причины разрушения минаретов Средней Азии и рекомендации по их сохранению 39
Хасанов А.З, Хасанов А.З.

Load transfer platform for column-supported embankment 48
B. E. Tuncer

load transfer platform for column-supported embankment 57
I. Towhata, T. Sasaki, Y. Taguchi

Papers

Studies and investigations on forts with Portuguese legacy 67
L. Ribeiro e Sousa, A. Viana da Fonseca, Karim S. Karam

Historical Development of Embankment Dams in Japan 73
T. Tanaka, M. Yoshiyuki, H. Tagashira

Geotechnical investigations of historical monuments of Kazakhstan 79
A. Zh. Zhussupbekov , T. O. Zhunisov

Stability analysis of masonry structure at Angkor Thom in Cambodia using elasto-plastic NMM-DDA 84
R. Hashimoto, T.Koyama, M. Kikumoto, S.Yamada, M.Araya, Y.Iwasaki, Y.Ohnishi

On the Burial Style of Ancient Tombs from the view Point of Seepage Water Measurements 90
K. Onitsuka, Y. Hara

Conservation of the naked stone chambers with restored soil mound at Garandoya Tumulus 97
M. Mimura, S. Fukumoto,M. Yoshimura,T. Terao

Salt damage mechanism in northeastern Thailand and proposal of repair methods 103
A. Iizuka, Sh. Nomura, K. Kawai

Preservation of Old Buildings in Tehran, Iran 111
S. Heidari

Some Problems of Foundations of Historical Buildings in St. Petersburg 117
R.A.Mangushev, A. Osokin

Proposals on stabilization of the inclined Nev'yansk tower 121
Lushnikov V.V.

Rehabilitation activities in Al-Kadhimayn mosque and shrine in Baghdad 125
N. Al-Saoudi

Basement floor construction in the historical building in Tobolsk 131
Y.A. Pronozin, R.V. Melnikov, M.A. Stepanov

Vulnerability Assessment of Jamma MAsjid, New Delhi: A Case study 134
N. Satyam. D. Prasanna kumar

Древняя ирригация Средней Азии 139
Д. Ниязов, Р. С. Мукимов

Устойчивость зданий и сооружений Казанского Кремля 143
В.Р. Мустакимов Р.И. Шафигуллин, С.Н. Якупов, А.В. Мустакимов

The secrets of endurance of Indian heritage structures 150
R. M. Madhav

Опыт решения геотехнических проблем реконструкции памятников архитектуры в республике Башкортостан 152
А. Л. Готман

Deformation of stupas measured by photogrammetry before and after Ayutthaya Flood in Thailand, 2011 157
Y. Fujii, K. Watanabe, U. Weesakul, N. Poovarodom, B. Bhadrakom, S. Kawano

Задачи инженерно-геологической диагностики деформаций памятников архитектуры 163
Е. М. Пашкин, В.Я. Ендржиевский

Characterization of strength variability of cement-treated soil column 172
T. Namikawa

Estimation of liquefaction from case histories 178
S. Gh. Jahromi, M. Gutierez

Осадки фундаментов промышленных объектов Карагандинского металлургического комбината 242
А.В. Филатов, А.С. Жакулип, АЛ. Жакулиua

Numerical Solutionfor 3D Contaminant Trough Anisotropy Soil/Rock Media 246
SA. Sadrnejad, M. Memarianfard

Инженерные проблемы сохранения Памятников архитектуры 252
К.С. Абдурашидов, СА.Саидий, З.С. Шадманова, Б.К. Рахманов

К вопросу эксплуатации зданий и сооружении на основаниях, сложенных просадочными лессовыми грунтами и рекомендхемые противопросадочные мероприятия 256
А. Сапаров

Роль техногенеза в изменении инженерно-геологических условий 200
Сапарова А., Сапарова МЛ.

Исследование закономерностей распространения лессовых пород по долине р. Чирчик на базе современных информационных технологий
М.Ш. Шерматов, А.С. Хусамитдипов, Б.Т. Курбанов, И.И. Усманходжаев

Разработка концепции схемы* солеотводящих сетей бассейна *р. Амударьи на базе интегрированных ГИС-технологий 273
Б.Т. Курбанов, А.Ш. Халматов

Применение современных информационных технологий при строительстве гидротехнических сооружений
Н.М. Джураев, А.С. Хусамитдипов, Ш.И. Ёдгоров ~ л
Б.Т.Курбапов, Усманходжаев И.И

Оптимизация параметров свайных фундаментов под стены гражданских зданий 278
МелиеваЛ.К., Усманходжаев И.И.

***Геоэкологические проблемы и инженерно-геологические* условия Южного Приарилья** 281
Г.С. *Дурдиева*

Influence of soil structure on consolidation of soft clays using vertical geodrains 285
M.V. Shah, A.V. Shroff

Проблемы сохранения памятников архитектхры Узбекистана и их реабилитация на основе композиционных материалов 291
АЛ. Ишанходжаев, АЛ. Ашрабов

Реологические свойства антропогенных грунтов в основании сооружений 296
Х.З. Расулов, С.М. Норбоев

Оползневые явления в откосах в результате разжижения грунтов 298
Х.З. Расулов, А.Х. Садиков

Сейсмопросадочная деформация лессовых грунтов 300
Расулов Р.Х.

Глубина разжижаемой зоны в основании зданий при землетрясении 303
А.У. Тошходжаев

Исследование устойчивого уклона исскуственных откосов при интенсивных колебаниях 306
Э. Казаков

Несущая способность оснований зданий при сильных землетрясениях 309
Х.З. Расулов, М. Бабажанов

Dilution of water-sated lousier soil at seismic influences 311
Расулов Х.З.

Длительная деформация медресы Амир Тура в г. Хиве 315
Норбоев С.М

Comparison of Geotechnical Freezing Characteristics between Korea and Kazakhstan Soils 319
E.C. Shin & B.H. Ryu A.Zh. Zhussupbekov & Zh.A. Shakhmov

Vulnerability assessment and seismic rehabilitation of stone masonry buildings using pipe bracing system 327
M. Mahmoudi, F. Ebadi

Resistivity profiles and foundation structure of Central Tower, Bayon in Angkor 333
K. Nakagawa, I. Shimoda, S. Yamada, R. Kanai, Y. Ogawa, Y. (Yasuda) Ohta, M. Fukuda, A. Jomori, T. Takahashi, Y. Iwasaki

Earthen heritages should be passed on to the future -Contribution of Geo-Engineering-

Kunio Watanabe
Geosphere Research Institute, Saitama University, Saitama,, Japan

Rasool Vatandoust
Department of Conservation, Faculty of Arts and Architecture, Azad University, Tehran, Iran

ABSTRACT: Earthen heritages in the world should be well preserved and passed on to the future generation because these earthen structures display not only ancient culture and civilization but also ancient geo-technology that may applied to the modern structures. As the earthen structures can be easily eroded by some natural processes such as rain, earthquake, salt weathering and etc., technology to conserve the heritages should be developed on the basis of scientific researches. As the examples of scientific researches, documentation by three dimensional graphics, analyses of earthen material and evaluation of typical deterioration processes are shown in this paper with presenting data mainly obtained at two historical sites; Choga Zanbil, Iran and Ajina Tepa, Tajikistan. The basic concept of the actual conservation works performed by UNESCO at the Ajina Tepa site is also reported. It is concluded that the Geo-Engineering should contribute more on the conservation of historical heritages in the world.

1 INTRODUCTON

Historical earthen structures in the world, denoted as heritages, have survived over a long period of time in different environmental conditions. Those structures were remained even in the seismic areas and even suffered by the heavy rainfalls. Those structures are informing;

(1) Ancient culture and civilization
(2) Ancient technologies of Geo-Engineering that are harmonized with the environmental condition given. If the technologies were not fitted the environment conditions, the earthen structures might be easily deteriorated and might be not survived.

Although earthen heritages could survive over a long period of time, these are still eroded and deteriorated by heavy rain, earthquake, salt weathering and etc. It is difficult to completely stop the deterioration process under the environmental conditions. Also, there is a possibility that the environmental condition around earthen structures will be change. For example, agricultural development around the earthen heritage sites rises the groundwater table in irrigation period and this condition may accelerate the salt weathering. In addition to these problems, the climate change due to the global warming may increase the rainfall amount and may accelerate the erosion.

In addition to the effects of these natural conditions, animal and insect can give severe damages to earthen structures and also human activity may destroy the structures.

Because historical earthen structures have important information, these structures must be properly conserved and passed on to future generations. It should be a big duty of Geo-Engineering to clarify the deterioration mechanism and to develop proper conservation techniques for historical earthen structures. In this paper, the important points in the conservation are summarized.

2 CONTRIBUTION OF GEO-ENGINEERING

There remain many problems for properly conserving the historical earthen structures. The major problems that are more or less related to Geo-Engineering field can be divided into four categories as follows;

(1) Documentation on the current condition of historical earthen structures
(2) Scientific researches on the materials used and the deterioration processes
(3) Plan and execution of conservation
(4) Maintenance after the conservation

All of these items are very important in any conservation works and relating to the Geo-Engineering. Brief explanations on those categories are given.

As the most important item in the documentation, mapping over the historical site is indispensable. Also, three dimensional geometry of earthen structure should be precisely recorded and visualized. Techniques such as photogrammetry (Linder, 2003) and laser scanning have been used for the mapping and 3-D visualization (Yastikli, 2007, Yilmatz et al., 2007,

Fuji et al., 2009, Fujii et al., 2012). Once the 3-D geometry is well documented, the overall deterioration of the structures can be evaluated with comparing the geometries made at different time.

Earthen structure is also damaged by human, animal, insect activities. The damages by these activities must be well documented as the damage assessment. Salt weathering is also an important process in the deterioration (Goudi et al., 1997, Kuchitsu et al., 1999, Topal et al., 2003, Fodde, 2007a, 2007b, Watanabe et al., 2011). Salt created on the surface of earthen walls should be analyzed and documented. On the basis of the documentation, the deterioration mechanisms can be scientifically studied. There are many questionnaires on the mechanisms, for examples;

*What is the physical, chemical properties of material of earthen structures ?
*How the earthen structures are deteriorated ?
*How rain erodes the structures ?
*How salt crystallization deteriorates the structures ?

Scientific researches mainly from the view point of Geo-Engineering are indispensable for answering to these questionnaires.

Any conservation work must be planned and designed on the basis of the scientific researches. For example, if the deterioration process is very rapid, a possible way of conservation is covering of the ancient structures with thick shelter coat. When the groundwater much influences the salt weathering and softening the material, some countermeasures to decrease the water content beneath the ground surface is needed.

Maintenance of the structures after the conservation is also important. The environmental conditions around the historical site must be well managed. For example, agricultural development in the vicinity of the site must be properly managed because irrigation brings about the increment of water content in soil and may accelerate the decay process by the salt weathering. Path way for tourists should be well prepared to avoid the artificial damage. Monitoring of the deterioration and continuous repair of the conserved structures are also very important.

As above mentioned, knowledge of Geo-engineering including soil mechanics, geo-chemistry, hydrogeology and etc. is indispensable to properly conserve the historical earthen structures.

3 DOCUMENTATION BY 3-D GRAPHICS

3.1 *Technique*

It is preferable to document the geometries of earthen structures by 3-D graphics. As mentioned, two major technical tools; laser scanning and photogrammetry, have been commonly used for making 3-D graphics. By using the technique of photogrammetry, 3-D graphics can be constructed from a pair of digital photographs (stereo photographs). Of course, the locations of several points on structures targeted must to be precisely measured by using a total station. A photograph does not give any information on the geometry behind the structure. It implies that only a part of structure can be visualized from a pair of stereo photographs. So that, a structure is visualized part by part and finally combine these parts. It has been pointed that the resolution of photogrammetry is less than laser scanning. Because a digital photograph is composed of many point data on every pixel, the resolution is depended on the area that one pixel is covering. Error is coming from other reasons such as torsion of photograph, lightning condition and so forth. In usual case, the resolution is the order of several cm when a structure of which size is about 10-20 m and the error in the perpendicular direction to the wall is larger than in the parallel direction. The accuracy (resolution) of laser scan is thought to be higher than the photogrammetry. However, Fujii et al. (2011) pointed out that the accuracy of both techniques are almost identical. The cost of the equipment for laser scan is more expensive as compared with it of photogrammetry including software used for making 3-D graphics. The appropriate technique must be selected with considering the objectives that 3-D graphics are used.

Figure 1 summarized the major objectives of the documentation using 3-D graphics. There may be three phases in which 3-D graphics are effectively used. Before the conservation, the 3-D geometry of earthen structures must be well documented. When 3-D graphics are made at different time, the change of structures could be evaluated with comparing those graphics and the deterioration processes can be evaluated. Of course, the deterioration processes, such as weathering, erosion and collapse of structures, are more or less continuing during the conservation work and even after the conservation. As the earthen structures are continuously deteriorated, the 3-D graphics should be made at some different times. From this view point, photogrametry was thought to be better than laser scanning because the stereo photographs can be easily taken at any time. Figure 2 shows two examples of 3-D.graphics of

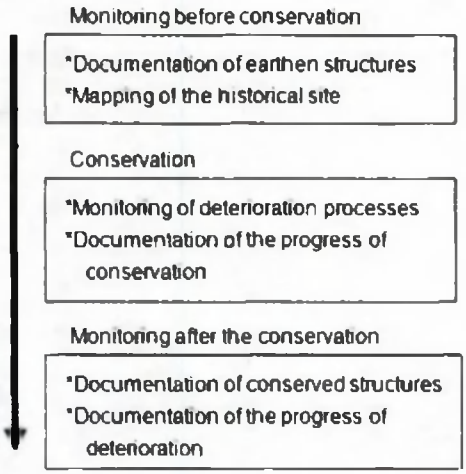


Figure 1. Documentation by 3-D graphics

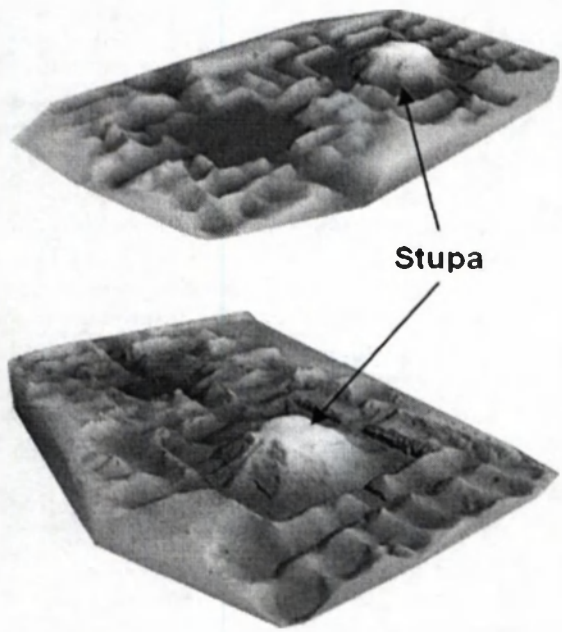


Figure 2. Two perspective views of Ajina Tepa

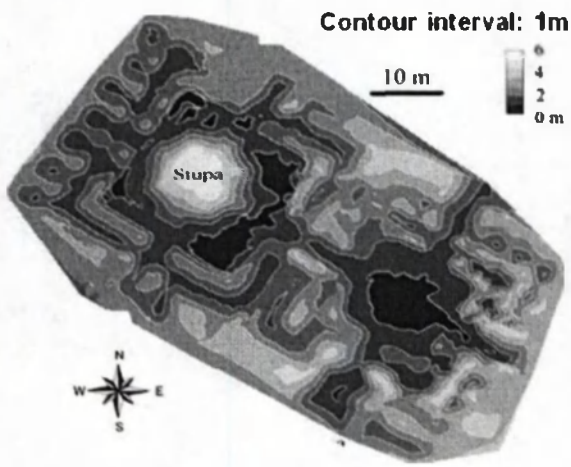


Figure 3.Map of Ajina Tepa

Ajina Tepa, Tajikistan. Figure 3 illustrates the contour map of this site constructed from the data obtained by photogrammetry. There is a big Stupa made of mud brick in this site. However, the selection of technique should be performed with considering the conditions of site, accuracy of the measurement etc. Combined use of photogrammetry and laser scanning may be preferable.

4 EARTHEN MATERIALS

4.1 *Two historical sites studied*

Any earthen material such as clay, silt and sand that are distributing near the sitse have been used as the construction material. The physical, chemical and mineralogical features of earthen material used should be clarified. Some important physical properties are presented with showing some data obtained from different two earthen materials in Ajina Tepa site, Tajikistan and Choga Zanbil site in Iran.

4.2 *Material in Ajina Tepa Sit, Tajikistane*

The Buddhist Monastery of Ajina Tepa, Tajikistan is located in a valley surrounded by hills that are part of the west foot of Pamir Mountains and at about 100km south of the capital city Dushanbe. The Ajina Tepa monastery was constructed along the ancient Silk Roads, and was archeologically excavated by Soviet archeologists led by Litvinskij during 1960-1975 (Litvinskij et al., 2004). On the basis of the archeological study, Ajina Tepa was defined as a typical combination of monastic and temple aeas of 7^{th}-8^{th} C AD.

The structures in the Ajina Tepa site were constructed by mud bricks and pakhsa (rammed earth). Mud brick and phkhsa specimens were sampled under the permission of Ministry of Culture of Tajikistan. Figure 4 illustrates typical grain size

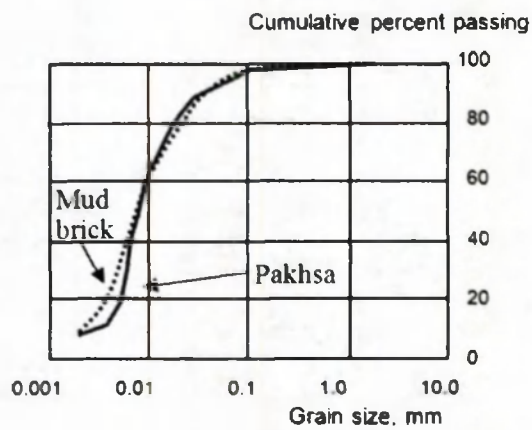


Figure 4. Grain size distribution

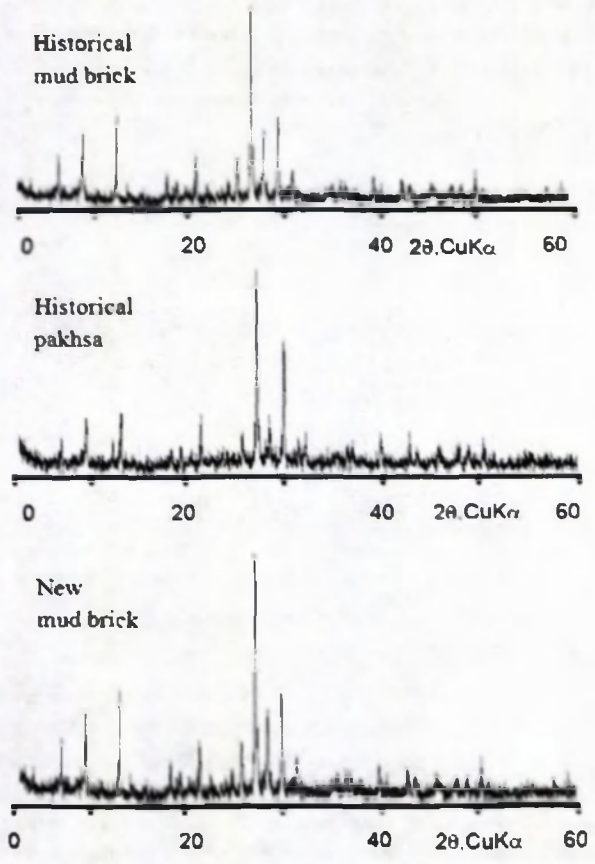


Figure 5. Mineral compositions


Figure 6. Production of new bricks

distributions of mud brick and pakhsa. It can be found that the grain size distributions of these earthen materials are almost identical. Figure 5 displays the mineralogical components of these materials that were analyzed by X-ray diffractometer. The major minerals are quartz, calcite, mica, plagioclase and chlorite. The mineral compositions of these materials are almost identical. The mineral composition of new mud brick that was used for the construction of shelter coat over historical structures is also displayed in this figure. New mud bricks were made from the soil distributing along some small canals locating in the vicinity of the site. Figure 6 shows the way of new mud brick making. It can be seen that the mineral composition of new mud brick is also identical to the ancient mud brick and pakhsa. From this fact it can be said that the historical bricks was made by using soil distributing around the site.

4. 3 Materials in Chogha Zanbile Site

Choga zanbil temple is a world heritage locating at the western part of Iran and composed of many important monuments such as a big ziggurat, three peripheral walls, palace, underground tombs, a water reservoir and so forth (Ghirshman., 1963, 1966, 1968). Most of those structures were composed of mud brick except for the water reservoir. The ziggurat was made of mud bricks but it was covered with fired brick layer of 1-2 m thick. The Choga Zanbil temple was constructed by the king Untash-Napirisha (1260-1235 BC) and abandoned in about 640 BC (Roef, 1990).

Figure 7 shows a ziggurat of the Choga Zanbil temple. Five samples of mud brick, joints fillings mortar were sampled undert he permission of Iranian government from the different points of Ziggurat as illustrated in Fig 8 (Watanabe, 2003).. In this figure, MB-1, MB-2 and MB-3 are mud bricks, MB-4 is the joint filling


Figure 7 Ziggurat in Choga Zanbil

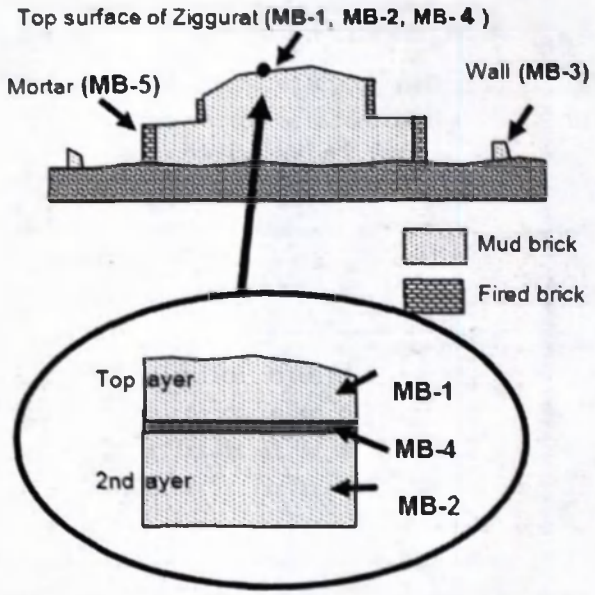


Figure 8 Sampling locations and names of specimens

mortar between mud bricks and MB-5 is the mortar between fired bricks. MB-1 and MB-2 were sampled from the top of the ziggurat and MB-3 was taken from the surrounding wall. MB-1 and MB-2 were sampled from the top layer and the second layer of ziggurat. MB-1 was more weath

ered as comparing with MB-2. It was reported that the surrounding wall was constructed at about 100 years before the construction of Ziggurat.

Figure 9 displays the grain size distribution of these mud brick and joint filling. It is found from this figure that the distribution of MB-1 and MB-2 are much different from MB-3 and MB-4. The distribution of fine sand (F-S) existing around the ziggurat was also illustrated in this figure. From the comparison among those distributions it can be thought that the materials for MB-1 and MB-2 were the mixture of the soil used for MB-3 and MB-4 and F-S. It can be said that the soil for making mud bricks were different even in one site.

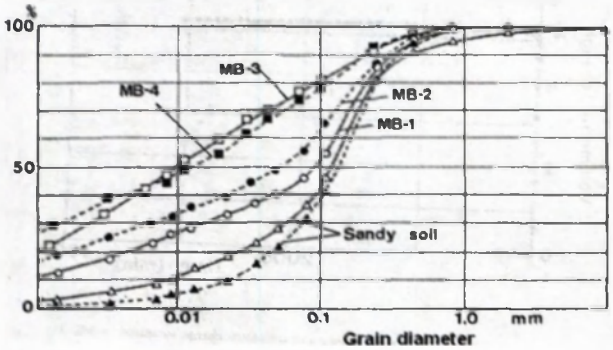


Figure 9 Grain size distribution

Table-1 displays the physical properties of those samples. Density, void ratio, hydraulic conductivity and so forth are summarized. The measurement of hydraulic conductivity was very difficult because mud bricks are rapidly decayed in

Table 1. Physical properties of specimens

Sample	Soil particle density (g/cm^3)	Density (g/cm^3)	Void ratio	Hydraulic conductivity (cm/s)
MB-1	2.706	1.750	0.563	3.43E-5
MB-2	2.732	1.707	0.642	1.39E-5
MB-3	2.750	1.813	0.594	4.10E-6
MB-4	2.761	1.848	0.530	-

water. Although a special mold was used for the measurement, the hydraulic conductivity was not so accurate. Table-2 illustrates the mineral compositions of mud bricks and mortars analyzed by the X-ray diffractometer. The mineral compositions of MB-2, MB-3, MB-4 and MB-5 are dis

Table 2. Mineral composition

Minerals	Samples			
	MB-2	MB-3	MB-4	MB-5
Smectite	+	+		
Chlorite	+	+	+	
Kaolinite	+			
Gypsum	+	+	M	L
Calcite	L	L	L	+
Dolomite	S	+		
Quartz	L	L	L	+
Plagioclase	S	+	S	
Palygorskite	+	+	+	
Nacl		+	+	
Mica	+	+	+	

L: Large amount, M: Middle amount,
S: Small amount, +: a little amount

played. The mineral compositions of mud bricks (MB-2, MB-3) and mortar (MB-4) between these mud bricks are almost identical. Swelling clays, that are mainly smectite and palygorskite, are contained in mud bricks and the mortar among mud bricks. Those swelling clays causes severe volumetric change of brick when in the wetting or drying processes (Fisher W.B.,1968). The mortar (MB-5) among fired bricks is almost composed of pure gypsum.

Figure 10 shows the water retention curves of MB-1, MB-2 and MB-3. The hysteresis. is clearly found for those specimens. And the retention curve of MB-1 (weathered mud brick) is much different from it of MB-2. The retention curve of MB-1 is considerably shifted toward the left hand side of this figure from MB-2. It can be concluded from the fact that the average size of pores in MB-1 was enlarged during the long term weathering process. However, as shown in Table-1, the void ratio of MB-1 is smaller than MB-2. From these facts the following processes occurred in the

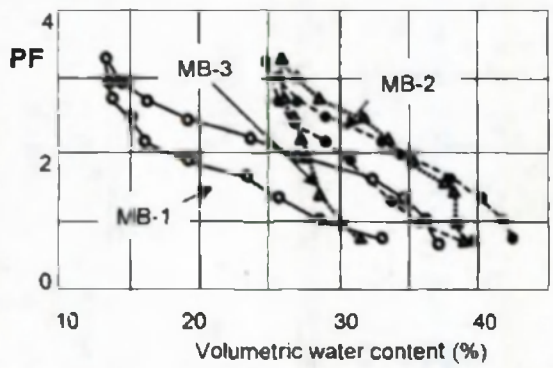


Figure 10. Water retention curves weathering;

*Reduction of total pore space
*Average pore size increased
It can be concluded that smaller spaces might be filled with salt crystallized during the weathering process. The hysteresis curve of MB-3 is distributing near the region of MB-2.

Earthen material can be easily decayed by the water infiltration. To know the decay process, slaking test was performed. Figure 11 illustrates the test procedure adopted. At the first, a small piece of mud brick is dried in an electric oven under the temperature of 60C during 24 hours, then, it was cooled down to the room temperature. This dried specimen is input into water and the de

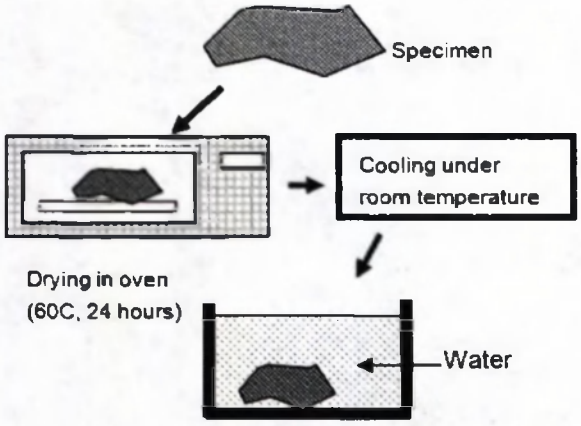


Figure 11 Slaking test for mud brick

cay process was observed. The decay process is divided into five conditions named as the slaking indices (see Fig. 12). MB-1, MB-2 and MB-3 were tested and the results displayed in Fig 13 were obtained. As illustrated in this figure, the ziggurat mud bricks MB-1 and MB-2 were rapidly

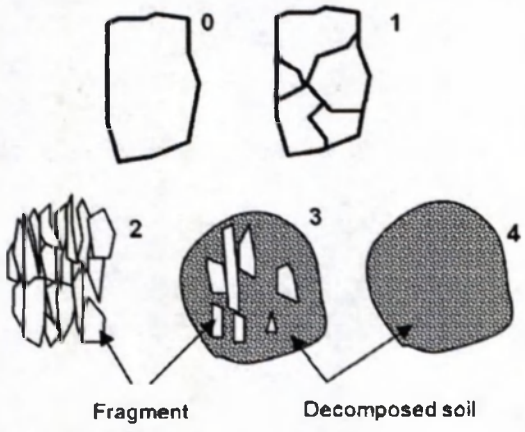


Figure 12. Slaking Indices

decayed soon after inputting into water and reached to the condition of the index 4 (completely decayed). On the other hand, for MB-3, it took

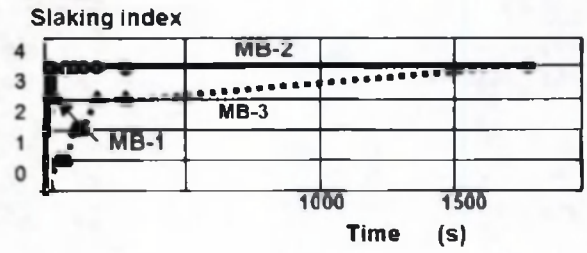


Figure 13 Result of slaking test

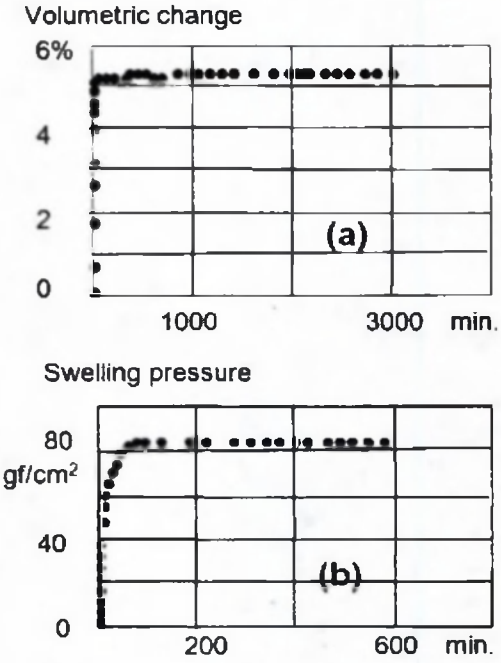


Figure 14 Results of welling tests. MB-2 was used. (a) volumetric change, (b) swelling pressure

longer time than 30 min. before reaching the index 4. It can be concluded that the durability of MB-3 is higher than MB-1 and MB-2.

Mud brick changes its volume during the wetting/drying processes because of the existence of swelling clays, and the swelling pressure is created if the brick is confined. The volumetric change and swelling pressure could deform the structure. Figure 14 illustrates the results of swelling tests. MB-2 was used for the tests. (a) is the volumetric change and (b) is the swelling pressure change. It is found that the swelling pressure reached to around 80gf/cm^2.

4.2 *Other important properties*

It is very important to clarify the physical, chemical and mineralogical properties of earthen materials used in the historical earthen structures. In addition to the properties mechanical properties such as strength and deformability of materials are needed to know the deterioration processes of historical structures. However sampling of enough

volume of historical materials for many tests is difficult because the material it self is also a component of heritage. Non-destructive techniques such as hardness test, penetration test and so forth, should be used for roughly estimating mechanical properties.

5 DETERIORATION MECHANISM

5.1 *Deterioration processes in the Ajina Tepa*

Earthen structures could be deteriorated during a long period of time if the conservation and maintenance works were not properly performed. The speed and extent of the deterioration are the function of physical and chemical properties of earthen material, climate condition, water content in soil around the sites etc. Figure 15 and 16 display some big cracks in an earthen wall and slides formed at the upper part of the Stupa. As the natural processes relating to the Geo-Engineering, surface erosion, salt weathering, fracturing, fail ures of a part of wall, tumbling of walls and surface sliding are commonly observed.



Figure 15. A historical wall having big cracks



Figure 16. Slides on the big Stupa

Many types of deterioration are observed in the Ajina Tepa site. The common symptoms of deterioration observed are: deposition of debris at base of wall (92.3%of all walls), soft crust of clay (91.3%), grass with deep roots (82.7%), hard crust of clay (88.9%) grass growth (62.9%), coving (48.2%), hole by animals (48.1%) man made damage (40.7%) preferential channels (25.9%), salt crystallization (17.3%), hole made by insect (14.8%), wide portion of missing wall (12.3%), missing wall (7.4%). As the salt crystals can not be easily observed by eye, the percentage of salt crystallization phenomena may be more than 17.3%. It can be concluded that many earthen walls in the world have been deteriorated not only by the natural process but also by the activities of plants, animal, insects and man.

5.2 *Failures induced by salt weathering*

Fujii et al (2009) reported that the salt weathering brings about the failure of wall. The typical process of salt weathering is schematically illustrated in Fig. 17. Water contained in the basement soil is upwardly transported by the evaporation as shown in Fig. 17(a). Salt is crystallized not only on the surface but also in many micropores just behind the wall surface. As the volume of the crystallized salt is larger than the micro pore spaces, wall is destroyed from the surface (Fig. 17(b)). As the evaporation is large at just above the ground surface, the foot part of wall is deteriorated and cove structure is formed (Fig. 17(c)).

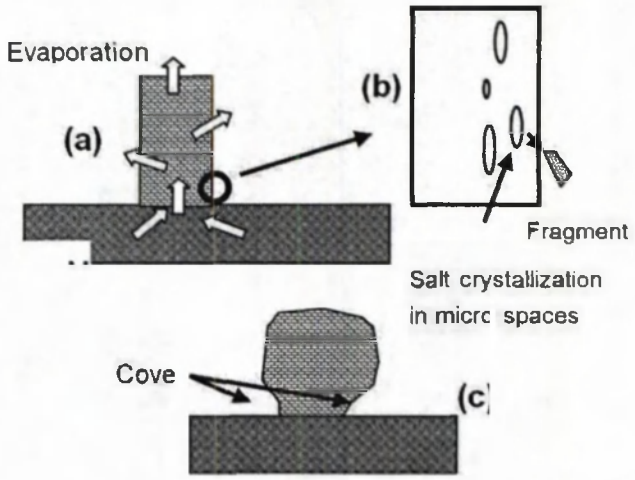


Figure 17 Damage by salt weathering

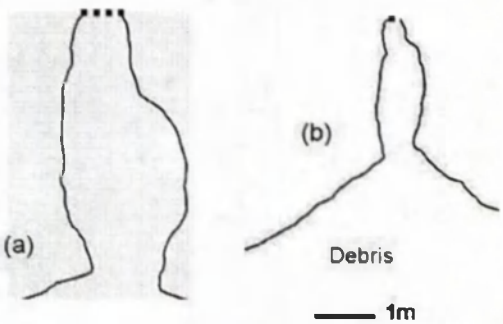


Figure 18. Two typical cross-sections of wall.. Foot parts of walls are eroded.

Fig. 18 displays two examples of the typical cross-sections of walls in the site. It can be observed that the lower parts of walls are deteriorated and eroded, then, the walls are unstable.

Fig. 19 displays the evaporation measurement equipment (Watanabe et. al., 2008) used in the site. Figure 20 illustrates the vertical profile of the evaporation rate along wall surfaces. It can be seen the evaporation rate was large near the ground surface and it decreased with height. From this fact it can be said that the salt weather ing is intense at the foot of wall as schematically shown in Fig.17.



Figure 19 Equipment for evaporation measurement.

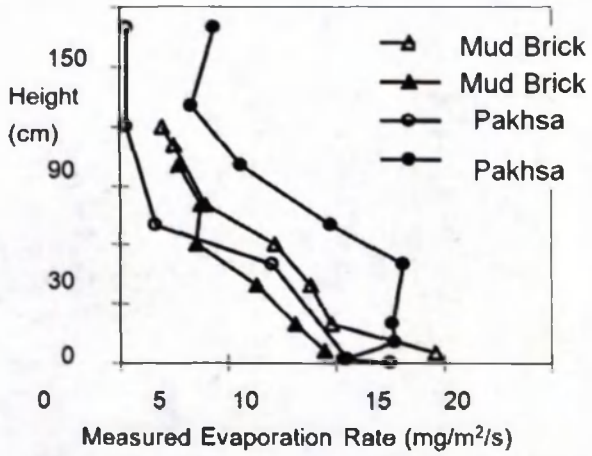


Figure 20 Evaporation profile along four walls



Figure 21 Two typical types of failure after the salt weathering

Figure 21 illustrates two possible failures of unstable earthen wall. Slide and the tumbling can be commonly occurred. Figure 22 and Fig. 23 show the examples of these types of failures. It can be concluded that the deterioration due to the combination of salt weathering and failures are very severe in the Ajina Tepa site.

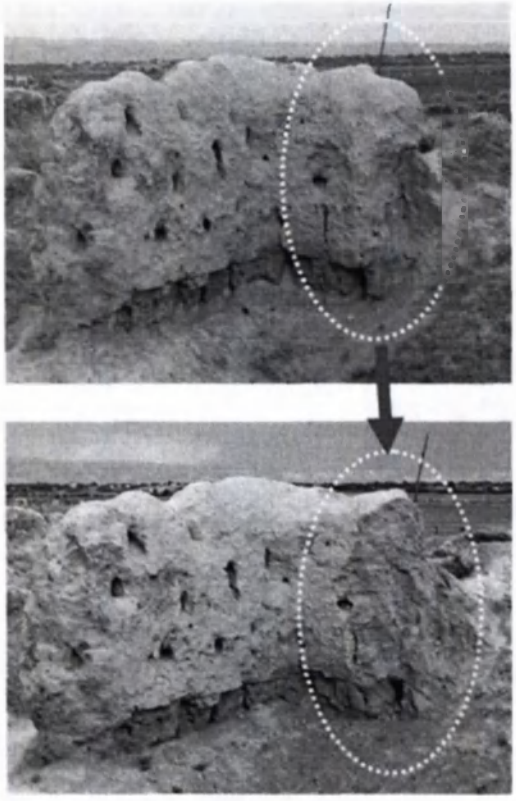


Figure 22.Slide type failure occurred during Aug. 2006 – May 2007

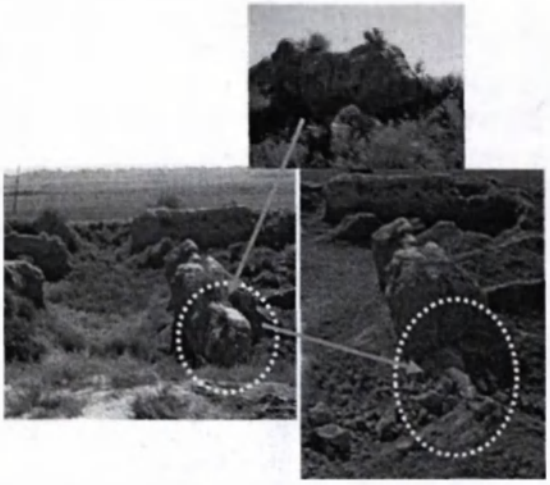


Figure 23. Tumbling type failure occurred during Nov. 2005 – June 2006. Unstable wall was collapsed.

5.3 Collapse by earthquake

Earthen structure is collapsed by seismic motion. Figure 24 shows the damage of Bam, Iran by the earthquake occurred in 2003 (donated by UNESCO). It can be seen that all of many historical

earthen structure, houses, mosques, barracks etc. were collapsed. There are many modes of failure by earthquake. One of the typical failures is the separation along joints. Strength of joint filling mortar and connection among mud bricks should be increased to prevent such type of failure.

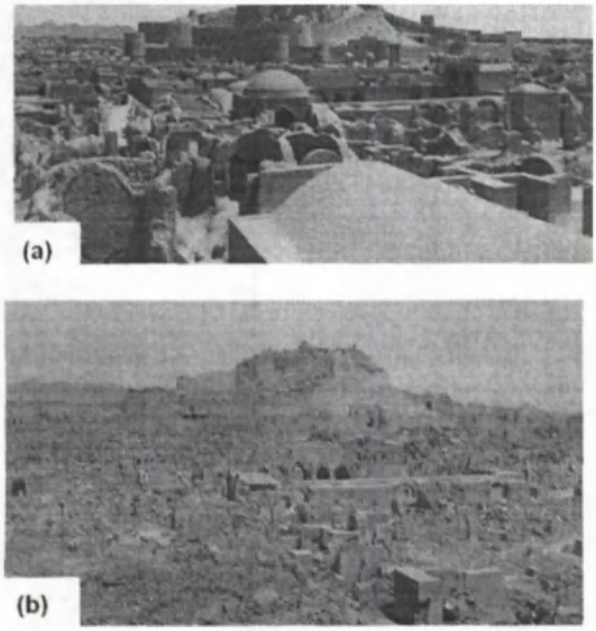


Figure 24 (a) before and (b) after the Bam earthquake (photographs were donated by UNESCO)

6 CONSERVATION

6. 1 *Buttress support and Shelter coat*

Shelter coating by using new earthen material is one of the most popular ways of the conservation if deterioration process is rapid. In the Ajina Tepa, because the deterioration process of earthen structures walls is rapid, the UNESCO/Japan Trust Fund Project was executed for the preservation of the Ajina Tepa Monastery during 2005-2008. In this project, shelter coating was adopted as the conservation technique. The procedure of shelter coating is schematically illustrated in Fig. 25. Shelter coat was composed of thick layers of new mud bricks and plaster. Unstable walls (Fig.25 (a)) were supported by the buttress walls made of mud brick as shown in Fig.25 (b). Then the walls are covered with thick mud brick layer as displayed in Fig.25 (c). Finally, the mud brick layer was covered with plaster (Fig.25 (d)). Figure 26 displays an example of conservation performed for a damaged wall. After the archeological cleaning, thick mud brick layer was constructed to cover the historical structure. Then, the mud brick layer was covered with plaster of about 10cm thick. Figure 27 and 28 also show the shelter coating of the other walls. The big Stupa was also covered with mud brick and plaster layers as shown in Fig. 29. There was a big argument on the shelter coating on these historical structures because shelter coat could change the landscape of the site. Finally, it was decided that the conservation was more important because the deterioration process was very rapid.

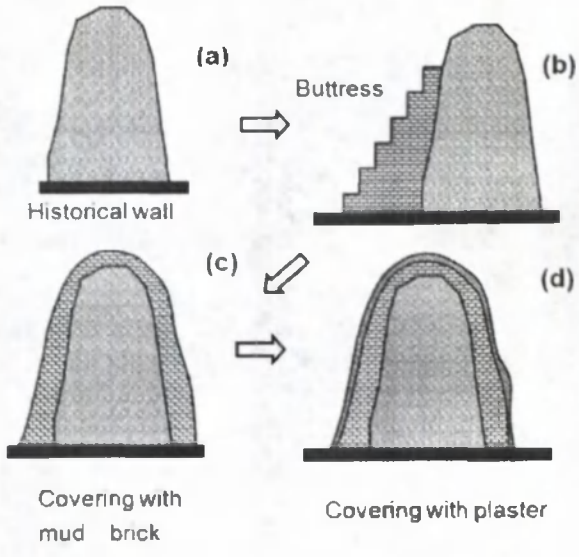


Figure 25 Concept of conservation for Ajina Tepa

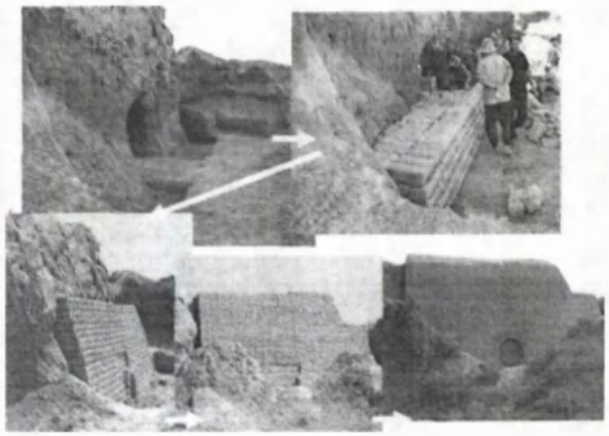


Figure 26 Conservation procedures after the archeological cleaning

3-D graphics of structures after the shelter coating is very important. In usual case, the shelter coat is constructed by the local people without measuring and reporting the thickness distribution of shelter coat. So that, the 3-D geometries be-

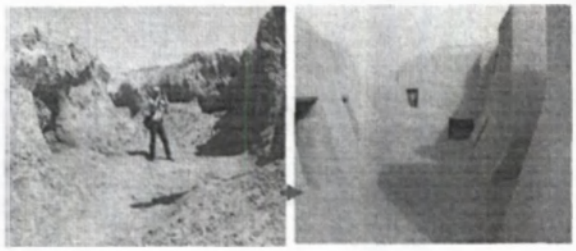


Figure 27. Before and after the conservation

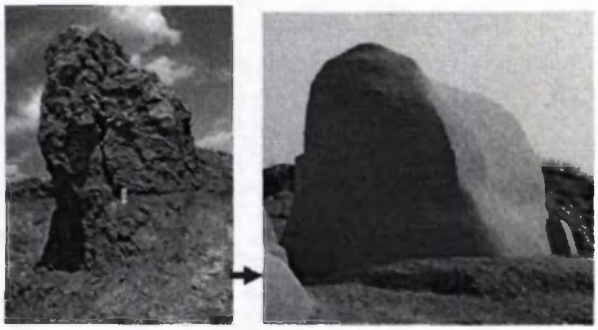


Figure 28. Shelter coating over an damaged wall with big cracks .



Figure 29. Shelter coating over the big Stupa.

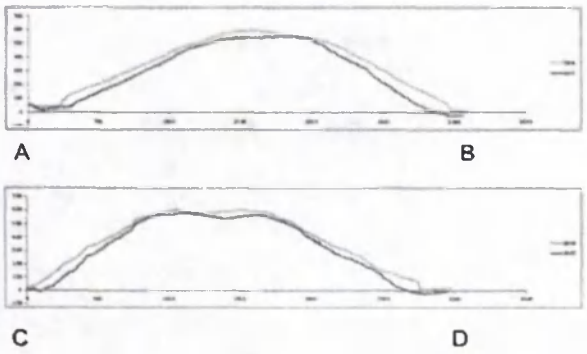


Figure 30. Cross-sections of the Stupa before and after the conservation

fore and after the conservation should be made. Through the comparison between two geometries, the thickness distribution of shelter coat can be estimated. This distribution is very important for the maintenance after the conservation. Figure 30 displays an example of geometrical changes of the big Stupa. Photogrammetry was adopted for making 3-D graphics.

6.2 *Prevention of salt weathering*

Although the deterioration of historical walls can be considerably prevented by thick shelter coat, salt weathering is still going on and decaying the shelter coat. After a long period of time, shelter coat may be deteriorated and disappeared. After that, the historical earthen structure may be decayed. It is important to protect the shelter coat. Figure 31 illustrates a possible way to prevent the salt weathering. The moisture movement from the basement induces the salt weathering. This movement could be considerably stopped by using impervious sheet as schematically illustrate in this figure. Figure 32 displays the effect of the impervious sheet. It can be clearly seen that the shelter coat below the sheet was highly damaged. On the other hand, shelter coat over the sheet was not so much deteriorated. It can be concluded the technique is good for decreasing the salt weathering effect.

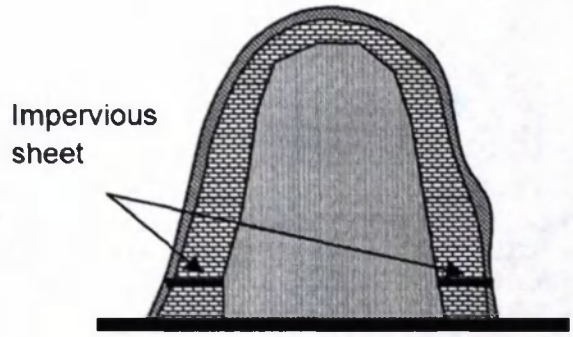


Figure 31 Way to reduce the salt weathering

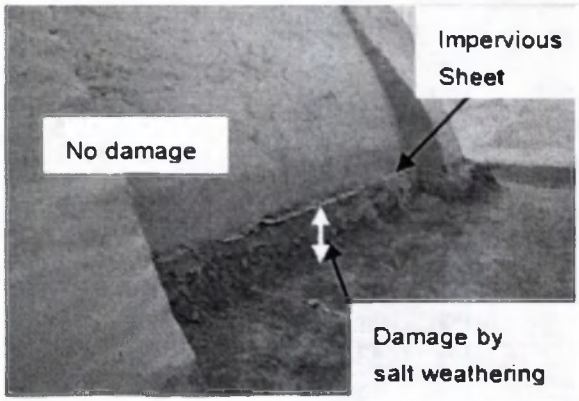


Figure 32 Effect of impervious sheet on salt weathering

The salt weathering becomes more severe by the irrigation around the site. The groundwater table is upwardly moved by the irrigation and the salt weathering is accelerated. Figure 33 displays the salt weathering in the irrigation period. Wide buffer zone to keep the groundwater table in lower condition is indispensable to decrease the effect of the salt weathering.

Alisher Navoiy nomidagi O'zbekiston MK
2013/15
1173

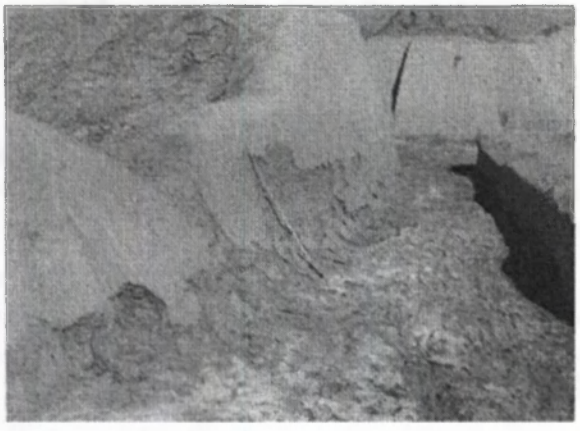


Figure 33 Damage of shelter coat by salt weathering

6.3 *Other possible techniques*

The use of Geo-textile may be a possible technique to conserve the historical earthen structures. Geo-textile or soft plastic net has been used to increase the earthquake resistance for new mud brick house (Neuman et al., 2007). For examples, it was proposed in Peru to wrap the earthen wall by plastic net and reported that this technique considerably prevented .the damage by earthquake. Geo-textile can also prevent the failure of earthen structures. However, the use of geo-textile is not technically established yet. More research works on the way how to use geo-textile is needed.

6 CONCLUSION

In this paper, techniques for making clear the earthen material and deterioration processes are presented with some actual data obtained in Chogha zanbile, Iran and Ajina Tepa, Tajikistan. Also, some examples of conservation techniques are reported. All of those techniques are tightly related to the field of Geo-Engineering. More research works are needed to develop the proper conservation techniques because ancient earthen structures are presenting not only ancient culture but also techniques that are harmonized with environmental condition.

ACKNOWLEDGEMENT

The authors reveal a sincere thanks to Mr. Yuri Peshkov of the UNESCO Cluster Office of Almaty, Dr. Enrico Fodde of BRE CICM, Bath University, UK and Dr. Yukiyasu Fujii of Fukada Geological Institute for their cooperation during the UNESCO/Japan Trust Fund Project.

REFERENCES

Fisher, W.B., (1968), "The Cambridge History of Iran", Volume I, Land of Iran, Cambridge University Press, pp. 259-263.

Fodde, E. (2007a), "Fired brick and sulfate attack: the case of Moenjodara, Pakistan", *Journal of Architectural Conservation*, 13, 69-80.

Fodde, E., (2007b), "Conserving sites in the Central Asian Silk Roads: the case of Otrar Tobe, Kazakhstan", *Conservation and Management of Archeological Sites*, 8, 77-87.

Fodde, E. (2007c),"Analytical methods for the conservation of the Buddhist Temple II of Krasnaya Rechka, Kyrgyztan", *Conservation and Management of Archeological Sites*, 8, 136-153.

Fodde, E., Watanabe, K., Fujii, Y. (2008), "Conservation and documentation of the Buddhist Monastery of Ajina Tepa, Tajikistan: heritage of the Silk Roads", *Terra 2008, 10th International Conference on the Study and Conservation of Earthen Architecture*, Getty Los Angeles: Conservation Institute.

Fodde, E. (2010), "Conservation and Conflict in the Central Asian Sirk Roads", *Journal of Architectural Conservation*, 16, 75-94.

Fujii, Y., Fodde, E., Murakami, K. (2009), "Digital photogrammetry for the documentation of structural damage in earthen archeological sites; The case of Ajina Tepa, Tajikistan", *Engineering Geology*, 105, 124-133.

Fujii,Y., Weesakul, U., Poovaradom, N. Bhadrakom, M., Watanabe, K., Kawano, S., (2012)."Deformation of stupas measured by photogrammetry before and after Ayutthaya Flood in Thailand, 2011." *4th Central Asian Geotechnical Symposium.(accepted, in printing)*.

Ghirshman, R., (1963), "L' Elm et les Recherches a Dur-Untash (Tchoga Zanbil) ", IA III, pp.1-21.

Ghirshman, R. (1966), "Tchoga Zanbil (Dur-Untash), Volume I, La Ziggurat", MDAI XXXIV, Paris: Paul Geuthner.

Ghirshman, R. (1966), "Tchoga Zanbil (Dur-Untash), Volume II, Temenos, Temple", Palais, Tombes, MDAI XL, Paris : Paul Geuthner.

Goudie, A., Viles, H. (1997), "Salt weathering Hazards", John Wiley & Sons, 241 pp.

Kuchitsu, N.,Ishizaki, T., Nishiura, T. (1999), "Weathering of the brick monuments in Ayutthaya, Thailand", *Engineering Geology*, 55, 91-99.

Linder, W., (2003)."Digital photogrammetry theory and applications."Springer,Berlin, 189pp.

Litvinskij, B., Zeimal, T.I., (2004), "The Buddhist Monastery of Ajina Tepa, Tajikistan", Isiao, Rome, 190pp.

Neuman, J.V., Torrealva, D, Blondet, M. (2007)"*Adobe Reforzado*", Fondo Editorial, 39pp.

Roef, M., (1990), "Cultural Atlas of Mesopotamia and the Ancient Near East", *Fact on File*, pp.143-144.Yastikli, N.(2007).Documentationof cultural heritage using digital photogrammetry and laser scaaing." *Jour. Cultural Heritage*,8,423-427.

Topal, T., Sozmen, B., (2003), "Deterioration mechanisms of tuffs in Midas monument", *Engineering Geology*, 68, 201-223.

Watanabe, K. Vatandoust R., Okada Y.(2003)" Physical, mineralogical and chemical properties of mud bricks and mud mortars of the Choga Zanbil, Iran." *Terra 2003, 10th International Conference on the Study and Conservation of Earthen Architecture*, Getty Los Angeles: Conservation Institute.

Watanabe, K., Maung, M..M., Fujii, Y., Fodde, E. (2008), "Evaporation measurement for the preservation of historical Buddhist Monastery, Ajina Tepa, Tajikistan", *Annual Journal of Hydraulic Engineering*, Japan Society Civil Engineering, 52, 19-24.

Watanabe, K., Fodde, E., Fujii, Y. (2011):"Deterioration and conservation of earthen walls in Ajina Tepa, Tajikistan." *Proc. Special Session on Geo-Engineering for conservation of cultural heritage and historical sites, 14th ARC,ISSMGE*, Hong Kong, pp.44-48.

Yastikli, N. (2007)."Documentation of cultural heritage using digital photogrammetry and laser scanning." *Jour. Cultural Heritage*,8,423-427.

Yilmatz, H. M., Yakar, M.,Gulec, S.A., Dulgerler, O. N.,"Importance of digital close range photogrammetry in documentation of cultural heritage." *Jour. Cultural Heritage*,8,428-433.

The Measurements of Temperature and Humidity in Ancient Tomb in Northern Dahshur, Egypt

Y.Iwasaki
Department of World Heritage, Cyber University, Fukuoka, Japan
Geo-Research Institute, Osaka, Japan
K.Yazawa and S.Yoshimura
Institute of Egyptology, Waseda University, Japan

ABSTRACT: Dahshur area locates some 30km south of Cairo, Egypt. Many ancient tombs have been excavated for archaeological study by Institute of Egyptology, Waseda University. Most tombs had been found after excavation of about 10m in depth from the ground surface. Some of the excavated tombs have been used as storage space for the excavated archaeological remains. Since the salting problem was realized in the storage space, measurements of humidity and temperature were carried out.

1 INTRODUCTION

Institute of Egyptology, Waseda Party led by Prof.S. Yoshimura has been engaged in archaeological excavation in several sites in Egypt. Northern Dahshur is one of these sites where many ancient tombs have been excavated. The excavated remains in the tombs have been studied and stored in some space that had been excavated already. Since the area is rather dry desert area, salting damage to the walls of the underground space as well as the stored remains were anticipated. To evaluate the environmental condition in the shaft, temperature and relative humidity in several shafts in Northern Dahshur area are measured and evaluated.

2. Northern Dahshur Area

Dahshur locates at 5km west of Nile River and 30km south of Cairo city, Egypt as shown in Fig.1.

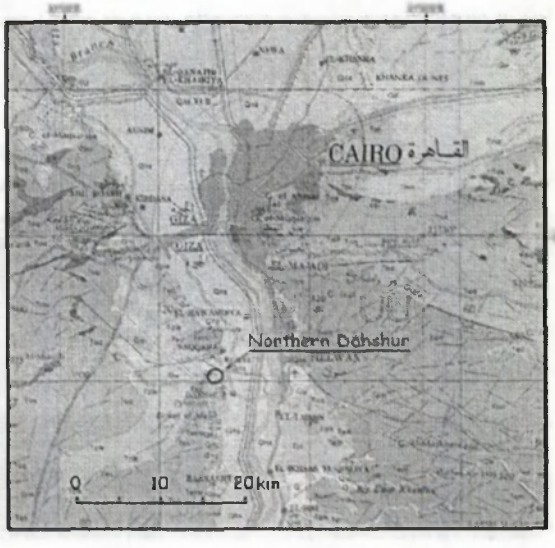


Fig.1 Dahshur site

The area had been studied by satellite image as well as by ground survey and identified as ancient group tombs in 1995.

Fig.2 Excavation site plan

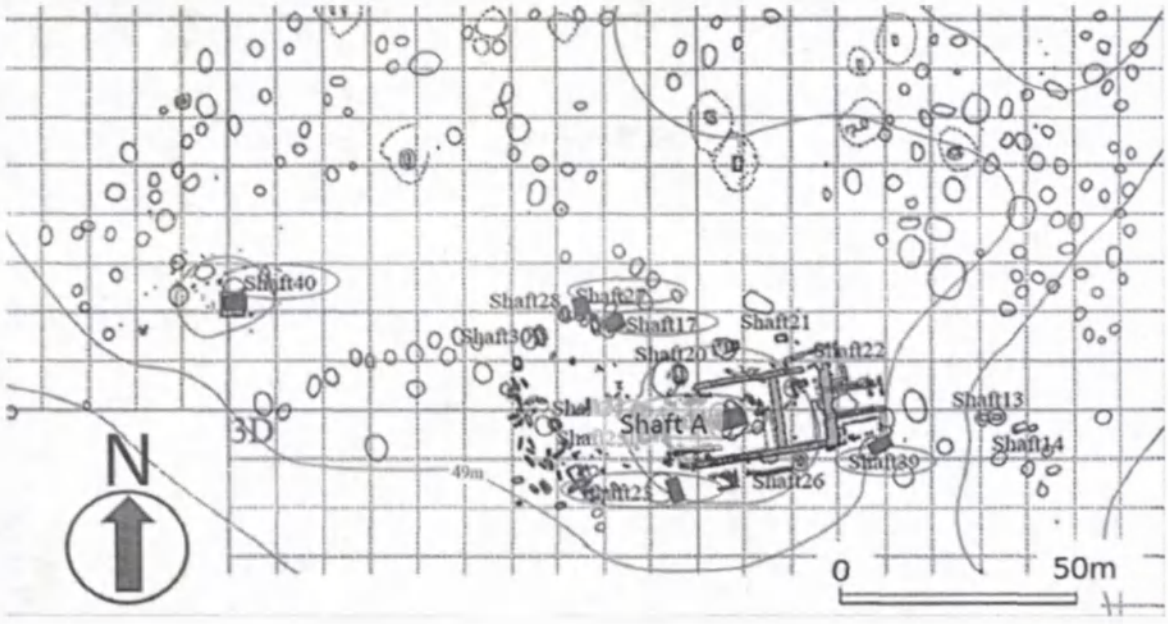




Fig.3 Digging of an ancient tomb

The study area at northern Dahshur is about 100m x 200m with a surface geology of Pleistocene geological period. The ground consists of gravel layer of a few meter in thickness followed by limestone of Tertiary geological period.

In this area, these ancient tombs are rather easy to locate at the site, because the backfilled soils covered with the surface are usually subsided compared to the surrounding ground. The circles in the Fig.2 are these subsided spots where tombs are expected to exist.

Local workers use a wind up wheeler with hand to lift up mucks that are produced during excavation a vertical shaft from the surface to reach the entrance of the horizontal drift where ancient coffin was buried. The depth of the coffin entrance is about 10m in depth. The shaft dimension in plan is about 1-2m by 5m.

3 Temperatures and Relative Humidity

3.1 Sensor

Sensor used at the site is a miniature scaled sensor that is commercially available as hygrochron.

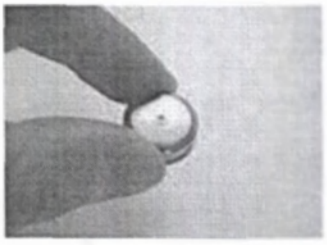


Fig.4 Sensor

A hygrochron sensor was put within a net bag with a

cable. Measurements were carried out by lowering the net bag from the top of the shaft for every 50cm with measuring 5min for each depth.

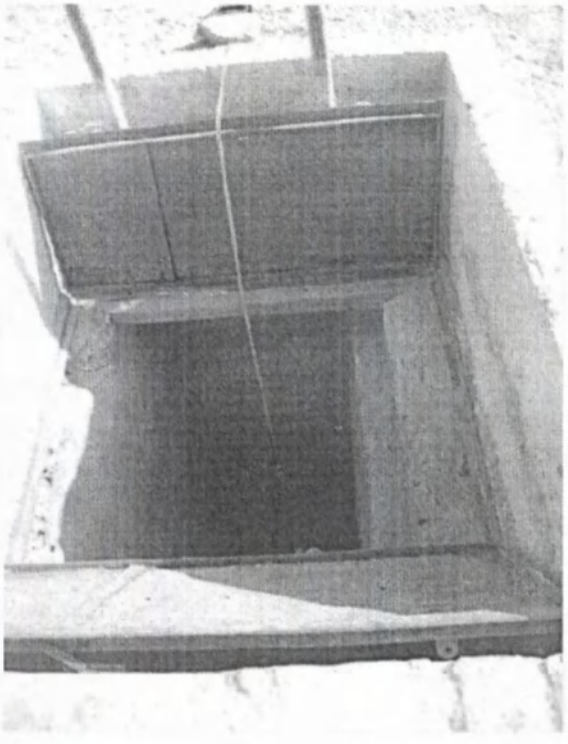


Fig.5 measurement in a shaft

3.1 Shaft No.17

A typical result of the measurement is shown in Fi.6 at Shaft No.17.

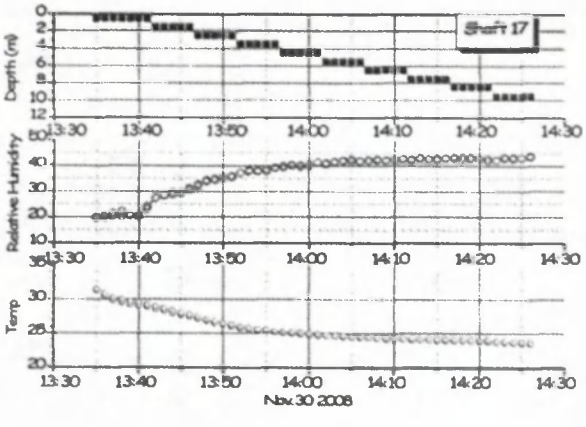


Fig.6 Temperature and RH at Shaft No.17

The results are shown in Fig.6. The temperature at the ground surface was about T=31 degrees in Centigrade with a relative humidity of RH=20%. The temperature decreased to about T=24 degrees and the relative humidity increased to RH= 42%.

3.2 Shaft A

Among many tombs that were dug about 10m in depth, a few tombs were found as much deeper and consist of several chambers. Shaft A is one of such tomb in the site and found with some remains of foundations for shrine as shown in Fig.2.

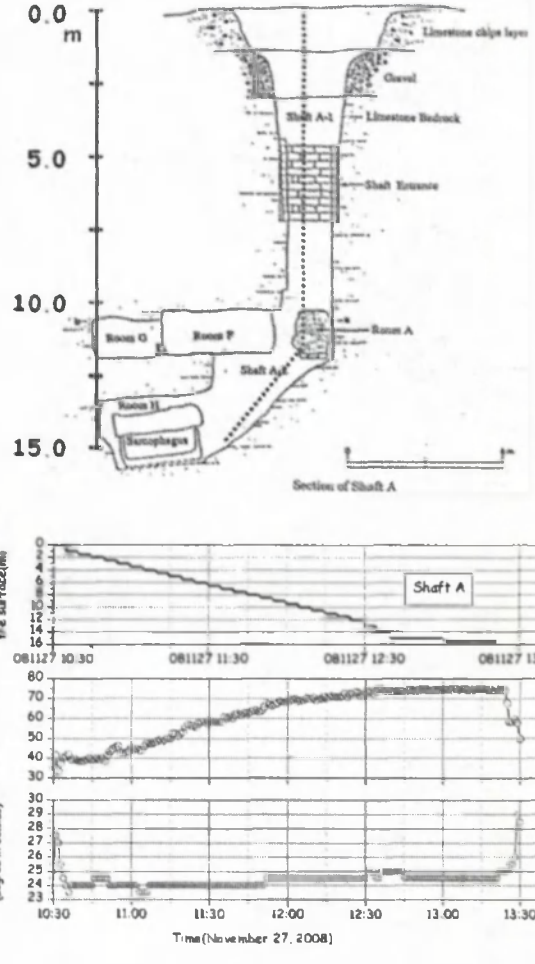


Fig.7 Vertical section of Shaft A and Measurements for Shaft A

The results of measurements for the Shaft A are

basically similar to Shaft no.17.

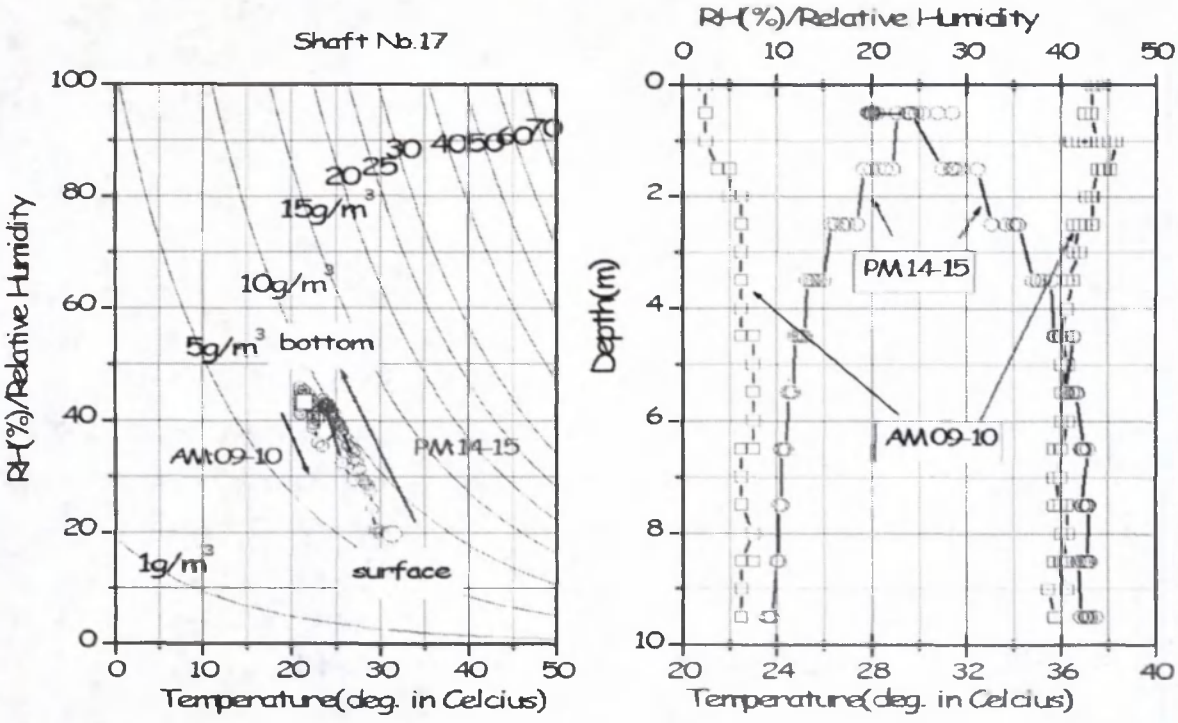


Fig.8 Vertical distribution of temperature and RH for Shaft 17

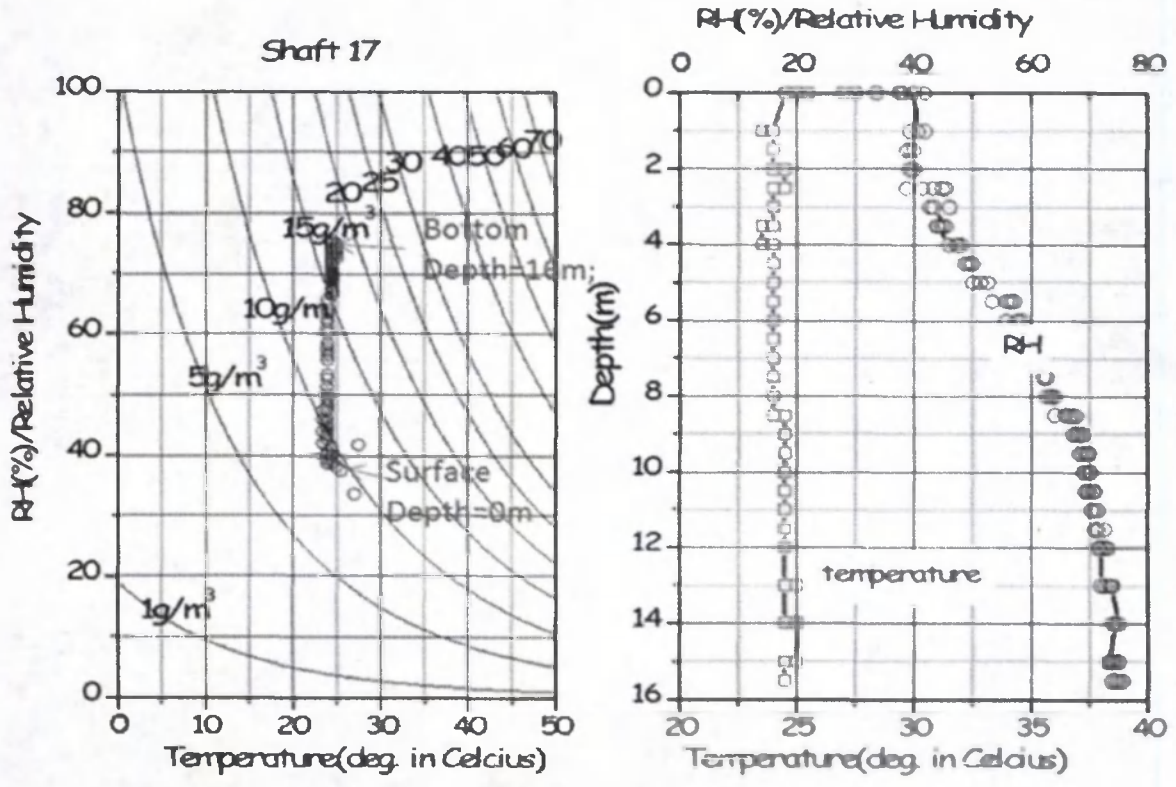


Fig.9 Vertical distribution of temperature and RH for Shaft A

4. Absolute Humidity

Fig.8 in the right shows comparison of temperature and relative humidity for different time of PM14-15 on Nov.30, 2008, and AM09-10 in the following day for the Shaft No.17.

Fi.8 in the left shows the distribution of the measured temperature and RH in the Temp-RH chart that shows contour lines of the absolute humidity of water mass per unit air volume.

The distribution of temperature and relative humidity in the morning is different from those in the afternoon for the depth shallower than four meters. At the same time, the absolute relative humidity shows rather constant value of about 8%.m^3. When the Shaft No.17 was excavated, the bottom of the shaft was found to be connected with the bottom of another shaft of a tomb nearby. These two shafts are connected each other and consist of tunnel tube. Air is easily flows into an entrance of one of the tunnel and flows out from the other tunnel.

The constant absolute water contents along the depth of the Shaft No.17 were caused by the steady flow of the air through the connected shafts.

Fig.9 shows the results for Shaft A where the temperature is rather constant from the just below the entrance. The relative humidity begins with RH=30% at the ground surface and then increased with the depth and reached around RH=75% at the depth of 14m.

The absolute humidity shows a different trend to the Shaft No.17. It begins about 8g/m^3 at the ground surface and keeps the same value until 2m below from the entrance then gradually increases with depth.

5. Effect of Closed Entrance of Shaft

The difference of the distribution of the absolute humidity may be from the several reasons. Since the site condition of geology and underground water is considered as the same, the difference must be caused other reasons. Shaft No.17 is open gate and the Shaft A has a gate that closes air flow from outside to inside to the shaft.

The constant value of the absolute water in air along depth in the Shaft No.17 suggests that the air is moving into the shaft from outside. The air temperature in the shaft is controlled by the surrounding ground. The relative humidity increased with the decrease of the temperature under the constant water content in the air.

On the contrary of the Shaft No.17, outside air of the Shaft A is blocked by the gate at the ground surface. The closed situation in the Shaft A does not allow air flow and keep the air rather at the same depth. During the time of measurement, the Shaft A was not completely closed but opened in the daytime and closed at night for some human activities.

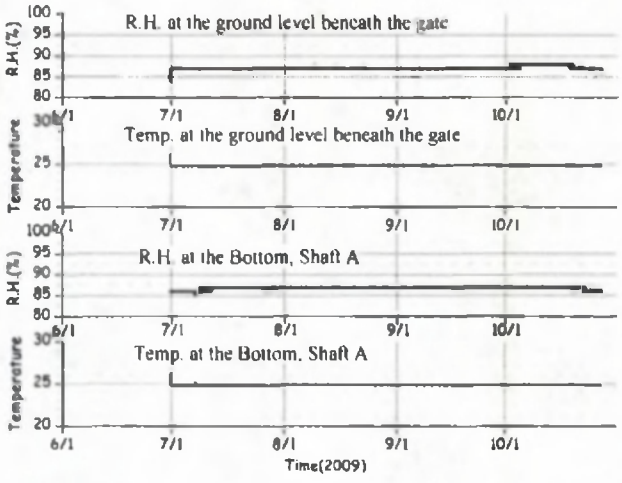


Fig.10 Temperature and R.H. for long term under the closed gate (2009)

In 2009, a continuous monitoring was carried out in the Shaft A. Two points were selected for measurement at top of the shaft just beneath the gate

and at the bottom Shaft from June 30 for about four months.

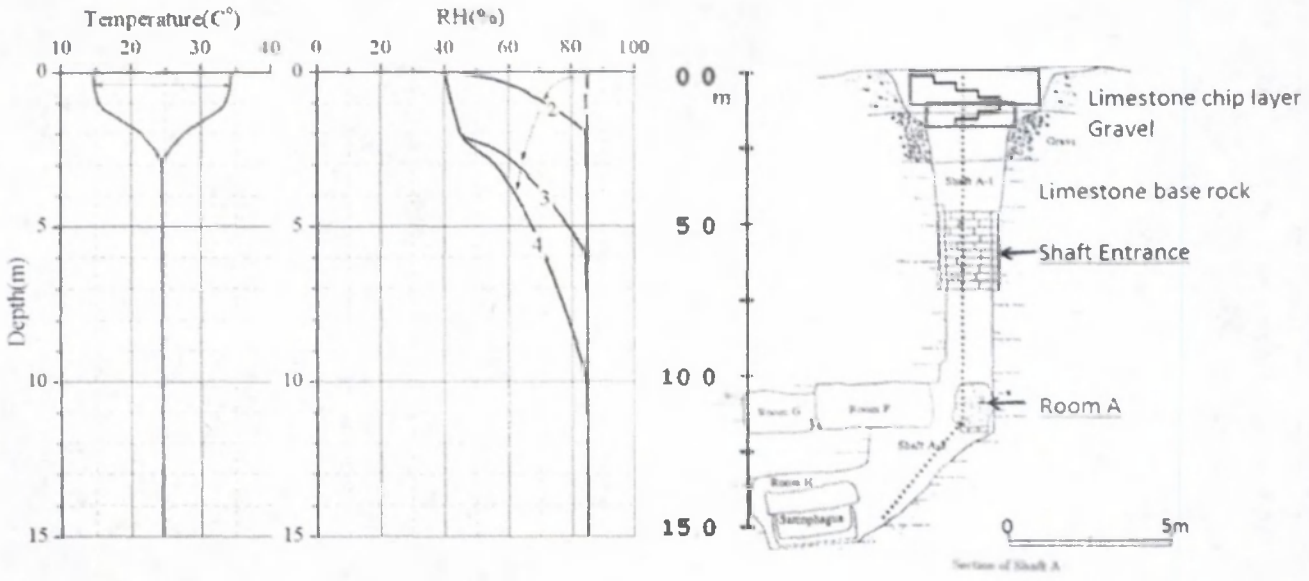


Fig.11 Estimated time change of distribution of temperature and relative humidity caused by opening

As shown in Fig.10. the data at the top of the shaft just beneath the gate and at the bottom of the shaft show almost the same value of 25 degrees and the relative humidity of 87%.

The constant value of 87% of the relative humidity was kept under the closed environment in the Shaft A. The depth variation of Shaft A shown in Fig.9 is considered due to some human action of introducing outside air into the shaft and mixed air was the results of increasing water contents from the gate to the bottom.

Fig.11 shows the effect of human activity to the temperature and relative humidity in the Shaft A under the condition of human activity for day time.

The temperature in the ground is the yearly averaged temperature outside the shaft. The temperature near the surface might fluctuate caused by the outside temperature but basically constant.

Change of the relative humidity is caused by human activity takes place at the top of the shaft in the first step. Since dry air is carried into the shaft and mixed with the existing air in the shaft.

Relative humidity decreases at the top zone of the Shaft A. The decrease of the relative humidity is schematically shown in Fig.11 as 1, 2, 3, to 4.

There is a step stairs with wide width in the top of the Shaft A from the ground to about 2m in depth where mixing air is easy and shown as a special zone in Fig.11.

6 Controlling Relative Humidity in the Shaft A

It is necessary to keep the relative humidity higher than the critical value to avoid any salting damage. As shown in Fig.11, drying air in the shaft starts from surface to downwards, relative humidity shall be monitored at some depth and human activity shall be limited based upon the monitored humidity.

7 Conclusions

Based upon measurement of the temperature and relative humidity in some shaft in Northern Dahshur.

two types are identified as free air flow and constrained flow shaft.

Free air flow type shows a constant absolute water content in the shaft and relative humidity changes with function of temperature distribution.

In constrained flow shaft, the temperature become the year average temperature and the relative humidity as high as 85% and they are more or less constant if the gate is closed and outside air is not allowed to flow in. However, the gate is open and some human activity brings outside air into the shaft, the relative humidity becomes to decrease from the top surface towards deeper depth with time.

The relative humidity of some level in the shaft shall be kept from decreasing by monitoring relative humidity in the upper level and to use it as to control human activity.

REFRERENCE

Yoshimura,S., Baba M.,Kondo J., Nishimoto S., Kashiwagi H. and Yazawa K.(2010) "Preliminary Report on the Waseda University Excavations at Dahshur North: Twelfth and Thirteenth Seasons." *The Journal of Egyptian Studies* Vol.16. pp.5-46 (in Japanese)

Preservation and Reconstruction of historical monuments with provisions for soil-structure interaction analyses

V.M. Ulitsky
Chair of TC207 "Soil-Structure Interaction. Retaining Walls", State Transport University, Saint Petersburg, Russia

A.G. Shashkin, C.G. Shashkin, M.B. Lisyuk
Georeconstruction Engineering Co. Saint Petersburg, Russia

ABSTRACT: Authors of the paper analyzed many important historical monuments in Saint Petersburg using soil-structure interaction (SSI) approach. Among them are the Admiralty building in central Saint Petersburg, St. Nicholas Naval Cathedral in the town of Kronshtadt near Saint Petersburg, and Kamennoostrovsky theatre on the Stone Island in Saint Petersburg. These projects are presented in the paper. It is shown that SSI is a very powerful tool in analysing historical monuments. The potential of this method lies in the complete description of the stress-state of the monuments and in possibility to develop measures of the monuments' remediation. To fulfil this method successfully a comprehensive survey of the monuments is needed. Essential parts of this survey are: survey of structural elements and foundations, geophysical research, soil sampling and testing, in-situ testing of soils. All these findings can be used in SSI analysis.

1 INTRODUCTON

The lecture deals with preservation and reconstruction of the most valuable historical monuments in St. Petersburg. Among them are the building of the Admiralty, Kamennoostrovsky (Stone Island) theatre, St. Nicolas Cathedral in Kronshtadt near Saint Petersburg and other important and valuable historical monuments in Saint Petersburg.

Analysis of historical buildings condition is very important for projects dealing with preservation or reconstruction of historical monuments and their foundations.

Such analysis should include the following major steps:

- Analysis of the actual stress - strain conditions of subsoil of preserved buildings, and, if necessary, of adjacent buildings;
- Estimation of the influence of present vibration background on settlement development;
- Estimation of ongoing settlements of buildings (under own weight and outside factors), that is defined through calculations or observations the location of geodetic marks and gauges;
- Estimation of the allowable additional settlement of the existing buildings during reconstruction works or new development.

For important projects it is also necessary to make historical analysis of foundation behaviour of preserved/reconstructed buildings and buildings adjacent to reconstructing object or to new development together with substructure behaviour of the existing buildings;

In all cases the principle of soil-structure interaction analyses was used with account of joint work of subsoil, foundations and superstructure.

2 ANALYSIS OF ST. NICHOLAS NAVAL CATHEDRAL IN KRONSHTADT NEAR SAINT PETERSBURG

St. Nicholas Naval Cathedral is located in the town of Kronshtadt (Fig. 1). It was built in 1902-1913 according to the project of V.A. Kossiakoff. In this cathedral an idea of a classical cruciform church with a domed roof was fulfilled. This idea was realized first in the famous St. Sophia Cathedral in Constantinople.

In fulfilling ancient architectural traditions new structural materials, introduced in the beginning of the 20 century, have been used. The main dome is supported by the system of steel beams. The dome is made of the reinforced concrete. Four big pillars are the main supporting elements of the cathedral.

Geological investigations were made in 1897 and 1902. Eighte*en boreholes were bored to the depth of 27.7 m. The bearing layer of subsoil is a coarse sand with pebbles (thickness of the layer is 1.1-4.3. m.). This layer is underlain by moraine loams with boulders (thickness 6.4 m) and hard clays.

Due to the presence of the boulders the author of the project decided to construct foundations made of cast-in-place reinforced concrete avoiding construction of piles.



Fig. 1. St. Nicholas Naval Cathedral in Kronshtadt.

Immediately after the construction completion the differential settlement was recorded with the value of about 4 cm.

During the Cathedral's life a lot of cracks have been developed. In May 2009 a sharp local increase of a crack in one of the abutments was observed. This endangered the stability of the whole structure. A special programme of cathedral structural survey, research and development of salvation measures was put forward. The key issue of this investigation was to find out the reasons of cracks development.

Some dangerous cracks in the cathedral's structures are shown in Fig. 2 and 3.

The scope of the survey works was the following:

- Full structural survey of the cathedral was completed

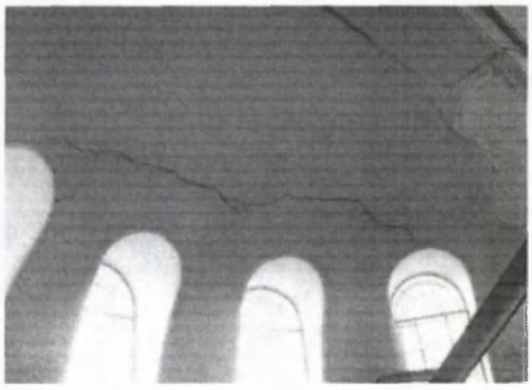


Fig. 2. Cracks in the vaults of the cathedral.

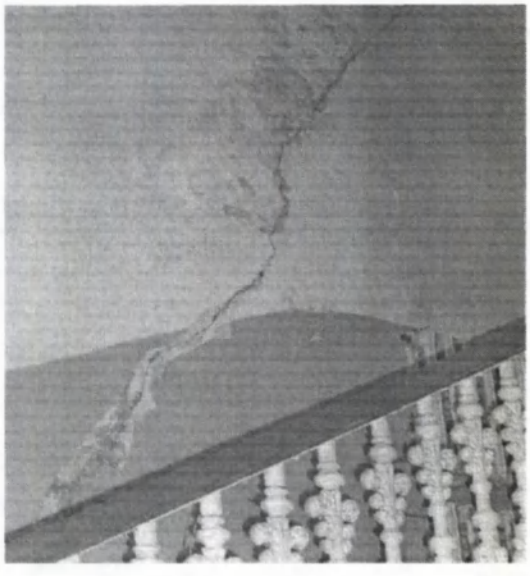


Fig. 3. Cracks in the wall of stairwell passage.

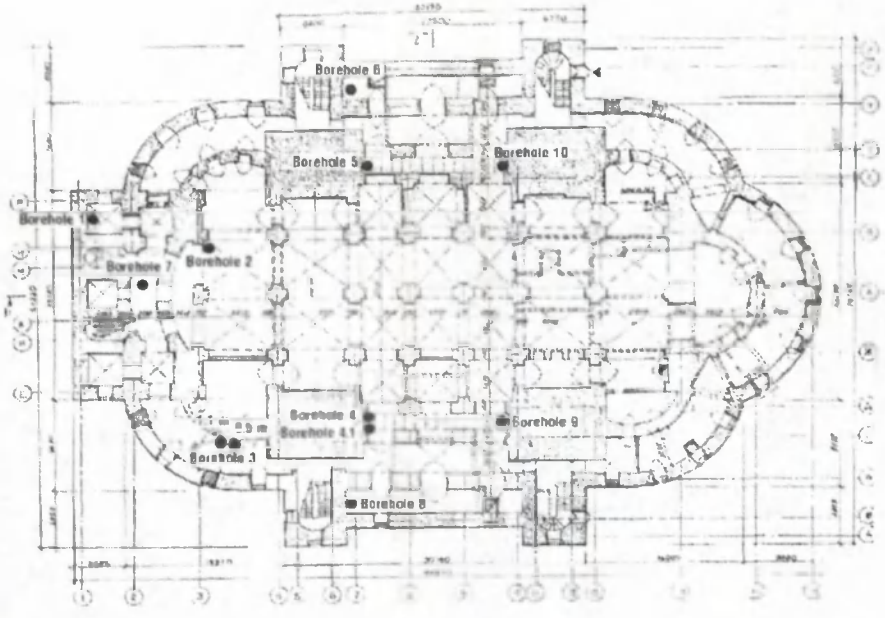


Fig. 4. Location of test boreholes drilled through foundation body to the subsoil.

- 11 holes have been drilled through the foundations body to the subsoil. Scheme of test boreholes is shown in Fig. 4. The condition of the foundations and subsoil was estimated.

- Dynamic sounding of the subsoil was made

- A detailed geophysical investigation was made. This investigation showed that there are several zones of subsoil local softening due to leakage of water. These zones are located in the vicinity of the engineering networks. Around the cathedral a partially decayed timber sheet pile wall was found out.

- Soil samples from the holes were taken: main properties of soil were determined.

It was found out that the condition of subsoil and foundations was satisfactory.

A series of soil-structure interaction computations has been performed with the help of FEM models 2.0 software (Ulitsky V.M. et al, 2003). The computation profile is shown in Fig. 5. All main structural elements, foundations, and subsoil layers have been incorporated in the computation profile. All main findings during the condition survey of structural elements, foundations, and subsoil have been taken into account in computations.

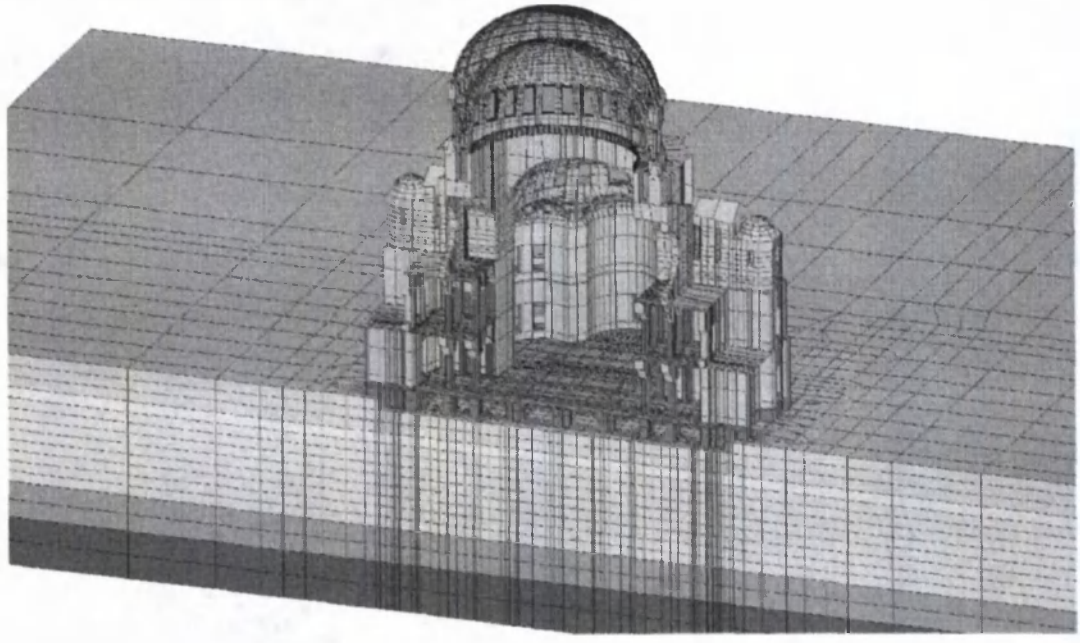


Fig. 5. Computation profile of the cathedral.

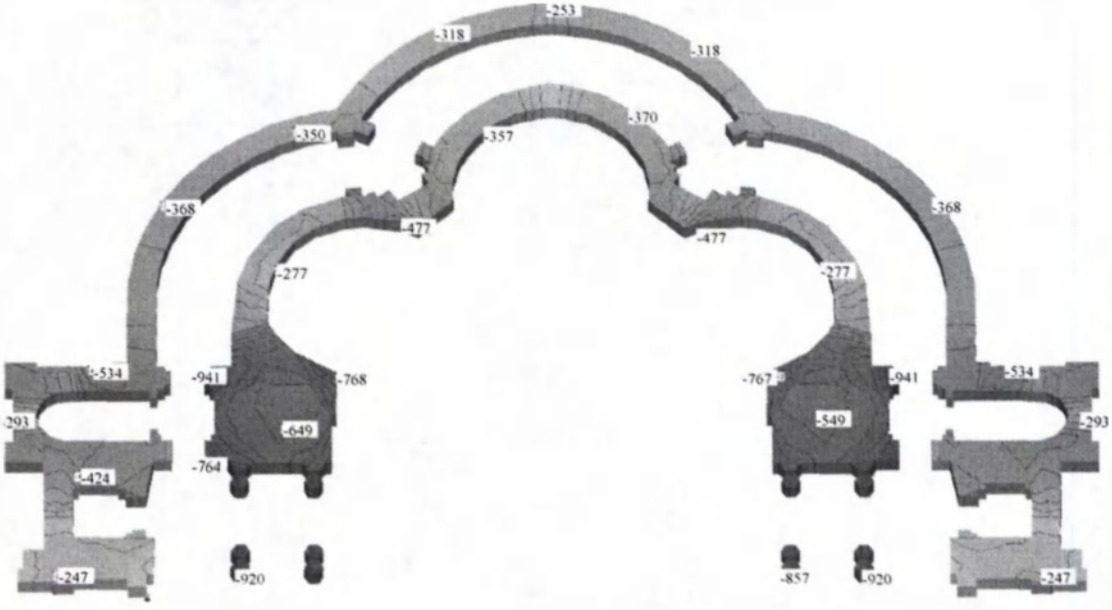


Fig. 6. Distribution of vertical stresses (kPa) in the main bearing structures of the Cathedral on the level of the 1st floor. The most heavily loaded are the main pillars, the least loaded are the walls of the outer galleries.

Soil-structure interaction calculations showed that the cathedral is subject to non-uniform settlements. The reason of these settlements is the different loads acting to the main bearing structures of the Cathedral (Fig. 6, 7). Such non-uniformity of loads is quite typical for the temples characterized by cross-cupola structural scheme. The most heavily loaded are central pillars by which the central cupola is supported. Hence, the pillars are subject to bigger settlements. The calculated non-uniform settlements (Fig. 7) correspond well to the results of the geodetic measurements. The observed settlement differential is about 13-22 mm.

Computations show that the zones of development of tensile stresses in brickwork well agree with the locations of actual cracks. In particular, taking into account non-uniform settlements we have a characteristic system of cracks in the semi-domes in altar and Western parts of the Cathedral (Fig. 8 and 9).

The main conclusion of the conducted investigations and SSI computations is that currently there is no danger of an immediate collapse of the Cathedral.

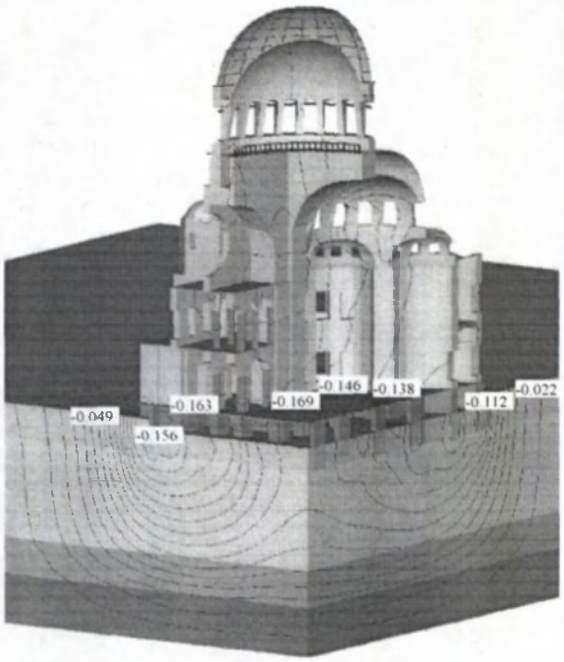


Fig. 7. Contours of computed of settlements of the Cathedral, cm.

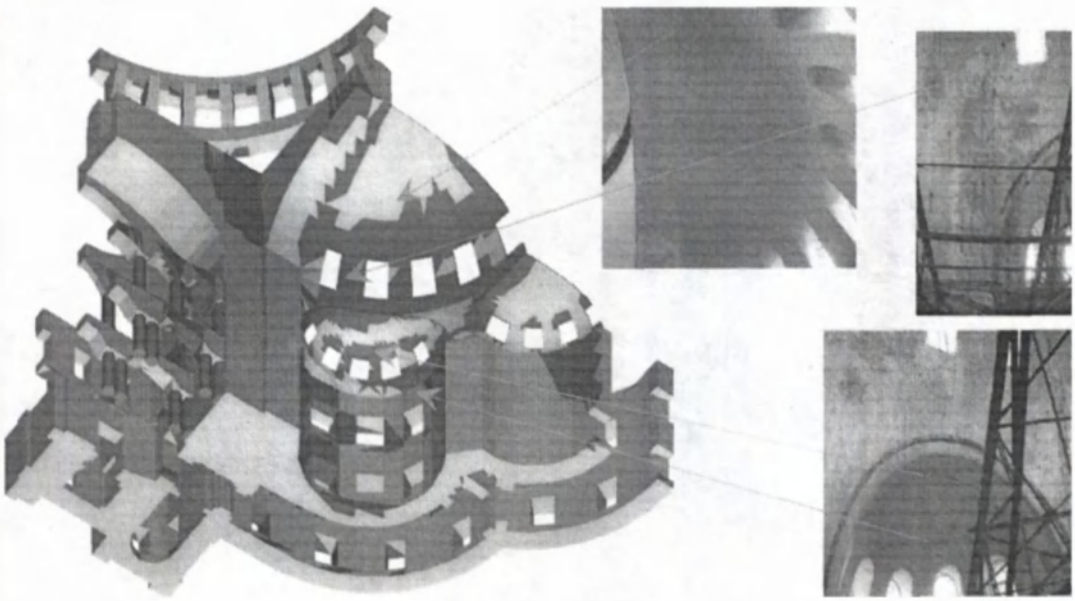


Fig. 8. Location of possible calculated cracks development and real observed crack locations.

Local mostly endangered structural elements are: the main dome, its supporting elements and semi-domes in Eastern and Western parts of the cathedral. Local reinforcement must be provided as soon as possible. This reinforcement must be based on the detailed analysis.

The computations of the system "subsoil-foundations-superstructure" show that all main cracks in the structural elements of the cathedral are caused by differential settlements of the monument (Fig. 7), conditioned by the non-uniform loading of the subsoil. The most dangerous cracks

caused by differential settlements are the cracks in semi-domes in Eastern and Western parts of the cathedral.

The Cathedral was successfully reconstructed. It was re-opened on May 2012.

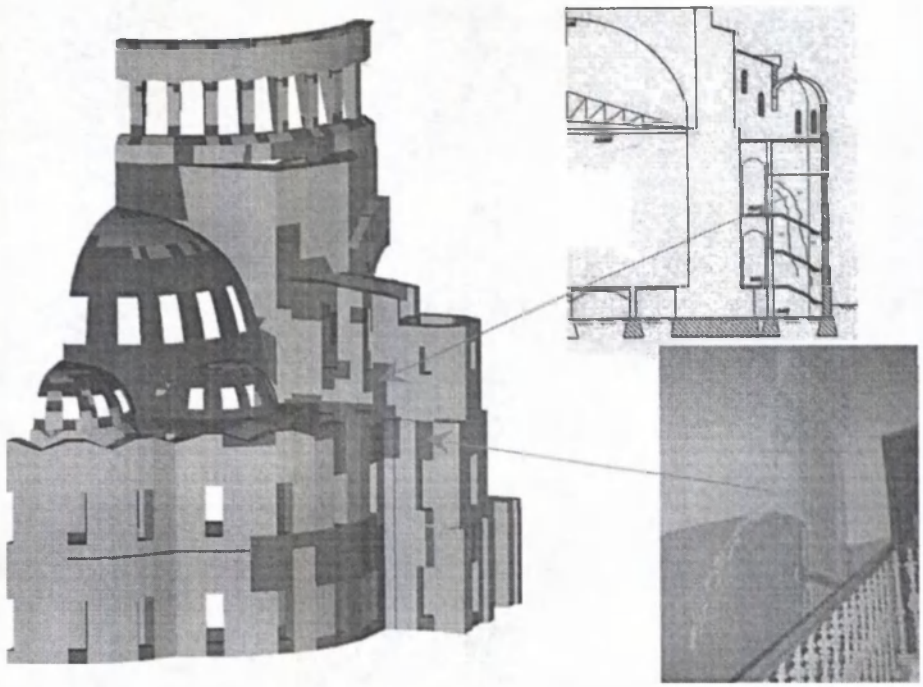


Fig. 9. Location of possible cracks development by calculations as compared with the real observed cracks.

3 ANALYSIS OF THE ADMIRALTY BUILDING IN CENTRAL SAINT PETERSBURG

First example deals with the Admiralty building in central St. Petersburg (Fig. 10). The building has well pronounced cracks. The purpose of the historical analysis in this case was to find out the reason of these cracks development to make decision about further strengthening or preservation of the monument.

(a)



(b)

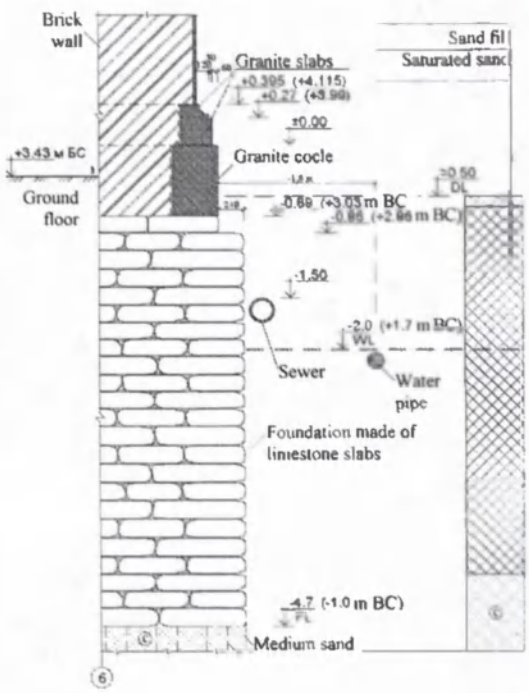


Fig. 10. (a) The building of the Admiralty, (b) historical foundation under the Admiralty tower.

The Admiralty tower was constructed in 1734 by I. Korobov. In 1811-1823 the Admiralty was reconstructed by A. Zakharov, who enlarged the tower and made some structural rearrangements.

The tower has a rigid structure. It rests on stone foundations supported by wooden piles (Fig 10b). The subsoil under the tower is loaded more than under the adjacent lower wings of the building. Therefore the tower suffered bigger settlement than the adjacent wings. The cracks appeared in the wings near the location of windows.

The subsoil of the Admiralty is comprised of fine-grained saturated sand of medium density and soft clayey sands. A thorough survey of the foundation has been made. The stone foundations were inspected by a mini TV camera lowered down the survey holes predrilled through the stone foundations.

It was found out that the average percentage of voids in the foundation body was in the range of 1 to 10%. General condition of the foundations was found to be satisfactory, except for one part of the foundation under a transverse walls of the tower.

The structural survey of the building made it possible to identify all cracks in the walls. It was discovered that many cracks appeared in the bearing walls of the tower.

To find out the reasons of the cracks development in the tower a 3D soil-structure interaction analysis has been performed. All findings made during the geotechnical and structural survey of the building have been taken incorporated into the design scheme.

Initial construction and consequent reconstruction of the building was modelled. First the deformations of old Korobov's Admiralty tower (1732) were assessed, and then the modifications of the design scheme were made with account of the added walls (1816) and additional loads (Fig. 11). Thus, the real construction history had been simulated.

The contours of settlements accumulated after reconstruction of the building are shown in Fig. 12. The total estimated settlements have a value of about 20 cm. It should be noted that the soil model used in the analysis can take into account a long-term creep of the Admiralty's subsoil.

The performed analysis has made it possible to identify the reasons of the cracks development in the structural elements of the building. The main crack appeared in the tower wall adjacent to the lower wing. The reason of this crack development is the non-uniform settlement of the building. The development of settlements may still go on, which can be explained by a long-term creep of the subsoil. The non-uniform settlement leads to the generation of shear stresses in the walls with their maximum values up to 235 kPa (Fig. 13a).

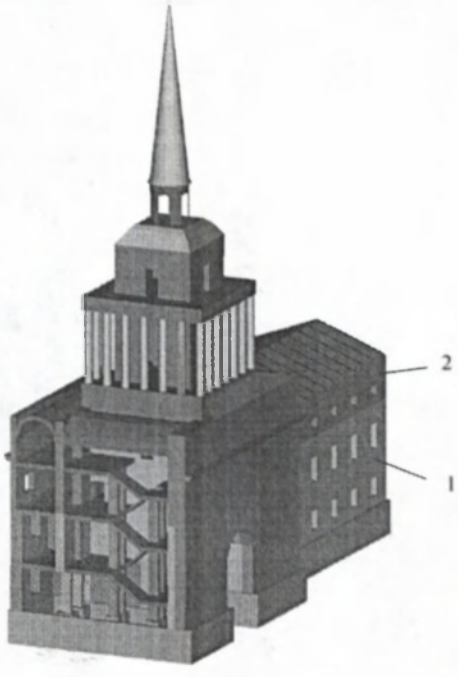


Fig. 11. Part of the calculation profile for the Admiralty building: 1 – masonry of 1732, 2 – masonry of 1816. Subsoil not shown but it is incorporated into the calculation profile.

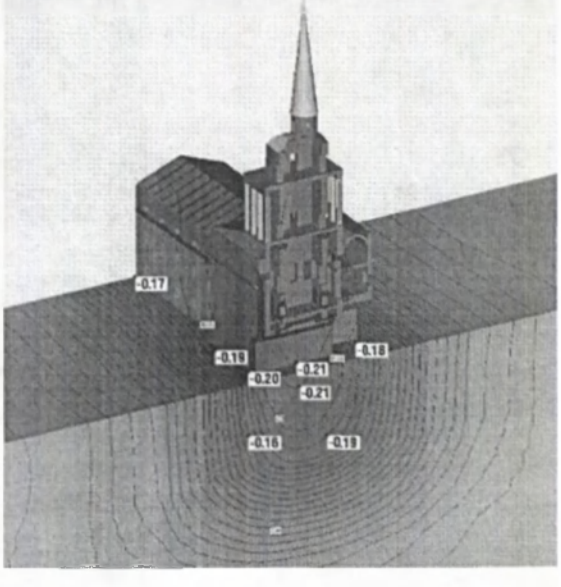


Fig. 12. Contours of computed of settlements of the Admiralty (cross section along the symmetry axis), cm.

The shear stresses cause the development of the cracks in the tower walls (fig 13b). There is a good correspondence between the soil-structure interac-

tion calculation results and the observed behaviour of the building (fig. 14).

Thus, the conducted historical analysis of this geotechnical problem taking into account joint behaviour of the Admiralty' structure and subsoil as well as the construction history helped to identify the reasons of the deformation of this famous monument in the central Saint Petersburg.

(a) (b)

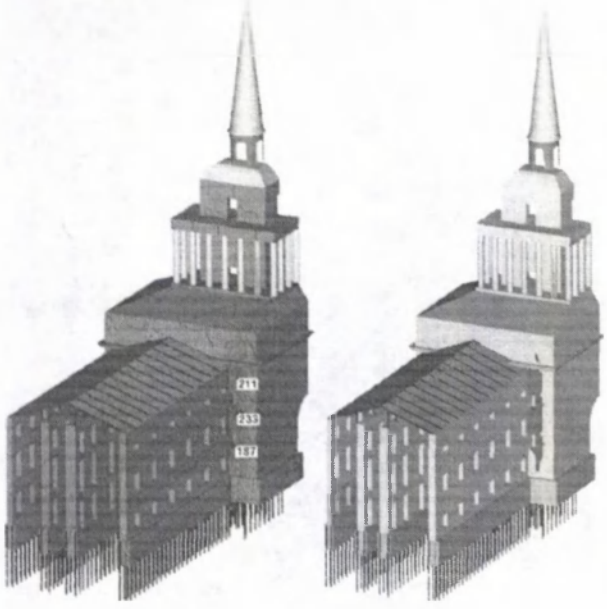


Fig. 13. Analysis of the structure of the building: (a) contours of the shear stresses in the masonry (kPa), caused by the differential settlement of the tower and the lower wing; (b) zones of the possible development of the cracks caused by shear deformations of the transverse wall.



Fig. 14. Development of cracks in the Admiralty tower.

4 RECONSTRUCTION OF HISTORICAL KAMENNOOSTROVSKY THEATRE

Kamennoostrovsky (or Stone Island) timber theatre was constructed in 1828, designed by architect S. Shustov to provide a temporary floor for the Imperial Opera and Ballet Troupe whilst reconstruction of the Bolshoi Masonry Theatre was ongoing (the latter was subsequently rebuilt into the St. Petersburg Conservatoire). The critics noted rare elegance of the structure and it was due to that elegance that following a decade and a half a decision was taken to preserve it by means of adding rubblework foundations (prior to that the lowest courses of the building rested directly on timber piles). The Russian-Italian architect Alberto Cavos believed he had managed to prolong the building's life by about 50 years. However the building was able to withstand the passage of time for as long as 180 years, surviving the tempestuous years of revolutions and wars. Until the 1930-s the Stone Island Theatre was used as a warehouse, when it was renovated and converted into a television theatre and later to a dance studio. In Russia only two timber theatre-structures have remained, the Stone Island Theatre being a world heritage site protected by the UNESCO (Fig. 15).

In 2006 it was decided to renovate the monument making it a theatre corresponding to all modern standards of stage technology and comfort.

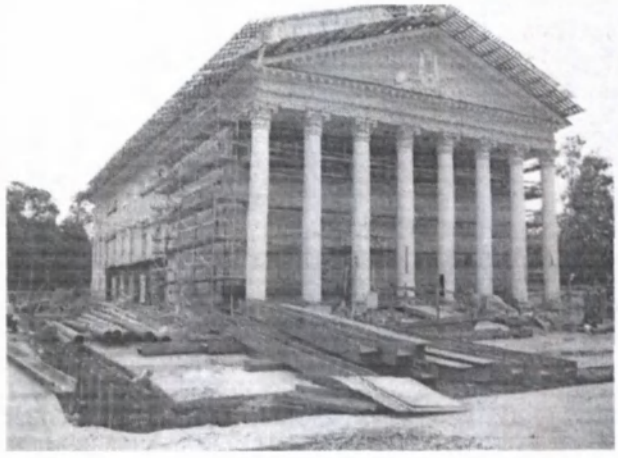


Fig. 15. Kamennoostrovsky theatre.

It was decided that an underground space should be provided under the theatre, keeping historical wooden structures intact. The dimensions of the underground part are 80×40 m. This underground space should be provided immediately underneath the historic superstructure. That space houses stagecraft facilities – upper and lower stage mechanics (e.g. stage terracing, orchestra pit, light-

ing arrangements, backdrop hoists, etc), as well as roomy foyers and cafes, convenient wardrobes.

The subsoil of the theatre is composed by lacustrine and glacial soft highly compressible clays underlain by glacial deposits of moraine and hard Wendian clay. Quaternary deposits extend down to 24.2...30,3 m, corresponding to absolute levels of -22.27...28.27 m BS (Baltic Datum), and are underlain by Wendian stratum, being firm silty clay.

Reconstruction implies provision of underground facilities under the entire footprint of the building and extending beyond its perimeter by 6.8 to 25 m (the size of the underground space is 80×40 m). The relative level of the underground structure is at minus 6 m (minus 2.9 m BS). In order to construct the underground area, excavation was necessary down to relative level -6.7 m (absolute level -3.6 m BS). The absolute planning level is at 2.0 m BS. Therefore, an excavation down to 5.6 m from the surface was necessary to accommodate the underground structure.

It should be noted that on all stages of design and works implementation Soil-Structure interaction analyses have been performed to ensure the safety of the building.

The sequence of works adopted for the project is shown in Figures 16-20. The works can be subdivided into 6 stages:

1. Drilling holes in existing walls to accommodate transverse beams of the unit responsible for temporary walls-to-piles loads redistribution.

2. Construction of bored piles, introduction of the transverse steel beams, preparation of rebar cages and concreting for reinforced concrete waling beams to facilitate load transfer. (Fig. 16, 17). Simultaneous construction of the sheet pile cofferdam. Bored piles were of 2-step construction "Titan" type: initiated with oscillation of the casing down to the level of the underground structure subsequently followed with pile construction as such. The casing was necessary to improve bending strength of the top half of the pile, which was needed during excavation for the underground structure.

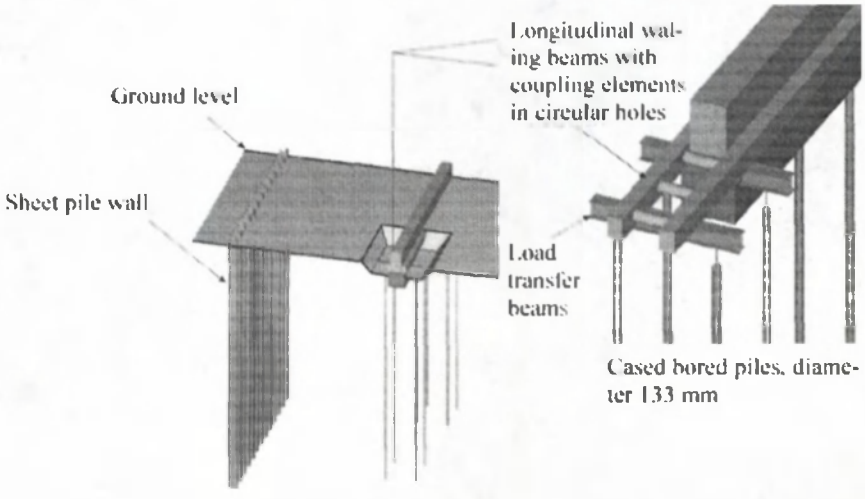


Fig. 16. Construction of sheet piles, bored piles, and the unit transferring the load from the walls to the piles.



Fig. 17. Introduction of beams underneath the waling and transferring loads onto piles.

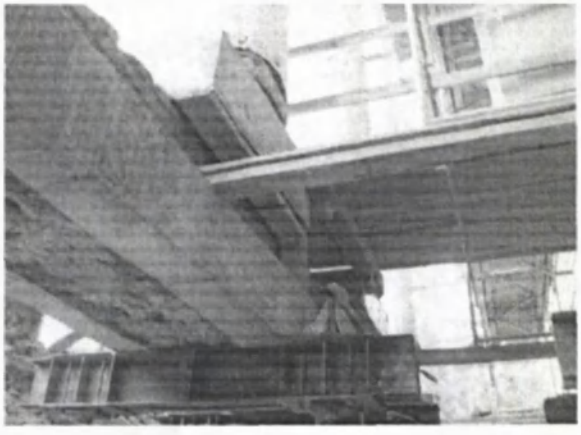


Fig. 18. All loads have been redistributed. Old foundations removed.

3. Application of jacking devices on the transverse beams, tightening retaining nuts on bars of the underpinning bored piles thereby engaging the piles to assume loads. Following this the lower sections of the building's rubblework foundations could be removed (Fig. 18). These works were to be carried out using maximum sparing methods, ruling out dynamic loading onto existing buildings. Following removal of the lower parts of the rubblework foundations a slab is to be cast directly underneath, forming a rigid disc at the level of the foundations (Fig. 19, 20). Stiffness strips are cast under the existing foundations to redistribute loads onto the slab. Bored piled also are embedded into the rigid disk slab. Following this step, the units described in 2 above are no longer required as the loads from the walls of the building are now transferred directly onto piles through the medium of the rigid disk.

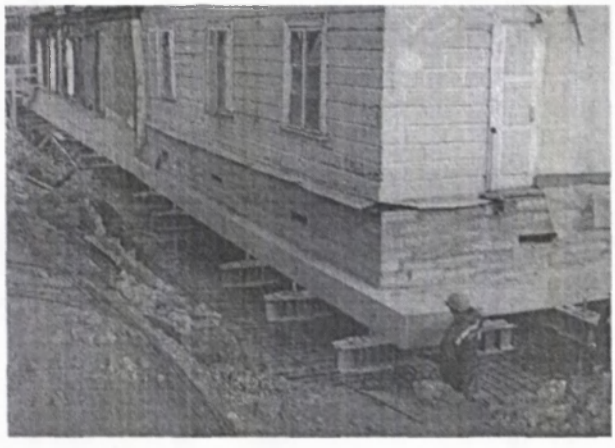


Fig. 19. Suspension of the building on the root piles to provide construction of the rigid disc slab.



Fig. 20. Construction of the upper rigid slab.

4. Excavation of the pit for the underground structure down to the designed level. Excavation is performed by layers starting from the strips closer to the outer perimeter. Thereat symmetry of excavation on various sections of the building is to be strictly observed. To provide for stability of the sheet pile cofferdam a waling beam and a shoring system are provided; those are to be supported by the rigid disk and mounted on special embedded elements in the slab. Following excavation of the perimeter strips light-duty machinery is introduced into the pit and excavation begins directly underneath the theatre building. As the soil is excavated the piles are propped by struts to form through-section columns and enhance stability.

5. Construction of bottom slab for the underground structure. Forming embedment slots for the bored piles in the bottom slab.

6. Concreting for the exterior walls, interior walls and columns of the underground structure. After concreting for the exterior wall of the underground structure and construction of the intermediate slabs at the perimeter sections the spaces between the sheet piles and the underground structure are backfilled. Following completion of the underground structure and backfilling the struts are taken down. As soon as supports are introduced under the rigid disk slab, temporary through-section columns of bored piles are dismantled at which point the loads come to be transferred through the bottom slab.

On all stages of the project a careful monitoring of the settlements of the theatre was performed. The values of the theatre' settlements were within acceptable limits. The project has been successfully completed. The Theatre was open in May 2011.

The Authors should also mention that on 17-20 November Leipziger Messe exhibition hall hosted another of its biennial Denkmal events — European Trade Fair for Conservation, Restoration and Old Building Renovation under patronage of UNESCO. A gold medal at this exhibition was awarded to Kammennoostrovsky Theatre Project.

5 INFLUENCE OF GEOTECHNOLOGIES ON ADJACENT BUILDINGS IN URBAN AREAS

When considering the issue of neighbouring buildings preservation or strengthening the following rule must applied: means of protection must be adequate to provisional impact.

Usually it is not too difficult to establish impact associated with loading or unloading of subsoil, while the influence rendered by technological factors is much more complicated to define. It is recommended to attempt calculation of impact generated by various piling technologies onto subsoil, to established the importance of relevant technological factors, as well as the dimensions of impact areas, for example, of pile jacking (oscillating), pile driving and vibration techniques of piling and

sheet piling in relation to existing structures have been also established (Poulos, 2003, Ulitsky, 2003). It is especially important for urban areas with marine soft soils which often are structurally unstable media inclined to remolding at externally generated impact which procedure is accompanied by reduction of their mechanical properties, such as bearing capacity and strength and increase of their compressibility.

As can be seen from analysis of deformed buildings in central Saint Petersburg, (Fig. 21), the portion of dilapidation brought about by works implementation drawbacks of adjacent construction is 39%.

Below we list an example of technological impact to an adjacent buildings. In 1998 one of the world's leading geotechnical companies was carrying out continuous flight auger (CFA) bored piling in central St. Petersburg. Resulting from impossibility to create proper drilling conditions, whereat one turn of the auger would correspond to downward advance of same auger by one flight, remoulding of subsoil of adjacent building was brought about.

Boreholes with geometrical volume of 8 m^3 would consume 12 m^3 of concrete, sometimes amounting to 24 m^3, and in two cases to as much as 50 m^3. Resulting from large scale piling the adjacent multi-storey building constructed in 1905 and located at 20 m from the excavation had started developing deformations which exceeded 30 mm by the beginning of 1999 (Fig. 22).

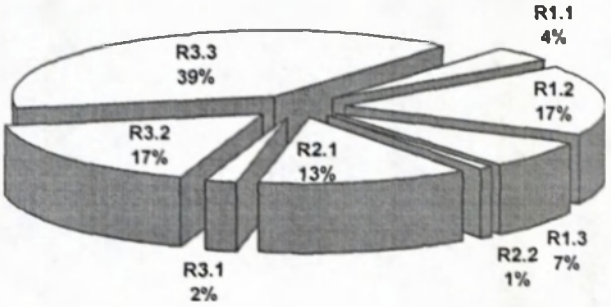
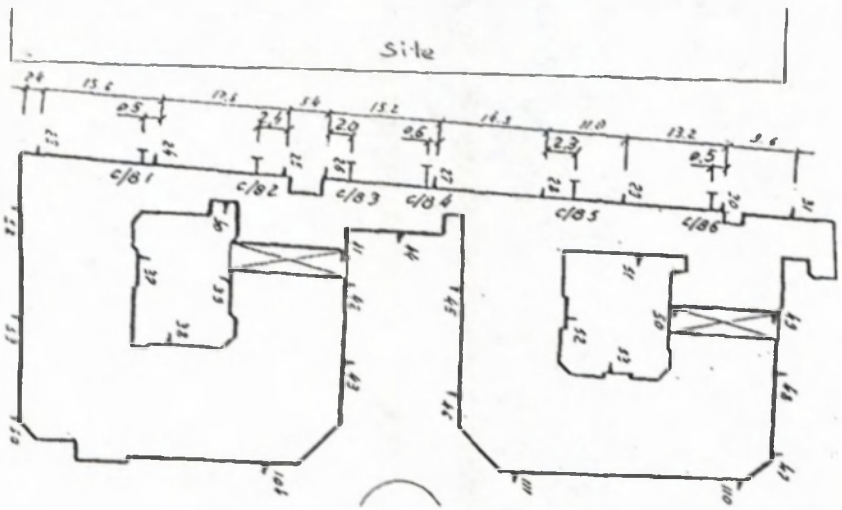


Figure 21. Causes for damage to existing buildings during adjacent construction in St. Petersburg:
R1.1 – deformation causes related to mistakes in site investigation/condition surveying; R1.2 – deformation causes related to faulty design; R1.3 – deformation causes related to faulty works implementation; R2.1 – deformation causes related to faulty maintenance of building; R2.2 – deformation causes related to faulty maintenance of adjacent area; R3.1 – prospecting/condition surveying drawbacks of adjacent construction; R3.2 – design drawbacks of adjacent construction; R3.3 – works implementation drawbacks of adjacent construction.



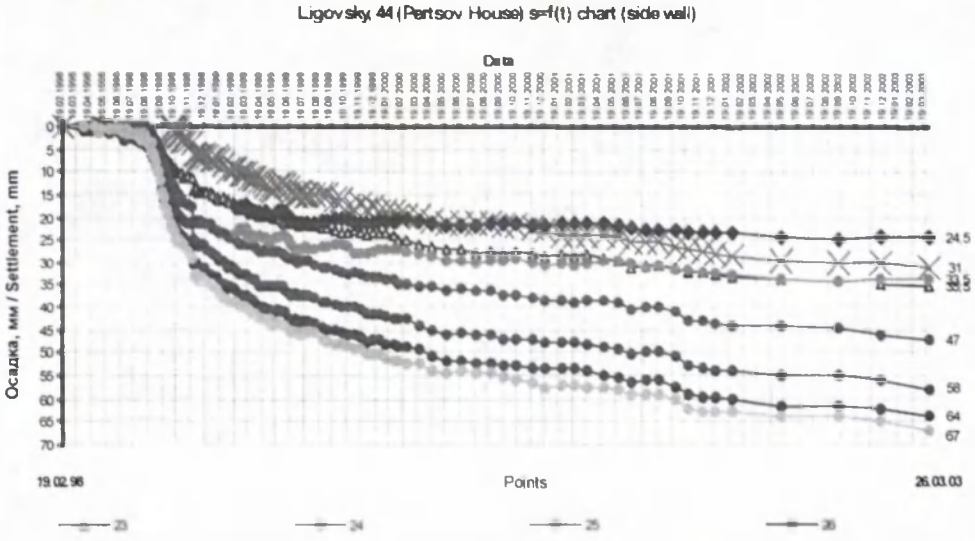


Fig. 22. Settlement development in time resulting from CFA piling (Ulitsky, 2003).

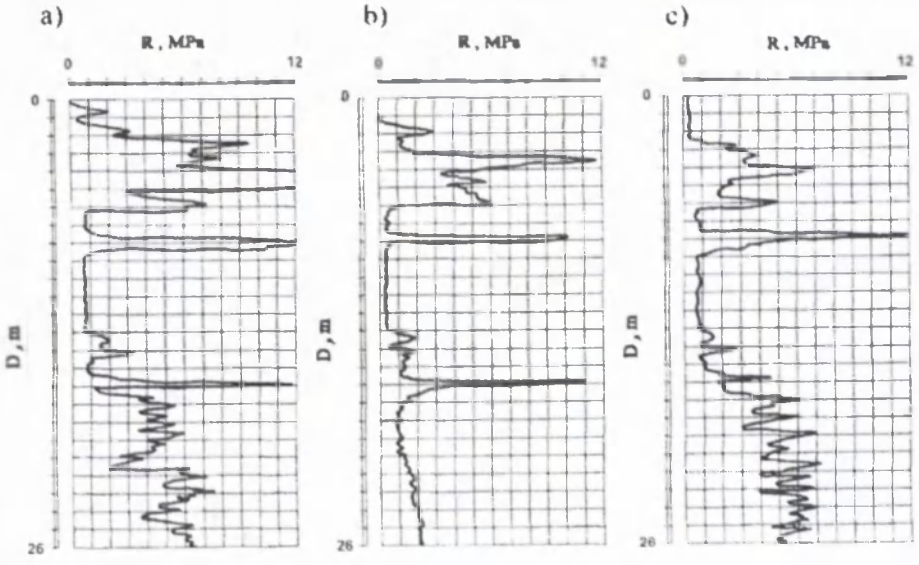


Fig. 23. Change of cone penetration resistance of soils: a) prior to commencement of piling; b) during piling; c) following completion of piling (Ulitsky, 2003).

The works were suspended owing to economical reasons and everyone had a possibility to observe 'pure' after effect of such piling. Currently the building has settled by more than 90 mm. Such nature of deformations corresponds quite well to our forecast provided before the works have started. Ground probing conducted prior to commencement of the piling, during the piling, and following site suspension produced interesting results. Following completion of piles construction the soils considerably reduced their cone resistance properties (Fig. 23).

Therefore domestic geotechnical codes of St. Petersburg, published after this case, hold as prerequisite for the designer to opt for such foundation solution of the new or reconstructed building and such corresponding construction technology which would be certain to result in no precarious situations with the existing buildings.

6 CONCLUSIONS

Examples of historical monuments analyses are presented in this paper. These examples show that it is very important to use soil-structure interaction approach in design of monuments preservation and renovation in urban areas. SSI approach is a very efficient at all stages of analyses of monuments. It is very powerful tool in prediction of behaviour of preserved buildings and structures.

Successful application of SSI approach requires a very comprehensive survey of the monuments. Essential parts of this survey are: investigation of the structural elements, foundations and subsoil, geophysical research and testing, soil sampling and

tesing, in-situ testing of coils. Results of these investigations must be used in SSI Analysis.

Choice of geotechnologies and foundation type should be influenced by the limitation of the additional allowable settlements both for the building under design and, not less importantly, for the adjacent structures.

REFERENCES

Burghignoli, A., Jamiolkowski, M., and Viggiani, C. 2007. Geotechnics for the preservation of historic cities and monuments: components of a multidisciplinary approach. General report. *Proc. of XIV European conference on Soil Mechanics and Geotechnical Engineering "Geotechnical Engineering in Urban Environments"*. Madrid. Volume 1.

Frank R. 2006. Some aspects of soil-structure interaction according to Eurocode 7 'Geotechnical design'. *Engenharia Civil Civil Engineering*. Universidade do Minho. Portugal. No. 25. pp.5-16.

Poulos, H. 2003. Effects of urban construction on existing pile foundation. State of the Art report. *Proceedings of the 13th European Conference on Soil Mechanics and Geotechnical Engineering*. Prague. 25-28 August 2003.

Powderham, A. 2003. Protecting historical infrastructure using the Observational Method. *Proceedings of the geotechnical conference "Reconstruction of historical cities and geotechnical engineering"*. St. Petersburg. 16-18 September 2003. Vol. 1. pp. 243-250.

TSN 50-302-2004. *Design of foundations for buildings and structures in St. Petersburg*. Local constructional codes for St. Petersburg. Government of Saint Petersburg. 2004.

Ulitsky, V., Shashkin, A., Shashkin, K., and Lisyuk, M. 2003. *Soil-structure interaction: methodology of analysis and application in design*. ASV Publishers. St. Petersburg – Moscow. 40 p. (in English)

Ulitsky, V. 2003. Geotechnical challenges in reconstruction of historical cities (as may be illustrated by St. Petersburg). *Proceedings of the geotechnical conference "Reconstruction of historical cities and geotechnical engineering"*. St. Petersburg. 16-18 September 2003. Vol. 1. pp. 13-28.

Construction of minarets in Central Asia, reasons of deformation and destruction
Конструкции минаретов Центральной Азии, причины их деформации и разрушения

A.Z. Khasanov & Z.A. Khasanov
Department of Geotechnics, roads and aerodromes, The Architectural and Civil Engineering Institute, Samarkand, Uzbekistan

АБСТРАКТ: В статье приводятся результаты исследования геометрических форм, конструкций минаретов, методы и технологии их возведения, а также анализ причин деформаций отдельностоящих и пристроенных минаретов. Информация об инженерно-геологических условиях площадки окрестности минаретов. Приводятся исторические сведения о методах выпрямления двух уникальных минаретов медресе М.Улугбека ансамбля Регистан. Анализируются основные причины повреждения минаретов Самарканда, Бухары и методы их выпрямления и усиления.

1. ИССЛЕДОВАНИЯ ГЕОМЕТРИЧЕСКИХ ФОРМ, КОНСТРУКЦИЙ МИНАРЕТОВ, МЕТОДЫ И ТЕХНОЛОГИИ ИХ ВОЗВЕДЕНИЯ

Минареты являются основными композиционными элементами комплексов мечетей и медресе, служащими для оповещения о начале богослужения, а также проведения культовых религиозных ритуалов.

Минареты архитектурных памятников Центральной Азии отличаются друг от друга геометрическими размерами и формой. По вертикали конструкции минаретов можно разделить на три части: фундамент, цокольная часть ствола и часть ствола с винтовыми лестницами, которая завершается круговым арочным павильоном или балконом. В некоторых случаях завершающим элементом служат такие архитектурные формы как гулдаста (коническое уширение характерное для памятников архитектуры Самарканда) и цилиндрическая форма с 5-10 открытыми проёмами арочного типа. Минареты возводятся, как правило, отдельно стоящими и примыкающими к углам зданий медресе и мечетей. Подробный анализ конструктивных решений минаретов представлен в литературе [1,2,7]. Проведенные нами исследования основных геометрических размеров минаретов архитектурных памятников показали, что отношение их высоты к среднему диаметру находится в пределах от 4 до 10, а отношение высоты надземной части к глубине заложения подошвы фундамента составляет 3 - 4. По мере подъема по высоте минарета происходит уменьшение диаметра. Уклон сужения приблизительно составляет 3-5%. Устойчивость минарета на опрокидывание обеспечивается за счет максимального понижения в низ его центра тяжести, который для большинства из них, находится на уровне 0,2-0,4 ее высоты.

Минареты относятся к очень

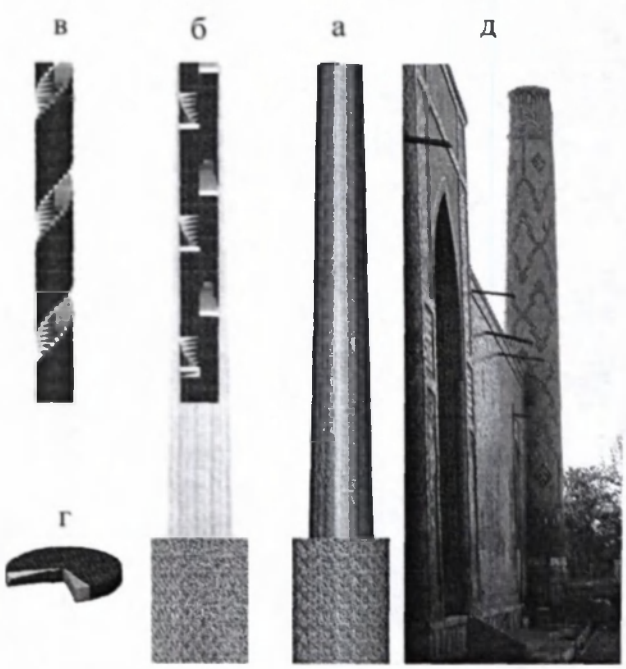


Рис. 1 3D графическая модель северо-западного минарета медресе М Улугбека (а, в), б - продольный разрез, г – диск (элемент лестницы, ствол и элемент кровли лестничной шахты) и д - общий вид.

сложной, с точки зрения ее геометрического построения форме. Помимо конической формы включают сложные винтовые лестницы внутри шахт (рис. 1 б, в). Очевидно, архитектурные мысли в чертежах излагались при помощи хандисов (математиков геометров), разрабатывающих основные принципы построения, которые, не исключено, приводились ими к очень простым для строительства решениям. Для выяснения принципа построения столь сложной конфигурации лестничных шахт авторами производилось компьютерное графическое моделирование. В качестве графического моделирования проекта минарета был взят не принцип технического построения винтовых поверхностей, основанный на современной геометрии, а метод моделирования аналогичный процессу строительства. На рис. 1, 5 представлены принципы графического построения на примере северо-западного минарета М.Улугбека в г. Самарканд и минарета «Калон» в г. Бухара. Как видно из рисунка, основным элементом строительства является круговой диск толщиной «h» с вырезанным сегментом. Диск состоит из трех частей: собственно лестницы, стволовой части и геометрического элемента, характеризующего потолок шахты. Основными параметрами этого элемента служат: ρ - нижний и верхний радиус минарета; η -коэффициент уменьшения радиуса по высоте; δ - угол сегмента (соответствующий параметрам лестницы, в данном случае треугольник $\delta = 15^0$, a=330 мм, l=1200мм и h=300 мм.). При формировании входной части (приблизительно равной по высоте росту человека 2-2.2 м.) производится послойное наложение слоев с постепенным увеличением угла сегмента. После достижения необходимой высоты наращивание угла сегмента прекращается и далее производится только его поворот на угол δ и уменьшение радиуса пластины на величину коэффициента η. В соответствии с этой технологией обязанности миссаха (измеритель) заключаются в слежении за вертикальностью оси ствола. При строительстве минарета использовались плоские кирпичи, укладываемые на ганчхоке. Фундаменты возводились из бутового камня (плоские сланцевидные), кирпичей или слоями того и другого материала. Кладка покрытия шахты минарета осуществлялось преимущественно ребром в радиальном направлении.

2.АНАЛИЗ ОСНОВНЫХ ПРИЧИН ДЕФОРМАЦИЙ МИНАРЕТОВ.

К основным факторам, влияющим на устойчивость минаретов, можно отнести следующие факторы: физическое состояние материалов и грунтовой среды, старение материалов, климатические условия и сейсмические воздействия. Именно по этим причинам происходит физический износ материалов, а вследствие этого деформация или потеря устойчивости. Отклонение минаретов от вертикали происходит длительное время (такой характер деформирования в классической механике носит название ползучий). Разрушение материалов и потеря устойчивости минаретов может произойти в двух случаях: при уменьшении коэффициента устойчивости менее чем 1.1 (отношение опрокидывающего момента к удерживающим) или, в случае возникновения в теле сооружения предельных напряжений, превышающих остаточную прочность материала $\sigma_{\substack{\max \\ \min}} \geq R_{ост}$.

Проведенный анализ показал, что минареты, примыкающие к зданиям мечетей, с течением времени имеют тенденцию к отклонению от него. Такое явление имеет место на медресе Улугбека в г. Самарканде. По нашему мнению, отклонение связано с постепенным накоплением дополнительных моментных усилий в вертикальной плоскости минарета действующего в направлении от здания. Это приводит к возникновению неравномерных нормальных напряжений по горизонтальному сечению ствола.

Снижение прочности и потеря устойчивости минаретов может произойти из-за недопустимых кренов или в результате исчерпания несущей способности каменной кладки в результате воздействия солевой эрозии. Известно, что чрезмерные отклонения от вертикальной оси произошли в северо-восточном и юго-восточном минаретах медресе Улугбека, которые были выпрямлены инженером М.Ф. Мауэром (1932 г) и проф. Э.М. Генделем (1964 г). Например, максимальное отклонение юго-восточного минарета до выпрямления составляло 178 см [3].

Полное разрушение одного из минаретов комплекса "ЧОР-МИНОР" в Бухаре в 1995 г. произошло в результате полного исчерпания прочности кирпичной кладки в её

цокольной и стволовой части, основной причиной чего явилась, очевидно, солевая агрессия. Концентрация солей в цокольной части связано с капиллярным поднятием влаги и отложением солей в процессе ее испарения. Состояние остальных трех сохранившихся минаретов комплекса "Чор-Минор" является также ненадежным и подлежит обследованию и усилению.

В результате влияния вышеуказанных причин в г. Бухаре и Хиве происходит постепенное наклонение других минаретов. На рис. 2. представлена фотография наклонившегося минарета мечети комплекса Боло-хауз в г. Бухаре. Этот минарет в настоящее время выпрямлен местными мастерами. Рядом с минаретом расположен хауз (водоем). Основанием под минарет служат слабые водонасыщенные, неоднородные по составу грунты антропогенного происхождения (суглинки с включением органики, бытового и строительного мусора). Горизонт грунтовых вод расположен на глубине 1-1,5 м. от поверхности земли. Грунтовые воды агрессивны к строительным материалам и содержат преимущественно ионы сульфата (954 мг/л). Глубина заложения фундамента 3.0 м. Фундаменты имеют цилиндрическую форму диаметром ориентировочно 3.5 м. Причем нижний слой высотой 2 м. каменный бут, а верхний слой 1.6 м. выполнен из битого кирпича на ганчевом растворе. Расчеты показали, что приблизительная масса минарета ориентировочно равна 235-240т. Центр тяжести минарета находится на расстоянии 3.6 м от уровня земли.

Предполагалось выпрямить минарет двумя способами. По первому методу по контуру существующего минарета должны были подготавливаться железобетонные фундаменты, а в тело минарета вмонтироваться металлическая рама. Домкраты устанавливаются в промежутке нового фундамента и рамы, после чего производится подъем и выпрямление минарета. По второму проекту вокруг фундамента минарета устраивается железобетонный кольцевой фундамент «L» образного сечения. В теле фундамента оставляются 5-6 отверстий, на которых устанавливаются металлические инвентарные сваи, которые задавливаются при помощи домкратов в грунт. Процесс надавливания свай начинается со стороны крена минарета. По этому методу предполагалось укрепить не только фундамент,



Рис. 2 Общий вид наклонившегося минарета Боло-хауз в г. Бухаре и его 3D модель.

но и основание. Также можно было использовать метод проходки горизонтальных скважин перфораторами (диаметр 50-60 мм) на уровне подземной части ствола.

Среди четырех минаретов медресе М. Улугбека в настоящее время наиболее наклоненным является северо-западный. Высота минарета составляет 26,75 м. диаметр ствола на уровне цокольной части - 4,0 м. а в верхней его части на отметке 26,75 м - 2,80 м. Отношение высоты минарета к его среднему диаметру составляет 7,84. Глубина заложения фундамента равна 6-7 м, поперечное сечение которого имеет круглую в плане форму. Отношение высоты минарета к глубине заложения фундамента составляет 3,0. Фундамент под минарет выполнен из бутовой кладки на ганчевом растворе. Удельный вес кладки фундамента ориентировочно равен 22,0 кН/м^3, а кирпичной кладки ствола - 19,00 кН/м^3. Крен минарета имеет северо-западное направление. Отклонение его верхней части составляет 1,13 м [4]. Ствол минарета до отметки 12,6 м. имеет сплошное поперечное сечение, выше которой выполнена винтовая лестница. Общая масса минарета на уровне обреза фундамента составляет 490 т. Инженерно геологическое строение грунтов : с поверхности до глубины 4-6 м, залегают грунты культурно городских отложений, ниже залегают природные лессовые суглинки с прослоями из крупнозернистых песков пролювиального происхождения. Глубина подземных вод 14,5 м. Удельный вес грунта



Рис.3 Вид медресе северо-восточного минарета медресе М.Улугбека и Тилла-Кори, (снимок конец 19 в.)

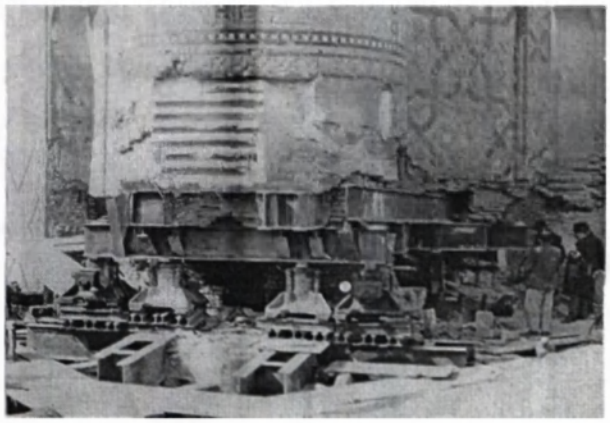


Рис. 4 Общий вид процесса выпрямления минарета Ю-В минарета медресе Мирза Улугбека под руководством проф. Э.М.Генделя

γ=15,5 - 16,5 кН/м3; пористость грунта n=0,85-0,9, природная влажность w=16-18%.

С целью установления прогнозируемой прочности и устойчивости накренившегося минарета, авторами был произведен статический и динамический расчет с учетом сейсмических воздействий и возможных просадочных деформаций. Прочностные характеристики принимались с учетом степени износа материалов несущих конструкций и элементов. Сейсмический расчет минарета выполнялся по программе "ЛИРА" в упругой постановке. Расчет был произведен на 7, 8 и 9 баллов. Как показали расчеты, наиболее опасным является сечение на высоте 12,60 м. Нормальные (σ) и касательные (τ) напряжения в кладке здесь равны: при сейсмичности 7 баллов $\sigma = 0.357 \pm 0.270$ МПа; $\tau = 0{,}034$ МПа. При 8 баллах $\sigma = 0.357 \pm 0.338$ МПа; $\tau = 0{,}043$ МПа. При 9 баллах $\sigma = 0.357 \pm 0.472$ МПа; $\tau = 0{,}061$ МПа. При сейсмическом воздействии более 8 баллов минимальные нормальные напряжения σ_{min} становятся растягивающими, что может привести к обрушению минарета. Предельными в этих случаях являются также и касательные напряжения τ .

Опасным может быть и сечение на отметке 21.4 м., где при сейсмичности равной 9 баллам нормальные напряжения σ_{min} также становятся растягивающими (σ_{min} =0,019 МПа). Нормальные напряжения в заделке у основания минарета во всех случаях остаются сжимающими.

Устойчивость минарета, определяемая соотношением удерживающего и опрокидывающего моментов при 9 баллах составила – $K=M_{уд}/M_{опр}=1{,}97$; при 8 баллах – K= 2,75; при 7 баллах K=3,43.

Как показывают статические и динамические расчеты, общая устойчивость минарета обеспечена. Однако имеющийся крен минарета ухудшает архитектурную выразительность и поэтому возникает необходимость в выпрямлении крена минарета. Ниже приводятся методы выпрямления минаретов выполненных М.Ф. Мауэром и Э.М.Генделем.

В 1932 г. инженером М.Ф. Мауэром [5] при участи известного механика В. Г. Шухова был выпрямлен северо-восточный минарет медресе Улугбека. На рис.3 представлена фотография, где явно прослеживается С и СВ уклон минарета. С обратной стороны на уровне кровли примыкающего к минарету здания медресе, прослеживается область возникновения разрушения. Это говорит о том, что устойчивость минарета тогда была на грани исчерпания своей несущей способности. К сожалению, в литературе нет информации об усилении этого участка кирпичной кладки. Но скорее всего, именно поэтому в настоящее время сохранился контр уклон с разломом прямой в этой области минарета.

По методу М.Ф.Мауэра на уровне цокольной части минарета, сквозь тело поочередно устанавливались металлические клепаные балки под железно – алебастровое кольцо. Несущие балки опирались на перпендикулярные им опорные элементы, расположенные за пределами контура минарета. Между подбалансирными плитами и высокими балками – прогонами размещались стальные плиты кругового очертания, между которыми укладывались толстые свинцовые полосы. Кладка минарета ниже уровня балок была разобрана и заменена. Процесс выпрямления осуществлялся по кинематической схеме, предложенной В.Г.Шуховым, методом переката над его центром тяжести при помощи поочередного удаления клиньев.

По методу Э.М.Генделя [3] минарет, был поднят со стороны крена на 418 мм десятью гидравлическими домкратами грузоподъемностью по 2000 кН. По верху и по низу домкратов размещались металлические спаренные двутавровые балки № 45. Подъем был осуществлен по отношению к четырем шарнирам, расположенным в теле кирпичной кладки пилонов. Процесс выпрямления сопровождался гидравлическим нивелированием. Кирпичная кладка на этом участке была заменена на железобетон (Рис. 4).

Анализ описанных методов выпрямления минаретов показал, что они громоздки, материала емкий и достаточно сильно повреждают существующие конструкции в местах их усиления. В связи с чем, для выпрямления СЗ минарета, авторами предлагаются два других варианта. Сущность первого варианта состоит в устройстве верхнего и нижнего кольцевых обжимающих поясов, между которым поочередно в нише кладки устанавливаются гидравлические домкраты и специальные фиксаторы [6], которые служат для автоматической стабилизации перемещений поясов. Выпрямление может осуществляться методом подъема или опускания. Устойчивость каменной кладки в опорных частях поясов обеспечивается за счет ее армирования и укрепления.

Сущность второго варианта состоит в многослойном армировании, ослабленной смятием и выветриванием, каменной кладки

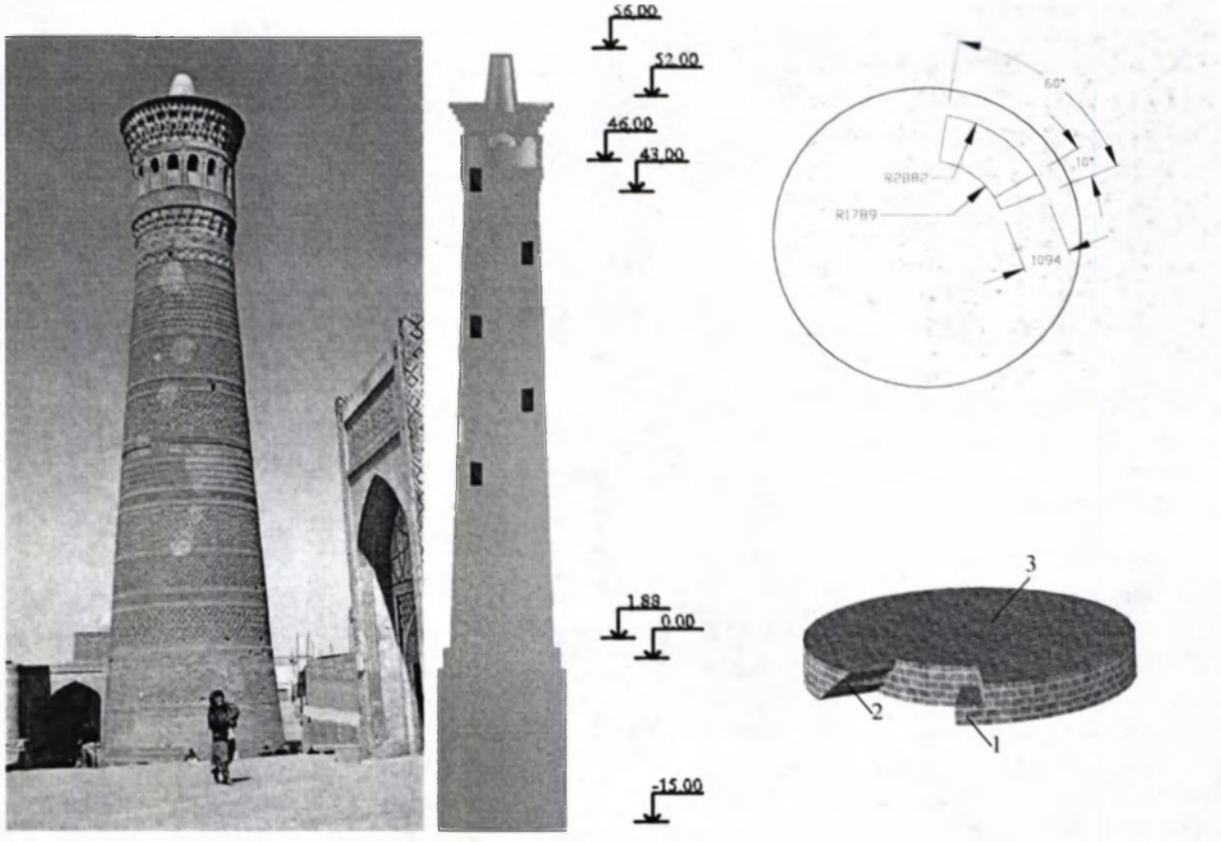


Рис.5 Общий вид минарета «Калон», продольный разрез с фундаментом, элементарный диск (1-элемент лестницы, 2-ствол и 3- кровля лестничной шахты).

минарета, устройством над домкратного опорного пояса из монолитного железобетона. Гидравлические домкраты и фиксаторы устанавливаются на отдельные фундаменты, расположенные по периметру минарета. Выпрямление осуществляется по аналогии с первым предложенным вариантом.

В случае отдельно стоящего наклонившегося минарета, как это показано на рис. 2, более эффективно использовать метод радиального сверления (перфорации) горизонтальных скважин с последующим их заполнением специальными материалами с заданными деформационными свойствами. При этом уровень (отметка от уровня земли) перфорируемых скважин зависит от кривизны минарета по ее высоте. В случае жесткого равномерного крена минарета желательно выпрямление производить ниже уровня цоколя, т.е. в подземной части. В любом случае при крене минаретов от вертикали необходимо вести мониторинг и производить техническое инструментальное обследование с целью выявления причин, вызывающих деформации.

Предлагаемые варианты выпрямления являются надежными, менее трудоёмкими и, поэтому авторы рекомендуют их осуществление на практике.

Одним из наиболее величественных минаретов считается минарет Калян построенный 1127-1129 гг в г. Бухаре. Несмотря на солидный возраст, он без крена сохранил свой первозданный вид. По этому, на наш взгляд, он интересен с точки зрения геометрических и механических параметров. Минарет имеет в плане круглое сечение. Радиус ствола основания минарета 4.90 м. а радиус у основания фонаря 3.4 м. Глубина фундамента ориентировочно равно 15м. Полная высота минарета от уровня земли 54.м. остальные геометрические размеры минарета представлены на рис. 5 Винтовая лестница начинается от уровня покрытия одноименной мечети на отметке 8,45м. Конструкция ствола отличается от вышерассмотренных. В центре минарета имеется полнотелый цилиндр (диаметр 3600мм), который прорезает ее по всей высоте. Соотношение среднего диаметра к ее полной высоте (без учета фонаря) составляет 0,21.

В отличие от вышерассмотренных минаретов в данном случае винтовая лестница начинается не с центра, а с боковой поверхности цилиндра. Элемент лестниц имеет

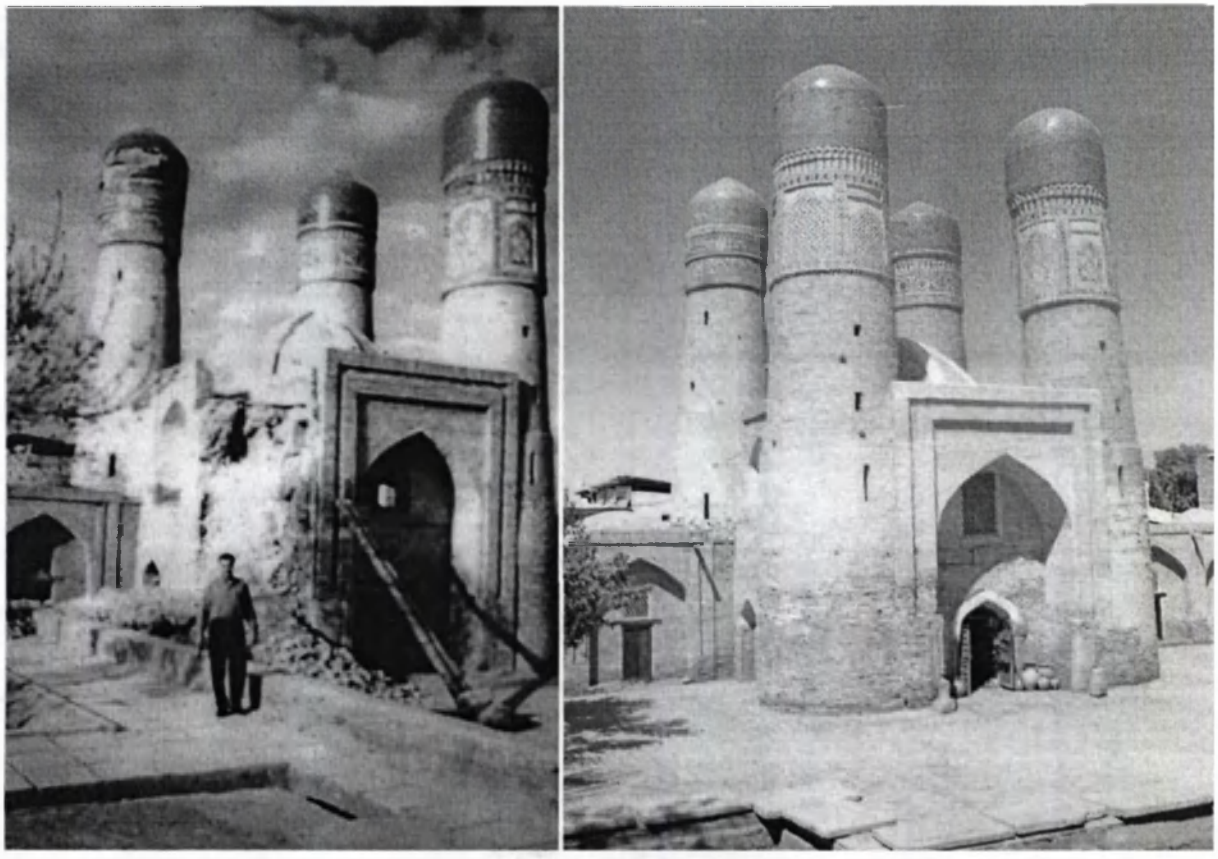


Рис. 6 Вид медресе Чор-Минор после разрушения (слева) и современный вид (справа).

форму трапеции с размерами 500x310x1093 и высотой подступни 375 мм. Угол поворота лестницы 10^0. На рис. 5 показана конструкция составного элемента диска лестницы. Угол сужения минарета $2,6^0$. Вес минарета выше уровня земли около 5000 т, вес фундамента 3100 т и общий вес минарета с фундаментом 81375 т. Центр тяжести минарета от уровня земли находится с фундаментом на высоте 12м, а без фундамента 22 м. Соотношение высоты центра тяжести минарета к ее общей высоте составляет 0,4.

2.1 Анализ причины разрушения минарета медресе Чор-Минор в г. Бухаре.

Медресе был построен купцом халифа Худойдом в 1807 году в г. Бухаре. Здание построено в строго симметричном виде с центральным квадратным залом размером в плане приблизительно 4,5x4,5 м. Вход в зал осуществляется с четырех сторон парадными порталами, а по углам размещены четыре башни минарета. Внутреннее пространство здания в первом этаже, как в ее центральной зальной части, так и внутри трех минаретов завершаются куполом. Только внутри одного минарета (с фасада на правом углу) предусмотрено винтовая лестница. На втором этаже центральный зал и в башнях размещены хозяйственные помещения и библиотека. Конструкция четырех башен, начиная с второго этажа выполнена в форме полого, слегка сужающего к верху усеченного конуса. Все четыре минарета с верху завершены в виде барабана завершенные куполом и покрыты голубой майоликой.

Инженерно геологическое сложение местности имеет следующее: сверху залегают культурно городские отложения. Грунты суглинистого состава имеют влажность превышающую 20%. В составе грунта встречаются останки строений и строительный мусор. Грунты вскрыты с поверхности до глубины 2,5 м. Ниже залегают водонасыщенные серые заиленные суглинки от мягко-пластичной до текучей консистенции. Грунты в глубине 4,5 м в виде тяжелых суглинок, плотные в туго-пластичном состоянии. Грунты водонепроницаемые и служат экраном для подземных вод. Здание в плане достаточно жесткое. Для этой местности удельное электрическое сопротивление грунта не превышает 18 Ом/м. Грунты засоленные сульфатными солями. Влажность каменной кладки до высоты 1 м. превышает 6-7%. Концентрация солей в кирпичной кладке постепенно увеличивается, что приводит к разрушению структуры кирпича и раствора "Ганчхока". Эти явления и послужили снижению несущей способности цокольной части всех четырех минаретов. В 1995 г. правый минарет потерял устойчивость (рис. 6). На месте данного минарета, по согласованию с ЮНЕСКО, было принято решение о его восстановлении. Минарет был восстановлен мастерами Бухары из старых кирпичей при соблюдении исторической технологии. По нашему мнению образование новых трещин (рис.8) связано с отсутствием укрепления грунтов основания и фундамента во время восстановления минарета.

Проведенные нами визуальные обследования медресе, показали, что кирпичная

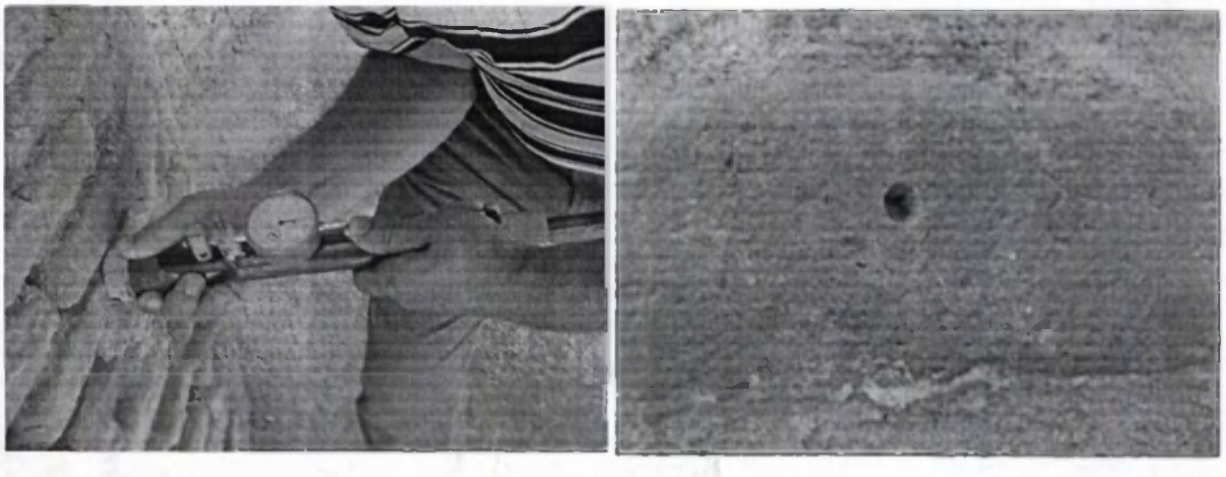


Рис. 7 Определение прочности кирпича по результатам динамического зондирования (с лева) и образованный отпечаток зондирования (справа). Медресе Чор-Минор, г. Бухара.

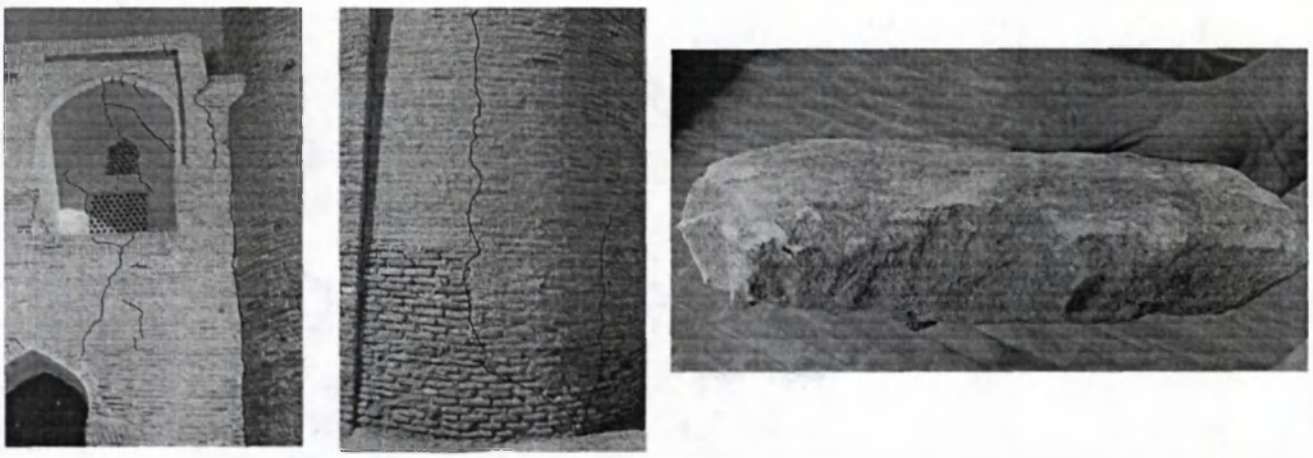


Рис. 8 Образование трещин в местах примыкания и в окрестностях вновь возведенного минарета, в теле правого минарета и состояние эродированного кирпича медресе Чор-Минор.

кладка на уровне цокольного этажа и на уровне пола второго этажа сильно эродированы (рис 7). Динамическое зондирование с конусным наконечником показало, что при одном ударе внедрение конуса внутрь кирпича для эродированного кирпича составил более 4 мм. (рис.7). При сравнении, для кирпича, в хорошем состоянии, глубина погружения конусного наконечника составило не более 1 мм. Это свидетельствует о том, что в наиболее нагруженных цокольных частях здания прочность кирпича снижена до 2-3 раз. Такое остаточное прочностное состояние, является угрожающим и для остальных минаретов.

Наличие вертикальных трещин в теле минаретов показывает, что величина тангенциальных напряжений местами превышают прочность кладки на растяжение. Эквивалентное внутреннее тангенциальное напряжение, которое может привести к разрыву (вертикальным трещинам) в кладке минарета цилиндрической формы с размерами внутреннего и внешнего радиусов 100 см и 185 см равно порядка σ_θ =150-300 кПа.

Здесь необходимо провести более тщательный анализ напряженного состояния кирпичной кладки, с тем, чтобы определить резервную остаточную прочность каменной кладки. В случае необходимости, в нужных местах по высоте минарета усилить металлическими натяжными поясами. В окрестности медресе так же рекомендуется устройство одного или двух вертикальных дренажных скважин, что позволит снизить уровень грунтовых вод до глубины 4-5м.

3. ВЫПРЯМЛЕНИЕ НАКЛОНИВШЕГОСЯ МИНАРЕТА В Г. САМАРКАНДЕ.

По окончанию строительства в 1993 г. стал заметно наклоняться минарет мечети, расположенной на территории акционерной компании «Сино» в г. Самарканде рис. 9. Отклонение верха от вертикали составило 670 мм, а крен достиг 0,04 и приобрел прогрессирующий характер, в следствии этого потребовалось срочное принятие мер по



9 Общий вид наклонившегося минарета в г. Самарканд

предотвращению наклона минарета с

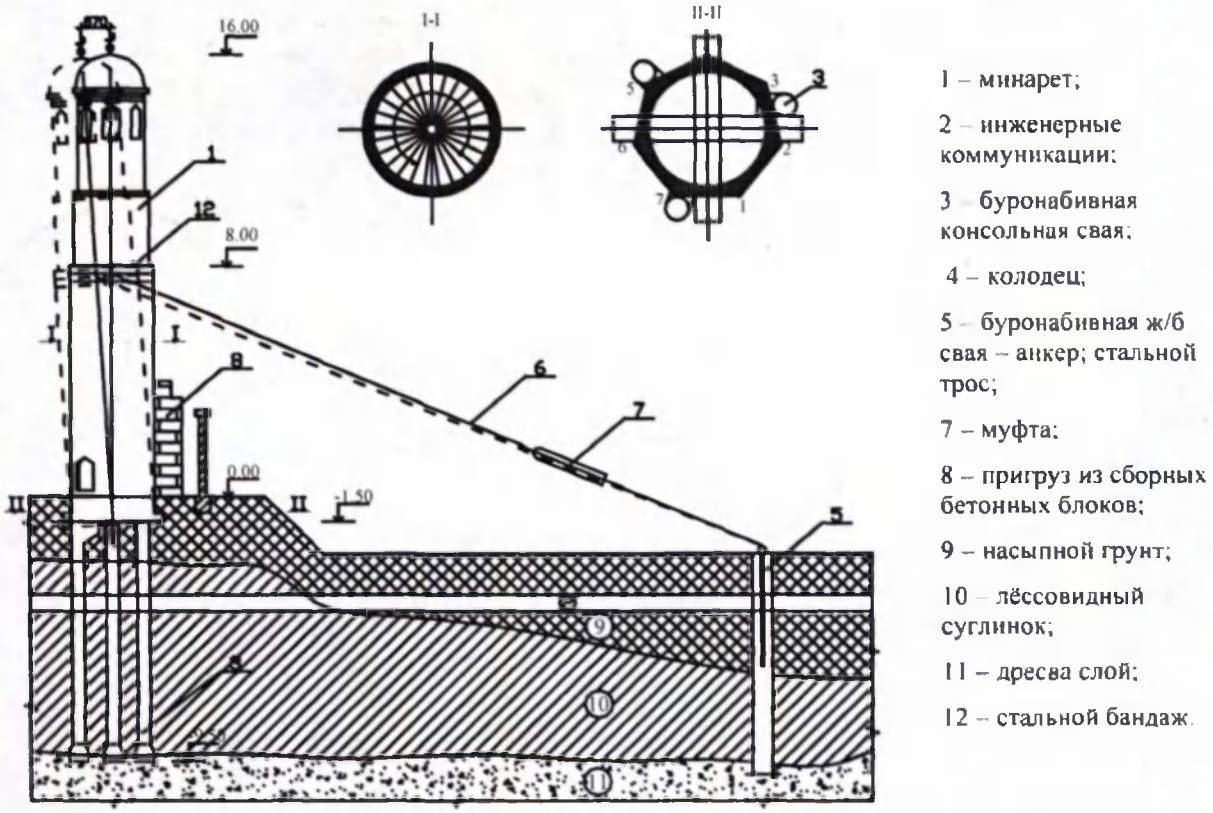


Рис . 10 Схема отклонившийся минарет в г. Самарканде.

последующим его выпрямлением до вертикального положения.

Высота минарета составляет 16 м. Стены минарета выполнены из кирпичной кладки на цементном растворе (кирпич М100, раствор М50). Фундамент представляет собой в плане семигранник толщиной стенок 0,5м, высотой 1,5 м, опирающийся, в свою очередь, на крестообразный фундамент размерами 4,5х4,5 м. Общий вес минарета составляет около 2000 кН.

В плане минарет (рис.10) имеет круглую форму. Участок территории строительства сложен с поверхности до глубины 3,7 м культурно-городским отложениями, включающими до 10...50% строительного и бытового мусора, непригодного для использования в качестве основания фундаментов. Ниже, до глубины 5,9 м. располагаются суглинки высокопористой твердой консистенции П типа по просадочности, подстилаемые дресвой кварцполевошпатного состава. Уровень подземных вод вскрыт не был.

Техническая документация и последующее визуальное обследование подтвердили исключительно сложные условия основания, на которое фактически опирался минарет. Для предотвращения опрокидывания минарета, в первую очередь было выполнено его временное крепление. Стабилизация производилась с помощью конструкций, состоящих из стального бандажа, натянутого троса и двух анкерных буронабивных сваи. Кроме того, край фундаментной плиты, противоположный крену, был пригружен бетонными фундаментными блоками весом около 150 кН. В результате этих срочных мероприятий был приостановлен прогрессирующий крен.

Для выпрямления минарета по его периметру были возведены 4 консольные буронабивные железобетонные сваи. Глубина свай равна 8 м., диаметр 0,6 м. Первая свая выполнялась на участке между марками 5 и 6. Последующие сваи возводились после достижения бетоном требуемой прочности и передачей на нее нагрузки от минарета. В конце изготавливалась свая, расположенная со стороны крена минарета (между марками 3 и 4). Отметка верха сваи не доводилась до подошвы фундамента на 70 см. с целью установки в этом промежутке основного гидродомкрата грузоподъёмностью 2000 кН. Рядом с основным домкратом располагался контрольно-страховочный домкрат грузоподъёмностью 500

кН. Все подготовительные работы были выполнены в течение месяца, а выпрямление минарета было осуществлено в течение четырех часов. При постепенном подъёме основного гидродомкрата в зазоры между подошвой фундамента и верхом всех свай одновременно вставлялись стальные диски и одновременно подтягивался страховочный трос. Вертикальность контролировалась двумя теодолитами.

СПИСОК ЛИТЕРАТУРЫ

1. Асанов А.А. Мечеть Биби-Ханым (краткая характеристика конструкций и перспективы их укрепления)/ Из истории искусства великого города (к 2500-летию Самарканда)- Сб. статей.- Ташкент: Изд лит и искусства им. Г. Гуляма, 1972.-с. 119-160.
2. Асанов А.А. Памятники архитектуры и их конструкции //Строительство и архитектура Узбекистана. -1973.-№7-с. 9-12.
3. Гендель Э.М. Инженерные работы при реставрации памятников архитектуры. – Москва: Стройиздат. 1980. с.199.
4. Кузибоев М.К. Отчет «Исследование кренов и осадок архитектурных памятников ансамбля Регистан» - Самарканд. 1989. с. 120.
5. Массон М.Е. Падающий минарет. – Ташкент. Изд. Узбекистан. 1968.
6. Хасанов А.З. Стриго Г.С. Устройство для фиксации зданий и сооружений А.С. IHDP 9600383.1
7. Hasanov A.Z Designs of architectural monuments of Samarkand. ISBN 3-931991-21-0. © the Publisher, 2003.

LTP. Fig. 2 illustrates schematic diagrams of the different LTPs. The focus in this paper is on GRLTP (i.e., catenary and beam LTPs).

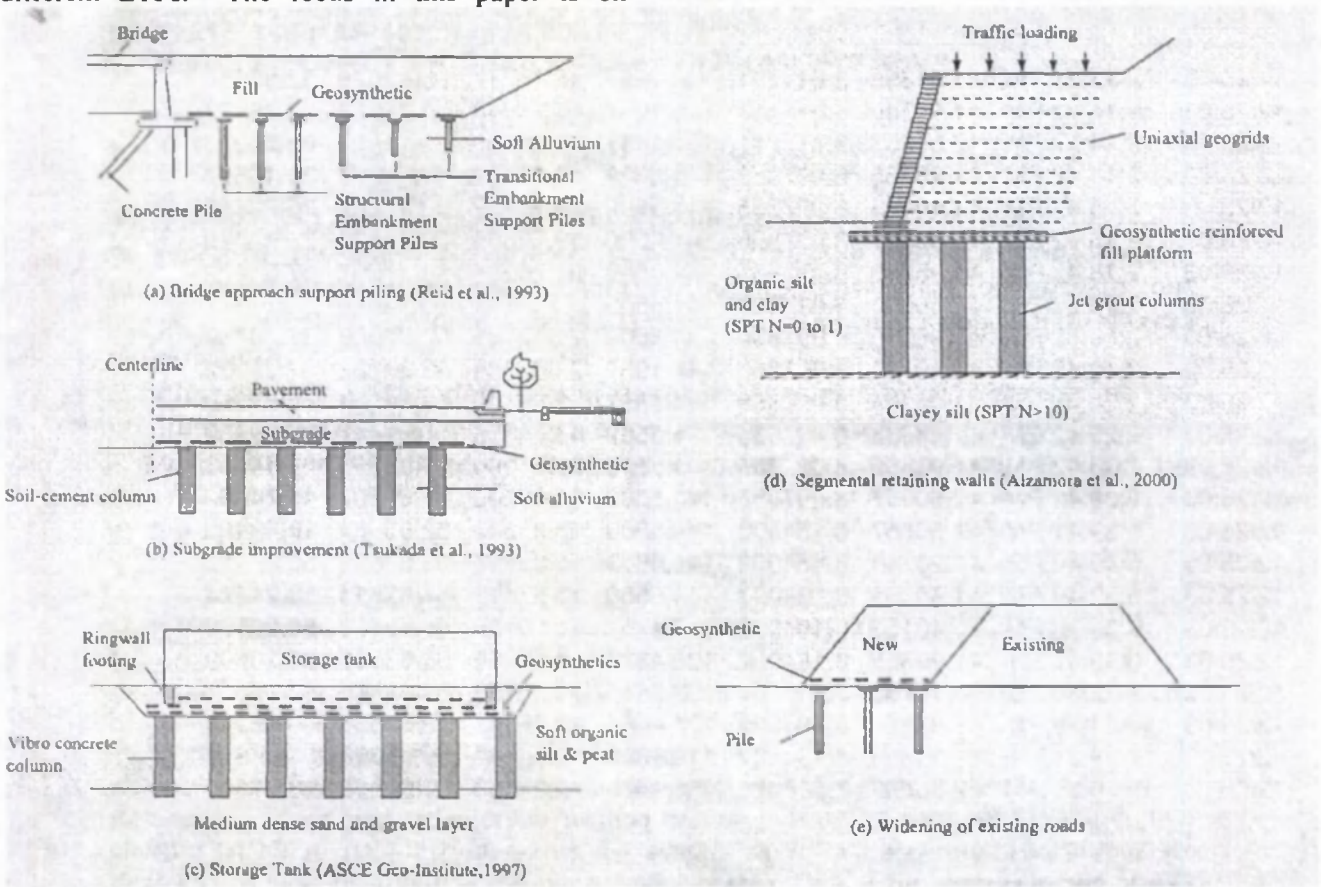


Fig. 1 The applications of load transfer platforms supported by columns (after Han and Gabr 2002).

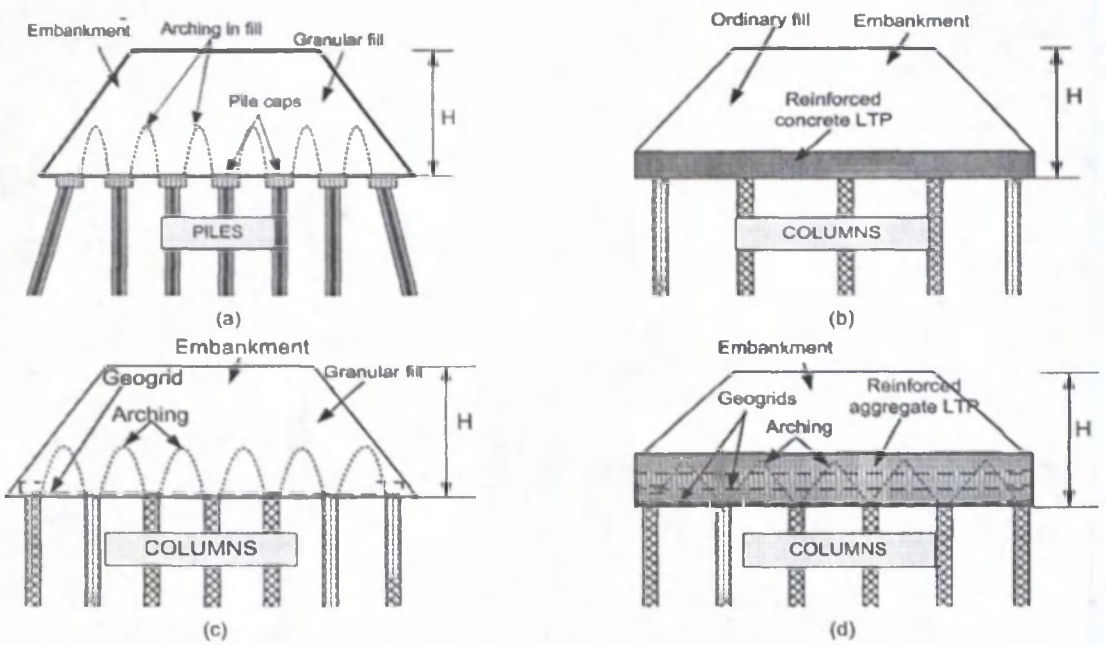


Fig. 2 Different types of load transfer platforms: (a) unreinforced granular LTP, (b) reinforced concrete LTP, (c) catenary LTP, and (d) beam LTP (after Abdullah 2007)

There are currently several different concepts for the design of GRLTP for column-supported embankments. However, there are two commonly used design concepts (Jenner et al 1998): 1) tension membrane approach (catenary LTP), and 2) improved arching approach (beam LTP). In the catenary LTP, only a single or at the most two layers of high strength geogrids are used as reinforcement. The reinforcement in essence behaves as a structural element and any benefits resulting from the creation of a composite reinforced soil mass are ignored (Collin 2004). In the beam LTP, three or more layers of relatively lower strength geogrids are employed as reinforcement within a select aggregate. It is assumed that there is interaction between different layers of the geogrids that result in a stiffer LTP with less differential settlement between the columns and the matrix soil in between the columns. The beam LTP is claimed to be stiffer than catenary LTP and therefore, theoretically is able to take more load with less deflection (sagging) at the base of the LTP and consequently, less deformation at the surface of embankment than the catenary LTP. However, this has yet to be verified because there are many factors that may affect the fill-LTP-column-subsoil interaction. Amongst them are the tensile stiffness of the geogrid or the stiffness of the LTP, column-subsoil stiffness ratio, stiffness of the column, the height of embankment, the spacing of the columns, support for the LTP by the subsoil, and the aggregate strength (angle of friction). Furthermore, the mechanism of load transfer from the embankment to the LTP and subsequently to the subsoil and the column is poorly understood. The major contentious issues include the appropriate arching theory/method to use; the manner load is transferred from the geogrids or LTP to the columns, and the proportion of the load supported by the subsoil. Russell and Pierpoint (1997) mentioned that the uncertainty for designers is reflected in different amounts and properties of geosynthetic reinforcement used in the LTP, for column-supported embankments with similar dimensions.

Another contentious issue is whether the support provided by the matrix soil should be included in the design. The British and Nordic design methods (British and Nordic methods) completely ignore the contribution by the subsoil, whereas in the German design method (German method) and the Collin beam design method (Collin method) contributions from matrix soil are considered. The supporters of the British and Nordic methods argue that there are uncertainties in either the magnitude of support that can be provided by the subsoil (over a large area), and also whether the subsoil support will always be present during the lifetime of the embankment. Love and Milligan (2003) and others contend that the support provided by the subsoil may vanish if the water table lowering causes excessive settlement of the subsoil such that the support is no longer rendered. Love and Milligan also assert that in as far as the magnitude of support that can be provided by the matrix soil, there is uncertainty in the consistency of the natural soils such that quantifying the magnitude of support will be a complex, soil-structure interaction matter.

Most of the design methods for GRLTP consider only stiff columns in their designs. The British and the Nordic methods are explicit in stating that only piles or columns of similar stiffness are to be used with their designs. The German method is silent on the types of columns that can be used to support the embankment. Collin (2004) presented a list of less stiff columns that can be used to support the LTP. Less stiff columnar system such as deep cement mixed columns, stone columns, and geopiers have been used as an alternative to piles in the construction of column supported embankment. These new columnar systems may be more suitable than piles since most of them have diameters many times more than those of piles; consequently, pile caps are not required. Piles are also many times stiffer and are able to carry higher load than necessary as opposed to the less stiff columns. In this study, rammed aggregate pier, called "geopier" foundation system, is focused as an alternative to piles. Geopiers are relatively new intermediate-depth columnar foundation introduced in the construction industry (Fox and Cowell 1998).

To obtain field evidence for the evaluation of the performance of the catenary and the beam LTPs, a heavily instrumented full-scale test embankment supported by rammed aggregate piers called "geopiers" was constructed over soft ground in Gebeng, Pahang State, Malaysia and the results are presented and interpreted. While there is a large database for use of geopiers as footing support for buildings where concentrated loads are involved, there are relatively few cases of embankment support by geopiers. The field test allowed evaluation of geopier performance as an embankment support based on the total settlement and its ability to resist lateral displacement under embankment loading. Additionally, numerical modeling of the column-LTP system was undertaken to clarify the appropriate arching theory.

2 GEOSYNTHETICS USED IN LTPS

The magnitude of force in the geosynthetics will vary depending on the application. In a steep slope

strengthened by a geosynthetic reinforcing layer, each reinforcement layer might have to support a tensile force of 10 - 40 kN/m; alternatively a single geotextile reinforcing layer at the base of an embankment on soft soil may be required to support a tensile force of 100 – 400 kN/m (Jones, 1995). The stress-strain characteristics of geosynthetics depend on the properties of the constituent materials and the geometrical arrangement of elements within the geosynthetic material.

The geosynthetics have to be relatively stiff in reinforcing soil so that the required force can be mobilized at a tensile strain, which is compatible with the deformation of the soil. The concept of strain compatibility between the reinforcement and the soil is implicit in any reinforced soil structure. The allowable strain in geosynthetics depends on the applications. For a reinforced soil under embankment, the allowable tensile strain of the reinforcement is likely to be between 5 – 10%. In the case of reinforced soil wall, the total extension may be between 2 – 4%. Jones et al. (1990) stated that a practical upper limit of 6% is imposed in the LTP supported columns to ensure maximum load transfer to the columns with negligible load transferred directly to the soft foundation. However, limitation of the long- term creep extension is critical to ensure that localized deformation do not occur at the surface of the embankment especially when the embankment is relatively low. Based on experience, Jones et al. (1990) set the limit on creep strain at 2%. Other catenary design methods (Nordic Handbook, Collin Method, and German Method) set the same maximum initial tensile strain of 6% and creep strain limit of 2%.

3 ARCHING

Soil arching is the ability of material to transfer loads from one location to another as a result of relative movement between locations. In column-supported embankment, for the design methods that ignores the support from the subsoil (i.e., British and Nordic method), the entire vertical load is assumed to be ultimately transferred to the columns. The weight of the soil (and surcharge) below the arch is assumed to be supported by the geogrid alone; or geogrid and the soil beneath the geogrid depending on the method that is selected. The main difficulty in the design calculations is the assessment of proportion of vertical load carried by the reinforcement between the columns and the proportion of vertical load carried by the columns. Various analysis techniques have been developed to determine the arching ratio in the fill for the calculation of the load on the geogrid. Major arching methods are considered in this study; three of them are commonly used for the design in the codes or design manual for GRLTP column-supported embankment. The four major arching methods are: 1) Terzaghi (1943) arching theory, 2) BS8006 (1995) – this is based on Marston's formula for positively projecting conduits, 3) Hewlett and Randolph (1988) arching theory, and, 4) Guido (1987) arching method. Terzaghi arching method has not been used for the calculation of the tension in the geosynthetic for GRLTP column-supported embankment by any of the known GRLTP design method but has been used by Giroud et al. (1990) for GRLTP over void.

In order to compare different design methods, a parameter known as arching ratio (ρ) as defined by Low et al. (1994) is used. Arching ratio is defined as the ratio of the average vertical stress over the reinforced area between the columns to the average vertical stress due to the embankment fill and the surcharge if any.

$$\rho = \frac{\sigma_g}{\gamma H} \qquad (1)$$

where σ_g is the average vertical stress on the geosynthetic, γ is the average unit weight of fill and H is the height of fill. It is important to note that the vertical loads induced by the vertical stress on the geosynthetic (σ_g) are partly apportioned to the geosynthetic by means of tensile force generated in the geosynthetic and partly to the soil underneath the geosynthetic (that is in contact with the geosynthetic).

4 TEST EMBANKMENT

A full-scale test embankment was constructed at Gebeng, Pahang in the east coast of Peninsular Malaysia (Abdullah and Edil, 2007). The test embankment site is located in a small flat flood plain some 8 km from the coastline adjacent to a pile-supported bridge. Site investigation indicated a soft silty clay/clayey silt layer as deep as 15 m at some locations. However, this layer generally extended approximately 5 – 6 m below the original ground level. The soils in this layer are composed of highly plastic clay and silt with natural water contents between 35–61%. Field vane tests indicated that the shear strength in this layer ranges 14 to 60 kPa, with most of the values less than 25 kPa and the sensitivity varies 3 to 11. The top clayey/silty soil is interspersed with thin organic and sandy layers that were sometimes detected during drilling for the installation of the geopiers. The top layer is underlain by stiff to hard gravelly silt, which, in turn, is underlain by firm

to stiff silt. The water table in this area is very high, at or just below the original ground level.

The length of the test embankment was approximately 90 m, the width was 14.5 m and the height was 3.5 m. The side slopes of the embankment were 1V:1.5H. The test embankment was divided into 4 major sections (Sections 1 through 4) and 2 control sections (C1 and C2) at the two ends of the embankment. Different types of LTPs supported on geopiers were used in the major sections. All the geopiers were installed in a square arrangement with a specific center-to-center spacing (from now on termed as spacing). The dimensions, the types of LTP, and the geopier square-arrangement spacing for each section are shown schematically in Fig. 3. The geosynthetic-reinforced LTPs consist of an aggregate layer with geogrid reinforcement within the aggregate. Section 1, has 1.5 m thick beam LTP with four layers of a biaxial extruded polypropylene geogrid (Tensar SS20 with 20 kN/m tensile strength) reinforcement spaced at 0.3 m apart vertically within the LTP, and supported on geopiers spaced at 3.25 m center to center square pattern. Section 2, has 1.0 m thick beam LTP but with three layers of the same geogrid as in Section 1 spaced at 0.3 m apart vertically, and supported on geopiers spaced at 2.5 m center to center square pattern. These beam LTPs were designed in accordance with the Collin Method. Section 3, has a catenary LTP with two layers of a uniaxial woven polyester high-strength geogrid coated with polyvinyl chloride (Miragrid 24XT with 370 kN/m tensile strength) spaced at 75 mm apart vertically. One layer placed in the transverse direction and the other in the longitudinal direction to the embankment. The section was supported on geopier elements spaced at 2.5 m apart center-to-center square pattern. The catenary LTP was designed in accordance with the British method. The bottom-layer geogrids in Sections 1, 2 and 3 were placed directly over the geopiers. The final major section, Section 4 was supported on 0.3-m thick continuous steel-reinforced concrete LTP and geopier elements spaced at 2.5 m center-to-center square pattern. The detailed layout of the LTPs for various sections is presented in Fig. 4. The concrete slab was constructed directly over the geopiers without any connection between the concrete slab and the geopiers. The control sections were not supported by the geopiers and were built directly over the ground. Geopiers were installed by drilling 0.6 m to 0.9 m diameter holes and filling them with select aggregate in thin layers. Each layer of the aggregate is rammed with a beveled shape rammer for about 20 seconds.

5 INSTRUMENTATION

The test embankment was heavily instrumented. Resistance wire strain gages were installed on the geogrids to measure strain of the geogrids at three locations: the edge of the geopier, in-between geopiers; and between a group of the geopiers. The strain gages were positioned in transverse and longitudinal directions to the embankment. Other instrumentation included settlement plates, earth pressure cells, piezometers, extensometers, and vertical and horizontal inclinometers creating a heavily and redundantly instrumented system. The test embankment was subject to heavy rain and flooding. However, most of the instruments performed reasonably well and provided invaluable field data. Approximately 83% of the 128 gages still functioned at the end of the construction and 70% and 44.5% after 6 months and 2 years, respectively after construction (Abdullah and Edil, 2008).

6 GEOGRID PERFORMANCE DESIGN VERIFICATION

The tensile strain in the geogrid is usually the main controlled parameter in the design of LTPs supported on columns. The strain also indicates the force in the geogrid. The geogrid strains measured at the edge of the geopiers were consistently higher than the strains measured at mid-distance between the columns. Numerical analyses by Pham et al. (2004) and Han and Gabr (2002) show that maximum tensile strain in the geogrids occurs at the edge of the columns and minimum tensile strain occurs at the center in between the columns supporting the field observation. The strains also vary depending on the geogrid layer as well as with the LTP section. The magnitude of strain in a geogrid depends upon the initial localized stress induced during the placement of the geogrid, additional stresses applied by the loads, and interaction between the geogrid and the aggregate. Due to the above factors, it is unlikely if the strain measured at different locations, under what is assumed to be the same conditions will yield the same strain. A case study reported by Rogbeck et al. (1998) showed that the measured strain of geogrid placed at different locations under similar conditions ranged between 0.5 % and 4.5%. They also reported that in the same area under similar conditions as in the first case, but where differential settlements were smaller (because of soil support) resulted in geogrid strains of -0.2% to 0.8%. Jenner et al. (1998) also reported similar finding i.e. the range of the strain in the geogrid under the same conditions varies from 0.5% to 2.8%.

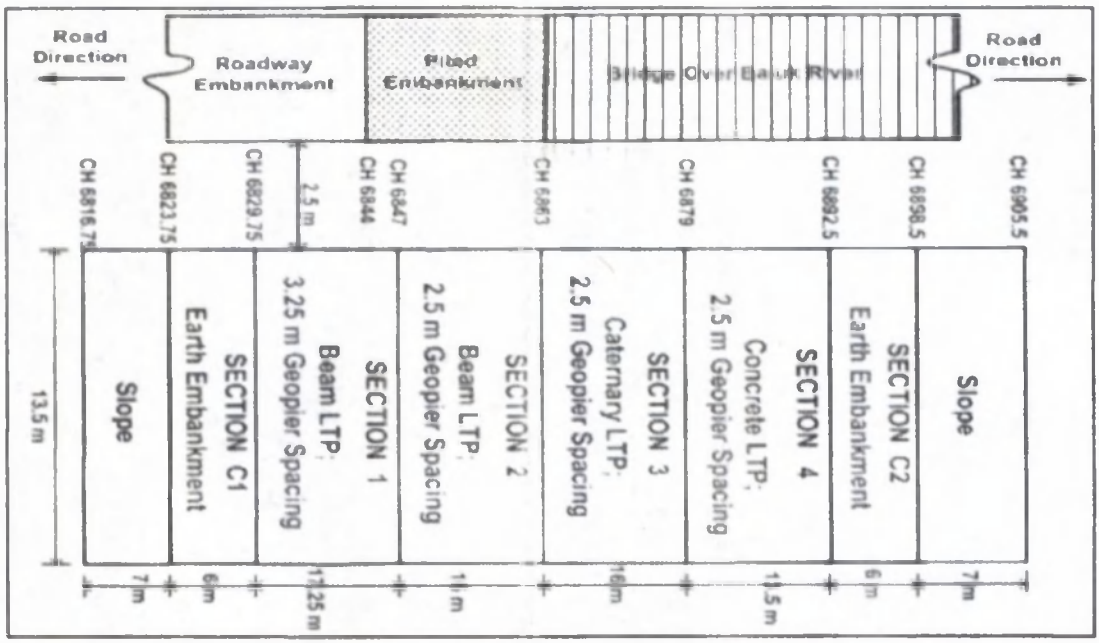


Fig. 3. Layout of the major LTP sections and the control sections

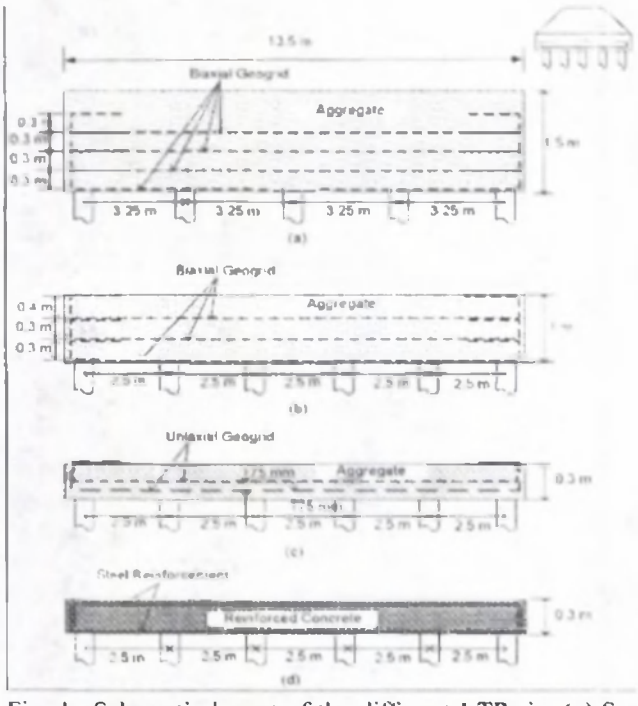


Fig. 4. Schematic layout of the different LTPs in: (a) Section 1- beam LTP; (b) Section 2 – beam LTP; (c) Section 3 – catenary LTP; and, (d) Section 4 – concrete LTP.

The measured transverse geogrid strains at the edge of the geopiers continued to increase after the completion of the embankment construction before they essentially stabilized at nearly constant values. The summary of the final strains in the transverse direction in the geogrids at the edge of the geopiers as well as between the geopiers for the bottom layer in Sections 1, 2 and 3 are given in Table 1. The strains in the geogrids in the longitudinal direction are not tabulated. There was insignificant difference between the tensile strain in the transverse and the longitudinal directions, with the strains in the transverse direction mostly being higher.

In Sections 1 and 2 (the beam LTPs), the general trend pointed to reduction in average tensile strain in the geogrids at the edge of the geopiers from the bottom layer to the top. Occasionally there are compressive strains recorded at the topmost geogrid layer. The measured strains in between the geopiers did not show any specific pattern. The tensile strain seemed to vary in a small range with the geogrid layer, except at the top layer where the tensile strain magnitude is lower than the rest of the layers. The maximum strain recorded in the geogrids (3.16% in Section 1) is still smaller than that assumed in the beam LTP design (i.e., 5%). The reduction in strain in the consecutive geogrid layers from bottom up indicate that correct assumptions are made in the design of the beam LTP i.e. the tensile force in the geogrids get smaller in the upper layers. The strains in the geogrids at the edge of the geopiers are higher than the strains in between the geopiers.

The data in Section 3 (the catenary LTP) also demonstrate that the tensile strains in the geogrid are higher at the edge of the geopiers than in between the geopiers. However, the tensile strain in the stronger machine direction of the uniaxial geogrid (transverse in Layer 1; longitudinal in Layer 2) was higher in the bottom layer than the top

Table 1. Strain in the transverse direction in geogrids at the edge of the geopiers and between geopiers

Geo-grid layer	Location of the strain gages	Range and average of strains in each layer of the geogrid (%) Section 1		Section 2		Section 3	
		Range	Avg	Range	Avg	Range	Avg
Layer 1 (bottom)	Edge of geopier	1.82-3.16	2.32	0.82-1.67	1.26	0.25-1.09	0.66
	Between geopiers	-0.57-1.15	0.59	-0.7-2.31	0.96	0.19-0.83	0.55

layer indicating slightly higher lateral force acting in the transverse direction. The maximum strain recorded in the geogrids is much smaller than that assumed in the catenary LTP design (i.e., 6%).

The design and field tensile forces in each layer of the geogrid are compared in Tables 2 and 3. The field tensile forces given in Tables 2 and 3 were calculated from the longitudinal tensile strains observed at the edge of the geopiers and the geogrid modulus in the same direction. The design tensile forces were also calculated from the specified tensile strains in each design method for load transfer (6% for the catenary LTP designs and 5% for the beam LTP design) and the relevant geogrid modulus. Table 2 shows that all of the design methods for the catenary LTP overestimate the tensile force in the geogrids. In the case of the German design method, the tensile force in the geogrid depends on the modulus of the subsoil. The values of tensile force from the German method are based on the minimum and maximum values of the modulus of the subsoil obtained from the laboratory and field tests (i.e. lower subsoil modulus results in higher tensile strain in the geogrid and vice versa). The British and Nordic method do not consider the support provided by the subsoil, therefore these methods are expected to be conservative. The tensile force in the geogrid from the British and Nordic methods are approximately 5 and 9 times the field tensile force, respectively. As for the German method, the calculated tensile force is only between 3 and 7.5 times the field value. For the beam LTPs, the calculated tensile force in the geogrid layers generally, are within the range of the values observed in the field (Table 3).

7 NUMERICAL ANALYSES AND ARCHING RATIO

Three-dimensional (3D) numerical analyses were conducted using PLAXIS 3D Foundation Program using coupled analyses in accordance with the construction program (Berilgen et al., 2010) to simulate the behavior of the load transfer platform and its effect on arching between the geo-pier columns. The analyses were conducted taking into account the non-linear elasto-plastic soil stress-strain model. The soil model parameters were obtained from the laboratory and field tests. In the finite element model, the geo-grid elements were represented as elastic plate elements that can support only tensile forces. For the geogrid elements a tensile modulus of 280 kN/m was used as recommended by the manufacturer (Abdullah and Edil, 2007). The analytical solutions compared well with the various field measurements such as settlement and lateral deformation obtained during the construction of the embankment and the investigation provided a better understanding of the mechanisms of load transfer to the foundation soil in such a complex arrangement involving geopier columns and an LTP. Additional understanding was gained relative to the load transfer between the columns, i.e., the arching ratio.

The arching ratios calculated by different methods and measured in the field as given by Abdullah (2007) are compared with the arching ratio value of 0.40 obtained from the 3D FEM analysis in Fig. 5. Section 3 was chosen for comparison with the field data because all of the arching methods can be applied to the catenary LTP. Fig. 5 demonstrates that the arching ratios from Terzaghi, Hewlett and Randolph, German, and Nordic arching methods are very close to each other. The difference in arching ratios is less than 6% between these methods. The arching ratio obtained from the 3D FEM is lower (approximately 2/3) of these ratios. The BS8006 overestimate the arching ratio by more than 40%, while Guido under estimate the arching ratio by more than 80%.

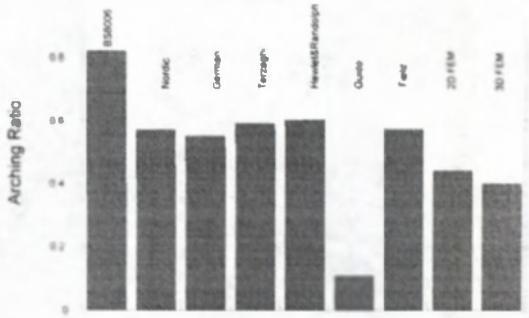


Fig. 5. Comparison of arching ratio by different arching methods

Table 2. Comparison of design and field tensile forces for the catenary design (Section 3)

Basis for tensile force	Tensile force (kN/m)
Field (maximum value)	15
British Method	141
Nordic Method	77
German Method*	47 - 112

*Range of tensile forces varies depending on the Young's modulus of subsoil used

Table 3. Comparison of design and field tensile forces for the beam design (Sections 1 and 2)

	Section 1		Section 2	
Layer number	Field tensile force (kN/m)	Design tensile force (kN/m)	Field tensile force (kN/m)	Design tensile force (kN/m)
Layer 1	2.9 - 6.2	4.9	0.7 – 6	3
Layer 2	3.1 – 6.8	3.4	2.3 - 3.2	1.6
Layer 3	0.6 – 3.0	2.1	1.3 - 5.5	0.5
Layer 4	0 – 3.1	0.7	NA	NA

8 SUMMARY AND CONCLUSIONS

Evaluation of the performance of different embankment load transfer platforms supported on geopiers are presented in terms of geogrid strains and forces, and arching ratio. The data collected at a test embankment supported by various load transfer platforms (LTP) indicated the following.

The use of LTPs together with rammed aggregate piers (geopiers) as the columnar elements in supporting a test embankment reduced total settlement of the embankment and more importantly, the differential settlement between the columns and the foundation subsoil were very small. The measured settlements within the beam LTPs are reduced or remain the same from the base up within the LTP. The use of more compressible columns (e.g. geopiers) together with LTP would be suitable for low embankment as this system results in low differential settlements.

The lateral shear displacement of the subsoil with the LTP system was small. Finite element analysis and empirical calculations show that without the LTP and the geopier subsoil the lateral shear displacements could be significantly (3-4 times) higher.

The test embankment was located in a very severe environment subject to heavy rain and flooding. However, most of the instruments that measure the performance parameters performed reasonably well and provided invaluable field data. The strain gages installed performed better than expected, where approximately 83% of the 128 gages still functioned at the end of the construction and 70% and 44.5% after 6 months and 2 years, respectively after the end of the construction of the embankment.

The tensile strains measured in the geogrids indicate that they are significantly higher at the edge of the geopier elements than mid-distance between the geopiers. The strains in different layers of the geogrid vary. Comparison of the field tensile forces estimated from the maximum strain in the geogrids and the design tensile forces shows that the various design methods overestimate the expected tensile forces by a very large margin (more than 3 times) in the case of the catenary LTP. For the beam LTP, the field and design tensile forces are more comparable.

Advanced numerical modeling with carefully measured soil and geosynthetic properties is demonstrated to be verifiable with the field data and can be used to investigate load transfer mechanisms, i.e., the arching ratio. The arching ratio obtained from the numerical analysis is 0.40 and much lower than assumed in the design methods and slightly lower than the field arching ratio.

Construction costs for geosynthetic-reinforced LTPs are likely to vary with locality; however, it appears that beam LTP offer a less costly approach with enhanced performance.

All of the current design methods for geosynthetic-reinforced LTP have provided a safe design but they can be refined so that the construction cost can be further reduced; in particular, a less conservative approach for catenary LTP (British, Nordic and German design methods) seems to be warranted.

ACKNOWLEDGMENTS

The author acknowledges Drs. C. Hassandi Abdullah and Mehmet M. Berilgen for their basic

work that enabled the writing of this paper. The Government of Malaysia funded the construction of the embankment. The late Dr. Ahmad Nazdri Hussein is acknowledged; without whom, it would not be possible to construct the embankment.

REFERENCES

Abdullah, C. H. (2007). Evaluation of Load Transfer Platforms and Their Design Methods for Embankments Supported on Geopiers. Ph. D. Thesis. Department of Civil and Environmental Engineering, University of Wisconsin-Madison.

Abdullah, C.H.,and Edil, T.B. (2007). "Behavior of Geogrid-Reinforced Load Transfer Platforms for Embankment Supported on Rammed Aggregate Piers," *Geosynthetics International*, Vol. 14, No. 3, 141-153.

Abdullah, C.H.,and Edil, T.B. (2008). "Performance of Instrumentation in Load Transfer Platforms for Geopier-Supported Embankment," *GeoAmericas 2008*, The First Pan American Geosynthetics Conference and Exhibition, Cancun, Mexico, CD-ROM.

Berilgen, M. M., Edil, T. B. and. Ozaydin, I. K. (2010). "3D Numerical Analysis of Embankments Constructed with Load Transfer Platforms over Geopier Rammed Columns," *ACE2010-GEO068. Proc.* 9th International Congress on Advances in Civil Engineering, Karadeniz Technical University, Trabzon, Turkey, (CD-ROM)

British Standard BS 8006. (1995). *Code of Practice for Strengthened/Reinforced Soils and Other Fills*, British Standard Institution, London.

Collin, J. G. (2004). *NHI Ground Improvement Manual – Technical Summary #10: Column Supported Embankments, National Highway Institute, Arlington, VA, USA.*

Fox, N.S. and Cowell, M. J. (1998). Geopier Foundation and Soil Reinforcement Manual. Geopier Foundation Company, Inc. Scottsdale, Arizona.

Guido, V. A., Knueppel, J. D., Sweeney, M. A. (1987). "Plate loading tests on geogrid-reinforced earth slabs." *Geosynthetics Conference '87*, Vol.1, 216-225.

Giroud, J.P. Bonaparte, R. Beech, J.F and Gross, B.A. (1990). "Design of soil layer-geosynthetic systems overlying voids." *Geotextiles and Geomembranes*, Elsevier, 9(1), 11-50.

Han, J. and Gabr, M.A. (2002). "Numerical analysis of geosynthetics-reinforced and pile-supported earth platforms over soft soil." *Journal of Geotechnical and Geoenvironmental Engineering*, Vol. 130, No. 2, 129-138.

Hewlett, W.J. and Randolph, M.F. (1988). "Analysis of piled embankments." *Ground Engineering*, 12-18.

Holmberg, S. (1978). "Bridge approaches on soft clay supported by embankment piles." *Geotechnical Engineering*, Bangkok, Thailand.

Jenner, C. G., Austin, R. A., Buckland, D. (1998). "Embankment support over piles using geogrids." *Sixth International Conference on Geosynthetics*, 763-766.

Jones, C.J.F.P. (1995). "The development and use of polymeric reinforcements in reinforced soil." *The Practice of Soil Reinforcing in Europe*. 1-31.

Jones, C.J.F.P., Lawson, C.R.,and Ayres, D.J. (1990). "Geotextile Reinforced Piled Embankments." *4th International Conference On Geotextiles, Geomembranes and Related Products*, The Hague, Holland, 155-160.

Love, J., Milligan, G. (2003). "Design methods for basally reinforced pile-supported embankments over soft ground." *Ground Engineering*, 39-43.

Low, B.K, Tang, S.K and Choa, V. (1994). "Arching in piled embankments." *Journal of Geotechnical Engineering*. Vol. 120, No. 11. 1917-1935.

Pham, H.T.V., Suleiman,M.T.,and White, D.J. (2004). "Numerical analysis of geosynthetic –rammed aggregate pier supported embankments." *Geotechnical Special Publication No. 126, ASCE. Vol. 1*, 657-664.

Rogbeck, Y., Gustavsson, S., Sodergren, I., and Lindquist,.D. (1998). "Reinforced piled embankments in Sweden-design aspects." *Sixth International Conference On Geosynthetics*. Atlanta, Georgia, 755-762.

Russell, D. and Pierpoint, N. (1997). "An assessment of design methods for piled embankments." *Ground Engineering*, 39-44.

Terzaghi, K. (1943). *Theoretical Soil Mechanics*. John Wiley and Sons, Inc., New York, pp 510.

Ting, W.H., Chan, S.F. and Ooi, T.A. (1994). "Design methodology and experiences with pile supported embankments." *Symposium On Developments In Geotechnical Engineering Bangkok/Thailand*. 419-430.

Behavior of Sandy Soils during the 2011 Gigantic Earthquake in Japan

I. Towhata
Department of Civil Engineering, University of Tokyo, Tokyo, Japan

Y. Taguchi & T. Hayashida
Fudo-Tetra Inc, Tokyo, Japan

T. Sasaki
Graduate Student, University of Tokyo, Tokyo, Japan

ABSTRACT: One of the research needs arising from experiences of the 2011 gigantic earthquake in Japan was the more accurate evaluation of liquefaction risk of sand with and without fines. The reason for this was the overestimation of liquefaction potential in current hazard mapping possibly without paying attention to age effects. In this regard, the present paper sheds lights on this issue by analyzing many bore hole data in order to quantitatively demonstrate the increase of liquefaction resistance with age. As for the effects of fines, a series of laboratory tests were conducted on loose sand that was collected from sites of liquefaction during the 2011 earthquake and was deposited in a loose state. The aim of undrained cyclic torsion shear tests was to assess the effects of many number of cycles that was induced by the earthquake of M=9.

1 INTRODUCTON

This chapter presents an overview of the earthquake damage. The earthquake event of magnitude = 9 in March, 2011 was an unprecedented event in modern cities where many types of structures and social systems exist together. Consequently, many lessons learned were new to the recent earthquake engineering and disaster mitigation practice. For example, the significant number of damage over a vast area interacted together and caused secondary but very significant problems. Because transportation networks were paralyzed at many places, supply of raw materials stopped and factories could not produce good that were needed to rescue. Shortage of fuel supply was another consequence of transportation stop.

In contrast, modern earthquake engineering was successful to a reasonable extent. Fig. 1 illustrates the center of Sendai City that is close to the rupture zone of the earthquake. Apparently there is no problem in a structural sense. Fig. 2 shows the quay wall of the Ishinomaki Harbor in the same area. Although tsunami attack caused significant scouring later, the earthquake shaking could not affect the alignment of the quay. What deserved attention was the very strong earthquake acceleration record of 2900 cm/s2 (Fig. 3) in Tsukidate, north of Sendai, where there was virtually no significant damage in ordinary structures (Fig. 4). This may imply that people's perception on the acceleration during earthquake being directly related with damage extent.



Fig. 1 Intact high-rise buildings in Sendai City.



Fig. 2 Straight alignment of quay wall in Ishinomaki.

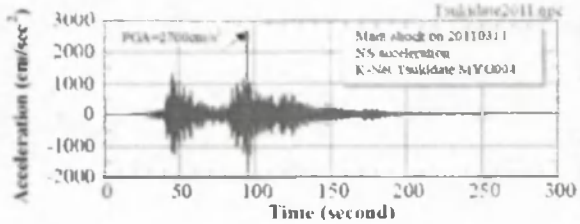


Fig. 3 K-Net Tsukidate record of acceleration.



Fig. 4 Street in Tsukidate Township three weeks after the earthquake.



Fig. 5 Tsunami-scouring behind sea wall (Noda Village).

2 DAMAGE IN GEOTECHNICAL STRUCTURES

In contrast to the aforementioned situation, damage in less expensive structures was significant. Typical examples are found in sea walls subjected to tsunami action, river levees, foundation of private houses, and lifelines for which earthquake resistant provisions cannot be fully installed due to financial limitations. Hence, there is a need to push the principle of seismic performance-based design by which an idea of appropriate earthquake resistance is sought for at a reasonable cost.

Figure 5 demonstrates significant scouring behind a sea wall in Noda Village. Although complete protection from high tsunami is not possible, stability of such a wall is essential in dissipation of overtopping water and mitigation of damage in the protected area.



Fig. 6 Tone River levee in Sawara resting on former river channel.

(a) Crest subsidence



(b) Lateral flow of slope



Fig. 7 Damage of Naruse River levee resting on clayey subsoil.

River levees were substantially damaged by subsoil liquefaction. Conventionally, those levees resting on liquefiable natural soil have been focused on; see Fig. 6 for such a levee in an abandoned river channel. In contrast, the Naruse-River channel near Sendai developed significant subsidence at the top (crest) and lateral displacement in the slope despite that there is no liquefiable sand in

the foundation (Fig. 7). This type of damage is currently interpreted as a consequence of liquefaction inside a levee. Because the levee was constructed on soft clayey subsoil, consolidation settlement resulted in the sandy bottom part of the levee being submerged in ground water and becoming liquefiable (Fig. 8).

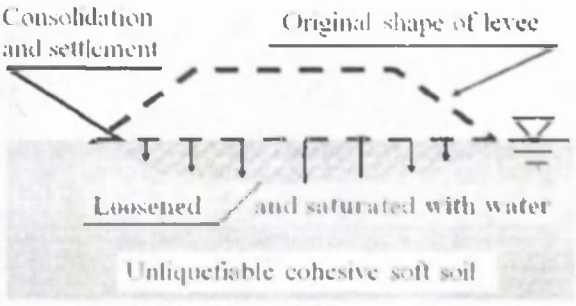


Fig. 8 Inferred mechanism of internal liquefaction in a body of levee.



Fig. 9 Liquefaction-induced subsidence and tilting of a private house (Hinode in Itako City).

Figure 9 indicates a typical damage of a house subjected to subsurface liquefaction. Tens of thousands of houses were affected in this manner, to different extents. First, note that there is no structural damage in this house except significant subsidence and tilting. Underground connection with lifelines was probably destroyed. Second, this particular area in Fig. 9 used to be a lake and was converted to an agricultural land in 1940s by removing the lake water. Thus, this area came to be called "reclaimed land" that is composed of aged lake-bed soil. Traditional geomorphological investigation has not called reclaimed land highly vulnerable to liquefaction. However, the area was further converted to a residential area in 1960 by filling sand at the surface. This sandy layer got saturated with rain water and liquefied in 2011. This type of "reclaimed land" should be considered as a more-liquefiable "manmade island" from the viewpoint of hazard assessment.

The most significant problem is that house owners wish to improve the liquefaction resistance of houses and foundations while keeping the houses at the ground surface. Obviously soil improvement under existing houses is very costly and cumbersome. Note that there is no good earthquake insurance in this country.

Sewage lifelines were affected significantly as well. Fig. 10 illustrates floating of a manhole caused by liquefaction of loose backfill. Further, the embedded sewage pipes were clogged by liquefied sand (Fig. 11) that came into pipes through disconnection of pipes or broken branch pipes that are less resistant against liquefaction. Cleaning of the clogged pipes took significant time after the earthquake and more reliable construction of sewage systems is desired.



Fig. 10 Floating of manhole caused by liquefaction.

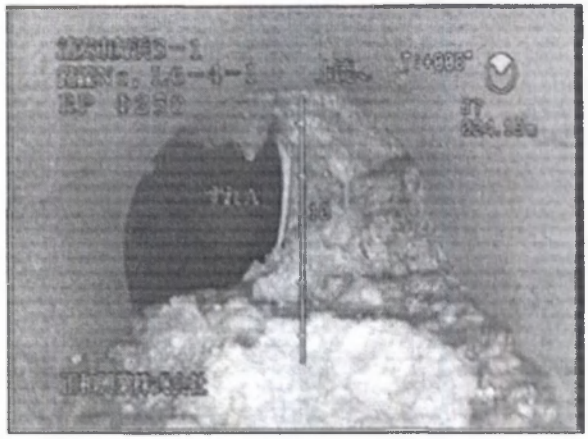


Fig. 11 Disconnection and sand clogging of sewage pipe (courtesy of Urayasu City Government).

3 EFFECTS OF SOIL AGE ON LIQUEFACTION PROABBILITY

3.1 Different behaviors of young and aged subsoil

One of the lessons learned from the present earthquake addresses the significant liquefaction in manmade islands in Tokyo Bay Shore that is in contrast with nearly complete lack of liquefaction in the more aged alluvial soils. Discussion in what follows concerns mostly the Urayasu City that is located to the east of Tokyo.

Figure 12 illustrate the distribution of liquefaction in Urayasu City. The northern tip of this city without liquefaction (Fig. 13) is situated upon a more-aged alluvial deposit, while the remaining part was constructed after 1960s by filling dredged seabed sand. Unless soil improvement was practiced, this young part of the city liquefied entirely (Fig. 14). Similarly, most liquefaction in the Tokyo Bay area occurred in recent manmade lands, while the older alluvial plane did not liquefy (Fig. 15). Thus, the effect of age on liquefaction vulnerability of sand is very important. Noteworthy is that hazard mapping in terms of soil liquefaction, that was made prior to the earthquake, designated the entire city as being prone to liquefaction.

Accordingly, the present study decided to investigate possible variation of liquefaction resistance of soil with age, which is not taken into account in existing design formulae.

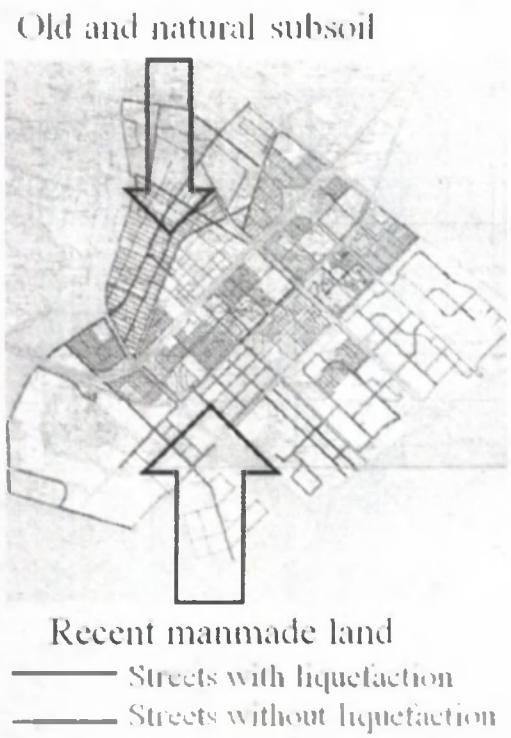


Fig. 12 Distribution of liquefaction in Urayasu City.



Fig. 13 Northern part of Urayasu City on aged soil without liquefaction.



Fig. 14 Significant liquefaction in middle part of Urayasu City.

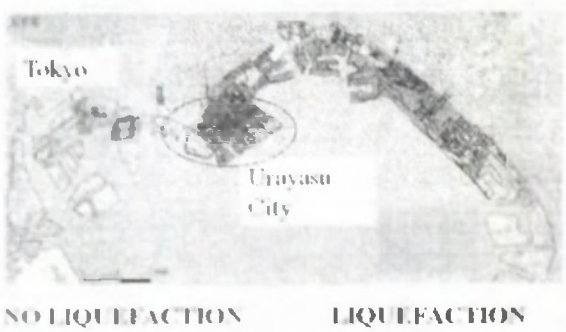


Fig. 15 Distribution of liquefaction along Tokyo Bay Shore (collaboration work my JGS and MLIT Kanto).

3.2 Ageing study by bore hole data

Effects of age on liquefaction resistance of sand were investigated by collecting bore hole data and calculating the factor of safety against liquefaction, F_L, at sites with and without liquefaction. Because the 2011 earthquake caused liquefaction in and around Tokyo where the history of land reclamation is rather well known since 17th Century, the ageing study was made possible.

Since design codes on liquefaction make use of SPT-N as the input soil index, one issue had to be discussed prior to the study. The issue is the time

when SPT-N was recorded. Fig. 16 illustrates the relationship among three important times; construction, SPT-N, and earthquake. The age of soil is determined by the period between construction and earthquake. Because it is supposed that the studied SPT-N stands for the soil properties at the time of the earthquake, the time lag between SPT-N and earthquake has to be reasonably shorter than the soil age or SPT data should not vary significantly during the time lag. For very aged soil, the first situation is the case and there is no problem. In young soil, in contrast, the variation of SPT-N with time was considered briefly by using SPT-N data in Niigata Airport.

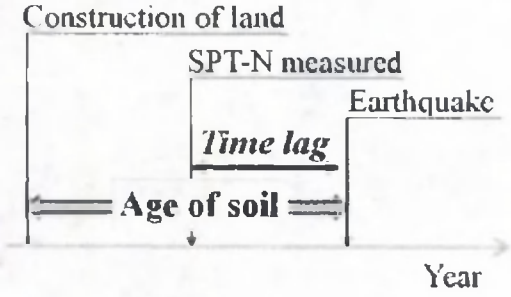


Fig. 16 Time difference between SPT-N and occurrence of earthquake.

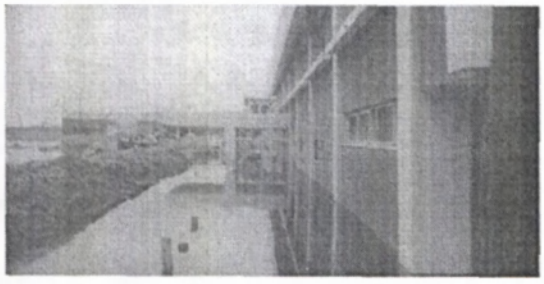


Fig. 17 Liquefaction-induced subsidence of terminal building in Niigata Airport in 1964.

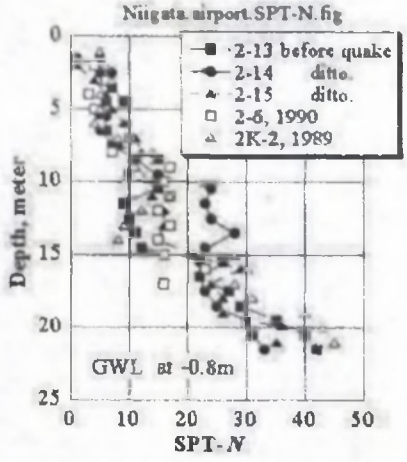


Fig.18 SPT-N profiles of Niigata Airport site (courtesy of then Ministry of Transport).

The site of Niigata Airport was probably filled with sand in the middle of 20th Century and liquefied in 1964 (Fig. 17). Fig. 18 compare SPT-N values that were measured at different times, prior to or after the earthquake. Virtually there is no significant difference among them. Hence, it is tentatively supposed that SPT-N does not change significantly in sandy soil, although more study is obviously needed. Note that deterioration of SPT-N is possible in such materials as crushed mudstone.

In practice, the factor of safety against liquefaction, F_L, is calculated by

$$F_L = \frac{R}{L} \tag{1}$$

in which R stands for resistance of soil and determined by SPT-N and fines content among others, while L is the earthquake load for design. The current research interest lies in the boundary value of $_FL$ between onset of liquefaction and no liquefaction. In principle, this boundary value is 1.0 but it is supposed that this value may decrease with age, preventing the onset of liquefaction even if the calculated number is less than unity.

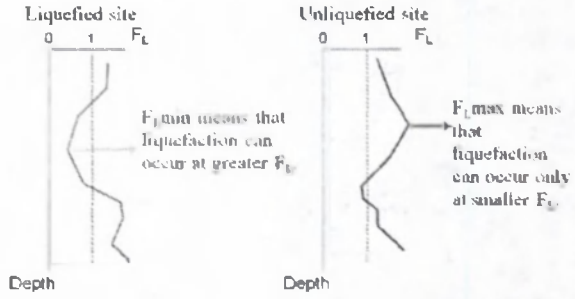


Fig. 19 Ideas of $F_L$min and $F_L$max in calculated F_L profile.

F_L values were calculated by using the Highway Bridge Design Code at many sites where the soil age is known to a certain accuracy. The input earthquake acceleration was obtained from nearby K-NET observation database. Note that the effects of possible increase in SPT-N is automatically taken into account by the use of design-code formula and the present study is investigating additional ageing effect which is not accounted for by design formula. Figure 19 illustrates the idea of the minimum value of F_L at sites of liquefaction as well as the maximum value of F_L at sites without liquefaction. At liquefied sites, the boundary F_L is greater than this minimum value because liquefaction did occur here. On the other hand at unliquefied sites, the boundary is less than the maximum value in the profile because the soil here did not liquefy. It is

thus intended to find out the boundary value between the minimum and maximum bounds.

Figure 20 plots the earthquake load, L, at depths of minimum of maximum F_L. Traditionally the border between data from liquefaction and no liquefaction designates the resistance of sand, R. As an overall view, there is only one border and consideration on age may not be necessary. This is, however, due to relatively small number of data from liquefaction of aged soil and more detailed study is described in what follows.

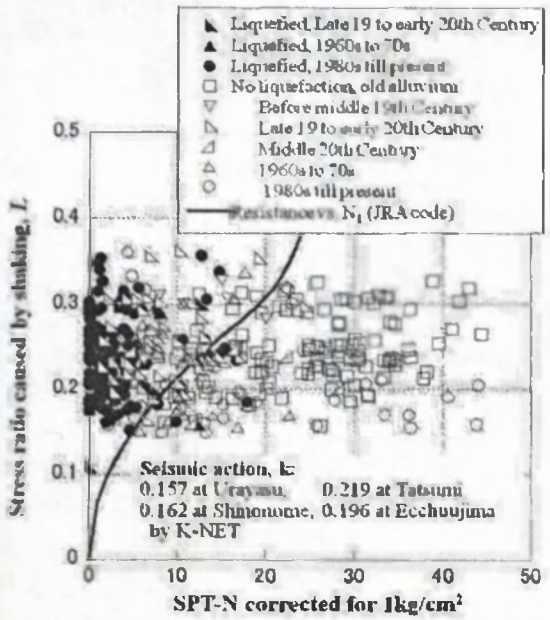


Fig. 20 Relationship between SPT-N and earthquake load at sites with and without liquefaction.

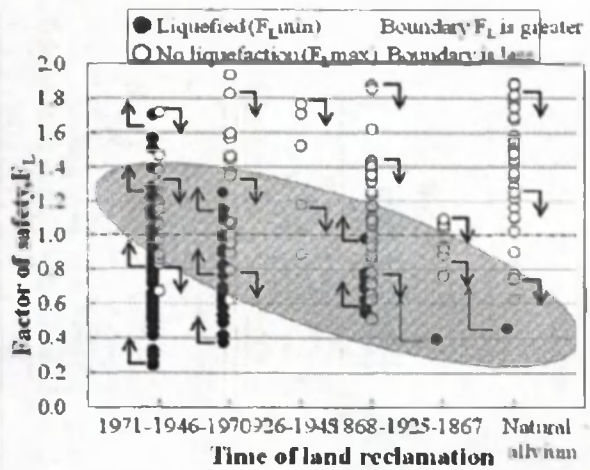


Fig. 21 Relationship of $F_L$min and $F_L$max with age of soil.

Figure 21 illustrates the variation of minimum and maximum values of F_L with age of subsoil (time elapsed since construction). The arrows in the figure indicate that the required boundary value lies between hollow and solid symbols. Because of the intrinsic nature of this type of study, engineering judgment is needed to determine any boundary. Noteworthy herein is that there are many hollow symbols, designating no occurrence of liquefaction, at construction times older than 1925. Possibly soils older than 100 years may have additional resistance against liquefaction.

Two red symbols in Fig. 21 designates liquefaction in relatively aged soils. It was not easy to find liquefaction in such aged soil and this probably infers that aged soil has good resistance against liquefaction. The left one at construction time prior to 1867 was obtained from Tsukiji site in Amagasaki City, near Osaka, where significant liquefaction occurred at the time of the 1995 Kobe earthquake. After the earthquake, additional soil was filled at the surface and the ground water was lowered by installing many drainage pipes so that future liquefaction risk would be reduced.

The other red symbol comes from Kozaki site near Tone River where liquefaction of aged alluvial sand occurred in 2011 near an abandoned river channel. The authors would like to keep some reserve about this site, supposing that the particularly liquefied sand might be younger, its age being hundreds of years possibly.

Consequently, the boundary between liquefaction and no liquefaction may be as shown by a hatched ellipse. It appears that aged soil has obtained additional resistance, which is not considered in design codes, and does not liquefy even under a small value of F_L.

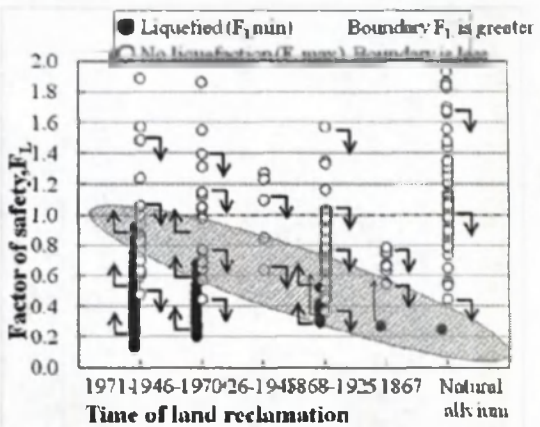


Fig. 22 Revised relationship of $F_L$min and $F_L$max with age of soil.

The range of uncertainty in the boundary value in Fig. 21 (significant width of ellipse) was not desirable. Hence, further study was conducted. First, the surface acceleration for calculation of L in Eq. 1 was obtained from nearby observation sites where liquefaction did not occur. It is likely that the significant amplification of ground motion in liquefiable soft soil is not fully considered in the

current calculation. According to the experiences in Urayasu City, the recorded motion in liquefied area was approximately 33% greater (4/3 times greater) than that on unliquefied soil. Considering this fact, the L values at liquefied sites were increased by 33%. Moreover, the liquefaction resistance, R, at all sites was reduced to 80% first by considering the elongated duration of shaking under M=9 earthquake, and, second, additional 10% considering the multi-directional (EW and NS) shaking in reality.

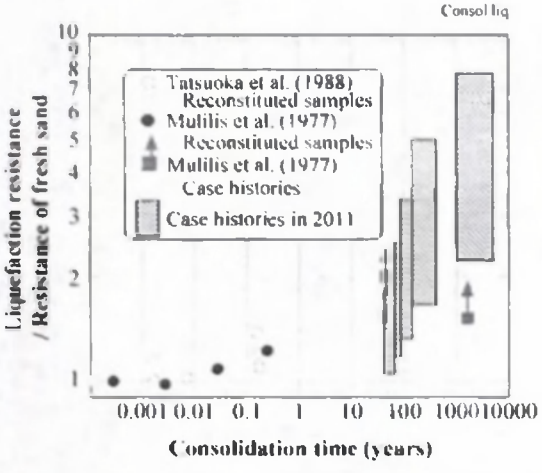


Fig. 23 Obtained ageing effect in liquefaction resistance.

The revised relationship is illustrated in Fig. 22. It is interesting that the boundary ellipse starts from F_L=1 for the youngest subsoil, and then decreases with age. Considering the uncertainties that still remain, it is reasonable that soils older than 150 years (construction before 1867) have liquefaction resistance two times greater than a what current design code gives out of SPT-N. Finally, Fig. 23 summarizes the findings in the present study (hatched rectangles) and compares them with previous studies. Tatsuoka et al. (1988) consolidated laboratory-reconstituted sandy specimens for several months and then ran liquefaction tests. Mulilis et al. (1977) ran laboratory tests as well and further analyzed cases. There are consistency among all the studies and it may be said that soils older than 100 or 150 years has two-times greater resistance against liquefaction than SPT-based design formula implies.

It should be stressed here that Fig. 23 should not be misunderstood as insisting revisal of design codes. What is important is that design codes and hazard assessment are different. For design, conservatism is the important issue and risk is often overestimated. In contrast, hazard assessment is required to predict the extent of risk as precisely as possible with only minor conservatism being allowed. It is stressed again, therefore, that ageing effect can be taken into account only in hazard assessment.

4 UNDRAINED CYCLIC SHEAR TESTS ON SAND WITH FINES

4.1 Aim and Method of Testing

The traditional design codes on liquefaction assumed magnitude of design earthquakes to be more or less 7.5. This means that the number of equivalent uniform cycles in earthquake loading is 15 to 20. This number is evidently much less than the real number of cycles that was produced by the M=9 earthquake (Fig. 24). Because provisions for a similarly gigantic earthquake are going to be required in the western part of Japan, it was considered essential to study the effects of increased number of cycles on liquefaction of sand.

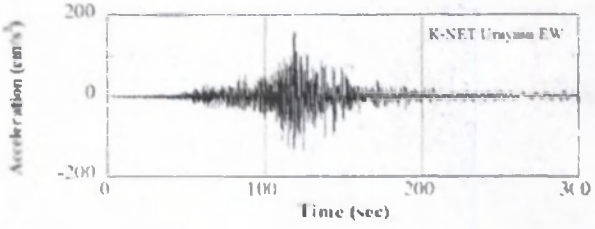
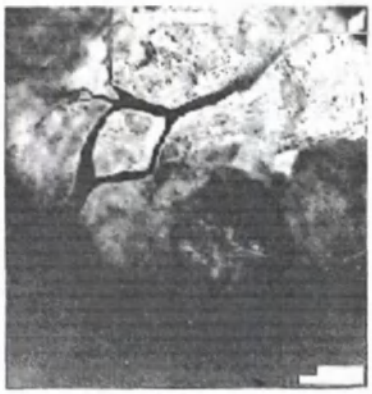


Fig. 24 Acceleration time history at unliquefied site in Urayasu City (K-Net record).

Boiled sand was collected from Urayasu City and tested. The physical properties of this sand is; Gs = 2.685, e_{max} = 1.40, e_{min} = 0.78, D_{50} = 0.1 mm, and fines content = about 30 %. The fines exhibited no plasticity. Because the research interest also addressed the original nature of the dredged sand (Fig. 25), the specimens were made very loose.

Hollow cylindrical specimens of outer diameter = 10 cm, the inner diameter = 6cm, and the height = 20 cm were prepared by air pluviation of dry sand at zero height of fall to achieve the relative density of 40 %. Water saturation of B>0.95 was achieved by the double vacuum method in which the negative pore pressure removed air, followed by circulation of de-aired water. After isotropic consolidation under 100 kPa, undrained cyclic shear tests with uniform amplitude as well as the irregular seismic load as recorded in the center of the liquefied area were conducted (Fig. 26).

in 1948:



in 1981:



Fig. 25 Air photos of Urayasu City prior to and at the end of dredging and land construction (website of Urayasu City).

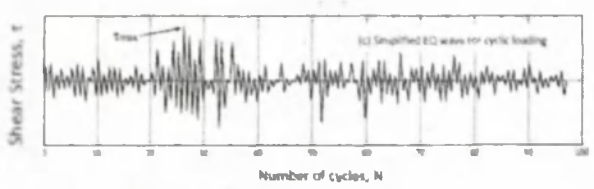


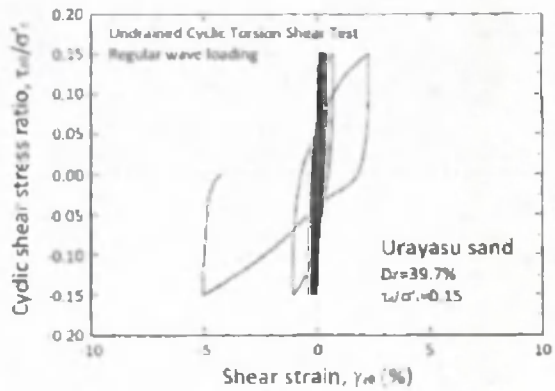
Fig. 26 Simplified stress history as loaded on sand specimens (recorded by ERI, Univ. Tokyo).

4.2 Results of cyclic undrained shear

Figure 27 indicates results of one of the tests with uniform stress amplitude with the cyclic stress ratio = 0.15. Because the fines do not have plasticity, the stress path reached the state of zero effective stress and the cyclic shear strain started to develop significantly. By repeating this type of tests with different stress amplitude, a liquefaction resistance curve was obtained as shown in Fig. 28. Because of the low density of sand, the cyclic resistance at the number of 20 is around 0.146. This number probably infers the liquefaction resistance of sand immediately after the construction stage.

Next, it was attempted to relate the effect of irregular seismic loading with Fig. 28. The first idea was running irregular undrained loading with varying stress amplitude on the similar type of specimens and detect the maximum shear stress that achieves liquefaction precisely at the end of loading. The test in Fig. 29 was conducted with the maximum shear stress ratio, τ_{max}/σ_o', being 0.204 in which σ_o' designates the initial isotropic consolidation stress of 100 kPa. At the end of loading, there still remained effective stress and therefore the strain amplitude was small. Thus, this stress ratio of 0.204 was not equivalent to the liquefaction curve in Fig. 28.

(a) Stress-strain relationship



(b) Stress-path diagram

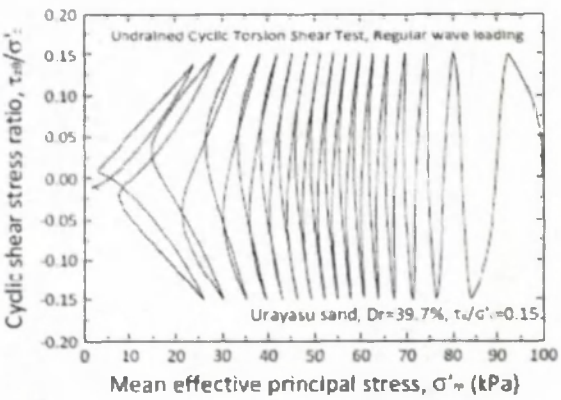


Fig. 27 Undrained cyclic shear test with uniform stress amplitude (cyclic stress ratio = 0.15).

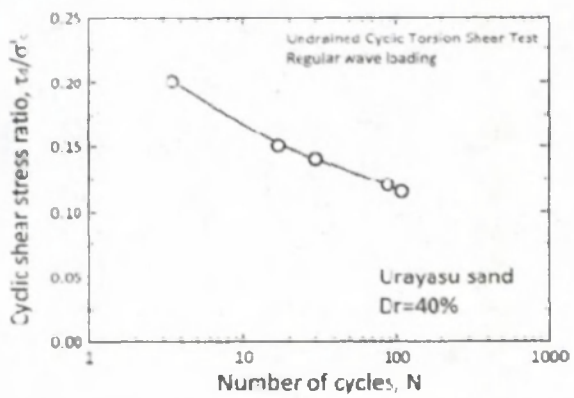
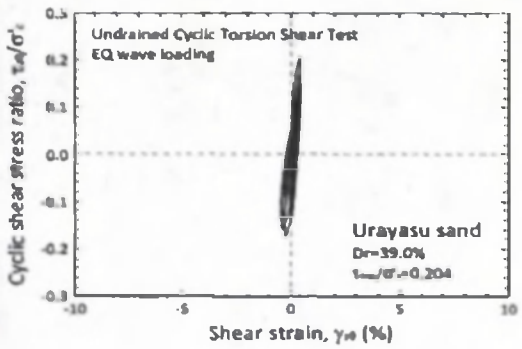


Fig. 28 Liquefaction curve of loose Urayasu dredged sand obtained under uniform amplitude of cyclic shear stress.

(a) Stress-strain relationship



(b) Stress-path diagram

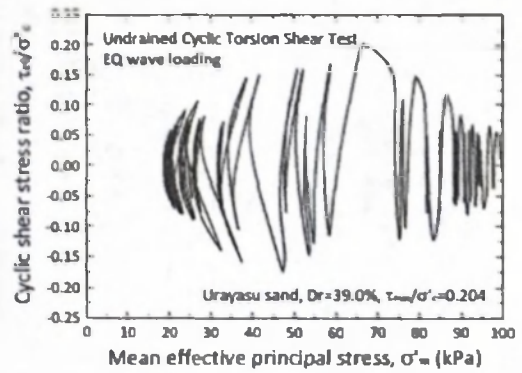
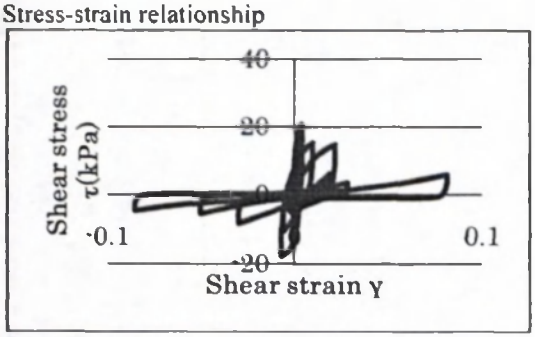


Fig. 29 Undrained cyclic shear test with irregular stress history (maximum cyclic stress ratio = 0.204).

(a) Stress-strain relationship



(b) Stress-path diagram

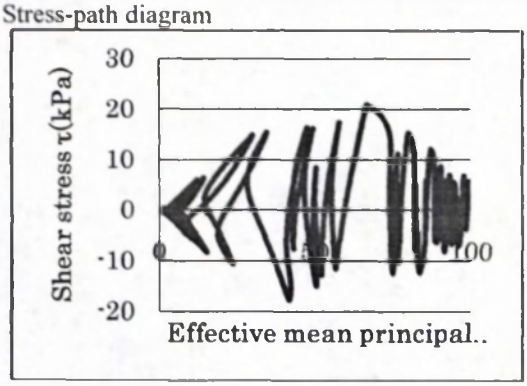


Fig. 30 Undrained cyclic shear test with irregular stress history (maximum cyclic stress ratio = 0.250).

The next irregular loading was performed under a slightly increased stress ratio of 0.208 The effective stress reached the state of complete liquefaction and the strain became large. Thus, the maximum shear stress ratio between 0.204 and 0.208 during the irregular loading is equivalent to the liquefaction curve and in particular the uniform stress ratio of 0.146.

The equality between the uniform and irregular loading thus studied was further investigated from the viewpoint of damage accumulation (Lee and Chan, 1972). In their idea, suppose that one cycle of loading with a stress ratio of τ_i/σ_o' is equivalent with $1/N_{Li}$ of complete liquefaction in which N_{Li} means the number of cycles to achieve liquefaction that is needed for this particular stress ratio in Fig. 28. By summing up $1/N_{Li}$ for all the stress cycles with different stress amplitude, the total effect of an irregular loading is determined;

$$Total\ effect \equiv \sum_i \frac{1}{N_{Li}} \tag{2}$$

The stress amplitude in the irregular loading history was varied to find out a particular value that achieved the total effect equal to unity. The obtained stress ratio, which is equivalent with liquefaction was around 1.4 which is similar to the valued obtained from experiments.

The Highway Bridge Design Code defines a soil parameter of Cw by;

$$C_w \equiv \frac{1+2K_o}{3} \frac{\left(\frac{\tau_{max}}{\sigma_o'}\right)_{irregular\ loading}}{\left(\frac{\tau}{\sigma_o'}\right)_{20\ cycles}} \tag{3}$$

where Ko stands for the earth pressure coefficient at rest and is equal to 0.5 typically. Moreover, the authors proposes the Cw number to be reduced by 10% to take into account the more severe condition of simultaneous EW and NS loadings. As a whole, the Cw parameter becomes around 0.9.

The obtained value of Cw is only slightly less than the current practice of 1.0 for an earthquake in the subduction zone. This minor difference in spite of the long duration of M=9 loading come from two facts;

1) most earthquake energy on March 11, 2011, was released from ruptures at far distance as evidenced by two seismic events in the northern area (Fig. 3) and the Tokyo area was affected by only one additional event (Fig. 24).
2) the employed sand was very loose and its liquefaction curve is nearly flat, making the difference among different stress ratios very small.

The second issue suggests that more aged sand would have Cw further less.

5 CONCLUSION

The behavior of loose sand during the gigantic earthquake in Japan was studied by means of bore hole data as well as laboratory tests. The following conclusions may be drawn.

1) Soil becomes more resistant against liquefaction after one hundred years. This effect is called ageing.

2) In spite of the elongated duration of shaking, the effect of the earthquake motion in Tokyo area is not much different from what has been supposed for conventional earthquakes in the subduction zone.

ACKNOWLEDGMENTS

The study on ageing was supported by advices by Prof. K. Wakamatsu. The tested Urayasu sand was obtained through assistance of Chiba Prefectural government. K-Net data for analysis was extremely important. The irregular loading history was supplied by the Earthquake Research Institute, University of Tokyo. The authors express their sincere gratitude to those assistances.

REFERENCES

Lee, K. L., and Chan, K. (1972). "Number of equivalent significant cycles in strong motion earthquakes. *Proc. Int. Conf. Microzonation for Safer Construction Research and Application*, pp. 609-627.

Mulilis, J. P., Mori, K., Seed, H. B., and Chan, C. K. (1977). "Resistance to liquefaction due to sustained pressure." *ASCE*, 103(GT7), 793-797.

Tatsuoka, F., Kato, H., Kimura, M., and Pradhan, T. B. S. (1988). "Liquefaction strength of sands subjected to sustained pressure". *Soils and Foundations*, 28(1), 119-131.

Studies and Investigations on Forts with Portuguese Legacy

A.Viana da Fonseca
Department of Civil Engineering, University of Porto, Porto, Portugal

Karim Karam
PhD, Sarooj, Muscat, Oman

L. Ribeiro e Sousa
Department of Civil Engineering, University of Porto, Porto, Portugal & SKLGDUE of China University of Mining and Technology, Beijing, China

ABSTRACT: Forts, including in this designation military castles, presents high complexity due to their its elevate nature. Methodologies followed in studies and investigations on forts conducted at University of Porto (UP) are briefly presented, as well studies concerning forts with Portuguese legacy. The first case is related with rehabilitation of foundations and walls of Guimarães castle, Portugal. An assessment of the causes of the appearance signs of holes or torn threads in the exposed face of the wall and tower of the extreme southwest of the castle was done. The intervention performed was focused on stabilization of rock mass and careful sealing of the massive network of high strength and consolidation of the most altered and fractured. The second is related with the protection of Jalali fort, in Oman. During 2007, cyclone Gonu caused substantial damage to the revetment adjacent to the fort. The study addresses the redesign of the revetment.

1 INTRODUCTON

Some medieval forts located in the northern region of Portugal evolved from primitive forts carved in rock formations, previous to the creation of Portugal in the 12th century, and are based on sets of high natural rock elevations that hinder their access, becoming difficult to take by storm. Today they function as a privileged point of view, but all as testimonies of local power and defense of those ancient times. Many of these fortified structures were built by warring monastic orders.

These castles are made by sectioned walls, over rock masses that may rise from the surface in height, overlapping the walls that tend to adapt to these erratic weathered profiles sweetening the foundations to these geologies (Fig. 1).

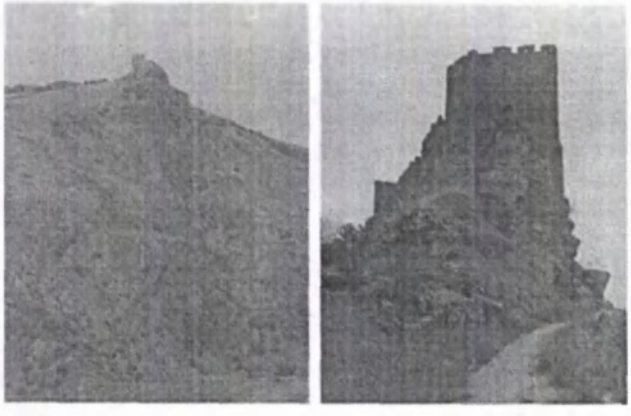


Fig. 1. Foundations of the medieval Fort of Algozo

Forts with Portuguese legacy are disseminated in all the continents. This is the case of fort of Mutrah in Oman, constructed by the Portuguese in the 17th century (Fig. 2).

In this paper, methodologies followed in studies and investigations on forts conducted at UP are briefly presented at section 2, as well studies concerning forts with Portuguese legacy. Section 3 is related to the rehabilitation of the foundations of foundations and walls of Guimarães castle in Portugal and section 4 to the redesign of the protection of Jalali fort in Oman. Finally a conclusion is presented in section 5.



Fig. 2. Fort of Mutrah, Oman

2 EXPERIENCE AT UP

The School of Engineering from UP have a considerable activity in the area of maintenance and rehabilitation of the ancient patrimony, includeing forts (Costa et al., 2010).

In a general format the activities involve the following phases (Fig. 3): i) *Knowledge phase* – considers rock and soil mechanics areas, including tests and the study of the geology, and intends to obtain information about the construction history and the evolution of the structural transformations, permitting subsequently to define the whole structural system of the forts. The main rock mechanics activities are summarized in Fig. 4; ii) *Analysis phase* – consists in the modelling activities regarding the choosing the appropriate tools and subsequent construction of the models. In modelling activities, the following itens should be considered: type of modelling (limit analysis, finite element models and discontinuity models using discrete element models); and type of analysis (static linear, static non-linear, dynamic, and 2D and 3D modelling); iii) *Rehabilitation phase* – includes the accompanying of the rehabilitation works with execution of reports, as well as the installation of a monitoring system sometimes with development of new monitoring equipments.

A protocol exists between UP and the Public Institute for Buildings and National Monuments (DGEMN). Fig. 5 presents the activities performed by UP for DGEMN since 2007 until March 2010.

For the calibration of numerical models it is fundamental to realize *in situ* and laboratory tests, for the deformability, strength and also for the evaluation of the discontinuity sets. In Fig. 6, it is summarized tests performed for modal identification of the Caminha tower (Silva et al., 2009).

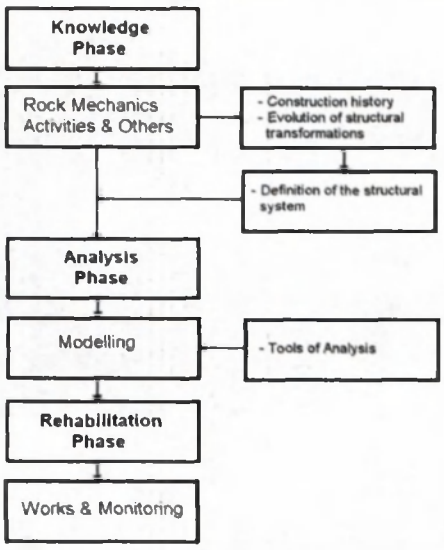


Fig. 3. Flowchart of activities at UP

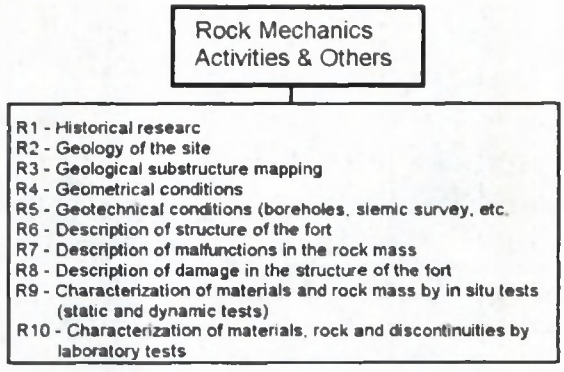


Fig. 4. Rock Mechanics activities

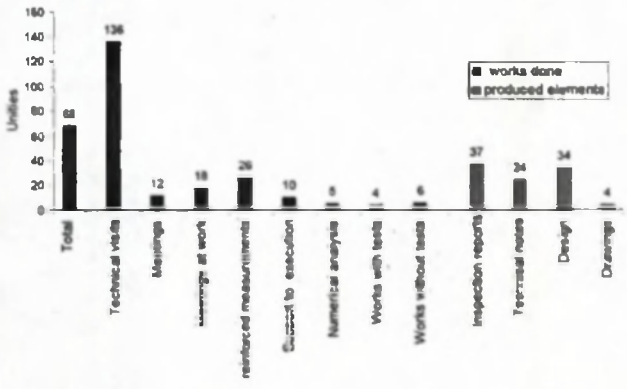
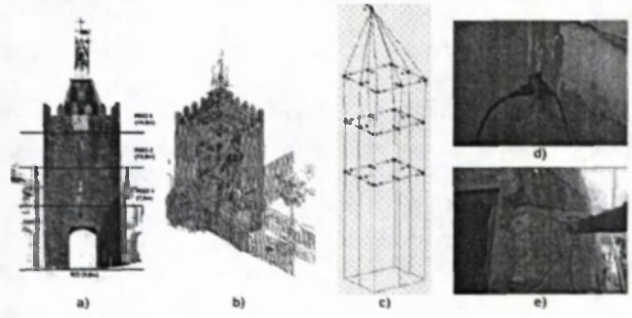


Fig. 5. Activities at UP for the rehabilitation of patrimony for DGEMN



a) image of tower; b) laserscanning; c) points for vibration tests; d) colocation of accelerometers; e) hammer

Fig. 6. Studies for the Caminha tower (Silva et al., 2009)

3 REHABILITATION OF FOUNDATIONS AND WALLS OF GUIMARÃES CASTLE

The Castle of Guimarães was founded in the Xth century for the defense of the monastery of Guimarães and the adjacent roads. From the primitive fort nothing survived to our days. The oldest traces still remaining are of the castle end of the XIth century (Fig. 7). In the last gothic phase, the southwest corner of the fence was reviewed, ad-

vancing on the walls of the village of Castle built between 1265 and 1318.

In the last century, starting in 1936, DGEMN made several restoration works on the monument. The works consisted of consolidation of the walls, restoration of the main door, replacement of masonry, demolition of elements 'newly built', and the reconstruction of the battlement stairs, parapets and battlements, reconstruction of wall panels, etc. These operations ended in 1971.



Fig. 7. A general view of the medieval castle of Guimarães

In November 2008, an intervention was requested by the DGEMN to UP to evaluate the causes of the development of fissures and fractures in the exposed facie of the main wall and tower in the Southeast of the Guimarães castle. A solution for these problems should be arisen from it, namely for the contention of these damages (Fig. 8). The tower presents an opening of the joints with a development in the vertice on the base of the wedge, reflecting a rotation in the base. On the North face, together with the opening of the joint, a singular fracture was observed with some losses of stone masonry indiciating a crashing by compression, as a consequence of the increase in stress resulting from the rotation of the wedge.

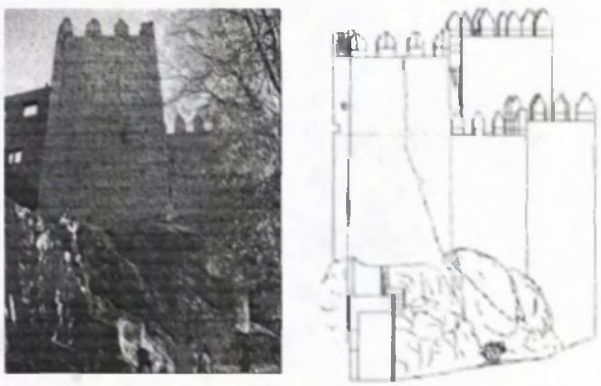


Fig. 8. Perspective of the instabilized foundations

The foundation of the wall, and specifically of this wedge, is a rocky system with an outcrop of around 3.5m above the surface and presents a clear fracturing system and a high degree of weathering, more intense in the base. The position and orientation of the system of discontinuities, explains fairly well the orientation of the fissuring in the masonry, especially along vertical joints in the North side of the fort as illustrated in Fig. 9. Therefore, from the performed analysis, where the geological-geotechnical studies have played an important role for the understanding of the structural mechanisms, it was concluded that an early cutting of the rock outcrops, executed in the decade starting on 1940, to enlarge the view of the fortified masonry in a urbanistic arrangement, might have been responsible for the instability verified in some of these outcrops. The intervention consisted in the insertion of a well selected high resistance nailing system, that could allow for stabilization of blocks and boulders of the rocky ground jeopardized by the unconfinement. The execution of a thorough net of nails sealed in the high resistance rock masses, aimed at avoiding the mobilization of the most weathered and unstable masses, which would be responsible for additional movements and settlements, responsible for the structural damages. The identification of the weak planes and fractures was the main concern of the geological-geotechnical studies, which were developed under the supervision of the geotechnical laboratory of UP (Viana da Fonseca, 2008). Both interventions were done, with the purpose of maintaining or recover the initial repos conditions, without jeopardizing the original architecture or its structural behaviour, for what it was decide to minimize as much as possible the ulterior works, namely the execution of prebored holes to insert the nails.

The presence of granite blocks is related to geological structures such as fractures, foliation or faults, where water can easily flow into and through, accelerating chemical weathering processes. They can be reasonable determined when a careful and rigorous geological-geotechnical site investigation campaign involving the all excavated volume, is carried out into the boreholes net, in order to construct a reliable geological-geotechnical model.

The study area is characterized by granite formations, whose matrix corresponds to a calc-alkaline granite two-mica biotite with predominant porphyritic texture with frequent, sometimes gneissica. An emphasis is due to the importance of masses of rounded blocks, consisting of granites low weathering levels (W_2), included in sound granitic masses.

The characterization of discontinuity contained in the unstable blocks was first made in a field survey and drilled cores. After the geological-geotechnical characterization, it became evident the need for adopting measures to stabilize the large block that supports the foundation of the

tower, in particular the west corner, dominated by a sub-horizontal facture with an unfavorable tilt angle, and where, apparently, there have been a very recent movement that evolved to the foundation of that part of the structure which leaned partially. Fig. 10 outlines the most likely mechanism of instability, and illustrates photos of areas of weakness.

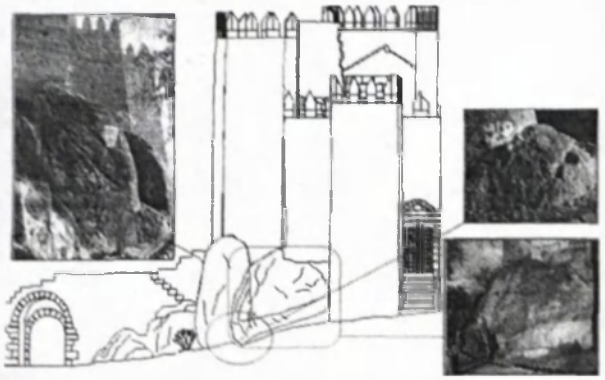


Fig. 9. Perspective of the granite massif that supports the foundation of the tower.

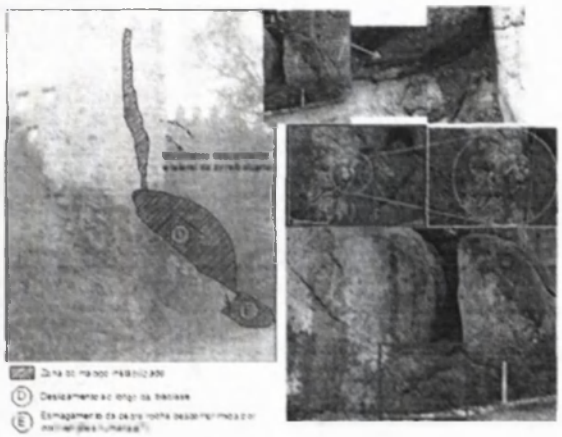


Fig. 10. Instability mechanism explaining the observed damage

The stabilization measures were intended, as a principle, to "sew" the two sides of the block and prevent future relative movements. Fig. 11 presents a scheme of stabilization - absolutely indicative and preliminary.

After studying various solutions that could be implemented in this case and taking into account the constraints of the site, a set of stabilization measures were proposed that, at first glance, would ensure the stabilization of the rock mass above the large fractured block by nailing the passive feature. These high resistance steel nails would be sealed with selective and repetitive injections in the area of fractures and faults, but also in the rest of the involved areas, looking to fill other discontinuities which would be identified in drilling process for installation of the nails. To this end the drilling procedure that has been prescribed would have to enable an integral sampling for characterization and classification of the underlying rock mass, in particular the foundation of the wall itself. The integral rotary technique that was used to execute the holes for the inclusion of the steel bars had the advantage of not transmitting significant vibrations to the structure. This drilling was extended deep enough so that the lengths of sealing guarantee a safe embeddedness in the sound to rock (W_2 to W_3). This was complemented with enough drilling extend to assure the nailing of the contiguous block, to ensure its attachment to the base, and finally, the mass sealed with microcement underlying the two major granite balls (identified in Fig. 10 as zone E). The space between the two blocks would still be filled with structural material cemented due to capping of the original stone material. Finally a thorough monitoring system was installed to evaluate a possible structural reinforcement of the tower and adjacent walls.

It is considered that nailing subject to cutting forces, should be introduced through the upper surface of the block, near the area of the foundation close to the walls, and that drilling openings should be spaced 1.5 m of the edge line, looking for a layout that was as orthogonal as possible to the gap plane (diagram in Fig. 11). The nailing elements to be adopted should consist of steel bars of high resistance so that they could establish the safety level imposed by design criteria an in number compatible with the available space. The injection procedure and inspection criteria are described below. The solution proposed required continuous monitoring, needed to adjust the solution in terms of length of the bars, arrangement and number depending on the recognition of the solid and weathered rock zones. This monitoring by the designer in works of this kind must be, in fact, an assumption in such of geotechnical works.

Fig. 12 shows some of the phases of the construction.

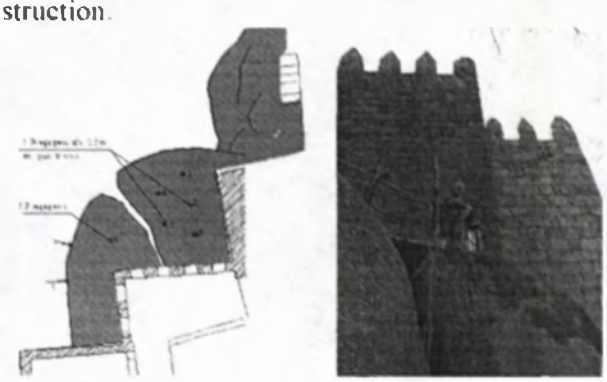


Fig. 11. Plan of nailing positioning and drilling

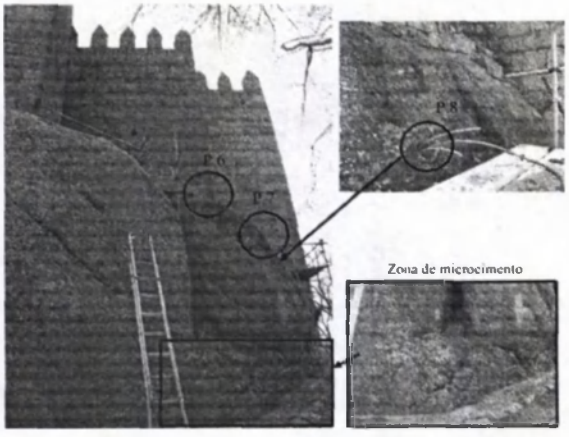


Fig. 12. Arrangement of nailings and consolidation zone with micro-cement.

The work should be started from injection upwards defining two injection steps: a first run by gravity purge tube up to the mouth; the second - performed immediately - by injection under pressure with the volume control (accompanied by a careful check upwelling). Two different types injections should be considered: injections in rock masses of good quality and injections in rock masses very altered and fractured soils. The injections were performed with cement grout to achieve the pressures defined in paragraph below, which ensured the consolidation of land and good sealing of the armor. The first hole injection would be used to assess the type of solution to be used and method of implementation of the injections. In the treatment of mass for the foundation and in the presence of soils or soft soils areas and highly weathered rock masses, selective and repetitive injections would be necessary in some sections specific. The multiple works in the repetitive injections are illustrated in Fig. 13.

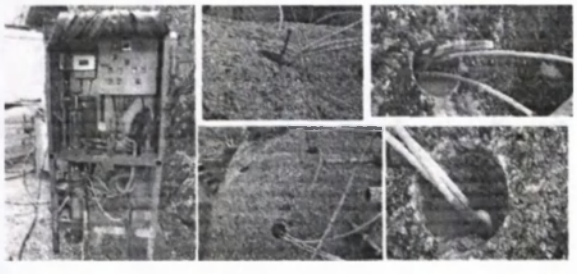


Fig. 13. Multiple works in the repetitive injections

Finally, all the mouths of the holes where they closed with cores that were cut with a diameter of 200 mm and that had been removed on the starting of the execution of the holes. Later, the space between was filled with large stone blocks cemented and built a dry stone masonry similar to the wall, this will faceting. At the base of the second block, where consolidation had been made with mortar and micro-cement very fluid - see above - proceeded in a similar way (Fig. 14).



Fig. 17. Stabilized situation of the Castle

4 PROTECTION OF JALALI FORT, MUSCAT

Jalali fort is the finest of Oman's historical fortification in the capital area and its environment (Fig. 15). The fort was originally built by Portuguese occupying forces in the early of the 16th century. Fort Jalali went through a series of transformation in design and fortification.

During 2007, cyclone Gonu caused substantial damage to the 300m long revetment adjacent to Fort Jalali, in Muscat, Oman (Fig. 16). The damage included destruction to 200m of the Shed concrete armour units, collapse of numerous 160 tonne concrete crest blocks and failure of the slope (Bentika et al., 2010). About seven hours before passing near the northeastern Oman coastline, Cyclone Gonu began affecting the country with rough winds and heavy precipitation, producing strong waves along much of the coastline, leaving many coastal roads flooded.

The revetment east of Fort Jalali was originally constructed in 1980. The original revetment was about 265m long. The revetment was armored by Dolos units in two layers with total thickness of 2.6m at a slope of 1:1.5 (V:H) laid on stone. A detailed inspection of the damage following cyclone Gonu was performed as referred in the publication of Bentika et al. (2010). The potential causes of failure included armor unit structural failure, toe failure and loss of underlayer leading to undermining of the units.

The revetment was redesigned using appropriate hydraulic models for simulating the extreme conditions for the waves. A model was constructed and tested in one of the random wave flumes and the tests were used confirm and optimize the design. The new revetment for protection is shown in Fig. 17, while in Fig. 18 the final configuration is presented.

The works involved in the construction comprised (Fig. 18): dredging the debris field at the toe of the revetment; lifting the large 175 tonne crest units, splitting them into two 80 tonne blocks and then lifting them into position to form the new toe;

re-profiling the slope and laying the large underalyer rock (The rock was sourced from Farfarah quarry, about 70km from Muscat); placing over 900 No 16m^3 AccropodeTM units on the slope. These were cast at Halban, about 90 km from Muscat. The dredging operation went well. As noted earlier, the existing toe was found to be in reasonable condition. The revetment successfully stood up to Cyclone Phet, albeit it is noted that Phet was much milder than Cyclone Gon.

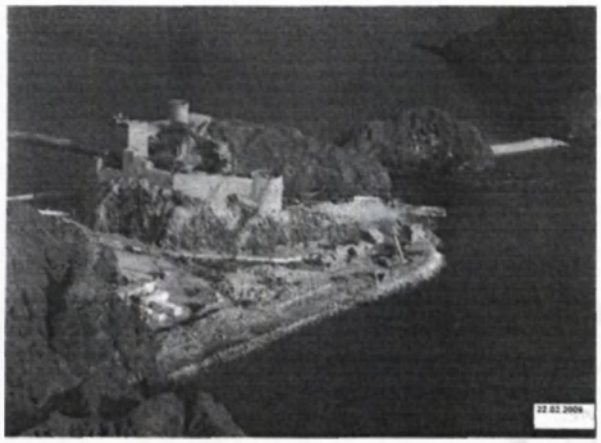


Fig. 15. View of Fort Jalali



Fig. 16. Fort Jalali. Location of the revetment (Bentika et al., 2010)

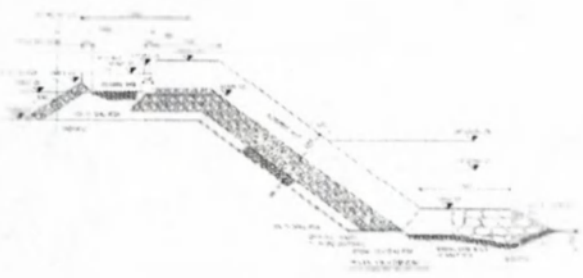


Fig. 17. Design configuration of the revetment (Bentika et al., 2010).



Fig. 18. Fort Jalali. View of the new protection

5 CONCLUSION

Studies and investigations on forts and castles with Portuguese legacy were presented with applications to the Guimarães castle in Portugal and to the Jalali fort in Oman.

Emphasis was also made to the methodologies followed by UP to these studies, particularly regarding geotechnical studies, tests and numerical modeling.

ACKNOWLEDGEMNTS

The authors thank the Department for the Cultural Heritage of DRCN (IGESPAR), in Portugal, in the persons of Mrs. Architect Paula Silva and Mrs. Ing. Anabela Carvalho, for creating the best conditions for the execution of the stabilization solution of the Guimarães Castle and the authorization for the publication of this work.

REFERENCES

Bentiba, R.; Crickshank, L.; Khalili, S. (2010). Failure during cyclone Gonu and reconstruction of the Fort Jalali Revetment, Oman. 2nd Int. Conf. on Coastal Zone Engineering and Management (Arabian Coast 2010), November 1-3, 2010, Muscat, Oman.

Costa, A.; Delgado, R.; Arêde, A.; Guedes, J.; Vila Pouca, N.; Romão, X.; Paupério, E. (2010). Patrimony interview – The experience of NCREP/IC from UP (in Portuguese). Congress of Patrimony, Porto, 16p (CD-ROM).

Silva, B.; Lopes, V.; Miranda, L.; Guedes, J.; Paupério, E.; Costa, A. (2009). Geometric and mechanical characterization of Caminha tower through visual inspection and NTD techniques (in Portuguese). 3rd Meeting on Patology and Rehabilitation of Buildins, Porto.

Viana da Fonseca, A. and Cruz, N. (2010). Geotechnical interventions in Patrimonium with reinforcement of foundations. The Castle of Guimarães. Congress "Rehabilitation 2010. CD-Rom: 31 pages (ISBN:978-972-752-123-4)

Viana da Fonseca, A., Carvalho, J.M., Ferreira, C., Santos, J.A., Almeida, F., Pereira, E., Feliciano, J., Grade, J. & Oliveira, A. (2006). Characterization of a profile of residual soil from granite combining geological, geophysical and mechanical testing technique. Geotechnical and Geological Engineering, Vol. 24, N°. 5, pp. 1307-1348.

Historical Development of Embankment Dams in Japan

T. Tanaka
The Japan Association of Rural Resources Recycling Solutions (JARUS), Tokyo, Japan
Y. Mohri & H. Tagashira
National Institute for Rural Engineering, Tsukuba, Japan

ABSTRACT: Embankment dams are the oldest irrigation infrastructure in Japan. The embankment dams have contributed to irrigation of rice crops. This paper describes the construction methods, compaction of materials and seismic aspects of main old earth dams. The compaction of materials of embankment dam body was known to be very important and construction works were carried out with extreme caution. Also the performance of small embankment dams including old embankment dams constructed in Edo period was reviewed

1 INTRODUCTON

Dry climate and water scarcity in India led to early development of water management techniques, including the building of a reservoir in 3000 BC. In Sri Lanka large reservoirs have been created by ancient Shinhalese kings in order to save the water for irrigation. The technologies of reservoir constuction tranfered to Japan via China and Southern Korea. In Japan reservoirs are important for irrigation of rice crops and many reservoirs are constucted as national projects. The ancient famous reservoir is Sayama-Ike Dam. This reservoir is still in use today but many improvement projects have been implemented at the dam over its long history.
In the Tumulus period from 3rd to 7th century, burial mounds of immense size called 'zenpokoenfun' were built, and these uniquely Japanese tombs were circular with a rectangular frontage. The most famous mound in this period is Tomb of the Emperor Nintoku. The length of the mound is 486 m and the height is 36 m. This mound is the world's largest burial site that has a ground size larger than the Great Pyramid of Giza in Egypt and the Imperial Mausoleum of Shih-Huang-Ti in China.



Fig. 1 Tomb of the Emperor Nintoku in Sakai City

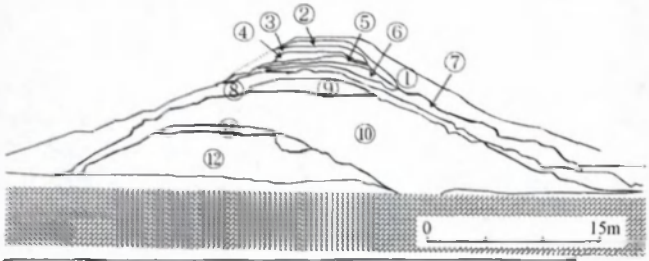
The tomb is surrounded by reservoir for the purpose of protection. The construction technology of these large burial mounds and old large reservoirs such as Sayama-Ike Dam in Osaka prefecture were closely interconnected.
Manno-Ike Dam is largest old type reservoir and constructed in the 8th century in Kagawa prefecture. In Edo period many reservoirs are constructed and Iruka-Ike Dam is second largest old-type reservoir in Japan and constructed in the 17th century in Aichi prefecture.
A recent study of the performance of embankment dams which have been subjected to earthquake shaking has thrown considerable light on some aspects of seismic behavior. A review of the performance of small embankment dams including old dams in Edo period was reported (Akiba and Senba, 1941) in the 1939 Oga earthquake in Akita prefecture. As a result of this earthquake 12 cases of complete dam failure occurred. This report is an important contribution to the earthquake resistant design of modern embankment dams.

2 SAYAMA-IKE DAM

2.1 *Background of the dam*

The Sayama-Ike Dam, built around 616 A.D., is considered to be one of the oldest irrigation reservoir in Japan. Remarkably, the reservoir is still in use today. At least 11 large-scale improvement projects have been implemented at the dam over its long history, as referenced in Fig. 1(JCOLD,2012). The flood control capacity of the river basin was reduced by changes such as land classification redistribution

accompanying urbanization, resulting in the frequent occurrence of flood disasters. The heavy rainfall brought by a 1982 typhoon gave rise to floods inundating more than 3,000 houses. To provide flood control measures against such issues in the future, the existing embankment of Sayama-Ike Dam was raised, adding flood control functions to the dam.



①~③	Improvements from Meiji to Showa Periods (1868-1964)
④~⑥	Improvements in the Edo era (1620-1859)
⑦	Improvements by Katusmoto Katagiri, a Feudal Load, 1608
⑧	Improvements in the Warring States Period (Mid-15th to Mid-16th Century)
⑨	Improvements by the high Priest, Chogen, 1202
⑩	Improvement in Nara Period (710 -794)
⑪	Improvement by the high Priest Gyoki, 731
⑫	Initial Dam Body, 616

Fig. 2 Improvement history of old dam (after JCOLD, 2012)

2.2 *Site Factors*

The Sayama-ike Dam was originally formed by damming up the relatively wide valley bottom plain with gently sloping hills on both sides. The dam site geology is dominated by strata of the consolidated clay to silt layer and sand and gravel layer. The absence of solid bedrock under the terraces on the left and right banks was the major cause of the repeated collapse of the spillway of the dam.

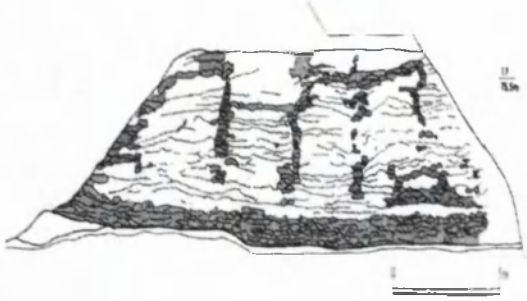


Fig. 3 Cross section of the initial dam body (after JCOLD, 2012)

2.3 *Dam technology from ancient times to the Middle Ages*

Many technologies from ancient times to the Middle Ages were discovered during the recent improvement work. The first dam body was directly embanked on top of alluvial strata. The entire bottom part of the dam body was formed by soilbags or soil blocks piled to a height of about 80 cm. There is evidence that the soilbags contained a mixture of soil and organic matter; this technique was presumably used to add strength and to prevent settlement on the soft ground. The soilbags were piled vertically every 3 to 4 m in the upstream-downstream directions. It is considered that these soilbag lines effectively demarcated the range for embanking work and served as a frame for each layer of soil (Fig. 3).
Prior to 762 A.D., the dam body was constructed using the foliage mulching method. In this filling method, a layer of leafy wooden materials was placed at every 10–20 cm of the embankment height, and is considered to drain and embankment reinforcement just as geotextiles (Fig. 4).

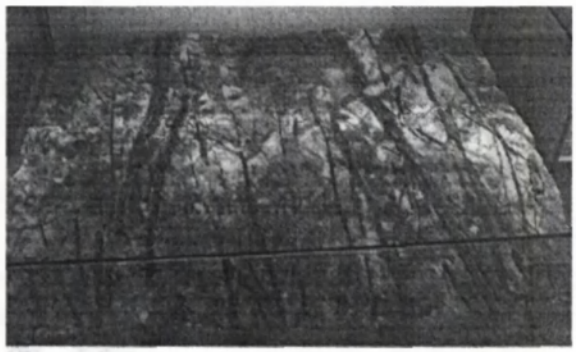


Fig. 4 Surface of the foliage mulching work (after JCOLD, 2012)



Fig. 5 Wooden cribs (after JCOLD, 2012)

Around the center sluice intake at the toe of the upstream side of the dam body, wooden cribs were constructed in lengths of 30 m (Fig 5). These seem to have been intended as a prevention measure against sliding of the dam body, erosion and sedimentation.
Artifacts discovered during the most recent improvement project, extracted examples of portions of the older facilities and the cut-out section of the old dam body are on display in the Osaka Prefectural Sayama-Ike Museum.



Fig. 6 After improvement work of Sayama-Ike Dam (after JCOLD, 2012)

3 MANNO-IKE DAM

3.1 *Site factors*

The peripheral foundation of Manno-Ike Dam is mainly composed of granite, although there are distributions of mudstone and sandstone in the left area. The gradient of the Kanakuragawa River is moderate, and while the river width near the dam body is narrow, the upstream side forms a flat plateau. These land features allow high storage efficiency.
The Manno-Ike Dam has undergone repeated improvements since its first construction. Due to the small catchment basin as well as the paucity of rainfall in the region, the storage capacity obtained as a result of the second and third dam body raising projects was derived from nearby rivers.
The dam bodies have frequently collapsed in floods or earthquakes since the first construction. New restoration work followed each instance of damage.

3.2 *Reconstruction in 821*

The methods used for embankment building at the time included the *hanchiku* method for mud walls, etc., in which wooden frames were filled with layers of soil jammed tight, and the method in which tree foliage and wooden materials were spread and stratified between compacted soil layers to promote consolidation. The government dispatched the High Priest Kukai (774–835) to take charge of the reconstruction of the dam.

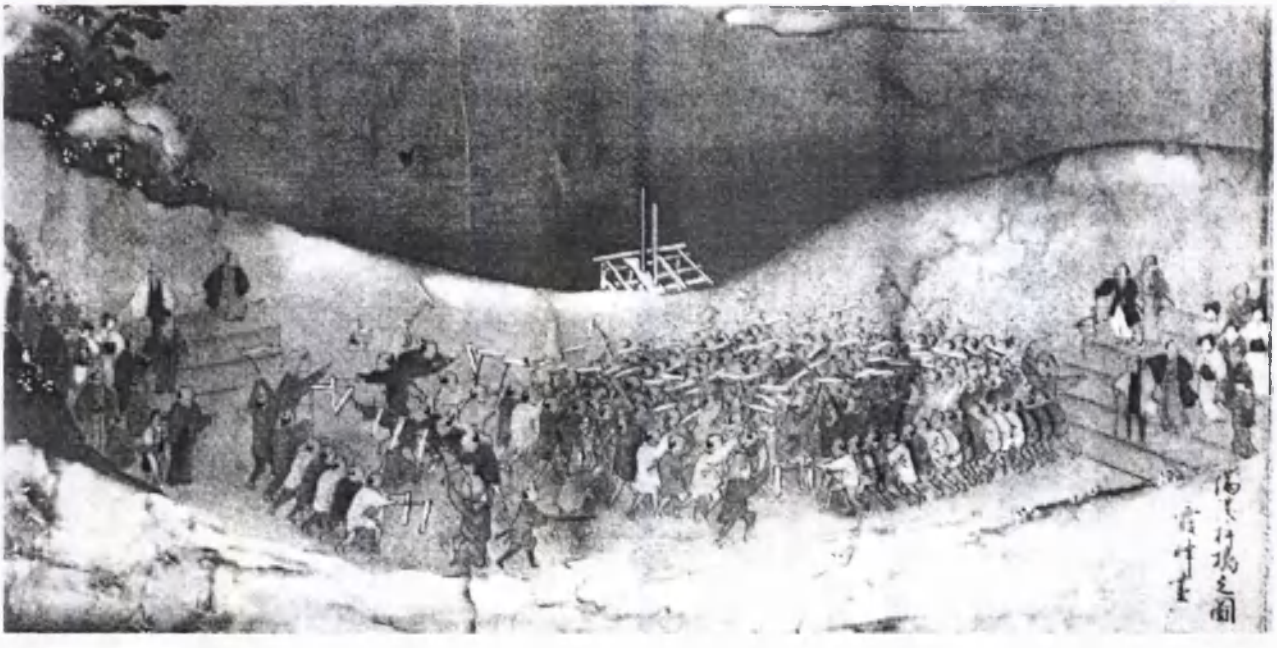


Fig. 7 Compaction works for old embankment dam body (after Agricultural Eng. Hist research Society, 1988)

Characteristics marking the construction work at the

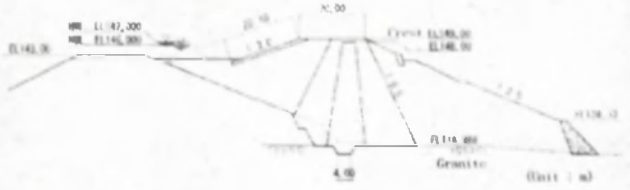


Fig. 8 Cross section change by dam body heightening (after JCOLD, 2012)

time included the following three points:

(1) Adoption of an arch type as the shape of the dam body.
(2) Installation of a spillway (built by excavating rocks on the banks).
(3) Installation of an apron at the water's edge on the upstream slope to protect against erosion.

Each marks an epoch-making innovation in embankment methods. We can deduce that the arch shape (1) was adopted rather than a straight dam body in order to prevent rocks used as a spillway from being buried in the bank, and also to reduce the total earth volume.

For (2), compared with the previous prevention measure against overflow during heavy rains, which depended on discharge via the bottom sluice, the installation of the spillway substantially contributed to the safety of the dam in flood conditions. This spillway remained in use until 1930. As for the apron (3), this prevented wave erosion of the dam body by placing a line of wooden piles driven into the ground at the edge of water, to which fascines, iron wire, bark, wood, etc., were bound.

This dam has problems of a decrease in storage capacity due to the inflow of silts and sands, increased water demand for irrigation, and limited influx in years of low rainfall due to the small size of the catchment basin. The efforts were made to heighten the dam body. Also this dam experienced many failures and repairs hitherto existing. Before Meiji period compaction works for embankment dam body were mainly depended on human feet or human power using pestles.

3.3 *Heightening construction works, 1940–1959*

There were droughts severe enough to dry up the Manno-Ike Dam in 1934 and 1939. These conditions led to a heightening project, to increase the storage capacity.

The most prominent design characteristic is the section design. All previous improvement work was of a homogeneous-type earth dam body, but in this work, a zone-type earth dam body with a central core was built on the downstream side of the old



Fig. 9 Wooden sluice pipe exchange works of Manno-Ike Dam (after Agricultural Eng. Hist research Sosiety, 1988)

dam (Figs. 8). With the raising of 6 m, the storage capacity generally doubled.
Today, 1300 years after its construction, the Manno-Ike Dam is still in service, making a tremendous contribution to irrigation in the region. The present reservoir volume is 15.43 million m^3 and largest old type reservoir (Tame-Ike) in Japan.
The wooden sluice intake pipe that was located under the center of dam body was exchanged periodically by open-cut method because of corrosion of wood materials. In this sluice intake exchange works a total 400,000 people were mobilized (Fig.9).



Fig. 10 General view of present Manno-Ike Dam (after JCOLD, 2012)

4 OGA EARTHQUAKE AND FAILURE OF OLD SMALL EMBANKMENT DAMS

The performance of small embankment dams in 1939 Oga earthquake in Akita Prefecture was investigated by Akiba and Senba. They investigated 58 embankment dams and about 30 % of these dams are constructed before Meiji period.
The conclusions of this investigation were. (1) There were very few cases of dam failures during the earthquake shaking, most of the failures occurring either a few hours or up to 24 hours after the earthquake. (2) The majority of the damaged and failed embankment dams consisted of sandy soils (3) No complete failures occurred in embankment dams constructed of clay soils. (4) At short distances from the epicenter, there were no complete failures of embankment dams constructed of clay soils. (5) At greater distances from epicenter there was a concentration of completely failed embankment dams with sand rich soils.
The Oga earthquake experience provides evidence of the stability of embankment dams constructed of clay soils under strong seismic loading conditions over those constructed of sand rich soils. In this earthquake, embankment dam failures are reported to have occurred some time after the earthquake motions had ceased. The critical period for an embankment dam subjected to earthquake shaking is not only the period of shaking, but also the period of hours of following the earthquake, because piping may occur through cracks induced by the earthquake motion or because slope failures may result from pore pressure redistribution.

5 CONCLUSION

We described the construction, rehabilitation, and conservation of historical irrigation embankment dams such as Sayama-Ike Dam and Manno-Ike Dam together with the burial mounds of immense size in ancient Japan. The compaction of materials of embankment dam body was known to be very important and construction works were carried out with

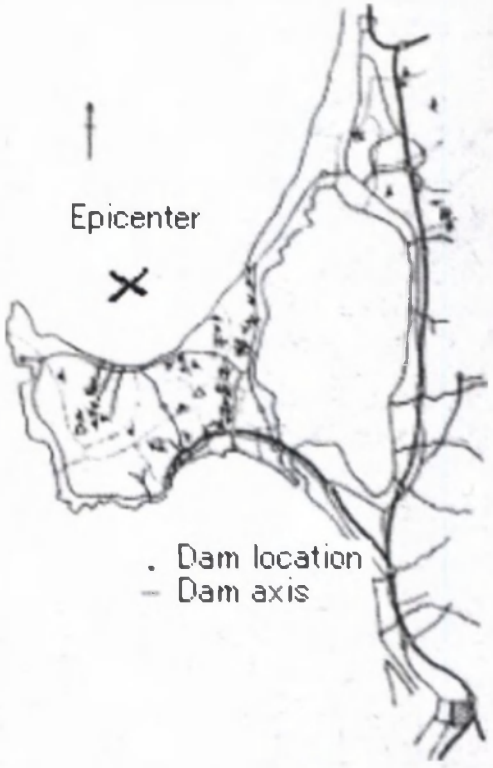


Fig.11 Epicenter, location of embankment dams and dam axis (after Akiba, M. and Semba, H.)



Fig. 12 Present Oga peninsula, Hachirougata Lake is now reclaimed

extreme caution. Also the performance of small embankment dams including old embankment dams constructed in Edo period in the 1939 Oga earthquake was reviewed.

REFERENCES

Akiba, M. and Semba, H. (1941). "The earthquake and its influence on reservoirs in Akita prefecture". J. Agric. Engng. Soc. Japan 13, No.1, 31-59.

Japan commission on large dams.(2012)."Sayama-ike dam". ,Dams in Japan",375-382.

Japan commission on large dams.(2012)."Sayama-ike dam". ,Dams in Japan",383-388.

Agricultural civil engineering research society,(1988)."Construction of small earth fill dam". Marking of the earth".126

Agricultural civil engineering research society,(1988)."Construction of small earth fill dam". Marking of the earth.126-163

Geotechnical investigations of historical monuments of Kazakhstan

A.Zh.Zhussupbekov
Department of Civil Engineering, Eurasian National University, Astana, Kazakhstan

T.O.Zhunisov
Department of Civil Engineering, Eurasian National University, Astana, Kazakhstan

ABSTRACT: Currently in the territory of Kazakhstan, it is revealed the existence of a total of about 25 000 immovable monuments-basically archeological objects-ancient sites of ancient settlements, barrows, burial grounds, parking, also objects of cult medieval architecture of Kazakhstan- the mausoleum, necropolises, ancient mosques- madrasah, place complexes etc.

This paper includes historical sites in south and central Kazakhstan, description of geological ground condition and also type of foundations. Technical survey methods, examples of technical diagnosis and significance of historical monument structure, such as mausoleums Arystanbab, Hodzha Ahmed Yassaui are also described in this paper. This geotechnical and structural investigations are important for the conservation of historical culture heritage in Kazakhstan.

1 INTRODUCTION

Architectural monuments, which are under the influence of geological environment, and also the engineering and economical activity of human, get two types of impacts. First is demolition of brickwork of a monument which brings to the deformation of base stock. Second is the demolition of monuments that takes place secretly and relates with changes, states and behavior of foundation soil. In the term of the second impact , the destruction occurs intensively with the changes cause of economical activity. This is the very factor which becomes more destructive for architectural monuments and as times goes by, its impact will increase up. These causes motivated of researching the man-caused impact on architectural monuments preservation to determine construction's induced deformation and diagnosis in order to choose the right treatment course and further partial and full 'convalescence'. This kind of treatment can be incorrect, and then man-caused factors impact can not be reduced but instead going up. Ignoring such impacts, which are often noticed during restoration because of lack of knowledge, take place on account of methodical literatures absence, absence of regulation documents on registration of man-caused factors for monument safety. As the impact of these factors has invisible character their appearance can be caught only on a final state of the monument's demolition process.

2 GEOTECHNICAL AND STRUCTURAL INVESTIGATIONS

Determination of the diagnosis of architectural monuments' deformation requires a clear view of the behaviors and structure of that geological environment that which consists of the subsystem sphere of interaction of geological environment with the architectural monument. So it is necessary to take the engineering and geological information into account, the content of which allows solving the issue by finding the cause and explaining the phenomena of researched object, and deformation of architectural monuments.

The importance of determining the role of hydrological factors in preserving the architectural monuments is considerable and has substantial meaning while diagnosing demolition causes of foundation soil behavior, foundations, and walls of monuments. On the other hand, diversity and uncertainty of impact conditions, appearances of these factors and their inadequate investigation are the main causes of interpreting the right reasons. And these cause this or that hydro geological factors. Such confusion sometimes brings to the acceptance of an absurd decision which can become the object of huge harm than to save the primary conditions [1].

Underground water adjacent to the surface and aeration zone are always the object of interest, i.e. those hydro geological objects that closely interact with the monument foundations and which determine the conditions of development of exogenous geological processes in terms of monuments

and geological environment interaction. The latter can be divided into aeration and logged zones. The permeable soil of the logged zone is waterlogged under hydrostatic pressure. And pore spaces of aeration zone are not filled by water under hydrostatic pressure but they can be filled by sporadic seasonal water (land water) which is formed on impermeable soil. If the impermeable soil is between logged and non-logged soil then it belongs to an aeration zone.

There is usually one aeration zone and one logged zone, where one of them is under the aeration zone. However, in some cases, there two or more zones of each belt can be apportioned. If there are two aeration zones then the lowest zone of aeration is situated between the highest and lowest logged zones.

Aeration zone according to its water content and its circulation can be divided into three belts: soil moisture belt, internal belt and last one is capillary cover belt [2].

The soil moisture belt is adjacent to the surface zone where water evaporates into atmosphere in a big amount. It transforms to plants and into air. Power of this belt is diverse according to its type and flora. Where there is a grass cover consisting of 0.1 – 0.15 m, and where there are gardens and parks this figure goes up rather higher. Moisture of soil belt depends on its hydroscopic water, of which its molecular adhesion saves from evaporation and also determines its balance with atmospheric vaporous water. Soil water is formed at the interaction moment of wet air with dry soil.

Capillary cover determines the belt which is above the logged zone, that contains capillary pores (0.1 mk) and is in pennanent contact with the waterlogged zone. Water of the capillary cover is above this zone and under the influence of capillary drains which rise up along the walls and pro rata to the pore soil diameter. That is why the height of capillary rise depends on soil behavior and its moisture. For dry sand, the height of capillary rise is only few dozens centimeters (in non granulated sands – 0.15-0.35 m, small granulated sands – 0.35- 1.0 m). In damp condition the height of capillary rise of sand reaches for 3-4 times higher (Engineering geology, 2004). Clay sand reaches 1.0 – 1.5 M., Uliginose soils – 2.4 m., loamy soil – from 3-to 4 m. Capillary water in clay can raise to 8.0 m., and in loess – 4.0 m.

Rising of water in soil through capillary pores can be defined by this formula:

$$H_k=0,3/d \qquad (1)$$

where: H_k–the height of capillary rising, cm; d–diameter of capillary, cm.

It should be mentioned that in the zone of soil compression foundations under the basis load the height of capillary rising naturally decreases with the expansion of soil volume weight. Thus, significant compression of clay soils can lead to the total stoppage of capillary rising of water, due to the compression, ultra pores, completely filled with fixed water are formed [5].

The height of capillary rising water in soils' spheres of monument's interaction can beof different magnitude, which corrects acceptance of these or those engineering decisions, which is directed to neutralization of negative condition changes of soil foundation, given by its moisture. So, for example, penetration into capillary water bases causes a decrease in its coherence and solidity.

Chemical structure of water also affects on the height of capillary rising; particularly as a result of chlorous and sulphureous natrium presence in water in moist integument loam raising these saline through capillaries happens differently. Penetration of these salines brings to that in lower part of loams where sulphates predominate, and in upper one – chlorides, greater maintenance of the latters in upper part of slit is connected also with the fact that chlorides diffuse faster than sulphates. It's especially important to take that into account now, when salt is used against the icy cover of pavements and roads, which then migrates up through seepage of surface water along the capillary.

In this case water first penetrates into foundation soil capillaries, into the construction materials of the foundation and the walls, consequently it causes the appearance of dampens not only on frame constructions and interiors, but also brings to the penetration of salty ingredients into whitewash, natural building materials, layer and their chemical destruction. Capillary water movement in soil goes not only from bottom to top, but also tends to impact the side of capillary force, which occurs on the boundary of different components: foundation soil and foundation material. On this basis there is molecular interaction of water and air with inner surface of ore space of brick work material, in its wetting and formation of meniscus pores, determining rising force.

Between soil water and capillary cover there is an interim belt of aeration zone. Water occurring onto this zone with its mass goes down to the logged zone or is kept in capillary pores of transition belt and is called water of intermediate belt. Up and down boundaries of internal belt is defined

according to local conditions stipulating for the peculiarity of soil dampness regime of aeration zone.

Intervening belt of aeration zone can be missed and then capillary cover closely gets to soil water. Such phenomenon appears at the time of historical territories' impoundment. In this case straight passage of ground water into atmosphere occurs with a help of evaporation.

Possibility of soil humidity changing aeration zone in the time and space depends on the influence of factors' influences that determine distribution of moisture in this zone. Particularly, soil humidity of aeration zone depends on absorbing ability of soil, and that ability primarily depends on its characteristics. The surface infrastructure condition which determines evaporation amount impacts on soil moisture. That is why in usual conditions soil moisture goes down when evaporation takes place. But soil moisture increases after rain. However if the surface is covered with steam-proof materials like concrete or asphalt, evaporation dramatically decreases and soil moisture distinctly increases in spite of atmospheric precipitates seepage exception. In this way natural soil moisture of aeration zone reflects influence both of soil content and seepage, and evaporation conditions [6].

Architecture monuments have great influence on evaporation way, under which it gets smaller or entirely excluded. This throws into augmentation of aeration zone, especially in the central part of the buildings. "People's" technology of buildings maintenance produced the struggle manners with moisture accumulation under buildings concluded in a facility of cellar which is ventilated in summer time. Such measure used to provide evaporation of moisture from soil pores and to exclude the capacity of fully absorbing ability of the grounds. This trick permitted to except moisture accumulation in soils under the monument's building and its further penetration into bearing constructions and interiors. An example, the foundations of "Arystan-Bab's" mausoleum(Fig. 1) walls [4].



Fig. 1 Mausoleum Arystan-Bab XII centiry

In the process of researching, geotechnical and restoration measures, escort of process and quality of geotechnical and engineering works, control of temperature-humidity conditions was organized.

Organization of constant monitoring works and environment has a great importance. Monitoring on Arystan-Bab's mausoleum must include:

- Supervision of UPV changing before and after dewatering,
- Constant control of old splits on the fronts and lurking of new one's appearance,
- Geodetic control of vertical and horizontal deformations of longitudinal and cross-cut walls, especially buttresses;
- Registration of a ventilation trench and pipes;
- Measurement of TVR parameters to define suitable exploitation parameters;
- Control of measuring the salinization of brick walls and foundations;
- Control on a change of chemical behavior of underground water and its link with agriculture land;
- Gynecological control on ground and underground space.

To provide these tasks it is necessary to be equipped with modern facilities.

We show some examples of pictures of architectiral monuments below (Fig.2,3,4,5,6).

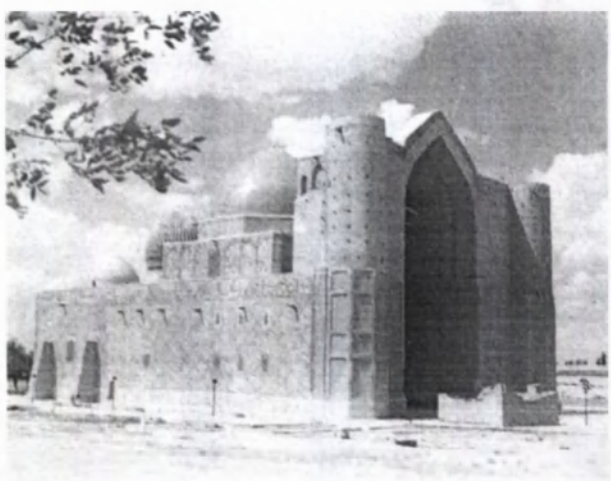


Fig. 2 Mausoleum of Kozha Ahmed Yassaui

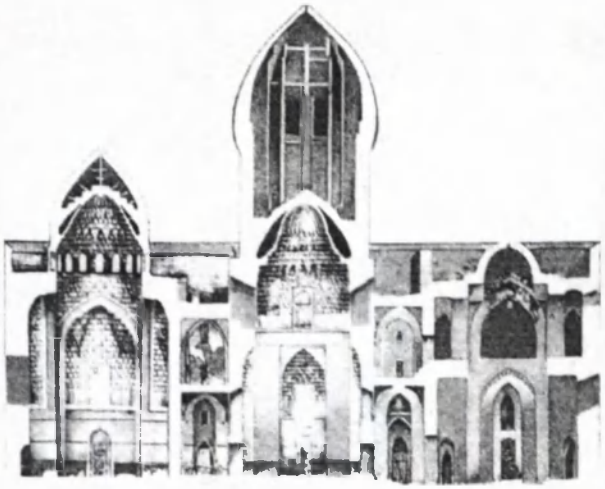


Fig. 3 Crosscut of Mausoleum of Kozha Ahmed Yassaui



Fig. 4 Historical monuments of the city Otrar



Fig. 5 Main view of the historical monuments of the city Otrar



Fig. 6 Mausoleum of Kalka-Ishan

3 CONCLUSION

As it is shown within practice, salinization process in favorable geological and hydro geological conditions takes place on many historical monuments, especially in regions with hot climate and with a notable temperature difference of atmosphere. The process takes place in a capillary zone in a cyclic way and it can be accompanied by soil grain recovery scoping with its extent (Massarsh K.P. 2004). This effect can cause a wall to crack, particularly on weak joint parts. One of the starts of solving this problem is decreasing capillary zone below the daytime surface.

Preservation of such monument as Aristan-Bab mouselum is a worldwide problem. It has a link with environmental and technological effects. In most cases geotechnical and hydro geological conditions play the most important role. Capillary water rise process in clay soil and pore materials with salinization is observed on most historical monuments, particularly in regions with hot climate and with a notable temperature difference of atmosphere.

In order to work out a special project on a regulation moisture regime of ground and underground soil damp of the underground parts of mausoleum frontward (Technological scheme of SR..., cipher 778-g/04) NIPI PMK has offered to use an evaporation method with the help of air ventilation through pore material backfilling outside, inside and particularly the lowest parts of the trench, and brick walls (foundations). Moisture ventilation and evaporation intensity is stimulated with a fixation of vertical asbestos-cement pipes with a diameter 100 mm [3].

The project worked out by NIPI PMK SR (2004) can not find all decisions connected with geotechnical problems of the monument. The most complex problem appeared to be fighting against salinization. There are many ways of finding a

solution of the problem, but detailed study of the object might be more useful.

REFERENCES

1. Abramov, S.K. (1973). Underground drainage in industrial and urban development. M.: Stroizdat, 280.
2. Under the editorship of Michailovskogo, E.V., (1977) Architectural monument restoration methods.– M.: Stroizdat.
3. A project work documentation on Mausoleum "Arystan-Bab's". NIPI PMK, Almaty city, (2004) (cipher 778-g/04).
4. Massarsh, K.P. (2003-2004). Preservation of Egyptian monuments of the pharaoh epoch. Reconstruction of cities and geotechnical construction #7. St.Petersburg, 60.
5. Pashkin, E.M. (2005). Engineering geology. M., Architecture-C, 264
6. Pashkin, E.M., and Bessonov G.B. (1984). Deformation diagnosis of architectural monuments. M., Stroizdat.

Stability Analysis of Masonry Structure at Angkor Thom in Cambodia using Elasto-plastic NMM-DDA

R. Hashimoto & T.Koyama
Department of Urban Management, Kyoto University, Kyoto, Japan

M. Kikumoto
Institute of Urban Innovation, Yokohama National University, Kanagawa, Japan

S. Yamada & M. Araya
Faculty of Creative Science and Engineering, Waseda University, Tokyo, Japan

Y. Iwasaki
Geo Research Institute, Osaka, Japan

Y. Ohnishi
Kyoto University, Kyoto, Japan

ABSTRACT: There are many historic remains in the world and many masonry structures in danger of collapse are included. In order to select suitable methodsforrestoration and preservation, it is important to evaluatethe stability of masonry structures considering interaction betweenfoundation ground and building and accurate calculation of stress distribution inside the masonry structuresis required. Hence, in this study, NMM-DDA (coupled Numerical Manifold Method and Discontinuous Deformation Analysis), one of the discontinuum based numerical methods,wasused for the stability analysis of PrasatSuorPrat N1 Towerin the Angkor monuments, Cambodia. Theelasto-perfectly plastic constitutive law was newly introduced to the original NMM-DDA code to consider the failure of soil. In the simulations, the effect of improved soil after restoration on the stability of masonry structure was also investigated. The simulation results were compared with the site observation/investigationand the applicability of newly developed elasto-plastic NMM-DDA wasalso discussed.

1 INTRODUCTON

Today there are large numbers of historic remains including masonry structures in the world and some of them are facinga danger of collapse due to natural and/or man-made factors. The Angkor monuments in Cambodia arenot an exception. Angkor is the ruins of Khmer Empire, which flourished from 9thto 13th century. The Khmer Empire was invaded by Ayutthaya Kingdomandit had been passed into oblivion until rediscovered by a French expedition in the 19th century. After the rediscovery, the conservation and restoration works have been conducted by many countries including Japan (JSA 2005).

For the restoration and preservation of masonry structures, it is greatly important to evaluate their stability considering the condition of foundation ground. In the case of Angkor, the monuments tend to be affected by the change of ground condition (wet-dry-cycle)caused by the annual rotations of rainy seasons and dry season. Some of the Angkor monuments tend to incline more during rainy season.

A masonry structure consists of many stone-blocks and the stress transmission mechanism/ stress redistribution plays important roles for the stability of masonry structures.In order to dealmasonry structures with many discontinuous planes properly,discontinuum based numerical methods such as DDA (Discontinuous Deformation Analysis)and/orNMM (Numerical Manifold Method) originally developed by Shi (Shi,1985, 1988, 1991 and 1992)will be appropriate. The DDA and NMM have been widely used in the field of rock-mechanicsfor both dynamic and static problems,such as rockfall simulations (Shimauchi*et al.*, 2009), and earthquake response analysis (Sasaki *et al.*, 2005; Koyama *et al.*, 2010) by DDA, and tunnel excavation (Miki *et al.* 2007) and stability analysis of cut slope (Koyama*et al.* 2012) by NMM. Also for the stability analysis of world heritages (especially masonry structures), DDA was applied to stability analysis of Masada, Israel (Hatzor, 2004), and DDA and NMM were separately used to stability analysis of Pyramid of the Pharaoh Khufu, Egyptand Pont duGard, France(Sasaki *et al.*, 2011).

However, it is difficult for DDA and/or NMM alone to analyze the stability of masonry structure and foundation ground simultaneously. In DDA, rigid body displacement/rotation and strain are defined at the gravity center of blocks and therefore, there is a difficulty to display the local stress/strain

inside blocks.On the other hand, since NMM does not treat rigid body rotation in the explicit form, NMM cannot treat large rigid body rotation properly.Therefore, to overcome these drawbacks of DDA and NMM, NMM-DDA (coupled Numerical Manifold Method and Discontinuous Deformation Analysis) was proposed(Miki*et al*, 2010).

In the previous study for the stability analysis of PrasatSuorPratN1 Tower in Angkor, Cambodia, NMM-DDA was firstly used to investigate the mechanism for the inclination of the tower (Koyama 2011). In the original NMM-DDA, all blocks and elements were treated as elastic material. Hence, the uneven settlement of foundation ground and inclination of the tower weremuch underestimated without considering the failure of the soil.

Therefore, in this study, elasto-perfectly plastic constitutive law was newly introduced to original NMM-DDA code, and applied to the simulations of PrasatSuorPratN1 Tower. The simulations performed under twodifferent ground conditions before/after restoration to investigate the effect of improved compacted soil on the stability of the tower.From the simulation results, the applicability of newly developed elasto-plastic NMM-DDA was also discussed.

2 BASIC THEORY OF NMM-DDA

Similarly to original DDA and NMM, the formulation of NMM-DDA is based on the principle so-called the minimization of potential energy (Miki*et al*.,2010).

The total potential energy of the whole system can be expressed as:

$$\Pi_{sys} = \Pi^{d}_{sys} + \Pi^{m}_{sys} + \sum_{B_i} \sum_{E_j} \Pi_{i,j} \qquad (1)$$

The first and second terms on the right side of Eq. (1) are the potential energy for DDA and NMM parts, respectively (which is exactly same as DDA and NMM alone). The third term represents the potential energy for the contacts between a DDA block *i*and a NMM element*j*. In the original DDA and NMM, the potential energy is minimised in terms of the displacement of the DDA blocks (D^d) and the NMM elements (D^m), respectively. This process is also applied to NMM-DDA, and the potential energy for the contacts between DDA blocks and NMM elements is minimised in terms of D^d and D^m, in NMM-DDA. Consequently, in the formulation of NMM-DDA, only defining the potential energy for the contacts between DDA blocks and NMM elements is newly required. The detailed explanations of NMM-DDA and derivation of the equations can be seen in the reference (Miki *et al*.,2010).

3 ELASTO-PERFECTLY PLASTICCONSTITUTIVE LAW

In this study, to consider the failure of soil, elasto-perfectly plastic constitutive law with Drucker-Pragermodelwas newly introduced to the originalNMM-DDA code. Following the associated flow rule, the yield function and the plastic potential can be expressed as

$$f = -\alpha I_1 + \sqrt{J_2} - \kappa = 0 \qquad (2)$$

$$\alpha = \frac{\sin\phi}{\sqrt{9 + 3\sin^2\phi}}, \kappa = \frac{3c \cdot \cos\phi}{\sqrt{9 + 3\sin^2\phi}} \qquad (3)$$

whereI_1 is the first invariant of the stress, J_2 is the second invariant of the deviatoric stress, ϕ is the internal friction angle, and c is the cohesion. Eq. (3) can beobtainedby assuming Mohr-Coulomb failure criterionunder planestrain condition.

4 OVERVIEW OF PRASAT SUOR PRAT N1 TOWER

There are 12 masonry towers of PrasatSuorPrat, which are arranged in a row at the east end of the Royal Plaza and face the Terrace of Elephants at the west end of Royal Plaza (Uchida *et al*., 2005).Since the N1 Towerhad the highest risk of collapse, restoration of the entire N1 Towerwas carried out from 2002 to 2005by JSA (Japanese Government Team for Safeguarding Angkor).In this paper, the N1 Towerwas selected as the target for stability analysis.

4.1 *The structuralfeature and ground condition of the N1 Tower*

Figure 1 shows the outward appearance of the N1 Tower (after restoration). TheN1 Tower consists of the main tower and the antechamber. The antechamber faces south and the bathing pond is located to the north of the N1 Tower.The main tower is composed ofthe platform,three stories (the 1st, 2nd and 3rd)and roof. The main building material of the tower is laterite blocks and sand stones are partially used.

The foundation ground of the N1 Tower consists of two parts: 1)natural ground and 2)compacted soil layers. The soil type of thenatural ground and compacted soil layers are cohesivesoil and sandy soil, respectively.

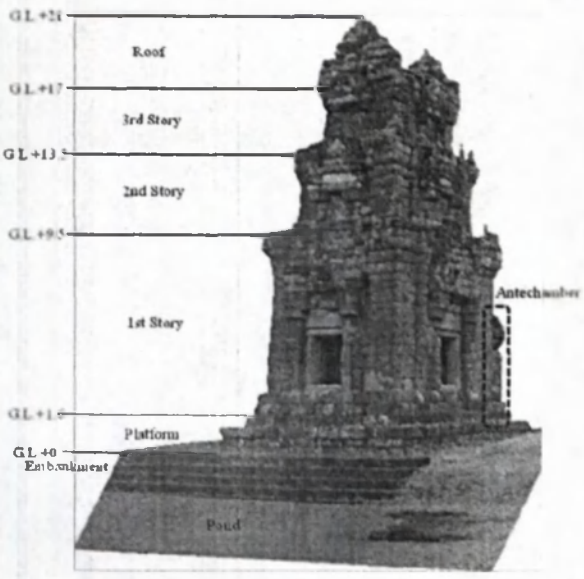


Fig. 1PrasatSuorPratN1 Tower (after restoration).

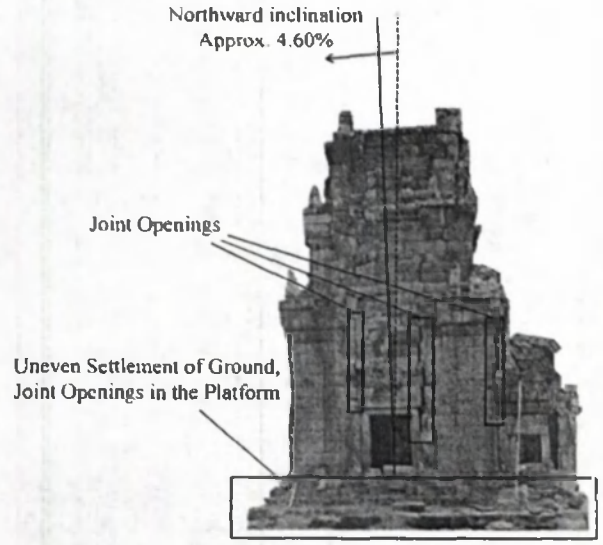


Fig. 2. The main damage of the N1 Tower (west side view, before restoration)

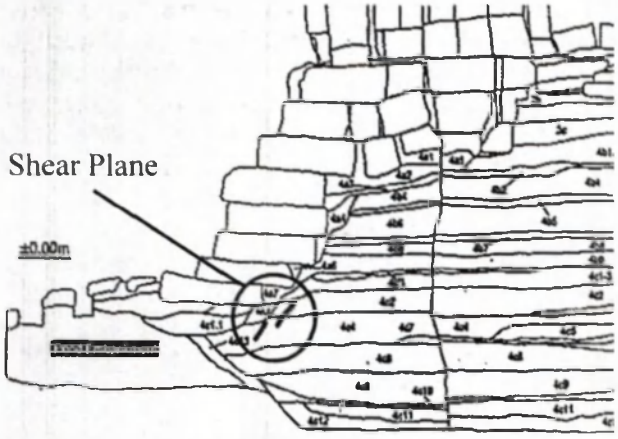


Fig. 3. The observed shear plane inside the compacted soil (west side view).

4.2 *The damage of N1 Tower before restoration*

The maindamage of the N1 Tower before restorationis summarized as follows (also see Figure2).

1) The tower inclined 4.96%/2.84°toward northwest(4.60%/2.63°towards north from the west side).
2) Some blocks fell down due to the inclination of the tower.
3) Some critical joint openings were observed in upper and lower platform, and on the wall of thetower (especially, along the windows).

Above mentioned damagemay be caused by uneven settlement of the foundation ground. Therefore, it is necessary to consider the interaction between masonry building and foundation ground for the stability analysis using accurate stress redistribution of masonry blocks. The following issues may be related to the uneven settlement of foundation ground.

1) A sliding toward the bathing pond by cutting slope and uneven soil pressure.
2) The erosion of sandy soil in the platform due to rainfallinfiltration.
3) Local stress concentration due to weathered laterite blocks and/or changes of the stress transmission paths.

5 STABILITY ANALYSIS OF PRASAT SUOR PRAT N1 TOWER

5.1 *Analytical domain*

Figure4 shows the numerical modelof the Prasat-SuorPratN1 Tower, which was created based on the sketchfrom west side after restoration (in 2-D, plane strain condition).

The masonry blocks, which may possiblycollapse during simulation, were modeled by DDA, and the foundation ground was modeled by NMM. This enabled to focus on the large displacement of the blocks (include joint openings) and the local distribution of stress/strain in the foundation ground. All masonry blocks were modeled as linear elastic material, and Drucker-Prager model (elasto-perfectly plastic model) was applied to the foundation ground.The displacements in both normal and horizontal directions, and only horizontal direction were fixed along the bottom and side edges of the analytical domain, respectively.

In the simulation, only the self-weight was considered the simulation was continued until the displacement of the blocksbecame stable.

The material properties used in the simulation which were obtained from the laboratory tests performed by JSA, were summarized in Table 1.

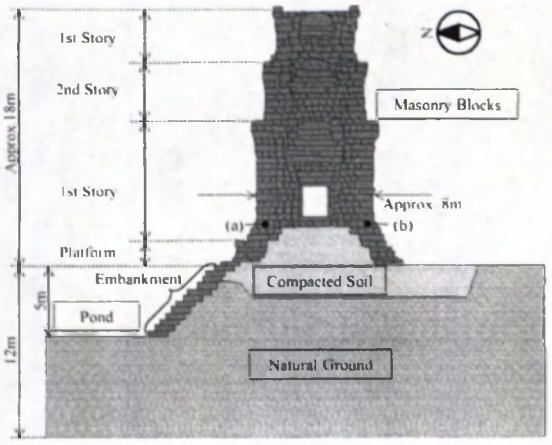


Fig.4. Analyticaldomain.

Table 1.Material properties for stability analysis.

	Masonry blocks	Compacted soil	Natural ground
Unit weight (kN/m^3)	30	18	18
Elastic modulus (kN/m)	1.0×10^6	2.5×10^4	1.0×10^4
Poisson ratio	0.2	0.3	0.3
Internal friction angle (°)	-	30	21.3
Cohesion (kN/m)	-	25	72
Surface friction angle(°)	36	36	36

5.2 *Simulation Results*

Figures 5 and 6 show the distribution of vertical displacement at the end of the simulation and the time evolution of the vertical displacement of the monitoring points (block (a) and (b) located in the bottom of the 1st story. see Fig. 4), located in the bottom of the 1st story. From these figures, the vertical displacement becomes larger(approximately 3.7 cm larger) in the northern part of the tower. This means that the ground settled unevenly and the tower inclined toward north. This uneven settlement also caused joint openings in the platform and on the wall of the 1st story as shown in Fig. 7.

Figure8 shows the distribution of the maximum shear strain at the end of the simulation. From this figure, shear bandis clearly observed in compacted soil under the northern platform, which shows the good agreement with the site observation before restoration (see Figure 3).

The NMM-DDA simulation could reproduce the inclination of the tower, joint opening along the wall and shear bands inside the foundation ground successfully. However, the calculated inclination of the tower is 0.50%/0.28°, which is smaller than the one observed before restoration (4.60%/2.63°).

As for the discrepancy in the inclination of the tower may be caused by other additional factors (such as erosion of compacted soil, more sophisticated soil behaviour under dry-wet-cycle, the effect of wind etc.) and should be studied further.

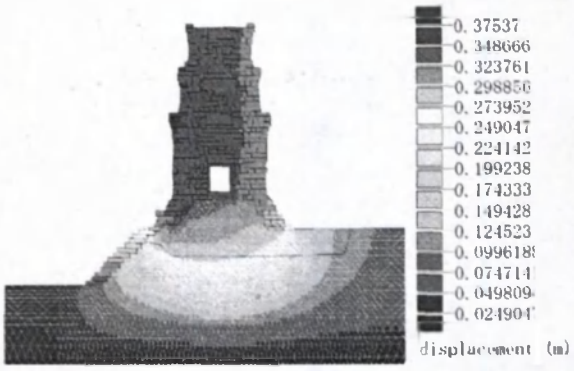


Fig. 5. Distribution of vertical displacement.

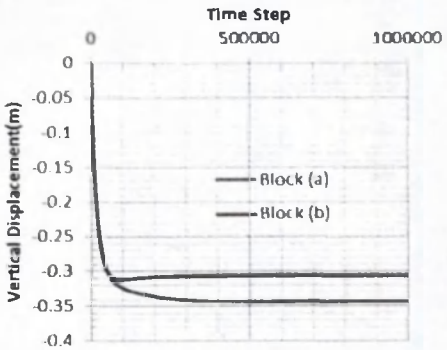


Fig. 6. Time evolution of vertical displacement for monitoring points.

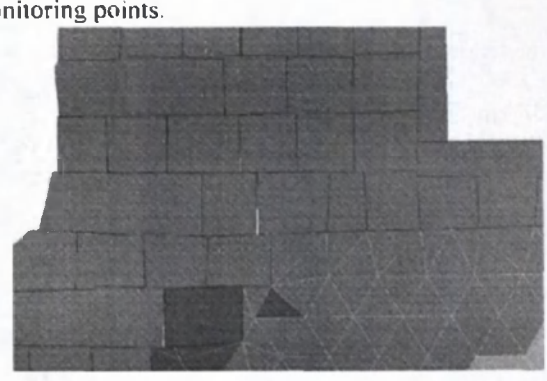


Fig. 7.Joint opening along the wall of the tower.

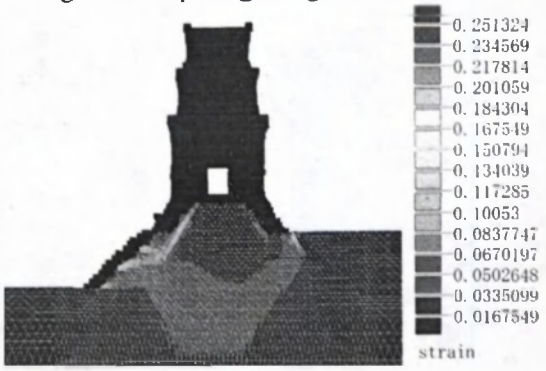


Fig. 8. Distribution of maximum shear strain.

6 STABILITY ANALYSIS AFTER RESTORATION– THE EFFECT OF IMPROVED COMPACTED SOIL

6.1 *Outline of simulations*

As mentioned before, the restoration of the entire N1 Tower was carried out. To reinforce the foundation ground slaked lime was mixed with the compacted soil (sandy soil) and geotextile was also introduced.In this section, to investigate the effect of improved compacted soil on the stability of the tower, additional simulations were performed using improved soil properties.

Table 2 shows the mechanical properties of improved compacted soil mixed with slaked lime (7 curing days) reported by JSA (2005).As shown in this table, after mixing slaked lime, the elastic modulus and cohesion were significantly improved.

Table 2.Material properties of improved compacted soil.

	Slaked lime mixed compactedsoil
Unit weight (kN/m^3)	18
Elastic Modulus (kN/m)	1.3×10^5
Poisson Ratio	0.3
Internal friction angle (°)	30
Cohesion (kN/m)	114

6.2 *Simulation Results*

Figure9 shows the distribution of maximum shear strain at the end of the simulation. Comparing with Fig.8 in the previous section, shear bandsunder the platform disappeared.

The distribution of vertical displacement at the end of the simulation and the time evolution of the vertical displacement ofmonitoring points (the block (a) and (b) in Figure 4) are shown in Figs. 10 and 11, respectively. From Fig. 11, the difference in the total vertical displacement between block (a) and block (b) was approximately2.4 cm, which issmaller than the one presented in the previous section. Therefore, uneven settlement became smaller and calculated inclination of the tower was significantly reduced to approximately 0.34%/0.19°. Consequently, no joint openings were observed along the wall(see Fig. 12).

From these results, the improvementof compacted soilwill be effective to control the slide of the foundation ground.In this study, the effect of geotextile was not considered. However, the inclination of the tower will become further smaller after introducing geotexile.

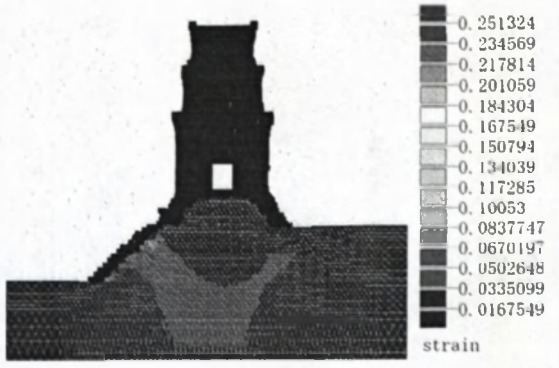


Fig. 9. Distribution of maximum shear strain after improving the compacted soil by mixing slaked lime.

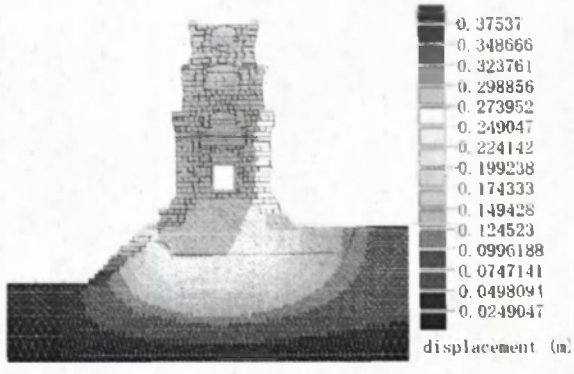


Fig. 10. Distribution of vertical displacement after improving the compacted soil by mixing slaked lime.

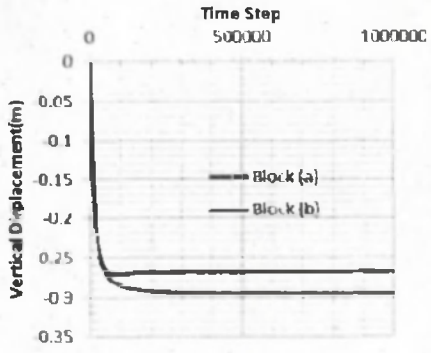


Fig. 11. Time evolution of vertical displacement for monitoring points after improving the compacted soil by mixing slaked lime.

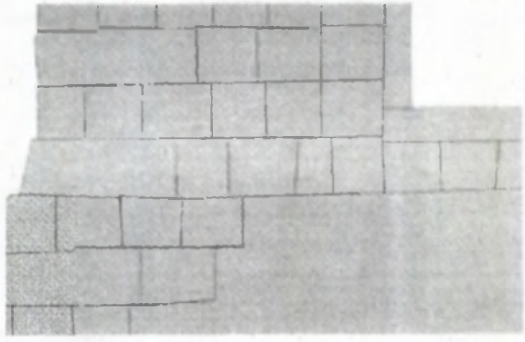


Fig. 12.Jointalong the wall after improving the compacted soil by mixing slaked lime.

7 CONCLUDING REMARKS

In this study, firstly, the stability analysis of the PrasatSuorPratN1 Tower was carried out using newly developed elast-plastic NMM-DDA.The effect of improved soil after restoration on the stability of masonry structure was also investigated. The findings obtained from this study can be summarized as follows.

- Since NMM-DDA can calculate the stress redistribution correctly by considering block movement, the interaction between masonry building and foundation ground properly.
- By introducing elastio-plastic constitutive law to the original NMM-DDA code, the failure of soil can be expressed more properly.
- The inclination of the tower, joint opening along the wall, as well as shear bands in the compacted soil observed at the site before restoration can be successfully reproduced by newly developed elasto-plastic NMM-DDA.
- The calculated inclination of the tower was still smaller than the one observed at the site.
- By using improved soil (mixing slaked lime with sandy soil), the vertical displacement and the inclination of the tower become smaller and shear bands observed in the compacted soil disappears after restoration.

For the further study, the following issues should be investigated.

- The effect of wet-dry-cycle and weathering on the strength of the soil should be considered.
- The effect of erosion of compacted soil on the stability of the tower.
- Coupled stress-flow behavior in the foundation ground including unsaturated soil properties.

ACKNOWLEDGMENTS

The authorsare really grateful to Dr. Shigeru Miki, Kiso-Jiban Consultants Co., Ltd, Dr. Takeshi Sasaki, Suncoh Consultants Co., Ltd., and Dr. Mitsuharu Fukuda, Geo-info evaluation, for their valuable comments and suggestions. .

REFERENCES (IN THE ALPHABETICAL ORDER)

Chen, Wai-Fah., Mizuno, E. (1990)."Nonlinear analysis in soil mechanics: theory and implementation", Developments in geotechnical engineering 53, Elsevier.

Hatzor, Y. H., Arzi, A. A., Zaslavsky, Y., Shapira, A. (2004). "Dynamic stability analysis of jointed rock slopes using the DDA method: King Herod's Palace, Masada, Israel." *Int. J. Rock Mech. Min. Sci.*, 41, 813-832.

Japanese Government Team for Safeguarding Angkor (2005). "Report on the conservation and restoration work of the PrasatSuorPrat Tower."

Koyama, T., Akao, S., Ohnishi, Y. and Nishiyama, S. (2009)"Earthquake response analysis for rock slope using discontinuous deformation analysis", *Doboku GakkaiRonbunshuu C*, JSCE, 63(5), 644-662 (in Japanese).

Koyama, T., Yasuda, Y., Yamada, S., Araya, M., Iwasaki, Y. and Ohnishi, Y. (2011). "The application of NMM-DDA to the stability analysis for the PrasatSuorPrat Tower, Angkor Thom, Cambodia"*Proc.* of the 45th US Rock Mechanics/Geomechanics Symposium, San Francisco, USA, 26-29 June, paper No.11-284, pp.1-6 (CD-ROM).

Koyama, T., Ohnishi, Y., Miki, S., Nakai, T., Maruki, Y., Yagi, K. and Kobayashi, T. (2012)"Application of Manifold Method (MM) to the stability problem for cut slope along the national roads", Geomechanics and Geoengineering, an international Journal, 7(1), 39-56.

Miki, S., Sasaki, T., Ohnishi, Y., and Nishiyama, S. (2007)."Applications of Manifold Method to geotechnical problems involving excavations."*Proc. the 8th Int. Conf. on Analysis of Discontinuous Deformation (ICADD-8)*, 275-280.

Miki, S., Sasaki, T., Koyama, T., Nishiyama, S., and Ohnishi, Y. (2010)."Development of coupled Discontinuous Deformation Analysis and Numerical Manifold Method (NMM-DDA)."*Int. J. Computational Methods*, 7(1), 1-20.

Sasaki, T., Hagiwara, K., and Horikawa, S. (2005)."Earthquake response analysis of rock-fall by Discontinuous Deformation Analysis."*Proc. ICADD-7*, 137-146.

Sasaki, T., Hagiwara, I., Sasaki, K., Yoshinaka, R., Ohnishi, Y., Nishiyama, S., and Koyama, T. (2011). "Stability analysis of ancient masonry structures using discontinuous deformation analysis and numerical manifold method.", Int. J. of Computational Methods, 8(2), 247-275.

Shi, G. H., and Goodman, R. E. (1985)."Two Dimensional Discontinuous Deformation Analysis", International Journal for Numerical and Analytical Methods in Geomechanics, 9, 541-556.

Shi, G. H., and Goodman, R. E. (1988)."Discontinuous Deformation Analysis—Anew method for computing stress, strain and sliding of block systems." Key Questions in Rock Mechanics, Cundall*et al.* eds., Balkema, 381-393.

Shi, G. H. (1991)."Manifold Method of material analysis."*Trans. the 9th Army Conf. on Applied Mathematics and Computing*, 92(1), U.S. Army Research Office.

Shi, G. H. (1992). "Modeling rock joints and blocks by Manifold Method." *Proc., the 33rd U.S. Symp.on Rock Mechanics*, A. A. Balkema, 639-648.

Shimauchi, T., Nakamura, K., Nishiyama, S., and Ohnishi, Y. (2009). "Concerning the influenced of velocity ratio and topography model on the result of rockfallsimulation." *Proc. ICADD-9*, 39-46.

Uchida, E., Suda, C., Ueno, A., Shimoda, I. and Nakagawa, T. (2005)."Estimation of the construction period of PrasatSuorPrat in the Angkor monuments, Cambodia, based on the characteristics of its stone materials and the radioactive carbon age of charcoal fragments", Journal of Archaeological Science, 32, 1339-1345.

On the Burial Style of Ancient Tombs from the View Point of Seepage Water Measurements

K. Onitsuka & Y. Hara
Nihon Kensetsu Gijutsu Co., LTD, Saga prefecture, Japan

ABSTRACT: Ancient burial styles and burial depth are different according to the era, climate (weather, topography and geology) and the buried person's status. These systems were strongly affected by the ancient people's seepage water measurements. Hence, change of burial styles and difference in burial depth in ancient China, the Korean Peninsula and Japan are reviewed and discussed from the view point of seepage water measurement. Almost of burial mounds in Japan preceding the Yoshinogari remains chose the Jiangnan's overground burial style which was a revolutionary change in the burial system from the under ground to the overground burial. This can be said as an excellent idea of ancient Japanese.

1 INTRODUCTION

Burial methods started with the pit burial and changed in the course of different eras to cairns (stone mound tombs), dolmens, Tudunmu (in Chinese, burial mounds in Jiangnan, the lower basin of Chang River (Chang Jiang or Yangtze River), China), burial mounds and Kofun (in Japanese, burial mounds with a big stone chamber). Burial matters also change from only human remains to those in coffins, chambers, brick chambers and big stone chambers. The materials of burial matters change from wood and stone to pottery and brick.

The burial location is under or over the ground. These styles and burial depth are different according to the era, climate (weather, topography and geology) and the buried person's status. These systems are strongly affected by the ancient people's seepage water measurements. Hence change of burial styles and difference in burial depth are reviewed and discussed from the view point of Geotechnical Engineering.

In the Yellow River basin which is under low temperature and humidity, burial matters are set under the ground even though a burial mound stands on the surface. This burial system propagated to burial mounds in Lesi country (B.C.108~) and burial stone mounds with wooden chamber in Sila Kingdom (A.D.6 hundred) in Korea. On the other hand, in the case of Jiangnan's burial mounds under high temperature and humidity, human remains or coffins are buried in the mounds over the ground in order to protect the burial matters from the seepage water. This burial system is a revolutionary change.

In the case of burial mounds in northern Kyusyu such as Yoshinogari burial mound (B.C.150), jars with human remains are set in the mounds over the ground. This burial system is an excellent idea by Yayoi people in the district which followed to the Jiangnan's burial system.

2 PIT BURIAL UNDER THE GROUND IN THE YELLOW RIVER AND CHANG RIVER BASINS

In early stages, it was in the pit burial where human remains were buried, and it gradually became the coffin burial and the compartments (boxes around coffins) burial. The burial style of Banpo remains (B.C.5.0~B.C.4.5 thousand), which are moat settlements in Yangzhao Culture

period in the middle Yellow River basin, was a pit burial and children were mainly buried in small jars. In Liangzhu remains, Liangzhu Culture period (B.C.3.3~B.C.2.2 thousand) in the middle Chang River basin, some wood coffins and wood compartments were found (Zhejiang Province Archeological Institute 1997).

3 CAIRNS AND DOLMENS IN THE NORTHEASTERN REGION OF CHINA

In the late New Stone age (B.C.8~B.C.2 thousand), cairn (stone mound) burials started, and dolmens and stone coffin burials followed (Mori et al.1995). Cairns are filled with river field stones, and human remains or coffins are set in the cairns.

The cairns in Niuheliang remains (Hongshan Culture period, B.C.4~B.C.3 thousand) , Liaoning Province are well known as early cairn burials shown in Fig.1. The cairn burials that appeared in just started Gogureo (Koguryo) which was founded in B.C.1 hundred year. After that, the cairn burials developed to large sized burials such as the General tomb (Shogunzuka, in Japanese, late A.D.3 hundred) which has a corridor-style stone chamber (Saotome 2000) in Jian, Jilin Province. The burial locates on just near North Korea. It is shown in Fig.2. Except for early cairn burials, generally human remains and coffins are buried in these cairns. Hence, it can be said that the burial location is over the ground.

The dolmens are found in around the world in the period from the late New Stone age to Stone-Metal Utilizing age. This is a large stone burial, where some stones on the ground support a large cap stone. Exactly speaking, the dolmen doesn't belong to the category of the burial mounds. The dolmens in China mostly exist in the Liangdong Peninsula and its neighborhood (Liaonin Province Archeological Institute 1994). The construction time is about B.C.1.5~B.C.0.5 thousand. The dolmens in China are classified into two groups, namely Stone Shelf and Large Stone Cap Burial. The stone shelf is a burial where three or four tall plate stones support a large ceiling stone. The large stone cap burial may be named so in that the ceiling stone looks like a cap because of low supporting stones.

Fig.3 is a typical stone shelf in the Liangdong



(a)



(b)

Fig.1 Early cairn burials in Gogureo (Koguryo,) Niuheliang remains, Liaoning Province, China (a):total view (b):stone coffin and cairns



Fig.2 General tomb in Jian, Jilin Province, China.



Fig.3 A typical stone shelf in Shipengshan, Gaizhou, Liaoning Province, China

Peninsula. It is known that dolmens exist also in Ruian, Zhejiang Province. These dolmens in Fig.4 were constructed from the West Zhou period to the Spring and Autumn period (B.C.1.1 ~ B.C.0.5 thousand). As explained later, many Tudunmus (in Chinese, burial mounds in Jiangnan, the lower Chang River basin) were constructed there in the same period.

4 DOLMENS IN THE KOREAN PENINSULA AND NORTHERN KYUSHU, JAPAN

Dolmens from the Northeastern region of China were introduced to the Korean Peninsula about B.C.8~B.C.7 hundred. Table-type (or northern type) dolmens appeared in the northwest and Go-table-type (or southern type) dolmens appeared in the southwest of the Korean Peninsula. The table-type dolmen as shown in Fig.5 is the same type of the stone shelf in China. It is called as the Northern type dolmen. And the go-table-type dolmen is similar to the large stone cap burial in China, and it is called as the Southern type dolmen (Saotome 2000).

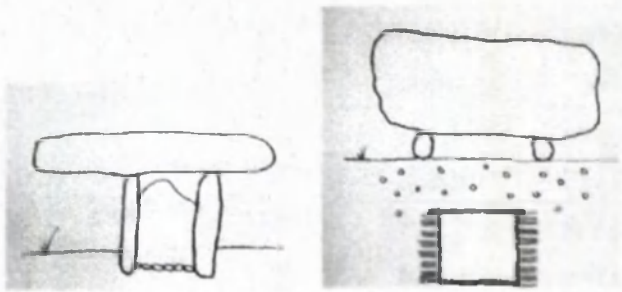
In Northern Kyusyu as well, dolmens were constructed from the late Jyomon period to early Yayoi period (about B.C.300). The shape is the same as the southern type dolmen in the southwest of the Korean Peninsula as shown in Fig.6.

The burial locations in both the stone shelf and the northern type dolmens are on the ground, and these in both the large stone cap burial and southern style dolmens are under the ground. Concerning the dolmens in northern Kyushu, human remains are buried in the pit under the ground. There are some cases in which a burial Jar is found in the pit.

There is a question that these dolmens in the southwest of the Korean Peninsula and in the northern Kyushu, Japan originated from the northeastern region of China, or from Zhejiang Province. The author thinks that dolmen's construction technique in Zhejiang Province propagated to the southwest of the Korean Peninsula and northern Kyushu, through the sea. This question is a big subject concerning the origin and propagation of the dolmen in Japan.



Fig.4 Big stone cap burial in Ruian, Zhejiang Province, China



(a) (b)

Fig.5 Dolmens in the Korean Peninsula (a): table (northern) type (b): go-table (southern) type



Fig.6 Dolmens in northern Kyushu, Japan (Maruyama remains, saga)

5 BURIAL MOUNDS OVER THE GROUND IN JIANGNAN, CHINA

Burial mounds in Jiangnan, the lower Chang River basin in China, were constructed during the West Zhou period to the Warring State period (B.C.1.1~B.C.0.2 thousand) (Onitsuka et al.2002, 2003;Onitsuka 2008;Lu 2002) . This is filled with soils as shown in Fig.7. Fig.8 is a normal sized burial mound where the author had some geotechnical investigations.

This is a revolutionary change in the burial system from the burial pit under the ground to the overground burial. The reason of change from

underground burial to overground burial is needless to say to protect the burial matters from the underground water and seepage water.

Jiangnan's burial mounds sizes in the Warring State period became larger for burials of aristocrats and kings. Their seepage water measurement became more elaborate. Fig. 9 is a vertical cross section of Yue King's burial mound (Shaoxing, Zheijiang Province) (Chin 1999; Lu 2003) which is well compared with the first Qin Emperor's burial mound. The Yue King's burial mound is constructed on the excavated natural mountain using Hanchiku compaction method. The wooden structured burial compartment has a triangle cross section of height taller than a person and of a 40m length. A large amount of charcoal is laid 1.8m in thickness under the wooden compartment and the compartment is rolled by barks 25cm in depth. And around the bark, charcoal is utilized to roll 1.0m in thickness. These are rolled by barks 10cm in thickness and finally around and over these parts, blue cohesive clay is put and yellow-brown soil is compacted by Hanchiku method. Two mallets used for the compaction of Yue King's burial mound were found.

The author considers that Jiangnan's burial mound is the root of Yoshinogari burial mound (about B.C.150) as shown later. Namely the construction technique of Jiangnan's burial mound propagated to the Shandon Peninsula. and these construction techniques of Jiangnan's or Shandon Peninsula's burial mounds propagated to Yoshinogari in northern Kyusyu, Japan through the sea, not through Korean Peninsula (Onitsuka et al. 2011). 」

6 WOODEN COMPARTMENT BURIALS UNDER GROUND AND BURIAL MOUNDS IN THE YELLOW RIVER BASIN

Large wooden compartments were built under ground in the Yellow River basin in the period from the West Zhou to the Spring and Autumn, and Warring State. Wooden compartments followed those in the Yellow River basin appeared also in the middle Chang River basin (Zhejiang Province Archeological Institute 1997). The

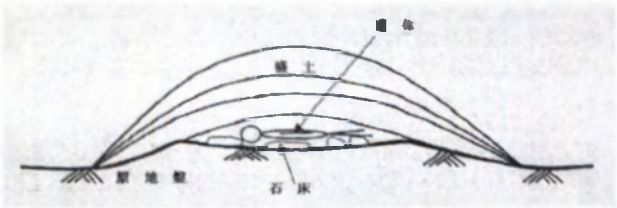


Fig.7 A schematic figure of burial mound in Jiangnan, China



Fig.8 A normal sized burial mound in Jiangnan, China

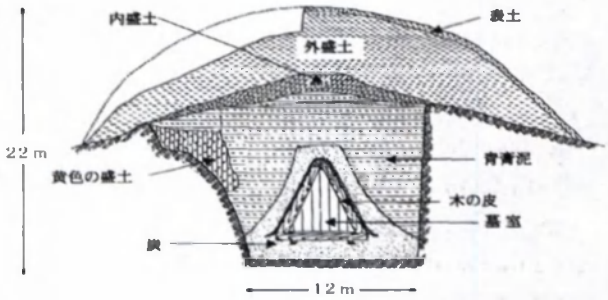


Fig.9 A vertical cross section of Yue King's burial mound in Shaoxing, Zheijiang Province, China

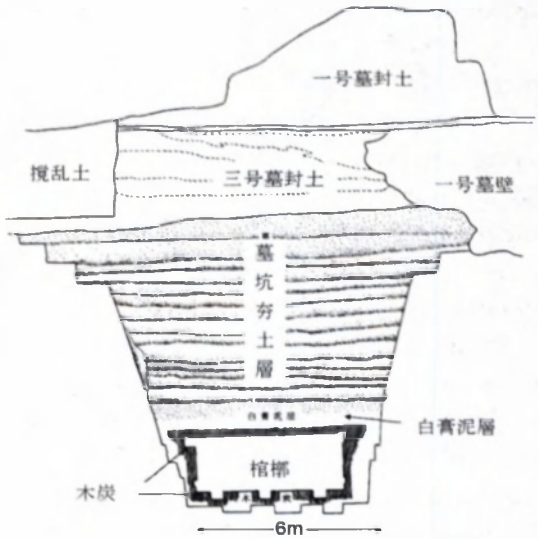


Fig.10 A vertical cross section Mawangdui Han style tombs with a wooden compartment in Changsha, Hunan province, China

Zenghouyi tomb in Chu (about B.C.450 year, Ruichow, Hubei Province) (Hubei Province Museum) which is a wooden compartment was installed in the deeply excavated large pit. Around the compartment, charcoal and white cohesive clay were compacted to prevent the seepage water.

The Mawangdui Han style tombs (Changsha, Hunan province) in the West Han period are similar to the Zenghouyi tomb. On the Mawangdui Han style tombs, the existence of burial mounds of about 10m height are confirmed. Fig.10 shows the vertical cross section of a Mawangdui Han style tomb with a wooden compartment (Hunan Province Museum, Hunan Province Archeological Institute 2004). It is a big question why wooden compartment burials were constructed in the middle Chang River basin under high temperature and humidity and much raifall,

An initial burial mound in the Yellow River basin is such as the Houguduisong tomb (about B.C.5hundred) in Gushi, Henan province in the late Spring and Autumn period (about B.C.5 hundred year) in Henan Province. The diameter is 55m and the height is 7m (Yang 1981). From the late Spring and Autumn period to Warring State period, very large sized burial mounds such as the first Qin Emperor's burial mound appeared. These burials matters and palaces are installed under the ground instead of in the mound. One of four reasons of burial mound construction is said to be the utilization of occurred soil by excavation for the construction of a large burial room under the ground (Yang 1981).

Burial mounds from the West Han to the East Han period (B.C.2 hundred ~A.D.2 hundred) in the Shandon Peninsula are very similar to Jiangnan' burial mounds in the view of location circumstances, shape and appearance. However, wooden compartments were laid under the ground in the Shandon Peninsula.

7 WOODEN COMPARTMENTS BURIALS UNDER GROUND IN THE KOREAN PENINSULA

The construction technique and burial methods of burial mounds in both the Yellow River basin and/or the Shandon Peninsula propagated to he

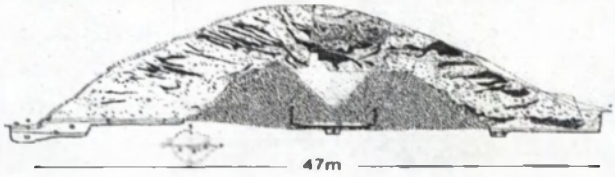


Fig.11 A vertical cross section of Heaven horse tomb with a wooden compartment, Gyeongiu, Korea.

Korean Peninsula after the setting of the Lesi country (B.C.108~A.D.313) in the West Han period. A lot of burial mounds near in Pyongyang which are called as Lesi burial mounds group have wooden or brick compartments under the ground.

In Silla of the Three Kingdoms of Korea period (late A.D.3 hundred~), many cairns with wooden compartment were constructed. These burials install a wooden compartment under the ground and fills stones on the ground, and finally covers around cairns (stone fills) with soils. Except of the Heaven horse tomb (Gyeongiu, early A.D.6 hundred) in Fig.11 (Korean Administration of Culture Publicity and Cultural Properties 1975), most of burial mounds in Gyeongiu have their wooden compartment under the ground. Like this, burial mounds which follow those in the Yellow River basin have a characteristic such as installing their compartment under the ground.

8 BURIAL MOUNDS OVER THE GROUND IN JAPAN

The oldest and large Yoshinogari burial mound in Japan was constructed at the highest location of the hill by Sochiku and Taichiku compaction method. After that, burial jars were laid on the dug hole and back filled very densely. It is an overground burial as shown in Fig.12. Hence this is similar to the Jiangnan's burial style which is different from the both Yellow River basin and Lesi burial mound styles. However, the large burial jars instead of coffin and compartment were utilized. This can be considered as an ancient Yayoi people's excellent idea in northern Kyushu to protect human remains and other burial matters from the corrosion due to the seepage water.

From the rectangular shaped burial mound in

Osaka Kami remains which followed Yoshinogari remains, 23 wooden coffins and from the burial mound in Fukuoka Yoshitake-Hiwatashi remains, 27 burial jars were found. These wooden coffins and burial jars were installed in the burial mounds, hence these burial mound style are similar to Jiangnan's and Yoshinogari's burial mound styles. However Tatetuki burial mound (A.D.1~2 hundred) , in Okayama prefecture, has a very rare wooden compartment at 1.5m depth under the ground.

In Japanese burial mounds (Kofun in Japanese) with a stone room in the Kofun period after above mounds in the Yayoi period, it is needless to say that the location of burial matters in the stone room is over the ground.

9 BURIAL MOUNDS IN KOREAN PENINSULA

It seems that Yeogsan River basin in the southwest of the Korean Peninsula (South Jeolla Province,) , jar burials with a mound were constructed in A.D.2 hundred (Saotome 2000; Pak 2001). The burial jars became larger in size in A.D. 4hundred and burial mattes became gorgeous (Saotome, 2000). Both in the basin of Geum River which flow through Buyeo, ancient Baekje's capital, and Yeungnam region , (Gyeonsang Province), Silla and Caya ancient country existed, human remains and burial matters were installed under the ground, and then a mound was filled. Namely, this is an underground burial style or the burial mound construction is antecedent style.

On the other hand, the basin and its northern basin, the human remains and burial matters were installed in the filled burial mound. This is an overground burial style or burial mound construction is postdated style. As shown above, Southwest region burial mound style in Korean Peninsula is similar to Yoshinogari remains and other remains in northern Kyushu. And similar style dolmens were constructed in both regions, it can be said that the south west region of the Korean Peninsula and northern Kyushu have a common burial system.

The horizontal chamber in the Korean Peninsula entered from China through the Lesi country in A.D.4 hundred. This may have propagated to

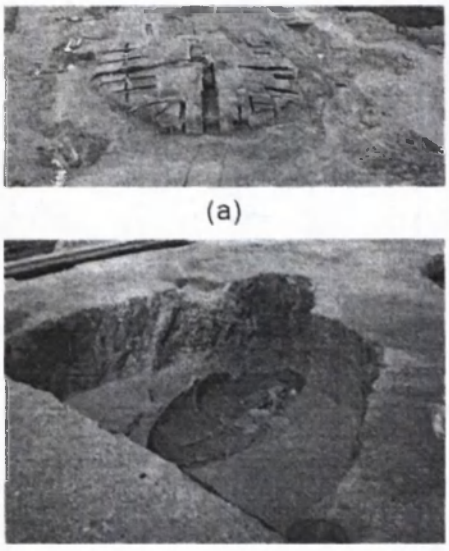


Fig.12 Yoshinogari burial mound (a):total view (b): burial Jar

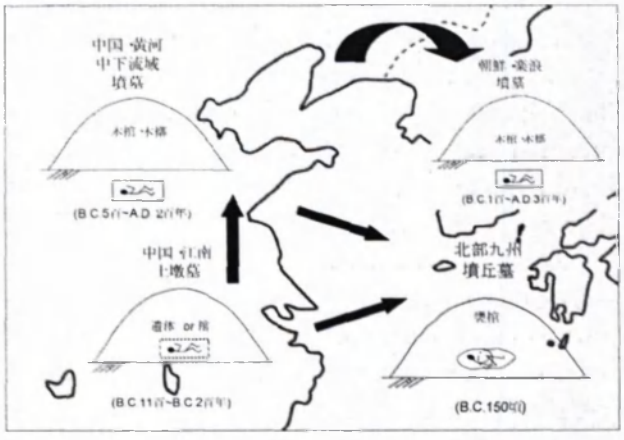


Fig.13 Burial style's differences and construction technique's propagations

Baekje and Silla in A.D.6~7 hundred. Especially in basin, many burial mounds which resembles to Keyhole-shaped burial mound in Japan concentrated (Saotome 2000 ; Pak 2001). The most of them have a horizontal chamber and the burial location is over the ground such as burial mound in Japan. There seems to be close relations between burial systems of Korea and Japan.

10 CONCLUSIONS

The burial mounds, which is filled with soils, were constructed in Jiangnan, China from the West Zhou period to the Warring State period. Burial matters were installed over the ground or in the

mounds, this burial system is a revolutionary change from the conventional burial method under the ground. Of course, this is an ancient people's idea considering the climate of high temperature, humidity and much rainfall.

On the otherhand, in the Yellow River basin in the climate of low temperature, humidity and less rainfall, coffins and compartments which were buried under the ground progressed. And these burial systems propagated to the Korean Peninsula following cairns and stone shelfs in the Northeast of China, which are overground burials. Hence, the wooden compartment with a burial mound in the Korean Peninsula, was installed under the ground. However, In the construction of both Yoshinogari burial mound in the middle Yayoi period and other late burial mounds in Japan, ancient people chose similar Jiangnan burial style which is the overground burial for climatic reasons. In Southwest of Korean Peninsula, dolmens which are similar to northern Kyusyu, and after the Yoshinogari burial mound, burial mounds with jars and keyhole-shaped burial mounds with a stone chamber were constructed. These are the same burial locations with burials in northern Kyushu.

Fig.13 summarizes the burial style and burial depth on soil burial mounds except dolmens and cairns, namely in Jiangnan (B.C.1hudred ~B.C.2hundred), middl –lower basin of the Yellow River (B.C.5~A.D.2hundred), the Lesi country (B.C.1hundred~A.D.3hundred) in the Korean Peninsula and Yoshinogari (B.C.150), northern Kyusyu in Japan. The arrows in the figure show the propagation of burial mound's construction technique.

The Yoshinogari burial mound's construction technique was considered to propagate from burial mound in Jiangnan, China or Shandon Peninsula through the sea, not through Korean Peninsula. However, concerning the burial depth, almost of burial mounds in Japan preceding the Yoshinogari remains chose Jiangnan's over-ground burial style. This can be said as an excellent idea of Ancient Japanese.

REFERENCES

Chin, Y.(1999). "Main archeological results of research during 20years on Shan and Zhou periods in Zhejiang." *The 20th anniversary proceedings of Zhejiang Province Archeological Institute*, Xiling publishers, pp. 116~122. (in Chinese)

Fuan, S. (2003). "Research on Han-tombs, Yuelu publishers."(in Chinese)

Hubei Province Museum "Zenghouyi tomb's valuables", Hubei art publishers (Wuhan) .(in Chinese)

Hunan Province Museum, Hunan Province Archeological Institute (2004). "Chansha Mawangdui 2, 3 Hang style tombs." Wenwu publishers.(in Chinese)

Korean Administration of Culture Publicity and Cultural Properties(1975). "Investigational report on Heaven horse tomb."(in Japanaese)

Liaonin Province Archeological Institute(1994). "Stone shelf," Liaonin Technological publishers.(in Chinese)

Lu, J. (2003). "Geotechnical characteristics and construction methods of Tudun tombs in China and Yoshinogari funkyu tomb in Japan," *Doctoral thesis, Saga University*. (in Japanaese)

Mori, K.(supervisor), Higashi?, U. and Tanaka, T. (1995). "History and remains of Gogureo", Chuokoronsha.(in Japanese)

Onitsuka K., Lu J., Tang X., and Kai D. (2002). "Geotechnical characteristics of Mound-tomb in Jiangnan area of China," *Tsuchi to Kiso*, Vol.50, No.9, 10-12. (in Japanaese)

Onitsuka K., Lu J., Tang X., Hara Y. and Kai D. (2003). "Geotechnical characteristics and construction methods of Yoshinogari fun-kyu tomb in Japan and Tu-dun tombs in China." *J. Geotech. Eng., JSCE*, No.736/III-63,1-17.

Onitsuka K. (2008). ."Construction technique of fills in ancient China", "Construction technique of fills in ancient Japan", *Symposium on the construction technique and preservative technique of historical soil structures*, 141-154. (in Japanese)

Onitsuka K. , Hara Y. , Lu J., Tang X. and Chen P. (2011). "Roots in China of construction methods of ancient Yoshinogari burial mound." *Proceedings of Special Session on Geo-Engineering for Conservation of Cultural Heritage and Historical Sites*, 14 Asian Regional Conference, ISSMGE, pp.13~18, Hong Kong, China..

Pak, H. (2001). "Burial mounds in the Yeongsan River basin, Archeology in the Eastern Asia and Japan," Burial system ①, .3-31, Doseisha. (in Japanese)

Saotome, M. (2000)."Archeology of the Korean Peninsula," Archeology in the world⑩, Doseisha. (in Japanaese)

Yang, K. (Nishijima, S. (supervisor), Ogata, I. and Ota, Y.(translator)) (1981). : Origin and Transition of Chinese Emperor's burial mounds, gakuseisha. (in Japanaese)

Conservation of the Naked Stone Chamber with Restored Soil Mound at Garandoya Tumulus

M. Mimura & S. Fukumoto
Graduate School of Engineering, Kyoto University, Kyoto, Japan

M. Yoshimura &. T. Terao
Soil and Rock Engineering Co. Ltd., Toyonaka, Japan

ABSTRACT: Garandoya Tumuli are located in Hita City, at the west of Oita Prefecture, Japan. It was constructed on the terrace of Mikuma River and famous for mural paintings on the chamber stones. The soil mound that originally covered the stone chamber has been destroyed and lost. Due to instability of the naked stone chambers as well as poor water protection for the inner mural paintings, it has been decided to restore the tumuli with soil mound that is thought to be round shape with a diameter of 25 to 30m. In the present paper, necessary factors for the restoration and conservation of Garandoya Tumulus in terms of stability, water proof system and heat conductivity of the restored earth mound are discussed on the basis of the model chamber tests.

1 INTRODUCTON

Garandoya Tumuli are located in Hita City, at the west of Oita Prefecture, Japan (see Fig. 1). They were constructed on the terrace of Mikuma River and famous for mural paintings on the chamber stones. Photo 1 shows the side view of Garandoya Tumulus. This is one of the three tumuli of Garandoya Tumuli. As is seen from the photo, the soil mound that originally covered the set of stone chamber has been destroyed. Due to instability of naked stone chamber as well as poor water protection for the inner mural paintings, it has been decided to restore the tumuli with soil mound that is thought to be round shape with a diameter of 25 to 30m. Because the environment will drastically be changed from in the open air to the buried structure, possible negative impact encountered after restoration has to be investigated.



Photo 1 Side view of Garandoya Tumulus

On the basis of the concept that cultural heritage should be open to the public, the stone chamber has been decided to be stored in the building with enough room for people to appreciate it. At the same time, the environment in the stone chamber has however to be kept appropriate. Hence we have to pay attention to the following factors, namely, drainage system against rainfall and seepage of underground water, temperature effect, and stability of the restored earth mound that will be constructed outside of the storing building. A series of laboratory chamber tests to evaluate the water proof system for the earth mound is conducted to assess the possibility to introduce "capillary barrier" for the earth mound. The chamber tests to investigate the heat conductivity of the earth mound is also conducted to derive the necessary and possible quality of the earth mound in order to conserve the environment inside the stone chamber as much as possible.

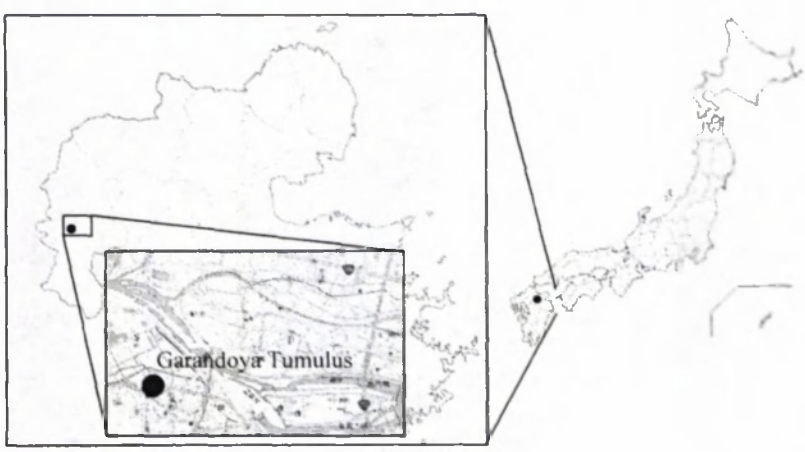


Fig. 1 Location of Garandoya Tumulus

The mechanical properties required for the stable structure of the earth mound is also discussed following the selection of the appropriate soil materials for the earth mound.

2 POSSIBLE PROBLEMS TO BE OVERCOME

2.1 *Intrusion of water*

Water intrusion into tumulus mound causes the deterioration of the structures. Fortunately, perfectly cohesionless materials like sand and pebble cannot be soil mounds because of their lack in cohesion. Generally, tumuli are made of well-graded materials with appropriate amount of fine contents that are well compacted. For such materials, water is not so easily intruded into tumulus mound because the permeability is low enough. However, cracks can be produced by dry shrinkage or natural disasters such as earthquakes and landslide etc. In the case, the inherent impermeability of mound materials are so easily broken that drainage systems are normally constructed in- or around mounds. The restored mound for Garandoya Tumulus should also be accompanied by the equivalent functions to protect the tumulus from water intrusion. Fig. 2 shows one example of water protection system for the restored mound. Highly permeable pebble layers are set overlain by the well-graded compacted earth materials with lower permeability. Water from falling rain is hence excluded because of the existence of highly permeable layer inside associated with the effect of "capillary barrier" at the border of two different soils.

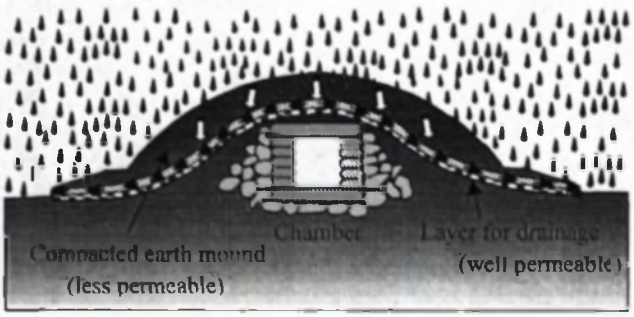


Fig. 2 Concepts of Protection against Water By Rainfall for the Restored Tumulus Mound

2.2 *Seepage of underground water*

Another concern related to water intrusion arises from seepage of underground water. The level of underground water changes related to rainfall. It is true tumuli were constructed on the dry foundation above underground water level but the unsaturated surface soils sometimes suck underground water up. Because this phenomenon occurs depending upon the soil types, we have to know the soil type and physical properties for the target layers situated below tumulus mounds. If the target layers are not relics but the original ground, samples should be taken for the necessary laboratory tests such as for particle size distribution of soils, density of soil particles, water retentivity of soils etc. Fig. 3 shows the schematic view of insert type RI-densimeter and moismeter test to detect the wet density and natural water content of the subsurface ground. Seasonal measurement can provide the significant information on the change in water retention of the target layers. If the effect of sucking up underground water cannot be discharged, the necessary countermeasure should be adopted to avoid increasing humidity inside the chamber.

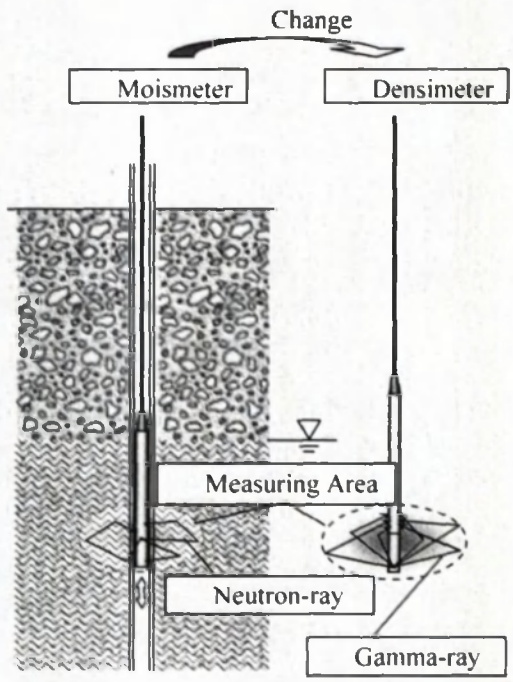


Fig. 3 Schematic View of Insert Type RI-densi and Moismeters

2.3 *Temperature effect*

The temperature variation of the inside of tumuli is of concern. High temperature assists the production and propagation of fungi and bacteria that cause the serious damage to the buried relics. The chamber is normally located about a few meters below the surface of the tumulus mound. The influence of the atmospheric temperature on the performance of the temperature inside the chamber depends upon the thermal properties of the mound soil. Temperature inside chambers should be constant with less variation because temperature fall causes dew condensation that is directly connected to the environmental degradation of chambers. The properties of heat conductivity of mound soils play significant roles to control the internal environ-

ment of stone chambers. In the case of Garandoya Tumulus, the earth mound is constructed covering the conservation building for the stone chamber. The property of heat conductivity for the selected soils has to be assessed.

3 IN-SITU MEASUREMENT OF THE LEVEL OF THE UNDERGROUND WATER

Intrusion of rainfall can be ruled out for Garandoya Tumulus because the indoor structure covered by compacted earth is planned. Then, the most serious problem is the intrusion of humidity from the underground because it gives harmful effect such as production of fungi and acceleration to weathering of stones. The capability of the underlain surface soil layer to suck underground water becomes a serious issue in this particular case. The authors hence carried out the inserting type RI-densimeter and moismeter tests in the existing borehole close to the tumulus (Mimura and Yoshimura, 2011). The measured results are shown in Fig. 4. The solid line denotes the result for rainy season whereas the hatched line denotes the one for dry season. The underground water level changed from G.L.-5m at the rainy season to G.L. -8.4m at the dry season. It is natural that the natural water content, w_n changed drastically. The values of 40 to 50% of w_n mean that the corresponding layer below the underground water is saturated. On the contrary, the natural water content for the overlying sand gravel layer (G.L. -1.6m to -3.6m) on which the stones of tumulus are set is almost unchanged irrespective of the underground water level. The authors have confirmed that the unsaturated surface sand gravel layer (G.L. -1.6m to -3.6m) do not suck underground water below. It is hence concluded that the water intrusion from the underlain sand gravel layer into the inside of the chamber can be discharged for Garandoya Tumulus even after restoration.

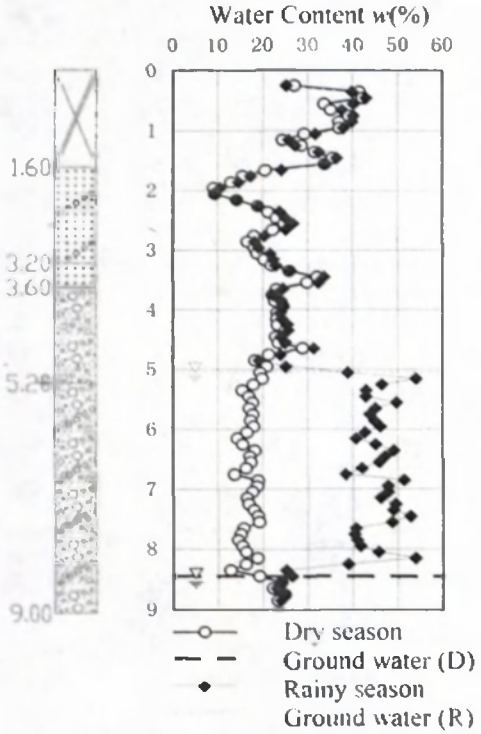


Fig. 4 Distribution of Water Content in the Original Ground of Garandoya Tumulus

4 EXPERIMENTAL ASSESSMENT FOR THE RESTORAION OF THE TUMULUS MOUND

Figure 5 illustrates the provisional shape of the restored Garandoya Tumulus. It is true the detailed design of the restoration will be conducted based on the experimental and numerical interpretation but the building was determined to be constructed to cover the present stone chamber with enough room for visitors to appreciate it by covering with the appropriate earth materials. In this chapter, the necessary and required quality of the restored earth mound is discussed based on the laboratory experimental results.

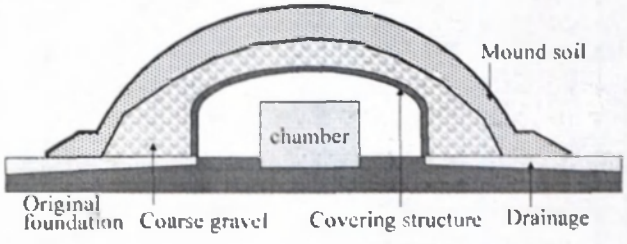


Fig. 5 Provisional structure of the restored Garandoya Tumulus

4.1 *Materials for the restored mound*

The experimental results of grain size analysis are shown in Fig. 6 for the selected soils for the mound as well as the coarse gravel (Mimura et al., 2012). The selected soil for the restored mound is well graded with the value of D_{50} is 2.0mm whereas the almost monotonic particle size of 20mm can be seen for the gravel. The natural moisture content, w_n is 11.3%. On the basis of the compaction test result, the optimum moisture content, w_{opt} and the maximum dry density, ρ_{dmax} are 13.5% and 1.90g/cm^3 respectively.

A series of compaction tests on the selected soil for the restored mound is conducted under the various compaction energies to determine the prescribed value for the dry density, ρ_d when the restored mound is constructed. The selected material is found to be well compacted with the increase in compaction energy. Considering the construction

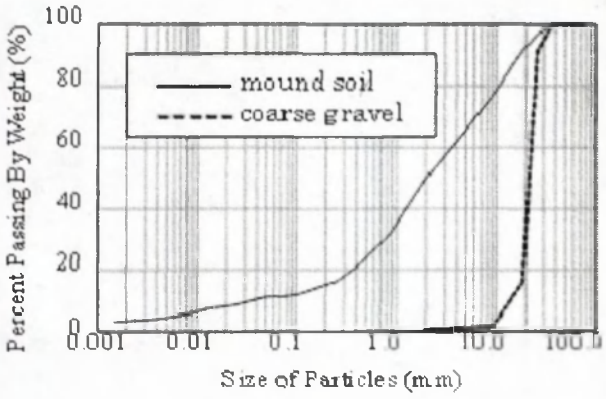


Fig. 6 Grain Size Accumulation Curves of the Selected Soil for the Mound and Gravel (Mimura et al., 2012)

procedure of the restored mound, the applicable energy is about 0.4 E_{cJIS}. The design value of the restored earth mound in terms of the dry density ρ_d is hence set to be 1.75 g/cm^3 based on the experimental results shown in Fig. 7.

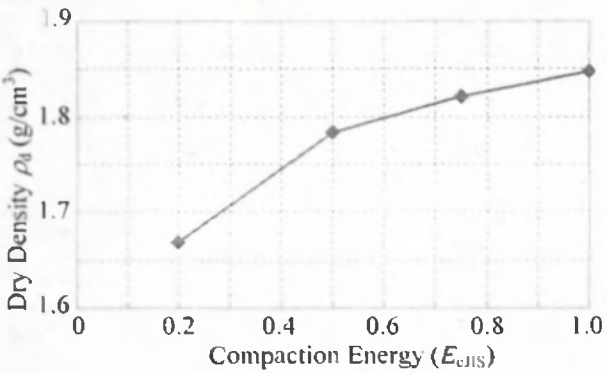


Fig. 7 Compaction Energy Dependency of the Dry Density, ρ_d of the Selected Soil for the Mound

A series of direct shear tests is conducted on the selected soil for the restored mound. As the initial condition, the dry density ρ_d of the specimen is set to be 1.75 g/cm^3 that has been derived as the prescribed value of the restored mound. The mechanical properties that are required for the soils of the restored mound are the ones under the relatively low stress level because the thickness of the restored mound is at most 1.5 to 2.0m. Considering the construction condition for effective compaction, the soil is planned to be compacted under the condition of natural water content (w_n = 11.3%) that is slightly smaller than the optimum water content. The vertical stress for the direct shear tests are determined as 30, 60 and 90 kN/m^2 in this particular case. The experimental results are shown in Fig. 8. The experimental results provide that the cohesion, c equal to be 54 kN/m^2 and the shear resistance angle ϕ equal to be 38 degree un-

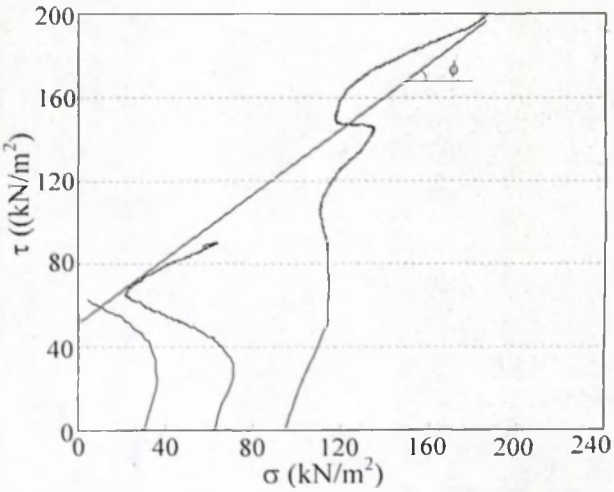


Fig. 8 Mechanical Properties of the Selected Soil for the Mound Based on the Direct Shear Tests

der the condition of the dry density of 1.75 kN/m^3 that has been determined for the prescribed value for the restored mound.

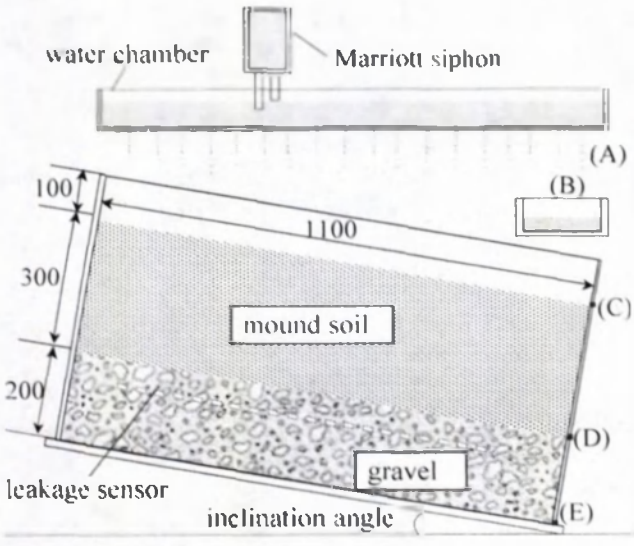
By applying these soil parameters to the conventional stability analysis, the factor of safety in terms of the critical angle of the restored mound is derived as 48 degrees for the prescribed thickness of the mound. This value guarantees the construction of the restored earth mound safely.

4.2 *Evaluation of water proof structure*

As is shown in Fig. 5, the restored Garandoya Tumulus has a house in which the present stone chamber is stored with a room for visitors. Water from rainfall can actually be cut off at the roof of the house. Drainage function in terms of well permeable coarse gravels is however constructed around the house to avoid leakage of water due to occurrence of cracks both in the mound and house itself. Finally on the surface, the restored mound is constructed by the well graded compacted earth materials. This provisional structure of the restored tumulus can provide the original shape of Garandoya Tumulus as a rounded earth mound associated with the inner room for the public to appreciate the stone chamber.

The layered mound structure with the compacted earth underlain by the coarse gravel includes the possibility of the occurrence of "capillary barrier" at the border of the layers. When infiltrative front invades the mound during the normal rainfall, suction force is mobilized depending upon the void among soil particles. In the present layered structure of the mound, the larger suction is mobilized in the outer mound soil than the inner gravel, which results in the possible generation of "capillary barrier" effect. The authors carried out a series of chamber model tests on the

generation of "capillary barrier" at the border of the layered soils Mimura et al., 2012). Figure 9 shows the schematic view of the chamber testing apparatus to evaluate the mechanism of the seepage and capillary barrier in the layered mound with the selected mound soil underlain by the gravel. The precipitation is controlled by the combination of the Marriott siphon and the number of needles for falling water to the surface of the foundation model. Drainage systems are equipped at the surface of the mound, at the border between the mound soil and the gravel and at the bottom of the gravel layer. If the capillary barrier is developed and functions well, no water can be found from the bottom of the gravel layer. The break of the capillary barrier is also monitored with the electric leakage sensors that can catch short-circuit due to submergence. The critical length L_c is defined as the length between the top of the slope to the breaking point of the capillary barrier (Steenhuis and Parlange, 1991).



(A): needle for water drop
(B): precipitation measurement apparatus
(C): drainage for the surface flow
(D): drainage for the boundary flow
(E): drainage for bottom flow
*The length is described in mm.

Fig. 9 Experimental Apparatus for the Development of Capillary Barrier

The experimental results are shown in Fig. 10. The experiments are conducted with the inclination angle, α of 4, 6.5 and 10 degree. The density of the mound soil is set to be the equivalent to the prescribed in-situ dry density of 1.75 kN/m^3. The intensity of precipitation is 3.6mm/h. As shown in Fig. 10, the critical length, L_c prolongs with the inclination angle of the mound. Although the thickness of the mound soil plays a significant role to control the critical length, it is provisionally concluded that the layered structure with the compacted earth mound underlain by the gravel has a possible capability to obstruct the intruded water into the buried stone chamber.

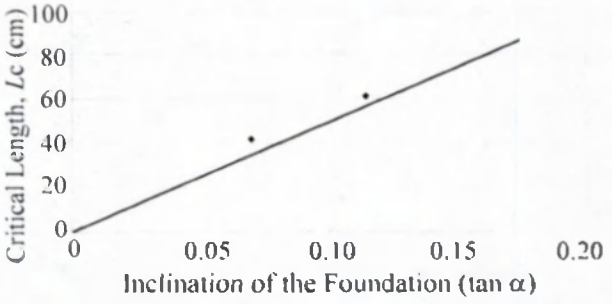


Fig. 10 Development of Critical Length with the Inclination of the Foundation

4.3 *Evaluation of heat conductivity*

Temperature in stone chambers is one of the most serious problems for the conservation of geo-relics because the high temperature causes the generation of fungi in the stone chamber (Kigawa et al., 2006). It is also noteworthy that the dew condensation due to the change in temperature causes the deterioration of stones as well as the generation of fungi. It is hence determined that the house is covered by the compacted earth materials not only for the purpose of water proof but also heat proof. A series of chamber tests on heat conductivity of the restored soils was conducted.

Figure 11 show the schematic view of the testing apparatus. Foundation model is constructed in the acrylic cylindrical chamber covered by the thermal insulation. The size of the chamber is 20

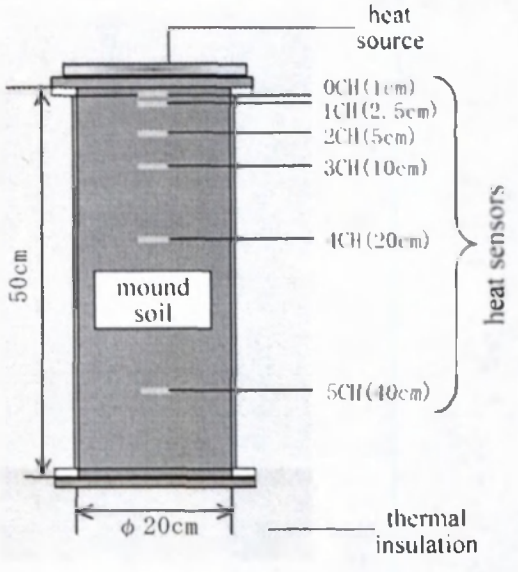


Fig. 11 Schematic View of the Experimental Apparatus for Heat Conductivity of Soils

cm in diameter and 50 cm in height. The soil for restoration of the mound is compacted every 5 cm under the condition of the natural water content, w_n=11.3%. The heat source is stored in the top plate and the heat sensors are set at the depths of 1, 2.5, 5, 10, 20 and 40 cm from the surface. The heat of 40 degrees are applied to the surface of the soils and kept for 8 hours followed by the removal of the plate with the heat source for 16 hours (15 degrees in the laboratory). This process is repeated 4 times and the change in temperature at the individual depths with time and the delay of the phases of them.

Figure 12 shows the time – temperature relations for the individual heat sensors in the mound soil. At the places close to the heat source such as CH0 (1 cm) and CH1 (2.5 cm), the increase in temperature can be observed immediately after the heat supply, followed by the increase at CH2 after 20minutes, at CH3 after 1.5 hours, at CH4 after 3 hours and at CH5 after 7 hours. When the heat supply is turned off, sudden drop can be observed for CH0 and 1 after the peak values of 36.7℃ and 34.6 ℃ respectively. Occurrence of the peak values of the temperature is observed after 30 min. for CH2 with 31.8 ℃, 1 hour for CH3 with 27.7 ℃, 3 hours for CH4 with 22.0 ℃ and 11 hours for CH5 with 17.9 ℃. The same process is found to repeat cyclically associated with the delay of the phases. The delay of heat conduction and the difference in the absolute values with depth are caused by the thermal properties of soils. Based on the experimental results, the coefficient of heat conduction, k can be derived as 8.04×10^{-3} (J/cm·s·℃). The heat supplied at the surface is found to be conducted to the depth of 140 cm for 10 hours if the heat supply continues. In the sense, covering by soils is effective to prevent the inner space from the increase in temperature. Quantitative assessment is required to maintain the appropriate environment in soils for conservation of geo-relics

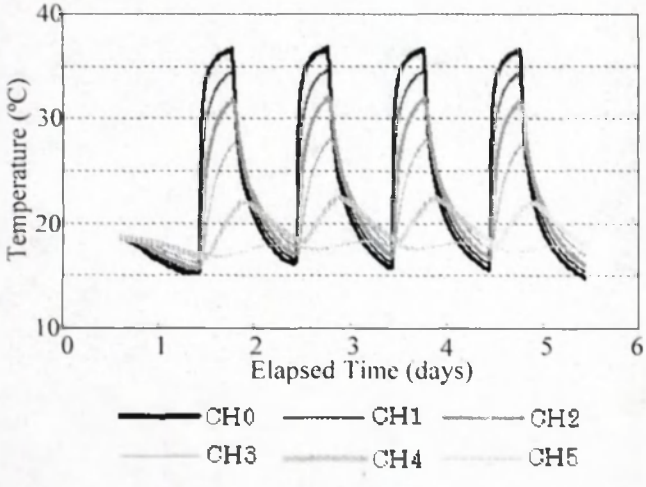


Fig. 12 Change in Temperature in the Mound Soil Due to Repeating Heat Supply

5 CONCLUSION

Geotechnical approach has been conducted to assess the restoration and conservation of Garandoya Tumulus where the naked stone chamber remains at present. The house structure is introduced to protect the naked stone chamber as well as to make a room for visitors to appreciate it. Compacted earth mound will be constructed around the house because it has been determined to retrofit the original tumulus mound. Water intrusion into the chamber through the earth mound from the underground water as well as rainfall has to be stopped to conserve the environment of the stone chamber. Double layered structure with the compacted earth underlain by the gravel has been introduced to flow the intruded water out. Here the capillary barrier effect is also expected. A few meters of the earth mound was found to provide the milder condition of the inner temperature of the stone chamber. In the short term, 1.4m of the thickness of the mound can produce the appropriate environment in the earth mound without remarkable change in temperature whereas the temperature at the surface of the ground increases. For the detailed program to restore Garandoya Tumulus, the additional geotechnical research is necessary.

REFERENCES

Kigawa, R., Sano, C., Ishizaki, T. and Miura, S. (2003). "Concept and Measures of the Conservation of Takamatsuzuka Tumulus for Thirty Years and the Present Situation of Biodeterioration." *Science for Conservation*, 45, 33-58 (in Japanese).

Mimura, M. and Yoshimura, M. (2011). "Geotechnical Contribution for Conservation of Compacted Tumulus Mounds", *Proc. 14th Asian Regional Conf. SMGE*, Paper No. ATC19_3.

Mimura, M., Fukumoto, S., Yoshimura, M. and Terao, T. (2012). "Experimental Study on Water Resistant Structure of Tumulus Mound Considering the Function of Capillary Barrier", Proc. 47th Annual Conf., JGS, pp.73-74 (in Japanese).

Steenhuis, T.S. and Parlange, J. Y. (1991). "Comment Diversion Capacity of Capillary BarriersBy Benjamin Ross". *Water Resource Research*, 27(8), 2155-2156.

Salt damage mechanism in northeastern Thailand and repair methods

A.Iizuka & K.Kawai
Research Center for Urban Safety and Security, Kobe University, Kobe, Japan

S.Nomura
Department of Civil Engineering, Graduate School of Engineering, Kobe University, Kobe, Japan

ABSTRACT: Approximately 20% of the land in northeastern Thailand has already been covered by saline soils, making 10% of the area completely unsuitable for any crops. This is considered to be one cause of poverty in this northeast region of Thailand. Furthermore, deforestation due to recent developments here has caused a rise in the saline ground water table. It now reaches up to the root zone of the vegetation, causing the plants to wither. Also, reduction of vegetation further influences evaporation from the ground surface, which has created a vicious cycle that has actually doubled the salt damage problem. In this paper, after simulating the salt damage mechanism by using the FE numerical simulator, some methods to prevent the salt damage are discussed. A method known as mulching, the spreading of relatively large-particle sized materials over the ground surface, is examined using the FE numerical simulator and an improved method of mulching to support less damaging ways of farming is also discussed.

1 INTRODUCTON

Northeastern Thailand is characterized by a dry plat-eau landscape. The amount of annual rainfall varies from 1100mm to 1500mm and the region is not exposed to extreme dryness. The ground surface is covered with relatively stiff, sandy soil. Rainfall is likely to penetrate deep and water retention is meager. Approximately 20% of the land in northeastern Thailand has already been covered by saline soils, making 10% of the area completely unsuitable for any crops. This is considered to be one cause of poverty in this northeast region of Thailand. Furthermore, deforestation due to recent developments here has caused a rise in the saline ground water table. It now reaches up to the root zone of the vegetation, causing the plants to wither. Also, reduction of vegetation further influences evaporation from the ground surface, which has created a vicious cycle that has actually doubled the salt damage problem. In this paper, presented is our investigation report on the salt damage in the northeastern Thailand. And, a trial to explain the salt damage mechanism in northeastern Thailand using FE computation technique based on unsaturated soil mechanics is presented. A mathematical modeling taking account of diffusion and advection in the deformable porous soil media in the framework of unsaturated soil mechanics is described and a FE numerical simulator in which the mathematical modeling is incorporated is developed. After simulating the salt damage mechanism by using the FE numerical simulator, some methods to prevent the salt damage are discussed. This paper is a digest of the keynote lecture entitled 'The role of unsaturated geomechanics in desertification due to salt damage' by Iizuka,A., Kawai,K., Nomura,S., Tachibana,S., Ohno,S. and Pipatopongsa,T., 5th Asia-Pacific Conference on Unsaturated Soils, 2012.

2 SALT DAMAGED IN NORTHEASTERN THAILAND

The largest rock salt layer in Southeast Asia was discovered between 1960 and 1970 at a depth of 150m to 300m under the large inland area that is home to the Sakonnakhon and Korat basins (Figure 1). A long time ago, before the continental drift, this salt layer was situated at the bottom of the tropical sea, but, rose with holding sea water in the bowl-shaped base. This water then evaporated and salt crystals settled to the bottom, resulting in a layer of sedimentary salt rock. After that, with subsequent rises in the sea level, sea water that was flowing into the basin formed an upper layer of salt rock. Due to salinity in the ground water, the ecological environment is more severe here than in other areas of Thailand, resulting in low agricultural productivity. During the dry season, local farmers have taken up the manufacturing of salt to

supplement their incomes. Moreover, due to an increasing demand for salt by the chemical industry, this salt rock, which consists of high purity sodium chloride, has the potential to be a promising industrial raw materials and mineral resources. For this reason, salt manufacturing continues to be encouraged, and an increase number of wells are being dug for it.

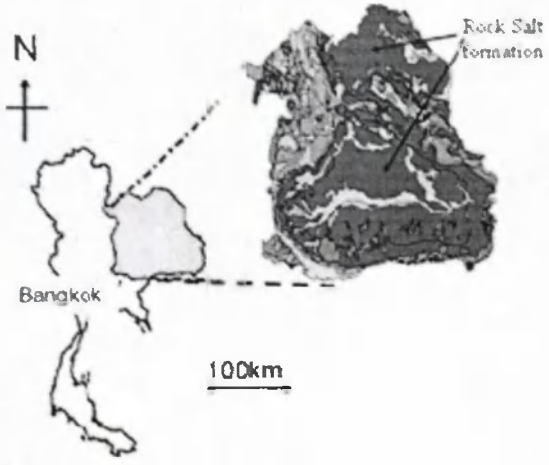


Fig.1 Geological map of northeastern part of Thailand (Sukchan,S.,2005)

Due to disorder of water cycle caused by deforestation, a rise in the saline ground water table occurs and the salt crystal appears on the ground surface as shown in Photo 1. According to Dr. Somsak Sukchan, International Training Center at Khon Kaen of Agricultural Department, this area is seriously suffered from the salt disaster, the salt disaster in this area were caused due to deforestation, which leads to unbalanced water circulation between the ground and the atmosphere. Once the water retention capability on the ground surface is lost by deforestation, the salt which is originally weak-contained in the ground water is pulled up and condensed on the bare ground surface by solar energy.

As for salt manufacturing, in the traditional method of salt production, salinity ground water is pumped up from a well, air-dried in a salt pan or boiled in a caldron (Photos 2 and 3). Regardless of the method employed, waste water with a high-concentration of salinity gets discharged into the irrigation facilities. This again causes salt damage to occur (Photo 4). Local farmers are effectively "strangling themselves" by being engaged in salt manufacturing during the dry season to compensate for their poor rice productivity, because the salt damage consequently becomes even worse. Moreover, pumping out so much ground water causes ground subsidence like the cave-in shown in Photo 5. Modern industrial facilities have more recently been constructed, whereby high quality



Photo 1. Salt on the rice field (Photo by Sukchan,S., 2005)

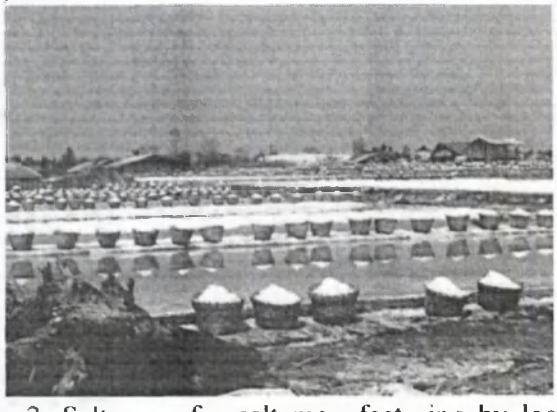


Photo 2. Salt pans for salt manufacturing by local farmers (Photo by Sukchan,S., 2005)

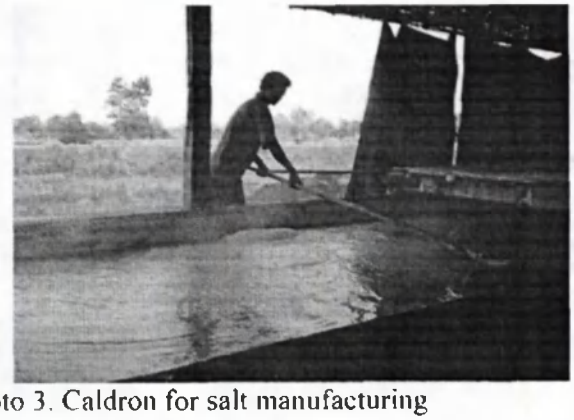


Photo 3. Caldron for salt manufacturing



Photo 4. Salt-damaged irrigation facility (Photo by Sukchan,S., 2005)

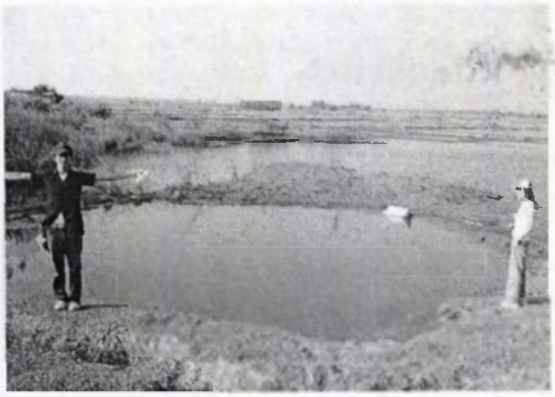


Photo 5. Ground subsidence due to excessive pumping of ground water

salt is extracted directly from the salt rock layer and waste materials are returned to the original position under the ground. While this does not cause further salt damage as mentioned above, it does not much improve the current livelihood situation of local farmers.

3 MATHEMATICAL MODELING TO SIMULATE THE SALT DAMAGE

When the salt damage encountered in north-eastern Thailand is simulated, the following conditions have to be taken into consideration.

1) Mechanical and seepage characteristics of saturated and unsaturated soils.
2) Stress/deformation and pore water flow coupling.
3) Water balance through precipitation, transpiration and evaporation.
4) Effect of vegetation on water circulation, namely transpiration from vegetation.
5) Advection and dispersion of dissolved materials.

Therefore, the mathematical formulation shown in Fig.2 is required. A three phase mixture, as symbolically shown in Fig.3, is employed and the following points are assumed in the formulation of mathematical modelling:

1) The soil is modelled as a three phase mixture consisting of solid, pore air and pore water.
2) The solid is an elasto-plastic material.
3) Water retention characteristics are described based on the water retention curve showing the relationship between suction and the degree of saturation. The hysteresis response in drying and wetting processes is taken into account.
4) Pore water is incompressible and its behaviour in the soils follows Darcy's Law, governed by water permeability and the gradient of total water head.

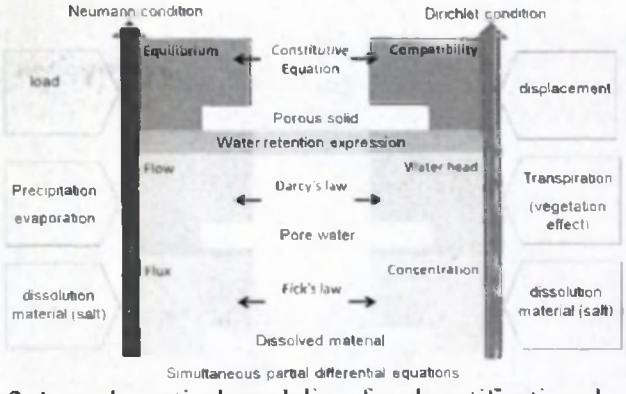


Fig.2 A mathematical modeling for desertification due to salt damage

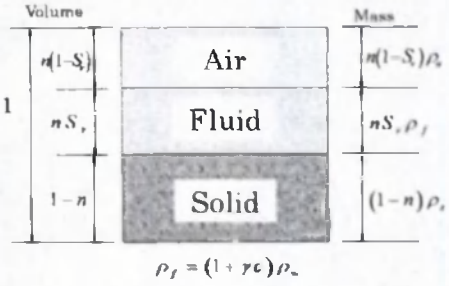


Fig.3 Soil model

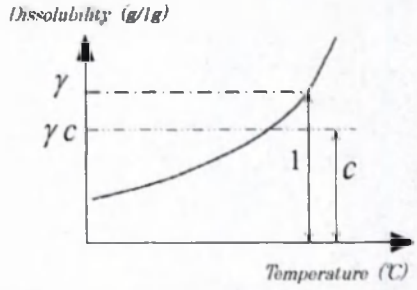


Fig.4 Definition of concentration

5) Pore air is compressible and its behaviour in the soils follows Darcy's Law, governed by air permeability and the gradient of air pressure.
6) Dissolved material does not cause a change in the volume of the liquid solution. Its behaviour follows Fick's Law for dispersion and Darcy's Law for flow of pore water for advection.
7) Concentration of dissolved material is de-fined by the unit mass ratio per its dissolubility limit under a specified temperature as shown in Fig.4.
8) Phase change due to temperature is out of scope.

The details of mathematical modeling are described in the original papers by Iizuka et al.(2012).

The mathematical expressions of the above 1) to 8) constitute the initial and boundary problem, in which continuity conditions govern the coupling phenomena. By simultaneously solving the gov-

erning equations under a set of initial and boundary conditions, various geoenvironmental problems such as desertification due to salt damage, etc., can be numerically treated using the finite element discretization technique.

The elasto-plastic constitutive model proposed by Ohno et. al. (2007) is employed for porous solid in the mathematical modeling. This model is called the *'Se-hardening model'* and is characterized by the strain hardening/softening rule in the unsaturated state, which is formulated by a function of the effective degree of saturation, *Se*. This model can seamlessly and continuously describe the mechanical behavior of soils from the unsaturated state to the fully saturated state. In the fully saturated state, this model is automatically reduced to the Cam-clay model for saturated soils. In this sense, it can be said that this model is an extension of the Cam-clay model for the unsaturated state.

In the mathematical modeling developed by the authors, water retention characteristics of unsaturated soils are modeled using logistic curves in the space of degree of saturation and suction, see Kawai et al. (2007). This model can express dependency of suction history.

The permeability of pore water in the unsaturated state is modeled as a function of the effective degree of saturation, *Se* after Mualem (1976):

$$k_r = S_e^{1/2}\left\{1-\left(1-S_e^{1/m}\right)^{m}\right\}^{m},\ k_r = k_u/k_s$$

in which k_s, k_u : the permeability coefficients in the saturated and unsaturated states, respectively, m : material parameter.

It is noted that the effective stress definition employed in this paper is:

$$\boldsymbol{\sigma}' = \boldsymbol{\sigma}^{net} + p_s \mathbf{1}$$

in which $\boldsymbol{\sigma}^{net} = \boldsymbol{\sigma} - p_a \mathbf{1}$, $p_s = S_e s$, $s = p_a - p_w$, $\boldsymbol{\sigma}'$:effective stress, s : suction, p_s : suction stress.

4 NUMERICAL SIMULATIONS OF SALT DAMAGE AND COUNTERMEASURES

A simple supposition is considered: that the ground water contains weak salinity and the water table is located 4m below the ground surface. Vegetation is not considered. The simulation ground is directly exposed to repeated drying and wetting from evaporation and precipitation. The FE model is shown in Fig.5. Salinity concentration of the ground water is assumed to be 0.03 in mass ratio as defined in Fig.4. Fig.6 indicates the climate condition used in the computation. Since the actual evaporation from the ground depends on the current moisture condition of the ground, the actual amount of evaporation imposed on the ground surface as a boundary condition is computed by multiplying the estimated evaporation with the effective degree of saturation in the ground surface. Ground material is assumed to be fine silt, mimicking the local soil found in this Thai region. Water retention characteristics of the soil used in the computation are shown in Fig.7. The initial suction in the ground is assumed to be proportionately distribute, equivalent to the height from the ground water table. Its corresponding initial degree of saturation in the ground is assumed to be the middle value of primary drying and primary wetting curves indicated in Fig.8. Simulated results obtained by Kawai et. al. (2009) are as follows:

Fig.8 represents the development of salt concentration in the ground. Salinity moves upward with the passage of time. Fig.9 shows the change in salt concentration over time in the unsaturated ground: Y indicates the vertical coordinate and $Y = 0$ is at the ground water level and $Y = 4m$ is at the ground surface. The repetition of rainy and dry seasons was found to have a remarkable influence on the salinity content in the ground closer to the surface ($Y = 4m$). After two years, the salinity completely reaches the initial value of salinity concentration, which the ground water contains in the ground. Following this, the salinity accumulates near the ground surface, its content reaches $c = 1.0$ (the pore water is saturated with salinity) within three years. Salinity then begins to appear as crystals on the ground surface, as shown in Fig.10. Fig.11 shows the total water head distribution in the ground. The direction of pore water flow in the ground varies to the repetition of rainy and dry seasons. Water balance in the ground is shown in Fig.12. Dehydration from the ground due to evaporation is found to surpass the water supply to the ground through rainfall. This leads to the accumulation of salt crystals on the ground surface because the salinity migration in the ground depends on the direction of the pore water flow.

In order to prevent the upward migration and accumulation of salinity, possible measures are considered. The amount of evaporation from the ground surface varies depending on the dry degree of soils. With this in mind, a method known as mulching, the spreading of relatively large-particle sized materials over the ground surface, has been widely employed in the field of agriculture. Since the materials used for mulching have low water retention capabilities, evaporation is suppressed and drying out of the ground is prevented. Such effects have been examined. Moreover,

overlaying soils on the mulching materials, an improved method of mulching, to sup-port less damaging ways of farming is also examined. Mulching and improved methods of mulching are shown in Fig.13. Silica sand is assumed for mulching materials, since it has a higher permeability and lower water retention than fine silt. Water retention characteristics employed for mulching materials are shown in Fig.14, with a comparison to that of fine silt.

According to simulation results, when the thickness of the mulching layer was assumed to be just 10cm, no increase in the concentration of salinity toward the ground surface was detected, Fig.15(a). Likewise, for the improved mulching meth-od, when the thickness of the mulching layer was changed and the simulation was carried out, a mulching of a 20cm thickness was found to be sufficient in preventing the progress of salt damage. Fig.15(b). A surface soil with a 50cm thickness for farming was also considered based on the fact that rice is widely planted in this region and the roots of the rice plant are known to grow approximately 50 cm deep. Thus the deterrent effects of both mulching and improved mulching as a measure to prevent the progress of salt damage can be confirmed. Fig.16 shows the change in ground salinity concentration over time. The salinity concentration changes only in elements that are just above the water table and no accumulation of salinity occurs in the upper layer. The change of salinity concentration at $Y = 0.05m$ is due to dispersion and will not lead to salt damage. Fig.17 shows a change in the degree of saturation in the surface soil element over time when mulching is and is not present. The degree of saturation for the mulching material remains at quite a low value and compared to fine silt holds a higher value for the degree of saturation. This depends on the difference in water retention capabilities. Since the actual amount of evaporation strongly depends on the amount of moisture in the soil, evaporation from the surface is reduced when the surface is mulch covered with a material that has low water retention. Therefore, the inflow by rainfall surpasses the outflow due to evaporation, as seen in Fig.18.

Fig.19 shows the distribution for total water head in the case of improved mulching. The flow of pore water is found to stop at the boundary of the mulching layer. In the surface soils above the mulching layer, the total water head significantly varies in relation to the repetition of drying and wet-ting. Contrary to this, however, in the ground situated under the mulching layer, the total water head remains almost constant and salinity migration in the ground is not yielded. Fig.20 indicates the change in the degree of saturation for

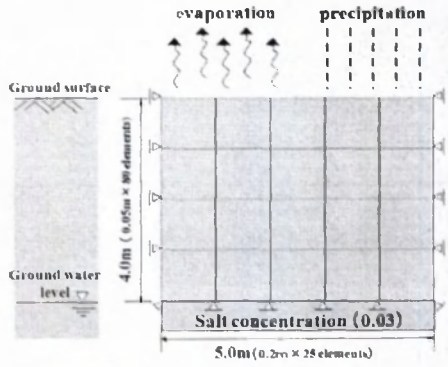


Fig.5 Supposed unsaturated ground

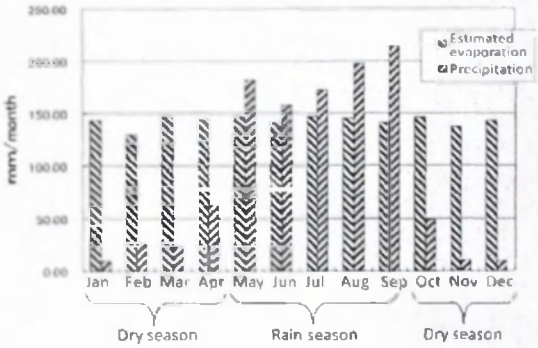


Fig.6 Climate conditions for simulation

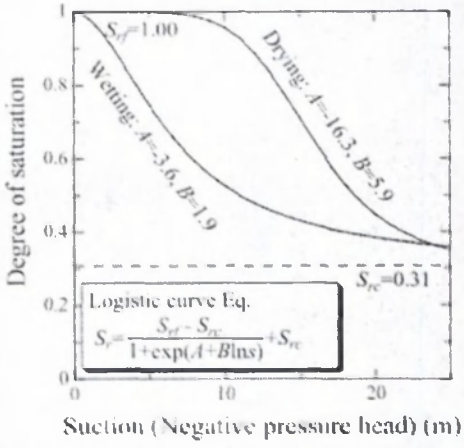


Fig.7 Water retention curves for simulation

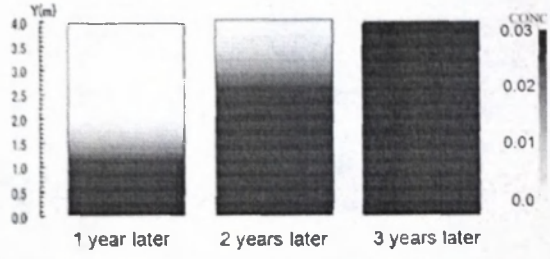


Fig.8 Development of salt concentration in the ground

the improved mulching layer. The degree of saturation remains at a relatively lower value. Fig.21 shows the relationship between the permeability of

mulching materials and the degree of saturation. Since the degree of saturation in the mulching layer remains low, the results of its corresponding permeability are also quite low. Therefore, the mulching layer appears to work almost as an impermeable layer that prevents the migration and accumulation of salinity.

Furthermore, the simulation also makes it possible to examine the purification of salinity contamination. An example of this is the 'flushing' effect, which is examined here. The FE model is the same as the example shown in Fig.5. It is assumed that the ground is entirely contaminated by salinity: $c = 0.03$. The climate conditions shown in Fig.6 are also taken into account in the simulation. However, the available amount of water for flushing is assumed to be restricted to an annual amount of $900l/m^2$. Three cases were then considered, all available water is flushed at once for a period of 31 days (Case A): available water is equally flushed every day for a period of one year (Case B): and available water is flushed only in the dry season from January to April and October to December (Case C). The computed results are shown in Figure 38. The case of flushing restricted only in the dry season (Case C) is found to show the highest effect for purification of salinity contamination. If a certain amount of water can be utilized for flushing, it is preferable that flushing is done in the dry season when the amount of rainfall is less than that of the possible evaporation.

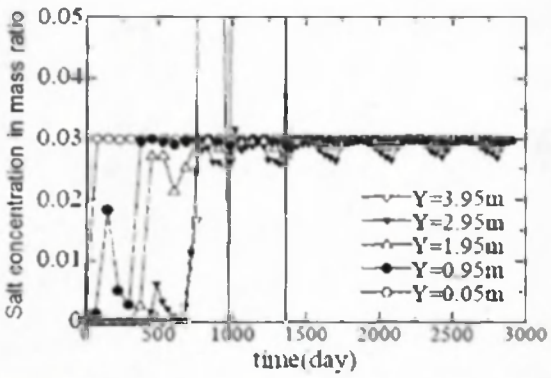


Fig.9 Change of salt concentration over time

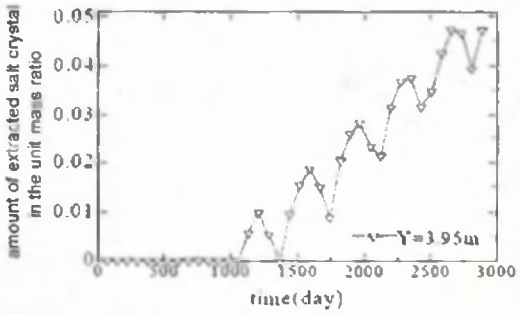


Fig.10 Accumulation of salt crystals near the ground surface

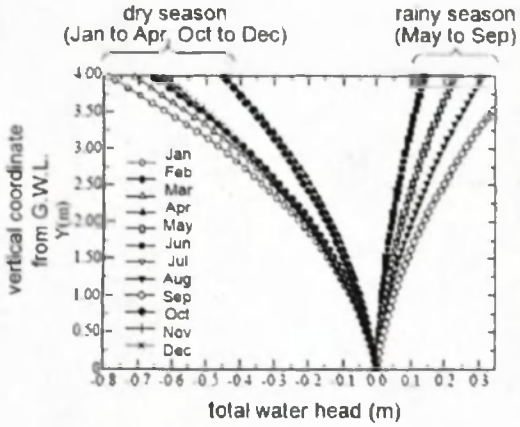


Fig.11 Change of total water head distribution

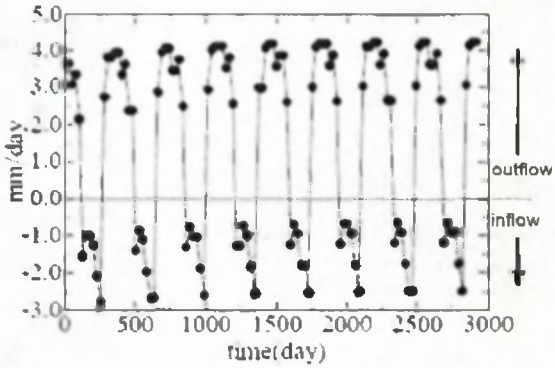


Fig.12 Water balance in the ground

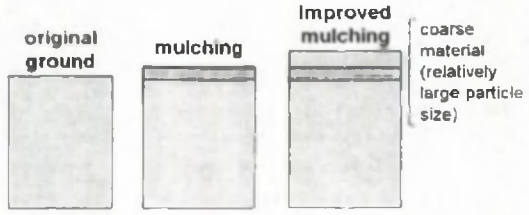


Fig.13 Methods for ground improvement

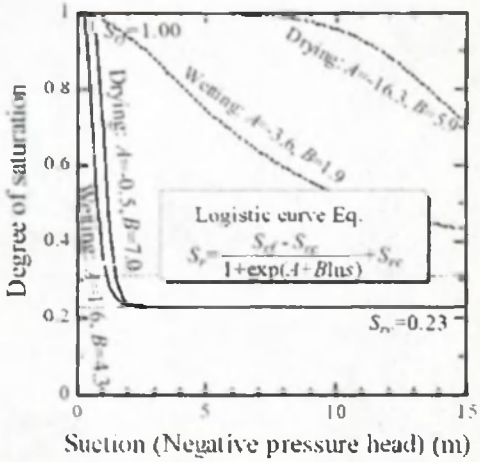
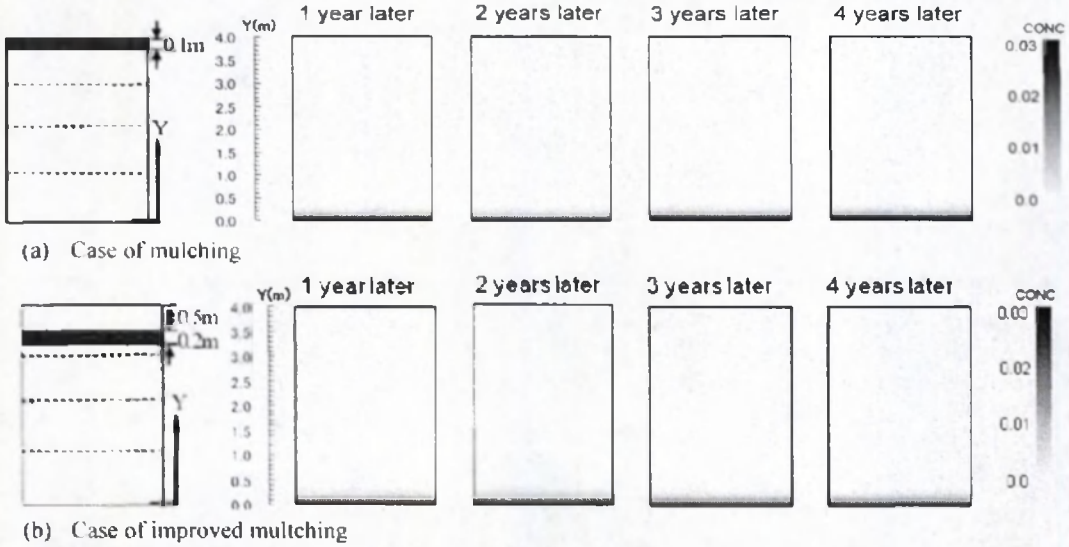


Fig.14 Water retention characteristics of silica sand

5 CONCLUDING REMARKS

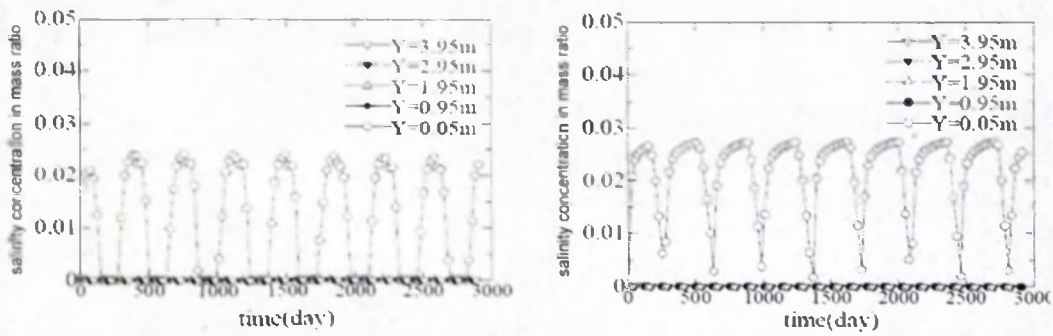
This paper is a digest of the keynote lecture at the 5th Asia-Pacific Conference on Unsaturated Soils (Iizuka, et al,. 2012) and describes the salt damage and possible countermeasures against it through a series of numerical simulations based on unsaturated geo-mechanics. Finally, the authors express their sincere acknowledgement to Dr. Somsak Sukchan, Soil Survey and Classification Division, Department of Land Development, Ministry of Agriculture and Cooperatives, Mr.Pramual Jenkunawat, Bureau of Mines and Conession, Department of Primary Industries and Mines, Ministry of Industry, Assoc. Prof. Supakit Nontananandh, Prof. Suttisak Soralump, Dr. Barames Vardhanabhuti, Dr. Apiniti Jotisankasa, Kasetsart University, and Dr. Pongsakorn Punrattanasin, Khon Kaen University, for their help and cooperation.



(a) Case of mulching

(b) Case of improved multching

Fig.15 Deterrent effect of mulching and improved mulching on development of salinity concentration



(a) Case of mulching

(b) Case of improved mulching

Fig.16 Salinity concentration change over time

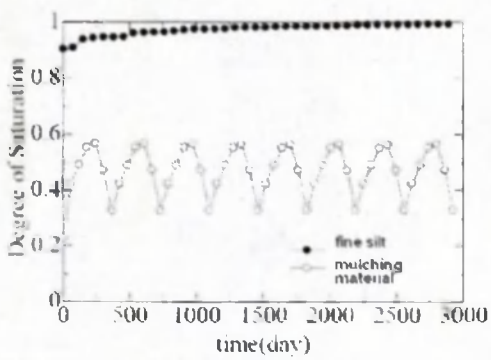


Fig.17 Change in degree of saturation at the surface element

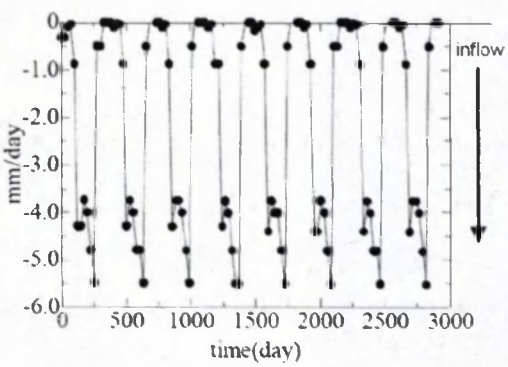


Fig.18 Water balance in the case of mulching

REFERENCES

Iizuka,A., Kawai,K., Nomura,S., Tachibana,S., Ohno,S. and Pipatopongsa,T.(2012) "The role of unsaturated geomechanics in desertification due to salt damage", *Proc. 5th Asia-Pacific Conference on Unsaturated Soils*, Pattaya, 31-44.

Kawai,K., Nomura,S. Ohno,S., Pipatpongsa,T., Tachibana,S., Kanazawa,S. and Iizuka,A.(2009) "Study of the stratigraphic architecture resistant for salt damage and the method to purify salty ground", *Journal of Applied Mechanics*, JSCE, 12:421-428 (in Japanese)

Maulem,Y.(1976) "A new model for predicting the hydraulic conductivity of unsaturated porous media", *Water Resources Research Journal*, 12:513-522.

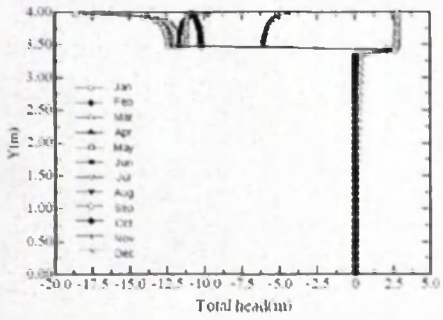


Fig.19 Total water head distribution in the case of improved mulching

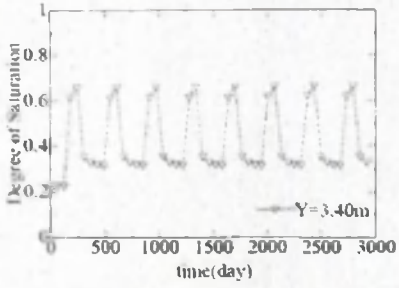


Fig.20 Change in degree of saturation at multing layer

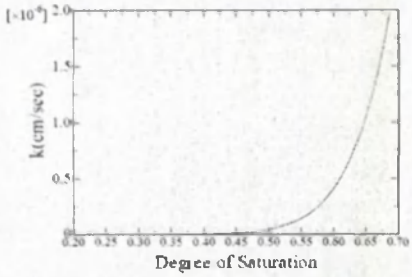
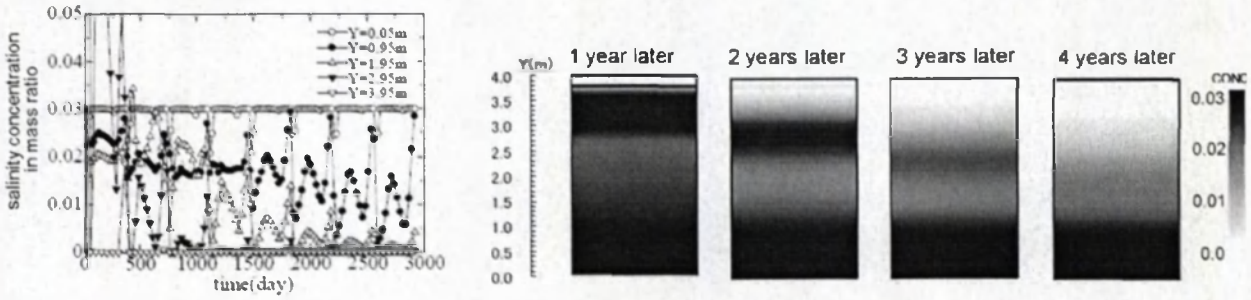
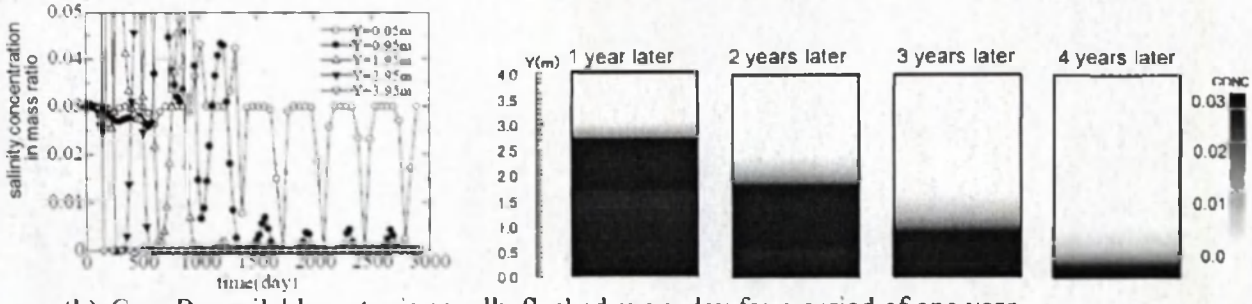


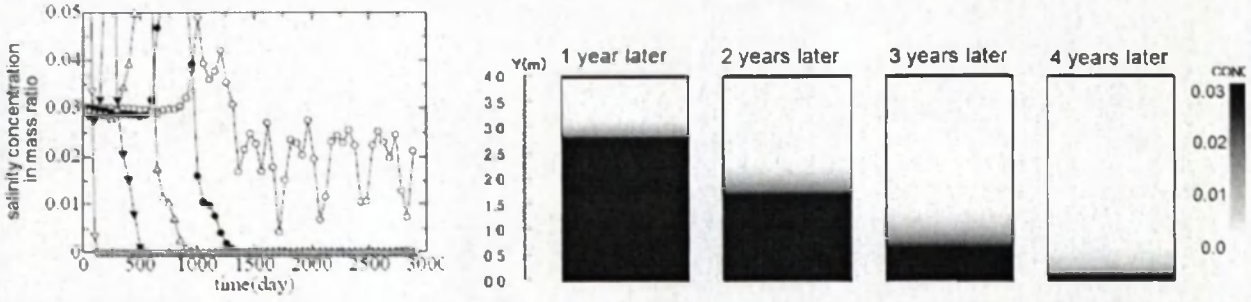
Fig.21 Permeability of mulching layer



(a) Case A: all available water is flushed at once for a period of 31 days



(b) Case B: available water is equally flushed every day for a period of one year



(c) Case C: available water is flushed only in the dry season from Jan to Apr and Oct to Dec

Fig.22 Effect of flushing for purification of salinity contamination

Preservation of Old Buildings in Tehran, Iran

S. Heidari
Civil Engineering Department, Islamic Azad University, South Tehran Branch

Iran is among the 10 countries which have the biggest number of historical monuments and sites in the world. On the other hands, Iran is located on the famous seismic belt of Alp-Himalaya and many large intensive earthquakes subsequently occur in the country. These are good reasons for qualified maintaining and preserving of old buildings and historical monuments. The oldness of this structures varies between decades to thousands years. Even though the city of Tehran, is not very historical but it has been the capital for recent three centuries and a lot of palaces and governmental or social buildings are consequently located there. During recent years, Iranian Cultural Heritage Organization as an involved office has worked on preservation, strengthening and renovation of these buildings, based on their physical condition and structural type. Preservation of footings and bases are very important due to their significance and the fact that there was less attention for evaluation of the soils and bases in the past.

In this paper, the above mentioned topics are reviewed and discussed while the renovation processes and the employed construction methods in preservation of three old buildings are presented and illustrated by photos.

1 INTRODUCTON

There are some old official buildings in Tehran which are still being used. According to this, preservation and maintenance of these buildings are important, so some efforts take place to perform these operations. From geotechnical point of view (Mills 1997) and in the cases where the bearing capacity is needed to be increased or there are settlement problems, it is recommended to stabilize the soil (employing the methods such as injection or installing micro-piles) instead of construction of any type of foundations. In this paper the preserving and maintaining works for three old buildings are explained and discussed in mentioned fields.

2 GENERAL SPECIFICATION

"Military Training Yard" (Meidan-e-Mashgh) was constructed near 200 years ago in "Ghajar Kingdom" but in primary "Pahlavi Kingdom" its function changed and subsequent buildings were gradually built within that:

- Military House Palace
- Police Office Palace
- Foreign Ministry Palace
- National Iranian Museum
- Iran-Britain Oil Company Office
- Central Post Hall
- National Garden Portal Monument

Among them, "Military House Palace" was the oldest and built in 1901 (Zomorshidi 1990) In this paper preserving and maintaining of "Police Office Palace" and "Iran-Britain Oil Company Office" (which is now used as Consular Building in Foreign Ministry Palace Complex) are explained and discussed. Preserving and maintaining of another old important building, "National Congress Building" in Tehran, is also considered for discussion.

2.1 *Police Office Building*

"Police Office Building" (Kakh-e-Shahrbani) is located in central part of Tehran (photo 1).



Photo 1. General view of the "Police Office Palace".

The construction process started in 1933 and finished in 1935. Architectural style of the building is named as National Neo-Classic Style which is a combination of pre-Islamic architecture and "Ghajar Kingdom" architecture and has some components of European Style. This style was popular for

a long period in Iran. "Police Office Building" may be called the best and the most perfect case of this architectural style. This building is in a great importance due to its construction time, architectural values, stylistics and history of Iranian Architecture.

2.2 *Foreign Ministry Consular Building (Iran-Britain Oil Company Office)*

"Foreign Ministry Consular Building" (photo 2) is constructed during years 1922 to 1925. It is located in an old street in the south of "Military Training Yard" and had been formerly named "Iran-Britain Oil Company Office".



Photo 2. Back view of "Foreign Ministry Consular Building".

2.3 *National Congress Building*

"National Congress Building" (Majles-e-Shoray-e-Melli) established at 1906 is also located in central part of Tehran (photo 3). The original site area is near 51000 m^2 including gardens, pools and roads between them. Infrastructure area is near 7000 m^2. The building includes near 200 rooms and halls which has been repaired several times during last years.

The display of the "Congress Library" and the glory of the "Mirror Room" are unique in the area.



Photo 3. General view of "National Congress Building".

3 TECHNICAL SPECIFICATIONS

3.1 *Police Office Building*

This Building has a vast area and includes a basement and two stories. The basement has brick shell ceiling and first floor has Tagh-Zarbi ceiling (small arched brick ceiling between parallel beams) where the floor consists of timber trusses which were eroded intensively. Load bearing system of the building is brick bearing walls (in Iran known as "Porter Walls") and some timber column supports.

3.2 Foreign Ministry Consular Building

Just an external shell had been remained in the building where the wooden structure was intensively eroded. Even the mortar had got porous in many places. Load bearing system of this structure was also brick bearing walls supported with timber columns where timber trusses and beams had been used in ceiling.

3.3 National Congress Building

The construction of this building began under the supervision of first Iranian educated architect and finished in 1879. Load bearing System of the structures were brick bearing walls and timber trusses floors.

4 STRUCTURAL PROBLEMS AND RECONSTRUCTION PURPOSES

4.1 Police Office Building

General weakness of the building made the whole building shaking. The reconstruction purpose of Police Office Building was to repair and resolve the risk of damages (based on international basics and laws). The building has got unweight and excessive attachments (like walls and rooms which were added afterwards) were omitted for this reason. Following this and finally a strengthening work process was performed within the building.

4.2 Foreign Ministry Consular Building

The reconstruction purpose of this building was to replace the wooden structure frame of the building while keeping its external shell (total view of building). With this structural replacement (wood to steel), strengthening of the building was also provided.

4.3 National Congress Building

The purpose of reconstruction project for this building was to repair and preserve the main building (based on international basics and laws) which

was locally damaged. The building obtained adequate stability by these operations, however some additional works was also done to strengthen and integrate the structure.

From geotechnical point of view, a continuous concrete footing was alternately constructed under all of the brick bearing walls.

Finally the wooden truss ceiling was replaced by a steel truss.

5 PRESERVATION OPERATIONS

5.1 Police Office Building

Preservation operations for the Police Office Palace building include:

I. Shallow soil excavation and construction of foundations for new steel columns (photo 4) or existing timber columns (photo 5).
II. Construction of new added steel columns between walls and truss beams between existing and/or new columns.
III. Replacement of some brick walls with substitution of steel columns.
IV. Construction of new "Tagh-Zarbi" (small arched brick ceiling between parallel beams) in places where the ceilings have collapsed or reinforcement of existing ones using welded rands.
V. Reinforcement of ceilings with crossed in-plane rods and new added horizontal steel beam frames (photo 6).
VI. Replacement of timber truss roof with steel one, equipped with suitable seats.



Photo 4. Construction of foundation for new steel columns.



Photo 5. Construction of foundation for existing timber columns.

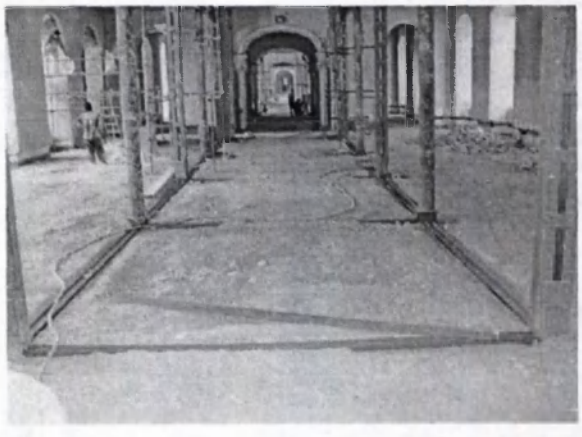


Photo 6. Reinforcement of ceilings with rods and new added steel frames.

5.2 Foreign Ministry Consular Building

Preservation operation for the Foreign Ministry Consular Building includes:

I. Shallow soil excavation and construction of foundations for steel columns (photo 7).
II. Construction of bored short piles under some selected shallow footings (photo 8).
III. Construction of new complete steel structure substituted with the eroded bearing walls with porous mortars (photo 9).

IV. Construction of new concrete ties or repair of old traditional "Shefteh" (clay-lime mixture mortar) ties and "Shefteh" footings (photo 10).



Photo 7. Shallow soil excavation and construction of new foundation.

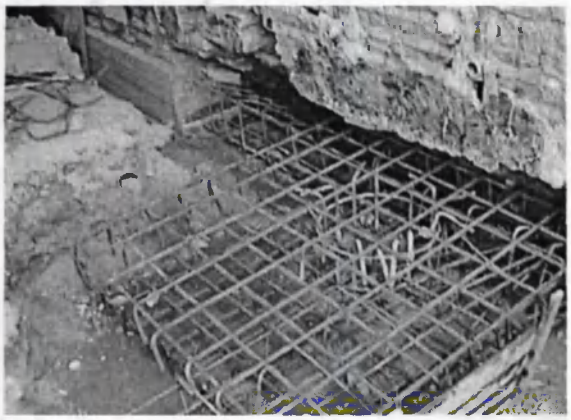


Photo 8. Construction of bored piles under footings.

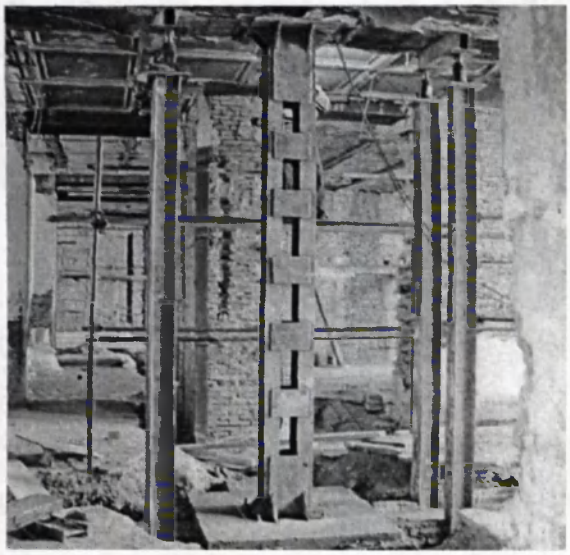


Photo 9. Construction of new steel structure.



Photo 10. Construction of new ties.

5.3 National Congress Building

Recent preservation operations for National Congress Building include:

I. Construction of concrete continuous footings under the bearing walls in alternate sequences (photo 11) and concrete drainage and equipment channels adjacent to the walls (photo 12).

II. Repair of brick foundation caps under brick pedestals (photo 13).

III. Replacement of existing timber trusses with steel trusses (photo 14).

IV. Fine works of internal elements (brick, stucco and mirror work) and works on outwards (photo 15).



Photo 11. Excavation for Construction of Continuous footings under the bearing walls.



Photo 12. Construction of continuous concrete footings and drainage channels.



Photo 13. Repair of brick foundation caps under brick pedestals.



Photo 14. Replacement of timber trusses with steel trusses.



Photo 15. Fine works in "Mirror Room".

6 CONCLUSION

The result would be obtained in a great way if the preservation and maintenance are performed precisely and technically. Subsequently, the building lifetime will be increased to more decades.

From geotechnical point of view, it is important and notable that subsurface soil is usually firm and cemented in Tehran. That was why no serious or

significant geotechnical problem observed in the above discussed buildings.

ACKNOWLEDGMENTS

The author acknowledges "Azar79 Construction Company" for their useful data and valuable photos.

REFERENCES

Azar79 Construction Company (2003). "Preservation of Historical and Old buildings in Tehran" *Technical Report, Tehran.*

Mills, E. (1997). "Building Maintenance and Preservation" *Architectural Press, New York.*

Zomorshidi, H. (1990). "Preservation and Maintaining of the Buildings" *Azadeh Books, Tehran.*

Some Problems of Foundations of Historical Buildings in St. Petersburg

R. Mangushev
Dr. Sc. Professor, Head of Geotechnical Department. Saint-Petersburg State Architectural and Civil Engineering University, Russia

A. Osokin
PhD, Docent of Geotechnical Department. Saint-Petersburg State Architectural and Civil Engineering University; General Director of Company "Geostroy", Russia

ABSTRACT: The engineering and geological conditions of the central part of Saint-Petersburg are considered. The analysis of the main characteristics of the foundations of historical buildings (18-19 Century) is made on the basis of field investigations. The data of dependence between the size of foundations, the number of floors, and the condition of soil are given. The pressure on the bottom of the foundation and the bearing capacity of the soil of the base are analyzed. The examples of the foundations of some historical buildings in St. Petersburg are given. This paper provides also monitoring results of behavior of historical buildings, especially, settlements of foundations. These characteristics of foundations that are important for understanding of interaction of historical old buildings with soft soil ground of Saint-Petersburg are described.

1 INTRODUCTON

The origin of the City is connected with the events of the North War (1700-1721) between Russia and Sweden. Peter and Paul fortress erected on one of the islands in Neva delta for the protection of the won territory became the first building in the future City.

Starting with 18th century all the buildings in the City were constructed from stone in accordance with project specifications. These specifications were developed with participation of Peter I - the founder of the City. The soil of the territory of the future City was characterized by thick layers of soft water saturated silty soil settled on the bottom of glacial Baltic lake and covered by alluvial soil formed by silty and fine sand from Neva.

2 TYPES OF THE FOUNDATION

According to these historical specifications it was recommended to use wood sills when making rubble foundations in soft soil below the level of underground waters. The pine, fur tree and larch trunks were used as wood sills. When the foundations of the old (18 century) buildings were opened it was revealed that the trunks located lower the level of the ground waters were in relatively good condition. In the areas with low level of ground waters rubble plates were done in opened trenches. The main types of the foundations used till the 30th years of the 20th century were rubble foundations formed from lime stone, sand, sometimes granite and diabase fragments, 80 cm diameter. The stones were carefully selected and laid on limy solution fitting each other.

Starting with 20th century the cement solution was used.

In 18 - 19th century in the central part of St. Petersburg where the soft soil prevail, wooden piles 10 m long were used.

3 SETTLEMENTS OF THE ST. ISAACS CATHEDRAL

St. Isaacs Cathedrial may be taken as an example. The period of the construction 1818-1858. Architect – A. Montferrand. It is one of the largest domed structures in the world 101,5 m high, having the area of 4 thousand square meters it can hold 12th. people. When erecting the foundation the 6 m piles were put under the rubble plate 7,5 m thick. The plate was laid in the depth of 5 m. Under the pylons the length of oak piles was 8,4 m. Totally 24 thousand wooden piles with average diameter 26 cm were used. Fig. 1.

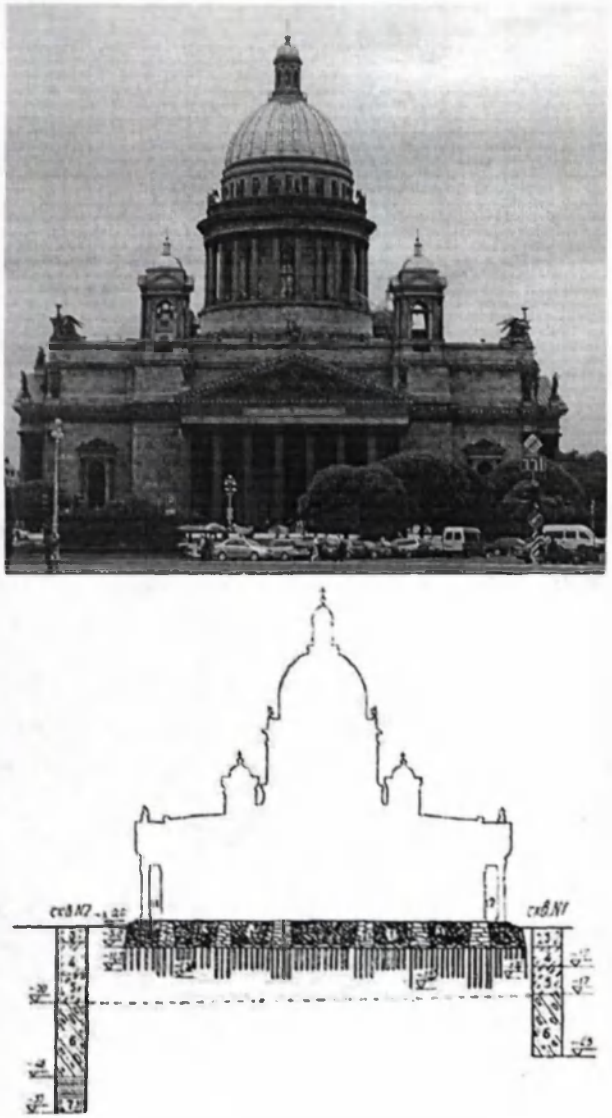


Fig. 1 General view of the Isaacs Cathedral and schematic cross section of the foundation.

Measured in the middle of 80-ies of the 20th century the difference in the surface marks near the building and 50 meters from the building was 85 cm and the slope of the plate towards the south-west was registered. The maximal difference between the surface marks at the distance of 78 m (L=78m) inside the Cathedral was 30 cm. (Fig. 2, 3)

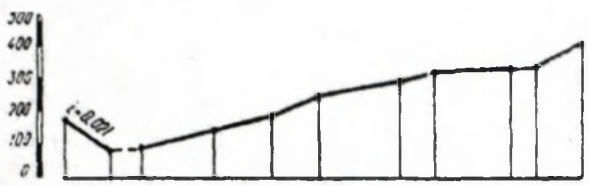


Fig. 2 The floor profile inside the Cathedral in the direction "A-A"

It means that the average settlement of the Cathedral during more than 150 years was less than 100 cm. But thanks to the rigidity of the structure of the Cathedral, there were no serious deformations of the upper structures and the there were no need in strengthening the foundation and bearing structures. The reason of the large foundation settlement was big vertical deformation of soft water saturated layers laid above till sediments. The thickness of soft soil with deformation modulus less than 10 MPa reached more than 45 meters in the construction area of the Cathedral.

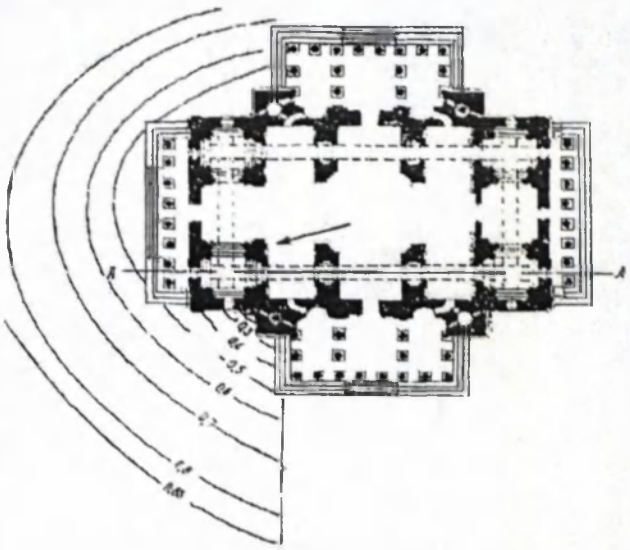


Fig. 3 The plan of the Cathedral on the floor level. The arrow shows the slope direction of the pile raft.

In our days the reconstruction and repair of the old buildings and also compact construction of new buildings in old parts of the City made it necessary to examine and monitor the foundations of old buildings. The average depth of the foundations in most of examined buildings was 1,5-3,4 meters and the depth of the artificial layer in some regions of St. Petersburg reach 3 meters.

The cross section of the typical belt and plate foundations of the civil and apartment buildings constructed before the 20th century in St. Petersburg are shown in Fig. 4.

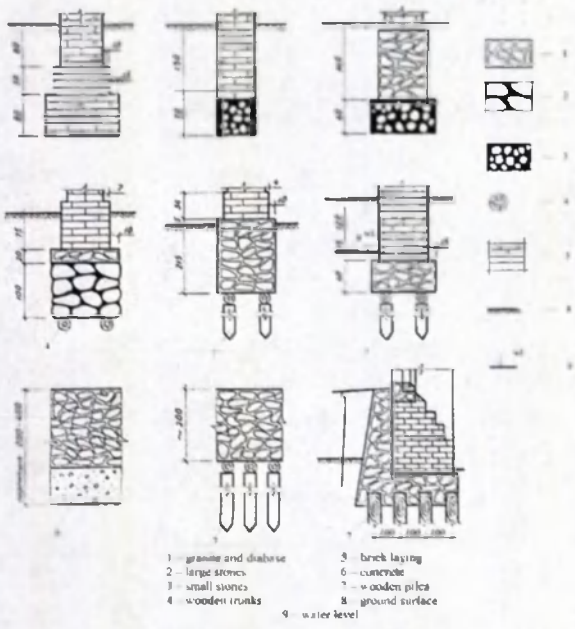


Fig. 4 Types of foundations of old buildings in St. Petersburg.

4 ANALYSIS OF RESULTS OF FOUNDATIONS INSPECTIONS

The generalized experience and the analysis of the inspection of 64 buildings constructed in the period of 18th – beginning of 20th century revealed some regularity which characterizes the buildings referring to this period and constructed in the central part of the City. The buildings usually have 2 -6 floors. The foundation of 44% of the buildings was laid on a silty soil, 56% on a sand of different course. The foundations of 82% are formed from rubble, granite or slime stones and only 18% from burned bricks. Wood sills were found under the foundations of 22 buildings (34%), and wooden piles under foundation of 9 buildings (14%). The photo of opened wood sills and wooden piles under 5 floor building is shown in Fig. 5.

The analysis allowed to estimate the main characteristics of the examined foundations depending on the number of floors in the building. Fig. 6 shows the dependence between the width of the foundation bottom made on sand and silty-sand base and the number of floors. Buildings with wood sills under the foundation bottom are marked by separate line.

The width of the foundation bottom in the inspected buildings "*b*" varied from 0,5 m till 2,8m for foundations on sand base and from 0,8 m till 2,3m for silty soil. The most common width of the foundation bottom is b=1-1,5 m (36% - sand base and 54% - silty soil) (Fig. 7).



Fig. 5 Photo of wood sills and wooden piles under the foundation of 5 floor building.

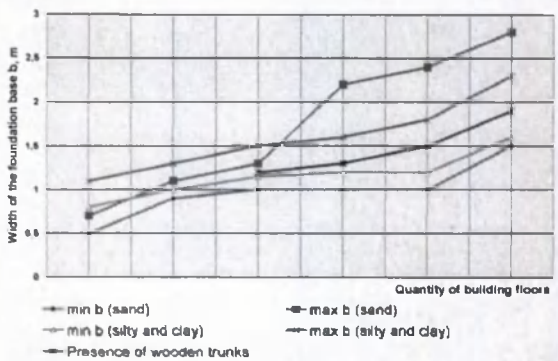


Fig. 6 Dependence between the width of the foundation bottom and the number of floors.

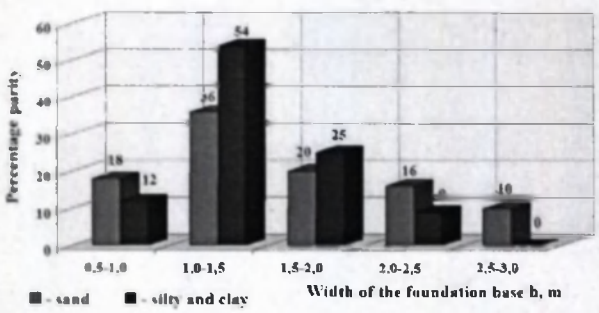


Fig. 7 Subdivision of the width of foundation bottoms in percentage

They followed by width of the foundation b=1,5-2,0 m, 20% and 25% correspondingly. The wood sills were found under the 2-6 floor buildings.

Besides there was a case when the width of the foundation bottom was 4 meters, it was rubble/concrete foundation under which the wooden piles were found Lobanov-Rostovsky House (Constructed 1817-20). Within two

centuries the building has not received any deformation.

The dependence between the depth of the foundations "*d*" and the number of the floors in the buildings are shown in the diagram (Fig. 8).

The depth of foundations varies from d=0,3 m till d=3,0 m for sand base and from 0,7m till 2,5 m for silty soil.

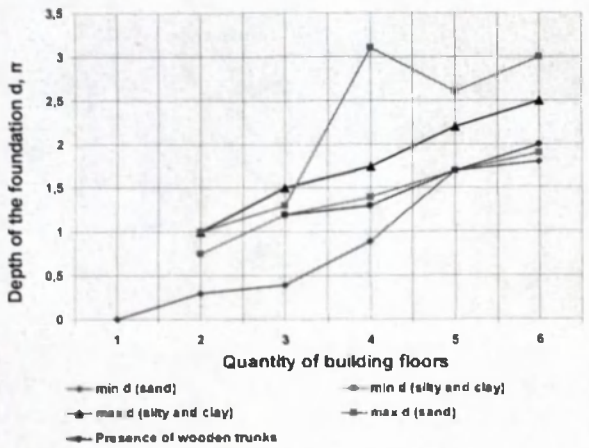


Fig. 8 The dependence between the depth of the foundation bottom and the number of floors.

As a rule the wood sills were found when the depth of foundation bottoms was 1,2 – 1,8 m.

The diagram of the subdivision of the foundation depth of examined buildings shows that the most common depth "d" is equal to 1,5-2,0 m. This depth corresponds to 44% of examined buildings on sand base and 53% on silty soil.

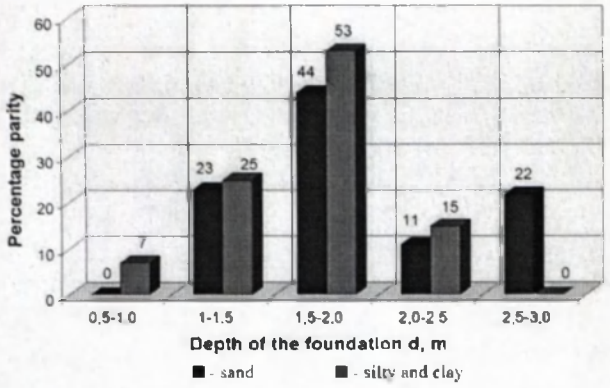


Fig. 9 Subdivision of the depth of the foundation bottom in percentage.

When you compare the action of the actual average pressure "***p***" on the bottom of the foundation of the inspected buildings and the pressure specified in the modern construction documentation, the value "***R***" in particular, it is possible to find the following (Fig. 10).

The value "*p*" for 62% of the buildings constructed on sand base in the central part of St. Petersburg exceeds the value "***R***" permitted by modern Russian Norms. It was registered in 34% cases of bases formed by silty soil.

These results do not correspond to the similar values for Moscow and Moscow region. According to his estimation the value $p/R > 1$ were registered in 8, 3% of examined buildings and 85,7% correspond to the value $p/R < 0,8$ that means that bearing capacity was not sufficiently used.

During the examination of the old buildings of St. Petersburg the value $p/R < 0,8$ was found in 24% of buildings on sand base and in 33% silty soil base.

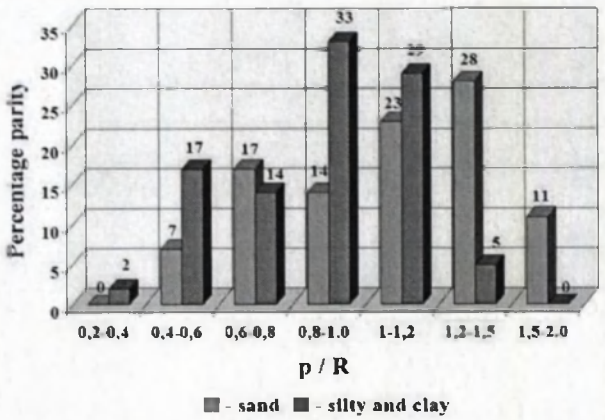


Fig. 10 Distribution of p/R value of examined buildings in percentage.

5 CONCLUSION

The results of the investigation confirm that most of the buildings of 18 - beginning of 20th century were constructed on such a way that the real pressure on the base of the foundation was larger than the bearing capacity of the soil base.

Evidently, this is one of the reasons of cracks and deformation of the upper structures of many old buildings.

REFERENCES

Dalmatov B. I. etc. the Bases and the bases. Uch-to for High Schools, Publishing house ASV, SPbGASU, 2002. – 387 p.

Konovalov P. A. The bases and the bases of reconstructed buildings. 4 edition. – Moscow: VNIINTPI, 2000, 317 p.

Mangushev R., Osokin A. Geotechnics of Saint-Petersburg. Publishing house ASV, 2010. 260 p.

Sotnikov S.N. Settlements of the Isaakievsky Cathedral in Leningrad //Fundamentostroenie in a moustache-lovijah weak soils: Interhigh school. LICI. Leningrad, 1986. pp. 7-18.

Proposals on stabilization of the inclined Nev'yansk tower

Lushnikov V.V.
Ural Scientific Institute of "UralNIIproekt RAASN", Yekaterinburg, Russia

ABSTRACT: The Nev'yansk Tower - a remarkable monument of history and culture of the Urals- built in the beginning of the XVIII century is among the well-known leaning structures. Measurements of the recent years have shown continuation of the Tower inclination, which produces real risk factors for its existence. In case the dangerous progress of its inclination is confirmed, engineering intervention in the destiny of the Tower may become necessary - like it has been done on the world famous Tower of Pisa. The report contains the description of the authors' proposals on possible ways of stabilizing spatial location of Nev'yansk Tower.

The Nev'yansk Tower is a remarkable monument of history and culture of the Urals built in the beginning of the XVIII century by industrialists Nikita and Akinfiy Demidov, which is among the famous inclined buildings. Data on the history of this monument and the information on the known along with the many unknown facts related to it was reported in the works published before (Shakinko,1989; Lushnikov, 2011), including the collection of works "Memorchilik va Qurilish Muammolari" (Lushnikov, Orzhekhovskii, Khadur, 2002), as well as the report (Lushnikov, Orzhekhovskii, Smetanin, Lukpanov, 2011) at the "Asian Conf. on Soil Mechanics and Geotechnical Engineering" international conference in Hong Kong.

The present report provides information on the continuation of the Tower inclination, which creates real risk factors for its existence. In case the dangerous development of its inclination is confirmed, there can appear a necessity for engineering intervention in the destiny of the Tower and for the developing projects of position stabilization, just as it has been done with the world-famous inclined monument of history and culture – the Leaning Tower of Pisa. The report contains a description of the authors' proposals on possible ways of stabilizing Nev'yansk Tower location.

The Leaning Tower of Pisa has been studied and has been accompanied by thorough observations and forecasts for many years. Finally, in 1990, when its stability was considered to be threatening, it was closed for tourists (Burland, Jamiolkowski , Vidggiani 2003).

At first the Tower of Pisa incline correction was planned to be carried out with the help of lead loads with a total weight of 690 tons, mounted on the Tower side opposite the tilt (Fig. 1). For some time (from 1993 to 1995.) it had been declining backward, but then it started to lean in the southern direction again (this time is shown by a circle in Fig. 1b).

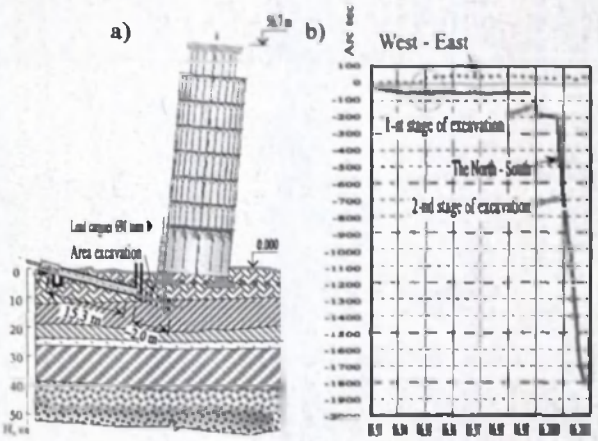


Fig. 1. Correcting the tilt of the leaning tower of Pisa:
a - the scheme of excavation of soil;
b - change the inclination of the Tower

In 1999 the realization of another project to rectify the incline of the Tower started. To do this, 42 inclined wells were drilled on the north side of the Tower (see Fig. 1), through which excavation of soil from under the edge of the foundation was carried out. The first cycle of excavation of 7 m^3 of soil resulted in the settling of the foundation north edge by 1.3 cm or reducing the tilt by 3' approximately (or 200 arc sec). The Tower "went back 30 years" in its leaning history. The second cycle of excavation (38 m^3) led to the returning of the Tower by 0.5° (or 1800 arc sec) and reducing the incline of the top by approximately 40 cm and "returning" it to the middle of XIX century. Threat of stability loss disappeared and in 2001 it was opened for visiting again.

On its plan the Nev'yansk Tower has an area of 18.10 x 9.60 m (together with the annex) and height of 57.5 m. It includes one "tchetverik" (four-sided base) and three "vos'merics" (octagons) crowned with a spire. Its spatial arrangement is shown in Fig. 2 together with one of the options for its stabilization.

Little is known by now about this Tower. For example, it is unknown what kind of foundation it

has – whether there are wooden piles under it or not, and it is dangerous to excavate the soil – it can aggravate its position.

There are a lot of theories concerning the Tower. The most stable of them is that the Tower was allegedly built intentionally inclined - like Pisa. However, there is definite evidence disproving this hypothesis. A polyline (sabre-like) longitudinal axis, continuous settling and deviations of the body of the Tower, different angles of floor tilt, window and door openings, tension bars, etc., all of these indicate that the Tower was intended to be vertical. But the instability of soil bed led to the nonuniform settling immediately after the beginning of its construction and each floor was built vertically but under the conditions of the continuous nonuniform tilt deformations.

Many experts believe that the stability of the Nev'yansk Tower is provided by its annex placed opposite the tilt side. They believe that it was built by the builders after the first signs of the Tower leaning from the vertical had appeared. Its mass is about 200 tons, and iron tension bars connecting the Tower with annex continue to constrain the inclination.

All the previously carried out measurements of the Nev'yansk Tower performed by almost only enthusiastic amateurs were episodic in nature and did not have any reliable basis for measurement.

There is evidence of the Tower top incline of 2½ "arshin" (1.778 m) in 1870, of 1.8 m in 1979. (Shakinko,1989) and of 2.35 m in 2000. (Lushnikov, 2011).

At different times the rate of the foundation inclination was estimated to range from 0.5 to 0.9 mm a year (which corresponds to the top tilt from 25 to 50 cm per 100 years). On this basis different predictions were made concerning the stability and possible time when the critical state of the Tower may occur, its condition being admitted dangerous when tilting the top by 2.5-3 m.

One of the predictions was published in the article (Zaretskii, Kapustin, Lushnikov, Sukhanov, 1981). According to this prediction the Nev'yansk Tower may lose its stability by 2200-2250.; by this date the stability coefficient can achieve critical value of $k_{st} = 1.0$; now the stability of the Tower is estimated by coefficient $k_{st} = 1.2$-1.3. A similar prediction for the leaning tower of Pisa in the same journal led to a critical coefficient $k_{st} = 1.0$ by 2150 far earlier than the Nev'ansk Tower. Naturally, then nobody could have taken into account the operations for the correction of its incline described above when its stability was estimated by a coefficient $k_{st} = 1.1$.

Since May 2003, when three benchmarks were installed near the Nev'yansk Tower, monitoring its foundation deformation has been continued . Location of marks on the foundation is shown in Fig. 2 and the results of measurements for the period from 2003 to 2010 are summarized in table. 1.

Table 1- Settling marks on the Tower (excluding annex).

Number of mark	05.2003	05.2004	05.2005	08.2005	11.2006	09.2007	12.2010
M–2	0	-0.9	-5.6	-3.8	-3.8	-3.5	-7.6
M–3	0	-0.8	-5.0	-3.2	-4.0	-4.2	-8.4
M–4	0	-0.5	-6.2	-3.0	-4.2	-4.5	-9.1
M–5	0	-0.7	-3.9	-2.6	-2.5	-3.4	-6.5
M–6	0	-0.6	-2.4	-1.8	-1.5	-1.7	-4.3
M–7	0	-0.8	-3.0	-2.4	-1.8	-2.2	-4.9
Average settling	0	-0.72	-4.35	-2.80 (-4.35)	-3.00 (-4.55)	-3.25 (-4.8)	-6.8 (-8.35)

However, in this table the values of settling contain errors - during the period from 05.2005 to 08.2005(this period is marked by grey tone) an apparent rise of the Tower had occurred which is in essence impossible (probably this is the result of marks damage). This could have led to some additional settlings being missed: under the mark M-4 - ΔM-4 = 3.2 mm, under the mark M-6-ΔM-6 = 0.6 mm (average of marks 1.55 mm). If one takes into account missed settlings, average Tower settling for the measurement period will increase up to 8.35 mm, and the inclinations will change as follows:

- for the period from 05.2003 to 05.2005- VΔS = 1.88 mm/per year;
- for the period from 08.2005 to 09.2007 they will rise to - VΔS = 1.87 mm/per year;
- for the period from 09.2007 to 12.2010- VΔS = 1.35 mm/per year;

– for the entire observation period from 05.2003 on 12.2010- VΔS = 0.97 mm/per year.

Thus, the deformation of the Tower is going on. A high rate of settling in 2003-2005 can be explained by the site buildup around the Tower, which was performed with the use of heavy road making machines, and restoration works on the Spaso-Preobrazhenskiy Cathedral. Later the rate of settlings has somewhat decreased, but the average rate for the entire observation period remains rather high, exceeding the rates obtained in the previous measurements (VΔS = 0.5-0.9 mm/year). One can assume that in the future the rate would gradually decrease, but the anxiety about the future of the Tower still remains.

Therefore sooner or later one must start searching for ways of stabilizing the Tower position. The author isn't aware of any serious proposals regarding this situation.

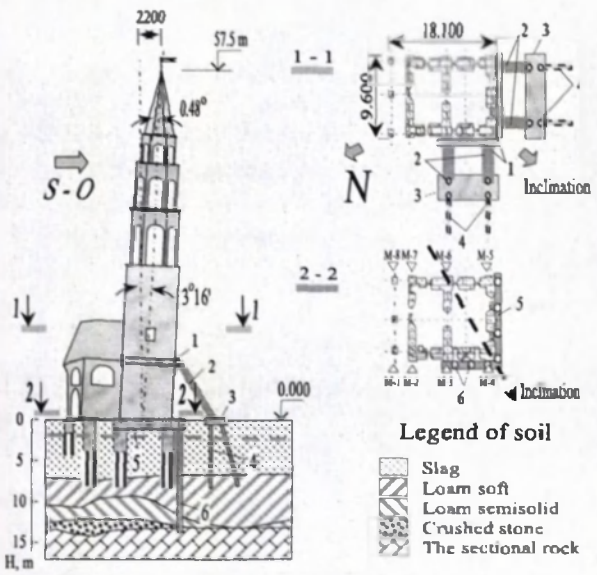


Fig. 2. The construction of bored piles:
1 – basic beam; 2 – inclined beam; 3 – plate;
4 – piles; 5 – bandage; 6 – chisel pile

Unfortunately, one can't apply the method of soil excavation as it has been done in Pisa because in the presence of wooden piles it is dangerous. Therefore the author suggests bearing in mind four possible ways of stabilizing the Tower given in Fig. 2 - 5.

The first two ways involve the strengthening of the foundation and soils under the Tower from the tilt side.

The first way consists in the construction of bored piles down to the rocky ground and their connection with the foundation of the Tower by reinforced concrete grillage (Fig. 2);

The second way consists in the injection of reinforcing mortars into the base under the foundation (Fig. 3).

Ways of soil solidification and construction restraints by means of poling bored piles from the Tower tilt side (Fig. 2) or injecting reinforcement mortars from the same side (Fig. 3) are widely practiced in the Urals. But these methods involve some risk factors that must be taken into account. A great amount of water penetrates together with cement-sand grout or with the piles concrete into the soil in injecting the solutions. Water is significantly weakening the ground until the cement-sand component of the mortar or piles concrete gain the necessary strength. In this period (it lasts from 10 to 30 days) further technological settlings can arise softening the soil and exacerbating the Tower tilt. Therefore, for the period of the injection or the piles construction it is necessary to protect the Tower from technological settling by constructing struts with feet on the ground (in the form of pile foundation grillage).

Two other ways use the idea of a counterweight to the Tower from the side of annex, which previously performed this function and is still performing it now:

The third way is the creation of a counterweight of bored piles (with widening at the bottom), built from the side of annex, coupling the piles with reinforced concrete grillage and the foundation, and tension bars - with the Tower itself (Fig. 4);

The fourth way - creating a counterweight of heavy loads, constructed from the side of the annex edge coupling them with grillage and the foundation of the annex and the same tension bars - with the Tower (Fig. 5).

Piles and heavy cantledges must create the torque opposite the tilt. Considering that by the mass of Nev'yansk Tower of G = ~ 3 thousand tons and by the deviation of its gravity centre by approximately e = ~ 1.1 m tilt back moment for the Tower is created M = G e = ~ 3 · 1.1 =~ 3.3 thousand t·m, then to stabilize the Tower it is enough to create the torque opposite the tilt with the value of about 0.5 thousand t m, which must be provided by the mass of the cantledges or pile capacity. The creation of this torque opposite the tilt should complement supporting functions of the annex. In the case of realizing the 3-rd and 4-th ways of stabilization it is also reasonable to provide for installment of temporary strut.

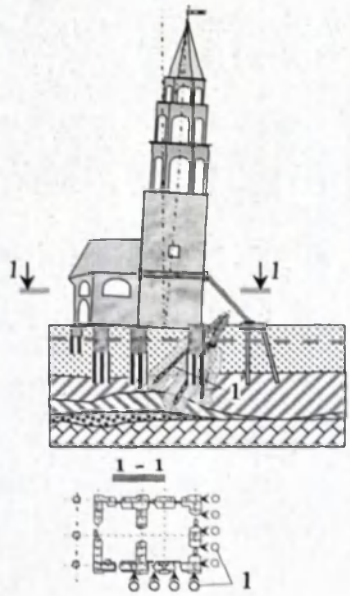


Fig. 3.
Injection reinforcement:
1 – iniector

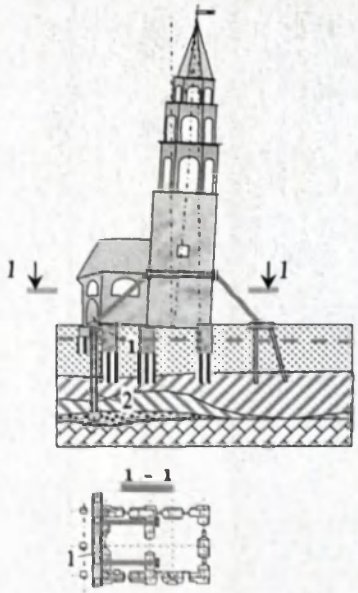


Fig. 4.
Device balances of bored piles:
1 – beam; 2 – chisel pile

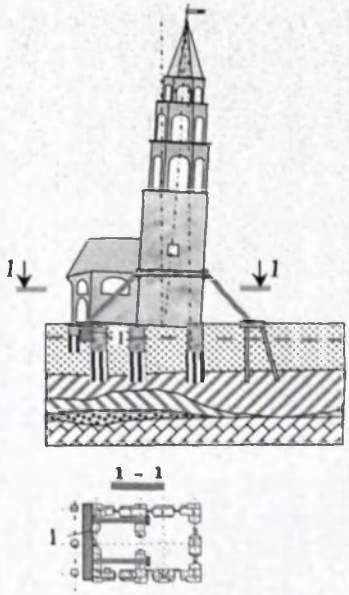


Fig. 5.
Device in They anti-balanced
blocks: 1 – counterbalance

CONCLUSIONS, SUGGESTIONS

1 At present, we can make a conclusion about the stability of the Tower and security of its present position, but it should be viewed as preliminary. But such a conclusion requires extensive verification, confirmation or refutation on the basis of regular high-accuracy instrumental observation and its competent analysis.

2 It is clear that nonuniform settling of the foundation and the incline of the Tower, accumulated since the beginning of its construction, and continuing up to the present time, sooner or later can lead to the need for engineering intervention in its future.

3 Given the huge historical and cultural significance of the Tower to the Urals, it is necessary to organize continuous monitoring of its condition using modern measuring equipment. Information concerning the continuation of its inclination should be widely available, as the analysis contains alarming findings, which should not be concealed from the public at large.

4 One way to attract the attention of the public could be the announcement of a contest for the protection of the Tower from the ongoing tilt, and the development of the projects for its stabilization. This should lead to activation of creative activity by professionals and enthusiasts, aimed at the preservation of this unique monument. Proposals described in this report must be included in the list of possible variants of stabilization of the Tower.

REFERENCE

Burland J.B., Jamiolkowski M., Vidggiani C. (2003). The stabilisaftion of theLeaning Tower of Pisa. – Proc. of Japanese Geotechical Socitty on Soils and Foundation. Vol. 43, No 5, pp. 63-80.

Lushnikov V. V. (2011). Whether the Nev'yansk Tower will fall? And as straightened Pisa Tower – Ykaterinburg. – 88 p.

Lushnikov V. V., Orzhekhovskii Yu. R., Khadur M.A (2002). The analysis of deformations and stability of an inclined tower in to Nev'yansk of Sverdlovsk region. // Memorchilik va Qurilish Muammolari (ilmiy-texnik jurnal). – Samarqand, № 3. pp. 14-18.

Lushnikov V. V., Orzhekhovskii Yu. R., Smetanin M.V., Lukpanov R. (2011). Analysis of deformation and stability of the Nev'yansk Tower. – Int. Asian Conf. on Soil Mechanics and Geotechnical Engineering. – Hong Kong.– pp. 93–100.

Shakinko I. M. (1989). Nev'yansk Tower (legends, history, hypothesizes, considerations). – Sverdlovsk: Middle-Ural Press. – 304 p.

Zaretskii Yu. K., Kapustin V. K., Lushnikov V. V., Sukhanov B. I. (1981). Prognosis for the stability of the Nev'yansk Tower. // Bases, foundations and mechanics of soils, № 6, pp. 19-21.

Rehabilitation Activities in Al-Kadhimayn Mosque and Shrine in Baghdad

N.K.S.AL-Saoudi

Department of Building and Construction Engineering. University of Technology, Baghdad, Iraq

ABSTRACT: Baghdad the capital of Iraq said to be founded on 30 July 762 by the Abbasid dynasty, led by Calipha al-Mansur. Baghdad contains many heritage buildings and religious places distributed in different parts of the city. Among these religious places are Al-Kadhimayn mosque and shrine. Historically Al-Kadhimaya town was the cemetery containing the bodies of Calipha al- Mansur's family. In 799 Immam Musa bin Jafar known as Al-Kadhim was buried in the cemetery and his grandson Immam Muhammad Al-Jawad who died in 834 was buried in the same place. The two Immams are descendants of the prophet Mohammad (pbuh). In 1515, the shrine was constructed on the site of the shrines of the two Immams and since then became one of the most important mosques in the Islamic world. The present paper sheds the light of the rehabilitation activities that took place on the Mosque and shrine after 2003 till now.

1 HISTORICAL BACKGROUND

1.1 Baghdad and Al-Kadhimeyya

Baghdad city known as the round city was founded on the west bank of the Tigris River by the Abbasid Caliph Abu Jafar Al- Mansour in 762 A.D. It was considered as the largest city in the world shortly after its foundation with more than one million estimated inhabitants at that time. During the generation of its founding, Baghdad became the center of learning and commerce and many cultural houses like the house of wisdom were established. Baghdad is distinguished by many historical and religious landmarks. Most of these sites are named after past political or religious figures or related with historical events.(Iraq Significant site 011 2009)

Al- Kadhimeyya is one of the oldest districts, located some 5 km to the north of the center of Baghdad. Before the construction of Baghdad the caliph Al-Mansour made that area as a cemetery named Qureish cemeteries; containing the bodies of his family (Strika and Khalil 1987). In 799 Immam Musa bin Jafar, the seventh Immam, died and was buried was buried in the cemetery and his grandson Immam Muhammad Al-Jawad, the ninth Immam who died in 834 was buried in the same place. The two Immams are descendants of the prophet Mohammad (pbuh). The shrine housing the bodies of the two Immams was constructed in1515.The shrine then became a pilgrimage site and one of the most important mosques in the Islamic world.

The name Al- Kadhimeyya was set because of the two Imams who were famous for their suppression of anger that the place was called Kazemain or the two Kazims. Currently Al-Kadhimeyya as a spiritual holy place is visited daily by 150000 people and exceeds 500000 on Fridays and Saturdays. (Alwan and El-Melh 2006)

Al-Kadhimeyya town, extended and developed to cover an area of 13300 m^2 surrounded by three sides of Tigris River became an integrated part of Baghdad city. It is famous by its Iraqi cultural heritage, the old gold souk, and the old houses with wooden balconies. Fig.1 shows the area covered by Al-Kadhimeyya and the location of the holy shrine.(Global security .org 2009)

1.2 *Al-Kadhimyya mosque and shrine*

The Kadhimyya mosque known also as Al-Kadhumayn is a distinguished landmark. A visitor approaching Baghdad from the north or west will be astonished by the four tall golden

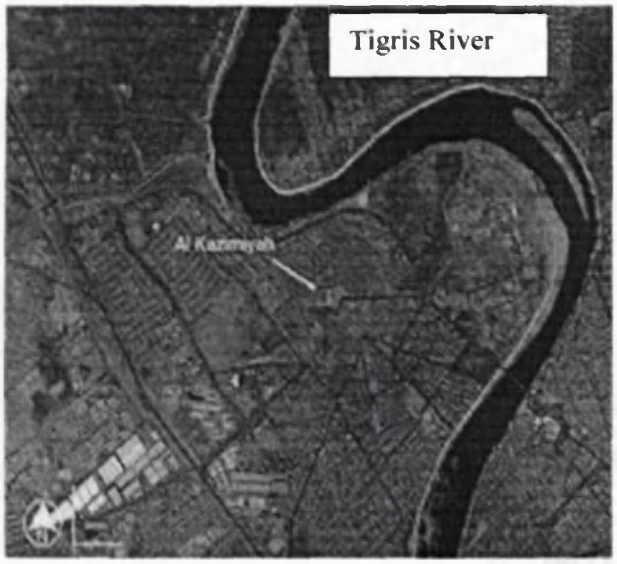


Fig. 1 The Kadhimyya town housing the shrine

minarets and the gilded domes.Fig.2 illustrates the main features of the outside. (Mashhad Al-Kazimia 2008)



Fig. 2 The Kadhimyya Mosque

Fig.3 is the overall section f the mosque and the shrine. The outside boundaries are 135m by 140m covering a square area 19575m^2. The structure containing the holy shrine is square in shape with dimensions 60m by 60m located at the center of the boundaries leaving the rest of the area as courtyards for prayer. Looking at the mosque from the inside, the basic structural elements are huge walls about 1.5 m wide and 8.5m high, made of brick, juss and lime supporting the two domes.



Fig.3 Horizontal section through the mosque

The open space close to the shrine is rectangular in shape of dimensions 28m in length and 7.5 m in width. The shrine of dimensions 6.75 in length, 5.2m in width and 3.5 m in height is located at the center. The area surrounding the shrine is left for the visitors to walk in circles around the shrine as part of their religious belief.(Report SECB 2008)

2. REHABILITATION AND MAMTAINANCE ACTIVITIES IN THE MOSQUE

After 2003 events, rehabilitation and maintenance of the shrine and mosque started. The development mission consists of several phases; some phases are concerned with modifications in the structural system of the mosque to provide more free space for the visitors or pilgrims to maneuver around the shrine. This was one of the critical structural problems that required complex structural analysis and high engineering judgment. The international center for technical research (ICTR) took the responsibility of the project. (Al Shahristany 2005)

The other important phase is the development and rehabilitation of the residential and commercial areas within 500m radius surrounding the mosque. This project was announced internationally and one of the consulting architectural offices was nominated as the best presentation that matches with history and culture of the holy city.

2.1 *Extension of the area around the shrine*

Al- Shahristany 2005 presented Fig. 4 showing two horizontal sections through the structure hosting the holy shrine before and after the extension. It is required to remove part of the columns holding the two domes as indicated in the figure to provide extra space for the visitors to walk around the shrine.

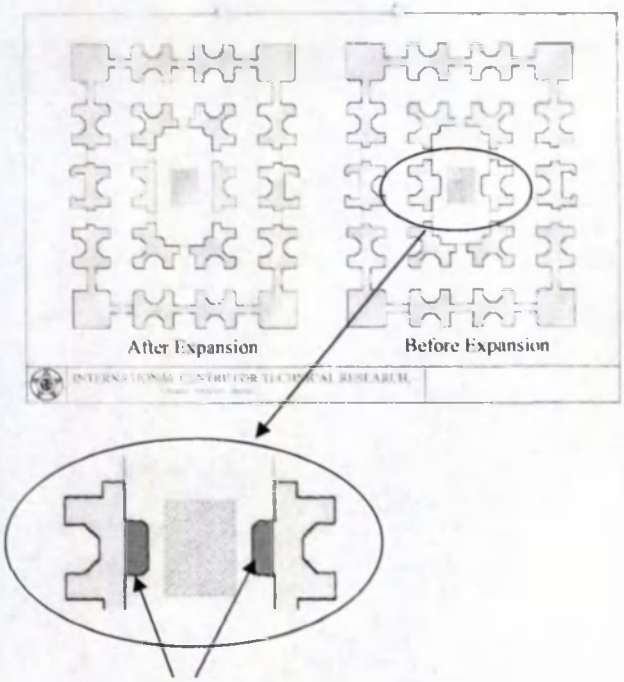


Fig.4 Section through ground floor before and after extension

Fig.5 illustrates the part of the columns to be removed from the inside of the mosque and very close to the shrine. The sequence in the construction steps of the structural elements forming the final skeleton of the structure is illustrated in Fig 6. The seven arches fixed in their respective positions, the two rings used to provide stability and rigidity, transfer and distribute the generated stresses from the two domes. The two columns at the middle and along the opposite sides of the shrine are wider and the indicated parts must be removed. The technique implemented for this job is illustrated in Fig.6.

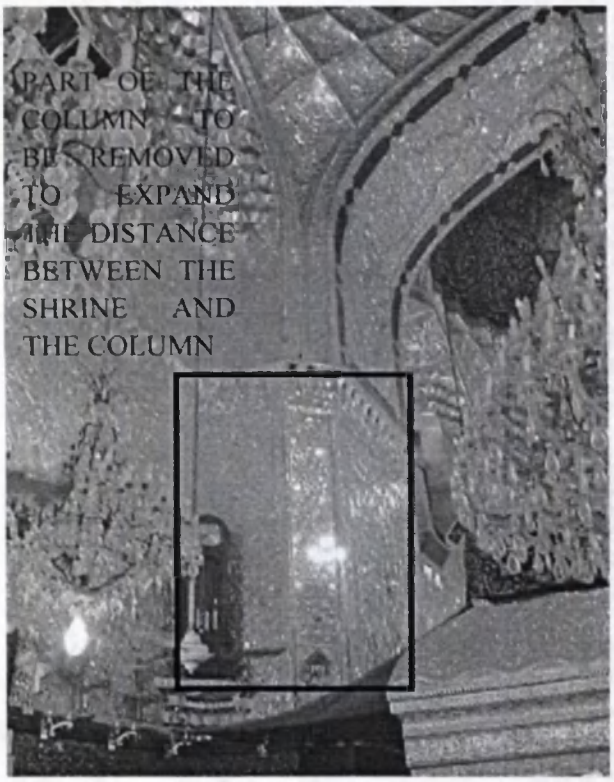


Fig. 5 Section of the column to be removed from the inside

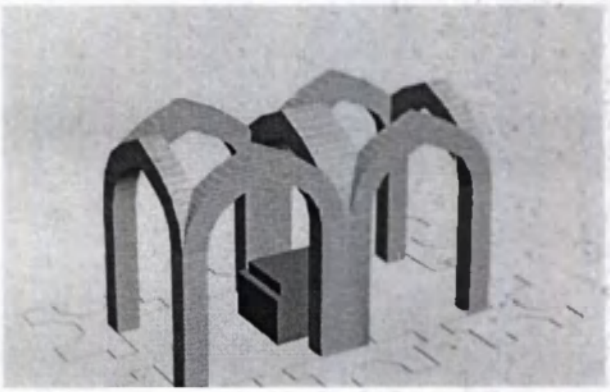


Fig. 6a Construction of the arches

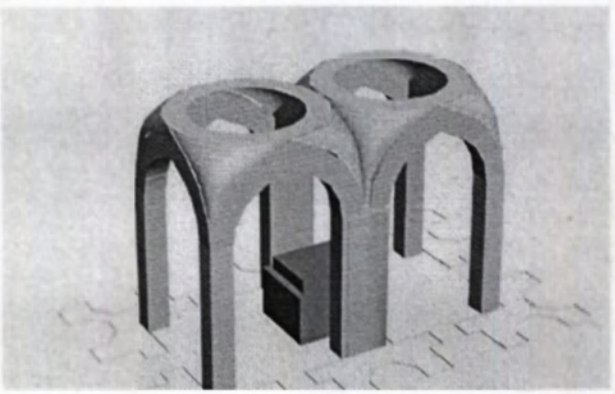


Fig 6b Construction the base of the circular rings

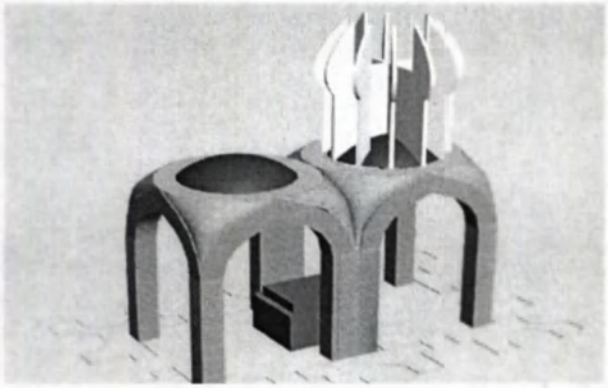


Fig. 6c Construction of the rings and domes

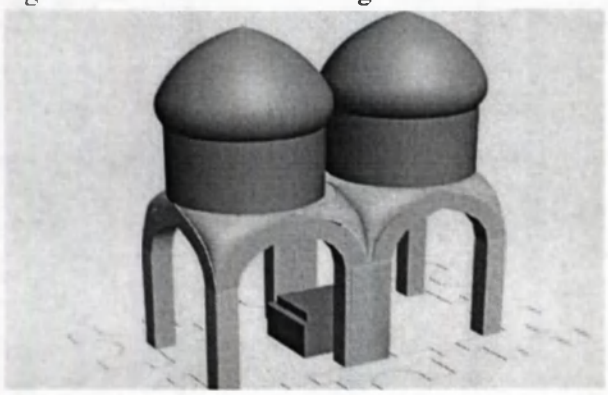


Fig. 6d Final stage of construction of domes

The first step was to get a clear analysis for the imposed loads from the domes to the contact area at the interface between the circular ring and the arches. The analysis revealed the area identified by the pink color shown in Fig 7.

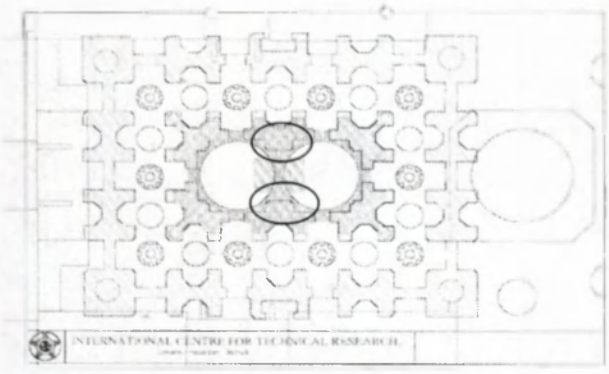


Fig. 7 Location of stress distribution

The consultant at this stage decided to replace parts identified by the two circles in figure 7 by two opposite reinforced concrete beams capable of supporting the imposed loads and distribute them evenly over the new contact area. A transverse section between the two domes, Fig 8, and a horizontal section, Fig 9, clarify the location of the two opposite reinforced concrete beams.

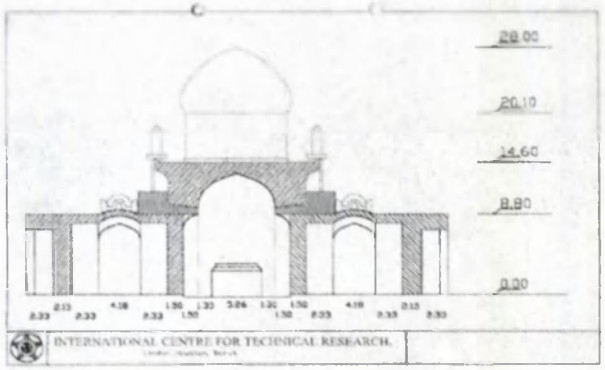


Fig. 8 Transverse section through the center of the domes.

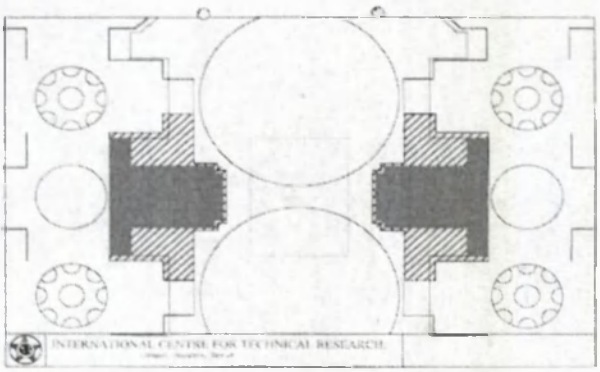


Fig. 9 Horizontal section through the domes

The reinforced beam that replaced the red zones in Fig 9 is shown in Fig 10

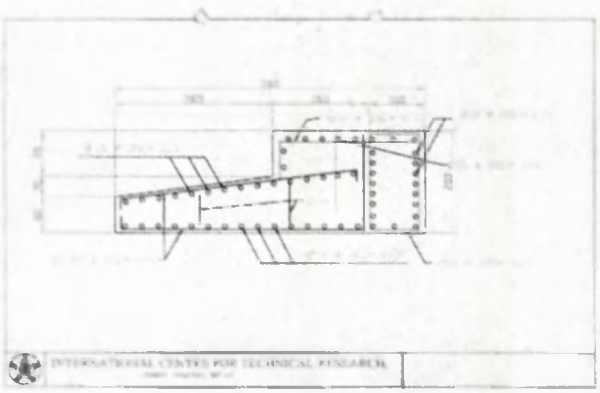


Fig. 10 Section through the reinforced beam

The beam consists of two parts with depth ranging in depth from 200cm to the right to 80 cm to the left with tapered part 285 cm in length. The construction of this huge beam started on the roof of the ground floor in three phases. The width of the beam was divided into three parts; the left part

was constructed first followed by the right part and finally the middle part. Fig. 11 illustrates the steps of construction.



Fig. 11a Drilling process



Fig. 11b Reinforcing the beam

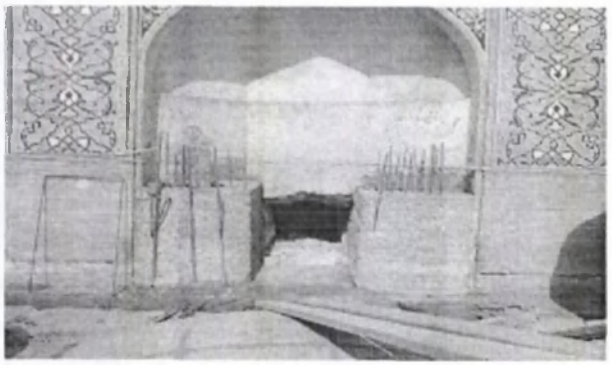


Fig. 11c Completion of the left and right parts

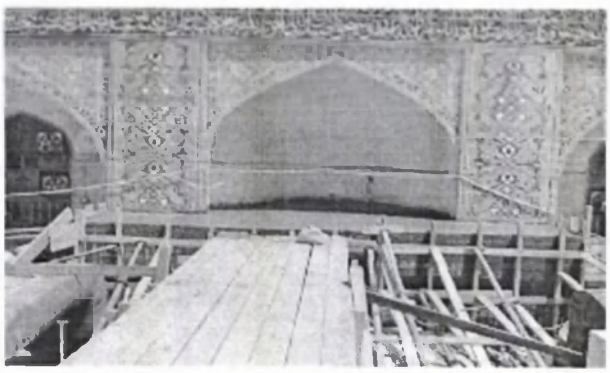


Fig. 11d Finished level of the beam

2.2 *Site characterization and geotechniques*

There are no available data about the geotechnical properties of the site. Inspection of the foundation along the boundaries of the mosque shed the light that all structural elements including the foundations are constructed from brick as a building unit and a mixture of juss and lime as a binder. It seems that these materials are highly durable and sustain various environmental conditions. It was hard to investigate the depth of foundations but it is expected to be more than 5 - 6m below natural ground level. It was even harder to estimate the width of the foundations of the columns and walls holding the domes.

Two boreholes were drilled in the courtyard outside the mosque to a depth of 25 m below ground level. Fig 12 demonstrates the variation

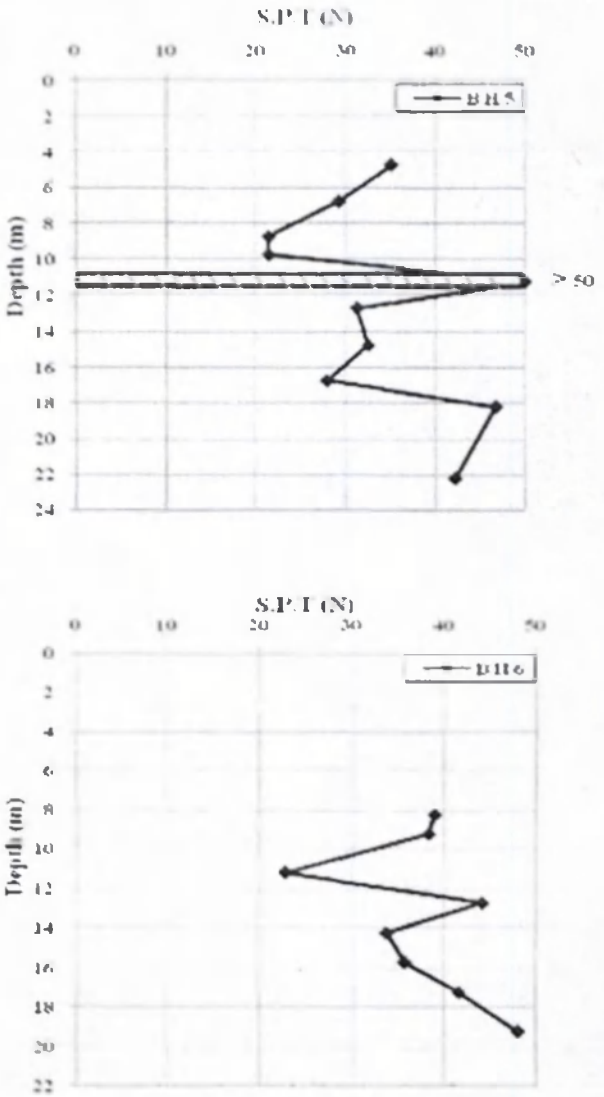


Fig. 12 Corrected SPT versus depth

corrected SPT versus depth. The top 4 to 5 m below ground level is fill material with crushed bricks and gypsum generated probably from accumulation of very old graves buried in this area. The second layer extends to a depth 15m below natural ground is stiff overconsloidated brown silty clay to brown clayey silt. The third layer extends from a depth 15m below natural ground till the end of boring. The majority of this layer is dense gray sandy silt with lenses of brown clayey silt. The average SPT along the depth of the two boreholes ranges between 35 to 40.

3 CONCLUSION

Al-Kadhumiyya mosque and shrine are world famous worship places and most important mosques in the Islamic world. Dealing with the structural problem of removing parts of the middle columns adjacent to the shrine, one must admit that such challenging problem was not easy to tackle. The geotechnical part of the paper indicates that high stresses from such huge structure acting on the underneath soil for such a long period of time made it very stiff. Any change in the skeleton of the structure within tolerable limits will cause minor influence in settlement.

ACKNOWLEDGEMENTS

The author is grateful to Al- Shahristany Association (The International Center for Technical Research) for providing all necessary details of the project. Sincere thanks are extended to Dr. Ihsan Al-Shahristany for reviewing the paper and providing the permission for publication. Last but not least thanks are extended to Eng. Hayder Al Assadi for his help and support.

REFERENCES

Al-Shahristany M. (2005). " The technical design of of the extension Al- Kaminiyya shrine" *report prepared by the International center of technical research ICTR* .

Alwan, W. and Melh, S. (2006). " Kadhimiya : City of Domes and Gilded Minarets"*Islamic Tourism*- issue 23 ,62-74.

Atlastours.net/Iraq/Baghdad "Shrines and mosques in Baghdad" www.atlastours.net/ Iraq/Baghdad

Global security, org " Mashhad Al-Kazimiya" www.globalsecurity.org/.../world Iraq

Iraq significant site 011-Baghdad www.cemml.colostate.edu/ cultural/09476/Iraq 05-09

Strika,V. and Khalil,J. (1987) " The Islamic architecture of Baghdad" *Instituto Universitario Orientale*

The scientific and engineering consulting bureau SECB (2008) "Surveying report of Al-Kadhumiyya" *University of Technology*/ Baghdad

Basement floor construction in the historical building in Tobolsk

Y.A. Pronozin, R.V. Melnikov &. M.A. Stepanov
Department of Construction Technology, Groundwork and Foundations, Tyumen State University of Architecture and Civil Engineering, Tyumen, Russia

ABSTRACT: The paper discusses the experimental results of the first basement floor in restorative renovation of cultural and historical heritage in Tobolsk. Works on deepening of the basement below the existing foundation footing have been done. This paper shows the results of basement floor computational modeling applying the Plaxis program with regard to step-by-step technology.

Tobolsk is a town in Tyumen Oblast, Russia, which was founded in 1587 during exploration of Siberia. It's located at the confluence of the Tobol and Irtysh Rivers. For three hundred years it was the capital of large Tobolsk Governorate, including the territory from the Urals to North America. Tobolsk is the only town in Siberia and one of the few ones in Russia which has a stone Kremlin. Tobolsk Kremlin is the unique monument of Siberian architectonics. A lot of trade routes from Eastern Part of Russia to China and Central Asia including "Great Silk Road" and "The Tea Road" passed through Tobolsk (Barabanova 1986).

Since foundation of the town, Tobolsk has been a sacred center of Siberia. The first Siberian eparchy is located in Tobolsk. It was founded in 1620. In 1994 The Holy Synod declared Tobolsk to be one of the three main sacred centers of Russia alongside with Moscow and Saint-Petersburg.

It is a unique monument-town in the open air with more than 200 historical and cultural landmarks. Not any other town of Russia can boast of such a great number of monuments.

Today careful attention is paid to conservation of Tobolsk cultural heritage and historical sites. The number of buildings, renovated between 2006 and 2010, is 68. In 2011 25 million dollars was spent on architectural monuments restoration. At present, restorative renovation of more than 30 town monuments is being carried out and about 90 are needed to be restored.

"Station hospital" (fig.1) is one of the historical and cultural landmarks, which is situated in the "upper" part of the town. It's included in restoration project of the region. There is a lot of contradictory information about the year of "Station hospital" construction, i.e. between 1794 and 1872.

Before 1917 Public assistance Prikaz was housed here. It was a charitable medical institution for the poor. Since the October Revolution of 1917 this building has been used as a hospital. In 1991 the building was closed because of critical conditions and after that "Station hospital" has been derelict.

"Station hospital" is a three-story building, which has a complex configuration in plan. Its dimensions are 43x28 m in plan without single-floor wings and dimensions of symmetrically located wings are 15x10 m in plan. The height of the face wall is more than 15 m, there is no basement in it. The total floor area is 1,375 sq. m. The structural layout is frameless with lateral load-bearing walls, which consist of clay brick and lime mortar. Floor decks are wooden.



Fig. 1 «Station hospital» before restoration (2006)

Today it is expected to be used for town authorities. Besides, there will be a dining room for 50 persons on the basement floor. For this reason, works on deepening of the basement below the existing foundation footing have been done in Tobolsk.

As preliminary work, depreciation analysis and inspection of the building load-bearing structures were made. It was established, that the building was out-of-commission and thus, it was necessary to renew roof construction and floor decks, partially to replace brick layout, repair cracks and reconstruct faces of the building walls. The foundations being walls' broadening and didn't have water isolation, but there were not any other construction defects.

The soil of the ground bed was composed of loams of various densities ranging from firm-stiff to soft-firm (consistency index Ic classification, ISO 14688). Physical-mechanical properties of the ground are presented in Table 1. The ground-water level was not found through 8m of depth from the ground level.

Table 1. Physical-mechanical properties of the ground

Depth of taking sample, m	Unit weight γ, kN/m^3	Water content W, d.f.	Liquidity index I_L, d.f.	Void ratio e	Angle of internal friction φ, °	Cohesion intercept C, kPa	Oedometric modulus E_{oed}, MPa
0-0,5	17,3	0,27	-	-	15	10	3,5
0,5-3,3	18,5	31	0,62	0,9	13	13	2,4
3,3-4,9	18,3	28	0,6	0,87	15	15	2,6
4,9-6,5	18,6	27	0,52	0,83	16	17	3,1
6,5-8	18,2	30	0,48	0,91	16	18	3,3

During restoration of "Station hospital", its painterly architectural look, agreeable with the time of construction, was recreated. Floor loading increase with basement floor building below the existing foundation footing was rather difficult geotechnical task. It was necessary to ensure durability and fixity of the "Station hospital" foundation during execution of work. If not, the whole of structure could undergo structural failure.

Basement floor construction was carried out by using gentle construction technology, embracing (fig. 2):

1. Soil densification of interior and external walls of strip foundation by root piles;
2. Removal of the ground to a depth of basement deck;
3. Installation of the caisson slab with connecting rods;
4. Placing of the welded mesh of caisson walls in the permanent position, combining it with caisson connecting rods and existing foundation rods (fig. 3);
5. Concreting of the caisson walls to basement floor beam;
6. Installation of the basement deck.

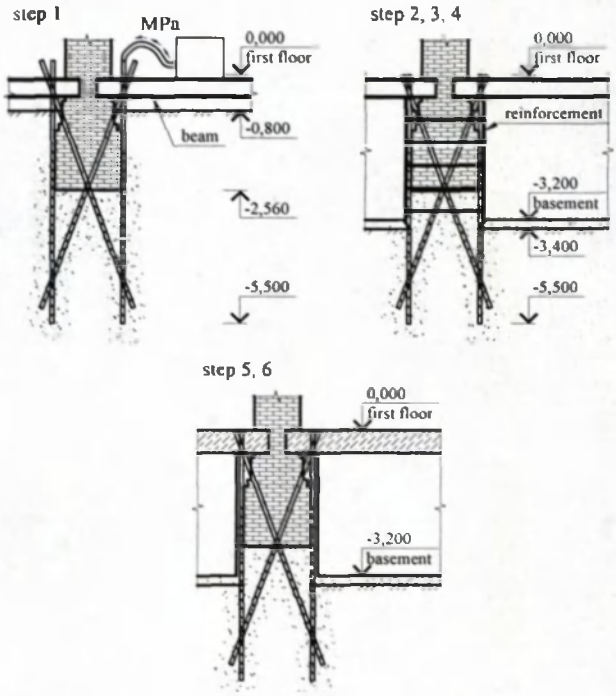


Fig. 2 Operation diagram.

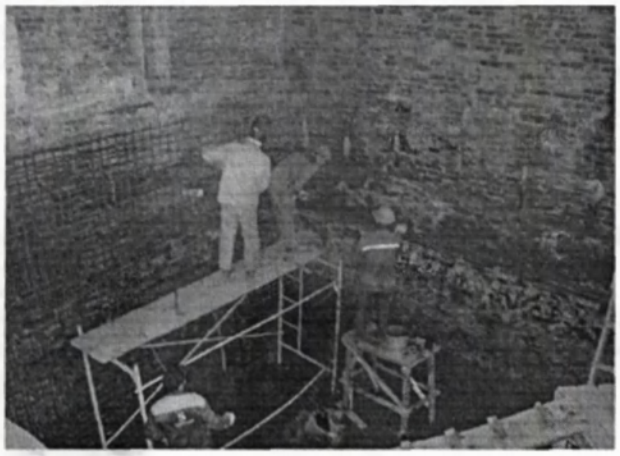
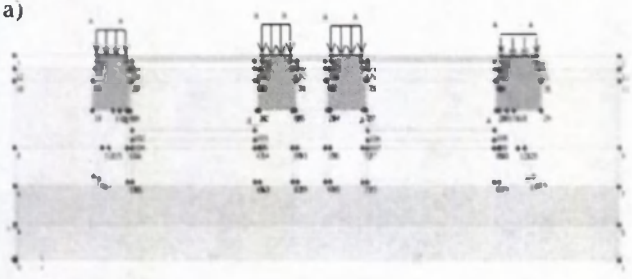


Fig. 3 Placing of the welded mesh of caisson walls in the permanent position.

Soil densification of "Station hospital" strip foundations was made by punched injection piles (root pile), 80mm in diameter. These piles were placed along the existing foundations passing under the angle through them. Injection pressure was from 0,5 to 0,7 MPa. The root piles depth was accepted using the results of the Plaxis 8.x. program computational modeling. Stabilization of the foundation and ground bed was considered. Mohr-Coulomb model was accepted by the standard engineering geology prospecting data in spite of the ground excavation modeling disadvantages. Diameter, root pile length and caisson thickness (stiffness of the structure) were designed by computational modeling. Fig.4 presents the design model.

a)



b)

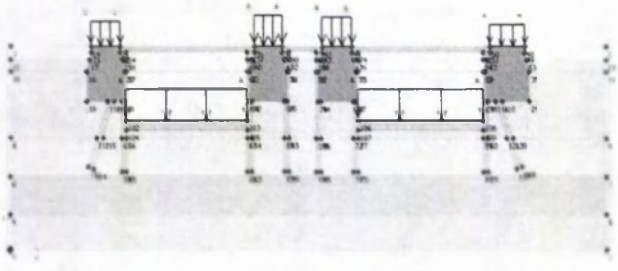


Fig. 4 Design model: a – before basement floor building, b – after basement floor building.

Computational modeling resulted in the following:

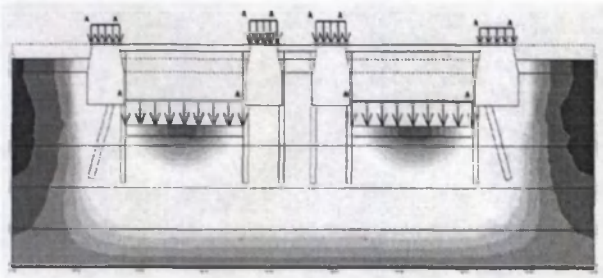
1. Caisson usage minimizes irregular settlements, because of foundation and walls combined action. Stiffness of the substructure increases. Caisson wall thickness equals 200mm, thickness of caisson slab equals 400mm;

2. Minimal pile depth is 5,500mm for regular settlements condition and uncritical advance of plastic strain zone in the basement. Pile diameter is 80mm.

3. Because of Mohr-Coulomb model drawbacks, soil behavior doesn't correspond to the real situation. According to computational modeling, ground raises in 20mm after 2,600mm of basement excavation.

4. Caisson usage balances the settlements of the whole of building (fig. 5b). Design settlement is 50mm. But there are some areas with more than 50mm settlements under the caisson. It happens because the Mohr-Coulomb model has no soil elastic modulus. There is only modulus of deformation in this model (Shashkin et al. 2005).

a)



b)

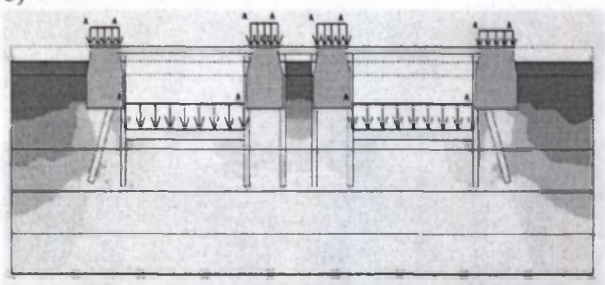


Fig. 5 a) Vertical stress isolines; b) Vertical displacement contours.

In April 2010 restoration work of "Station hospital" started. The authors monitored construction technology of basement floor building such as injection pile generation, soil excavation, erection of insitu reinforced concrete caisson.

Geotechnical monitoring resulted in the following:

- This method of basement floor building excluded limit pressure rise in building structural members;
- Maximum settlement was 20mm, average settlement was 16mm;
- Practical injection pile shape was different from pile shape used in computational modeling. It had root shape with lots of hydraulic fracturing.

This method of basement floor construction excluded critical additory deformation of the structure, cracks in bearing constructions and can be applied in analogous conditions. In November 2011 restoration work of "Station hospital" was finished and the building was ready to be housed by the town government. Fig.6 presents the exterior of "Station hospital" after restoration.



Fig. 6 «Station hospital» after restoration.

REFERENCES

Barabanova, L. P. (1986). A study about (is dedicated to the 400 years of Tobolsk), Sverdlovsk.

Shashkin A. G., Shashkin K. G. (2005). "Elasto-visco-plastic model of unstable structural clay soil." J. Urban redevelopment and geotechnical engineering, 9, 221-228.

Vulnerability assessment of Jamma Masjid, New Delhi: a case study

Neelima Satyam.D and Prasanna kumar.M
Earthquake Engineering Research centre.

ABSTRACT: This paper discusses seismic analysis of a historical building Jama Masjid located at Delhi (falling in seismic zone IV according to Indian seismic code) to predict the state of damage in case of earthquakes. The seismic analysis is done by using SAP2000 and ANSYS, which are usually very helpful to analyze the dynamic behavior and to interpret the experimental results. The results that contains large uncertainties such as the structural size of the various elements cannot be evaluated with the needed accuracy, the material characteristics such as the tension–strain relationship and strength are not known, the structure and materials often exhibit inelastic behavior whose effectiveness in connecting walls is uncertain and neither the depth of the foundation nor their geometry and material properties are known. Often the depth is variable as well as the soil characteristics. A model is designed for detailed analysis which helps to have an idea about the dynamic properties of the building. Then dynamic analysis and time history analysis are made by giving the mechanical properties of the stone used in the construction of the building then the experimental results are compared with those obtained by means of a simplified finite element model that reproduces the complex nature of the building. The results obtained are very useful to predict where the stresses could be concentrated and where cracks or damage could initiate under seismic actions. Such an analysis is very important both to identify areas in the structure particularly vulnerable to earthquakes and to plan an effective building retrofit program to resist seismic effects.

Keywords: seismic vulnerability, vulnerability function, response spectrum, mode shapes.

INTRODUCTION

Most of the structure codes in the world explicitly or implicitly accept structural damage to occur in a structure during strong earthquakes as long as there is no hazard to life. Many earthquakes have caused such damage in the past seismic design codes which were improved after each earthquake disasters, but old constructions were unprotected by new technology. The damage to built environment during recent earthquake in India has demonstrated the need for seismic risk assessment that is capable of predicting the consequences of earthquakes. The collapse of man-made, engineered and non-engineered structures during an earthquake is the chief contributor to the loss of lives and injuries to the people.

Given that the historical importance fabric their specific vulnerability which relates not only to the level of high damage leading to collapse, but also to losses associated with medium damage, caused by moderate earthquakes. The idea of strengthening historical structures to improve their resistance to earthquakes is not new. Throughout the history of structure there have been devices used to enhance earthquake resistance, particularly in those areas of India where occurrence of damaging earthquakes is more frequent.

For instance, the use of corner return stones of bigger dimension walls, to ensure integrity and transfer of actions between walls. In this paper our object of concern is Jama Masjid located in Delhi, which falls under zone IV (IS 1893). Figure 1 represents the seismic zoning map of India.

A preliminary model is studied with the objective of finding elements of the structure which are weak and analysis is done which will be helpful in suggesting any retrofitting methods to be employed.



Figure 1: Seismic Macrozonation Map of India (IS 1893:2002)

1) Seismic Vulnerability

Seismic vulnerability is a measure of damage caused in case of an earthquake by both seismic and induced hazard. A vulnerability assessment needs to be made for a particular characterization of the ground motion, which will represent the seismic demand of the earthquake on the structure.

The ground movement due to an earthquake does not happen in a fixed direction. For regular structures, it is common practice in to consider the earthquake action separately in two orthogonal directions, usually corresponding to the principal axes of the structure. Thus, for one structure two vulnerability functions are calculated. For earthquake scenarios, the direction of an earthquake is usually not taken into account and based on the two vulnerability functions in the two principal directions; a single representative vulnerability function of the structure has to be calculated. This representative vulnerability function should describe the overall behavior of the structure and hence should be some sort of 'mean' of the two vulnerability functions in the two principal directions. Choosing the most unfavorable vulnerability function of the two would lead to a worst case scenario which is not desired in the case of earthquake scenarios, as it can be assumed that on an average the structure behaves better. For very irregular structures the two vulnerability functions in the two principal directions might be very different and thus the direction of the earthquake action plays an important role.

A vulnerability function is a relationship which defines the expected damage for a structure or a class of structures as a function of the ground motion. The two key elements of vulnerability analysis are the capacity of the structure and the seismic demand. In order to estimate the damage, the ability of the structure to resist constraints (capacity of the structure) must be compared with the constraints on the structure due to the earthquake ground motion (seismic demand).

The capacity of a structure to resist seismic action is represented by a capacity curve which is defined as the base shear acting on the structure as a function of the horizontal displacement (Δ) at the top of the structure (also often referred to as a pushover curve). The shear capacity of the structure refers to the maximum base shear the structure can sustain and the displacement capacity refers to the ultimate displacement at the top of the structure.

Seismic demand is determined by using response spectrum. Response spectrum represents the maximum response of single-degree-of-freedom systems (SDOF) as a function of their frequencies. A displacement S_d response spectrum is used with regard to force based design and assessment procedures. Varying the intensity of the seismic demand by increasing the spectral displacement continually from zero onwards, the displacement demand of the structure increases continually and a curve of S_d - Δ is obtained. Only when the damage is taken into account, the vulnerability function is obtained. The top displacement must therefore be associated with a measure of damage.

2) Jama Masjid

Jama Masjid of Delhi is the largest mosque in India. Originally called the Masjid-i-jahan-numa, or 'mosque commanding view of the world', it stands at the center of the erstwhile capital city of the mughals, Shahjahanbad and across the road in front of the red fort. The Masjid is located on a mound in the heart of the old city and projects beautifully into the old-Delhi skyline. It is one of the last architectural works of the mughal emperor Shah Jahan.

The Masjid has three great gates, four towers and two 40 m-high minarets constructed of strips of red sandstone and white marble. The mosque faces west. It's three sides are covered with open arched colonnades, each having a lofty tower-like gateway in the centre. The mosque is about 261 feet (80 m) long and 90 feet (27 m) wide, and its roof is covered with three domes with alternate stripes of black and white marble, with its topmost parts covered with gold. Two lofty minarets, 130 feet (41 m) high, and containing 130 steps, longitudinally striped with white marble and red sandstone, flank the domes on either side. The minarets are divided by three projecting galleries and are surmounted by open twelve-sided domed pavilions. On the back of the mosque, there are four small minarets crowned like those in the front. The mosque stands on a platform of about five feet (1.5 m) from the pavement of the terrace. Figure 2 shows the elevation of the Jama Masjid.

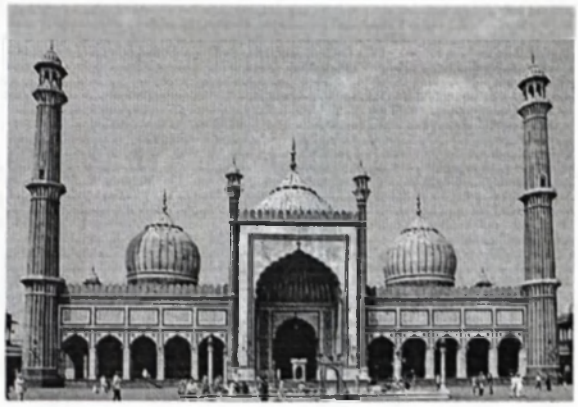


Figure 2: Picture of Jama Masjid, New Delhi

3) Modeling and Analysis

Various models with different characteristics are applied to estimate the behavior of structures ranging from very simple elastic models to complicated elasto-plastic finite element models which take the effects of cracks into account. Apparently the accuracy of the estimated behavior of adobe structures depends on considering different characteristics of the material. But there is another important point which may affect the accuracy of a model that is the 'uncertainty' and 'diversity' of dimensions and materials used in rural houses.

A linear model of Jama Masjid is produced using SAP2000 to investigate its seismic behavior and evaluate different retrofitting method. In the model plan area of the Masjid is taken as 80mx27m and three domes and were modeled, while eah minaret is teken as 41m.The structure was modeled with uniform elements representing the Delhi red sand stone. Shell elements with 4 nodes and 6 degrees of freedom in each node were applied using SAP2000. These shells have the ability to take into account the thickness (thick-plate shells). Shells which were used for roofs have different thicknesses according to the real Jama Masjid structure. Later, the mechanical properties of uniform elements i.e., red sand stone are taken as in Table 1. Sandstones are physically very hard, compact, fine grained, equi-granular homogeneous rocks of sedimentary nature.

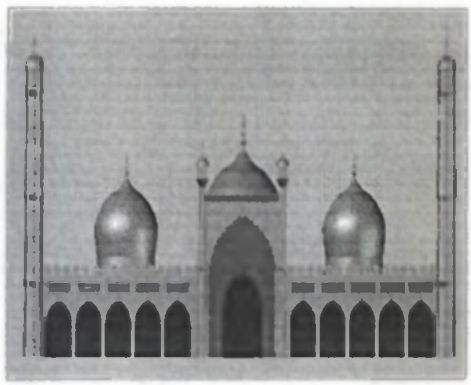


Figure 3: 3D-Model of the Jama Masjid

Table 1: Mechanical properties of red sand stone

Color	Minor color tonal variations exist but within the tolerance limit.
Hardness	6.5 to 7 on Moh's scale
Density	2.3 to 2.4 Kg/cm^3
Compressive Strength	90 to 140 N/mm^2
Modulus of Rupture	16-40 N/mm^2
Water Absorption	1.0 - 1.2 %
Porosity	Low to very low
Weather Impact	Resistant

2001 Bhuj recorded earthquake data with a magnitude 7.7 is considered in the present study using SAP2000 and time history analysis is carried out for the structure and response spectra curves are traced out at different joints of the structure and deformed shapes at different modes are taken.

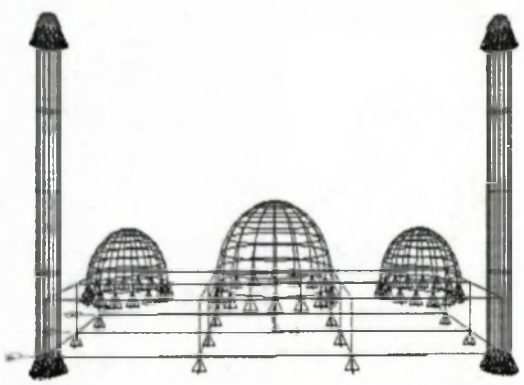


Figure 4: 3D Skeletal structure of Jama Masjid (SAP2000)

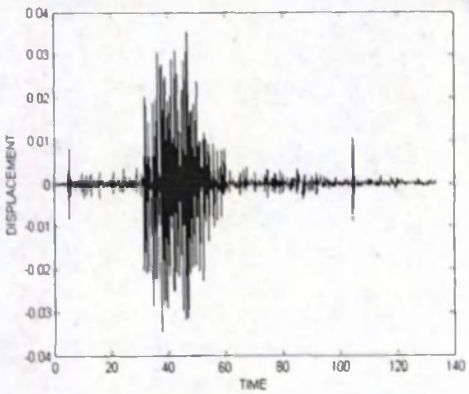
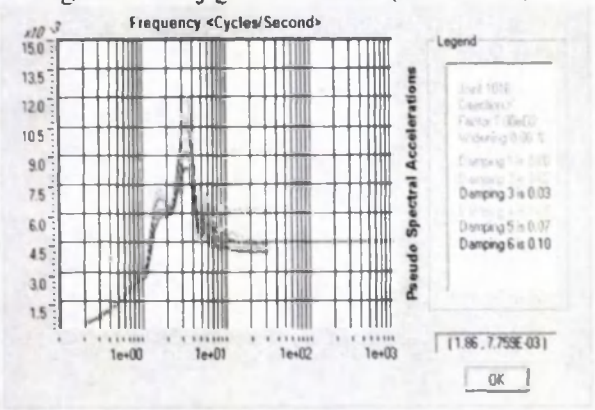
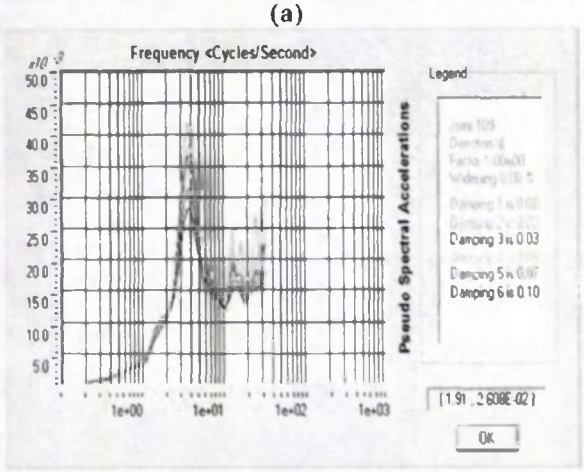


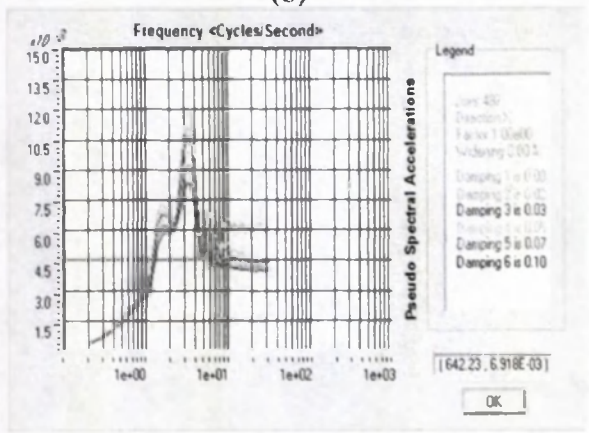
Figure 5: Bhuj ground record (MATLAB)



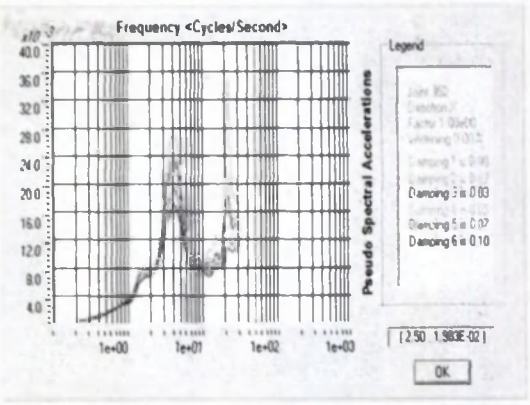
(a)



(b)



(c)



(d)

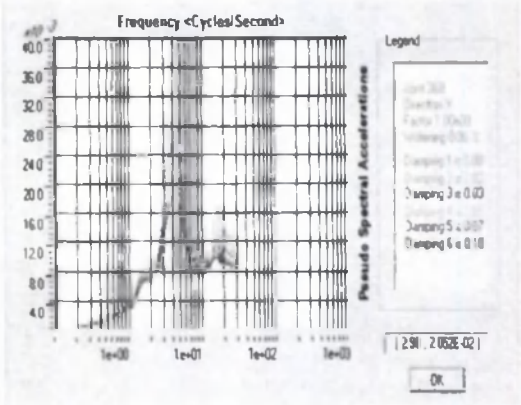


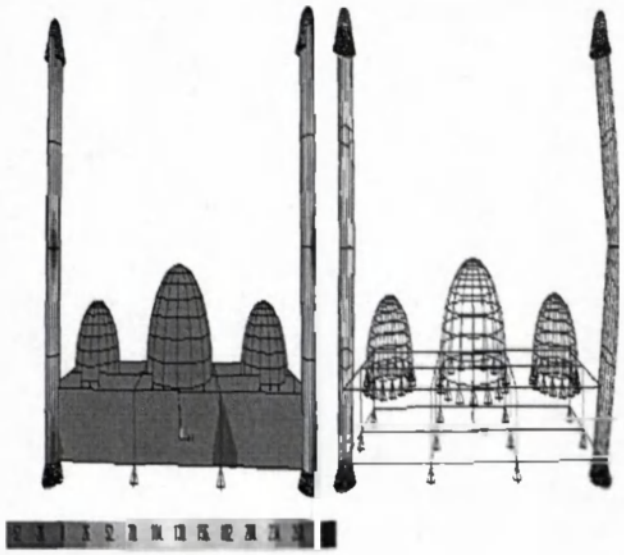
Figure (e)

Figures 6(a), (b), (c), (d) and (e): Response Spectrum curves at different joints

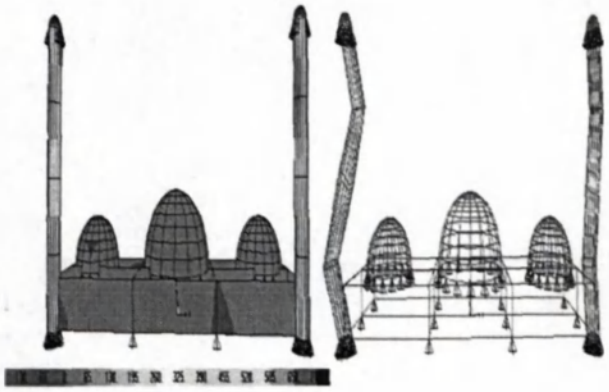
4) Results:

In the study of vibration in engineering, a mode shape describes the expected curvature (or displacement) of a surface vibrating at a particular mode. After the analysis was done, the structure deformed shapes are taken down and depending on the stress range graph, maximum damage at different areas for different mode shapes are found out and at that damaged areas joints are taken and response spectrums are traced out.

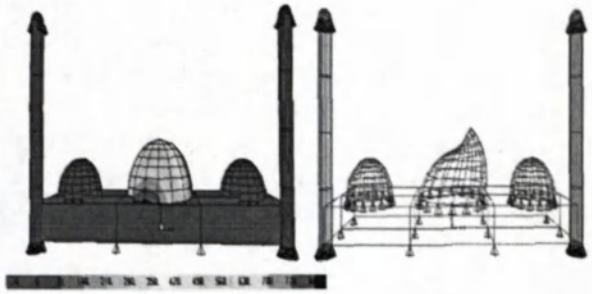
In the first mode shape as in Fig. 7(a) stress concentration at the center of the minarets are more; so, when earthquake occurs mainly the minarets are prone to damage. In the second mode shape Fig 7(b), stress concentration near top and base of the minarets is more. Mode shape 3 in Fig. 7(c) shows that the stress concentrations is more on left edge of middle dome and in mode shape four Fig.7 (d), it is more on the left edges of two small domes. By observing the mode shapes of the structure, it has been found out that the above mentioned sections of the structure are prone to damage when an earthquake occurs and hence retrofitting is suggested.



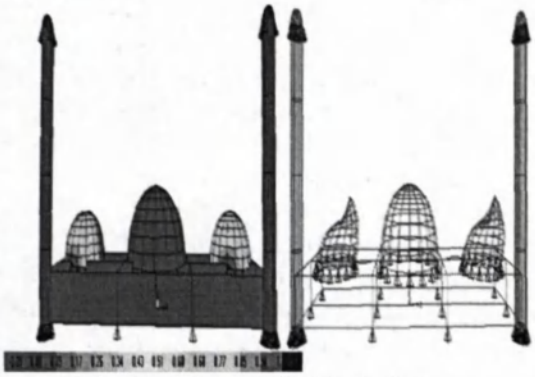
(a)



(b)



(c) (d)



Figures 7(a), (b), (c) and (d): Mode Shapes

CONCLUSION

Seismic vulnerability is dependent on the possibility of implementing strengthening programs. Given the cultural and economic value attached to the historic structures, however, interventions should be tailored to suit structural requirements of each building type, and provide sufficient reliability of performance in future earthquakes.

In light of this Jama Masjid of Delhi which is one of the monument with great historical importance has been considered. Its model is developed using SAP2000 with Bhuj earthquake data as input. Response spectrum curves are traced and mode shapes are taken to observe the stress concentration on the structure for seismic forces during the earthquake and vulnerability functions are derived the results obtained predicted the stress concentration, cracks propagation or damage under seismic loads.

Hence, in this study areas in the structure particularly vulnerable to earthquakes has been identified and retrofit program to the weak sections viz, miners and domes is suggested. This is an application to show the capability of the procedure to quantify reduction in vulnerability associated with strengthening implementations for different typologies.

REFERENCES

1. IS 1893:2002 ;criteria for earthquake resistant design of structures
2. (Part1) General provisions and buildings.
3. MATLAB; Developers THE MATHWORKS.
4. SAP2000; Developers Computers and Structures, Inc.
5. M.A. Ghannad, A. Bakhshi, S.E. Mousavi Eshkiki, A. Khosravifar. Y. Bozorgnia,
6. A.A. Taheri Behbahani; 'A study on seismic vulnerability of rural houses in Iran'; 3-8 September 2006;First European conference on earthquake engineering and seismology;Geneva; Switzerland.
7. Shunsuke Otani; 'Seismic vulnerability assessment methods for building in Japan'; September-2000; Earthquake engineering and engineering seismology.

Древняя ирригация Средней Азии

Джафар Ниязов
Институт истории, археологии и этнографии им. А. Дониша АН РТ
Рустам Мукимов
Таджикского технического университета имени академика М.С. Осими.

АННОТАЦИЯ: Древние гидротехнические сооружения Центральной Азии являются уникальными инженерными сооружениями которые с успехом служили в течение нескольких десятков веков и сохранившись до настоящего времени, что свидетельствует об их неповторимости и высоком инженерном искусстве мастеров прошлого. Эти сооружения несут в себе множество положительных традиций, достойных изучения историков, археологов, инженеров.

Инженерное искусство Центральной Азии имеет давние традиции. В частности, уже в эпоху бронзы (III – середина II тысячелетия до н.э.) и раннего железного века на территории Средней Азии (низовьях Мургаба, среднем течении Зеравшана, Северном Афганистане и др.) местное оседло-земледельческое население сооружало каналы, дамбы, водораспределительные устройства, акведуки, водохранилища для искусственного орошения сельскохозяйственных угодий.

Территория Таджикистана, занятая большей частью горно-предгорным рельефом и обладающая высокой сейсмической активностью, несколько тысячелетий назад также выработала устойчивые традиции инженерного и гидротехнического строительства, которые почти без изменений дошли до средневекового периода. Так, уже в эпоху энеолита (V- сер. IV тысячелетия до н.э.) и бронзы было осуществлено строительство оросителя в бассейне реки Зеравшан с регулированием отвода воды в искусственные каналы в районе поселения Саразм в близи современного Пенджикента. После строительства отводного канала на территории поселения появились водоёмы (самый крупный имел диаметр около 50 м и глубину более 3 м).

Большинство оросителей (среди них и подземные водоводы, прорубленные в скалистом грунте - каризы) эпохи античности проведено по крутым склонам саев и ущелий. Их относительно хорошая сохранность является свидетельством того, что древние гидростроители были знакомы с последствиями частых землетрясений, знали простейшие измерительные инструменты и были сведущи с основными методами прикладной геометрии.

Самый ранний кариз, исследованный археологами, является Санги Сурох, датируемый II в. до н.э. в Зеравшанской долины. Тоннель подземного водовода прорублен зигзагообразно. У каждого зигзага с боку тоннеля прорублено отверстие, предназначенное для выброса породы при строительстве и очистки от ила в период эксплуатации. Боковые отверстия закрывались камнями и дерном. Постепенно, как пишет археолог
У. Эшонкулов, оно было усовершенствовано, т.е. отверстия уже прорубались под углом, и наполненный водою тоннель эксплуатировался надежно.

Наибольшее количество ирригационных сооружений в зонах с просадочностью грунтов и высокой сейсмичностью сохранилось с раннесредневекового периода (в горных районах Бутгама в верховьях Зеравшана, в предгорных долинах рек северного склона Туркестанского хребта, т.е. Уструшане, в равнинных долинах Вахша и др.). В средневековом Востоке в целом сформировались четыре вида искусственного орошения: ручьевое, речное (с помощью искусственных самотечных каналов, водоподъемных сооружений и водохранилищ), каризное (с выводом грунтовых вод наружу при помощи водосборных галерей) и колодезное. В Уструшане, согласно исследований А.И. Билалова, имелись речное, ручьевое и каризное водоснабжение. Причем, с учетом местных особенностей (горно-предгорный рельеф, просадочность грунтов, сейсмичность и др.) здесь также строились каналы, проведенные по склонам гор, каризы с горизонтальными очистительными колодцами, подземные каналы с вертикальными колодцами и каналы на равнинах.

Один из русских исследователей XIX века с восхищением писал следующее: «Мы изумляемся, видя, что столь неразвитый в техническом отношении народ сумел отвести

на свои поля воду в крутой гористой местности...мимо гор и долин...удивляемся при виде каналов...исподволь спускающихся к долине вдоль отвесных стен, на половинной высоте их, и высеченных в твердой каменной массе...». При строительстве этих каналов применялись различные приемы, способствующие беспрепятственной подаче воды и обеспечивающие удлинение срока службы каналов. Так, в необходимых случаях каналы укреплялись каменными стенами, снабжались акведуками в виде лотков-желобов на деревянных подпорках. Многие из этих гидротехнических и инженерных сооружений приходилось нам наблюдать во время участия в археологических экспедициях в Северном и Центральном Таджикистане.

Так, во многих горных селениях Средней Азии, в том числе, например, в верховьях Зеравшана, имеются древние арыки, которые берут начало в глубине ущелий и питаются из родников и крупных рек. Они часто проходят выше селений с тем расчетом, чтобы можно было орошать удобные для посевов склоны горы. Орошение в горных ущельях уходит своими корнями вглубь веков. Например, канал Джуи Бекарон в восточной части правобережья Верхнего Зеравшана был проложен ещё в VII-VIII вв. Сохранились названия многих древних каналов, например, Мугобод в Палдораке, канал Охуна в Кабудбуид, канал Баходура (Верхний Зеравшан). В Нуратинских горах известны каналы Аманнулло-арык, Кунсулув, Мурадин тарнов, Оккоя-ата тарнов и другие.

Нехватка воды вынуждало жителей гор искать пути решения этой проблемы путем строительства отводных каналов, плотин, акведуков. Водоёмы устраивались в широком месте сая. Во избежание повреждения плотин водой её часто возводили не поперек сая, а наискось, под острым углом, в сторону орошаемого поля. Плотина (сарбанд) возводилась из камня в несколько рядов с тем, чтобы вода её не прорвала. Толщина небольших плотин обычно составляла около 2 м.

Одним из подобных сооружений является водохранилище «Хонбанди» в ущелье Асмансай Зеравшанских гор, где плотина имеет высоту более 15 м с длиной осования 24,3 м. Водохранилище было сооружено в X веке и просуществовало до конца XII века.

В долине Сох (верховья Исфары-сая) широко пользовались водоподъемными сооружениями типа чигирями – «чархи фалак», который состоял из трех основных частей6 из колеса-«чарх», обода и поперечных лопастей – «парак».

Обязательным компонентом арыков-каналов были акведуки. В Самарканде известен свинцовый акведук, снабжавший водой городище Афрасиаб с античных времен до прихода монгольских войск, разрушивших эту систему водоснабжения. Акведуки были и в виде сводчатых галерей, а также из гончарных труб – кубуров.

Своеобразные акведуки обнаружены в горных селениях Нураты Самаркандской области. Здесь они представляют собой высокие стены, выложенные из камня, по верху которых проложен арык. Эти стены с арыком называются «аржам» и «тарнов». Подобная подпорная стена-тарнав часто имеют длину до 30 м и высотой – 6 м. Их строительство исследователи относят к XVI-XVIII вв. Переброска воды через пересеченную местность с помощью подпорной стены бытовала и в Горном Бадахшане. Подтверждает это стена с многоводным каналом высотой 20 м в селе Намгути Поён в Ишкашимском районе. Специалисты считают, что каменная стена с каналом поверху более устойчива при ливнях и оползнях. Поэтому горцы возводили стену, примыкающую к оврагу, которая функционально и конструктивно оправдала себя и прошла проверку веками. Все подпорные стены имеют толстые основания с утонением кверху. Для устойчивости стены у основания сажаются деревья, стволы которых подпирают подпорную стену.

В горах Бахмала обнаружены акведуки, где деревянные желоба-тарнов поддерживаются каменными стойками в виде пирамиды высотой 1,2-2 м, установлены они через каждые 10-15 м. Акведук такой конструкции из Хуфской долины изучен этнографом М.С.Андреевым в 30-х годах XX века. Высота каменных устоев достигает здесь 6-7 метров.

В Сохе при проведении каналов по обрывистым склонам в них вбивали деревянные или железные клинья, используя специальные углубления. На клинья-кронштейны накладывали доски, а над ними прибивали стойки – «тиргак». Поверх досок укладывали три-четыре слоя дерна. Затем прокладывали неглубокие канавки для протока воды. Здесь, в бассейне реки Сох 1935 году был сооружен многоярусный акведук деревянной

конструкции. Высота нижнего яруса было около 6 м, ширина - 4-5 м. Наращиваемые ярусы уменьшались по высоте и по ширине. Общая высота сооружения составила около 40 м. На последнем ярусе был устроен деревянный водосток. Этот акведук снабжал водой жителей села Хушьёр до 1943 года.

Каризы, проводимые в горной местности, имели ширину 1,5-2,3 м при высоте 1,3-2,0 м. Вертикальные очистительные колодцы были круглые диаметром 1,5 м, их глубина составляла в зависимости от рельефа местности 7-40 м. Длина же каризов было от несколько сотен метров до 25 и более километров. Строительство таких водоводов (например, Токсанкариз, Ишанкариз, Обхурак и другие в верховьях Зеравшана или в Шахристане, Басманде, Ганчи, Дахкате и др.) помимо громадных затрат труда, требовало определенных инженерных знаний и опыта. Это обстоятельство подметил Садриддин Айни, основоположник таджикской советской литературы, первый президент Академии наук Таджикистана, написавший статью «Туксонкариз» ещё в 1940 году (древнейший кариз в верховьях Зеравшана, который в 1871 году в течение 10 месяцев был восстановлен)

В частности, он писал, что подобная работа представляла физическую трудность, но было ещё труднее с научной точки зрения, так как канал, проходящий от начала до конца под землей, нужно было проводить так, чтобы вода проходила беспрепятственно. Если бы строители не опирались на научную основу, то или излишек воды смыл бы сооружение, или ил и камни, несомые водой, в течение недели закупорили бы канал и тем самым уничтожили бы многолетний труд.

В средневековый период на территории Таджикистана практиковались подземные водоводы из керамических труб – кубуров диаметром до 50-60 см. Примером может служить самотечный 40-ка километровый кубурный водовод в Аштском районе, который в IX-XI вв. доставлял воду из предгорий Кураминского хребта в средневековый город Хаджистан и его округу с соляными промыслами близ озера Аксукон.

Из других средневековых видов гидротехнических сооружений следует назвать сардобы и водоёмы. Сардобы-цистерны в основном были распространены вдоль торговых путей в пустынных и степных районах Средней Азии.

По конструкции сардоба представляла собой подземный резервуар, выложенный жженым кирпичом и перекрытый куполом или сводом, предохраняющим воду от загрязнения и испарения. Для того, чтобы вода не просачивалась грунтовыми стенками, их выкладывали жженым кирпичом и покрывали специальным гидравлическим раствором, называемым «кыр». На территории Таджикистана цистерна-сардоба изучена археологами А.М. Беленицким и Е.А. Давидовичем близ Куляба.

В Северном Таджикистане в средние века стоились и плотины. Как отмечает В.В. Бартольд, только в бассейне Зеравшана, в округе Самарканда, было 8 каналов, на которых было устроено 680 плотин. Остатки плотины для регулирования подачи воды в сети других каналов замечены в окрестностях Ругунда близ Истравшана.

Несомненный интерес представляют остатки плотины Сар-и-Банд, обнаруженные в Сурхандарьинской области Узбекистана, входившими в ареал распространения таджикоязычного населения. Его единственным и притом нерегулярным водным источником является Кофрун-Сай, который заполняется водой только во время зимних дождей и весенних селевых потоков. Для сохранения этих вод и их разумного использования в сельском хозяйстве здесь и было сооружено водохранилище. В настоящее время большая часть плотины водохранилища разрушена до основания. Сохранились лишь ее боковая северо-восточная часть, упирающаяся в обрывистый песчано-глинистый берег сая, а также часть основания.

Помимо плотин таджикские гидростроители сооружали и специальные водохранилища, где собиралась вода и затем распределялась для орошения полей системой наземных и подземных каналов. Всего же только в Уструшане А.И. Билалов отмечает свыше 3 тысяч ирригационных сооружений, которые орошали более 200 тысяч гектаров земли. Подобная сеть ирригационных сооружений существовала и в долине реки Зеравшан, в её горной части.

Одним из творений инженерного искусства в историческом прошлом Таджикистана являются также водоподъемные устройства – чархпалак или чигирь. Они сохранились с незапамятных времен и до сих пор исправно служат во многих селениях и городах из-за простоты конструкции и

эксплуатации. Такие водокачки нами обмерены в Исфаринском и Пенджикентском районах, их можно увидеть и сейчас в городе Душанбе и в других местах Таджикистана, Узбекистана, Кыргыстана и т.п. Например, чархпалак в Исфаре представляет собой большое деревянное колесо с радиальными связями-лопастями, выходящими за пределы его внешнего контура. На концах этих лопастей укреплены гончарные сосуды с широким горлом. Колесо устанавливается вертикально на горизонтальную ось (диаметр колеса – чарх зависит от глубины уровня воды канала), которая покоится на двух стойках, вбитых в дно реки.

Под напором воды лопасти колеса приходят в движение, поднимая вверх наполненные водой сосуды. На верхних отметках сосуды опоражнивают воду на лоток, устроенный на стойках со стороны берега, с лотка вода вытекает в канаву, ведущую на огород или сад сельчанина. При необходимости водоподъемное колесо можно застопорить, тем самым, прекращая подачу воды на лоток. Для уменьшения количества воды, подающей на арыки-каналы, достаточно приоткрыть щель в лотке, откуда вода вытекает обратно в реку, а необходимое количество воды подается на орошаемое поле или участок.

Подобные чархпалаки можно устанавливать по несколько штук в ряд вдоль обоих берегов реки для каждого домовладения в отдельности. Чрезвычайная простота конструкции, безопасность и высокий коэффициент полезного действия позволили широкому распространению этих гидротехнических устройств по всей Средней Азии. Их можно увидеть и сейчас во многих селениях и городах, где высокие берега рек или каналов не позволяют устраивать водоотделительные сооружения.

Таким образом, можно заключить, что инженерные сооружения, построенные в прошлом на территории стран Центральной Азии, с успехом служили на протяжении многих веков и некоторые из них сохранились до настоящего времени. Это свидетельствует о том, что эти уникальные инженерные сооружения, построенные в сложных климатических и геологических условиях региона, несут в себе множество положительных традиций, достойных изучения и преемственности, как с точки зрения истории, археологии, также и инженерно-технических наук.

Литература:

1. Айни С. Канал Туксонкариз. // Точикистонн сурх, 15 мая 1940 года.
2. Андреев М.С. Таджики долины Хуф. Душанбе: Дониш, 1958, вып. 2, с. 29.
3. Бабаханов А. О некоторых древних водохозяйственных сооружениях Узбекистана. // Изв. АН Узб.ССР: серия общественных наук. – 1959, № 4, с. 42-49.
4. Бартольд В.В. Туркестан в эпоху монгольского нашествия. Географический очерк Мавераннахра //Соч., т.1. – М.: Наука, 1963, с., 140.
5. Беленицкий А.М., Давидович Е.А. Сардоба около Куляба. // Тр. АН Тадж.ССР, вып. 13.– Сталинабад, 1956, с. 101.
6. Билалов А.И. Из истории ирригации Уструшаны. – Душанбе: Дониш, 1980, с. 88.
7. Булатов М.С. Геометрическая гармонизация в архитектуре Средней Азии IX-XV вв. – М.: Наука, 1988, с. 1-30.
8. Гулямов Я.Г. Кушанское царство и древняя ирригация Средней Азии // Центральная Азия в кушанскую эпоху. Т.1. – М.: Наука, 1974, с. 119.
9. Литвинский Б.А. Водопровод Так-Языра. // В кн.: Культура и искусство народов Средней Азии. – М.: Наука, 1979, с. 79-84.
10. Миддендорф А. Очерки Ферганской долины. – СПб, 1882, с. 165.
11. Масон М.Е. Проблема изучения цистерн-сардоба. // Материалы Узкомстариса, вып. 8. – Ташкент, 1935.
12. Мукимов Р.С., Мамаджанова С.М., Мукимова С.Р. Инженерное искусство Таджикистана. – Душанбе: Мерос, 1996, с.37.
13. Назилов Д.А. Зодчество горных районов Средней Азии. – Ташкент, 1999, с.140.
14. Петрушевский И.П. Земледелие и аграрные отношения в Иране XIII-XIV вв. – М.-Л.: АН СССР, 1960, с. 117.
15. Ртвеладзе Э.В., Исхаков М.Х. Плотина Сар-и-Банд. // Строительство и архитектура Узбекистана, 1977. – Ташкент, № 1, с. 18-20.
16. Эшонкулов У. История ирригации Верхнего Зеравшана (с древнейших времен до начала XX в. - Автореф. дисс... канд. истор. наук. – Самарканд, 1989, с.5.
17. Эшонкулов У.Э. Оросительные системы восточной части правобережья Зарафшана. // АРТ, вып. XXI (1981 год). – Душанбе: Дониш, 1988, с.126-146.

Устойчивость зданий и сооружений Казанского Кремля

В.Р. Мустакимов
Казанский государственный архитектурно-строительный университет, Казань, Россия.
Р.И. Шафигуллин, С.Н. Якупов, А.В. Мустакимов
ГУП «Татинвестгражданпроект», Казань, Россия.

АННОТАЦИЯ: Приведена краткая историческая палеогеография формирования холма Казанского Кремля, анализ изменения топогеодезических, инженерно-геологических и гидрогеологических условий грунтов в основании зданий и сооружений, расположенных в пределах Казанского Кремля. Изложены результаты расчетов устойчивости пригруженных сооружениями откосов с учетом прогнозного увеличения влажности грунта. Предложены эффективные способы закрепления откосов.

ABSTRACT: The short historical geology of formation of a hill of the Kazan Kremlin, the analysis of change of topogeodezic, engineering and geological and hydro-geological conditions of soil is given in the basis of buildings and the constructions located within the Kazan Kremlin. Results of calculations of stability of the slopes loaded with constructions taking into account look-ahead increase in humidity of soil are stated. Effective ways of fixing of soil of the slopes.

Историческая палеогеография формирования холма Казанского Кремля

В истории формирования и накопления антропогенных отложений на территории Казанского Кремля в соответствие фондовых материалов ГУП «Татинвестгражданпроект», Казанского ТИСИЗ, выделены шесть крупных исторических периодов: 1-й период с 1100 по 1236 г.г., характеризуемый возникновением города Казани и его развитием, как одного из северных городов Волжской Булгарии; 2-й период с 1236 по 1445 г.г. – город Золотоордынско-булгарского княжества; 3-й период с 1445 по 1552 г.г.–город ханского булгарско-татарского княжества; 4-й период с 1552 по 1772 г.г. – столица христианско-татарской вотчины Руси; 5-й период с 1772 по 1917 г.г. – столица Казанской губернии Российской империи; 6-й период с 1917 по 1995 г.г., включая современный период – столица Татарстана в составе СССР, СНГ и России. Следует отметить современный период, с 1995г по настоящее время, в течение которого, проведены и продолжают проводиться геофизические, инженерно-геологические и археологические исследования.

В качестве северного форпоста Волжской Булгарии, Кремлевский холм, представляющий собой мысовый выступ третьей надпойменной террасы реки Волги, был выбран с учетом его стратегического, географического и ландшафтного положения. В результате длительной техногенной деятельности на территории холма, его общий вид и палеогеография подверглись значительному изменению, которые можно разделить на пять условных этапов.

В течении первого этапа - 12-16 в.в., Казанский холм, впервые был подвергнут техногенному воздействию. Произведено увеличение крутизны откосов.

Второй этап датируется 1552 г, с момента покорения Казани Иваном Грозным. К началу XVII века деревянные стены Кремля были заменены массивными кирпичными или каменными стенами и возведено 13 каменных башен. Вместо оборонительных деревянно-срубовых стен Булгарского и Ханского периодов, на старых фундаментах возведены тяжелые белокаменные крепостные стены и семь дозорных башен. К концу второго периода, мощность насыпи или антропогенных отложений, в Кремле достигла до 2,50-3,50м.

а



Рис. 1. Казанский Кремль. Первая половина XVI века. Реконструкция по материалам Н.Ф. Калинина.

В течение третьего этапа (16-20 в.в.), который характеризуется расширением русской империи и христианизации (16-17 в.в.) и превращения Казани в центр огромной Казанской губернии (18-20 в.в.), общая нагрузка на холм возрастает за счет увеличения более тяжелых каменных новостроек. Мощность антропогенных отложений достигла 2,60-4,50м.

К четвертому этапу (1920-1940 г.г.) относится советское время, в течение которого произошли значительные изменения. Почти все христианские памятники архитектуры и культуры были разрушены или снесены. Произош-

ло перераспределение статических нагрузок на грунты. В 30-ые годы на территории Кремля был проложен центральный водопровод, в результате чего усилилось периодическое неравномерное увлажнение насыпи. К концу этапа мощность антропогенных отложений составила 3,00-12,00 м. Важно отметить, что с постепенной утратой крепостными каменными стенами своей функции, как фортификационных сооружений Кремля, и накопления антропогенных отложений с внутренней стороны холма, они превратились в подпорные стены. Произошло изменение расчетной схемы каменных конструкций стен Кремля. Образовался дополнительный комплекс внешних нагрузок и воздействий, включая: боковое давление от собственного веса грунтовой насыпи и пригрузки; интенсификация транспортных потоков по периметру основания откоса и холма; накопление подземной влаги за внутренней гранью «подпорной» стены. В конструкциях периметрально расположенной стены и сторожевых башнях, образовались трещины, а также горизонтальные и вертикальные деформации.



Рис. 2. Рисунок Казанской крепости, выполненный Э.Турнерелли в XIX веке.

Пятый этап (1940-1995г.г., включая, современный период [1-4], оценивается как период с отрицательным дисбалансом геологических и гидрогеологических условий.



Рис.3.

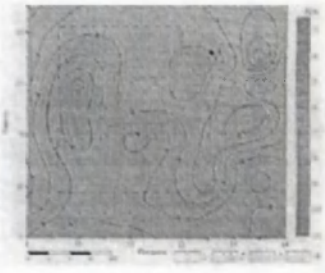


Рис.4.

Рис. 3. - Схема объемной модели рельефа холма Казанского Кремля. Рис. 4. - Карта мощности насыпных отложений по данным электромагнитного зондирования участка башни Сююмбеки; 1-пикеты зондирования; 2-скважина; 3-контуры пилонов Башни Сююмбеки; 4-изолинии мощности антропогенных (насыпных) отложений, м

Объясняется это тем, что проявляется нарушение условий естественного отвода ливневых и паводковых вод с увлажнением антропогенных отложений. В приакваториальной зоне города Казани, после создания в 1956 году Куйбышевского водохранилища, уровня подземных вод повысился на 11 метров. Это является причиной постоянного и более интенсивного подрыва устойчивости потенциально карстующихся инженерно-геологических элементов Казани, включая, массив холма Кремля.

Современные геофизические методы исследования грунтов при помощи электромагнитного зондирования по глубине массива холма Казанского Кремля [3], позволили с высокой достоверностью построить модель рельефа холма, а также горизонтали-изолинии кровли коренных пород и повысило точность инженерных и геотехнических расчетов. Отдельные результаты геофизических исследований геометрии холма и изолиний кровли коренных пород, приведены на рис. 3; 4.

Историко–хронологические и геотехнические сведения о Башне Сююмбеки

Башня Сююмбеки расположена в северо-западной части вершины Кремлевского холма, перед его крутым северным склоном. Участок Башни Сююмбеки находится в зоне потенциально опасных инженерно-геологических процессов, включая: оползневые, карстово-суффозионные.

Высота башни до верха шпиля составляет 58 м, площадь основания 227 м^2. По композиции башня состоит из семи ярусов. Первые три яруса прямоугольные, заканчивающиеся каждый уступами, обходными террасами, идущими вокруг башни. Террасы ограждены кирпичными парапетами.



Рис.5. Башня Сююмбеки. Фотоснимок XIX века -*а*; Фотоснимок 2004 года -*б*; схема башни с разделением на семь ярусов по высоте -*в*

Четвертый и пятый ярусы восьмигранные, шестой ярус представляет собой восьмигранную усеченную пирамиду, на вершине которой, размещен седьмой, дозорный ярус, с шестигранным шпилем, увенчанным небольшим шаром с иглой. В первом ярусе башни имеется проезд шириной 6,55 м, который раз-

деляет ярус на два пилона, северный и южный. Каждый из пилонов представляет собой сплошной массив кладки размером в плане 13,13х5,30м. Проезд перекрыт кирпичным сводом толщиной 27,5 см и двумя арками несущими южную и восточную стены башни.

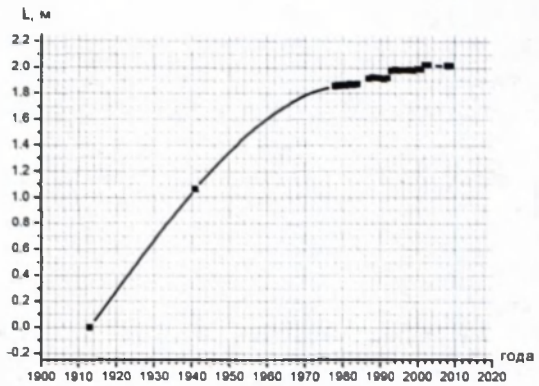
Стены и перекрытия выполнены из кладки керамического кирпича. Размеры полнотелых керамических кирпичей, составляют 295х148х80мм, уложенные на известково-песчаном растворе толщиной кладочного шва 20-25 мм, под расшивку швов. Освидетельствованная авторами, методами неразрушающего контроля, прочность керамических кирпичей, составляет в пределах от 50 до 75 кг/см^2 (марка М50-М75), а кладочного известково-песчаного раствора М15-М25.

Результаты мониторинга за деформациями Башни Сююмбеки

Первые сведения о техническом состоянии башни опубликованы в 1914 г (Ю.Б. Монфред). Отмечался вывал части кирпичной кладки южной торцевой стены, образование и развитие трещин в арочной кладке над проездом. В этот период был выполнен стальной пояс – бандаж на заклепках и металлические стяжные анкеры, а также была заменена часть кладки южной стены. В 1947г, по данным того же автора, на башне были зафиксированы: крен в «ЮВ» направлении с отклонением замка свода перекрытия 7 яруса от геометрического центра горизонтальной проекции основания башни на 1300 мм, а по замерам СНРПМ, отклонение составило на 1280 мм. Исследователями установлена: осадка юго-восточного угла башни и образование сквозных трещин в кирпичных конструкциях стен и сводов на первых 3-х ярусах со стороны восточного и западного фасадов; образование и развитие сквозной вертикальной трещины в южной стене вдоль проходной лестницы; сеть волосяных трещин вдоль замковой части арки проезда, а также разрыв крайней западной затяжки в арке над проездом. В 1957 г произведен ремонт башни и выполнена замена части кладки I яруса. В 1978 г исследователями ГУП ТИГП (О.И. Берим, А.И. Исхаков) было зафиксировано: увеличение отклонения шпиля башни по горизонтали в том же «ЮВ» направлении на величину 1710 мм.

По данным исследований КазТИСИЗ хронология развития крена башни, позволяет установить, что в период с 1913 по 1930 г.г, отмечен быстрый темп образования крена, составляющий 50-52 мм/год. В период с 1930 по 1941 г.г., скорость образования крена снижается до 16,4 мм/год. В течение 1941-1946 г.г., интенсивность крена возрастает и достигает величины 36,0 мм/год. Следовательно, за период с 1913 года по 1946 год накоплено 60% доли отклонения оси башни по горизонтали, которую имеет башня на период последнего замера и в 2010г. равную 2018 мм (рис. 6).

а



б

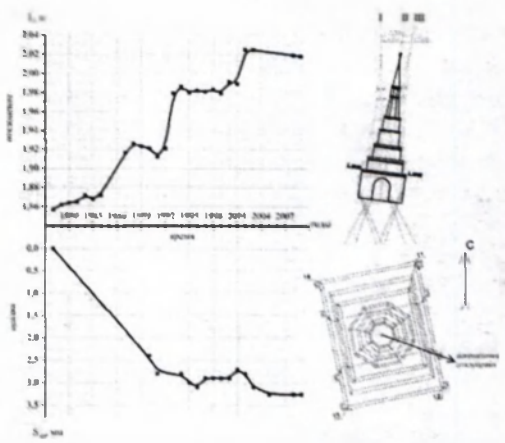


Рис. 6. Зависимость горизонтального отклонения "*L*"оси шпиля Башни Сююмбеки за период с 1913 года по 2010 год (с замеренной величиной отклонения *L*=2018 мм)–*а*; и графики отклонения "*L*"оси башни и осредненной осадки "*S*" Башни Сююмбеки-*б*

В следующий период с 1946 г по 1977 г отклонение практически прекратилось. Возобновление крена с весьма большим темпом 185 мм/год наблюдался в период с ноября 1977 года по декабрь 1978 года. Только за один год этого периода накоплено 10% от общего отклонения. Характер последнего отрезка кривой зависимости $L=f(t)$ показывает спад темпа до нуля и наступление очередного цикла стабилизации крена. Анализ графиков осадок настенных реперов №1234, 1250, 1526, 1900, установленных на конструкциях стен башни, позволяет отметить следующие особенности деформации во времени:

-максимальная общая осадка в период с 1950 г по 1979г.г. произошла на ЮВ углу башни на репере № 1526 – 5,5 см, меньшая осадка на СВ углу на репере № 1250 – 3 см, еще

меньше на ЮЗ углу на репере №1900 – около 2 см и не было практически осадки на СЗ углу на репере №1234;

-кривые по всем реперам имеют одинаковое увеличение темпа осадки в период с 1973 по 1978г.г., составляющей до 3 мм/год; реперы №1250 и 1526, с наибольшей общей осадкой S=1,5см, которая была накоплена в период с 1953 по 1967г.г.; репер №1234 с нулевой общей осадкой S=0,0см в период с 1955 по 1974г.г., испытывал незначительный подъем на 1,5 см относительно начала и конца наблюдений, т.е. в этот период наблюдалось его небольшое перемещение по вертикали вверх, при одновременной осадке другого репера с противоположного угла. По результатам нивелирования трех ярусов башни, можно сделать следующие выводы:

-разница отметок СЗ угла I-го яруса башни, имеющего нулевую осадку, по отношению к осадке ЮВ угла, имеющего максимальную неравномерную деформацию осадки S=90,393-90,097=0,296м=29.6см. Значения абсолютных отметок углов, имеющих идентичную ориентацию по сторонам света одинаковые, то есть: пониженные ЮВ углы, повышенные СЗ, следовательно, ось башни имеет уклон в юго-восточном направлении, как и крен башни "i";

-уклон "i" верха первого (I), второго (II) и третьего (III) ярусов башни, соответственно составил: i_I=0,016 м/м, i_{II}=0,05 м/м, i_{III}=0,1 м/м, то есть верхние ярусы по отношению к нижним, наклонены более круто, следовательно, наблюдается дугообразный изгиб башни вдоль оси. Направление уклона ярусов несколько различается: каждый верхний повернут относительно нижнего на одинаковую величину угла, равную по 10^0 против часовой стрелки. Это означает, что башня при неравномерной её осадке испытывает левосторонний крутящий момент "$M_{кр}$". Принимая во внимание особенность конструкци`и башни, можно смоделировать причинно следственную связь формирования внутренних напряжений в элементах башни и образования трещин, имеющих СВ азимут падения с максимальным их раскрытием в сторону действия крутящего момента "$M_{кр}$".

-основная доля крена продольной оси Башни Сююмбеки (60% от общей величины крена), произошла в период с 1913 по 1946 г.г., затем до 1977 г. – наблюдалась временная стабилизация, а с 1977 по 1979 г.г. крен возобновился и составил 10% общего крена со спадом темпа к началу 1979 г.

Анализ и оценка причин деформаций конструкций, крена и осадки Башни Сююмбеки

К основным причинам формирования и развития имеющихся деформаций конструкций, крена и осадки башни, следует отнести следующие процессы и явлений, в порядке их значимости: физико-геологические, гидрогеологические, конструктивные, гидрологические, антропогенные, природно-климатические, древние и современные техногенные воздействия с учетом современной урбанизации среды (археологические раскопки; реконструкция, ремонт и новое строительство объектов и инженерных коммуникаций; обустройство покрытий асфальтом; вибрационно-динамические воздействия от движения автотранспорта и электричек казанского метро). Среди физико-геологических причин, следует выделить: наличие нерегулярно, расположенных под фундаментом башни, насыпных грунтов, составляющих примерно 30% площади подошвы; возобновление древней карстово-суффозионной деятельности.

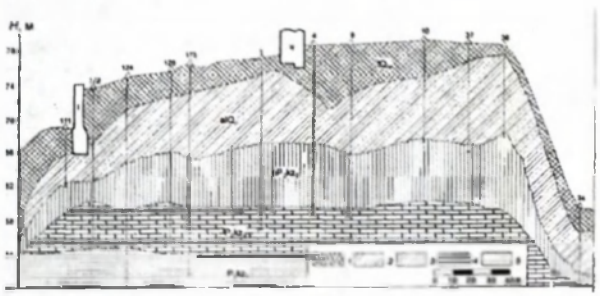


Рис. 7. Схематический геологический профиль холма Казанского Кремля. 1-насыпь преимущественно супесчаная, супесчано-суглинистая с органическими веществами (антропогенные отложения tQ_{IV}); 2-песок пылеватый, супесь твердая, пластичная, суглинок тугопластичный (alQ_{II}); 3-глинисто-карбонатная мука с дресвой и щебнем, с прослоями глины твердой консистенции (eP_2kz_2); 4-доломит, известковистый доломит, известняк (P_2kz_2); 5-песчаник сильно известковистый (P_2kz_1); I-крепостная стена; II-Башня Сююмбеки.

Насыпь преимущественно супесчаного состава, с включениями строительного мусора, кирпичного боя, костей, черепков. До 25% имеются включения в виде фракций песка и дресвы с развитием в восточной трети южного пилона и северо-восточном секторе северного пилона. Мощность насыпного грунта ниже подошвы фундамента, по результатам исследований, составляет 2,5 м.

Вскрытая археолого-геологическими выработками насыпь под подошвой фундаментов пилонов, датируется первой половиной XV века по материальной культуре монгольских и булгарских времен. Вблизи от фундамента, ниже его подошвы, археологическими исследованиями установлена, культура конца XII начало

XIII веков, а на более низкой отметке, вскрыта погребенные грунты. Исследованиями подтверждена гипотеза о наличии древних захоронений под восточной частью южного пилона и непосредственно к югу от него.

Насыпь под СВ углом башни, предположительно, имеет функциональную связь с обрушивающимися древним подземными ходами, либо с захоронением (Мавзолеем). Насыпные грунты, при их увлажнении, значительно снижает свою несущую способность, поэтому ЮВ и СВ углы башни приобрели наибольшую неравномерную деформацию осадки.

Исследование и анализ процесса суффозии аллювиальных и насыпных глинистых грунтов в подстилающие грунты, позволяет установить основные предпосылки к его образованию, включая: благоприятной для суффозии последовательностью расположения инженерно-геологических элементов (ИГЭ) сверху вниз - супесь, песок пылеватый (с прослоями мелкого), крупнообломочные доломитовые элювиальные грунты; возможностью скопления и струйной инфильтрации поверхностных вод в районах мощной насыпи. Следы химической и механической суффозии, в виде минеральных частиц «выноса», обнаружены в песках ИГЭ №3. На расстоянии 50 метров к ССВ от башни расположена граница карстово–суффозионного провала.

Воды верховодки значительно снижают несущую способность грунтов основания, являясь причиной деформации грунта. По результатам метеонаблюдений, в течение XX века были отмечены сверхнормативное выпадение атмосферных осадков в периоды: в 1926 году с осадками -580 мм/год; в 1941 году с осадками -556 мм/год; в 1977-1978 г.г. с осадками до 600 мм/год. Именно с этими годами связаны либо начало, либо высокий темп осадки и крена башни. График зависимости величины отклонения оси башни от вертикали за длительный период эксплуатации с 1913 года по 2009 год (с величиной отклонения L=2018 мм), приведен на рис.7.

К конструктивным причинам следует отнести: снижение пространственной и локальной жесткости и устойчивости конструкции башни, в результате неравномерной осадки с изгибом и креном-кручением II-го и III-го ярусов башни; снижение прочности конструкций фундаментов обоих пилонов башни, выполненных из кладки постелистого бутового камня на известково-песчаном растворе поверх наброски из рваного бута на глиняном растворе, в результате вымывания кладочного раствора подземными водами; гниение оголовков деревянных свай, расположенных под подошвой фундаментов нарушение целостности с разрывом стяжного пояса, выполненного на уровне I-го яруса башни.

К антропогенным причинам, вызвавшим деформацию башни, следует отнести: многочисленные археологические раскопки вокруг башни, некачественное выполнение реставрационных работ; локальное увлажнение грунтов основания башни в результате утечки хозяйственно-питьевых и технических вод; наличие вскрытых исследованиями заброшенных подземных ходов и укрытий в непосредственной близости от башни.

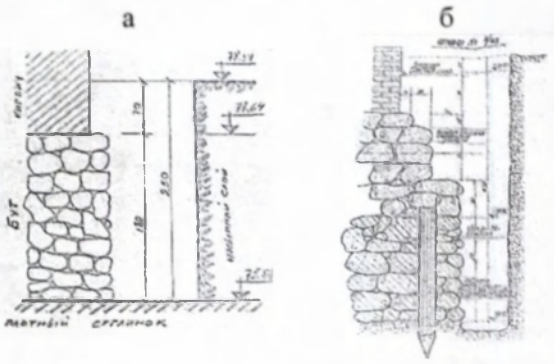


Рис. 8. Разрезы по фундаментам пилонов башни Сююмбеки

Мероприятия по упрочнению грунта основания и усилению фундаментов Башни

По расчетам авторов, общий вес Башни Сююмбеки, составляет - 4133,44 т. По данным других авторов (КазТИСИЗ) -5500 т. Расчетная схема башни приведена рис. 11. Теоретический центр тяжести башни, расположен на высоте 1,36 м от границы 2 и 3 ярусов. Отклонение центра тяжести от вертикали составляет ≈0,7м.

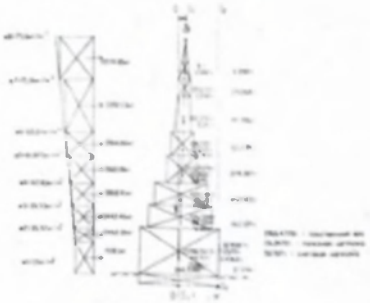


Рис. 9. Расчетная схема Башни Сююмбеки

Для установления предельной устойчивости башни от опрокидывания (на период до проведения работ по усилению сваями) были определены удерживающие и опрокидывающие моменты относительно точки «*M*» которые, соответственно составили: $M_{уд}$=42234,835 т·м и $M_{опр}$=592,84 т·м.

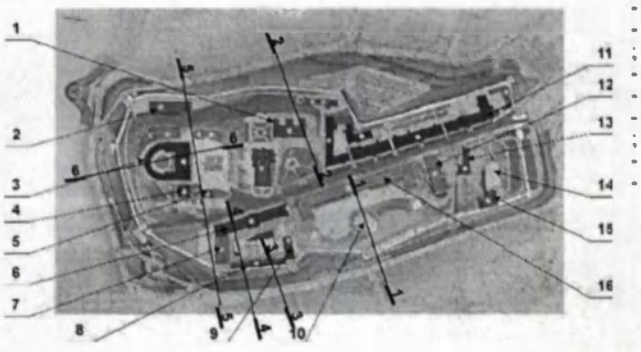
Следовательно, при условии стабилизации положения накренившейся башни, с отклонением центра тяжести на 700 мм, устойчивость обеспечивается, так как удерживающий момент $M_{уд.}$ более чем в 70 раз превышает опрокидывающий момент $M_{опр.}$ Принимая во внимание уникальность памятника архитектуры средних веков, которым является Башня Сююмбеки, для его сохранения и восстановления, были привлечены различные ученые и специалисты, которые выдвинули две основные тенденции из многочисленных вариантов, включая: I-усиление опорных ярусов конструкции башни, включая пилоны фундамента и упрочнение грунтов основания с сохранением накренившегося положения; II-усиление опорных ярусов конструкции башни, включая пилоны фундамента и упрочнение грунтов основания с устранением крена и приведением оси башни в вертикальное положение [9. 10]. Практическую реализацию получила первая тенденция.

В 1992 году фундаменты здания Башни Сююмбеки, были усилены при помощи устройства корневидных буроинъекционных железобетонных свай (БИС) длиной 20 м. Опирание концов БИС осуществлено на коренные породы представленные доломитами. Из 145 запроектированных БИС, фактически выполнено 64, что, как показывает опыт мониторингового наблюдения за устойчивостью башни, в течение 20 лет (рис. 6), является достаточным. По состоянию на апрель 2012 года исследуемая башня имеет стабилизированный крен и сохраняет устойчивое равновесие.

Моделирование НДС откосов и устойчивость склоновых зон холма Казанского Кремля

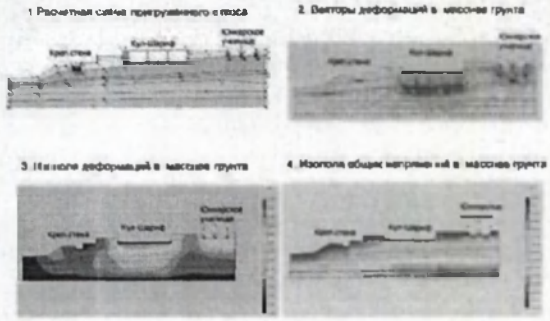
Авторами были проведены теоретические исследования напряженно-деформированного состояния (НДС) пригруженного внешними нагрузками грунтового холма и склоновых зон.

а)

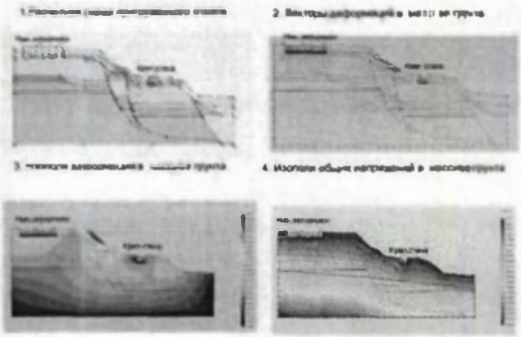


При помощи программных расчетных комплексов «*Плаксис*», «*Лира*» и «*Микро FE*» произведен сопоставительный расчет и осуществлено геотехническое моделирование НДС массива холма, пригруженного зданиями с прогнозируемым увеличением влажности ИГЭ до полного водонасыщения.

Створ 1-1



Створ 2-2



Створ 6-6

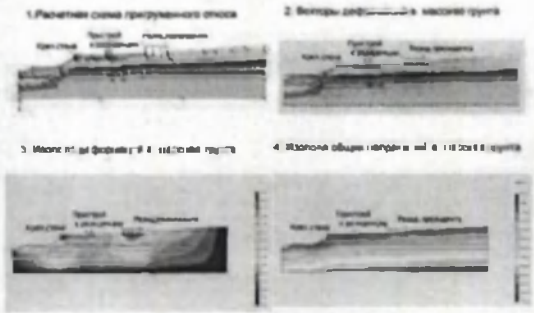


Рис. 10. Результаты расчетов устойчивости грунтовых откосов, пригруженных внешними нагрузками от зданий и сооружений, по характерным створам 1-1 и 2-2.

Таблица №1

№ расчетного створа	Результаты расчета напряженно-деформированного состояния				Результаты расчета устойчивости склонового массива		
	Макс. деформации (см)	Макс. деформации (см)	Макс. напряжения (кг/см²)	Заключение	Коэффициент устойчивости	Угол откоса / Угол внутреннего трения	Заключение
1-1	220	220	47	Устойчив	-	9°/29°	Устойчив
2-2	464	200	425	Не устойчив	К 1.0	-	Не устойчив
3-3	100	100	58	Устойчив	-	9°/24°	Устойчив
4-4	133	133	73	Устойчив	-	9°/23°	Устойчив
5-5	270	190	210	Не устойчив	-	9°/42,8°	Не устойчив
6-6	247	240	105	Не устойчив	-	9°/41,5°	Устойчив

ВЫВОДЫ И РЕКОМЕНДАЦИИ

В современных геологических и гидрогеологических условиях пригруженного внешней нагрузкой грунтового массива холма Казанского Кремля с учетом комплекса техногенных факторов (влияния метро, движения большегрузного транспорта в основании холма, строительных и археологических работ, покрытие территории асфальтом, полив зеленых насаждений) происходит длительный во времени оползневый процесс в комплексе с вертикальными деформациями приводящий к потере общей устойчивости склоновых зон и деформациям зданий и сооружений. Поэтому, для обеспечения надежной устойчивости откосов, авторами предложено: в пределах расчетной зоны развития напряжений массива грунта холма рекомендуется произвести упрочнение грунта при помощи вертикального и горизонтального армирования методом струйной геотехнологии, позволяющий сохранить гидрогеологический баланс и предотвратить увлажнение карстовых пород с обеспечением требуемой устойчивости грунтового массива и эксплуатационной пригодности объектов.

ЛИТЕРАТУРА

1. Салихова Ф. В. Башня Сююмбики и истоки цивилизации булгаро-татар. - Казань: РИЦ «Школа», 2005.- 104 с.
2. Мустакимов В.Р. Проблемы геотехники в современном строительстве и реконструкции зданий и сооружений Казани. Известия казанского государственного архитектурно-строительного университета. №2(6)/2006, КГАСУ, Казань, с. 66-68.
3. Слепак З.М. Геофизика для города. (На примере территории г. Казани). - Тверь, Издательство ГЕРС, 2007 г.–240с.
4. Хасанов А.З., Стриго Г.С., Мустакимов В.Р., Гаппаров Р.М. Опыт выпрямления наклонившегося минарета в сейсмически активном регионе. Марказий Осие шароитида бино ва иншоотларнинг зилзилабардошлиги муаммолари (анжуман якуни буйича илмий маколалар тупламы) 27-29 апрел, 1994й., Сам ДМКИ, Самарканд, 1994, 61-63.

The secrets of endurance of Indian heritage structures

A.S. Nene
JNT University, India

M.R.Madhav
IIT, Hyderabad, India

ABSTRACT: The paper presents the secrets of endurance of heritage structures and preservation and restoration aspects of substructures. Case studies of two Indian heritage structures are presented in this paper.

INTRODUCTION:

UNESCO has declared till today 125 structures as heritage structures and the responsibility of preservation and maintenance of these structures lies with the respective country within which these structures are located. Sixteen heritage structures in India are being maintained by the Archeological Society of India (ASI).

THE SECRETS OF ENDURANCE: Proper selection of three things is essential for durability of any heritage structure.

1. The Site
2. Construction materials used and
3. Construction techniques.

These points are briefly described below.

Site: In ancient days availability of a good site was not a problem. Most of the puranas (ancient scriptures) had a separate chapter called *Deshnirnaya* or site selection. Simple field tests on soils to determine their suitability of a foundation were described. All such tests were based on sound scientific principles. Site investigation was well known to ancient India. Most of the texts discuss in detail about site selection and investigations in their preliminary chapters. *Matsyapooran* quotes "First explore the site and then plan for the structure". A site is considered unsuitable for a town or a building if it is situated near a cremating ground, fissured, full of cracks, porous because of tree roots, full of ant hills, dead bodies, hairs, bones, corn husk, etc. *Mayasamhita* describes a cone penetration test which is similar to the one used by modern geotechnical engineers. As per the ancient practice a wooden cone is driven into ground by striking with a hammer. The markings on the cone indicate the amount of penetration. Smaller penetration indicates denseness of the stratum. The depths of foundations were between 1.5 m to 7 m depending upon the height or importance of the proposed structure. A simple thumb rule was to lay foundation on rock or just above the water table.

Construction materials: The construction materials used for heritage structures were stones, bricks, timber, lime mortars, paints and pigments.

Stones- Ancient Indian texts mention classification of stones according to color, age, gender. The stones with high compressive strength (male) were used for columns and the stones with high flexural strength (female) were used for beams. Building stones were closely examined for defects by applying herbal extracts to detect micro cracks and cleavage planes. For very important monuments, stones were tested by immersing them into boiling milk. There are religious traditions to apply protective coatings (Vajralepa) to the idols after every 12 years. Polishes made of coconut are applied frequently to impart shining of stone surfaces. Mud packs made out of *Multani mitti* and rose water are applied to white marbles to remove stains due to air pollution

Bricks: Preparations of brick earth molding and firing of bricks was described in ancient Indian text such as Rig Veda. Excavations at Mohenjodaro, Harappa and Lothal clearly indicate that the ancient bricks were far superior to modern bricks. Bricks were water cured for six months and then were used for construction. Many quality control tests such as sound test, water absorption and strength tests were mentioned in ancient Indian texts. Special organic additives such as algae, extracts of tree barks, decoctions of dry fruits (*Trifala*), jute fibers etc., were used in preparations of brick earths. These additives enhance the quality of bricks (sharp edges, strength and distortion free shape). Bricks of specific shapes and dimensions were developed taking into considerations the shape, form and function of the superstructure. To stagger the vertical joints and proper interlocking many types of bricks bonds were used in the construction of brick masonry.

Timber: Ancient text *Mayamat* mentions 84 types of suitable trees for wood work in superstructures. Ancient texts elaborately describe various aspects of timber, such as tree selection, preservation, wood defects and wood preservatives. One can find description of various types of wood joints in such texts. Application of wood polishes and oil based paints were essential parts of wood constructions.

Lime and lime preparations: Lime was extensively used as mortar for stone or brick masonry.

- Quick lime was prepared from lime stone, sea shales, mother of pearls etc. Quenching of lime was done using coconut water, Trifala decoctions, etc.
- Lime mortar was prepared at site, by grinding slaked lime and sands of various sizes using lime grinding mill operated by bulls. Various natural polymers were added during grinding. The natural polymers comprised of egg shales, hairs of goats, animal blood, decoctions of cereals (black gram) etc. Red lime mortar was prepared from saline soils.
- Plaster material was prepared by mixing lime with brick or marble powder. Many plasticizers such as ripe bananas or pulp of ripe fruits.

Colors and color pigments for walls were made out of natural ingredients. Five basic colors, white, red, yellow, green and black were prepared and then various shades of different colors were used with combinations of two or three colors.

Technical studies at the Baroda Museum revealed that three kinds of pigments were used by the ancient painters;

a) Mineral - including red lead, vermilion, yellow ochre, gold powder, Lapis lazuli, Azurite (blue), Malachite (green), calcium sulphate, white lead, silver powder, and zinc (white).

b) Vegetable - including indigo blue and madder red (derived from the manjistha plant, considered suitable for textiles and not for paintings).

c) Artificial - lamp black, verdigris green and ivory black.

Most pigments were minerals available locally: red ochre, vivid red, yellow ochre, indigo blue, chalk white, terra verte and green. Only Lapis lazuli was imported. Lamp-black was the only non-mineral. Following ancient texts deal with colors and pigments.

- Brihat-samhita (6th century)
- Kama-sutra (6th century)
- Vishnu-dharmottara (7th century)
- Samarangana-sutra-dhara (11th century)

Construction techniques: Time and cost constraints were not considered for the construction of heritage structures. Indigenous techniques were used to maintain the quality of construction. Few techniques are discussed below;

a. Compaction of foundation stratum - Durability of the structure depends upon proper compaction of foundation stratum. Well graded materials (cobbles, gravels, sands and clays) were properly compacted by rammers of the size of elephant foot.

b. Leveling of various layers: Very close quality control on levels and verticality of surfaces, was maintained. Special tools were developed to check the levels and heights of various components.

c. Proper load distribution: Structural loads were properly distributed with series of columns and beams. Roofs were prepared by proper interlocking of building elements (stones or bricks).

Опыт решения геотехнических проблем реконструкции памятников архитектуры в республике Башкортостан

А. Л. Готман, Ю.М.Шеменков
Уфа, Россия

АННОТАЦИЯ: В статье рассматриваются особенности грунтовых условий республики Башкортостан и проблемы, возникающие в ходе реконструкции зданий, являющихся памятниками архитектуры. Решение возникающих вопросов, в том числе увеличение несущей способности существующих фундаментов и восстановление эксплуатационной надежности здания, рассмотрено на примере реконструкции ряда зданий, являющихся памятниками архитектуры.

1. КРАТКАЯ ХАРАКТЕРИСТИКА ПАМЯТНИКОВ АРХИТЕКТУРЫ НА ТЕРРИТОРИИ РЕСПУБЛИКИ

В Башкирии в качестве памятников старины и архитектуры состоят на учете более 300 зданий. Самые древние из них построены в середине 18 века, большая же часть была построена в 19 и начале 20 веков.

Здания, как правило, кирпичные, 2-3 –этажные, на бутовых ленточных фундаментах. Конструкции перекрытий кирпичные, сводчатые, дверные и оконные проемы перекрыты арочными кирпичными конструкциями. Большинство зданий имеет подвал. Свайных фундаментов выявлено не было. «Действующие» заселенные здания обычно в удовлетворительном состоянии, хотя многие подвержены в той или иной степени разрушительным воздействиям времени. Неэксплуатируемые («заброшенные») здания разрушаются довольно быстро, и для их восстановления и реконструкции требуются серьезные инженерные мероприятия.

Восстановление и реконструкция этих зданий осуществляется по специальной республиканской программе Министерства культуры Республики, при этом для решения геотехнических проблем по каждому зданию привлекаются специалисты-геотехники из института «БашНИИстрой».

2. ОСОБЕННОСТИ ГРУНТОВЫХ УСЛОВИЙ РЕСПУБЛИКИ

Башкирия занимает юго-западную часть Урала и находится в основном в бассейне рек Белой и Камы.

Характерной чертой инженерно-геологического строения большей части территории Башкирии, в том числе той ее части, где исторически закладывались поселения, выросшие впоследствии до крупных городов, следует считать наличие мощных пластов пермских отложений на глубине нескольких десятков метров. В ряде районов они достигают дневной поверхности. Эти породы представлены песчаниками, известняками, гипсами, иногда глинами с прослойками песчаников или известняков. Обычно эти породы покрыты слоем четвертичных аллювиально-делювиальных отложений. В ряде районов встречаются неогеновые породы (обычно глинистые), залегающие под четвертичными. Аллювиально-делювиальные образования в основном представлены глинистыми отложениями от мягкопластичной до полутвердой консистенции. В пойменных террасах распространены крупнообломочные породы. На юге республики, а также в г.Уфе, встречаются макропористые просадочные (I типа) грунты. Однако значительно большее распространение имеют водонасыщенные глины при уровне грунтовых вод обычно на глубинах от 2 до 5 м.

Горные выработки в республике практически отсутствуют, но в ряде районов распространены карстовые явления. Особенно типичен карст в районах высоких берегов р. Белой. Чаще всего карстовые процессы являются затухшими, но встречаются участки с активными процессами (преимущественно в г.Уфе).

Согласно существующей классификации карста на территории г. Уфы развиты следующие классы карста [1].

1. Кластокарст, обусловленный наличием загипсованных песчаников (рис.1). Следствием развития кластокарста является образование в толще гипсоносных песчаников каверн, мелких полостей (высотой до 1 м), а на поверхности земли образование пологих оседаний и мелких карстовых провалов (диаметром до 2 м).

2. Карбонатный карст связан с известняками и мергелями уфимского яруса, в разрезе которых преобладают карбонатные породы (известняки, мергели), часто разрушенные до рухлякового состояния (рис.1). Скорости развития карста в карбонатных породах невелики, но при высоких градиентах фильтрации породы легко подвергаются суффозии, особенно в приконтактной зоне со скальными плитчатыми известняками, что резко ускоряет карстовые процессы.

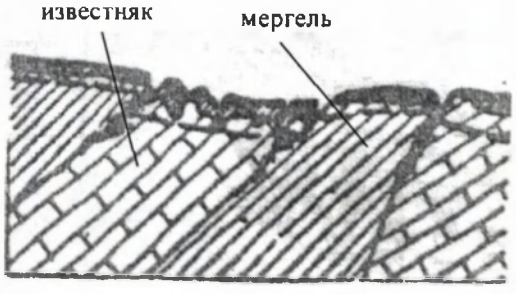


Рис. 1. Характерный профиль карбонатного карста связанного с известняками и мергелями уфимского яруса

3. Сульфатный класс карста связан с интенсивным растворением гипсовых (сульфатных) отложений (рис.2). Обычно наиболее закарстованной является приконтактная часть гипсов с вышележащей известково-мергелистой или глинистой толщей разреза. Это наиболее активный вид карстообразований, так как сульфаты имеют высокую скорость растворения в воде.

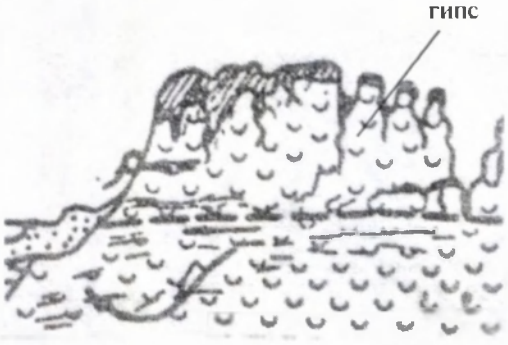


Рис. 2. Характерный профиль сульфатного класса карста

Таким образом, на селитебной части территории Башкирии имеют место следующие виды сложных, природно-неустойчивых грунтов:

- водонасыщенные сильносжимаемые глинистые;
- просадочные;
- закарстованные.

3. ГЕОТЕХНИЧЕСКИЕ ПРОБЛЕМЫ, КАК ОСНОВНАЯ ПРИЧИНА ДЕФОРМАЦИЙ И РАЗРУШЕНИЯ ЗДАНИЙ

При длительной (100 и более лет) эксплуатации зданий, построенных в другую историческую эпоху на основе технического уровня развития строительной отрасли того времени, имеются предпосылки для целого ряда причин потери эксплуатационной надежности здания и постепенного разрушения несущих и ограждающих конструкций.

Так, архитектурно-планировочные решения зданий 19 и более ранних веков представляют собой арочные и сводчатые кирпичные или каменные конструкции, чувствительные к малейшим неравномерным деформациям основания, так как не обладают пространственной жесткостью.

Фундаменты возводились, как правило, ленточными в виде бутовой кладки на известковом вяжущем основании, без уширенной части в подошве. Такие фундаменты являются абсолютно «гибкими», не работают на восприятие изгибающих моментов, поэтому при малейшей разности осадок в пределах здания в стенах появляются трещины.

Строить «солидные» здания старались на «сухих, прочных» грунтах, каковыми являются (в сухом состоянии) лессовые просадочные грунты, мергели, загипсованные песчаники, в изобилии залегающие на территории Башкирии.

Об особенностях же поведения таких грунтов при их замачивании в то время не было известно, равно как не учитывалась сама возможность сильного замачивания грунтового основания. Не было так же известно о повсеместном залегании на глубине 10 и более метров карстующих пород (сульфатов и карбонатов).

Совокупность этих факторов при длительной эксплуатации зданий является основой для потери эксплуатационной надежности старинных зданий (памятников архитектуры).

На основе опыта реконструкции и восстановления зданий (памятников архитектуры) последних 15 лет можно рассмотреть и проанализировать причины сверхнормативных деформаций старой постройки на территории республики.

1. Основными причинами сверхнормативных деформаций несущих конструкций старинных зданий являются замачивание просадочных грунтов и их просадка. Как правило, имеет место техногенный источник замачивания – локальные утечки из водонесущих коммуникаций в течение длительного времени. В результате грунтовое основание под какой-то частью здания дает осадку, что сразу сопровождается возникновением трещин в стенах здания. Отмечены также случаи, когда замачивание просадочных грунтов происходило в результате подъема уровня грунтовых вод. В этом случае осадки имеют более равномерный характер по всему зданию, однако такая «подвижность» здания тоже приводит к возникновению трещин в конструкциях.

2. Суффозионные явления. В случае подъема уровня грунтовых вод и природной организации разгрузки водных потоков в пределах сжимаемой толщи под зданием в суглинках, супесях, а также более прочных грунтах (мергелях, известняках, выветренных до состояния «рухляка») в течение длительного времени происходит вынос (механическая суффозия) пылеватых и мелких песчаных частиц с образованием протоков и мелких полостей, и просто ослабленных разрыхленных зон в массиве.

Подобные процессы происходят также по техногенным причинам. Например, в результате утечек из коммуникаций вода скапливалась в подвале здания, и ее откачивали мощными насосами, создавая тем самым принудительную механическую суффозию, а поскольку зачастую это продолжается многие годы происходит существенное «ослабление» несущего слоя грунтового массива с последующими неравномерными деформациями здания.

3. Карстовые проявления (химическая суффозия).

Образование в грунтовом массиве крупных карстовых полостей с выходом их на поверхность (провал) имеет место довольно редко и при проектировании рассматривается лишь как гипотетическое, как самый крайний случай. На практике наиболее распространенной формой карстопроявления является образование в грунтовом массиве «ослабленных зон», включающих небольшие пустоты, протоки и разрыхление основания. Подобные «дефекты» в грунте могут образовываться в течение нескольких десятков лет, т.е. за время, вполне соизмеримое со сроком эксплуатации здания, особенно старинного здания. Это и является одной из причин медленного разрушения старинных зданий, построенных на таких грунтах.

4. ПРИМЕРЫ РЕШЕНИЙ ГЕОТЕХНИЧЕСКИХ ПРОБЛЕМ

Объемы работ по реконструкции и восстановлению зданий, являющихся памятниками архитектуры, из года в год возрастают. Сотрудниками института «БашНИИстрой» в последнее время проводится большая работа по обследованию зданий различного назначения в разнообразных инженерно-геологических условиях. Из всего объема обследованных зданий можно выделить наиболее значимые и интересные в инженерном плане следующие объекты: здание бывшего медеплавильного завода (XVI в.) в с.Зилаир (год постройки 1748г.), здание Национального музея в г.Уфе (бывшее здание Крестьянского поземельного банка) 1906-08 г.г., здание медицинского института в г.Уфе (первоначально в здании находились присутственные места – суд, канцелярия и т.д.) 1854 года постройки, здание Государственного академического ансамбля народного танца им. Ф.Гаскарова в г.Уфе и т.д.

Обследуемые здания эксплуатируются в течение длительного времени, постепенно в несущих и ограждающих конструкциях зданий возникают различные деформации: трещины, разрушение кладки стен и т.д. Если за время эксплуатации деревянные конструкции в здании были подвергнуты, как правило, капитальному ремонту, то стены здания и фундаменты остались в первоначальном состоянии.

Причинами возникновения трещин в кирпичной кладке несущих стен зданий (памятников архитектуры), как правило, являются следующие:

- сезонное и аварийное колебания уровня грунтовых вод, включая верховодку, с образованием капиллярного подсоса влаги в капиллярно-пористой системе кирпичной кладки на известковом растворе;
- просадки, оползни и карстовые проявления;
- земляные работы и строительство в непосредственной близости или примыкание новых сооружений, расширение и надстройка исторических объектов;
- вибрация конструктивных элементов зданий под влиянием динамических нагрузок и т.д.

Основными проблемами, связанными с реконструкцией памятников архитектуры, являются вопросы, усиления фундаментов и упрочнения их оснований. Если основные строительные работы, связанные с реконструкцией надземной части зданий, у инженеров-проектировщиков не вызывают вопросов, то наибольшее затруднение вызывают работы, связанные с элементами здания, расположенными ниже поверхности грунта, и основаниями.

Решение возникающих вопросов, в том числе увеличение несущей способности существующих фундаментов и восстановление эксплуатационной надежности зданий, рассмотрим на отдельных примерах реконструкции зданий, являющихся памятниками архитектуры.

1. Здание Государственного академического ансамбля народного танца им. Ф.Гаскарова находится по ул.Гоголя в г.Уфе.

Здание дореволюционной постройки, двухэтажное. Здание примыкает с южной стороны к жилому дому, с восточной стороны – к зданию Филармонии более поздней постройки.

Здание имеет размеры в плане 11 х 15 м. Общий вид здания до реконструкции показан на рис.3.



Рис. 3. Общий вид здания Государственного академического ансамбля народного танца им. Ф.Гаскарова в г.Уфе до реконструкции

С целью оценки технического состояния несущих конструкций здания и возможности их дальнейшего использования было выполнено обследование, включающее следующие работы: шурфовку фундаментов с отбором монолитов грунта из-под подошвы, бурение изыскательской скважины, обследование несущих конструкций надземной части здания.

В результате шурфовки фундаментов выявлено, что для устройства фундаментов применен естественный строительный материал – постельный бутовый камень, а выше (для цокольной части и стен) хорошо обожженный глиняный кирпич. Ширина бутового фундамента в уровне подошвы равна 920 мм. Высота бутовой кладки фундамента – 1250 мм, глубина заложения – 1820 мм от существующей отмостки здания, а от пола 1-го этажа – 2070 мм.

Устоявшийся уровень грунтовых вод на момент откопки шурфа находился выше подошвы фундамента на 300-400 мм.

Отбор монолитов грунта из-под подошвы фундамента здания показал, что там непосредственно залегает суглинок обводненный, макропористый бурокоричневого цвета, мягкопластичный, тяжелый, пылеватый.

В наружных кирпичных стенах здания имелись сквозные трещины по ослабленным оконными проемами сечениям.

Для предотвращения дальнейших деформаций и раскрытия трещин в стенах здания было выполнено усиление фундаментов и стен, включающее следующие мероприятия:

- выполнены монолитные железобетонные пояса в уровне сопряжения бутовой и кирпичной кладки фундаментов;
- выполнена замена деревянных перекрытий на монолитные железобетонные;
- выполнено усиление стен накладками и тяжами (рис.4);
- осуществлена надстройка одного этажа.

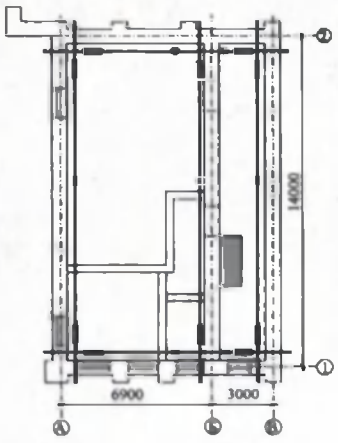


Рис. 4. Схема расположения металлических тяжей усиления наружных стен здания Государственного академического ансамбля народного танца им. Ф.Гаскарова в г.Уфе

Общий вид здания после реконструкции показан на рис.5.



Рис. 5. Общий вид здания Государственного академического ансамбля народного танца им. Ф.Гаскарова после его надстройки и реконструкции

2. Здание по ул.Фрунзе,45 в г.Уфе.

Здание построено в 1854 г. с применением традиционных строительных материалов, широко использовавшихся в строительстве со второй половины XIX века – хорошо обожженный кирпич-железняк, бутовый камень, дерево и металл.

Первоначально в здании находились присутственные места (суд, канцелярия и т.д.), а до настоящего времени была стоматологическая поликлиника мединститута.

Здание эксплуатировалось в течение почти 145 лет.

В ходе эксплуатации здания в бутовой кладке фундамента, несущих кирпичных стенах и межоконных простенках образовались многочисленных трещины. Имеющиеся деревянные междуэтажные перекрытия полностью исчерпали свою эксплуатационную надежность, и требовалась их замена.

В ходе работ по реконструкции здания были выполнены следующие работы:

- выполнены монолитные железобетонные пояса в уровне сопряжения бутовой и кирпичной кладок фундаментов (рис.6);
- выполнена замена деревянных перекрытий на монолитные железобетонные;
- выполнено обрамление оконных проемов из металлоконструкций;
- выполнена надстройка одного этажа.

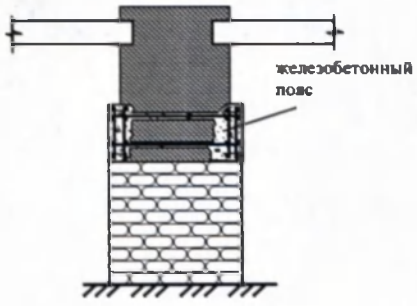


Рис. 6. Схема конструктивного усиления фундамента здания по ул.Фрунзе,45 в г.Уфе

При этом сводчатые кирпичные перемычки окон заменены на балочные, что существенно изменило архитектурный облик здания в ущерб архитектуре XIX века.

На рис.7 показан общий вид здания после надстройки дополнительного этажа.



Рис. 7. Общий вид здания по ул.Фрунзе,45 в г.Уфе после надстройки одного этажа

3. Здание Национального музея по ул.Советской в г.Уфе.

Строительство здания велось в два этапа: более старая часть была построена в 1908 году, а более новая часть (пристрой) – в 1943 году.

Фундаменты здания бутовые ленточные, с бутовым (местами кирпичным) цоколем. Бутовый камень на цементном растворе. Гидроизоляция фундаментов от стен из цементно-песчаного раствора.

В старой части здания стены цокольного этажа выполнены из красного кирпича толщиной 900 мм, а в пристрое – из бутового камня толщиной 780 мм.

Несущие наружные и внутренние стены старой части выполнены из красного глиняного кирпича толщиной 750 мм и 510 мм, а в пристрое – 640 и 380 мм.

В результате локального замачивания грунтов основания из водонесущих коммуникаций, проходящих вблизи стен, произошло снижение прочностных и деформационных характеристик суглинков в 1,6-1,7 раза, что вызвало неравномерные осадки и деформации в конструкциях фундаментов и надземной части

здания с образованием трещин с шириной раскрытия до 6-7 см.

Для восстановления эксплуатационной надежности здания и предотвращения дальнейшего раскрытия трещин в стенах здания было выполнено усиление стен металлическими тяжами и на уровне цоколя, в несущих стенах выполнены железобетонные пояса (рис.8).

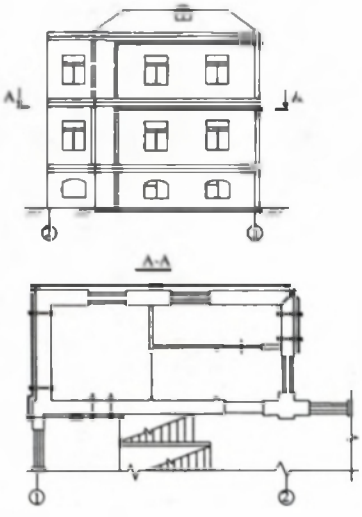


Рис. 8. Схема конструктивного усиления металлическими тяжами наружных стен здания Национального музея в г.Уфе

5. ЛИТЕРАТУРА

ТСН 302-50-95. РБ. Инструкция по изысканиям, проектирвоанию, строительству и эксплуатации зданий и сооружений на закарстованных территориях / Госстрой Республики Башкортостан. Уфа, 1996, 40с.

Deformation of stupas measured by photogrammetry before and after Ayutthaya Flood in Thailand, 2011

Y. Fujii
Fukada Geological Institute, Tokyo, Japan

U. Weesakul, N. Poovarodom &. M. Bhadrakom
Department of Civil Engineering, Thammasat University, Thailand

K. Watanabe, S. Kawano
Geosphere Research Institute, Saitama University, Saitama, Japan

ABSTRACT: Ayutthaya is one of the UNESCO World Heritage Sites in Thailand. The scientific documentation of some stupas in the site of Ayutthaya had been carried out by digital stereo-photogrammetry in April, 2011. After that, Ayutthaya province had been suffered from the big flood during October to December, 2011. Temples and constructions in Ayutthaya were inundated for approximately two months. After this flood, the same stupas were documented by the same technique in January, 2012. A stupa in Wat Yai Chaimongkhon had leant at an angle of 2-3 degrees in April, 2011. The inclination of the upper part of the stupa has increased a little in January, 2012. Many ruins in Ayutthaya have been deteriorated year after year. The documentation by photogrammetry could be very valuable for monitoring them and it also produces important basic data for restoration and preservation of Ayutthaya ruins.

1 INTRODUCTON

One of the aims of the Convention Concerning the Protection of the World Cultural and Natural Heritage is to protect and conserve heritage which is of such outstanding universal value for current and future generations. The first step to protect heritage is documentation, which includes archival research, observation and recording. Recently, the new methods of digital photogrammetry and terrestrial laser scanning are used to investigate and record cultural heritage as scientific three-dimensional (3-D) documentation (Koutsoudis et al., 2007; Yastikli, 2007; Yilmaz et al., 2007). On the basis of 3-D information taken by two different times, it's possible to get the change or deformation of the same heritage (Fujii et al., 2009). In the case of digital photogrammetry, it's possible to collect not only 3-D information but also digital images of the heritage simultaneously. We can take more information from the comparison of images taken by two different times.

In this study, the documentation of some stupas in the historical city of Ayutthaya had been carried out by digital stereo-photogrammetry before and after the flood in 2011. During the flood, many ruins in Ayutthaya were inundated for approximately two months. The 3-D models of the same stupa recorded before and after the flood could be compared through these documentations.

2 STUDY AREA

2.1 *Ayutthaya Historical Site*

Historic city of Ayutthaya is about 80 km north from Bangkok, the capital city of Thailand, and located in the valley of the Chao Phraya River (Fig. 1). The city was founded by King Ramathibodi I in 1350, and had been developed as a port city surrounded by rivers during about 400 years. It was reflected in the palaces and the multitude of ornate temple buildings (including stupas) showing its wealth of art and prosperity (Fig. 2). After the complete destruction by the war in 1767, they had been left as ruins. In 1969, the Fine Arts Department began with renovations of the ruins, which became more serious after it was declared a historical park in 1976. The park was declared a UNESCO World heritage site in 1991. The conservation and preservation of them has been continued. However the historical city is so large, therefore some of them have been deteriorated year after year.



Fig. 1 Location of Ayutthaya in Thailand (Map Data ©2012 Google, Tele Atlas, SK M&C, ZENRIN).



Fig. 2 Photograph of the precinct of Wat Yai Chaimongkhon in the historical city of Ayutthaya.

3 METHOD

3.1 *Digital Photogrammetry*

Photogrammetry is the process of deriving metric information about an object through measurement on photographs of the object (Mikhail et al., 2001). Obviously, two-dimensional co-ordinate can be gained from a single photo (two-dimensional plane). If we have two photos of the same object from different directions, we can get three-dimensional co-ordinates of the object (Linder, 2003).

Historically, photogrammetry has been employed to construct topographic maps from stereo-photographic pairs of aerial photographs. The technique of photogrammetry can be applied to close-range observations with a hand-held camera and lens. The close-range photogrammetry has been applied to fracture surfaces in granite (Fujii, 2007a, Fujii 2007b), cultural heritages (Yilmaz et al., 2007, Fujii et al., 2009), and many kind of objects (Mikhail et al., 2001, Linder, 2003).

3.2 *Construction of 3-D surface model from a pair of stereo-photographs of stupa*

A 3-D morphology can be produced from a pair of overlapping stereo-images. The information of camera positions and orientations (X, Y, Z, ω, φ, κ for left and right cameras) are needed to get the 3-D co-ordinates of the target object (Fig. 3). However, it is difficult to get the accurate positions and directions at the same time when taking a pair of photographs. Control points, of which the 3-D co-ordinates are measured in advance, are included in the photograph (Fig. 4). Total Station was applied to measure the control points. The Total Station (TS) is an optical measurement for surveying that is formed by an electronic theodolite, an electronic distance measuring tool and an external computer.

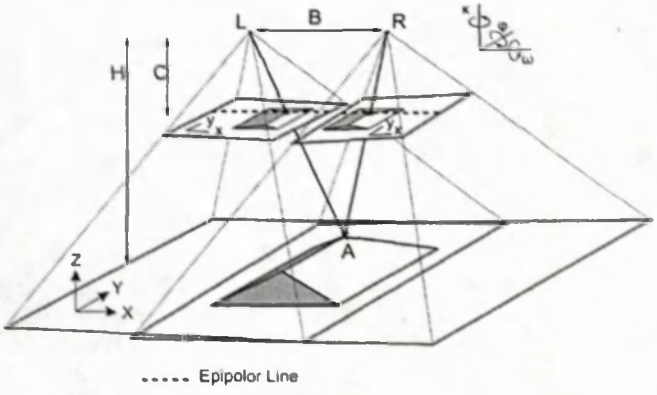


Fig. 3 An overlapping pair of stereo-photographs and a target object.

The camera positions and directions can be inversely calculated from the control points by means of least-square adjustments (LSA) with 3-D digital photogrammetric software. At least five control points, which might be spread over the object, can be needed for the calculation of the camera positions and directions. After the LSA in the stereo-photogrammetric program, the residuals can be calculated for each pair of stereo-photographs. The root mean square of residuals is about 30 mm for the stereo-pairs of southwestern-side photographs of Stupa (Fig. 4). The resolution of photogrammetry can be calculated as follows,

$$\sigma_{xy}=(H/C)\delta_{CCD} \quad (1)$$

$$\sigma_z=(H/B)\sigma_{xy} \quad (2)$$

where σ_{xy}: the resolution parallel to the photo-plane, x is horizontal and y is vertical on the photograph. σ_z: the resolution vertical to the photo-plane. δ_{CCD}: the resolution of CCD of the camera. H: the distance from the cameras to the object. B: the distance between two cameras. C: focal length of the camera (lens). In the above case, H is about 25 m, B is about 3 m, and C is about 6.1 mm (Figure 3). So σ_{xy} is about 8 mm, and σ_z is 70 mm. The above residual from the calculation of LSA is 30 mm, and it is less than σ_z. Therefore, it is thought that the calculation of camera positions and directions has been successfully done.

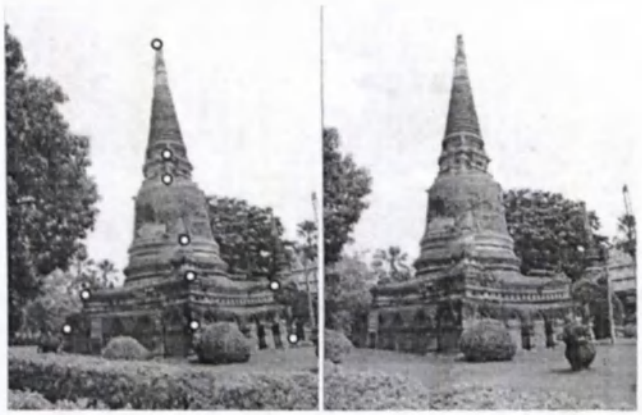


Fig. 4 A pair of stereo-photographs of a stupa, which is located at the right side in Fig. 2. White circles on the left photograph show control points.

After the calculation of camera positions, the software can make epipolar images (Fig. 5). Lens distortion is calibrated on the pair of stereo-photographs and each calibrated photographs are rotated and paralleled to the epipolar line. The epipolar lines are two lines where epipolar plane intersects a pair of overlapping photographs. The epipolar plane is known as the plane defined by the three points L, R, and A (Fig. 3).

The softwasre can give matching of the same positions on epipolar lines over a pair of epipolar images by means of the difference of color and contrast, and generates 3-D coordinates of the points. The 3-D data of about 10,000 points were generated on the surface of stupa. These points are connected with each other and a 3-D surface model of the stupa is composed of them as TIN (Triangle Irregular Network, Fig. 6). This model is called DTM (Digital Terrain Models, Fig.7a). The great advantage of digital photogrammetry is to put the photo images together with the DTM. The results is a texture mapping model, this can be viewed from arbitrary directions (Fig. 7b).

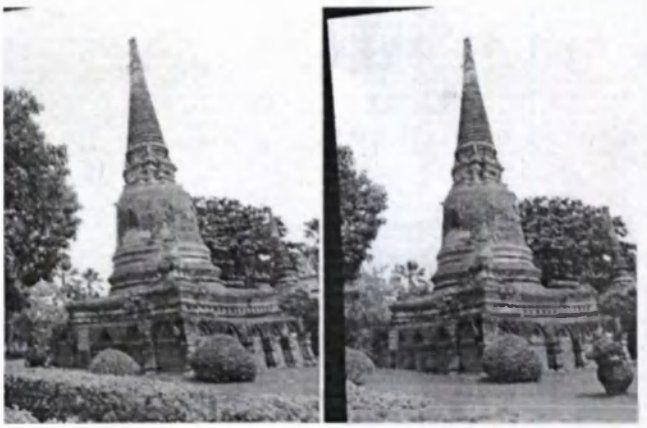


Fig. 5 Pair of epipolar images of the stupas.

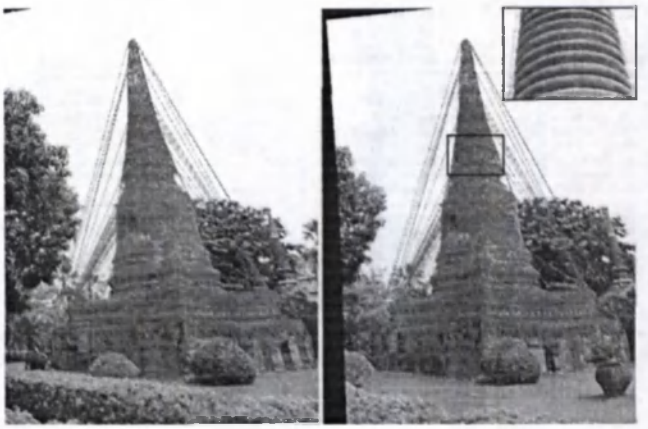


Fig. 6 3-D surface model of the stupa on the epipolar images.

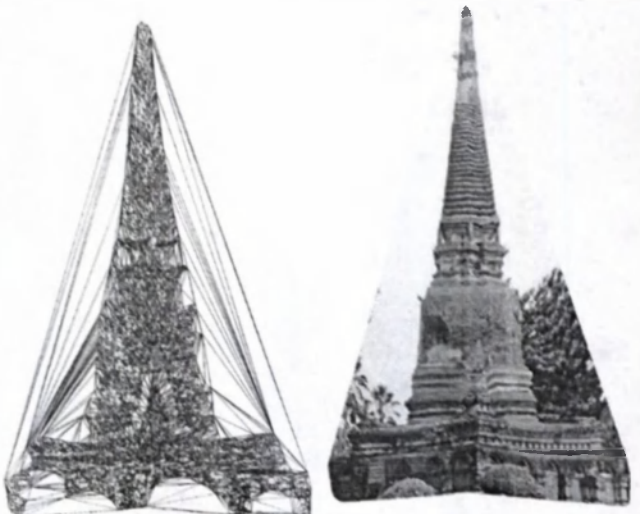


Fig. 7 a: DTM of the stupa composed of TIN.
b: Texture mapping model of the stupa.

4 RESULTS

4.1 *Displacement of the photogrammetric control points on the stupa before and after the flood*

Northwest side of a stupa, its height is about 25 meter, in Wat Yai Chaimongkhon was measured in 3-D with digital photogrammetry in April, 2011 (Fig. 7). After that, Ayutthaya province had been suffered from the big flood during October to December, 2011. Many ruins, including the above stupa, in Ayutthaya were inundated for approximately two months. About a month later from the recovery of this flood, the same stupa was documented by the same photogrammetric technique in January, 2012.

Some benchmarks had been already set on the ground around the stupa in Wat Yai Chaimongkhon for the geodetic references in 2011 (Fig. 8). In this study, TS was used for measuring the geodetic reference benchmarks and the photogrammetric control points (see Fig.4 for control points) both in 2011 and 2012. If the benchmarks are assumed not to be deformed before and after the flood, we can compare the deformation of the control points on the stupa between 2011 and 2012. Figure 9 shows the displacement of the photogrammetric control points on the stupa in the vertical direction.

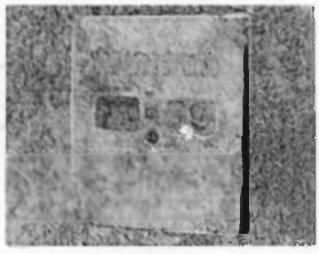


Fig. 8 An example of benchmarks in Wat Yai Chaimongkhon. The width is about 200 mm.

Except the control point No.1, there is more large displacement in the vertical directions as higher part of the stupa. About No.1 control points, the position might be a little miss-located between 2011 and 2012. About No.10 control points at the top part of the stupa, it is too high to be measured from the location of camera position by TS.

4.2 *Sections generated form DTMs of the stupa*

The northwest side of the stupa was measured in 3-D with digital photogrammetry in January, 2012 again. Another pair of stereo-photographs was taken in the very similar situation of the case in 2011. In addition same analysis was applied to the pair of photographs (Fig. 4 to 6), and a similar DTM was constructed from the photographs.

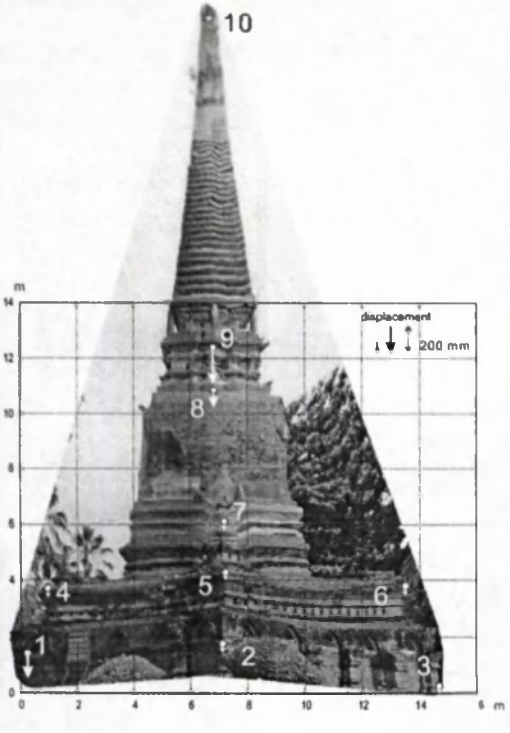


Fig. 9 Displacement of the photogrammetric control points on the stupa. White circles and numbers mean the photogrammetric control points

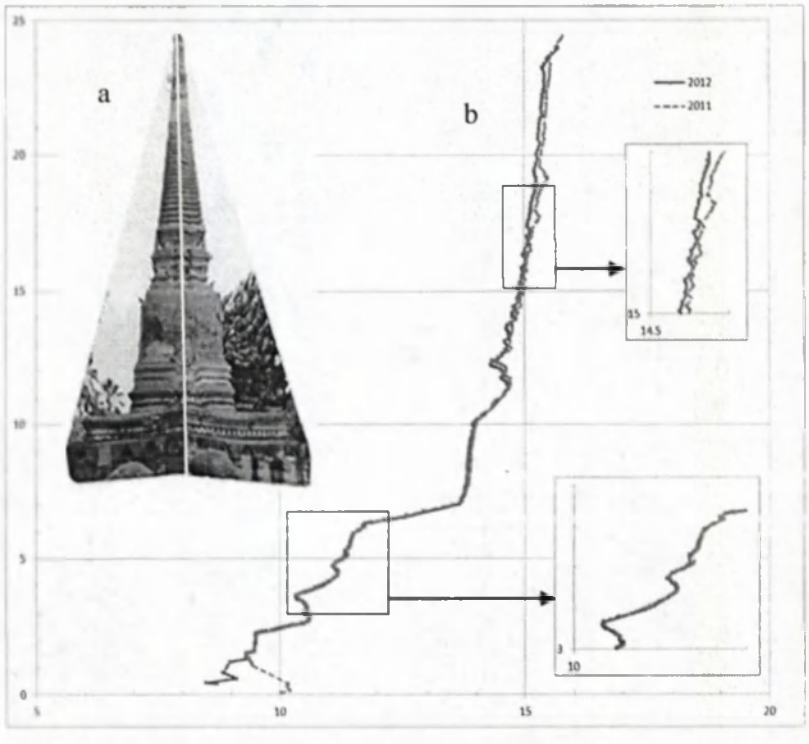


Fig. 10 a: Location of a vertical section on DTM in 2011. b: A comparison of vertical sections between 2011 and 2012. Horizontal axis is exaggerated than vertical axis.

Fig. 10 shows a comparison of vertical sections between year of 2011 and 2012. Each section is generated from each DTM in 2011 and 2012. The lower part of the stupa, which is less than 10 meter height, has no deformation. However the upper part of the stupa is deformed and has more lean to the direction of northwest. This deformation reflects the result of the displacement of the photogrammetric control points.

5 DISCUSSION

5.1 *Displacement of the stupa before and after the flood*

The stupa in Wat Yai Chaimongkhon had already been leaning at an angle of 2-3 degrees to the northwest direction in 2011. After the big flood, the inclination of the upper part of the same stupa has increased a little in January, 2012 (Fig. 9 & Fig. 10b). At the lowest part of the stupa in Fig. 10b, the sections between 2011 and 2012 have been changed. This is caused by a bush just at the front of the stupa. The bush has been grown in spite of the inundation of the flood. The flood level was about 1 meter from the ground here, and the height of the bush is about 1.2 meter.

At the lower part of the stupa, less than 10 meter height, there is no deformation in Fig. 10b. At the height of about 13 m around the No. 9 control point, the displacement is 150 mm in the vertical direction and about 50 mm to the northwest in the horizontal direction. At the top part of the stupa more than 20 meter, the displacement is 300 mm in the vertical direction and about 130 mm to the northwest in the horizontal direction. Those displacements are enough large compare to the residual (30 mm) from the calculation of LSA in photogrammetry and the resolution σ_z (70 mm) of photogrammetry.

It must be true that the leaning of the upper part of the stupa has been increased a little during the flood of 2011. However it is uncertain that the leaning is caused by the flood directly. The data of geological and underground water around Ayutthaya might be considered in the future study.

5.2 *Deterioration of stupa in Ayutthaya historical city*

There are many ornate temple buildings, including many stupas, in the historic city of Ayutthaya. Fig. 11 shows three different stupas in Wat Phra Si Samphet. This figure shows conceptual deterioration progress for historical stupa. The left stupa in Fig. 11 has not been so deteriorated and it's similar to the stupa in Wat Yai Chaimongkhon. About the center stupa in Fig. 11, its surface is deteriorated and some of fired bricks have been fallen down to the ground. About the right stupa, its upper part has totally collapsed and only the basement has been left with deteriorated fired bricks. In Wat Yai Chaimongkhon, there are also some stupas that have been left with only those basements (Fig. 2). Therefore the conceptual deterioration progress suggests that the stupa, which is documented in this study, will be collapsed in the future. The estimation of that time might be another future study for historical monument in Ayutthaya.

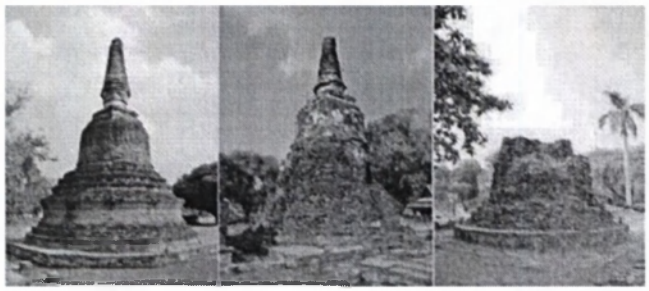


Fig. 11 Conceptual deterioration progress for historical stupa. Those stupas are in Wat Phra Si Samphet.

6 CONCLUSION

A stupa of Wat Yai Chaimongkhon in historic city of Ayutthaya has been documented with digital stereo-photogrammetry before and after the 2011 flood in Thailand. The stupa had leant at an angle of 2-3 degrees in April, 2011. The inclination of the upper part of the stupa has increased a little in January, 2012. Consideration of other stupas in the historic city, a conceptual deterioration progress is considered. The documentations by photogrammetry could be very valuable and important as basic data for restoration and preservation of Ayutthaya ruins.

ACKNOWLEDGMENTS

We thank to the Fine Arts Department in Bangkok for permitting us to survey in historic city of Ayutthaya. This research was supported by research subsidy project of Japan Construction Information Center.

REFERENCES

Fujii, Y., Takemura, T., Takahashi, M., Lin, W. (2007a). "Surface features of uniaxial tensile fractures and their relation to rock anisotropy in Inada granite." *International Journal of Rock Mechanics and Mining Science* 44, 98–107.

Fujii, Y., Takahashi, M., Hori, S. (2007b). "Three-dimensional topography of fracture surfaces obtained by a digital photogrammetric technique." *International Journal of the JCRM*, 3, 29–34.

Fujii, Y., Fodde, E., Watanabe, K. and Murakami K. (2009). "Digital Photogrammetry for the Documentation of Structural Damage in Earthen Archaeological Sites: the case of Ajina Tepa, Tajikistan." *Engineering Geology*, Vol. 105, 124-133. doi: 10.1016/j.enggeo.2008.11.012.

Koutsoudis, A., Arnaoutoglou, F., Chamzas, C. (2007). "On 3D reconstruction of the old city of Xanthi. A minimum budget approach to virtual touring based on photogrammetry. " *Journal of Cultural Heritage*, 8, 26–31.

Linder, W., 2003. Digital Photogrammetry Theory and Applications. Springer, Berlin. 189 p.

Mikhail, E. M., Bethel, J. S., McGlone J. C. (2001). Introduction to modern photogrammetry. John Wiley & Sons, Inc., New York, 479p.

Yastikli, N. (2007). "Documentation of cultural heritage using digital photogrammetry and laser scanning." *Journal of Cultural Heritage*, 8, 423–427.

Yilmaz, H.M., Yakar, M., Gulec, S.A., Dulgerler, O.N. (2007). "Importance of digital close range photogrammetry in documentation of cultural heritage." *Journal of Cultural Heritage*, 8, 428–433.

Задачи инженерно-геологической диагностики деформаций памятников архитектуры

Е.М. Пашкин, В.Я. Ендржиевский
«Реконфисс», г.Москва, Россия

АННОТАЦИЯ: За последние четверть века в России были отработаны основные требования к диагностированию состояния памятников архитектуры. В общем виде они ограничивались сбором и анализом ретроспективной историко-архитектурной и инженерно-геологической информации по территории памятника. Практика последних лет показывает, что диагностирование должно быть направлено на выявление изменений инженерно-геологических условий в сфере взаимодействия памятника, на выявление дефектов, возникших за период его существования, к отражению результатов взаимодействий в рамках их причинной зависимости. Особое место должно быть отведено выполнению специальных инженерно-геологических исследований причинности и отражения деформаций памятников архитектуры в структуре исторических природно-технических систем. Подчеркивается преимущество метода инженерно-геологической диагностики деформации памятников архитектуры, позволяющего при отсутствии стандартизации инженерно-геологических исследований исторических территорий решать задачи получения необходимой информации для их сохранения.

ВВЕДЕНИЕ

Грамматика исследований памятников архитектуры и диагностика их сохранности должны формировать свои правила, во многом опирающиеся на информацию обратной связи о состоянии исторических реальных систем. Это важное положение должно отражать существо сложившихся взаимоотношений элементов исторических систем в рамках их организованности, способной сохранять их устойчивость, а также информировать о различных периодах их реконструкций.

Условия сохранения памятников архитектуры, обусловленные многовековыми естественными изменениями исторических территорий, осложняются развитием техногенных процессов. Скрытый характер их развития, неполнота знаний о них не позволяли выявить в течение длительного периода направленность их действий, масштаб внесенных изменений в структуру грунтов оснований и фундаментов памятников архитектуры. Результаты действия скрытых процессов отмечаются лишь после возникновения тех или иных деформаций в конструкциях памятника или грунтов основания.

Инженерные исследования на объектах архитектурного наследия должны стать изысканиями нового типа, поскольку у них возникают свои специфические цели и задачи. В центре их интересов становится не оценка инженерно-геологических условий территорий, как например, для проектируемых сооружений, а изучение и понимание состояния реальных ИПТС, проживших несколько жизненных циклов, отводимых современным инженерным сооружениям. Они включают в сферу интересов не традиционные для инженерной геологии исследования, а изучают причинно-следственные отношения конструктивных элементов с инженерно-геологическими процессами. В рамках целевой ориентации инженерно-геологической диагностики причин деформации памятников такой подход требует расширения круга приложений инженерной геологии в области сохранения объектов культурного наследия. Поэтому проблема их сохранения как элементов реальных исторических систем связана, прежде всего, с оценкой продукта взаимодействия, отражающего совокупность изменений в структуре ИПТС, адекватных внешнему воздействию. Становится очевидным близость понятия отражения к причинно-следственным отношениям ИПТС. В связи с этим главное при изучении исторических систем – определение причинности возникающих в их структуре событий.

При диагностировании деформаций памятников архитектуры положены методы, позволяющие обнаруживать в рассматриваемых ИПТС деструктирующие начала, формирующие адекватный образ взаимодействий. Эта задача решается на основе анализа деформаций несущих конструкций с учетом взаимодействия природных факторов с ними, а также с грунтами основания. При этом важно знание об основных этапах воздвижения памятников архитектуры, наличие в их основании остатков бо-

лее древних сооружений и развитие в связи с этим в них деформаций в прошлом, деструкции примыкающих исторических территорий под влиянием техногенеза и изменений гидрогеологических и гидрологических условий. К сожалению, в последнее время ИПТС как объективная целостность исчезает из рассмотрения и остается лишь предмет исследования, определяемый полностью условиями конкретной задачи, например, изучением только технического состояния конструкций памятника, либо изучением лишь свойств грунтов основания. Отсутствие связности в изучении элементов системы, не позволяющее исследовать ее системные свойства, приводит к тому, что многие памятники архитектуры остаются не полностью исследованными, а многие проблемы нерешенными.

Для познания сущности взаимодействующих явлений, имеющих свою индивидуальность и структуру, признание лишь наличия взаимодействий в ИПТС недостаточно. Физическое состояние многих памятников архитектуры предъявляет вызов, на который необходимо дать ответ не только в виде фактографического набора информации, но и полного понимания и осмысления результатов взаимодействий. Их понимание и есть отражение проявления свойств реальных ИПТС воспроизводить в своих особенностях особенности взаимодействующих с ними других систем и явлений. В контексте ИПТС отражение рассматривается как продукт взаимодействий. Наконец, отражение позволяет формировать цели и задачи последующих исследований и самое главное определять образ будущих управляющих действий. В работе [1] отмечается, что существует определенное сходство отражения с причинно-следственными отношениями между объектами. Таким образом, познание процессов и явлений в структуре ИПТС должно сводиться к познанию взаимодействий внутри системы и в ее связи с окружающей средой при изучении продукта взаимодействий.

Поскольку отражение служит своеобразным инструментом превращения увиденного в идею, то очевидно подобное превращение может определяться лишь в процессе практики. Отметим также, что отражение действительности не может исключать и такие специфические процессы как абстрагирование, идеализация, воображение. Но наиболее важной формой отражения является принцип причинности. Рассмотрим на отдельных примерах некоторые формы отражения причинной зависимости событий, наблюдаемых в структуре ИПТС.

При их изучении вопросы структуры взаимодействия связанных элементов этих систем стали самыми востребованными. Структура исторических систем – важнейший диагностический признак, позволяющий выявить слабые звенья, как продукты длительного взаимодействия между элементами системы. Для выявления характера взаимоотношений в созданной веками структуре ИПТС, как показывает опыт их исследования, необходимо оценивать сложившуюся упорядоченность элементов, поскольку устойчивость ее бывает обусловлена тем, каким образом она организована.

Так, в ряде случаев возникает необходимость оценивать сохранность и несущую способность сохранившихся фундаментов более древних построек. Эти фрагменты, как реликты, позволяют после обследования ответить на вопросы, что случилось со зданием памятника, его фундаментом и грунтом основания, насколько возможно повторное использование старого фундамента и как они при взаимодействии с фундаментами новых построек повлияли на их устойчивость. Если фундамент сохранил несущую способность, и целостность его структуры не изменилась, то можно предположить, что и после возведения нового сооружения на прежнем месте он сможет воспринимать первоначальные нагрузки. Однако если несущие конструкции создаваемых вновь зданий оказались за контуром старых строений, то в этих случаях возникают иные условия взаимодействия, и в структуре построенных сооружений формируются слабые звенья, которые со временем приведут к серьезным деформациям. В этих деформациях проявляются свойства реальных ИПТС воспроизводить в особенностях сложившейся структуры особенности взаимодействующих элементов этой системы, например старых и вновь созданных фундаментов. Подобные причинные зависимости могут быть проиллюстрированы рядом примеров.

ПРИМЕРЫ ПРИЧИННОЙ ЗАВИСИМОСТИ ЯВЛЕНИЙ

В связи с этим уместно вспомнить слова И. Ньютона: "При изучении наук примеры не менее поучительны, нежели правила". Правил в инженерно-геологической диагностике пока нет. Обращение к наиболее ярким примерам установления диагноза отдельным памятникам может послужить основой для обогащения опыта изучения причинно-следственных свя-

зей, определяющих природу и механизм их деформаций. Подобный подход ценен еще и тем, что, как правило, не требует больших затрат.

Известно, что часть стен Нового города Кирилло-Белозерского монастыря возводилась в два этапа. Первый относится к 50-м годам XУ11в., второй – к 70-м. Первый участок стены мог быть пристроен к еще существовавшей тогда башне более раннего Ивановского монастыря, а на втором этапе возведения стены большая часть башни была разобрана, а оставшаяся часть вошла в структуру новой фортификации [2]. Об этом свидетельствует и геометрия трещины, идущей до валика, и составляющая часть высоты угловой башни (рис.1).

Вошедшая в стену Нового города старая стена башни могла послужить ослабленным звеном при образовании трещины. Вскрытый фундамент башни XУ1в. не был разрушен строителями и был сохранен в качестве усиливающего элемента в основании стены Нового города, фундаменты более ранней постройки которой, опираются на фундаменты башни и грунты, уплотненные сохранившимися деревянными сваями. Это
и стало причиной появления деформации стены из-за дополнительной ее осадки, поскольку грунты под ней не были уплотнены более ранними постройками. Необычность условий взаимодействия между элементами разновременных построек нашло отражение и в проявлении необычной геометрии трещины.

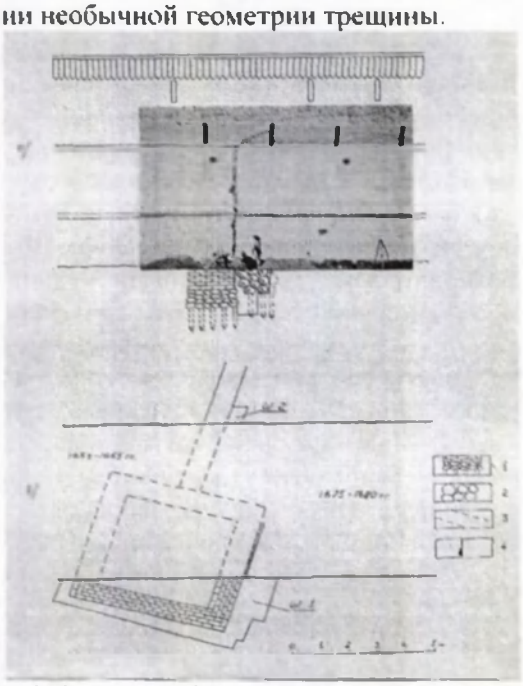


Рис. 1 Характер деформации стены Нового города Кирилло-Белозерского монастыря: а – развитие трещины на фасаде стены; б – положение трещины в плане: 1 – положение несущих конструкций угловой башни Ивановского монастыря; 2 – валунные фундаменты; 3 – положение фундаментов угловой башни в стене Нового города; 4 – трещина в стене

Прием использования старых фундаментов при строительстве более поздних сооружений может использоваться в разных случаях. Так, возникает возможность при наличии скрытых фундаментов ранее построенных сооружений, характерных деформаций в конструкциях более поздних памятников архитектуры, оценивать совокупность изменений, адекватных сложившейся причинности. В качестве примера может служить история Успенского собора Рязанского кремля, построенного в конце XУ11в. Но уже в начале следующего века, после двух сильнейших ураганов, пришедших с северо-западной стороны и сорвавших барабаны и кровлю, образовалась огромная трещина, разделившая здание собора на две части (рис. 2 и 3).

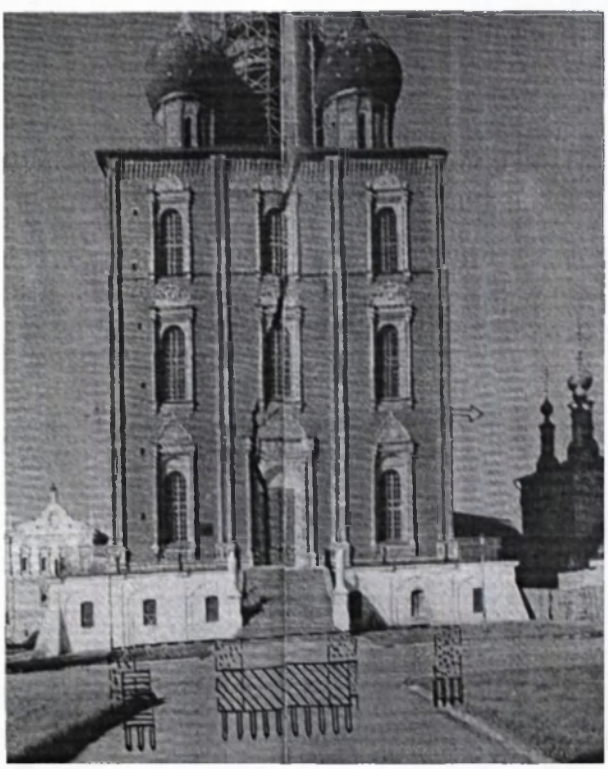


Рис. 2 Трещина на западной стене Успенского собора в Рязанском кремле: 1- трещина; 2- фундаменты разобранных построек; 3 – фундаменты Успенского собора; 4 – направление перемещения южной стены собора.

Объяснение этой деформации в то время и в последующие годы связывали с якобы слабыми и неоднородными грунтами в основании, что не нашло подтверждения материалами последующих изысканий. Однако при этом не обращалось внимания на два важных обстоятельства:

первое – северная и центральная часть Успенского собора были построены на месте разобранных строений старого Успенского собора и бывшей Зелейной палаты, существовавших с XУ1в. При строительстве Успенского собора здания старого собора и палат были разобраны, но фундаменты и сваи от них сохранились [2] . Поскольку площадь нового собора была больше, то дополнительный фундамент южной части собора пришлось включать в работу с грунтами под нагрузкой 0,5 МПа, которые до строительства не испытывали никакого уплотнения.

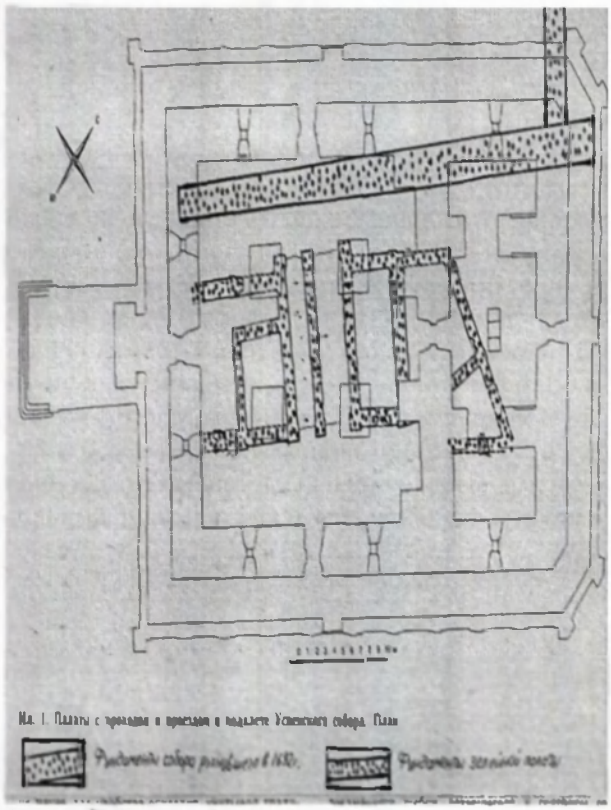


Рис. 3 План Успенского собора Рязанского кремля с положением сохранившихся фундаментов ранее разобранных построек: 1 – линия, разделившая собор на два блока; 2 - сохранившиеся фундаменты разобранных построек.

Это, безусловно, создавало иные условия взаимодействия фундаментов с грунтами оснований, чем в центральной и северной части собора. Это привело уже в первые годы к десинхронизации осадок собора между участками с сохранившимися старыми фундаментами и участками с новыми фундаментами. Разница осадок привела к образованию крупных трещин, расколовших собор на два архитектурно-тектонических блока, которые впоследствии оказались под воздействием других причин. Второе обстоятельство было связано с отмеченными ранее ураганами, воздействие которых на северную стену собора оказалось весьма значительным из-за большой ее парусности (более 1200м2). В результате воздействия ветровой нагрузки во время ураганов здание памятника могло создавать дополнительную кратковременную нагрузку на грунты основания южной части собора. Эта нагрузка превышала допустимую почти в 1.5-2.0 раза, что совместно с создавшимися условиями взаимодействия фундаментов привело к неравномерной осадке и образованию трещины. По заключению Б.П.Попова и П.П.Ротерта (1951г.), эти деформации собора могли быть связаны с возникновением напряжений в грунтах основания, а перемещение стены к югу на 10см были обусловлены более сложным характером деформаций. По мнению автора, эти деформации могли произойти в результате образования воздушной подушки при создании в соборе области повышенного давления воздуха после разрушения ураганом глав собора и возникновения зоны пониженного давления с южной (подветренной) стороны собора. Это привело к разнице давления воздуха на южную стену и созданию отрицательного давления (отсоса), под воздействием которого часть стены оказалась выдавленной наружу. Таким образом, проанализировав информацию в виде возможного продукта взаимодействий, отразивших внешние воздействия, удалось уйти от шаблонной оценки причинности событий, приведших к столь крупным деформациям собора.

Отражение причинной зависимости событий в ИПТС раскрывается порой состоянием отдельных элементов памятников архитектуры, их особенностями, предопределяющихся рядом условий. К ним можно отнести, например, колокольни храмовых построек, отличающихся от других элементов конструктивными особенностями, заключающимися в том, что имеют четыре пилона со столбчатыми фундаментами, на восточную пару которых влияет тепловое воздействие трапезной (рис. 4). Примыкание восточных пилонов к трапезной исключает промерзание фундаментов и морозоопасных грунтов, от которого зависят условия проявления сил морозного пучения. Но эти условия сохраняются для западной пары пилонов и определяются несколькими факторами: дисперсностью грунтов, теплофизическими свойствами материала кладки фундаментов, глубиной и скоростью их промерзания, скоростью влагопереноса и условиями накапливания конденсационной влаги вблизи фундаментов.



Рис. 4 Формирование теплового поля под фундаментами колоколен.

Кроме того, существенную роль определяет экспозиция пилонов западной пары, поскольку количество тепла, поступающего от прямой и рассеянной солнечной радиации на их поверхность не одинаково. Так, для северного пилона этой пары из-за его затененности северная и восточная грань получают минимальную рассеянную солнечную радиацию (1179 Вт/м2) и практически нулевую прямую радиацию, тогда как только северная грань южного пилона это пары находится в таком положении, а остальные грани получают и прямую и рассеянную радиацию от 1442 до 3048 Вт/м2 [4]. Таким образом, созданная предзаданность при формировании теплового поля под пилонами организует под северным пилоном условия для максимального промерзания. Пониженная тепловая инсоляция северного пилона западной пары изменяет температурно-влажностный баланс грунтов его основания и фундамента и приводит к увеличению скорости промерзания и снижению скорости их оттаивания, усилению их вымораживания, что увеличивает проявление морозного пучения и создает условия для инерции полного оттаивания северных пилонов, достигающей одного-полутора месяцев. Рассмотренные условия определяют возможность неравномерных по времени и величине осадок западной пары пилонов, которые приводят к значительным деформациям, прежде всего северного пилона и крену колоколен в северо-западном направлении. О подобной причинно-следственной связи свидетельствует пример состояния колокольни ц. Рождества в с. Поярково в Подмосковье (рис.5).

Примером проявления уникальных причинно-следственных отношений в организации условий сохранения устойчивости памятника архитектуры может служить факт замещения кальцитом гниющей древесины свайного основания храма Вознесения в Коломенском. Храм имеет ступенчатый плитный фундамент, сложенный из белокаменных блоков на известковом растворе, максимальная мощность которого достигает 7м. Процессы разложения древесины свай, растворения и выноса карбонатов из фундамента в местах активной инфильтрации атмосферных осадков проходили одновременно. Возникли условия для направленного массопереноса продуктов выщелачивания белокаменной кладки плитного фундамента и метасоматоза деструктируемой древесины свай, в результате чего произошло замещение древесины кальцитом [5]. Этот процесс самоорганизации привел к появлению продукта взаимодействия в виде кальцитовых свай и свидетельствует о направленном изменении структуры первоначального свайного основания.

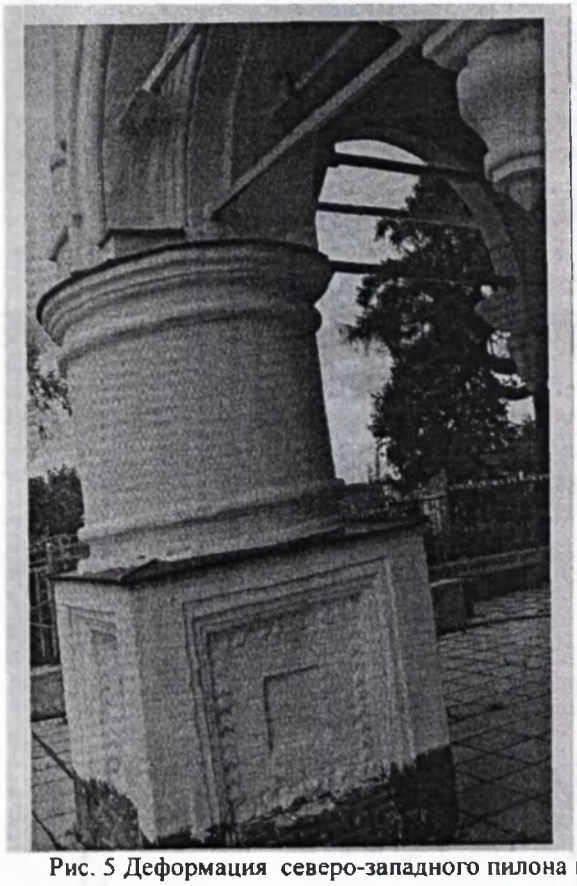


Рис. 5 Деформация северо-западного пилона колокольни церкви в с. Поярково в результате морозного пучения.

Приведенные примеры подтверждают ценность ретроспективной информации и информации обратной связи, отражающей сущность сложившихся в течение столетий взаимодействий между элементами ИПТС – информации, которая не может быть получена традиционными методами изысканий и может стать достоянием исследователя лишь в результате проведения инженерно-геологического диагноза о состоянии исторической природно-технической системы.

Польза от анализа примеров в любом деле совершенно очевидна. Особенно это важно в тех областях практической и научной деятельности, где получение информации сопряжено с большими трудностями. Поскольку жизнь памятников растянута на многие сотни лет и информации об их состоянии за прошедшие годы в большинстве случаев нет, то сказанное имеет прямое отношение к ним.

Памятники архитектуры, не имеющие нормированных сроков существования и по своему назначению призванные служить человеку вне времени, должны иметь надежное основание, нарушение которого влечет за собой деформации конструкций памятников, а иногда и их гибель. При этом надо иметь в виду, что наиболее длительный срок работы испытывали грунты в основании именно памятников архитектуры, которые за период их существования в течение многих сотен лет чаще других сооружений испытывали влияние различных изменений в окружающей среде.

Поэтому проведению реставрационных работ должно предшествовать тщательное инженерно-геологическое изучение состояния грунтов оснований, подвергшихся влиянию антропогенных изменений.

Воздействие человека на окружающую геологическую среду и состояние грунтов велико. В городах глубина вертикальной зоны антропогенных изменений грунтов под влиянием гражданского, коммунального, транспортного и гидротехнического строительства в настоящее время достигает 10-12м, а с учетом строительства метрополитена и эксплуатации водоносных горизонтов - 40-60 и более метров.

Глубина антропогенных изменений обуславливается:

а) глубиной заложения подземных коммуникаций и сооружений, перераспределением напряжений в массиве от строительства открытых и подземных горных выработок, под действием вибраций от транспорта и других источников;

б) Глубиной уплотнения или изменения грунтов в результате дренирования подземных вод или при подъеме уровня подземных вод ("самоподтопление" городов).

Антропогенные воздействия на грунты оснований могут быть разделены на механические (динамические нагрузки, суффозия) и физические; прямые (строительная деятельность человека) и косвенные (изменения грунтов при создании депрессионных воронок); обратимые (тиксотропные изменения грунтов) и необратимые; кратковременные и вековые; местные и региональные; приповерхностные и глубинные. Все эти воздействия в совокупности изменяют состояние, структуру грунтов в основании памятников

Ниже приведены примеры влияния на сохранность памятников архитектуры наиболее характерных антропогенных факторов.

I. Трапезная палата Андроникова монастыря в г. Москве.

В годы Великой Отечественной войны произошла значительная деформация объема трапезной (с последовательным образованием блоков I, II и т.д.), вызванная резким разуплотнением основания и просадками конструкций в связи с устройством под западной стеной палаты бомбоубежища, объемом до 200м^3. Оно имело вход со стороны набережной и находилось приблизительно на глубине 9м ниже уровня пола подвала. После войны, поддерживающие деревянные конструкции бомбоубежища и входной штольни были частично разобраны. Произошло постепенное обрушение бревенчатого перекрытия с соответствующей просадкой вышележащих слоев песка и насыпного грунта. Нет сомнения, что разрыхление основания под западной стеной Трапезной произошло уже в момент выработки грунта под бомбоубежище. К тому же в отрытый объем, видимо, было "выпущено" достаточное количество песка из вышележащего слоя, о чем свидетельствует большая толщина засыпки (до 5,5м) под полом подвала и характерное местное "истощение" песчаного слоя. Можно предположить, что этот прорыв произошел при проходке вентиляционной шахты или вдоль ранее существовавшего колодца. Обрушение грунта в бомбоубежище и заполнение его объема (даже неполное) привело к еще большему разрыхлению основания и увеличению площади осадки поверхности. Первоначально подстилающий песок "вытек" из-под фундаментов западной стены, частично центрального столба и внутренней стены подвала трапезной, а также и из-под юго-западного

угла Северной палаты. Эти фундаменты оказались висящими (по свидетельству отчетов за 1947-1948г.г.) или опирающимися на засыпку. Так, под западной стеной трапезной палаты на участке протяженностью 16м образовался отрыв грунта основания от подошвы фундамента на величину 0,1-0,15м. Отрыв грунта привел к появлению в сводах палаты крупных трещин и воронкообразных провалов в земляном полу подвала глубиной 0,2-0,25м. Меры по устранению просадок проводились в первые же послевоенные годы, когда заполнялись пустоты непосредственно под фундаментами; в конце 50-х годов произведено заполнение возможных не засыпанных полостей в откосе закачиванием в скважины цементно-глинистого раствора. Тогда же выполнено усиление надземных конструкций трапезной палаты - проведена чеканка трещин, перекладка обрушенных фрагментов сводов, восстановление воздушных связей и др.

Принятые меры по укреплению основания оказались своевременными, поскольку позволили устранить возможность развития дальнейших катастрофических деформаций и восстановлена рабочая схема конструкций.

Причиной последующих, ныне наблюдаемых деформаций, происходящих по старой "канве" (хотя и медленно) является действие следующих факторов нарушения основания:

а) продолжение естественного разрушения (гниение) деревянных конструкций бомбоубежища (зафиксированных скважинами 1948 и 1953г.г.) с образованием пустот;

б) суффозионный процесс при инфильтрации атмосферных осадков сквозь массив участка бомбоубежища и северного откоса (наблюдаемый в период дождей или таяния снега). Данное обстоятельство способствует явному оползанию досыпанной в 50-х годах части откоса, что особенно заметно в районе трапезной палаты, где берма получила прогибы и наклон к откосу, а покрывающее ее асфальтовое покрытие - продольные разрывы и сдвиги;

в) постоянная вибрация откоса при интенсивном движении тяжелого грузового транспорта вдоль набережной Яузы.

Регулярное затопление участка между стеной и Трапезной палатой (талыми и дождевыми водами и прорывом канализации) являлось в последние годы основной причиной осадок конструкций палаты, пристройки и примыкающего прясла монастырской стены. Протечки канализации имеют место и в междуэтажных перекрытиях, в частности, над сводом подвала трапезной палаты.

Предупреждение дальнейших осадок потребует выполнения комплекса работ по укреплению всего откоса, а также основания непосредственно под фундаментами наиболее деформированных частей здания. Представляется, что наиболее эффективным мероприятием было бы проведение повторной закачки цементно-глинистого раствора в пустоты, которая стабилизировала на время грунтовый массив. Однако, по мере гниения засыпанных деревянных конструкций, осадки могут возобновиться и будут продолжаться до тех пор, пока образующаяся в пределах бывшего бомбоубежища пустотность не будет полностью ликвидирована.

Одновременно с укрепительными работами должна быть решена проблема вертикальной планировки и водоотвода с поверхности территории монастыря.

II. Государственный музей изобразительных искусств им. А.С. Пушкина.

Начиная с 1936 года здание ГМИИ им. А.С.Пушкина стало воспринимать динамические нагрузки от проходящих в непосредственной близости поездов московского метрополитена. Наименьшее расстояние в плане от здания музея до тоннелей метрополитена составляет 9м (юго-западный угол музея, где расположен Египетский зал), максимальное удаление трассы тоннелей от главного фасада составляет менее 30м. Влияние динамических нагрузок на юго-западную часть музея усиливается тем, что на ближайшем к нему перегонном тоннеле начинается торможение поездов метрополитена, которое приводит к усилению динамических нагрузок.

Результатом передачи динамических нагрузок на грунты основания явилось их местное переуплотнение, появление неравномерных осадок, деформаций в стенах и перекрытиях музея. Особенно остро на вибрационные нагрузки реагировал наиболее хрупкий строительный материал, используемый при строительстве музея - искусственный мрамор, который в результате этих нагрузок покрылся паутиной микротрещин (Белый зал).

В 1956г. при обследовании Египетского зала, зала Древнего Востока и ряда других залов были зафиксированы кулисообразные трещины в полах с раскрытием до 3-4мм и смещением по ним блоков в вертикальном положении до 4-5мм. Характер относительных перемещений блоков пола, понижение абсолютных отметок пола в юго-западном направлении свидетельствует о продолжении развития осадок здания от вибрационных нагрузок метрополитена. В за-

лах, где динамические нагрузки ощущаются особенно остро, развитие трещин продолжается до настоящего времени. Опрос сотрудников музея, работающих в этих залах, показал, что появление новых трещин наблюдалось и в 1978 году.

Все это свидетельствует о том, что динамический процесс развития осадок грунтов оснований и фундаментов, процесс развития трещин в несущих конструкциях залов музея, расположенных в непосредственной близости от тоннеля метрополитена, продолжается.

В 1976г. по заданию ГПИ "Гипротеатр" Мосгоргеотрест провел дополнительные (первое обследование фундаментов было проведено в 1953г.) исследования фундаментов здания музея. В результате этих исследований было установлено, что фундаменты находятся в удовлетворительном состоянии, за исключением участка калориферной, где шурфами были зафиксированы горизонтальные трещины с раскрытием до 2-10мм. Причину появления этих трещин Мосгоргеотрест связывал с насыпными грунтами, якобы залегающими ниже подошвы фундамента на глубину 1,4м и рекомендовал выбрать на эту глубину грунт и заполнить новой кладкой.

В ноябре 1979 года при выполнении работ по подводке новых фундаментов на участке калориферной под Греческим залом был обнаружен отрыв нижней части фундамента на 0,6м (рис.6), а под противоположным фундаментом была зафиксирована просадка грунта на ту же величину на участке длиной около 12м. При этом было установлено, что грунты, залегающие в основании фундаментов, представлены так же, как и под фундаментами всего здания, древнеаллювиальными песками.

Ошибочная диагностика причин деформации фундаментов (неравномерное обжатие насыпных грунтов под подошвой фундаментов) явилась следствием несовершенной методики, принятой Мосгоргеотрестом при исследовании оснований (бурение скважин в рыхлых грунтах без обсадки трубами ручным буром искажает фактическое строение, состав и структуру грунтов), а также тем, что не были изучены и учтены при анализе деформаций возможные источники локального увлажнения грунтов оснований вблизи калориферной.



Рис.6 Отрыв грунтов основания от подошвы фундамента Греческого зала музея изобразительных искусств им. А.С.Пушкина.

При проходке шурфов ошибочность выявленных Мосгоргеотрестом причин трещин в фундаментах стала очевидной. Было установлено, что основание сложено древнеаллювиальными песками с характерной для них текстурой и структурой, во-вторых, было установлено, что природа просадки грунта на 0,6м с сохранением фундамента в первоначальном положении благодаря "мостовому эффекту" намного сложнее, чем просто "обжатие насыпных грунтов". Опрос рабочих калориферной показал, что в прошлом неоднократно были случаи значительной утечки воды из ванн и труб, которая удалялась под фундаменты на участке проявления максимальных деформаций.

Таким образом, наиболее вероятной причиной осадок грунтов основания явились суффозионный процесс - вынос мелких частиц грунта, вызванный утечкой воды из калориферной. Вынос песчаных частиц из переуплотненных вибрационной нагрузкой песков (в пределах активной зоны основания мощностью 5-6м), сосредоточенный в одном месте утечкой воды, привел к их разуплотнению, резкому увеличению пористости и просадке.

Значительные просадки грунтов основания на участке длиной около 12м могли бы привести к значительным деформациям и обрушениям даже при подведении бетонных фундаментов-подушек, поскольку грунты на глубине около 6-8м оказались в результате суффозионных процессов в рыхлом состоянии.

ЗАКЛЮЧЕНИЕ

Рассмотренные примеры диагноза свидетельствуют, что методы инженерно-геологического диагностирования должны основываться на изучении конкретных проявлений деструкции и дестабилизации, т.е. на оценке определенных заболеваний изучаемых систем. Историческую систему, состоящую из двух взаимосвязанных подсистем, нельзя изучать только конструктором или только инженером геологом. При диагностике должны проявляться глубокие взаимопроникновения опыта и знаний, но не должна допускаться подмена одних другими. Все задачи при диагностировании состояния элементов системы должны решаться на профессиональном уровне.

Принципиально важно отметить следующее положение. В последние годы в этой области определилась тенденция на преодоление сложившейся ложной научности, крайнего примитивизма и откровенного непрофессионализма. Подобную практику необходимо подкрепить продуманной и целенаправленной деятельностью инженеров геологов по совершенствованию общей методики диагностирования исторических систем.

ЛИТЕРАТУРА

1. Коршунов А.М. «Теория отражения и творчество». М.:Политиздат. 1971.
2. Пашкин Е.М., Кувшинников В.М. , Панкратов А.В. ,Пономарев В.В. «Особенности эволюционных изменений контакта фундамент-грунт церкви Вознесения в Коломенском.» «Геоэкология». №4. 2003.
3. Пашкин Е.М., ПодборскаяВ.О. «Исследование нижних частей несохранившейся угловой башни XVI в. Кирилло-Белозерского монастыря. Тр. С-Петербургского отделения института археологии РАН.2002.»
4. СНиП 23-01-99
5. Хворостова Е.Л. «Палаты с проходом и проездом в подклете Успенского собора Рязанского кремля. Реставрация и исследования памятников культуры.» Вып. 4. М., Стройиздат. 2001.

Characterization of Strength Variability of Cement-treated Soil Column

T. Namikawa
Department of Civil Engineering, Shibaura Institute of Technology, Tokyo, Japan

ABSTRACT: The probabilistic character of the unconfined compression strength of the cement-treated soil was examined using data sets of the cored samples retrieved from in-situ columns by deep mixing method. The spatial variability character of the unconfined compression strength is mainly studied in the present paper. The normal and lognormal distributions are adopted for the probability distribution of the cement-treated soil strength. Assuming the stationary random field with an exponential type autocorrelation function for the spatial variability of strength in a cement-treated column, we estimate the autocorrelation distance of the cored-sample strength by the maximum likelihood method. Moreover, the goodness of fit for the normal and lognormal distributions against the cored-sample strength date is evaluated using Kolmogorov-Smirnov (K-S) test and Akaike's Information Criterion (AIC). These statistical analyses reveal the probabilistic character of the strength of the cement-treated soil column.

1 INTRODUCTON

The strength of soil treated by the cement deep mixing varies widely, even at a single column, owing to variability of in-situ soil properties, variability of mixing effectiveness, and other factors. Therefore the rational design for ground improvement by deep mixing requires characterizing the strength variation. In this study, the probabilistic character of the unconfined compression strength is examined using data sets of the cored samples retrieved from in-situ cement-treated columns by the deep mixing method.

The spatial variability character of the unconfined compression strength is mainly studied in the present paper. The normal and lognormal distributions are adopted for the probability distribution of cement-treated soil strength. Assuming the stationary random field with an exponential type autocorrelation function for the spatial variability of strength in a cement-treated column, we estimate the autocorrelation distance of the cored-sample strength in the vertical direction by the maximum likelihood method. Moreover, the spatial anisotropy of the strength in a cement-treated column is studied using the strength data in the vertical and horizontal directions. The anisotropy of the autocorrelation distance is evaluated using the Akaike's Information Criterion (AIC) (Akaike 1974). Furthermore, the goodness of fit for the normal and lognormal distributions against the cored-sample strength date is evaluated using Kolmogorov-Smirnov (K-S) test and (AIC). These statistical analyses reveal the probabilistic character of the strength of the cement-treated soil column.

2 AUTOCORRELATION CHARACTER OF CORED SAMPLE STRENGTH

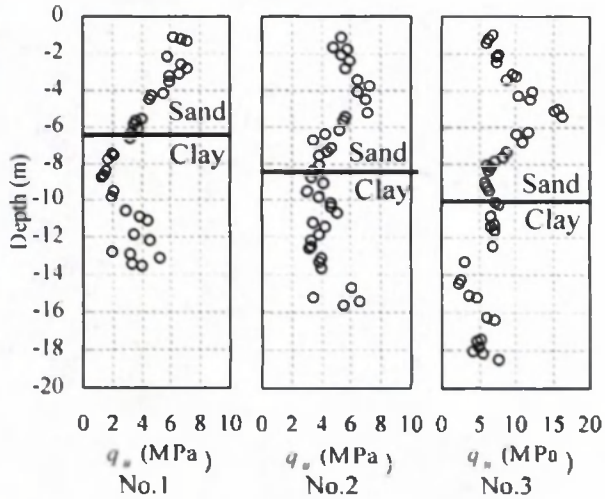
2.1 *Strength of cored sample*

The probabilistic character of the unconfined compression strength q_u in the in-situ cement-treated column by the deep mixing method is examined using the data sets of the cored samples retrieved from columns in two sites, Site 1 and Site 2. The cored samples at Site 1 were retrieved from three columns constructed at a site located at the coastal area in Japan. The data of cored sample strength at Site 2 was referred to Hibino (1985). The cored samples in Site 2 were obtained from two boreholes at the single column.

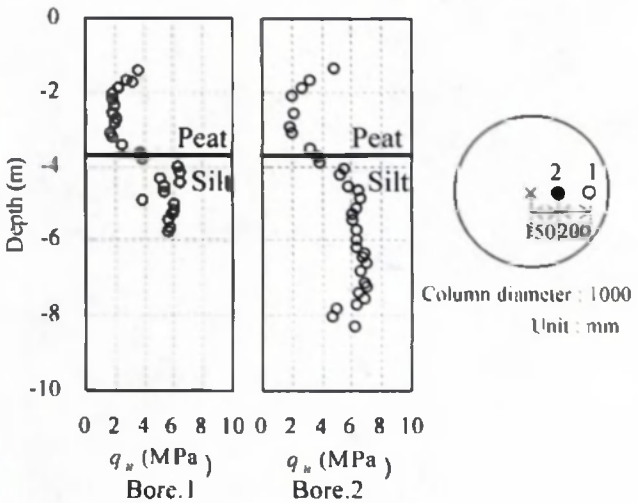
The distributions of q_u of the two data sets are shown in Figure 1. The soil profile at Site 1 consists of the upper sand and lower clay layers. Since the cement-treated soil strength depends on the soil character, the data were divided into the two groups at each sampling location. The soil profile at Site 2 consists of the upper peat and lower silt layers. Therefore, the data were divided into the two groups. The sample value of the mean, standard deviation σ and the coefficient of variation V_q, which is the standard deviation divided by the mean value, is shown in Table 1. The value of V_q ranges from 0.2 to 0.4.

2.2 *Evaluation method for autocorrelation distance*

The autocorrelation distance of unconfined compression strength of cement treated soils was calculated using the data shown in Fig. 1.



(a) Site 1



(b) Site 2

Fig. 1 Profile of unconfined compression strength q_u of cored samples

Table 1. Basic Statistics for q_u

	Column	Soil type	Mean (MPa)	σ (MPa)	V_c
Site 1	No.1	Sand	5.39	1.34	0.250
		Clay	2.92	1.17	0.401
	No.2	Sand	5.43	1.10	0.202
		Clay	4.20	0.95	0.227
	No.3	Sand	10.47	3.20	0.306
		Clay	6.07	1.67	0.274
Site 2		Peat	2.54	0.83	0.326
		Silt	5.90	0.89	0.151

The stationary random field with an exponential type autocorrelation function is assumed for the spatial variability of q_u in a cement-treated column. The exponential type autocorrelation function describes reasonably well the correlation characteristics of cement-treated soil strength (Honjo 1982). Moreover, in this study, the unconfined compression strength q_u field is assumed to follow the normal and lognormal distributions. The exponential type autocorrelation functions for q_u following the normal and lognormal distributions are defined as

$$\rho_{qu}(d) = \exp\left(-d/\vartheta_{qu}\right) \quad \text{for Normal} \qquad (1)$$

$$\rho_{\ln qu}(d) = \exp\left(-d/\vartheta_{\ln qu}\right) \quad \text{for Lognormal}$$

where $\rho_{qu}(d)$ and $\rho_{\ln qu}(d)$ are the correlation coefficients for q_u and $\ln(q_u)$, d is the distance between two points, and θ_{qu} and $\theta_{\ln qu}$ are the autocorrelation distances for q_u and $\ln(q_u)$.

The autocorrelation distance in Eq. (1) can be estimated by the maximum likelihood method (Honjo and Kazumba 2002). When q_u is assumed to follow a multivariate normal distribution, the probability distribution is expressed as

$$f_{qu}(\boldsymbol{q}_u|\theta_{qu}) = (2\pi)^{-n/2}|V_{quij}|^{-1/2} \exp\left[-\frac{1}{2}(\boldsymbol{q}_u - \boldsymbol{\mu}_{qu})^T V_{quij}^{-1}(\boldsymbol{q}_u - \boldsymbol{\mu}_{qu})\right] \qquad (2)$$

$$\boldsymbol{q}_u = \begin{bmatrix} q_u(r_1) \\ \vdots \\ q_u(r_n) \end{bmatrix}, \quad \boldsymbol{\mu}_{qu} = \begin{bmatrix} \mu_{qu} \\ \vdots \\ \mu_{qu} \end{bmatrix},$$

$$V_{quij} = \sigma_{qu}^2 \exp\left(-\frac{d_{ij}}{\theta_{qu}}\right)$$

where n is the number of the data, μ_{qu} is the mean of q_u, σ_{qu} is the standard deviation of q_u and d_{ij} is the distance between points i and j.

When q_u is assumed to follow a multivariate lognormal distribution, the probability distribution is expressed as

$$f_{qu}(\ln \boldsymbol{q}_u|\theta_{\ln qu}) = (2\pi)^{-n/2}|V_{\ln quij}|^{-1/2} \exp\left[-\frac{1}{2}(\ln \boldsymbol{q}_u - \boldsymbol{\mu}_{\ln qu})^T V_{\ln quij}^{-1}(\ln \boldsymbol{q}_u - \boldsymbol{\mu}_{\ln qu})\right] \qquad (3)$$

$$\ln \boldsymbol{q}_u = \begin{bmatrix} \ln q_u(r_1) \\ \vdots \\ \ln q_u(r_n) \end{bmatrix} \quad \boldsymbol{\mu}_{\ln qu} = \begin{bmatrix} \mu_{\ln qu} \\ \vdots \\ \mu_{\ln qu} \end{bmatrix}$$

$$V_{ln\,qui} = \sigma^2_{ln\,qu} \exp\left(-\frac{d_{ij}}{\theta_{ln\,qu}} \right)$$

where μ_{lnqu} is the mean of $\ln(q_u)$, σ_{lnqu} is the standard deviation of $\ln(q_u)$.

The log likelihood function of the multivariate normal distribution is given as follows

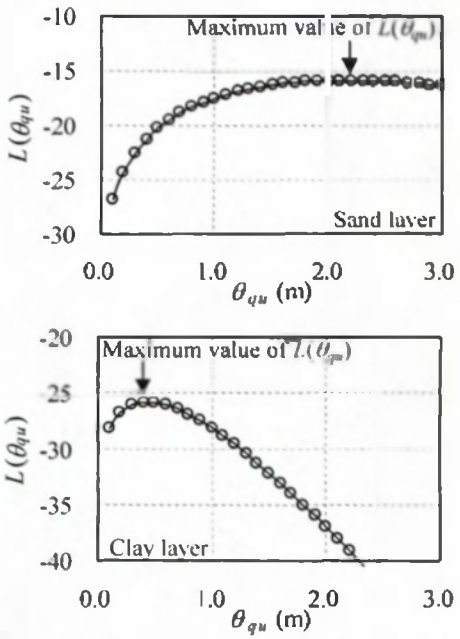
$$L(\theta_{qu}) = -\frac{n}{2}\ln(2\pi) - \frac{1}{2}\ln|V_{quij}| - \frac{1}{2}(q_u - \mu_{qu})^T V_{quij}^{-1}(q_u - \mu_{qu}) \quad (4)$$

In this methodology, the value of θ_{qu} giving the maximum value of $L(\theta_{qu})$ is identified as the maximum likelihood estimate. Similarly, the log likelihood function of the multivariate lognormal distribution is given as follows

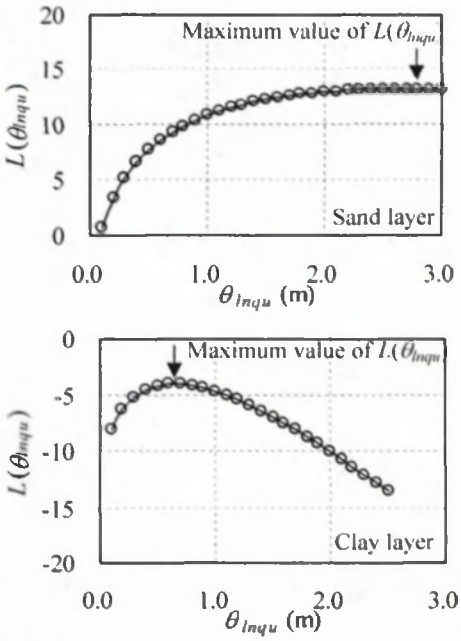
$$L(\theta_{lnqu}) = -\frac{n}{2}\ln(2\pi) - \frac{1}{2}\ln|V_{lnquij}| - \frac{1}{2}(lnq_u - \mu_{lnqu})^T V_{lnquij}^{-1}(lnq_u - \mu_{lnqu}) \quad (5)$$

2.3 *Autocorrelation distance in vertical direction*

The values of the log likelihood function for each autocorrelation distance were calculated using the data at Site 1. An example of the calculated values of $L(\theta_{qu})$ for the data is shown in Fig. 2(a). Since the cored samples were retrieved in the vertical direction at Site 1, Fig. 2(a) shows the log likelihood function for the autocorrelation distance only in the vertical direction. In these figures, the values of θ_{qu} giving the maximum values of $L(\theta_{qu})$ are identified as the optimum values for θ_{qu}. An example of the calculated values of $L(\theta_{lnqu})$ is also shown in Fig. 2(b). The evaluated optimum values for θ_{qu} and θ_{lnqu} in the vertical direction are summarized in Table 2. It can be seen that there is little difference between the optimum values of θ_{qu} and θ_{lnqu} in each layer. The optimum values of θ_{qu} and θ_{lnqu} were in a range of 0.3 m to 2.7 m. Honjo (1982) calculated the autocorrelation distance of the strength of cement-treated soils and found that the autocorrelation distance in the vertical direction is in the range of 0.4 m to 4.0 m. The calculated θ_{qu} and θ_{lnqu} values in this study fall within that range. Table 2 also indicates that the autocorrelation distance of q_u for the cement-treated sand is greater than that for the cement-treated clay. Since cohesionless soils are usually easier to mix than cohesive soils, the spatial correlation of the cement-treated sand might become stronger than that of the cement-treated clay.



(a) $L(\theta_{qu})$ for q_u



(b) $L(\theta_{lnqu})$ for $\ln(q_u)$

Fig. 2 Example of calculated log likelihood function (Site 1, No.1)

Table 2. Maximum likelihood estimator of autocorrelation distance (Site 1)

	Column	Soil type	θ_{qu}	θ_{lnqu}
Site 1	No.1	Sand	2.2 m	2.7 m
		Clay	0.4 m	0.6 m
	No.2	Sand	1.2 m	1.2 m
		Clay	0.3 m	0.3 m
	No.3	Sand	2.1 m	2.4 m
		Clay	1.1 m	1.4 m

2.4 *Spatial anisotropy of strength*

The spatial anisotropy of the strength in a cement-treated column is studied using the data at Site B where the cored samples were retrieved from two boreholes at the single column. The normal distribution is assumed for q_u here. The exponential type autocorrelation functions for the vertical and horizontal directions are defined as

$$\rho_{qu}(d_v, d_h) = \exp\left(-\frac{\sqrt{d_v^2 + \alpha^2 d_h^2}}{\theta_{qu}}\right) \quad (6)$$

where d_v and d_h are the distance in the vertical and horizontal directions, and α is the parameter associated with the spatial anisotropy. When $\alpha = 1$, denoting the spatial isotropy of q_u, the exponential type autocorrelation functions can be expressed as Eq. (1). When Eq. (6) is adopted for autocorrelation functions, the matrix of the covariance in Eq. (2) is rewritten as

$$V_{quij} = \sigma_{qu}^2 \exp\left(-\frac{\sqrt{d_{vij}^2 + \alpha^2 d_{hij}^2}}{\theta_{qu}}\right) \quad (7)$$

where d_{vij} and d_{hij} are the distances in the vertical and horizontal directions between two points.

The calculated log likelihood function for the normal distribution is shown in Fig. 3 and Fig. 4. Fig. 3 shows the values of the log likelihood function for θ_{qu} on the assumption of spatial isotropy. Fig. 4 shows the values of the log likelihood function for θ_{qu} and α on the assumption of spatial anisotropy. The maximum value of $L(\theta_{qu}, \alpha)$ for the peat layer is observed for $\theta_{qu} = 0.63$ and $\alpha = 0.5$; the maximum likelihood estimator of α is smaller than 1. This indicates that the autocorrelation distance in the horizontal direction is larger than that in the vertical direction. On the other hand, the maximum value of $L(\theta_{qu}, \alpha)$ for the silt layer is observed for $\theta_{qu} = 0.25$ and $\alpha = 1.3$; the maximum likelihood estimator of α is larger than 1, indicating that the autocorrelation distance in the horizontal direction is smaller than that in the vertical direction. This difference in the results of the maximum likelihood estimator implies that the characteristic of spatial anisotropy of q_u is not determined unambiguously.

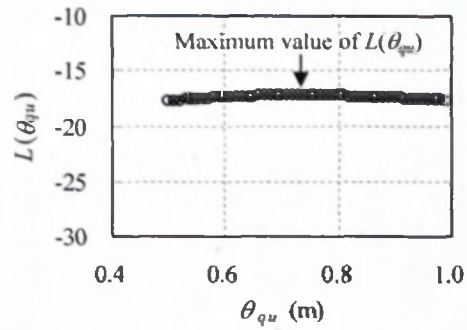
Fig. 3 and Fig. 4 show the log likelihood function on the assumption of spatial isotropy and anisotropy. However, while one parameters, θ_{qu}, is used on the assumption of spatial isotropy, two parameters, θ_{qu} and α, are used on the assumption of spatial anisotropy. Therefore, instead of the log likelihood function, Akike's Information Criterion (AIC) is employed to evaluate the spatial anisotropy of q_u (Akaike 1974). AIC is calculated from the log likelihood function for the normal distribution as

$$\text{AIC} = -2L(\theta_{qu}) + 2k \quad \text{for} \quad \text{Isotropy} \quad (8)$$

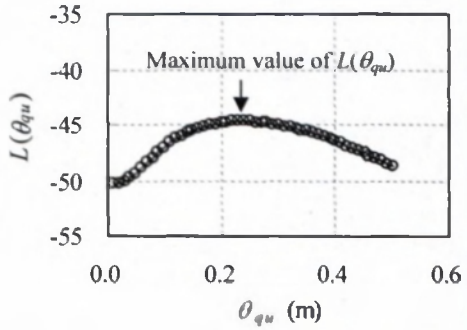
$$\text{AIC} = -2L(\theta_{qu}, \alpha) + 2k \quad \text{for} \quad \text{Anisotropy}$$

where $L(\theta_{qu})$ and $L(\theta_{qu}, \alpha)$ are maximum log likelihood and k is the number of parameters. The low value of AIC denotes the adequate model for the data.

The calculated values of AIC for the maximum likelihood estimators are shown in Table 3. For both the soils, the AIC values for the isotropic model are smaller than those for the anisotropic model; the model on the assumption of the spatial isotropy fit the data of q_u better than that on the assumption of the spatial avisotropy. This result indicates that the spatial isotropy can be assumed on the cored sample strength of the cement-treated soil column.

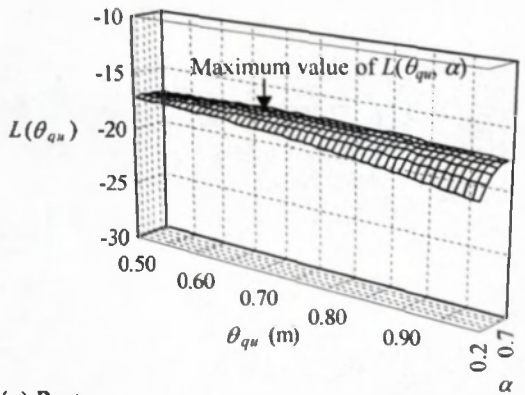


(a) Peat

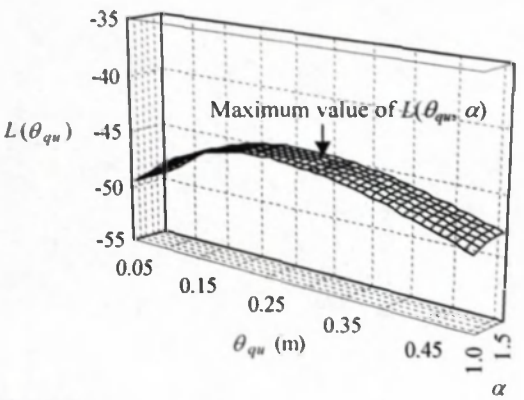


(b) Silt

Fig. 3 Calculated log likelihood function (Isotropy)



(a) Peat



(b) Silt

Fig. 4 Calculated log likelihood function (Anisotropy)

Table 3. AIC on maximum likelihood estimator (Site 2)

	Soil type		AIC	θ_{qu}	α
Site 2	Peat	Isotropy	36.6	0.73 m	-
		Anisotropy	37.7	0.63 m	0.5
	Silt	Isotropy	91.4	0.24 m	-
		Anisotropy	93.3	0.25 m	1.3

3 PROBABILITY DISTRIBUTION OF CORED SAMPLE STRENGTH

In the previous section, the normal and lognormal distributions were adopted for the probability distribution of the cement-treated soil strength. Fig. 5 shows an example of the histogram of q_u for the No.2 sand layer in Site 1. From such histogram, it is difficult to determine which of the distributions fits the probability distribution of q_u better. Here the Kolmogorov-Smirnov (K-S) test is used to evaluate the goodness of fit for the normal and lognormal distributions against the two data sets. The results of the K-S test are shown in Table 4. In this table, the D statistic is defined as

$$D = \max|F(x) - S_n(x)| \tag{9}$$

in which $S_n(x)$ is the sample cumulative distribution function and $F(x)$ is the target cumulative distribution function with the sample mean and variance. The P-value is calculated based on the test statistic, and denotes the threshold value of the significant level in the sense that the null hypothesis will be accepted for all values less than the P-value. Low values of the D statistic indicate a better fit of the data to the distribution than do high values. From these test results, it cannot be decided which of the distributions is the better one. The K-S test also shows that the P-values are larger than 0.1 in all the cases of the normal and lognormal distributions, indicating that the null hypothesis that these distributions are suitable for the probability distribution of q_u can be accepted at the 10 % significant level.

AIC is also used to evaluate the goodness of fit for the normal and lognormal distributions against the two data sets. Unlike the K-S test result, the effect of the spatial correlation is considered in the results estimated by AIC. Here the spatial isotropy is assumed in the analysis for the Site 2 data. The calculated AIC values are shown in Table 5. These values are calculated with the maximum likelihood estimators of θ_{qu} and θ_{lnqu}. As mentioned previously, the low value of AIC denotes the more adequate probability distribution for the data. The calculated AIC also indicates that it cannot be decided which of the distributions is the better one. The results of the K-S test and AIC suggest that there is not much to choose between the normal and lognormal distributions for the probability distribution of the cored sample strength.

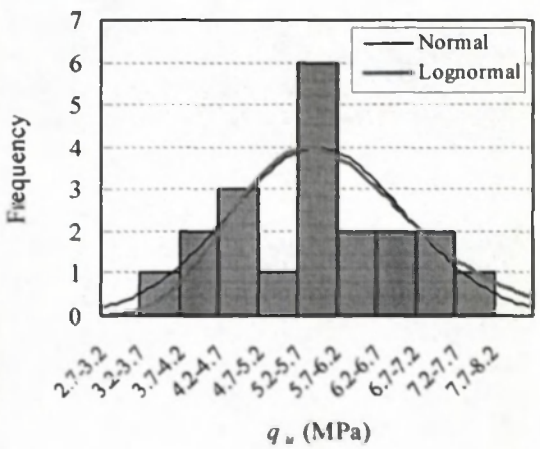


Fig. 5 Histogram for cored sample strengths q_u

Table 4. Kolmogorov-Smirnov Test results for cored sample strength q_u

Site	Column	Soil type		D	P-value
1	No.1	Sand	Normal	0.148	0.799
			Lognormal	0.182	0.563
		Clay	Normal	0.206	0.348
			Lognormal	0.167	0.606
	No.2	Sand	Normal	0.096	0.984
			Lognormal	0.135	0.810
		Clay	Normal	0.190	0.386
			Lognormal	0.156	0.633
	No.3	Sand	Normal	0.136	0.852
			Lognormal	0.137	0.844
		Clay	Normal	0.145	0.526
			Lognormal	0.196	0.188
2		Peat	Normal	0.227	0.209
			Lognormal	0.210	0.288
		Silt	Normal	0.137	0.602
			Lognormal	0.157	0.431

Table 5. Calculated AIC Values for cored sample strength q_u

Site	Column	Soil type		AIC
1	No.1	Sand	Normal	33.7
			Lognormal	31.8
		Clay	Normal	53.5
			Lognormal	47.8
	No.2	Sand	Normal	45.9
			Lognormal	46.6
		Clay	Normal	55.2
			Lognormal	50.8
	No.3	Sand	Normal	68.9
			Lognormal	64.8
		Clay	Normal	88.5
			Lognormal	92.6
2		Peat	Normal	36.6
			Lognormal	27.4
		Silt	Normal	91.4
			Lognormal	98.9

4 CONCLUSIONS

The probabilistic character of the unconfined compression strength q_u in the in-situ cement-treated column by the deep mixing method is examined using the two data sets of the cored sample strength. The autocorrelation distance of q_u was estimated by the maximum likelihood method. The optimum values for the autocorrelation distance were in a range of 0.3 m to 2.7 m. Moreover, the spatial anisotropy of the strength in a cement-treated column is studied using Akike's Information Criterion (AIC). The calculated AIC indicated that the spatial isotropy can be assumed on the cored sample strength of the cement-treated soil column.

The Kolmogorov-Smirnov (K-S) test and AIC were used to evaluate the goodness of fit for the normal and lognormal distributions against the two data sets. The results of the K-S test and AIC suggest that there is not much to choose between the normal and lognormal distributions for the probability distribution of the cored sample strength

REFERENCES

Akaike, H. (1974). "A new look at the statistical model identification." *IEEE Trans. Automat. Contr.*, Vol.19, 716-723.

Hibino, S. (1985). "Construction example. Chemical solidification work by Teno-column method." *Dobokuseko*, 26(14), 153-161. (in Japanese)

Honjo, Y. (1982). "A probabilistic approach to evaluate shear strength of heterogeneous stabilized ground by deep mixing method." *Soils and Foundations*, **22**(1), 23-38.

Honjo, Y., and Kazumba, S. (2002). "Estimation of autocorrelation distance for modeling spatial variability of soil properties by random field theory." *The 47th Geotechnical Engineering Symposium*, JGS, 279-286.

Estimation of Liquefaction from Case Histories

Saeed Ghaffarpour Jahromi
Department of Civil Engineering, Shahid Rajaee Teacher Training University, Tehran, Iran

Marte Gutierez
Colorado School of Mines, Golden, CO, U.S.A

ABSTRACTA critical parameter in the evaluation of the liquefaction of soils is the residual or liquefied shear strength. Liquefaction of granular soils can have extremely detrimental effects on the stability of soil slopes and deposits, and on structures founded on them. This liquefied shear strength determines the magnitude of the deformation that the soil will undergo once it has liquefied. Current procedures for estimating the liquefied shear strength are based on laboratory testing programs or from the back-analysis of case histories of liquefaction failures where in-situ test data were available. The case-histories approach is the procedure that is preferred in practice. However, it has several limitations including the very limited amount of data available, the significant uncertainties involved in the back-calculation of the liquefied shear strengths, and the lack of consistent and rational methods in the use of the available data. To address these current limitations, this paper proposes new probabilistic liquefied shear strength criteria for liquefiable soils from case histories.

1 INTRODUCTION

According to Seed (1987), the two important aspects related to the liquefaction of soils are the stress conditions that trigger liquefaction, and the consequences of the liquefaction. The first one requires the determination of the liquefaction shear strength, and the second one the post-liquefaction shear strength. It is now increasingly being recognized that the determination of the undrained residual shear strength could be more important than the determination of the stress conditions that trigger the liquefaction itself (e.g., Ishihara 1993; Stark et al. 1997; Finn 2000). The undrained residual or liquefied shear strength is the main factor which controls whether flow failure or large deformations will occur. As pointed out by Seed (1987), it may be adequate and economically advantageous simply to ensure the stability of an earth deposit or structure against post-liquefaction failure after the strength loss has been triggered than to prevent the triggering itself.

There are currently two methods for estimating the residual strength of soil deposits. One method is the case histories approach where the liquefied shear strength is back calculated from known cases of liquefaction in soil zones where in situ test data (e.g., Standard Penetration Tests results) were available.

The other approach for determining the residual shear strength is the laboratory procedure. Poulos et al. (1985) have developed a procedure for flow liquefaction using the results of monotonically loaded, consolidated-undrained triaxial tests. Ideally, the residual shear strength should be determined using undisturbed samples. However, it is often difficult to obtain high-quality undisturbed soil samples needed to determine the residual shear strength. More importantly, the costs of sampling and laboratory testing required in the laboratory approach are generally prohibitive, making the procedure applicable only for critical and large projects. Although the use of field data and case histories should be preferred in practice, there are several limitations of the case histories approach; first limited amount of data on back-calculated residual shear strengths from field case histories, second significant uncertainties involved in the backcalculation of the residual shear strengths, and third lack of consistent and rational methods to use the available data on residual shear strength of granular soils. In order to address the current limitations in evaluating the liquefied shear strength of cohesionless soil deposits using in situ tests, this paper aims to first re-evaluate and expand the available database on residual shear strengths of liquefied soils, second clearly delineate and systematically analyze the magnitudes of uncertainties involved in evaluating post-liquefaction shear strength, third develop robust, reliability-based procedures for back-calculating residual shear strength from case histories and forth present new probabilistic liquefied shear strength criteria for post-liquefaction stability analysis of cohesionless soils.

2 CASE HISTORIES AND METHOD OF BACK ANALYSIS

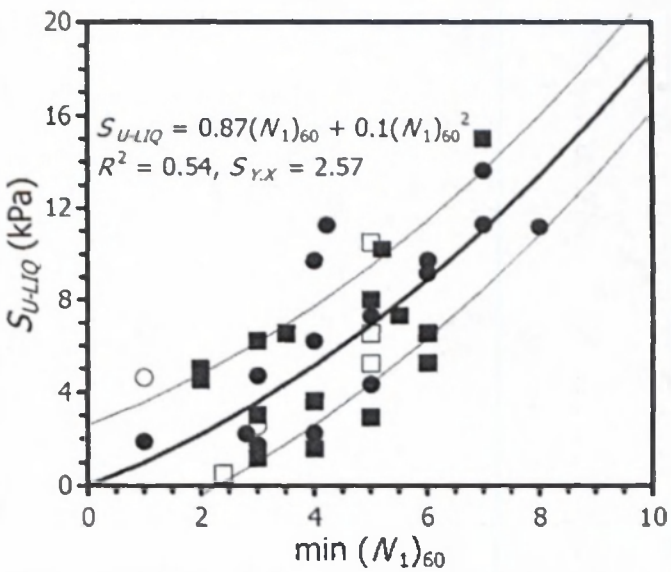
Thirty-eight case histories of flow liquefaction failures of natural and engineered slopes, including earth dams and embankments were analyzed to obtain data on liquefied shear strength of cohesionless soils. The case histories are composed of 18 failures which were analyzed with the infinite slope model and 20 cases which were analyzed using the more general Spencer's (1967) method of slices. Only case histories with sufficiently good quality data to perform the probabilistic backanalysis were included. The case histories include re-analyses of cases that were included in the study performed by Olson & Stark (2003), and nine new cases from recent earthquakes, including the 1993 Kushiro-oki Earthquake, 1993 Hokkaido-Nansei-oki Earthquake, 1995 Hyogoken-Nambu Earthquake, and the 1999 Kocaeli/Izmit Earthquake. The re-analyses differ from the analyses done by Olson & Stark (2003) in the following aspects; first the re-analyses did not account for kinetic forces, second the minimum instead of the average value of $(N1)_{60}$ was used, third the SPT blow counts were not corrected for fines content and forth the liquefied shear strengths were not normalized with respect to the initial effective vertical stress.

The post-failure geometries were used for the back-analyses since the liquefied shear strength is mobilized in conjunction with the post-failure geometry (i.e., after liquefaction has been triggered). The undrained shear strength in each field case was systematically adjusted until the slope stability model matches the observed field post-failure geometry. Best estimates of parameters required in the slope stability analyses were used.

The slip surface for the infinite slope cases was defined by the depth to the water table and the height of water above the failure surface. These values are assessed based on available cross-sections and measurements of the likely zone of liquefied material. For the analysis of the complex cases, the slip surfaces for back-calculating the liquefied shear strength are determined by finding the minimum factor of safety surface corresponding to the liquefied shear strength resulting in a factor of safety of unity. This provides a consistent means for selecting a slip surface for analysis as the slip surface in the field does not necessarily correspond to limit equilibrium slip surface.

Figure 1 shows the back-analyzed undrained liquefied shear strengths $S_{u\text{-}LIQ}$ vs. $\min(N1)_{60}$ obtained from the 38 case histories. It was found that the best correlation between $S_{u\text{-}LIQ}$ Sand $\min(N1)_{60}$ is obtained when the SPT blow count is not corrected for fines content. Also as discussed by Fear & McRoberts (1995) and Wride et al. (1999) the use of average SPT blow counts typically provides conservative values of liquefied shear strength. They proposed the use of the minimum SPT blow count as the "weakest-link-in-the-chain" measure. The $\min(N1)_{60}$ values turn out to correlate well with the undrained shear strength that leads to liquefaction flow failure.

Different types of regression were tried to develop the best approximation of the back-analyzed liquefied shear strengths $S_{u\text{-}LIQ}$ vs. the SPT blow count $\min(N1)_{60}$ data obtained from the case histories. The correlations included: linear, power, logarithmic, exponential, and second order polynomial equations. It was found that the second-order polynomial shown in Figure 1 provides the best-fit. Figure 1 also shows the corresponding to plus and minus one standard error of estimate. The R^2 value for the best fit curve is about 0.54. Approximately 71% (27 of 38 cases) of the case histories fall within the one standard error of best fit curve. In conventional analysis, the best fit line can be used to provide the best estimate of $S_{u\text{-}LIQ}$ from the measured value of $\min(N1)_{60}$.



Fige 1. Relationship between liquefied shear strength and SPT blow count from case histories of flow liquefaction.

3 PROBABILISTIC PROCEDURES

The First-Order Reliability Method (FORM) and Monte Carlo Simulation (MCS) are used to probabilistically analyze the failure case histories. Probabilistic analyses are needed to account for the

influence of uncertainties and variabilities in soil properties and in situ test data on the reliability of the backcalculated relationship between S_{u-LIQ} and $min(N1)_{60}$. The probabilistic analyses provide estimates of the probability of failure PF for cases of flow liquefaction failure in addition to the traditional factor of safety FS estimates. The FORM and MCS probabilistic procedures are used in conjunction with the infinite slope and Spencer's (1967) stability models.

Calculation of probability of failure requires definition of a performance function. Performance functions provide a limit surface which defines the boundary between failure and safety. Typically failure is defined as factors of safety FS less than 1 and safety is defined as factors of safety greater than 1. Therefore, the performance function G(x) used to assess the reliability is given as:

$$G(x) = C_1 FS - 1 \quad (1)$$

where FS is a function of all parameters involved in the slope stability analysis and the liquefied shear strength. The C1 term accounts for uncertainty in the performance function, and is discussed in more detail below. Failure corresponds to $G(x) \leq 0$ and safety corresponds to $G(x) > 0$.

3.1 First-Order Reliability Method

FORM involves calculation of the reliability index β, which is a measure of the standardized distance between the "mean" point (all inputs are assigned mean values) and the failure surface. Several procedures are available to compute β most of which involve developing the first derivative of the performance function. This task can be quite cumbersome as the performance function becomes complex. Low & Tang (2004) present an ellipsoidal approach where formulation of the first derivative is not required, and correlated and non-normal parameters are easily incorporated in a spreadsheet format. Equation (2) is used to calculate the minimum β:

$$\beta = \min_{\underline{x} \in F} \sqrt{\left[\frac{x_i - m_i^N}{\sigma_i^N}\right]^T [R]^{-1} \left[\frac{x_i - m_i^N}{\sigma_i^N}\right]} \quad (2)$$

where x is a vector representing the random variables in the slope stability calculations, F is the failure domain, [R] is the correlation matrix, and m_i^N and σ_i^N are vectors of the equivalent-normal mean and standard deviation computed from Rackwitz-Fiessler (1978) transformations. When calculating reliability indices using Equation (1), it is important to consider the deterministic FS, as only positive values of β can be obtained. If the deterministic FS is less than 1 (i.e., within the failure domain) the computed reliability index should be made negative. If the deterministic FS is greater than 1 (i.e., with the safe domain) the computed reliability index should be positive.

The probability of failure PF is normally computed with the notional probability concept, which assumes that the probability of failure can be computed from the reliability index β according to:

$$P_F = 1 - \Phi(\beta) = \Phi(-\beta) \quad (3)$$

where $\Phi(\beta)$ is the cumulative normal distribution.

3.2. Monte Carlo Simulation

MCS consist of generating a large number of samples, typically in the order of 10,000 to 100,000, from probability density functions (PDFs) of the parameters involved in the slope stability calculations. MCS then calculates the performance function for each group of samples using a prescribed stability model. Several commercially available software packages, such as @RISK (Palisades 1996), can be used to perform the simulations within Microsoft Excel. The Package @RISK was used for the infinite slope stability calculations. In addition, the slope stability software SLIDE from Rocscience (2006) combines MCS with several stability models. This software was used to analyze the Spencer-type cases of flow failure. In the context of slope stability, MCS provides a distribution of the factor of safety against failure. The P_F is then computed as the area under the factor of safety probability density function less than 1, or the probability that the performance function (Equation 1) is less than zero. When the MCS and FORM models have the same setup, the resulting P_F values should be identical as shown by Low & Tang (1997).

3.3. Uncertainties in Parameters

For all case histories that were back-analyzed, the magnitudes of uncertainties involved in evaluating the liquefied shear strength from field data have been carefully delineated and systematically analyzed. Probability Distribution Functions (PDFs) representative of the various parameters involved in the stability analyses were developed through available data from each case history or from historical catalogs of parameter uncertainty. For those case histories where the variations in site specific data distributions are not available, published representative values of probabilistic parameters will be used. Normal and lognormal PDFs are two widely used distributions.

While most data in nature appears to follow these distributions, they both can provide unreasonable values for geotechnical problems. The normal distribution spans from negative infinity to positive

infinity. When modeling parameters such as shear strength, friction angle or unit weight, negative and very high values are not reasonable. The lognormal distribution spans from zero to positive infinity. While the lognormal PDF does address the problem with negative values, very high values approaching infinity can still lead to unrealistic results and numerical problems. In addition, for most geotechnical parameters, lower bounds greater than zero are desirable. For example, the friction angle will likely never approach zero for drained sand in the field. To address the shortcomings of both normal and lognormal distributions and to avoid artificially truncating the PDFs, the Beta distribution is employed. The Beta distribution is defined by four parameters: the minimum and maximum values, the mean value, and the standard deviation. Note that truncating both the normal and lognormal distributions will also require a similar number of parameters as the Beta distribution.

4 PROBABILITIES OF FAILURE FOR CASE HISTORIES

The deterministic FS for each case is computed using the mean input values, which gives the best-fit line shown in Figure 1. The PDF of minimum SPT blow counts for each case is used to compute the distribution of liquefied shear strength from the relationship presented in Figure 1. The P_F and deterministic FS calculated for all cases are mapped using a Bayesian Mapping (BM) technique described by Juang et al. (2006). The BM procedure is based on regression analyses with the logistic function in Equation (4):

$$P_F = \frac{1}{1+(\frac{FS}{A})^B} \qquad (4)$$

where A and B are mapping coefficients.

Incorporating uncertainties in the performance function with the C_1 term (Equation 4) provides a rigorous approach to computing the probability of failure. As shown by Juang et al. (2006), P_F values may be inaccurate if model uncertainties are not accounted for. To assess the model uncertainty term, parametric studies were performed by changing the mean (μ_{C1}) and standard deviation (σ_{C1}) of C_1. The values are varied until the P_F computed from the FORM or MCS match those calculated from the PDF of the reliability index. Based on the parametric studies, the model uncertainty term has a μ_{C1} of 1.0 and σ_{C1} of 0.4. Figure 2 presents the PF, which accounts for the C_1 term, as a function of FS for the liquefaction failure cases presented in Figure 1. Figure 2 shows that as the deterministic FS increases the P_F decreases, as expected. The best-fit parameters A and B are equal to 1.048 and 2.908, respectively. As can be seen, the logistic function given in Equation (4), with P_F accounting for model uncertainty through parameter C_1, provides a good representation of the mapping between P_F and FS from the back-analyzed case histories.

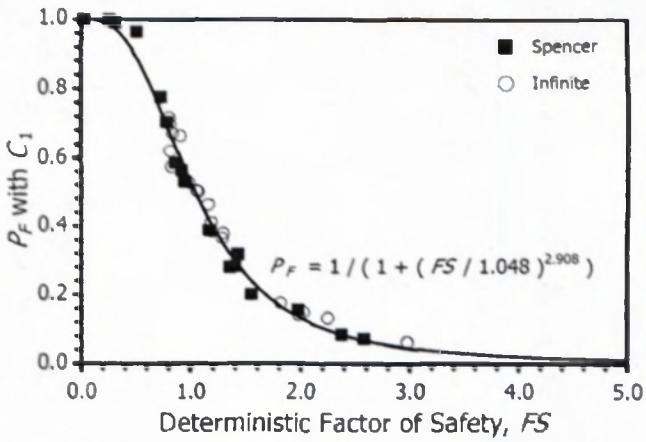


Fig 2. Mapping of P_F and FS. P_F is computed with FORM for infinite slope cases and MCS for Spencer-type cases including the C_1 term with μ of 1.0 and σ of 0.4.

5 PROBABILISTIC LIQUEFIED SHEAR STRENGTH CRITERIA

Equation (4) can be rewritten so as to plot contours of P_F on a $S_{u\text{-}LIQ}$ vs. $(N_1)_{60}$ plot:

$$\frac{S_{u(N_1)60}}{FFD} = A(\frac{1}{P_F} - 1)^{\frac{1}{B}} \qquad (5)$$

where $S_u[(N_1)_{60}]$ is the liquefied shear strength from the relationship shown in Figure 1, and FFD is the flow failure demand, which is the shear stress acting on the post-failure geometry of failed slope. The parameter FFD is analogous to the parameter CSR (cyclic shear stress ratio) in liquefaction evaluation. The FFD can be estimated from the slope stability analysis. Equation (5) gives a relationship for estimating the liquefied shear strength $S_{u\text{-}LIQ}$ for a given probability of failure PF for liquefiable cohesionless soils.

Probabilistic $S_{u\text{-}LIQ}$ versus minimum $(N_1)_{60}$ criteria are presented in Figure 3 with P_F contours corresponding to 2%, 16%, and 50%. As can be seen, the P_F=50% relationship is very close to the best fit second-degree polynomial derived in Figure 1. Figure 3 can be used in several ways to perform quick and simple probabilistic analyses of slopes and embankments containing potentially liquefiable soils: 1) with a minimum SPT blow count and FFD, the P_F can be estimated; 2) with a minimum SPT and a desired P_F the corresponding

FFD can be estimated; and 3) with the minimum SPT blow count PDF, the distribution of the liquefied shear strength can be estimated for use in probabilistic slope stability calculations.

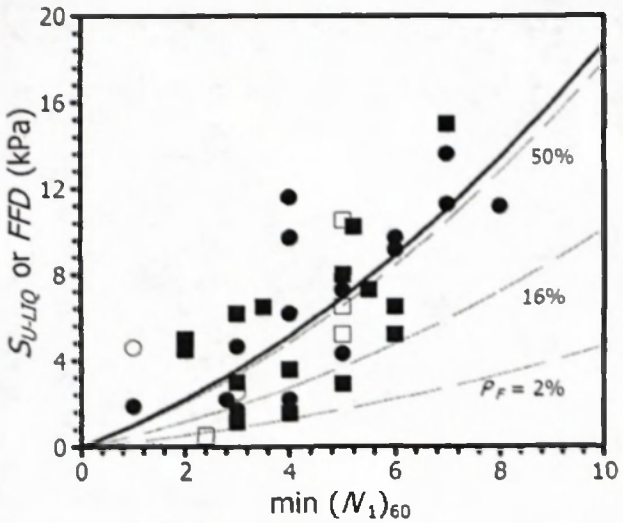


Fig 3. Contours of P_F computed with the liquefied shear strength relation shown in Fig. 1 including model uncertainty.

6 CONCLUSIONS

The paper presented probabilistic undrained residual or liquefied shear strength values of liquefiable soils as function of SPT blow count. The liquefied shear strengths were back calculated using slope stability analysis of previous case histories of flow liquefaction failures. Probabilistic procedures, including the First-Order Reliability Method (FORM) and Monte Carlo Simulations (MCS) were used in combination with limit equilibrium methods to analyze case histories of flow failure presented in the deterministic companion paper. Depending on the post-failure geometry of the case history, either the simplified infinite slope stability analysis or the more general Spencer method of slices analysis was used in the back analysis. The Beta Probability Density Function was used to model the statistical distributions and uncertainties in the geotechnical parameters involved in the probabilistic analyses. For FORM, a Bayesian Mapping procedure is used where values of PF are computed from the probability density function of the reliability indices of flow failure. The logistic mapping function is obtained by relating the deterministic factor of safety FS to PF for the liquefied shear strength relationships. A parameter C1was introduced to account for model uncertainty in the reliability calculations.

Probabilistic $S_{u\text{-}LIQ}$ versus minimum $(N_1)_{60}$ criteria were presented for P_F contours corresponding to 2%, 16%, and 50%. It was shown that the P_F=50% relationship is very close to the best fit relations obtained from the deterministic analysis of the case histories. The probabilistic $S_{U\text{-}LIQ}$ versus minimum $(N_1)_{60}$ criteria provide a more rational procedure for estimating the post-liquefaction stability of cohesionless soils deposits by providing estimates of the probability of failure in addition to traditional values of factor of safety. The probability of failure can account for the different uncertainties in the back calculation of the liquefied shear strength values from case histories, and the natural variability and uncertainties and properties of soil deposits.

7 REFERENCES

Fear, C.E. and McRoberts, E.C. (1995). Reconsideration of initiation of liquefaction in sandy soils, Journal of Geotechnical Engineering ASCE, Vol. 121(3), pp. 249-261.

Finn, W.D.L. 2000. Post-liquefaction flow deformations. Soil Dynamics and Liquefaction (2000), R.Y.S. Pak and J. Yamamuro (eds.), ASCE Geotechnical Special Publication No. 107, pp. 108-122.

Ishihara, K. (1993). Liquefaction and flow failure during earthquakes -33rd Rankine Lecture, Geotechnique, Vol. 43(3), pp. 351-415.

Juang, C.H., Jiang, T. and R.D. Andrus (2002). Assessing probabilitybased methods for liquefaction potential evaluation, Journal of Geotechnical and Geoenviromental Engineering ASCE, Vol. 128(7), pp. 580-589.

Low, B.K. and Tang, W.H. (1997). Reliability analysis of reinforced embankments on soft ground, Canadian Geotechnical Journal, Vol. 34, pp. 672-685.

Low, B.K. and Tang, W.H. (2004). Reliability analysis using object-oriented constrained optimization, Structural Safety, Vol. 26, pp. 69-89.

Olson, S.M. and Stark, T.D. (2003). Liquefied strength ratio from liquefaction flow failure case histories. Canadian Geotechnical Journal, Vol. 39, pp. 629-647.

Palisade Corporation, 1996. RISK: Risk analysis and simulation addin for Microsoft Excel or Lotus 1-2-3, Palisade Corporation, Newfield, N.Y.

Poulos, S.J. (1981). The steady-state of deformation, Journal of Geotechnical and Geoenviromental Engineering ASCE, Vol. 107(5), pp. 553-562.

Rackwitz, R. and Fiessler, B. (1978). Structural reliability under combined random load sequences, Computers and Structures, Vol. 9, pp. 484–494.

Rocscience, Inc. 2006. SLIDE version 5.025: 2-D limit equilibrium analysis of slope stability, Rocscience, Inc., Toronto, Ontario.

Seed, H.B. (1987). Design problems in soil liquefaction, Journal of Geotechnical and Geoenviromental Engineering ASCE, Vol. 113(8), pp. 827-845.

Spencer, E. (1967). A method of analysis of the stability of embankments assuming parallel interslice forces, Géotechnique, Vol. 17(1), pp. 11-26.

Stark, T.D., Kramer, S.L. and Youd, T.L. (1997). Post-liquefaction shear strength of granular soils, Proceedings NSF Workshop Postliquefaction Shear Strength of Granular Soils, National Science Foundation Grant CMS-95-31678, unpublished.

Wride (Fear), C.E., McRoberts, E.C. and Robertson, P.K. (1999). Reconsideration of case histories for estimating undrained shear strength in sandy soils, Canadian Geotechnical Journal, Vol. 36, pp: 907-933.

Assessment of the dynamic stability of the vibration dilute water-saturated soils foundation in the conditions of simulated earthquakes

I.T. Mirsayapov & I.V. Koroleva

Department of bases, foundations, dynamics of buildings and engineering geology, The Kazan State University of Architecture and Engineering, Kazan, Russia

ABSTRACT: The article presents the results of the evaluation of resistance vibration dilution water-saturated sands of the foundation of the scenario earthquakes in the city Kazan.

The concept of the Universiade - 2013 involves placing objects along the Grand Kazan Rings, including the right Bank of the Kazanka river. The location of the construction along the river consists of water-saturated Sands at a depth of up to 12 meters. These soils can be sensitive to seismic effects, in this case, the manifest dilution or thixotropic properties. The presence of such soils may indicate the need to increase in seismic activity of separate sites of accommodation facilities according to the results of seismic microzonation.

In accordance with the new map of seismic zoning of the SRF 97 on the territory of the city. Kazan is predicted an earthquake with an intensity of 7 points on the "middle ground". This fact requires the use of anti-seismic reinforcement of the design and construction of buildings and evaluate the dynamic properties of the soils of the grounds for the implementation of research.

The results of the works on seismic micro zoning of the construction site show that the seismic activity of the platform when data is the foundation soil is measured as magnitude 7.0 on a scale MSK 64 with acceleration = 143 cm^2/sec for short and medium periods of oscillations (Mirsayapov and Koroleva 2010).

Study of dynamic stability of the layer of water-saturated sands were performed in laboratory conditions. The possibility of their liquefaction under seismic impacts has been assessed. Impact consistent with the design of seismic activity site (Mirsayapov and Koroleva 2010). The conditions, when the soil is exposed to earthquake, are modeled before the test. In the result is calculated the expected seismic load. Use the technique of determining the amount of seismic load, which was proposed by Seed (1996) and Idriss (Ishihara 2006). In accordance with the methodology (Seed 1996; Ishihara 2006) of seismic load is assumed to be characterized by the value of the cyclic stresses shift (CSR) under the condition that the earthquake will be prescribed recurrence period:

$$CRS = \frac{\tau_{av}}{\sigma_v'} \qquad (1)$$

where

τ_{av} – the mean value of the expected cyclical pressures shift in the magnitude;

σ_v' – vertical stress.

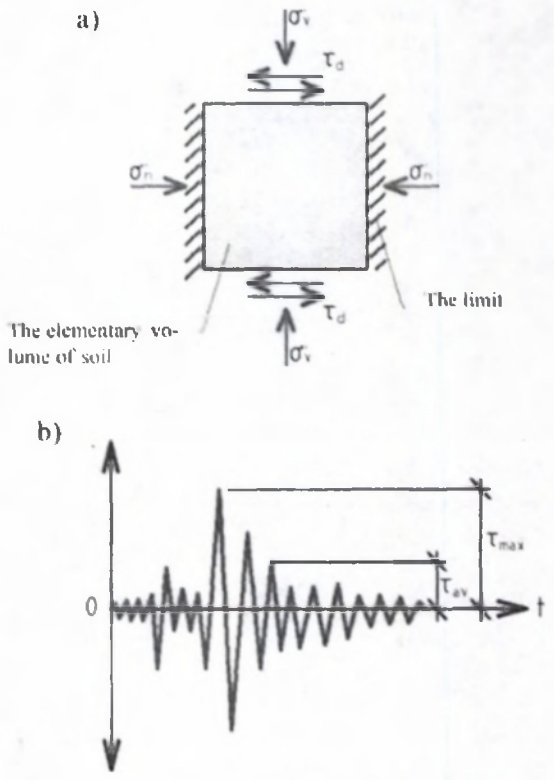


Fig.1.a) The stress condition of the soil in field conditions during the earthquake;
b) The irregular character of change of shear stresses in the earthquake.

The real dynamic loading of the soil is of a casual nature in the earthquake (Fig. 1b). In practical calculations is given to an equivalent in power against the regular (usually sine wave) law.

Tangential stresses are changing in time. This change occurs in the vertical passage of seismic shear waves through an array of ground with a smooth surface. This change will not periodic, and will be in different directions when viewed in the horizontal plane. For the quantitative assessment of the characteristics of the dilution of layers of water-saturated sands in the complex loading conditions is introduced several correction factors for the cyclic strength, which is obtained with regular cyclic loading (C_2 and C_5) (Seed 1996; Ishihara 2006). The coefficient C_2 takes into account the impact is not the frequency of the load, which operates in one direction only, the coefficient C_5 – the impact of multi-directional seismic loading. The product of the $C_2 \cdot C_5$ reflects the combined impact of non-periodicity of the load and its multi-directional. If you use these coefficients can be expressed by the relative maximum shear stress $\tau_{max.l}/\sigma_0'$, which causes a certain deformation of the shift, with different directions of non-periodic loading. The value of relative maximum shear stress is expressed through the relative cyclical stress (τ_{de}/σ_0'), which causes the same deformation for the same number of cycles of a regular one-way loading:

$$\frac{\tau_{max.l}}{\sigma_0'} = C_2 C_5 \left(\frac{\tau_{de}}{\sigma_0'} \right) / \sigma_0 \qquad (2)$$

where

τ_{de} – the amplitude of regular cyclic shear stress, causing a deformation shift;

$\tau_{max.l}$ – the peak value of the tangent of non-periodical voltage at the non-periodic change of the shear stress in the seismic loading, which causes the same deformation.

Thus, the average values of shear stress caused by the earthquake on depth, is determined from the expression.

$$\tau_{av} = (0.65 \cdot \gamma h / g) a_{max} \cdot r_d \qquad (3)$$

This expression allows you to evaluate the potential dilution of the water-saturated sandy ground in practical calculations.

The value a_{max} is passed in accordance with accelerogram earthquakes in peak vertical accelerations for the horizontal components of oscillations (Mirsayapov and Koroleva 2010).

Peak vertical accelerations when the simulated earthquake significantly less than the horizontal components and may not be taken into account when assessing the vibro dilution soils (Mirsayapov and Koroleva 2010).

When simulated seismic impact, the number of loading cycles (N) in a laboratory experiment depends on the time of the earthquake, and, consequently, the magnitude of the earthquake. It is presented in (Stavnitzer 2010; Voznesensky 1997; Seed 1996; Ishihara 2006). The above calculation gives the maximum value of the expected cyclical pressures shift in the earthquake (τ_{av}), which in carrying out three-axis dynamic tests corresponds to half the dynamic axial load.

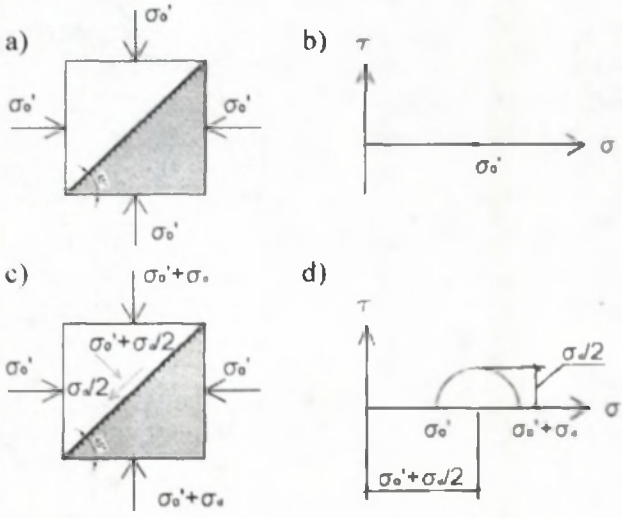


Fig.2. Modeling geostatic and cyclic stresses in the sample of the soil in conditions of triaxial compression (Ishihara 2006)
a and c) of the Stress state in the sample of the soil;
b and d) Community ultimate strength

Laboratory research of water-saturated sandy soils held in the instrument triaxial compression STF - 76/38. It is part of the measuring and computing complex ASIS. The unit is modernized for carrying out of tests in conditions of a three-axle cyclic loading on a specially developed technique. This method provides for the imposition of the static stress state of the samples of soil dynamic stresses, amplitude, frequency and duration of which are equivalent to the current simulated seismic impact. Tests were conducted in accordance with the methodology of GOST 12248-2010

on non-drained scheme with control voltages, pore pressure, vertical and radial deformation.

Equivalent seismic loading tangents cyclic loading are determined by the formula (3). The maximum acceleration shall be taken in accordance with (Mirsayapov and Koroleva 2010), equal to A=146см^2/ sec as the maximum out of all possible options. The frequency of load application 2Hz. The number of loading cycles in accordance with (Stavnitzer 2010; Voznesensky 1997; Seed 1996; Mirsayapov and Koroleva 2010) is assumed to be equal $N = 30$ cycles. Amplitude dynamic loading σ_d shall be equal to the $2\tau_{av}$ i.e. $\sigma_d = 2\tau_{av}$. The numerical values of the amplitudes of the equivalent dynamic cyclic loading shall be taken depending on the depth of the soil layer and intensity of earthquakes. The sequence of dynamic three-axle test is shown in figure 3.

In the working chamber is created comprehensive static pressure. It imitates a natural stress state in accordance with the conditions of selected soil samples (γ, h, K_0).

$$\sigma_0' = \sigma_1 = \gamma_i h_i = \sigma_2 = \sigma_3 = K_o \gamma_i h_i \qquad (4)$$

The deviator loading is made by steps until it reaches the value equal to the maximum dynamic load σ_d.

Cyclic loading is performed with the given amplitude and frequency with the supervision of the relevant stress and strain to the specified number of cycles $N = 30$ cycles.

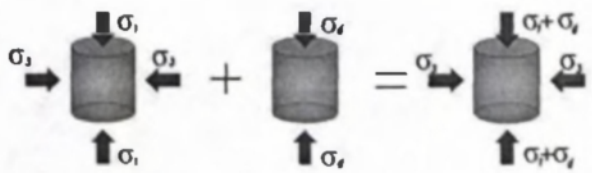


Fig.3. The sequence of loading the sample

In each series is tested at least three samples of twins with identical parameters of loading. The benchmarks are taken as average for the three samples. The main control characteristics are the maximum and minimum values of stresses (supported by the constant during the test) and deformation in the laboratory research of soils in the process of cyclic loadings.

The experimental researches have allowed to establish regularities of the development of deformations under equivalent cyclic loading and character of fatigue fracture of samples.

The character of changes of deformations at the equivalent of cyclic loading is presented in figure 4. On the charts clearly shows increasing strain during cyclic loading at the constant values of the maximum vertical load $\sigma_{1\max}$.

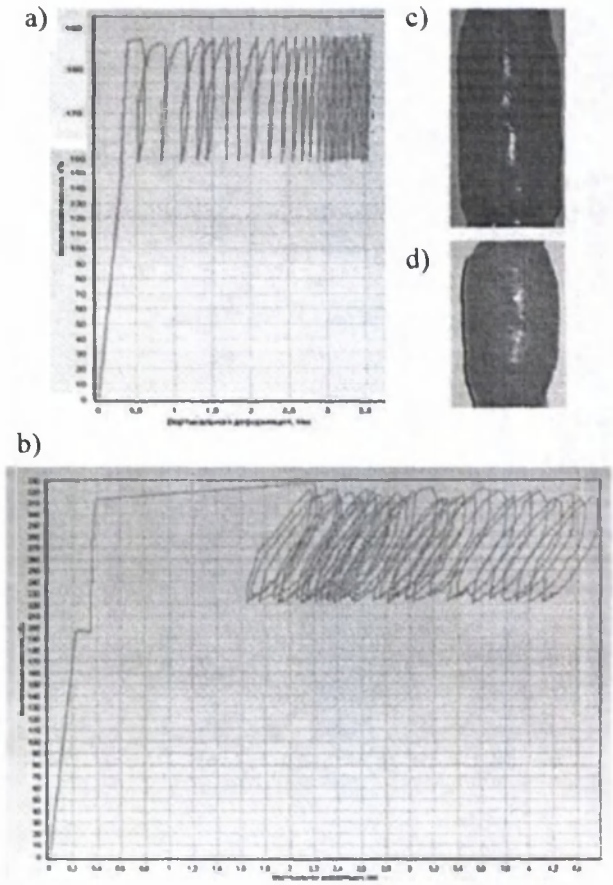


Fig.4. a) The schedule of dependence of change of linear deformations of growth of vertical stresses after 30 cycles during cyclic loading, equivalent to the current scenario earthquake with intensity magnitude 7.0;
b) The schedule of dependence of change of linear deformations of growth of vertical stresses in the destruction (more than 30 cycles) during cyclic loading, equivalent to the current scenario earthquake with intensity of more than 7.0;
c and d) The appearance of the sample of the soil after the test

Analyzing the obtained results we can conclude that, in a cyclic compression of samples sandy water-saturated soil when the parameters of the equivalent of seismic loading with the intensity magnitude 7.0, there is a development of deformations with varying intensity. At the initial stage of the development of deformations is intensively due to compaction sample, then strain stabilize.

It is established that the decrease of the amount of the effective stress in the skeleton of the soil

and the accumulation of shear deformation, which affect the degree of approximation to the limit condition, depend on:

a) intensity of cyclical effects;

b) static stress condition, if it is formed till the moment of application of the cyclical effects;

c) the possibility of additional soil compaction;

d) the ratio of the exposure time and the velocity dispersion of pore pressure.

Thus, the call criterion dilution in the form of a numerical parameter is not possible.

In connection with the use of the engineering method of evaluation of the vibro dilution.

The mechanism of the beginning of dilution water-saturated sandy soils is determined by the behavior of the standard sample of the soil, to which the device triaxial compression is applied cyclical stress with a constant amplitude of oscillations in the not drained conditions until the occurrence of a certain axial deformation.

According to the typical results of the cyclic triaxial tests (Stavnitzer 2010; Voznesensky 1997; Seed 1996; Ishihara 2006), in the process of application of cyclic axial stress pressure pore water constantly increases and reaches a value equal to the initial full pressure. This leads to the development of the axial deformation of about 5%. Such a state can be called the primary dilution or just dilution.

Accordingly, the occurrence of 5% of the axial deformation in a cyclic loading can serve as a criterion to determine the condition of cyclic decompression or dilution of water-saturated sandy soils.

As a result of research Stavnitzer (2010) established, that the principal value characterizing the dilution of the water-saturated sandy soils is the ratio of pore pressure $\beta = p_w/\sigma_{cp}$.

The criterion of dilution is $\beta \approx 1$, if $\beta \leq 0.6$ resistance to dilute provided.

Many experimental studies show that the axial deformation of the ground on the stage of the seals are reduced to the extent of increasing the number of loading cycles. If at some moment of time the return increase in strains (i.e., increasing the width of the hysteresis loop) that this moment can be conditionally accepted as a beginning of the process of dilution, i.e. $\Delta\varepsilon_{30} > \Delta\varepsilon_{29}$ although in this case the limit resistance is not achieved.

If $\Delta\varepsilon_{30} < \Delta\varepsilon_{29}$ resistance to dilute provided, i.e. $\frac{\Delta\varepsilon_{30}}{\Delta\varepsilon_{29}} < 1$.

In all samples tested during cyclic loading, equivalent to the current scenario earthquake with intensity magnitude 7.0, the magnitude of the axial deformation does not exceed 3.5 mm (4,6%) (fig. 4 a), the coefficient of pore pressure 0,3, the ratio of $\frac{\Delta\varepsilon_{30}}{\Delta\varepsilon_{29}} = 0{,}97 < 1$. In the course of the tests is not set external signs achieve maximum resistance education (drums and the inclined plane shift).

By testing samples for cyclic loading with the values of parameters is more than the specified settlement earthquake with intensity magnitude 7.0 (fig. 4b) the development of deformation occurs with varying intensity depending on the size of dynamic stress σ_d. At the initial stage there is an intensive development of deformations due to compaction soil, then it is a slowdown, and the stabilization of deformations. Later, if the limit is reached resistance liquefaction, begins decompaction of the soil and, as a consequence, the opposite is true increase in value of the strain in the cycle of loading.

The results of the test of the second series of samples to show that the primary vibro dilution begins with higher values of the dynamic stresses exceeding the dynamic stresses, the relevant settlement scenario earthquakes with intensity magnitude 7.0 from 3,0 up to 5.7 times.

REFERENCES

Ishihara, K. (2006). "Soil Behaviour in Earthquake Geotechnics" Publishers GRF. Saint-Petersburg.

Mirsayapov, I.T. and Koroleva, I.V. (2010). "The football stadium for 45,000 spectators, Chistopolskaya str. Laboratory of dynamical studies of soils under simulated earthquakes construction site." Report on research work, Publishers KSUAE, Kazan.

Seed, H.B. (1996). "Soli liquefaction and cyclic mobility evaluation for level ground during earthquakes" Journal of ASCE., 105, T2, P. 201-255.

Stavnitzer, L.R. (2010). "Seismic resistance of bases and foundations" Publishers ASV, Moscow.

Voznesensky, E.A., (1997). "The behavior of soils under dynamic loads" Publishers MSU, Moscow.

Subsurface cavities detection using surface waves

T. Akhlaghi
Faculty of Civil Engineering, University of Tabriz, Tabriz, Iran

ABSTRACT: Surface waves carry significant information about the properties of the media they propagate in, and therefore can be used for determination of geotechnical features of various sites. In this paper, surface waves dispersion characteristics have been used to theoretically investigate the presence and detection of subsurface cavities located in a homogeneous half-space. The surface waves are generated by an impact applied on the ground surface of the site under investigation. The propagating waves in the medium are simulated using finite elements in order to obtain the required numerical solution. A half-space with cavities of different sizes and embedment depths are investigated. The results show fluctuations in the dispersion curve near the cavity. The phase velocity ripples demonstrate the presence of the cavity and the pattern of the ripples can be interpreted to predict the location of the cavity.

1 INTRODUCTON

The surface wave procedure is a new rapidly developing and nondestructive testing method typically used for exploration and evaluation of geotechnical characteristics of layered systems such as soil deposits and pavement structures. The method is based on the dispersion features of Rayleigh waves in layered media. The aim of the surface wave testing is to obtain the Rayleigh wave dispersion curve, which illustrates the correlation between the phase velocity and frequency or wavelength, and then through the process of inversion to determine the shear wave velocity profile of the system.

Surface waves are generated by an impact source which produces a broad range of waves propagating with different frequencies. The nature of surface wave propagation in layered media is very complex and therefore a number of simplifying assumptions are made. One of the main assumptions made is that the layered system consists of infinite homogeneous layers with constant thicknesses. This assumption is violated whenever discontinuities such as cracks, obstacles and cavities exist in the system. Discontinuities reflect surface waves and cause fluctuations in the dispersion curve (Gucanski et al. 1996).

Limited findings are available on the effects of cavities on surface wave dispersion. Al-Shayea et al. (1994) utilized surface wave testing for detection of an artificially created underground cavity in a sand bin. They showed that the shear wave velocity determined from surface wave testing in the presence of a cavity in the soil is less than that of a soil without cavity. Gucanski et al. (1996) reported that subsurface obstacles reflect surface waves through far and near faces and cause fluctuations in the dispersion curves, particularly for long wavelengths. The procedure described herein for the cavity detection does not require the inversion of the dispersion curve, but numerical solutions of the equations of the motions are employed to determine the surface response of the system.

2 NUMERICAL MODEL

A 2-D axisymmetric finite element model has been developed to study the surface wave testing by using ANSYS computer program. Assuming that the wave propagation occurs in a vertical plane and there are no lateral reflected waves, the surface wave testing can be considered as an axisymmetric problem with an impact source at the origin of the system. As the strain level during the surface wave testing is very low, the soil is described to behave as linearly elastic material. To simplify the analysis, the soil is also defined as homogeneous and isotropic material. The analysis consists of implicit time integration of the motion equations. In order to make sure that the finite element analysis accurately simulates the surface wave testing and that the system response is not contaminated by waves reflected from the boundaries of the model, a few conditions are considered and imposed. These conditions are as follows:

(1) The element size should be small enough to capture short wavelengths, and

(2) The model should be large enough to allow propagation of large wavelengths to eliminate the effect of the boundaries on the wave field close to the cavity. The cavities with different sizes, shapes and embedment depths used for investigation in this study in a homogeneous half-space are shown in Fig. 1.

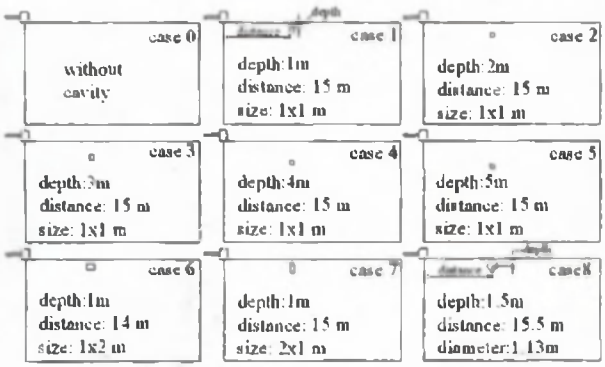


Fig. 1 Geometric specifications of cavities

The homogeneous half-space model used for this study has 50 m length and 45 m depth (Fig. 2) with 50 m/s shear wave velocity and 0.3 Poisson's ratio. Also shown in Fig. 3 is the finite element mesh model for case 1.

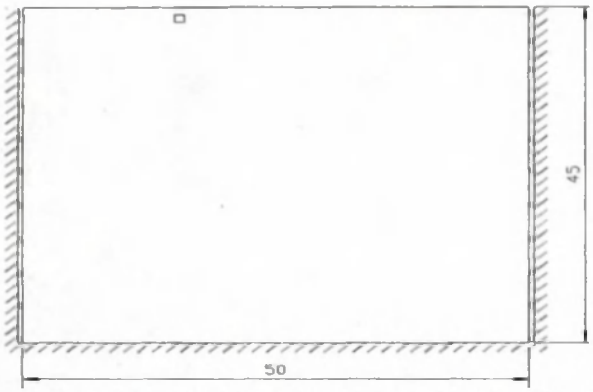
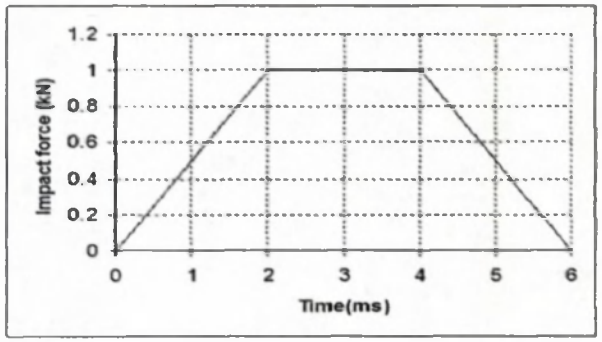


Fig. 2 Geometric Dimensions and Boundary Conditions of the Model

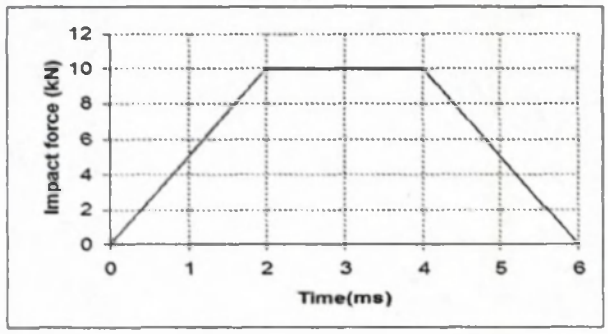


Fig. 3 Finite Element Mesh for Case 1

The impact is applied by an impulse of a trapezoidal shape with 1 kN and 10 kN amplitude and 6ms duration, as shown in Fig. 4.



(a)



(b)

Fig. 4 Model of Impulsive Loading (a)–1kN, (b)–10kN

$$\hat{f} = \frac{f}{C_s} \quad ; \quad \hat{C}_{ph} = \frac{C_{ph}}{C_s} \qquad (1)$$

For the sake of generalization, the frequency (f) and phase velocity (C_{ph}) of the waves are generalized according to the following expressions:

where C_S is the shear wave velocity of the half-space soil. In order to verify the finite element model, the dispersion curves obtained from the FE results and theoretical analysis of the half-space for case 0 (without cavity) are shown in Fig. 5. The error in phase velocity is less than 5%.

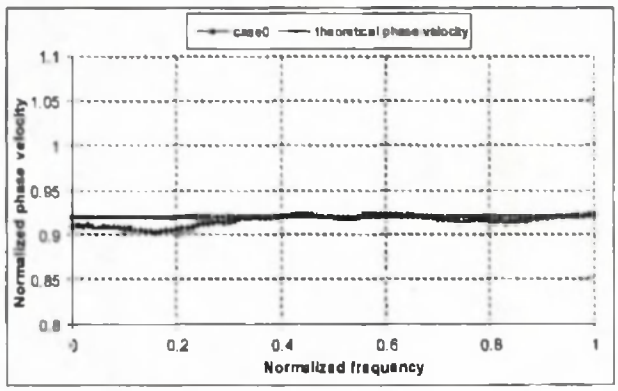


Fig. 5 Normalized Dispersion Curves for a Half-Space without Cavity

3 FINITE ELEMENT RESULTS

Various configurations of modeled cavities are shown in Fig. 1. For each case the phase velocity is first calculated as a function of the frequency and then the normalized phase velocity and frequency are determined based on the relationships given above.

Fig. 6 shows the phase velocity as a function of both first receiver location and frequency for case 1. This figure reveals that ripples are present in the dispersion curve indicating a distinct change in the phase velocity in front of the cavity. A signal recorded in front of the cavity is a superposition of the incident and reflected waves. The reflected waves, traveling toward the source, interact with the incident wave in a constructive or destructive manner, depending on the difference in their phases. The wave field is dominated by incident wave. However, reflected waves cause ripples in the overall amplitude, phase, and phase velocity. Close to the cavity, the reflected wave amplitude is comparable with respect to the incident wave amplitude, leading to more severe fluctuations. Fluctuations are far less pronounced beyond the cavity because there are no reflected surface waves in this region. The magnitude of the ripples decreases with frequency, as shown in Fig. 6. This is indicating a less pronounced effect of the reflected waves, which is generally due to three reasons. First, the phase associated with high-frequency wave components is so high that the effects of fluctuations are negligible. Second, the high-frequency waves attenuate more rapidly. Third, they do not extend deep enough to hit the cavity. The influence of the receivers spacing on the ripple magnitude is illustrated in Fig. 7.

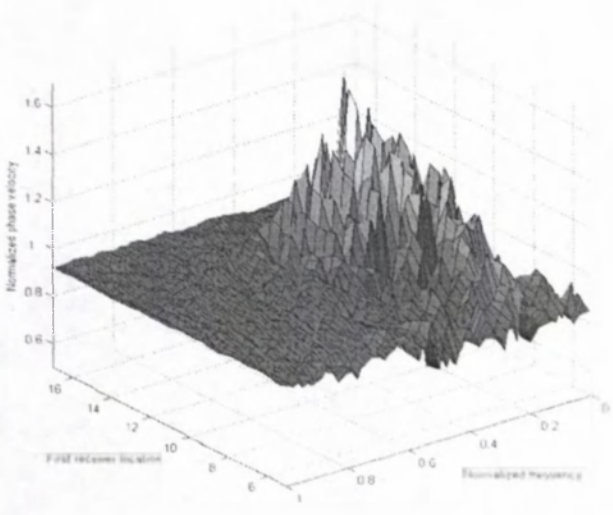


Fig. 6 Variation of Normalized Phase Velocity as a Function of Normalized Frequency and First Receiver Location for Case 1

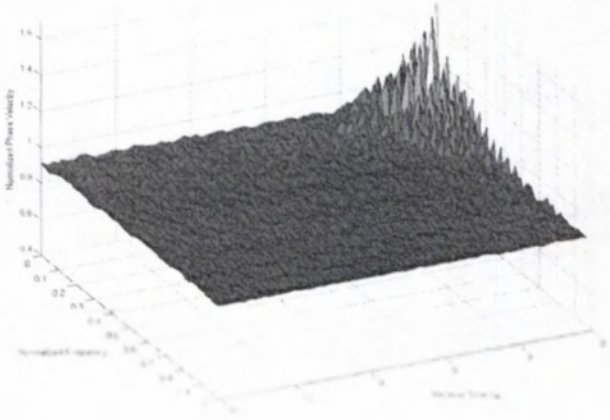


Fig. 7 Effect of Receivers Spacing on Phase Velocity in the Dispersion Curve

Evidently, ripples are more pronounced in certain frequency ranges. The magnitude of the ripples increases for shorter receiver spacing. This is due to the fact that, for small receiver spacing, the phase difference is small, thus any change in the phase will affect the total phase difference significantly. The severe variation of the phase velocity for a short receiver spacing can be used to identify the presence of a cavity. In this research work, the distance between two receive has been taken 25 cm which is retained constant for all studies.

In an attempt to correlate the size and depth of the obstacle to the dispersion curve fluctuations, the dispersion curves for cases 1-7 are investigated and compared in Figs. 8, 9 and 10. It can be seen that an increase in the height or decrease in the depth of the cavity affect considerably the magnitude of peaks and troughs, but insignificantly their location. The maximum amplitude of the ripples increases with the cavity height and decreases with the cavity depth. The effect of width of the cavity on the dispersion curve is also studied and it can be concluded that the position of the ripples does not change significantly, and the amplitude does.

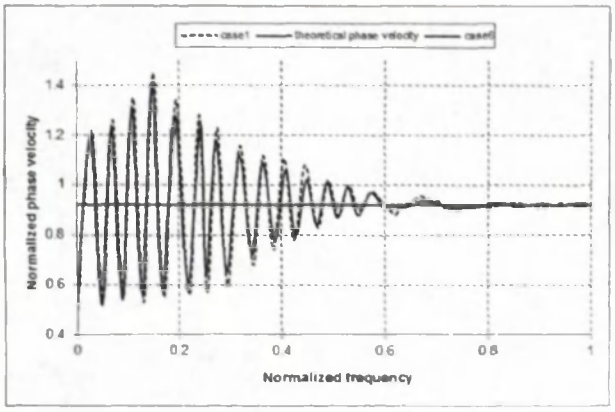


Fig.8 Effect of Cavity Width on Dispersion Curve

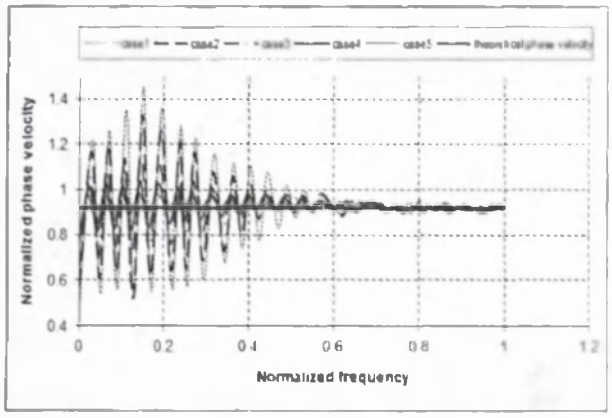


Fig.9 Effect of Cavity Embedment Depth on Dispersion Curve

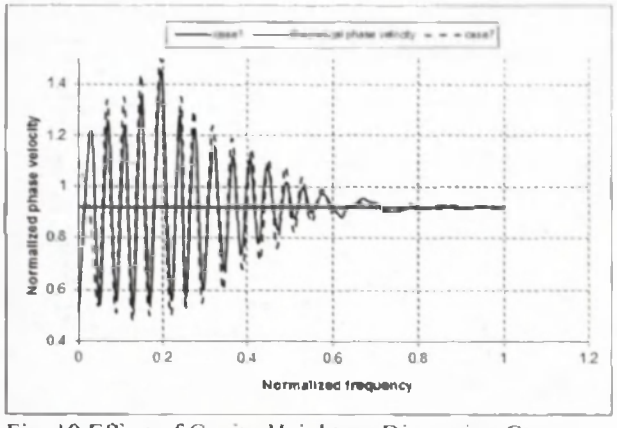


Fig. 10 Effect of Cavity Height on Dispersion Curve

The effect of the cavity shape on the dispersion curve for case 1 and 8 is also investigated and the results are illustrated in Fig. 11. The cavity in both cases has the same center and cross section area. It is evident from the figure that the cavity shape effect on the dispersion curve is insignificant and thus negligible.

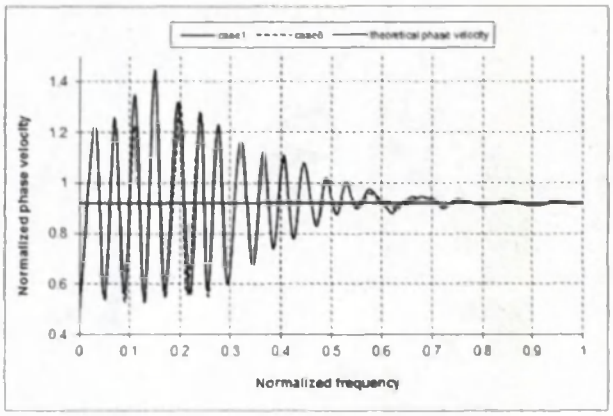


Fig. 11 Effect of Cavity Shape on Dispersion Curve

Finally the effect of source impact energy on the dispersion curve has been studied and investigated. A wide variety of impulsive sources can be used to generate surface wave energy over the desired frequency range. They should be able to generate Rayleigh waves over a wide range of frequencies with adequate amplitude so that they can be detected by the receivers. Source selection should be based on the range of frequencies (or wavelengths) that can be sufficiently excited to adequately sample the site. Waves having high frequencies (or short wavelengths) carry information about the properties of the media they propagate in from shallow depths, while waves with low frequencies (or long wavelengths) reflect the information from deeper layers. Small receiver spacings are used to obtain short wavelengths (high frequencies) and thus characterizing shallow depths, while large spacings are used to obtain long wavelengths (low frequencies) and thus profiling large depths. The most common types of sources used to date have been simple hammers or dropped weights which impact the ground surface and create transient wave containing a broad range of frequencies. These sources, in addition to being reasonably portable, have worked well at numerous sites.

In this research two types of impulsive source with 1 and 10 kN amplitude and 6 ms duration have been utilized. The results for cases 9-11 under 10 kN impulse amplitude is shown in Fig. 12.

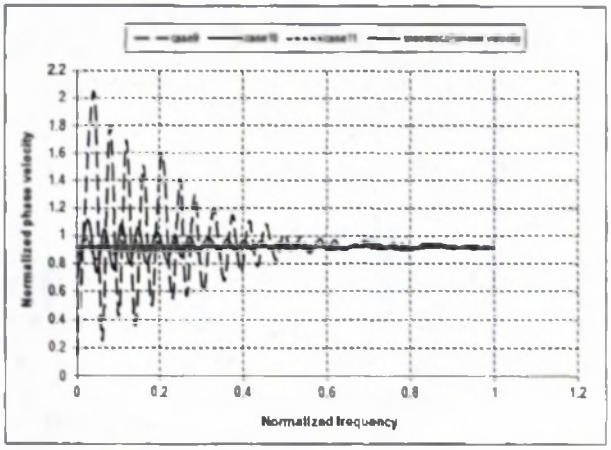


Fig. 12 Effect of Cavity Impulsive Source Energy on Dispersion Curve

It can be seen that the maximum amplitude of the fluctuations for case 9 occurs at 0.04 normalized frequency which is corresponding to 23 m wavelength. If we consider that the sampled depth is roughly attributed to 1/2 – 1/3 of the wavelength (Stokoe and Nazarian , 1985), then it can observed that fluctuations almost vanishes for depths larger than 8-12 m. It implies that this amount of energy can be used to detect cavities situated at depths smaller than 12 m. In other words, the waves generated with this amount of impact energy do not extend deep enough to hit the cavities located at depths larger than 12m. The same trend happens using 1 kN impulse amplitude for investigating other cases as well. As can be seen from figure 9, the maximum amplitude of the fluctuations for approximately all case occurs at 0.15 normalized frequencies which correspond to the wavelength of 6.23m. The attributed sampling depth is about 2-3m and implies that the waves are reflected less for wavelengths larger than 6m or for depth larger than 2-3m.

4 CONCLUSION

There are many circumstances that necessitate the detection of subsurface cavities. The surface wave testing is a new nondestructive procedure developed in the past twodecades and is mainly used for determining the elastic moduli and profile of layered systems. In this study, the surface wave testing has been simulated using finite element computer program ANSYS and employed for investigation of detection of subsurface cavities located in a homogeneous half-space. Several cavities with different sizes, shapes and embedment depths are analyzed and investigated. The results show fluctuations in the characteristic dispersion curve near the cavity. The fluctuations are a result of wave reflections from cavity's boundaries and the reflected waves traveling toward the source interact with the incident wave. Also the magnitude of amplitude in the normalized dispersion curves are increased with an increase in the height or decrease in the depth of cavity, but the effect of the cavity shape on the dispersion curve is negligible.

REFERENCES

Ah-Shayea, N. A., Gilmore, P., and Woods, R. D. (1994)."Detection of buried objects by the GPR method."*Proc., 5th Int. Conf. on Ground Penetrating Radar.* Kitchener, Ontario, Canada.

ANSYS,The Finite Element Software Package. (1995). Swanson Analysis Systems Inc.

Belesky, R. M., and Hardy, H. R. (1986)."Seismic and microseismic methods for cavity detection and stability monitoring of near-surface voids."*Proc.,27th US Symp. Rock Mech.*, Univ. of Alabama, 248-258.

Carlo, G. L., Glenn, J. R., Sebastiano, F., and Vitantonio, R. (2002)."Simultaneous measurement and inversion surface wave dispersion and attenuation curves."*J. Soil Dynamic and Earthquake Engineering*, ELSEVIER, 22(2), 923-930.

Dravinski, M. (1983)."Ground motion amplification due to elastic inclusions in a half-space."*J. Earthquake Engrg. andStruct. Dyn.*, 11, 313-335.

Glenn, J. R., Carlo, G. L., Catalina, Orozco, Gregory, L. H., and Vitantonio, R. (2001). "Recent advances in surface wave methods for geotechnical site characterization."*Proc. XV Internat.Conf. Soil Mech. &Geotech.Engrg.* Istanbul, Turkey.

Gucunski, N., and Woods, R. D. (1992)."Numerical simulation of the SASW test."*J. Soil Dyn. Earthquake Engng.* 11, 213-227.

Gucunski, N., Krstic, V., and Maher, A. (1996)."Field implementation of the surface wave for obstacle detection (SWOD) method."*J. Soil Dyn. and Earthquake Engrg.* 15, 223-231.

MATLAB, The Math Software Package. (1999). The Math Works Inc.

Vitantonio, R. (2001). "Soil properties and site characterization by means of Rayleigh wave." PhD Thesis, Thechnica-lUnivercity of Turin.

Determination of Elastic, Viscous, Plastic Characteristics of Soil on the Basis of Tests Results

K.S.Sultanov

Dynamics of Soils and Simulation of Complex Loading, Institute of Mechanics and Seismic Stability of Structures of the Academy of Sciences of the Republic of Uzbekistan, Tashkent, Uzbekistan.

A.A.Bakhodirov &. U.K.Abduraimov

Dynamics of Soils and Simulation of Complex Loading, Institute of Mechanics and Seismic Stability of Structures of the Academy of Sciences of the Republic of Uzbekistan, Tashkent, Uzbekistan.

ABSTRACT: Principal mechanical characteristics of soil, to be determined from results of tests, are: elastic characteristics, that is modulus of elasticity under dynamic and static loads, Poisson coefficient, modulus of shear; viscous characteristics, that is coefficients of viscosity, internal friction; plastic characteristics, that is modulus of unloading, plasticity limit. These characteristics of soil were determined by comparing results of experimental and theoretical studies on dynamic compression of soil samples.

At present the solution of various practical problems of construction of different engineering objects, structures and buildings, stability of natural slopes, foundations of existing architectural monuments requires the knowledge of mechanical characteristics of soil. An increase in engineering works connected with soil explains acute actuality of the problems of reliable and more exact determination of mechanical characteristics of soil.

Principal mechanical characteristics of soil, which should be determined from results of tests, are: elastic characteristics, that is modulus of elasticity under dynamic and static loads, Poisson coefficient, modulus of shear; viscous characteristics, that is coefficients of viscosity, internal friction; plastic characteristics, that is modulus of unloading, plasticity limit. These characteristics of soil are determined on the basis of two sources: A – tests, B – models of soil deformation (laws of soil deformation).

Source A is obtained by carrying out tests in laboratory and field conditions. Methods of carrying out of these tests are given in [1-4]. In most cases in tests physical-mechanical characteristics of soil (density, moisture content, granulometric composition, etc.) are determined, and components of stresses and strains are measured. As a result of these measurements the diagrams of soil compression $\sigma_{ij}(\varepsilon_{ij})$ are built, where σ_{ij} - are components of stresses, ε_{ij} - components of strains, $(i,j = 1,2,3,)$. Diagrams $\sigma_{ij}(\varepsilon_{ij})$ - are basic results of experiments on dynamic and static tests of soil.

Source Б includes the equations of state of soil, adequate to experimental compression of soil samples, that is mechanical characteristics of soil are determined on the basis of concrete model of soil. The values of these mechanical characteristics of soil not always could be applied to other models. That is why when selecting the model of soil with certain mechanical characteristics it is necessary to take into account an adequacy of selected model to corresponding processes of soil deformation.

Results of tests and models of soil determine elastic, plastic and viscous characteristics of soil, entering selected model of soil deformation. Models in most cases are divided on laws of volume and shear deformation and mechanical characteristics are determined separately for each law on the basis of different tests.

Mechanical characteristics of loess soils found in seismic zones of the world (Central Asia, Middle East, China, Central America and others) and their behavior under seismic load are not sufficiently studied. The level of seismic stresses in loess soil during the earthquake with magnitude 9 does not exceed 0,5 - 0,7 MPa. The aim of our study to establish which properties of soil are revealed under these loads, which models of soil describe these properties and how to determine the

parameters of these models (mechanical characteristics).

As mentioned above to determine mechanical characteristics of soil it is necessary to draw experimental regularities $\sigma_{ij}(\varepsilon_{ij})$. To do this the Institute of Mechanics and Seismic Stability of Structures has acquired the installation of dynamic loading UDN-150; a number of tests to determine the dependencies $\sigma_{ij}(\varepsilon_{ij})$ under axial dynamic compression of soil samples were carried out.

Tests on UDN-150 measure axial (longitudinal) stresses σ_1 and strains ε_1, and lateral stresses σ_2. The measurement of these components is carried out by special sensing elements of membrane type on tenso-resistors (sensors of stresses and strains).Before the beginning of the tests the sensors of stresses were gauged in oil chamber, and sensors of strains – with micro-meter.

In UDN-150 tested sample is located in a special ring with bore diameter 150 mm, and height 30 mm. Soil sample is supported on immobile piston with tensometers (in center and at the edge) to measure basic axial stress. Dynamic (impact) load is transmitted on the soil sample through upper piston, located in directing cylinder. In the center of upper piston there is another tensometer to measure stress σ_1. Lateral or basic radial stresses in cylinder sample of soil with thickness 30 mm are measured by tensometers installed into the ring. Face surface of these sensors contacting with soil has the same curvature as a ring has.

In tests displacement of upper piston is fixed with three deflection-meters (strain sensors); using these records we may determine the deformation of soil sample in axial direction. Under impact dynamic load which is created by dropping the load down from a certain height, axial basic stress σ_1 is measured by 4 tensometers, located under (3 sensors) and above (1 sensor) soil sample, and lateral (radial) basic stress – by two tensometers. Axial deformation ε_1 is determined by three deflection-meters; the value of total load is measured with tensometric tumbler. In UDN-150 ten tensometric sensors are fixing stresses and strains of soil sample under dynamic load: using the records of these sensors we may built the dependencies $\sigma_1(t)$, $\sigma_2(t)$, $\varepsilon_1(t)$, and $\sigma_1(\varepsilon_1)$.

On the basis of results of a number of tests we have dynamic and static diagrams of compression of soil samples $\sigma = \sigma(t)$, which characterize the law of volume compression of loess soils. According to diagrams $\sigma = \sigma(t)$ in laws of deformation of loess soils viscous and plastic properties of soil are seen even at $\sigma_{1\max} = 0{,}5 - 0{,}7$ MPa.

On the basis of experimental dependencies $\sigma = \sigma(t)$, G.M.Lyakhov's model of viscous-plastic media [3] is taken as the closest one to tests data. Further new methods of definition of parameters of viscous-plastic model of soil, that is viscous and plastic characteristics of loess soil are proposed.

The essence of proposed model consists in determination of dependency $\sigma = \sigma(t)$ theoretically, using closed system of equations of soil motion, subjected to tests on UDN-150. Here approximate values of parameters of a model, determined from tests results, are used. Comparing theoretical and experimental diagrams $\sigma = \sigma(t)$, the values of parameters of soil model are corrected. After several approximations sufficient and required accuracy of coincidence of test and design diagrams $\sigma = \sigma(t)$ is reached.

The statement of the problem of dynamic compression of soil corresponding to the statement of experiment and to the case of propagation of plane wave in soil sample, limited on a certain distance from the surface of soil by rigid immobile wall (obstacle) is given below.

Dynamic load is acting on the surface of soil sample:

$$\sigma = \sigma(t) \qquad (1)$$

the dependency (1) is determined from tests results. On immobile obstacle (under soil sample) the following boundary condition is given:

$$\upsilon = 0, \qquad (2)$$

υ - is a velocity of soil particles, t – time.

An equation of soil motion, corresponding to this case, has the following form:

$$\rho_0 \frac{\partial \upsilon}{\partial t} - \frac{\partial \sigma}{\partial x} = 0, \quad \frac{\partial \upsilon}{\partial x} - \frac{\partial \varepsilon}{\partial t} = 0 \qquad (3)$$

G.M.Lyakhov's model of elastic-viscous-plastic media has the following form:

$$\frac{d\varepsilon}{dt} + \mu\varepsilon = \frac{d\sigma}{E_D dt} + \mu\frac{\sigma}{E_S}$$

at $\frac{d\sigma}{dt}>0,\ \frac{d\varepsilon}{dt}>0$;

$$\frac{d\varepsilon}{dt} + \mu\varepsilon = \frac{d\sigma}{E_R dt} + \mu\sigma\left(\frac{1}{E_S} - \frac{1}{E_D} + \frac{1}{E_R}\right) + \mu\sigma_m\left(\frac{1}{E_D} - \frac{1}{E_R}\right)$$

at $\frac{d\sigma}{dt}<0,\ \frac{d\varepsilon}{dt}>0$; (4)

$$\frac{d\varepsilon}{dt} = \frac{d\sigma}{E_R dt} \quad \text{at} \quad \frac{d\sigma}{dt}<0,\ \frac{d\varepsilon}{dt}<0;$$

where E_D- is the modulus of dynamic compression of soil, E_S- modulus of static compression of soil, E_R- modulus of unloading, μ- parameter of viscosity, connected with coefficient of viscosity by relation:

$$\mu = \frac{E_D E_S}{\eta(E_D - E_S)}, \qquad (5)$$

where η - is a coefficient of viscosity of soil under the change of its volume, σ_m- maximum stress in soil particle.

The system of equations (3), (4), which describes dynamic and quasi-static deformation of soil is a closed system. The solution of equations (3), (4) with boundary conditions (1), (2) and condition on the fronts of waves allows to determine the change of $\sigma(t)$, $\varepsilon(t)$ and $\upsilon(t)$ theoretically. It is necessary to state, that in test dependencies (1) sharp ruptures (fractures), that is the drops of stresses under the impact of load on soil sample are not observed; so all fronts of waves are the lines of weak rupture. On these lines the following condition is fulfilled:

$$\sigma = -c\rho\upsilon = 0, \quad \upsilon = -c\varepsilon = 0 \qquad (6)$$

where c – is a velocity of propagation of longitudinal waves in soil.

The methods of determination of the value of parameter of viscosity μ, proposed in this paper, is based on tests measurement of soil deformation. Comparing the values of test and design dependencies $\varepsilon(t)$, one may determine rather exact value of μ.

To carry out design on worked out program and to solve dynamic problem in application to UDN-150, a constant and initial value is a density of soil ρ_0, determined according to traditional methods, as the value of ρ_0 is taken as the most reliable one.

Further, approximate values of mechanical characteristics of loess soil, that is E_S and E_R are used in design. The value E_D is determined from formulae $E_D=\gamma E_S$. Approximate value of μ, is determined by the following way.

On the basis of the first equation (4) the parameter of viscosity may be approximately determined from formulae [1], assuming that $d\varepsilon/dt$ and $d\sigma/dt$, as well as E_D and E_S, are constant and known values:

$$\mu = \left(\frac{d\varepsilon}{dt} - \frac{d\sigma}{E_D dt}\right)/\left(\frac{\sigma}{E_S}\right) \qquad (7)$$

From tests results it is known that $d\varepsilon/dt = 1s^{-1}$, $d\sigma/dt = 100kg/cm^2sec$. At $E_D=140kg/cm^2$ and $E_S=65kg/cm^2$, the values $\sigma=0,24kg/cm^2$ and $\varepsilon=0,02$ for linear part of dynamic diagram $\sigma(\varepsilon)$ based on formulae (7) we will obtain $\mu=20s^{-1}$. This value μ is considerably less than the value μ, given in [3,4]. So in design we take $\mu=100s^{-1}$. The value $c=\sqrt{E_D/\rho_0}$.

Using approximate experimental values E_D, E_S, E_R, c and μ on the basis of numeric solution of the problem we will obtain theoretical dependencies $\sigma(t), \varepsilon(t), \sigma(\varepsilon)$. Trying to achieve more exact comparison of theoretical and experimental dependencies $\sigma(t)$, $\varepsilon(t)$ and $\sigma(\varepsilon)$ we will equal the values of mechanical characteristics of soil.

The methods proposed in this paper are rather complicated. But they are more exact than any other existing now methods of determination of mechanical characteristics of soil. These methods liquidate any possible contradictions in values of mechanical characteristics of soil. Besides they are based on concrete equation of state of the media (soil); that excludes arbitrary determination of values of mechanical characteristics of soil. Mechanical characteristics of soil, not connected with the equation of state, complicate their further application in theoretical design. Besides, the methods, proposed here, determine full range of mechanical characteristics of soil according to equation of state (of the model) of soil (4).

Let us make the values of mechanical characteristics of soil more precise. As the value of static compression of soil Es, is taken as a principal parameter in design, so in the first turn

we will change its value: E_S=8,3 MPa. Here the values of other mechanical characteristics of soil are as follows: E_D=20,75 MPa, μ=200 s^{-1}, β=0.5 , γ=2,5 , C =116,5 m/s.

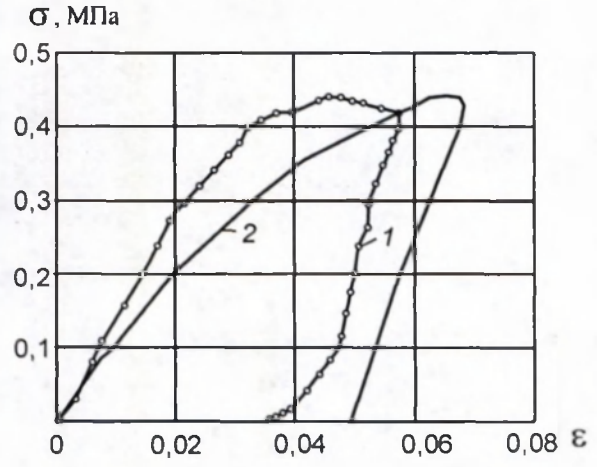


Fig.1. Experimental and theoretical stress-strain dependencies

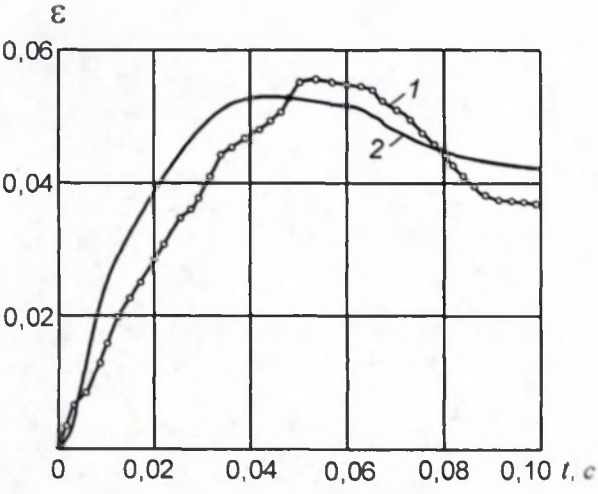


Fig.2. Experimental and theoretical dependencies of strains on time

Results of design, obtained with these initial data, are given on Fig.1, 2. In this case test and design dependencies $\varepsilon(t)$, $\sigma(\varepsilon)$ (curves 1 - test, curves 2 - theory) have good agreement. Their difference is about 10%. To our opinion this is a rather good agreement of experimental and theoretical results. To obtain final exact agreement several calculations were carried out with another parameters of mechanical characteristics (E_D, E_S, E_R, μ).

So, comparing results of experimental and theoretical studies on dynamic compression of soil samples, given in [5], we may with sufficient accuracy determine the values of mechanical characteristics of soil.

From results of theoretical investigations it is known, that satisfying the condition of quasi-statics [6] of the process of deformation of soil on UDN-150, test and design dependencies $\sigma(t)$ completely coincide. Evidently, varying the values of mechanical characteristics of soil, it is necessary to achieve the coincidence of test and design dependencies $\varepsilon(t)$, $\sigma(\varepsilon)$.

REFERENCES:

1. Kulinich Yu.V., Naroghnaya Z.V., Rykov G.V. Mechanical Characteristics of Sand and Clay Soils with Account of Their Viscous-plastic Properties under Short-term dynamic loads.// Moscow. : Preprint IPMech Ac.Sci.USSR, 1976 , N69 . 50p .
2. Rykov G.V., Skobeyev A.M. Measurement of Stresses in Soil under Short-term Loads.//Moscow : Nauka, 1978 , 168p .
3. Lyakhov G.M. The Basis of Dynamics of Explosion Waves in Soils and Rock Mass.// Moscow: Nedra, 1974. 192p.
4. Lyakhov G.M. Waves in Soils and Porous Multi-component Media.// Moscow: Nedra, 1982. 288p.
5. Sultanov K.S., Bakhodirov A.A. Experimental and Theoretical Methods of Study of Mechanical Characteristics of Composite Materials,// Composite materials. 2000, №1, P.63-68.
6. Sultanov K.S., Bakhodirov A.A. Substantiation of Quasi-static Experiments to Determine Mechanical Characteristics of Soil.// Composite materials. 2001, №1, P.50-53.

Reconstruction of foundations for new equipment of main building of Ekibastuz power station

L.V. Nuzhdin
Department of Engineering Geology, Bases and Foundations, Novosibirsk State University of Architecture and Civil Engineering (Sibstrin), Novosibirsk, Russia

O.V. Koneva
Architectural and Constructional Department, «COTES KAZAKHSTAN PLC », Pavlodar, Kazakhstan

ABSTRACT: The article considers engineering proposal of reconstructing foundations and underground facilities of the scrubbing department of Ekibastuz power station (EGRES-1), connected with disassembling scrubbers and replacing electrostatic precipitators with modern double-flow four-pole precipitators produced by "ALSTOM" firm. The task is not restricted by replacing the broken down equipment. We take an opportunity to improve ecological, operational and economic performance of the generating unit of the scrubbing department of Ekibastuz power station. This article is a part of a complex research and design work carried out for reconstruction and modernization of Ekibastuz power station.

1 INTRODUCTON

Ekibastuz power station (EGRES-1 named after Bulat Nurzhinov) is situated in the Republic of Kazakhstan, Ekibastuz District, Pavlodar Province. The power station was designed by the Novosibirsk branch of Design Institute "Teploelectroproect". The construction began in 1977. The first thermal generating set was launched into service in 1980. Most of production equipment of the power station was put out of action in the middle of the 1990's. The previous 15 years had been marked by numerous emergency stopping of production including stoppage of turbogenerating sets of the main boiler-turbine generators. The down-time without preservation of equipment was nearly sixteen years. Today most units of basic and auxilary equipment are dismantled. Some equipment is dismantled and the other equipment fell into disrepair.

The need for reconstruction and return to operation of Ekibastuz power station is determined by projected heat power balance and capacity of the northern regions of the Republic of Kazakhstan, the country in whole and Russian boundary regions. A complex of research and design work is being carried out now to reconstruct and modernize the power station.

One of the strands of reconstruction work is return to operation of the boiler-turbine generator of the scrubbing department of the power station. It had also been idle for more than 16 years. Most of auxiliary equipment of this boiler-turbine generator is missing as it is being used for carrying out reconstruction work of other boiler-turbine generators. There is obsolescence of the boiler, the turbine and other units of auxiliary equipment. They have undergone corrosion severity and erosive wear and they are not suitable for further operation. The boiler, the turbine, excitation system for the generator, the equipment of the compound system of ash cleaning flue gases and electrical equipment are worn out and obsolete. This equipment needs replacing and dismantling.

2 RECONSTRUCTION OF THE SCRUBBING DEPARTMENT OF THE POWER STATION

Taking into account the current technical condition of the boiler-turbine generator of the scrubbing department of Ekibastuz power station, it was decided not only to replace the equipment that broke down, but also to take an opportunity to improve ecological, operational and economic performance, as well as to modernize the

combustor and to update the ash-handling system by reducing ash emission into the atmosphere.

That is why "Ekibastuz GRES-1 named after Bulat Nurzhanov" PLC has concluded a contract for delivery a new boiler unit, a turbine and an excitation system for the generator. "COTES" CJSC and "COTES KAZAKHSTAN" PLC are working out project documentation for reconstruction.

Electrostatic precipitators should be replaced with modern double-flow four-pole precipitators produced by "ALSTOM" firm, which remove ash from boiler flue gases. This reduces dustiness of stack effluents to 400 mg/nm^3. This improves baseline ecological performance.

External upright collecting gasmain from the electrostatic precipitators to the smoke exhauster also has to be replaced. Scrubbers are dismantled as well.

As a result, there is a need of carrying out a complex of construction and installation jobs aimed at reconstructing existing structures, including reconstruction of foundations for new equipment.

3 GEOTECHNICAL SITE CONDITIONS

Environmental conditions of Ekibastuz power station enable construction. The site of the power station is situated on a hilly ground in the juncture of the southern margin of the West Siberian Lowland and the northern margin of Kazakh Highland. This territory is characterized by the hilly relief that changes into a slope and undulated relief of the Irtysh lacustrine-alluvial plain. Relative altitude of the hills is about 15...50 meters.

In terms of geology, the territory is situated on the boarder of the Western Siberian Plate and Kazakh folded structure. The Western Siberian Plain has a two-deck structure when horizontal Meso-Cenozoic loose soil spans complex rocky aggradation of Paleozoic base. Kazakh folded structure consists of rocky Paleozoic and Proterozoic rocks. The base of foundations is solid loam of hard and medium consistency including gruss, gravel and pebble. Engineering-geologic elements are portioned depending on an amount of inclusions (up to 15%; 25% and 40%). Their width is persistent and close to horizontal layers. According to in-situ tests data, the deformation modulus of loam is E = 27-45 MPa depending on an amount of inclusions; the angle of true internal friction is $\varphi = 26^0$-35^0; specific cohesion force is c = 20-33 kPa. Loam is underlain by conglomerate and a collapsing rock consisting of gravelstone and tuff breccia. The site has the highest groundwater level of about two meters.

The scrubber department is situated in the main building of Ekibastuz power station. All foundations of the scrubber department are shallow and have a natural base of different depth varying from 1.6 to 3.93 meters.

4 SURVEY OF EXISTING FOUNDATIONS

The main reason for reconstructing foundations for equipment is dismantling scrubbers. Exhaust ducts footings from the tubular air heater to electrostatic precipitators will be installed instead of the scrubbers at ground level. On-site investigation proved that the existing foundations of scrubbers have a depth of 3.93 meters. The foundations are circular plates. They are 7.00 meters in diameter and their width is 600 mm. Rings are leaned on them. The external diameter of the rings is 6.30 m and their width is 600 mm. The rings are composed of foundation wall blocks at depth of up to 1.5 m and at lower depth they are composed of in-situ reinforced concrete.

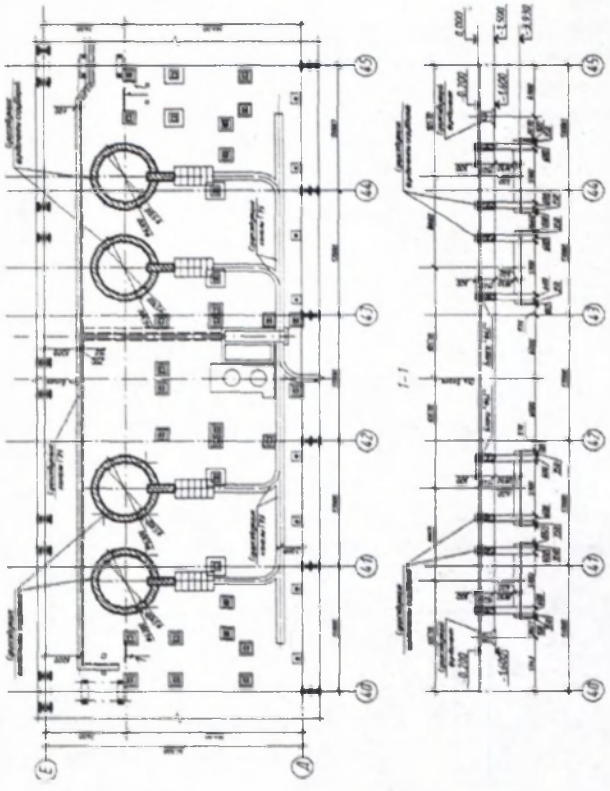


Fig. 1 The scheme of the main existing foundations of the scrubber department.

Figure 1 shows the scheme of placing the main foundations of the existing equipment. Installation

of new foundations was complicated by ash sluiceways which had to be preserved for further industrial use.

5 RECONSTRUCTION OF EQUIPMENT FOUNDATIONS

Exhaust duct footings are steel lattice towers that have a height of 17.66 m. Their variable cross-section along the height is from ground level to +12.660. Their uniform cross-section is from +12.660 to +17.660. The axis of exhaust ducts footings coincide with the axis of the dismantled scrubbers.

Several variants have been considered and analyzed when designing new foundations for exhaust ducts footings.

5.1 *Variant 1*

Complete dismantlement of the existing foundations of scrubbers and placing new foundations on natural soil. Considerable footing depth makes it possible to lessen plan dimension of the foundations. It also affords to make them separate for each footing. However, taking into account the necessity of interconnected operation of the whole system "exhaust ducts – footings – foundation", this variant is considered to be impractical.

5.2 *Variant 2*

Partial dismantling of existing foundations of scrubbers up to the top of the plate by part at level of -3.330. It was decided to use foundation plates only as bases for new subfoundations. This reduces the scope of work, but several new foundations will be supported by the soil. Consequently, there is a necessity to carry out special work not to allow differential settlement and displacement of the system.

The variant of using the existing plates as a constituent part of exhaust duct settings provided with interconnected operation with newly-formed parts of foundations was not considered by the general contracting design organization.

5.3 *Variant 3*

Dismantling only those units that are composed of foundation wall blocks of the top parts of the existing foundations of scrubbers up to the level of -1.500. Each new foundation is composed for two footings that have a form of a solid plate which is imposed on two site-cast concrete rings and rigid firm soil between them. This variant was taken as the main one after consideration.

The width of the foundation plate for the footings of the collecting gasmain was equal for the whole area – 800 mm. The footing depth is 1.00 meter, the level of foundation is -0.200. An intermediate made-close sand blanket having a width of 400 mm and a B3.5 concrete blinding having a width of 100 mm. were done under the plate. Production capabilities defined the plan dimension of the plate.

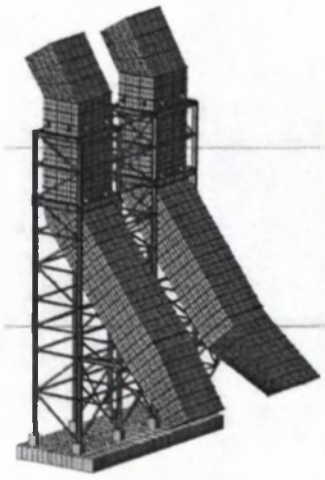


Fig. 2 3D design model of the structure "exhaust ducts – footing – foundation plate"

The ash-sluiceway, which had to be preserved, restricted the size of the foundation plate from one side. The sides of the new foundation touched the existing stanchion foundations of the boiler accessories. That is why it was possible to expand its size only one-way. Load on foundation from the structure of the footings and the exhaust ducts became nonsymmetrical and had a great eccentricity.

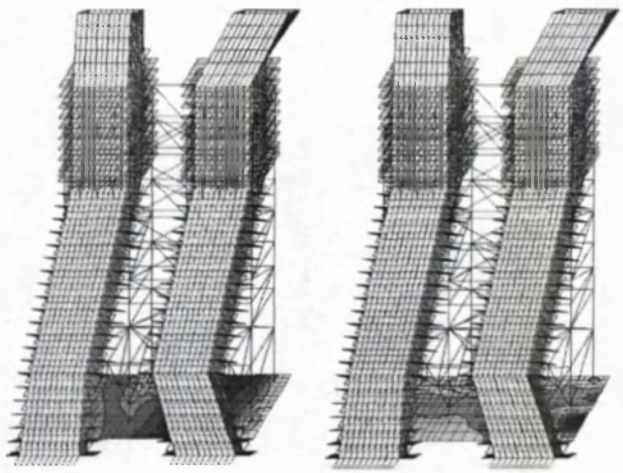


Fig. 3 Example of stress patterns M_x и M_y.

Calculation was carried out in a three-dimensional scheme by means of the finite-element

method using software solution "Lira". A 3-D model of the structure "exhaust ducts – footing – foundation slab" was created for calculating (see figure 2).

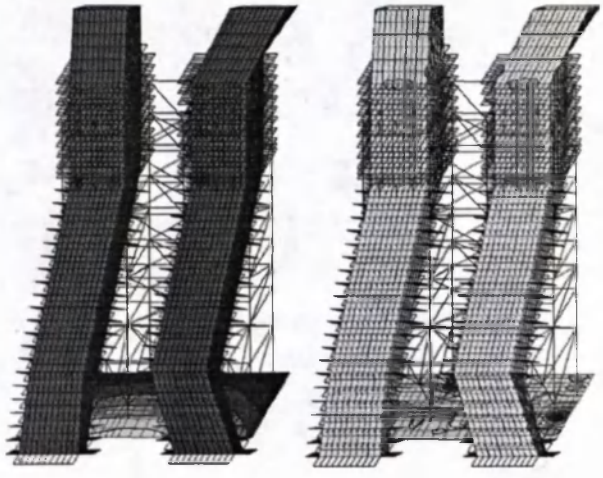


Fig. 4 Example of stress patterns R_z и Q_y.

Several types of elements were included into the design model: universal special axial element (type 10); universal triangular (type 42) and quadrangular (type 44) shell finite elements; stiffening of finite brace. The main calculation was carried out for static loading. Dead load and superimposed dead load were taken into account. Possible temperature drop, that was more than 130°C, delta-p (p = -1150 Pa), variation in ash load from 2000 Pa to 7200 Pa. Figures 3, 4 and 5 show the examples of stress patterns in the foundation plate and above ground structures of the 3-D design model.

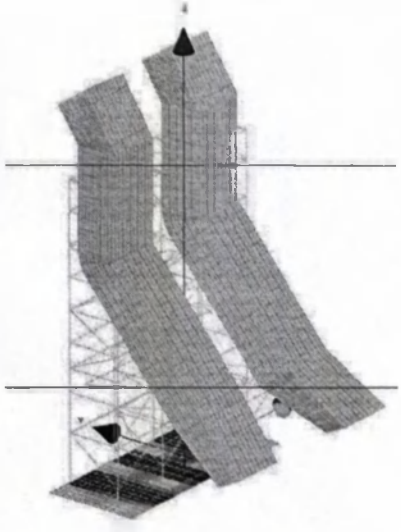


Fig. 5 Example of stress patterns M_x in foundation plate

Calculations showed that the sizes of the foundation slabs 19.45×8.10 m provide stability to the structure of the footings in case of all kinds of loading. The maximum pressure on the base under the foundation was 17 kPa. The foundation settlement and deformation of the system are within tolerable limits. The foundations were reinforced by two nets on two levels according to the result of calculation. Space frames were installed across them. Much attention was paid to a safe fixation of the base of footings of exhaust ducts. They were fixed with anchor bolts which must be installed into the foundation plate before concrete casting. Special anchor bolt templates should be used as they fix safely and provide bolts with proper location during concrete casting. The places where the new foundations touch the existing ones are provided with punches that have a gap of 50 mm.

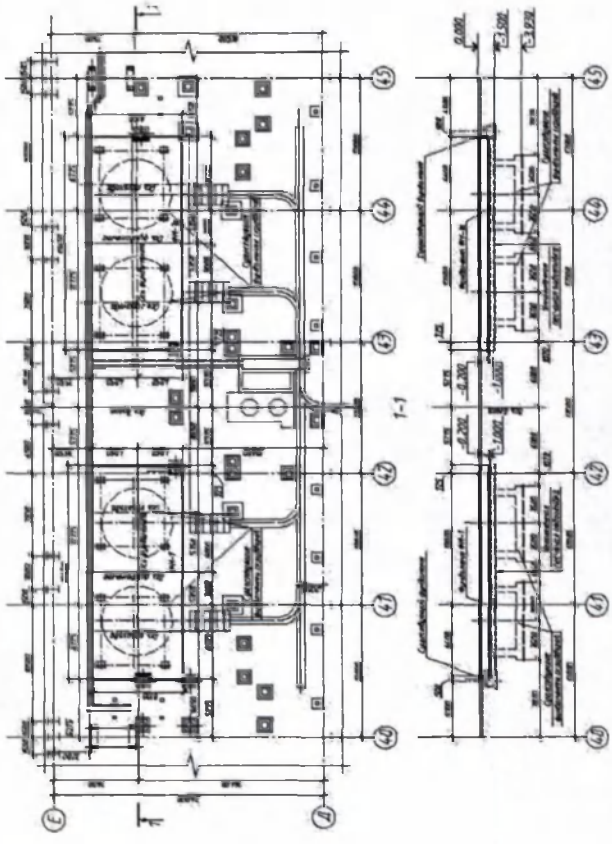


Fig. 6 Scheme of reconstructing foundations of the scrubber department.

Figure 6 shows the pattern of reconstructing equipment foundations. Ash sluiceways extending from scrubbers to air lift chambers, broken by installation of new foundations for exhaust ducts are not reconstructed. They are used in the hydrocleaning system. Other ash sluiceways and hydrocleaning channels broken when reconstructing the scrubber department are restored completely. The wearing cement floor in the

departments is dismantled and the new tile floor is laid. The remained ash sluiceways and hydrocleaning channels are taken into account.

6 CONCLUSION

Reconstruction of equipment foundations takes a great extent of responsibility and is quite a complicated task. Possible accidental situations or unscheduled shutdowns caused by an incorrectly designed foundation can lead to a great economic damage incomparable with reconstruction work expenses. Consequently, given data must be absolutely reliable, the design solution should have a comprehensive theoretical basis; construction work should be carried out by highly qualified specialists. Construction work should be qualitative and follow the designed project.

The existing geotechnical situation should be studied carefully before designing new equipment foundations on the site of the dismantled ones. Ground condition should be analyzed taking into account possible ground mobility in the process of the previous operation of the object, quality of construction work when forming existing foundations is also studied. Much attention is paid to defects and faults of the foundations, conformance of working loads and deformations to the design load. Usage of reliable data and modern methods of structural analysis, correct consideration of technological characteristics of construction let us obtain not only reliable, but also cost-effective solution.

REFERENCES

Technical report on expert inspection of condition survey of ash collectors in axes "35-45". 944-11K/ПИР-СК-ТС. RK, Pavlodar, "COTES KAZAKHSTAN PLC", 2011.

Nuzhdin, L.V., and Koneva, O.V. (2011). "Натурное обследование фундамента турбоагрегата Экибастузской ГРЭС-1 для восстановления его эксплуатационной пригодности. (in Russian)" *Proc., Int. Conf. "Deep foundations and problems of the using underground space"*, PNSPU, Perm, 303-310.

Nuzhdin, L.V., and Koneva, O.V. (2012). "Реконструкция фундаментов и подземного хозяйства скрубберного отделения ЭГРЭС-1. (in Russian)" *Mat., V All-Russian Sc.-techn. Conf. "Topical problems of the construction industry"*, NSUACE (Sibstrin), Novosibirsk, 36-40.

Application high-pressure directional injection method for strengthen soil base

M.L. Nuzhdin

Center of Engineering Surveys, Inspection of Buildings and Structures of Novosibirsk State University of Architecture and Civil Engineering (Sibstrin), Novosibirsk, Russia

L.V. Nuzhdin

Department of Engineering Geology, Bases and Foundations Novosibirsk State University of Architecture and Civil Engineering (Sibstrin), Novosibirsk, Russia

ABSTRACT: The last decades, construction in Russia has been steadily developing in the direction of fuller development of urban space. In the central districts of Siberian cities there are lots of earlier undeveloped sites characterized by thick filled soils with non-uniform bedding and by weak and collapsible soils. Perspective way to strengthen soil base for new construct and reconstruct objects is cement-sand mixture high-pressure directional injection method. The method essence contains injection cement-sand mixture into the ground under high-pressures exceeded the ground structural strength. High-pressure directional injection makes it possible to control distribution of the injected grout and to create vertically and horizontally oriented injection bodies, it reinforce and consolidate surrounding soil base massif. To date made more than 80 objects by the cement-sand mixture high-pressure directional injection method in Novosibirsk and Siberian region.

1 TECHNOLOGY OF HIGH-PRESSURE DIRECTIONAL INJECTION METHOD

The method of high-pressure injection of flowing cement and sand mixes for strengthening of soil foundations has been widely used in Novosibirsk and the Siberian region of Russia since the middle of the 1990s. The principle of the method consists in pumping of a flowing cement-sand grout through an injector under pressure exceeding structural strength of the soil. The result is discontinuity of the soil massif and development of tension cracks which are filled with a cement-sand grout. The mix is hardened forming solid bodies reinforcing the soil foundation and thus significantly reducing its deformability and to some extent compacting the surrounding soil. An essential limitation of injection through one injector is that it is impossible to forecast the distribution of the pumped mix in the soil.

The authors of the article have developed a technology to strengthen soil foundations using a method of directed high-pressure injection (M.L. Nuzhdin and L.V. Nuzhdin 2003, 2004). This method makes it possible to control distribution of the injected grout and to create vertically and horizontally oriented injection bodies in the soil foundation. The injection bodies are almost discal in shape.

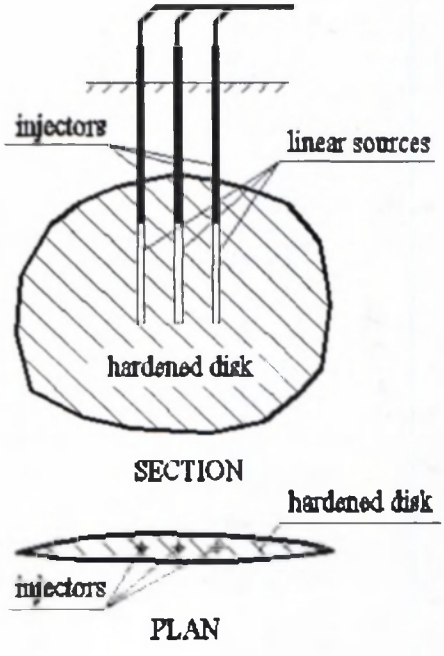


Fig. 1. Scheme of vertically oriented injection bodies.

The principle of the method consists in pumping a flowing grout simultaneously through several injectors arranged in a certain geometrical order. Three and more injectors are arranged along one line to form vertically oriented injection bodies. A

linear vertical injector with perforation height at least 10 times the injector diameter is used in each injection point. The best results are obtained using double direction perforation injectors.

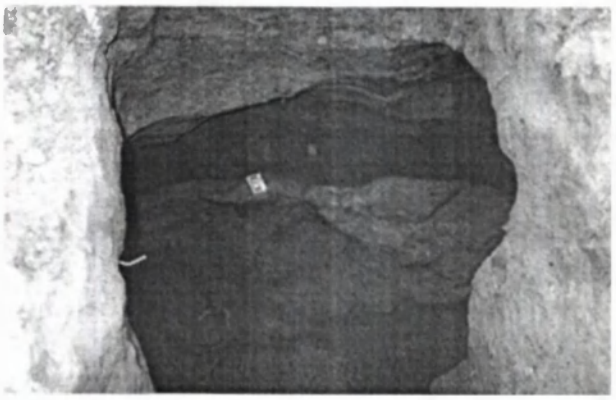


Fig. 2. Vertically oriented injection body.

When injectors are located at the corners of an imaginary equilateral triangle and point injection cavities are formed as a result of raising the injectors by 1-2 diameters, a horizontally oriented disk is formed in the soil foundation during pumping.

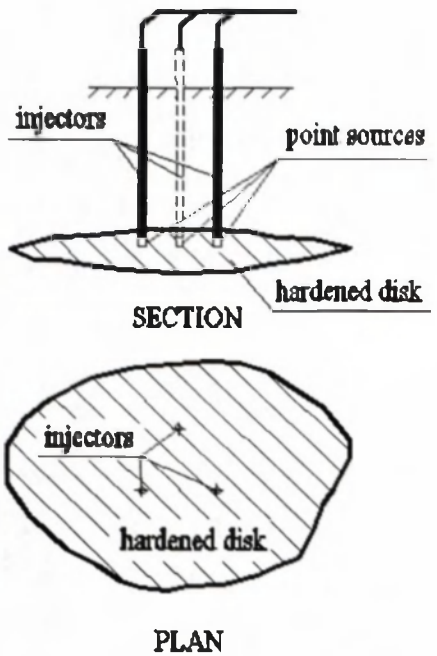


Fig. 3. Scheme of horizontally oriented injection bodies.

The technology for reinforcing the soil foundation by means of the method of directed high-pressure injection has a number of basic principles.

1. Cement-sand grouts are pumped into "weak areas" of the soil massif first. The number and the depth of such "weak areas" are determined using foundation testing and diagrams of cone penetration tests. Actual heights of the injection horizons are defined more exactly using the results of dynamic penetration tests – speed of immersing injectors into the soil (during their driving in or vibropiling).

2. The pumping process on each injection horizon is controlled by the change of pressure during injection and by the volume of the pumped grout. The works are completed with gradual increase of the supplied pressure by 40-50% in comparison to the working pressure. (Working pressure is determined after breaking the continuity of the soil massif, cracks formation and the beginning of the injection bodies formation). Continued injection process may result in repeated rupture of the soil massif continuity and uncontrollable distribution of the injected grout. Another criterion for completing the injection works in the given site is the volume of the pumped mix which should not exceed the volume of 2-2.5 m^3.

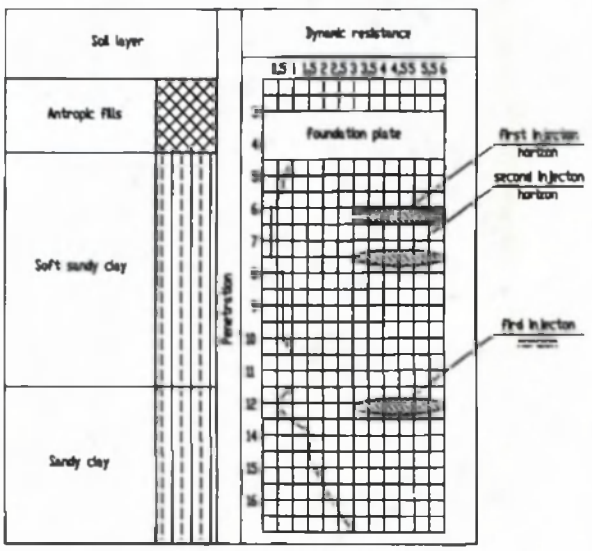


Figure 4. Location of injection horizons according to the results of static penetration tests and measuring the speed of injector immersion into the ground.

3. Optimum composition of the pumped grout depends on many factors: engineering and geological conditions of the site, technological parameters of the equipment used, volumes of the injection works, required strength of the injection bodies. The following grout composition is frequently used: cement M200 – 1 part, bentonithic clay – 1 part, small or medium size sand – 7 parts, water – as required to achieve the necessary plasticity. Grout of such composition has the flow ability that meets the requirements of injection equipment and has M10 strength which is sufficient for injection bodies in a soil massif.

4. In order to refine the design solutions, to fine-tune the technology and to increase the efficiency

of injection works it is recommended to organize works on a test field -a site that has similar soil conditions, usually in close vicinity to the construction site.
The principles of calculating the soil foundation include evaluation of its deformability before and after its reinforcement. The calculated value of the massif's integrated deformation module depends on the implemented method of the soil foundation reinforcement and the new value of soil density. Thus during the calculation, horizontally oriented injection bodies located on the same height are modeled by low tensile layer of certain thickness having mechanical characteristics that depend on the type of used injection grout. Integrated deformation module is calculated as equivalent for the foundation. The foundation consists of soil layers and low tensile layers with preset geometrical parameters - thickness and deformation module.

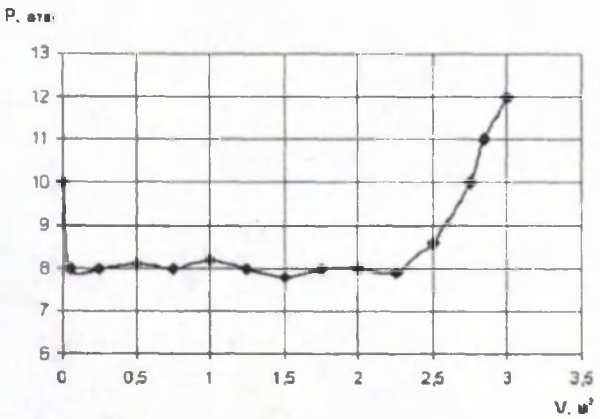


Fig. 5 Typical dependence supply pressure to pumped mortar volume.

Reinforcement of the soil foundation with vertically oriented injection bodies leads to formation of a cased wall of certain depth in the soil. Operation mode of the soil foundation is close to compression conditions. The soil massif deformation module is calculated by the value of the soil massif density consisting of soils density before reinforcement, injected grout volumes and correction factors taking into account change in the foundation operation mode.
Separate vertical injection bodies are rigid reinforcing elements. The top of these elements carries the load and the bottom transfers it to the underlying soils. As a result, we can speak of a new layer – reinforced soil that has a sufficient number of injection bodies in its massif. Deformability of reinforced soil is estimated taking into account possible soil slippage along the reinforcing elements in the top part.

2 STRENGTHEN SOIL BASE OF SHALLOW FOUNDATIONS

The method of directed high-pressure injection is widely used to reinforce shallow foundations.
Injection usually consists of two stages. The first stage includes the formation of vertically oriented injection bodies on both sides of the wall foundation.

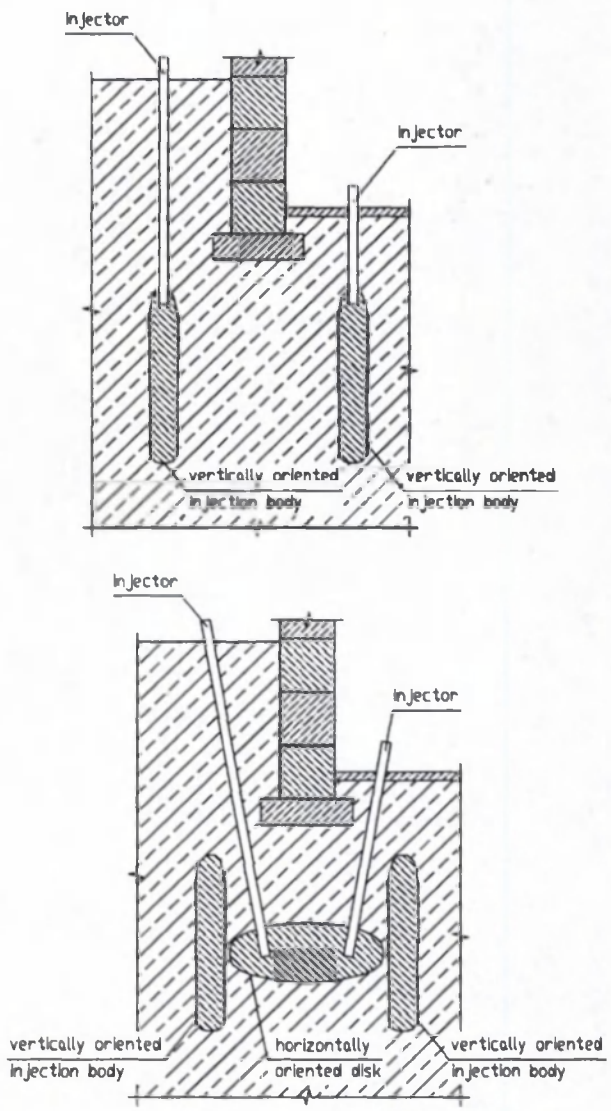


Fig. 6 Scheme of strengthen soil base of shallow foundations. First stage – formation vertically oriented injection bodies, second stage – formation horizontally oriented disk.

Works for separate column or slab foundations are carried out along their four sides. After that underside soils start working in the conditions close to compression ones. It contributes to stabilization of the foundation deformations. Depending on the soils type and technical conditions of the building the works on foundation

reinforcement can be discontinued. The second stage includes pumping the grout under the base of a wall (or column) foundation between the "compression walls". It makes possible to reinforce the soil significantly and even to create excessive pressures allowing "to level up" the foundation.

Injectors are immersed near the bearing walls in groups of three within increments of 1.5-2.0 m and may be inclined to the vertical axis in case of wide foundation base. The number of injection points and other parameters are specified by the project and depend on the specific situation.

Application of the method of directed high-pressure group injection is particularly effective to reinforce foundations of low-rise buildings due to high reliability of the obtained result and fairly low financial expenses.

3 STRENGTHEN SOIL BASE OF PILE FOUNDATION

Pile foundations are usually reinforced in order to prevent the development of additional deformations with increasing loads or deterioration of physical and mechanical characteristics of the soil. It is also possible to carry out such works to decrease deformability of back-up soil layers during construction. Reinforcement is done by pumping flowing cement-sand grout into the back-up soil layer all the way down the compressible thickness. The works also include two stages.

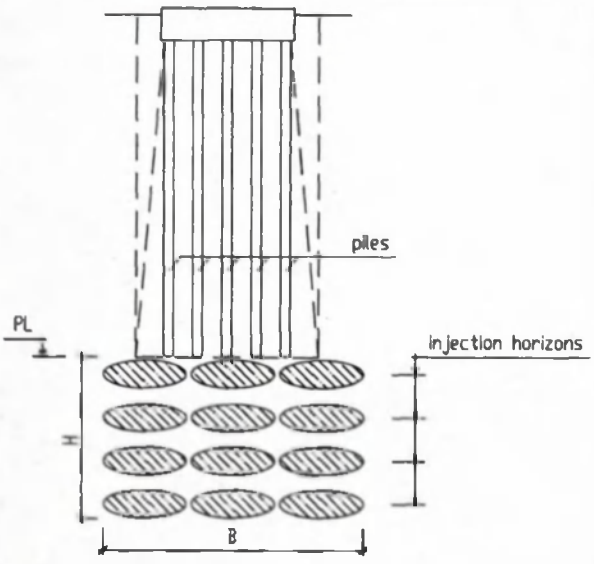


Fig. 7 Scheme of strengthen soil base of pile foundations.

During the first stage the flowing cement-sand mix is pumped along the perimeter of the pilework to form vertical walls and create compression conditions. During the second stage it is pumped directly under the pile foundation. Pumping, as a rule, is done bottom-upwards on several injection horizons.

Distance between the injectors in plan, the number and the height of injection horizons, volumes of pumped cement-sand mix are determined according to the analysis results of the engineering and geological conditions of the site, geometrical dimensions of the pile foundation and value of actual loads.

4 STRENGTHEN SOIL BASE OF BUILDINGS ON PLATE FOUNDATION

Foundation slabs are most often reinforced for timely correction of tilts and vertical position of buildings and structures by elimination of occurring deformations irregularity (both during the process of construction and during the first years of their operation). Injection conductors are placed in the body of the foundation slab when erecting it. It is done to enable injection of the cement-sand grout in the soil foundation under the building. The injection conductors are metal or asbestos-cement industrial injection pipes with internal diameter sufficient for immersing injectors through them. The bottom of the injection conductors is embedded in natural soil and their top towers over the edge of the foundation slab.



Fig. 8 Injection conductors situated in foundation plate body.

As a rule, conductors are usually arranged along a regular grid. The layout and the distance between the conductors depend on soil conditions of the construction site, loads on the foundations and design features of the building. In case of occurring irregular deformations exceeding the design values, grout is pumped in the soil foundation under the foundation plate in the direction the building tilt. The injection area in

plan, heights of injection horizons, their number and the required pumped grout volume are determined in a special design solution. The solution is carried out on the basis of analysis of the results of geodetic measurements and engineering-geological conditions of the site. Application of this method also significantly reduces the risk of negative consequences in case of construction of closely located buildings and structures.



Fig. 9 Many-storey buildings on plate foundation with injection conductors in Novosibirsk city.

There is also a method developed enabling to control the rigidity of the soil foundation. It includes engineering preparation of the foundation using the method of high-pressure injection in order to average its deformability, to decrease the risk of irregular yielding and also to reduce pressures occurring in the body of the foundation slab and in overground structures. The results of combined calculation of the system including the soil foundation – foundation slab show that overground structures identify the areas with highest tensions in the body of the slab. Such areas may appear due to irregularity of the soil foundation and due to irregularly distributed loads from load-carrying elements of the building. Analysis of available data makes it possible to determine the design parameters of the soil foundation and carry out pumping cement-sand grouts. Local reinforcement of the soil foundation makes it possible to eliminate vertical distortions of the foundation slab and to decrease the level of tensions both in the body of the foundation slab and in the overground constructions. Injection works in the process of construction are possible due to installation of injection conductors in the body of the foundation slab during its erection.

CONCLUSION

To date made more than 80 objects by the cement-sand mixture high-pressure directional injection method in Novosibirsk and Siberian region.

REFERENCES

Nuzhdin M.L. «Prevention of non-uniform settlements of foundation plate by means of high-pressure injection» (in Russian) // Experience of construction and reconstruction of buildings and structures on weak soils: Materials of International Scientifical and technical conference – Arkhangelsk: Publishing house of Arkhangelsk State University, 2003. – p. 119-122.

Nuzhdin M. L. «Use of cement-sand grouts to consolidate of soil foundations by means of directed high-pressure injection» (in Russian) // International Scientific and Technical collection of Scientific works (education) – Issue 59 – Kiev, 2003. – p. 430-433.

Nuzhdin M. L. «Application of injection conductors to prevent occurrence of foundation plate tilts above the permitted standard by means of high-pressure injection» (in Russian) // Geotechnical problems of large-scale and unique objects construction: Works of International Geotechnical Conference devoted to the Russian Federation Year in Kazakhstan. Almaty, Published by Kazakh State Academy, 2004. – p. 351-354.

Nuzhdin M.L., Nuzhdin L.V. « Experience of high-pressure injection method application for erection buildings on plate foundation» // From Research to Design in European Practice: Proceedings of the XIVth Danube-European Conference on Geotechnical Engineering. Key lectures, main lectures and abstracts of papers (Bratislava, Slovak Republic, 2nd-4th June 2010) – Bratislava: Published by Slovak University of Technology 2010. – 312 p. P.302 (on CD).

Nuzhdin M.L., Nuzhdin L.V. « Erection many-storey buildings one plate foundation with application high-pressure injection method» // Soil Mechanics and Geotechnical Engineering: Challenges and Solutions: The 14th Asian Regional Conference on Soil Mechanics and Geotechnical Engineering (Hong Kong, China, 23-27 May 2011) – Hong Kong: Published by The Hong Kong Geotechnical Society, and Department of Civil and Structural Engineering, The Hong Kong Polytechnic University, 2011. – 520 p. P.219 (on CD).

Patent for invention No. 2352723 of the Russian Federation. «Method of adjustment of the vertical position of buildings and structures on plate foundations» / Nuzhdin L.V., Nuzhdin M.L. – Published on April 20, 2009. – Bulletin No.11.

Effect of Drying and Remolding on Undisturbed Expansive Soil in Baghdad on Swelling Characteristics

Raddi M AlZubaidi
Associate professor, Department of civil Engineering ,College of Engineering, University of Sharjah

Kawkab H.S.AlRawi
Formerly Assistance Professor ,University of Technology ,Baghdad

Ahmed J.AlFalahi
MSc student,University of Technology ,Baghdad

ABSTRACT: Expansive soils can create damaging movements shrink and swell to foundations and structures. Many buildings in northern and middle of Iraq have been damaged by movement of superficial expansive clays These movements originate from changes in soil moisture .Extensive study carried out on Al-Rashdiya expansive soil in Baghdad (Iraq), this soil was silty clay and can be classified as (CH) .The degree of expansion was found to be ranged from low to medium depending on the free swell and swell pressure tests. Effect of drying and remolding of the undisturbed soil samples on Al-Rashdiya expansive soil was extensively investigated at different periods by performing free swell and swell pressure tests. The results showed that the swelling characteristics for the remolded samples were higher than those of undisturbed samples for different periods of testing (time effect)

Also the results showed a distinctive increase in the swell potential of the undisturbed sample when loosing moisture (drying samples). The final swell percent and swell pressure increases as the initial moisture content decreases for both remolded and natural undisturbed samples .Also been noticed that the remolded samples gave higher swell percent and swell pressure than those undisturbed samples. The effect of initial dry density is distinctive on swelling potential of both undisturbed and remolded samples. It is been found that the final swell percent and swell pressure increases as the initial dry density increase for both remolded and natural undisturbed samples.

1. INTRODUCTION

Expansive soil distributed in different parts of the world, these types of soils are confined to the semi –arid regions of the tropic and temperature climate zones where annual evapotranspiration exceeds the precipitation. Expansive soils contain minerals such as smectite clays that are capable of absorbing water. When they absorb water they increase in volume. The more water they absorb the more their volume increases. Expansions of ten percent or more are not uncommon. This change in volume can exert enough force on a building or other structure to cause damage. Cracked foundations, floors and basement walls are typical types of damage done by swelling soils. Damage to the upper floors of the building can occur when motion in the structure is significant. Expansive soils will also shrink when they dry out. This shrinkage can remove support from buildings or other structures and result in damaging subsidence. Fissures in the soil can also develop. These fissures can facilitate the deep penetration of water when moist conditions or runoff occurs. This produces a cycle of shrinkage and swelling that places repetitive stress on structures

Soils are composed of a variety of materials, most of which do not expand in the presence of moisture. However, a number of clay minerals are expansive. These include: smectite, bentonite, montmorillonite, beidellite, vermiculite, attapulgite, nontronite, illite and chlorite. There are also some sulfate salts that will expand with changes in temperature. When a soil contains a large amount of expansive minerals it has the potential of significant expansion. When the soil contains very little expansive minerals it has little expansive potential. Alonso E.E. et al (2005) investigated into expansive clay buffers in radioactive waste disposal designs experience cyclic drying and wetting paths during different stages of their design life. Clayey soils subjected to these processes develop swelling and shrinkage deformations, which give rise to the accumulation of compression or expansion strains during suction cycles.

Gupta et al (2008) studied the formation of longitudinal cracks induced in pavements constructed over highly plastic, expansive clay

subgrades The mechanisms leading to the development of the classical longitudinal cracks are expected to be due to tensile stresses induced by flexion of the pavement during settlements caused during dry seasons (moisture migration).

Lü Hai-bo et al (2009) conducted experimental studies on an expansive soil from Nanning (China) area in order to establish relationship between shear strength indices and cyclic drying and wetting parameters. It is found that the shear strength of expansive soil decreases with increasing number of cycles and finally reaches to a constant state. The value and cyclic number of the constant state reduce with increase of amplitude of variation of water content.YANG He-ping, et al (2006) studied the effect of cyclic wetting and drying under loading condition for the undisturbed expansive soil obtained from Ningming(a city in southern Guangxi,China) was carried out, and the variation of deformation and strength were also observed It was concluded that the swelling-shrinkage deformation of expansive soils was not completely reversible. In certain range of variation of loading, during the same cycle, the total or relative ratio of the expansion and shrinkage decreased along with the increase of loads. Shear strength increased along with the increase of load, and decreased as the cycle number increase under the same load. However, the larger the pressure was, the attenuation rate of shear strength became smaller during cyclic wetting and drying. The effects of load in certain range were to restrain the swelling-shrinkage deformation and the attenuation of shear strength.

Zornberg, J.G.etal (2010) reported that the expansive soils in semi-arid and arid regions of Texas are subjected to moisture fluctuations due to seasonal variation causing large volumetric changes. These ground movements are observed in the form of heave during wet season and shrinkage during dry season. They use of geosynthetic reinforcements, both geogrids and geotextiles, to minimize the development of longitudinal cracks in the pavements.

2. EXPANSIVE SOILS IN IRAQ

Iraq located in the arid to semi-arid zone and influenced by the Mediterranean climate, according to these circumstances expansive soils are presented in Iraq. Due to several severe problems created by these soils to the existing building, a number of researchers devoted their concerned to study and proposed some remedies

Rashid(1985) investigated the swelling characteristics of clay soils of Mousl(Iraq) area ,he studied the index properties ,classification ,X-ray diffraction analysis of the clay minerals in three sites ,Hammam Al-Aleel ,Noor and Shallalat area . Rashid concluded that the swelling percent in compacted Mousl clay is high. Sabaa, (1987) investigated the location and characteristics of the expansive soils in eight cities in the mid part of Iraq utilized the results collected from National Center of Laboratories .The results were analyzed and the degree of expansion was estimated depending on the classification system that proposed by Chen,(1975) .Sabaa concluded that degree of expansion of the expansive soils in mid part of Iraq from low to medium ,except in Kalis district in Diyala east of Iraq ,the degree of expansion ranged from medium to high..

Ibrahim,(1989) studied the expansion properties of the expansive soils in Al-Anbar city west of Iraq which contains a large percent of montmorillonite clay minerals .He concluded that the degree of expansion of the expansive soils in Al-Anbar city ranged from medium to high. Also he found that the swelling pressure ranged from 400 to 600 KN/m^2 and the swelling percent ranged from16% to 20%.Witwit ,(2001) estimated the degree of expansion for all the cities in Iraq for the expansive soils depending on reports from the National Center Laboratories using different classification systems .

2-1 Experimental Work

The site for the present research located at the east side of Baghdad city in Al-Rashdiya district .The description of the soil was stiff to hard lean to fat clay ,the water table encountered at 1 m depth below natural ground surface. The physical properties, grain size distribution and classification of the soil are shown in Table .1. Al-Falahi (2002)

Depth(m)	L.L (%)	P.L (%)	P.I (%)	L.S (%)	A(%)	Silt (%)	Clay(%)	Sand(%)	U.S.C	AASHTO
0.5-1	39.12	19.73	19.39	10.83	1.01	76.36	19 2	4.44	CL	A-6
1.5-2.0	51.01	19.58	31.43	13.09	1.31	63.64	24	12.26	CH	A-7-6
2.5-3.0	56.14	22.23	33.91	11.23	0.92	55.22	36 8	7.98	CH	A-7-6
3.5-4.0	60.23	27.92	32.31	13.29	0.77	57.82	42	0.18	CH	A-7-6
4.5-5.0	62.24	23.65	38.59	14.12	0.92	55.96	42	2.04	CH	A-7-6
5.5-6.0	63.25	23.11	40.14	11.31	1.43	60.44	28	11.56	CH	A-7-6
6.5-7.0	56.58	24.93	30.53	11.25	1.24	73.36	24 6	2.04	CH	A-7-6
7.5-8.0	62.45	26.05	37.52	14.19	1.25	60.78	30	9.22	CH	A-7-6
8.5-9.0	65.29	22.61	42.68	14.18	0.95	54.76	45	0.24	CH	A-7-6

Table(1) Physical properties of Al-Rashdiya soil

Depending on the physical properties of undisturbed samples from Al-Rashdiya soil, the clay content (< 0.002 mm) ranges from 19.2% to 45%, the silt content ranges from 54.76% to 76.36% ,the liquid limit ranges from 39.12% to 65.29% ,the plastic limit ranges from 19.58% to 27.92% ,the plasticity index ranges from 19.39 to 42.68% ,the activity ranges from 0.77% 1.43% and the linear shrinkage of the samples ranges from 10.83% to 14.19%. According to the classification chart modified by Van Der Merwe (1975) that depends on clay
fraction (< 0.002 mm) and the plasticity index .The degree of expansion of Al-Rashdiya soil was high to very high. X-ray diffraction test was carried out to determine the proportion of the various minerals present in the soil as shown in Table (2).Chemical tests also carried out as additional method to identify mineralogical composition of the soil as shown in Table (3)

Non-Clay Minerals	Mineral	percentage
	Quartz	24
	Calcite	34
	Feldspar	2
Clay Minerals	Montmorillonite	20
	Playgorskite	8
	Kaolonite	12

Table (2) X-ray of Al-Rashdiya soil

Compound		Percentage by weight
Silica	SiO_2	40.66
Alumina	Al_2O_3	9.82
Iron Fe_2O_3		1.09
Lime	CaO	28.98
Magnesia	MgO	0.99
Soda	Na_2O	3.10
Potassium	K_2O	0.74
Loss on Ignition	L.O.I	13.93
	PH	7.8

Table (3) Chemical Compounds of Al-Rashdiya Soil

2-2 Predictions of Swelling Characteristics by Direct Method

The most satisfactory and convent method for determining the swelling potential and the swelling pressure of an expansive soil is the direct method, where free swell and swell pressure tests were conducted on undisturbed and remolded samples from Al-Rashdiya soil.

3. VARIATION OF SWELL POTENTIAL WITH TIME FOR UNDISTURBED SAMPLES

In order to investigate the effect of drying on swell potential on undisturbed with time of Al-Rashdiya soil a 27 tests of undisturbed samples at original state and a 20 tests for undisturbed samples cured at air temperature (20) °C for one day were carried out as a trial to decrease the initial water content and modify the swelling characteristics of the samples.

As inTable (4) the results shows the variation of swelling potential with time for different depths for undisturbed samples .It can be noticed that the swelling percent increase with depth ,this is may be attributed to the increase percent of clay particles with depth.

Another set of swelling tests carried out on undisturbed samples but these samples were curried at the temperature room 20 °C for one day, the results can be seen in table (5) .The results showed an increase in the swell potential than those carried without drying(curing)

Depth in m	0.5-1	1.5-2	2.5-3	3.5-4	4.5-5	5.5-6	6.5-7	7.5-8	8.5-9
Time in Min.	Swell %	Swell %	Swell %	Swell %	Swell %	Swell %	Swell %	Swell %	Swell %
0	0	0	0	0	0	0	0	0	0.3
2	0.16	0.15	0.16	0.15	0.15	0.15	0.12	0.18	0.4
4	0.16	0.18	0.18	0.22	0.18	0.16	0.15	0.21	0.42
8	0.20	0.20	0.2	0.23	0.2	0.18	0.18	0.3	0.6
18	0.20	0.20	0.21	0.25	0.21	0.19	0.2	0.4	0.85
30	0.22	0.20	0.22	0.3	0.22	0.22	0.22	0.42	1.18
130	0.22	0.21	0.24	0.5	0.9	0.4	0.24	0.8	1.75
1500	0.22	0.22	0.85	1.15	1.8	0.5	0.28	1.3	4.8
3000	0.23	0.22	1	1.18	2	0.55	0.4	1.4	5.1
5500	0.23	0.22	1	1.2	2	0.58	0.4	1.4	5.5
6500	0.23	0.23	1	1.2	2.1	0.6	0.4	1.4	5.5

Table (4) Relation between swell potential and time for undisturbed samples (no curing)

Depth in m	0.5-1	1.5-2	2.5-3	3.5-4	4.5-5	5.5-6	6.5-7	7.5-8	8.5-9
Time in Min.	Swell %	Swell %	Swell %	Swell %	Swell %	Swell %	Swell %	Swell %	Swell %
0	0	0	0	0	0	0	0	0	0.28
2	0.10	0.10	0.10	0.10	0.20	0.10	0.10	0.10	0.42
4	0.16	0.15	0.15	0.20	0.30	0.15	0.15	0.15	0.70
8	0.18	0.19	0.22	0.30	0.40	0.18	0.20	0.20	1.0
18	0.20	0.20	0.24	0.40	0.50	0.20	0.21	0.40	1.20
30	0.22	0.22	0.40	0.50	0.58	0.22	0.28	0.60	1.60
130	0.22	0.22	0.50	1.40	1.50	0.40	0.30	1.30	3.00
1500	0.23	0.22	1.20	2.60	3.30	0.70	0.40	2.20	5.70
3000	0.23	0.24	1.22	2.70	3.50	0.75	0.50	2.30	6.20
5500	0.23	0.24	1.26	2.80	3.60	0.75	0.50	2.40	6.40
6500	0.24	0.25	1.28	2.80	3.60	0.75	0.50	2.40	6.50

Table (5) The Relation between swell potential and time for undisturbed samples cured for one day at 20 ° C

The primary swell was achieved at two days while four days was sufficient to complete the secondary swelling. The variation of swell with depth as

shown in Figs.(1) and (2) may be attributed to the difference in the initial water content and initial dry density ,also there is unique relation between the clay percent and the plasticity index with the swelling characteristics of the samples, since the maximum swell was at the maximum percent of the clay and plasticity index while the minimum swell was at minimum percent of the clay and plasticity index ,because of the clay particles are more able to absorption of water from other particle, thus the swelling increased with increasing the clay percent.

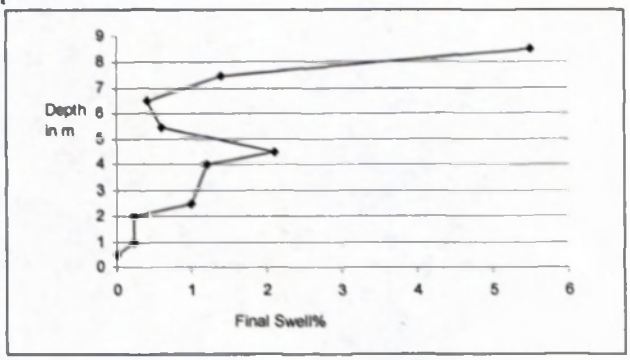


Fig. (1) Variation of swell percent with depth for undisturbed samples (no curing)

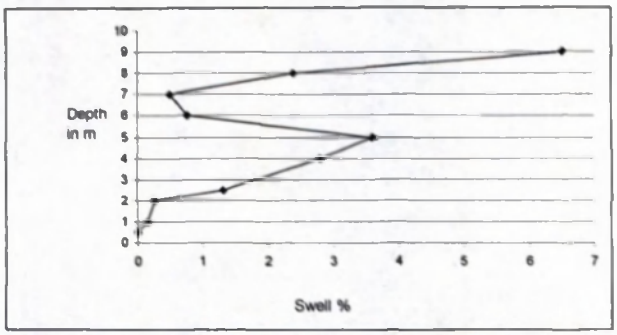


Fig. (2) Variation of swell percent with depth for undisturbed samples cured for One day at 20 ° C

3-1 Variation of Swelling Pressure for Undisturbed Samples

Figs. (3) and(4) show the relation between the swelling potential and the surcharge pressure for undisturbed both ordinary and cured samples respectively with depths.

The intersection of these curves with abscissa indicates to the required pressure for zero volume change during swelling, when these samples get wet. This pressure represents the swelling pressure. It can be noticed that the samples with maximum swell percent posses the maximum swell pressure while the samples with minimum swell percent posses the minimum swell pressure There are distinctive increase in the swell pressure values for undisturbed samples of the same depth cured with one day at 20 ° C than those with out curing ,this attributed to the lose of moisture (drying during curing).The values of the swell pressure for undisturbed sample for the cured and uncured samples showed a distinctive variation with depths. The swell pressure variation may be attributed to the initial in situ condition and clay content of the samples, drying process leads to increase the initial dry density of the sample that leading to increase the swell pressure.

4. EFFECT OF DRYING PERIODS ON SWELLING CHARACTERISTICS OF UNDISTURBED SAMPLES

Another type of tests were carried out to examine the effect of drying process on the swell potential of undisturbed samples, (12) free swell and swell pressure tests were conducted .

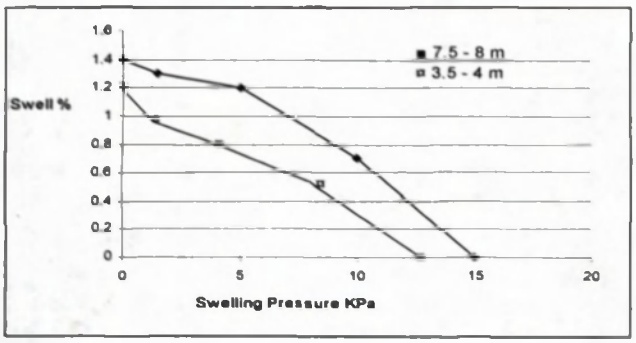
Tests were performed on dried samples at different period ranging from 1 to 7 days at air temperature (20) ° C.

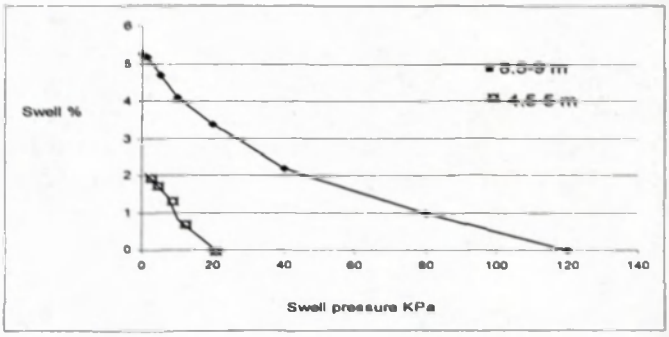
Fig.(5) shows the variation of swelling with time for undisturbed samples .The values of maximum swelling percent at the end of the tests were varied considerably depending on the initial condition ,but generally (48) hours were sufficient to complete the primary swell ,while (4) days were sufficient for the secondary swelling for curing period of (7) days .It can be noticed that the swelling percent increases with increasing the period of curing for the undisturbed samples .Table (6) shows the values of swell pressure for different curing period for undisturbed samples .It is clear that the values of the swell pressure increases with increasing the period of curing.

Increasing of swell percent and swell pressure with drying time may be attributed to initial water content and initial dry density ,thus when the drying time is increased ,the shrinkage increased ,i.e the amount of dried soil to unit volume will increase inside the consolidometer ring, and the amount of water interaction will increased during the test, on the other hand when the shrinkage is started ,the initial water content will decrease ,therefore the change in water content that necessary to accomplish the swelling will increase ,thus the volume expansion and the swell pressure will increase with increasing the initial dry density and decreasing the initial water content.

5. EFFECT OF REMOLDING ON SWELLING CHARACTERISTICS FOR DIFFERENT DRYING PERIOD

12 free swell and swell pressure tests were conducted on remolded samples , since from each mould 3 samples were extruded from top, middle and bottom of the mould, these samples were dried by keeping the samples curing in the temperature room 20 ° C for different period ranging from 1 day to 7 days .Fig.(5) shows the variation of swell potential with time for the remolded samples .the maximum rate of the swell was completely in (48) hours while the required time to finish the swelling was approximately (6) days .Table (6) summarized the swelling percent and the required swell pressure for both disturbed and remolded samples at initial water content and initial dry density condition ,it can be seen that the remolded samples developed higher swell potential and swelling pressure as compared with undisturbed samples. This tendency can be attributed to the fact that the initial dry density is most important factor effecting on swelling characteristics of the samples. For undisturbed samples the dry density represents the in-situ characteristics ,therefore the swelling pressure at in-situ dry density can be used directly to describe the swelling characteristics .For remolded samples , the distortion of structure of the soil was occurred and a newly rearrangement of the particles in the structure of the soil was taken place during the compaction .Therefore the swelling characteristics varying with the degree of compaction since the swelling potential depending on the maximum density of the samples ,then the swell pressure of the disturbed soil can be defined as the pressure require to keep the volume of the soil constant at its superimposed density.





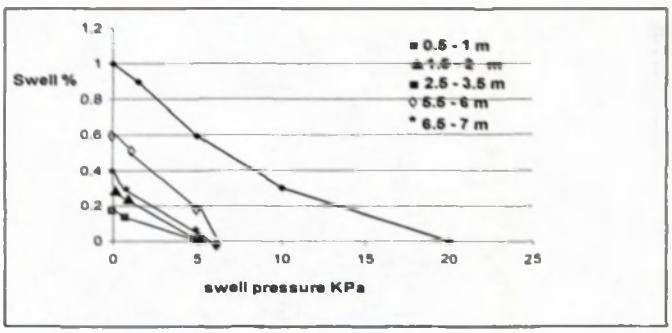
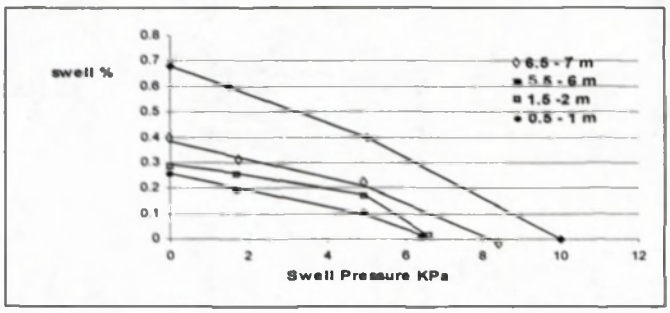
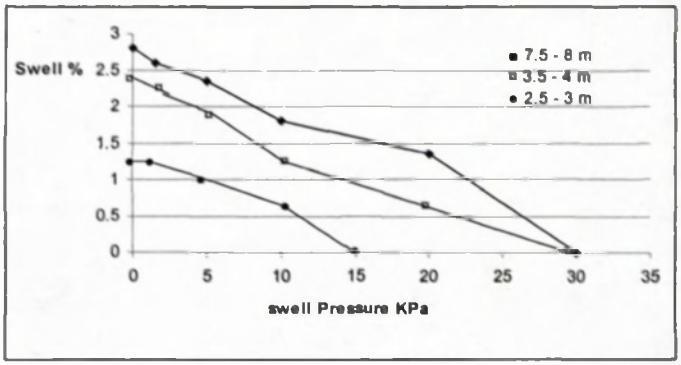


Fig.(3) Swell potential against surcharge pressure for undisturbed samples for different depths(no curing)





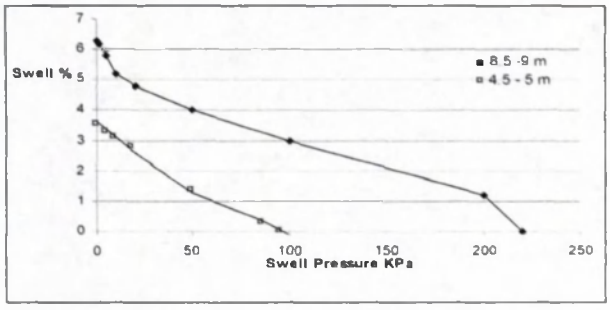


Fig.(4) Swell potential against surcharge pressure for undisturbed samples Cured for one day at 20 ° C for different depths

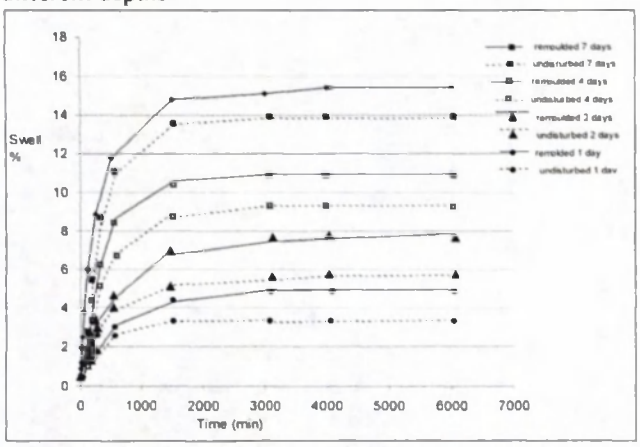


Fig. (5)Swell pressure against time (min) for undisturbed and remolded samples for different curing periods

Initial water Content (%)	Dry density (gm/cm^3)	Swelling percent		Swelling pressure KPa		Drying period (days)
		Undisturbed	Remolded	Undisturbed	remolded	
22.9	1.59	3.62	4.81	95.6	134	1
20.52	1.62	5.92	7.96	213.34	270	2
18.2	1.65	8.79	10.4	312.5	375	4
12.6	1.71	13.5	15.26	460.9	515	7

Table (6) Variation of swelling characteristics of undisturbed and remolded samples for different curing period

5-1 Variation of final swells percent and swell pressure with initial water content and dry density

The research also examine the effect of initial water content and dry density on swelling potential of both undisturbed and remolded samples .Fig.(6) and Fig.(7) show the effect of initial moisture content on swell percent and swell pressure for remolded and undisturbed samples .It is clearly shown that the final swell percent and swell pressure increases as the initial moisture content decreases for both remolded and natural undisturbed samples .Also it can be noticed that the remolded samples gave higher swell percent and swell pressure than those undisturbed samples.

As shown in Fig.(8) and Fig(9) the effect of initial dry density is distinctive on swelling potential of both undisturbed and remolded samples .

It is clearly concluded that the final swell percent and swell pressure increases as the initial dry density increase for both remolded and natural undisturbed samples.

The effect of drying process on swelling percent and swell pressure as a result from decreasing the volume of the wet soil and increasing the initial dry density inside the consolidometer ring, therefore the swelling characteristics were increased.

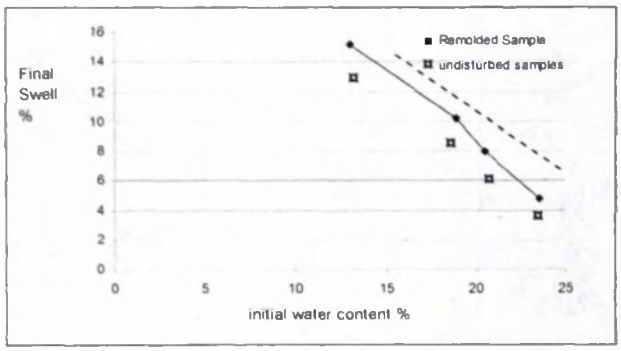


Fig.(6) Variation of final swell percent with initial moisture content for air dried samples

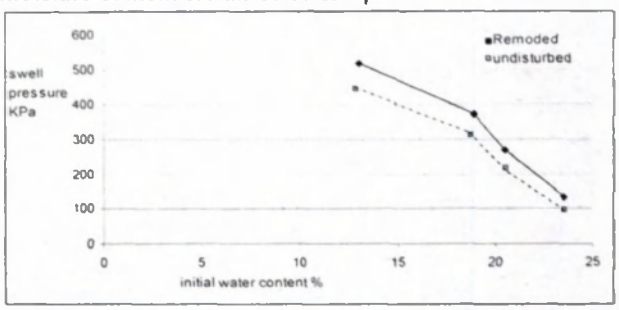


Fig.(7) Variation of final swell pressure with initial moisture content for air dried Samples

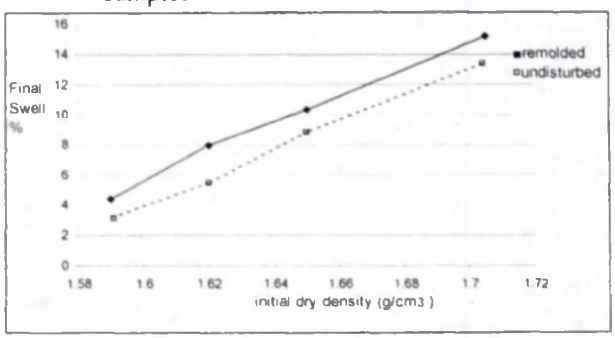


Fig.(8).Variation of final swell percent with initial dry density for air dry samples

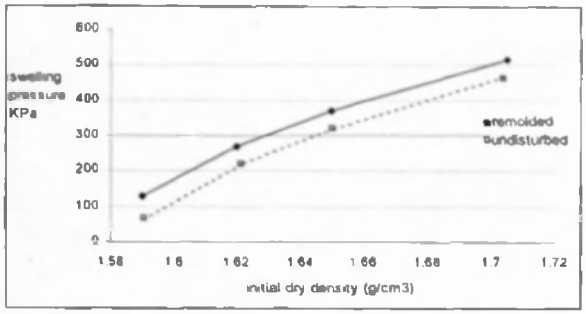


Fig.(9).Variation of swell pressure with initial dry density for air dry samples

6. CONCLUSIONS

Extensive study carried out on Al-Rashidya expansive soil (in Baghdad), the research includes the effect of drying and remolding on the swell potential of undisturbed samples, during this research the followings can be concluded:

1- The percentage of clay fraction for Al-Rashidya soil varied widely from 19% to 45% with depth, where the indirect method showed a degree of expansion from high to very high while direct method showed that the degree of expansion ranging from low to medium .

2- The free swell tests for Al-Rashidya expansive soil showed that (48) hours were sufficient to complete the primary swelling, while (4) days were sufficient to complete the secondary swelling

3-The results of undisturbed soil samples tested in the free swell tests produced a considerable increase in the swelling percent with depth as the clay fraction increases.

4- The undisturbed samples with one day curing at 20 ° C tested with free swell tests showed an increase in the swelling percent as compared with those for the same depth but with out curing.

Also the cured undisturbed samples result showed a considerable increase in the swelling percent with depth.

5-The values of swell percent and swell pressure showed extensive increase with increasing the period of curing where drying of the sample increases .So extensive care must be taken during sampling of expansive soil and the sampling tube must be sealed completely with wax and the undisturbed samples should be tested as reached to the laboratory where storing the sample for long time may decrease the original moisture content of the samples.

6- The values of swell percent and swelling pressure of the remolded sample are higher than those of undisturbed samples for the same depths .This needs to take a great care when extruding undisturbed samples from site investigation, the cutting shoe for the sampler should be sharp and thin in order to prevent any type of disturbance to the samples.

7- Effect of moisture content on the swelling potential also examined .The results showed that the final swell percent and swell pressure increase as the initial moisture content decrease for both remolded and natural undisturbed samples.

8-Effect of dry density on swelling potential also studied .It is concluded that the final swell percent and swell pressure increases as the initial dry density increase for both remolded and natural undisturbed samples.

The effect of drying process on swelling percent and swell pressure as a result from decreasing the volume of the wet soil and increasing the initial dry density inside the consolidometer ring, therefore the swelling characteristics were increased.

REFERENCES

Al-Falahi, A.J. ,(2002) "The Use Of Cement Dust to Reduce Swelling" M.Sc. Thesis, Department of Building and construction, University of Technology ,Baghdad, Iraq

Alonso, E.E. E. Romero, C. Hoffmann and E. Garcia-Escudero (2005)" Expansive bentonite–sand mixtures in cyclic controlled-suction drying and wetting "Engineering Geology, Volume 81,Issue3,14 November 2005, Pages 213-226,Issues in Nuclear Waste Isolation Research

Chen, F.H. ,(1975). "Foundation of Expansion Soils" .1st edition, Elsevier Science Publishing Company .New York

Gupta, R., McCartney J.S., Nogueira, C.L. and Zornberg, J.G., (2008)"Moisture migration in geogrid reinforced expansive subgrades", Geoamericas, Cancun, Mexico.

Ibrahim, I.A, , (1980). "Expansive properties of Akashat Soil" M.Sc Thesis, Department of Building and Construction, University Of Technology, Baghdad, Iraq

Lü Hai-bo, (2009) ZENG Zhao-tian and Yan-lin "Experimental studies of strength of expansive soil in drying and wetting cycle" Chinese Journal Rock and Soil Mechanics Vol.30 No.12

Rashid, K.A (1985) "Swelling Characteristics Of Compacted Soil in Mousl Area" M.Sc Thesis, Civil Engineering Department, College Of Engineering, University Of Mousl, Mousl, (Iraq)

Sabaa, M.R. (1987) "Evaluation of Soil Expansion Properties in Mid Part of Iraq. M.Sc Thesis, Department of Building and Construction, University of Technology, Baghdad, Iraq

VanDerMerwe, D.H, (1975). "Current Theory and Practice for Building on Expansion Clays," Pro.6th Reg. Conf. for Afr. On Soil Mech. And Found, Eng.Vol.2 .pp.160-167

YANG He-ping, HANG Rui, and ZHENG Jian-long (2006) "Variation of deformation and strength of expansive soil during cyclic wetting and drying under loading condition" Chinese Journal ofGeotechnical Engineering, vol.11

Zornberg, J.G., Gupta, R .and Ferreira, J.A.Z (2010) "Field performance of geosynthetic reinforced pavements over expansive clay subgrades" 9 International Conference on Geosynthetics, Brazil.

Witwit, A.M , (2001) "Expansion Soil In Iraq-Location, Properties and Treatment Method "M.Sc .Thesis, Department of Building and Construction, University of Technology, Baghdad, Iraq.

The Calculation Of The System "Plate- Base" With Taking Into Account Nonlinear Deformed Soil

E.A. Isahanov
Almaty, Kazakh Academy of Transport & Communication (named after M.Tynyshbayev)

S.Kh. Dostanova
Almaty, Kazakh Leading Academy of Engineering and Architecture

The elastic plate and three models bases are considered. The algorithm of the calculation of the system "plate-soil base" with taking into account the equations of the state and rheological characteristics of soil is presented.
The keywords: plate, soil base, elasticity, plasticity, rheology, equations of state, geotechnical engineering.

1 INTRODUCTON

The working of any building depends on strength properties of the soil array, above which it is raised. There is the relationship between an elevated part of building and the main basis when considering system "plate- soil base". When designing buildings in usual soil condition, when average pressure on base under sole base or road plates and aerodrome captive from loads does not exceed the design value, it can be satisfied by result calculation of base in linear stating.

How the practice and numerous experiments for majority type of soils show the dependences between stresses and deformation have a nonlinear nature so it is important to know the participation of the nonlinear behavior of the soil in working of the designs in comparison with the other model of the soil base. The calculation of the system "plate- soil base" with taking into account the complicated way of deformed base represents the complex mathematical task. So in present work following approach for calculation of the system "plate- soil base" is offered.

Knowing behavior of the soil base under the action of external load, it may consider the inverse task on the interaction supporting design with the soil base. These tasks are of great importance for designing and building deep in soil construction. Using available experienced data, it is possible to describe the behavior of a soil base with sufficient accuracy and choose the respective algorithm of the calculation. So considering the plate as more flexible, the settlements of the base under the action of loads, directly attached to base are defined [6].

2 THE CALCULATION OF THE SYSTEM "PLATE- SOIL BASE"

The calculation of the system "plate- soil base" consists of two interconnected tasks.
The stating of the first task.
We shall consider soil array (H- thickness, L,B- sizes in plan), residing under the action of average pressure q_0, attached on rectangular square $A=a \cdot b$, where a, b - sizes of the square.
They are considered as three models of the basis:
1) linear - deformed space;
2) nonlinear - deformed space (the heterogeneous base);
3) base with taking into account the creep of soil (under constant speed of the intensities of the deformation).

For calculation of the first model of the base the decision of Bussinesku [6, 3]is used, it is generalized on event of the uneven load by means of summations corresponding to decisions.

For calculation of the second model of the base the variation method with using the equation of the state, which links between itself intensities deformation, intensities of the stresses and average stress is used. This equation is received experimental or as a result of laboratory tests of the soil on the three axial compressions in the stabilometer and it has a nonlinear nature [4]. If the experienced data is lacking the relationship between generalized stress and generalized deformation is assigned approximately in the manner of power-mode dependency, their coefficients are defined by simple tests.

In nonlinear decision the soil is considered as heterogeneous elastic array, where dependences

of Genki for spatial task are satisfied. The theory of small elastic-plastic deformation is used, i.e. the task of theory of plasticity can be considered as task to theory of elasticity, but for heterogeneous elastic body, so parameters of elasticity in each point in general event depend on properties tense-deformed state. The decisions of such nonlinear task are built on combination of two methods: variation and method of the successive approximations in the form variable parameters of elasticity.

For the third model of the basis it is used also variation method with using rheological equations of the state, which link the intensities of deformation, intensities of stress, average stress and speeds of deformation between them. These equations are received experimental as a result of laboratory tests of the soil on the three axial compressions in the stabilometer for each type of soil separately and they also have a nonlinear nature [4]. At calculation the speed of intensities of deformation is assigned, it depends on speed of deformation and load basis, in general event it can change with time (step-like load in process building constructions or buildings).

In numerical calculation of the basis the settlements of surfaces are defined, further they will correspond to values of sagging the plate in nodes of the imposed net $w(x_i, y_i)$ i=1 ...N, where N is an amount of nodes taken on the external of the surface. These dates can be used for calculation of the same plate. They present themselves as deformed surface of the base and in view of the full contact of the plate with base it is possible to accept for deformed surface of the plate. At calculation of the plate by method of the finite elements (MFE) it is possible to give displacements on lower verge of the plate equal received settlements on the surface of the soil basis. At calculation of the plate by analytical method it is possible to receive the reactive pressure, corresponding to the deformed surface of the basis with use of the power-mode rows [2].

At calculation soil array with taking into account the equations of the state according to the main premise of the nonlinear theory of elasticity, as well as theory of small elastic-plastic deformation under simple load [1], the connection of intensity of the stress with intensity deformation for each point of the body under complex tense state is taken in this way, as connection of the axial stress with deformation of lengthening at simple tension of the body, i. e.

$$\sigma_i = E' \varepsilon_i \qquad (1)$$

where E' is a shear module to deformation of the first type. In theory of plasticity under simple load, in condition of the small deformation, this expression gives an opportunity to use the physical equations in the form of dependencies of Genki [1].

Using theory of small elastic-plastic deformation, mathematical device itself presents collection of six physical equations, three steady-state equations of the balance and six equations of the continuity deformation. It is necessary to find such decision of the task, which satisfies for each point of the deformed body above mentioned equations and, besides, on border of the body satisfies border conditions. The task of theory of plasticity is considered as task of theory of elasticity, but for heterogeneous elastic body, parameters of elasticity — E, μ, G in each point of the body in general event depends on properties in tense-deformed state [1]. The decision of such nonlinear task is to build on method of the successful approximations. In zero approximations $E^{*(0)}, \mu^{*(0)}, G^{*(0)}$ are equal to E, μ, G and, solving linear task to theory of elasticity, the components of the stresses and deformation are found.

From equation of the state the values of intensity stress and average deformation $(\sigma_i^{(0)}, \varepsilon_{cp}^{(0)})$ are defined, moreover in right part the found values $\varepsilon^{(0)}{}_i, \sigma^{(0)}{}_{cp}$ are used, then the values of parameters $(E^{*(1)}, \mu^{*(1)}, G^{*(1)})$ in the first approximation are defined. Then the task to linear heterogeneous theory of elasticity is solved. Using dependencies of Genki in each point the components of the stresses and deformation in the first approximation are defined. On base of the equation of state the solution $(\sigma_i^{(1)}, \varepsilon_{cp}^{(1)}, E^{*(2)}, \mu^{*(2)}, G^{*(2)})$ corresponding to new approximation, is defined. The equations of the state help goal-directed to vary the stresses and deformations in all point of the body, saving invariant dependencies.

For determination of settlements basis, corresponding to indicate to model, the variation method in combination with method of the elastic decisions in the form variable parameter is used. It is possible to consider the base as heterogeneous array with changing modules. Now, soil array is considered, it introduces in the manner of collection of separate elements (for example, the

parallelepipeds for spatial task or rectangles for flat task), their full energy is summarized from separate energy of each element. Varying values three node displacements by means of variable modules deformation [4], it is possible with sufficient accuracy to define final values of the displacement, corresponding to accepted model of the base, which minimize the functional energy E from full convergence. Values of the full potential energy of the body are defined in each n-approximation. The criterion to convergence of the decision is an energy principle, according to balance state $\Im = \Im_{min}$ [1]. The variation equation introduces in the manner $\delta\Im = 0$, in integral form it expresses condition of the balance of the deformed body, it consists of differential equations of the balance together with conditions of the balance on surfaces of the body (the border conditions). As independent varying parameters the variable parameters of elasticity E^*, μ^*, G^* are given, the stresses and deformations are connected with them corresponding to dependencies from theory of elasticity [1]. Components of displacement toward axis's x,y,z are connected with deformations on the base of the dependencies of Koshi [1]. These conditions express the continuity and indissolubility of the deformation. Using equations of state, components of the stresses $\vec{\sigma}$ vary in all point of the body and, accordingly, components of vectors deformation $\vec{\varepsilon}$ and displacement $\vec{u}$. Having sorted in all chosen points of the body vectors $\vec{\sigma}, \vec{\varepsilon}, \vec{u}$, the new state is received. The possibility of this state is defined by functional of full potential energy of the body.

In each approximation the stresses and deformations vary only in internal points of the body (in nodes of elements). On surfaces the stresses and deformations do not vary since in these points steady-state and kinematical conditions are to satisfy.

As zero approximation for nonlinear decision and at account creep of soil the linear decision is taken. In each node point all necessary components of the stresses and deformations and value of the full potential energy of the array in zero approximation are defined. Further the procedure of the approximation by means of variation components of stress and components of deformation in each node point begins. In zero approximation the full energy of the system is equal $\Im_0$, in each following approximation the energy $\Im$ is minimized by variation of the stresses and deformations in all node points. For each element the values of the stress $\vec{\sigma}$, deformation $\vec{\varepsilon}$, displacement $\vec{u}$ in all nodes are found. Having sorted all points, the decision, i.e. new approximation and corresponding value of the full energy of the body is received in this state.

The given algorithm allows solving linear (elastic) and nonlinear tasks, as well as taking into account the speed of deformation $\dot{\varepsilon}_i$, i.e. considering the process at time. Considering unceasing process of deformation at time, it is possible to solve the tasks with variable speeds of the stress and deformation in day, month and year. On print it is possible to give result in interesting moments of time or final results for period of time T.

At process of deformation at time it is taken into account the speed of intensity deformation which is possible to present in certainly-difference type. In given work value $\dot{\varepsilon}_i$ is given and constant:

$$\dot{\varepsilon}_i \cong \frac{(\varepsilon_i)_{k+1} - (\varepsilon_i)_k}{\Delta t}, \qquad (2)$$

where $\Delta t = t_{k+1} - t_k$, $(\varepsilon_i)_{k+1}$- an intensity to deformation in (k+1) moment of time; $(\varepsilon_i)_k$ - an intensity to deformation in k-moment of time.

According to (2) it is possible to write:

$$(\varepsilon_i)_{k+1} = (\varepsilon_i)_k + \dot{\varepsilon}_i \Delta t \qquad (3)$$

Using iterations on time t, it is possible to express the intensity to deformation in (k+1)- moment of time through intensity deformation in previous i.e. in k- moment of time. Considering process for interval of time T, it is possible to divide it on separate intervals $\Delta t = \frac{T}{n}$, where n - integer number. On base of the iterations on t in each interval Δt full picture of tense-deformed state is received in accordance with above-mentioned algorithm.

As a result of calculation the picture of the change for settlements and horizontal displacements for basis plates depending on type soil, speed factors deformation and load, intensities attached on surfaces forces is received.

Now algorithm for calculation of the bases of the buildings presents, where hard or thick

plates with taking into account the transverse shear are considered.

The stating of the second task.

The elastic plate, residing under the action of normal distributed load of the intensity q is given. The plate liberally rests upon soil basis. The contact of the plate with basis is realized in the manner of issues of the normal reactive pressures (the steady-state conditions). Friction between plate and basis neglects. The reactive pressures, sending on plate, depend on values of settlement, they are determined from the first task. The kinematical conditions on the internal surface of the plate are possible to express through displacements equal found settlements in node points.

The analysis of the stresses on thickness of the plate shows that collection of the normal stresses σ_x , σ_y results in bending pairs with moments M_x, M_y; the collection of the tangent stresses τ_{xy} results in turning pair with moment M_{xy}; the collection of the tangent stresses τ_{xz}, τ_{yz} results in resultant transverse forces Q_x, Q_y. Tangent shear stresses τ_{xz}, τ_{yz}, consequently and shifts γ_{xz} , γ_{yz} change on parabolic law, changing in zero on upper and lower border surface of the plate $z=\pm h/2$, and reach most values at middle surface. Consequently, rectilinear elements of the plate in process of the deformation, staying normal to upper and lower border surfaces of the plate are curved. The most degree of the curve corresponds to the part of the element, residing in close proximity from the neutral layer. The system of the external forces in general event can be presented by transverse load of intensities q(x,y), bending moments m_x, m_y, created by tangent stresses on internal surface of the plate, reactive pressure on the part of basis p(x,y). In general event with taking into account the deforming of shift system of three differential equations for functions of sagging and two tangent stresses, acting in middle plane of the plate is received [1-5]. Since function of sagging is known from decision of the first task, that use certainly-differenced relations for unknown tangent stresses, their values in all node point of the superimposed net can be defined. By means of border conditions recorded in certainly-differenced type, the outside of sidebar points through internal points of the middle surface of the plate can be expressed.

Disregarding deformation of shift the task is simplified and for their decision the theory of Kirchhoff can be used. If it is considered the three-dimensional task, then it is possible to use the variation approach [5]. For decision of the variation task the method of the finite element is used [2]. The proposed algorithm was realized for calculation of the base on the Almaty relay television station, located on peak of the mountain Kok-Tube near Almaty [4].

CONCLUSION

On the base of offered method of calculation of the system "plate-soil base" the following summary is possible to make:

1. The proposed algorithm of the calculation with taking into account the real behavior of soil basis is easy for realization on computer and it is possible to consider whole process deformation at time.
2. The mechanical characteristics of the soil change on nonlinear law, which is defined by experimental or assigned on some law, close to real behavior of the system.
3. The regularity in behavior of the soil is defined initial and changing parameters of soil basis at time depends on speed of the deformation and load.
4. The behavior of the system "plate-soil base" under given speeds of intensity of the stress or deformation is possible to forecast short-term and long-term.

REFERENCES

Alexander A.V., Potapov V.D. (1982). The bases of the theory of elasticity and plasticity. Moscow, High school, 216.

Fadeev A.B. (1987). The method of the finite element in geomehanics. Moscow. Depths, 221.

Gorbunov-Posadov M.I., Malikova T.A., Solomin V.I.(1984). The calculation of design on elastic basis.-Moscow, Stroyizdat, 679.

Isahanov E.A. (2000). Rheological characteristics of dense clay soil and calculations of design. Almaty, 144.

Perelimuter A.V., Slivker V.I. (2002).The accounting models of the buildings and possibility of their analyses. Kiev, "Steel", 597.

Zytovich N.A. (1963). Mechanics of soil. Moscow, 636.

Учет механических показателей грунтового основания при расчете дорожных конструкций

Б.Б. Телтаев
АО «Казахстанский дорожный научно-исследовательский институт» (КаздорНИИ), Алматы, Казахстан

АННОТАЦИЯ: Несмотря на то, что в нормативных документах предусмотрено проектирование конструкций дорожных одежд и их грунтового основания выполнять совместно, в настоящее время недостаточно уделяется внимание на учет состояния и механических показателей грунтового основания.

В настоящей работе, используя данные экспериментального изучения водно-теплового режима конструкции нежесткой дорожной одежды на автомобильной дороге «Астана - Бурабай» и решение осесимметричной задачи теории упругости слоистой среды, показаны принципиальная возможность и практическая важность одновременного учета величины и фазового состава влаги в грунтовом основании и температуры асфальтобетонных слоев при определении показателей напряженно-деформированного состояния в характерных точках дорожной конструкции.

1 ВВЕДЕНИЕ

В бывшем Советском Союзе был разработан и в 1983 году введен в действие нормативный документ по проектированию дорожных одежд нежесткого типа (ВСН, 1985). С 2007 года в Казахстане действуют Строительные нормы по проектированию нежестких конструкций дорожных одежд (СН РК, 2007). В казахстанском нормативном документе основные методические положения по расчету конструкций нежестких дорожных одежд остались практически такими как в (ВСН, 1985). В указанных выше нормативных документах одним из ключевых положений в расчете дорожных конструкций является совместное рассмотрение дорожной одежды автомобильной дороги и её грунтового основания. При этом конструкции дорожных одежд капитального типа должны рассчитываться на прочность по следующим критериям:

- по допускаемому упругому прогибу всей конструкции дорожной одежды;
- по допускаемому сдвигу в грунте земляного полотна, слабосвязных слоях дорожной одежды и асфальтобетонных слоях;
- по допускаемой величине растягивающего напряжения при изгибе в монолитных слоях дорожной одежды.

Несмотря на то, что дорожные одежды и грунтовое основание автомобильных дорог рассчитываются совместно при проектировании дорожных конструкций и грунт земляного полотна автомобильной дороги рассчитывается на прочность по отдельному критерию, на наш взгляд, в настоящее время недостаточно уделяется внимание на учет состояния и, как следствие, механических показателей грунтового основания.

2 НОРМАТИВНЫЕ ЗНАЧЕНИЯ ДЕФОРМАЦИОННЫХ И ПРОЧНОСТНЫХ ХАРАКТЕРИСТИК ГРУНТОВ

При расчете конструкций дорожных одежд согласно СН РК 3.03.19-2006, пользуются табличными данными расчетных значений модуля упругости Е, сцепления С и угла внутреннего трения φ грунтов, которые нормированы в зависимости от расчетного значения относительной влажности грунта в пределах 0,5…0,95 от $W_т$ ($W_т$ - предел текучести грунта, %) (таблица 1).

Наличие расчетных значений характеристик грунтов в нормативном документе привело к тому, что практически все проектировщики при расчете конструкций дорожных одежд на прочность пользуются только ими, т.е. не приводятся испытания с целью определения механических характеристик грунта.

Таблица 1. Характеристики грунта

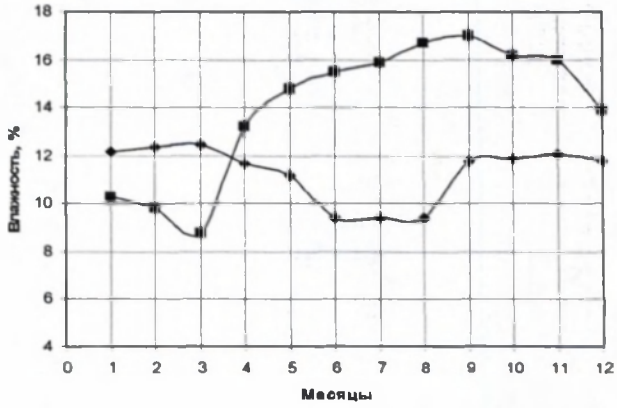
Грунт	Характеристика	Пределы изменения
Супесь песчанистая	E, МПа	70 … 40
	φ, град.	37 … 33
	C, МПа	0,015 … 0,007
Песок пылеватый	E, МПа	96 … 43
	φ, град.	38 … 31
	C, МПа	0,026 … 0,008
Глина, суглинок, супеси (кроме песчанистой)	E, МПа	108 … 23
	φ, град.	32 … 9
	C, МПа	0,045 … 0,004

3 ВЛАЖНОСТЬ ГРУНТОВОГО ОСНОВАНИЯ

Известно, что влажность грунтового основания автомобильной дороги не остается постоянной в течение года (Золотарь и др. 1971). Изменение влажности грунта носит сезонный характер и тесно связано с температурным режимом дорожной конструкции. Для наглядности на рисунке 1 показаны графики изменения средней влажности грунтового основания автомобильной дороги «Усть-Каменогорск - Самарское», км 17 (Восточно-Казахстанская область) в 2003 году и автомобильной дороги «Астана - Бурабай», км 76+30 (Акмолинская область) в 2010 году. При этом в зимний период для автомобильной дороги «Усть-Каменогорск - Самарское» показано содержание влаги в грунтовом основании, включающей как замерзшую, так и незамерзшую воду. А для автомобильной дороги «Астана - Бурабай» влажность грунтового основания в зимний период представлена только незамерзшей водой.

Конструкция дорожной одежды на автомобильной дороге «Усть-Каменогорск - Самарское» состоит из двух слоев асфальтобетона суммарной толщиной 10 см и слоев из природных гравийных и песчаных материалов общей толщиной 54 см. Грунтовое основание сложено из суглинка. Грунтовые воды залегают глубоко (ниже 3,5 м от поверхности дорожного покрытия).

Видно, что на влажность грунтового основания в указанных условиях некоторое влияние оказывают весеннее оттаивание и летнее высыхание. При этом максимальная влажность имеет место в марте (12,5 %), а минимальная - в июне-августе (9,5 %). В течение всего остального периода влажность грунтового основания остается постоянной (около 12 %).



■ - Астана-Бурабай, км 76+30, 2010 г.
♦ - Усть-Каменогорск-Самарское, км 17, 2003 г.

Рисунок 1. Изменение средней влажности грунтового основания автомобильных дорог

Конструкция дорожной одежды на автомобильной дороге «Астана - Бурабай» включает 2 слоя из щебеночно-мастичного (6 см) и пористого (9 см) асфальтобетонов, черный щебень (12 см), щебеночно-песчаную смесь, укрепленную цементом 7 % (18 см), слои из щебеночно-оптимальной смеси (15 см) и песка дробления (20 см). Общая толщина конструкции 80 см. Грунтовое основание сложено из суглинка тяжелого песчанистого (влажность на границе раскатывания W_p = 18,7 %, на границе текучести $W_т$ = 34,8). Грунтовые воды залегают глубоко (ниже 3,0 м от поверхности дорожного покрытия).

Как видно, влажностный режим грунтового основания на автомобильной дороге «Астана-Бурабай» существенно отличается от такового на автомобильной дороге «Усть-Каменогорск - Самарское». Здесь количество незамерзшей влаги в период январь - март составляет 9-11 %. С наступлением потепления количество жидкой влаги увеличивается. В период полного оттаивания грунтового основания в апреле её средняя влажность составляет 14 %. Следует заметить, что средняя влажность основания повышается с дальнейшим течением времени и максимальная влажность, равная 17 %, отмечена в сентябре, что объясняется влиянием атмосферных осадков в виде дождя.

На основе сказанного выше можно сделать вывод о том, что влажность грунтового основания автомобильных дорог и её фазовый состав не остаются постоянными в течение годового цикла. Следовательно, механические (деформационные и прочностные) показатели

грунта основания также изменяются во времени. Так как автомобильные дороги работают круглогодично в течение проектного срока службы, необходимо учитывать закономерности изменения механических показателей грунтового основания при их проектировании.

Согласно нормам проектирования нежестких дорожных одежд (СН РК, 2007), конструкции дорожных одежд рассчитываются на воздействие суммарного количества прохода расчетных автомобилей за весь срок службы дорожной одежды. Но, вопреки реальным условиям, принято, что все механические воздействия осуществляются в течение так называемого расчетного периода, за которого принимается короткий период наибольшего ослабления грунтового основания в весенний период в момент и после его оттаивания. Это нормативное положение исключает возможность рассмотрения особенностей работы дорожных конструкций в другие периоды в годовом цикле. В настоящее время по причине отсутствия надежных данных о поведении грунтового основания в зимний период, этот сложный и важный период в работе дорожных конструкций открыто игнорируется!

Далее попытаемся показать важность учета сезонного изменения влажности, следовательно, и механических показателей грунтового основания при расчете напряженно-деформированного состояния дорожных одежд.

4 НАПРЯЖЕННО-ДЕФОРМИРОВАННОЕ СОСТОЯНИЕ ДОРОЖНОЙ ОДЕЖДЫ

Для рассмотрения принята инструкция дорожной одежды первой автомобильной магистрали в Казахстане «Астана - Бурабай». Выбрано шесть характерных временных моментов, в которые определены показатели напряженно деформированного состояния дорожной одежды (прогиб поверхности асфальтобетонного покрытия, растягивающее напряжение и деформация растяжения в нижнем асфальтобетонном слое и вертикальная деформация поверхности грунтового основания). Схема дорожной конструкции и анализируемые показатели напряженно-деформированного состояния показаны на рисунке 2.

Расчетные значения модуля упругости грунтового основания автомобильной дороги назначены с учетом фактического изменения его влажности в годовом цикле и средней температуры, которые определены путем

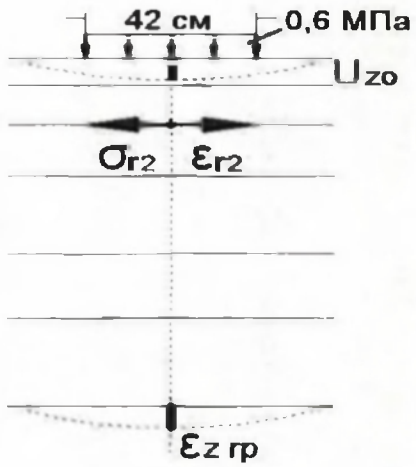


Рисунок 2. Схема дорожной конструкции

закладки специальных датчиков влажности и температуры в автомобильную дорогу «Астана - Бурабай» в 2010 году и периодического мониторинга водно-теплового режима. Значения модуля упругости грунта основания при положительных температурах назначены по нормативному документу (СН РК, 2007), а при отрицательных температурах - по данным проф. Н.А. Цытовича с учетом содержашейся незамерзшей воды (Цытович, 1973) (таблица 2). По причине отсутствия надежных данных, значение коэффициента Пуассона грунта основания принято постоянным и равным 0,35.

Таблица 2. Расчетные значения модуля упругости и коэффициента Пуассона суглинка тяжелого песчанистого

Расчетная дата	Средняя влажность, W, %	Средняя температура, °С	Модуль упругости E, МПа
22.11.2010	14,5	6,6	137
22.01.2011	9,9	-6,3	8300
25.02.2011	8,9	-5,9	7800
14.04.2011	13,2	1,3	151
14.06.2011	15,5	12,5	126
14.09.2011	17,0	18,0	112

Известно, что механические свойства асфальтобетонов сильно зависят от температуры. Расчетные значения модуля упругости асфальтобетонов при максимальных и минимальных суточных температурах вычислены с помощью корреляционной модели М. Витчака (ARA, 2004; Телтаев, 2010 а). Расчетные значения коэффициента Пуассона асфальтобетонов также определены по корреляционной формуле Руководства (ARA, 2004) в зависимости от величины модуля упругости. Вычисленные значения модуля упругости и коэффициента Пуассона

асфальтобетонов приведены в таблицах 3 и 4, в которых в числителе даны значения указанных показателей при максимальных, а в знаменателе - при минимальных температурах. Принятые в расчетах значения модуля упругости и коэффициента Пуассона материалов других слоев дорожной одежды представлены в таблице 5.

Таблица 3. Расчетные значения модуля упругости и коэффициента Пуассона плотного асфальтобетона

Расчетная дата	Температура, °С	Модуль упругости Е, МПа	Коэффициент Пуассона
22.11.2010	-2,6	13590	0,15
	-7,0	17100	0,15
22.01.2011	-17,0	25150	0,15
	-23,0	29130	0,15
25.02.2011	-11,2	20570	0,15
	-17,3	25370	0,15
14.04.2011	25,8	1680	0,38
	9,2	6240	0,20
14.06.2011	31,4	1090	0,41
	14,9	4030	0,27
14.09.2011	28,0	1410	0,40
	13,7	4430	0,26

Напряженно-деформированное состояние рассматриваемой дорожной конструкции под действием нагрузки на ось Q = 13 т (D = 42 см, q = 0,6 МПа) вычислено с помощью решения осесимметричной задачи теории упругости для слоистой среды (Приварников, 1973; Телтаев, 2010 б).

Результаты вычисления представлены на рисунках 3-6.

В результате анализа приведенных выше зависимостей установлено, что:

1. Показатели напряженно-деформированного состояния (НДС) дорожной конструкции не остается постоянным в течение года.

2. Прогиб дорожного покрытия, деформация растяжения в нижнем асфальтобетонном слое и вертикальная деформация на поверхности грунтового основания имеют качественно одинаковый характер изменения в годовом цикле. Так, наименьшие их значения отмечены в зимние месяцы (январь, февраль), когда грунтовое основание находится в наиболее замерзшем состоянии и асфальтобетонные слои также имеют наибольшую жесткость из-за низких температур. С наступлением потепления значения указанных показателей НДС увеличиваются. Наибольшие значения прогиба покрытия и вертикальной деформации грунтового основания имеют место в июне месяце, т.е. в момент времени, когда

Таблица 4. Расчетные значения модуля упругости и коэффициента Пуассона пористого асфальтобетона

Расчетная дата	Температура, °С	Модуль упругости Е, МПа	Коэффициент Пуассона
22.11.2010	-5,3	14510	0,15
	-10,6	18570	0,15
22.01.2011	-16,0	22590	0,15
	-18,5	24300	0,15
25.02.2011	-11,0	18880	0,15
	-18,0	23970	0,15
14.04.2011	23,2	1890	0,37
	11,2	4930	0,24
14.06.2011	35,4	730	0,42
	20,0	2450	0,35
14.09.2011	25,7	1550	0,39
	16,7	3200	0,31

Таблица 5. Расчетные значения модуля упругости и коэффициента Пуассона материалов слоев дорожной одежды

Материал	Модуль упругости Е, МПа	Коэффициент Пуассона
Черный щебень	600	0,25
Щебеночно-песчаная смесь, укрепленная цементом 7 %	500	0,25
Щебеночно-оптимальная смесь	230	0,30
Песок дробления	120	0,30

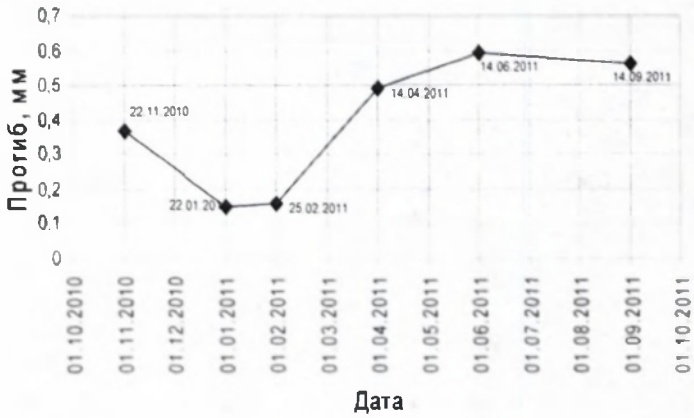


Рисунок 3. Прогиб асфальтобетонного покрытия

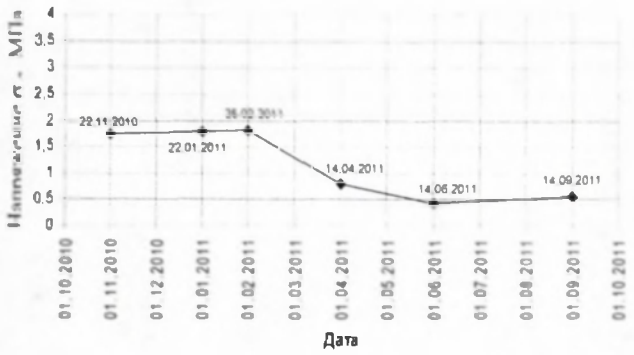


Рисунок 4. Растягивающее напряжение в нижнем асфальтобетонном слое

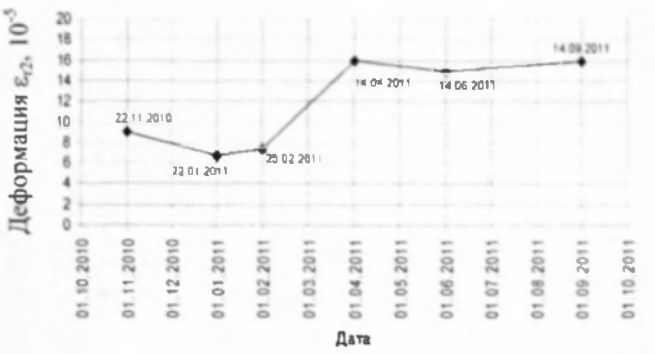


Рисунок 5. Деформация растяжения в нижнем асфальтобетонном слое

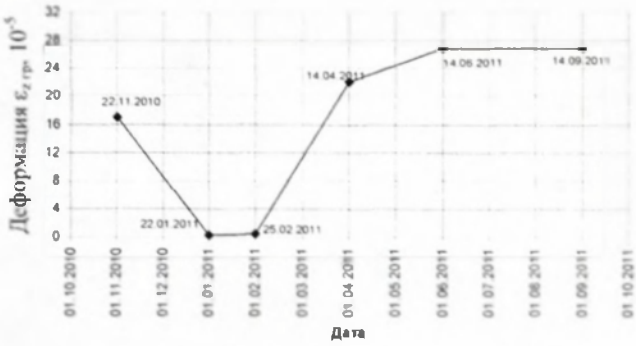


Рисунок 6. Вертикальная деформация на поверхности грунтового основания

асфальтобетонные слои дорожной одежды имеют наименьшую жесткость из-за высоких температур. При этом установлено, что в летний период прогиб дорожного покрытия и вертикальная деформация грунтового основания увеличиваются 3,9 и 7,5 раза соответственно в сравнении с зимним периодом. Наибольшая величина деформации растяжения в нижнем асфальтобетонном слое имеет место в течение длительного периода с апреля по сентябрь, которая больше 2,4 раза, чем в зимние месяцы.

Осенью указанные показатели НДС имеют промежуточные значения, несколько большее, чем зимой.

3. Изменение растягивающего напряжения в нижнем асфальтобетонном слое качественно отличается от рассмотренных выше показателей НДС. Оно в течение всего осенне-зимнего периода сохраняет своё наибольшее значение. С оттаиванием грунтового основания и уменьшением жесткости асфальтобетонных слоев величина растягивающего напряжения уменьшается в 4,3 раза и наименьшее его значение остается практически постоянным в течение всего летне-осеннего периода.

ЗАКЛЮЧЕНИЕ

Полученные в настоящей работе результаты позволяют сделать следующие выводы:

1. Влажность грунтового основания автомобильных дорог и её фазовый состав существенно изменяется в годовом цикле.

2. Результаты расчетов показали, что концепция расчетного периода, принятая в действующих дорожных нормах, является причиной необоснованного игнорирования особенностей работы дорожных конструкций и их грунтового основания в летний, осенний и зимний периоды года.

3. Показатели напряженно-деформированного состояния дорожных конструкций в их характерных точках при учете величины и фазового состава влаги в грунтовом основании и температуры асфальтобетонных слоев существенно и качественно неоднозначно изменяются в течение года.

ЛИТЕРАТУРА

ARA, Inc. ERES Consultants Division. (2004). Guide for Mechanistic-Empirical Design for New and Rehabilitated Pavement Structures. Final Report. NCHRP Project 1-37A. Transportation Research Board of the National Academies. Washington, D.C.

ВСН 46-83. (1985). Инструкция по проектированию дорожных одежд нежесткого типа. Транспорт. Москва.

Золотарь, И.А., Пузаков, Н.А., Сиденко, В.М. и др. (1971). Водно-тепловой режим земляного полотна и дорожных одежд. Транспорт. Москва.

Приварников, А.К. (1973). «Пространственные деформации многослойного основания». *Устойчивость и*

прочность элементов конструкций. Днепропетровск, 27-45.

СН РК 3.03-19-2006. (2007). Проектирование дорожных одежд нежесткого типа, Астана.

Телтаев, Б.Б. (2010 а). «Анализ расчетных значений модуля упругости асфальтобетонов». *Дорожная техника*. 130-137.

Телтаев, Б.Б. (2010 б). «Слоистое упругое полупространство при действии равномерно распределенной по площади круга вертикальной статической нагрузки». *Тр. Межд. науч.-практ. конф. «Механика и строительство транспортных сооружений»*, Алматы, 106-110.

Цытович, Н.А. (1973). Механика мерзлых грунтов, Высшая школа, Москва.

Особенность проектирования архитектурных памятников в условиях подработки территории Карагандинского угольного бассейна

Базаров Б.А. Калданова Б.О.
Казахстан. Карагандинский государственный индустриальный университет

Архитектурные памятники города Караганды, как часть материальной культуры дают обширную информацию тем, кто неравнодушен к истории нашего необычного края.

Так как одним из основных направлений экономического и социального развития Казахстана на ближайший период является дальнейший рост добычи угля в стране, одним из резервов, которого является более полное извлечение его под застроенными территориями. Город Караганда, например в существующих границах, за небольшим исключением, целиком расположен на залежах угля с запасами свыше 1,5 млрд. тонн, что более чем 1,2 раза превышает добычу угля за время существования угольного бассейна.

Поэтому строительство на подрабатываемых территориях, в частности архитектурно-жилищное, является в настоящее время предметом значительных теоретических исследований и проектных проработок ряда специализированных научно- исследовательских организаций.

Застройка этих территорий архитектурными памятниками различного функционального назначения представляет собой важную проблему, основа которой заключается в создании специальных строительных мер защиты, обеспечивающих долговечную и надежную эксплуатацию.

На кафедре «СиТ» КГИУ ведется разработка специальных фундаментных конструкции, обеспечивающих безопасность эксплуатации архитектурных памятников и сооружений при горнотехнических разработках.

Модельные исследования работы конических фундаментов с разными углами врезания

Модели фундаментов конической формы изготавливались из алюминиевого сплава и представляли собой коническое образование, угол врезаемой поверхности которых находился в диапазоне 70°, 80°, 90° (рис 1.1; 1.2).

Выбор различного угла врезания обосновывал определение оптимального угла врезания в подрабатываемое грунтовое основание, в результате неравномерного оседания цокольной части здания в грунтовый массив по гибкой схеме [192, 193, 194, 195, 196, 197, 198, 199, 200, 201, 202].

Диаметры подушек конических фундаментов, использованных в эксперименте равнялись:
d= 80 мм при α= 90, h= 40 мм;
d= 78 мм при α= 80, h= 46 мм;
d= 74 мм при α= 70, h= 53 мм.

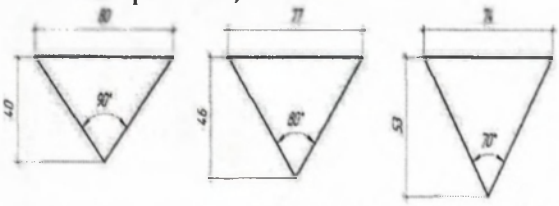


Рисунок 1.1 – Геометрические размеры модельных конических фундаментов с разными углами врезания

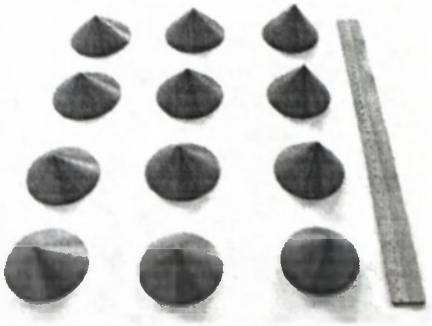


Рисунок 1.2 – Модели конических фундаментов с углом врезания 90^0, 80^0, 70^0

Линейный масштаб моделей и натурных фундаментов определялся соотношениями прочностных свойств (сцепления) суглинка, эквивалентного материала и равен 1:40.

Для сравнения механизма работы конического фундамента и традиционного столбчатого фундамента были использованы для экспериментов штампы идентичных диаметров с коническими фундаментами на контакте с грунтовой толщью (рисунок 1.3).

1-коническая часть, S_1-площадь конического фундамента на контакте с грунтовым основанием; α-врезаемая часть фундамента, угол которых составляет 90^0; 80^0; 70^0; h-глубина погружения, равная соответственно 30мм, 46мм, 53мм

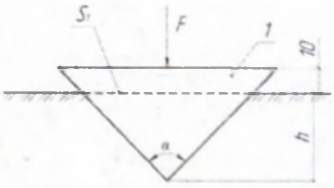


Рисунок 1.3 – Конструкция испытуемой модели фундамента перед испытанием

Эквивалентный материал укладывался в объемный стенд слоями по 5 см и уплотнялся катком (10 полных циклов укатки). В процессе подготовки основания контролировалась плотность материала по величине удельного веса.

Осадки штампов и конических фундаментов измерялись прогибомерами Аистова типа 6ПА0, перемещения грунта возле моделей фундаментов фиксировались индикаторами часового типа. Нагрузка передавалась статически ступенями и выдерживалась до условной стабилизации осадки, за которую принимали осадку не менее 0,01 мм и за последние 15 мин наблюдений (рисунки 1.4; 1.5).

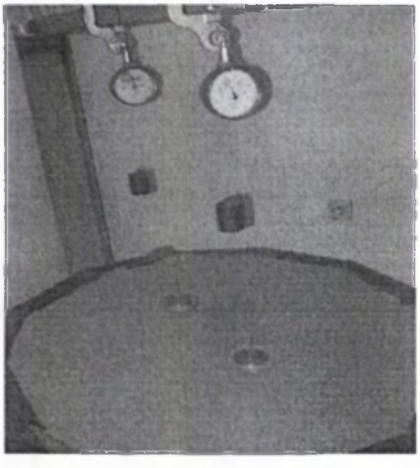


Рисунок 1.4 – Фрагмент испытаний на радиальном стенде



Рисунок 1.5 – Фрагмент испытаний на объемном стенде

Горизонтальные деформации основания в процессе подработки определялись микрометром путем измерения расстояния между марками, расположенными на поверхности материала через 5 см друг от друга. В соответствии с принятой программой модельных исследований были проведены следующие испытания:

а) нагружение моделей фундаментов на грунтовом основании без влияния подработки;

б) нагружение конических фундаментов и штампов на грунтовом основании, предварительно деформированном в одном горизонтальном направлении до величины $\varepsilon = (3;6;9;12)*10^{-3}$.

При этом в сериях а) и б) предусмотрено начало нагружения моделей конических фундаментов на грунтовом основании с величины врезания, которая равна 0,75R; где радиус фундаментной подушки (оставшаяся высота конического фундамента находится на дневной поверхности.

Надо особо отметить, что при этом диаметр на контакте с грунтом у конического фундамента и штампа (имитирующего столбчатый фундамент) равны между собой.

Сравнительные модельные эксперименты были проведены с целью получения фундаментов для определения несущей способности и податливости грунтового основания.

При рассмотрении графика "нагрузка-осадка" (рисунок 1.6, кривые б, в) врезание конического фундамента при горизонтальных деформациях растяжения земной поверхности происходит более интенсивно и при этом несущая способность также незначительно уменьшается. График "нагрузка-осадка" (рисунок 1.6, кривая а) характеризуется более медленным врезанием в грунтовый массив. Различие разных углов врезания компенсируют осадку здания в различных его частях. В краевых частях здания берется более повышенный угол врезания, а к центру – уменьшенный угол врезания. Сочетание в комплексе различных углов врезания (рисунок 1.6, кривые а, б, в), характеризует наиболее благоприятную работу конических фундаментов на подрабатываемом основании, т.е. обеспечивается плавное и равномерное врезание с достаточным уменьшением несущей способности деформируемого основания.

Модельные исследования показали, что несущая способность конических фундаментов увеличивается с увеличением угла врезания и

диаметра подушки (рисунок 1.3). При этом наиболее оптимальной глубиной "предварительного" внедрения конического фундамента является глубина, равная 0,75 радиуса подушки (рисунок 1.3). Исследования показали, что при таком начальном эксплуатационном нагружении фундамента четко выявляется характер врезания конструкции в толщу грунта, при котором несущая способность возрастает прямопропорционально врезке конических фундаментов (рисунки 1.7; 1.8; 1.9).

Кроме того, экспериментальные исследования показали, что несущая способность и осадка моделей конического и столбчатого фундаментов одинакова в упругой стадии деформирования (рисунок 1.9).

а – конического фундамента, угол врезания которго 90^0
б - конического фундамента, угол врезания которго 80^0
в - конического фундамента, угол врезания которго 70^0
г – столбчатого фундамента диаметром 60мм
α – угол врезания
– – – – – – кривая, полученная МКЭ при $\xi = 0$

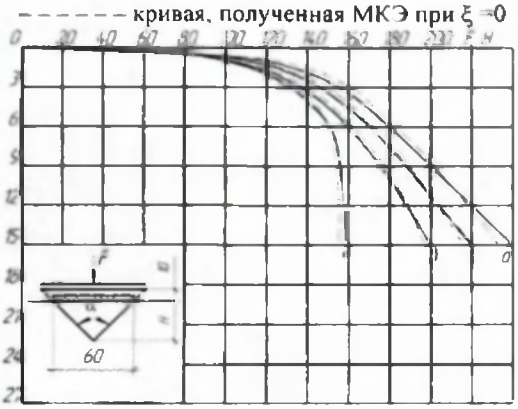


Рисунок 1.6 – графики «нагрузка - осадка» испытуемых моделей фундаментов

Однако при дальнейшем увеличении величины нагружения моделей фундаментов врезаемость конического фундамента уменьшается из-за увеличения контакта с грунтовой толщью, что не наблюдается у столбчатого фундамента (рисунок 1.6).

S, мм

а – при горизонтальных деформациях растяжения $\xi = 0$
б – при горизонтальных деформациях растяжения $\xi = 3*10^{-3}$
в – при горизонтальных деформациях растяжения $\xi = 6*10^{-3}$
г – при горизонтальных деформациях растяжения $\xi = 9*10^{-3}$
д – при горизонтальных деформациях растяжения $\xi = 12*10^{-3}$

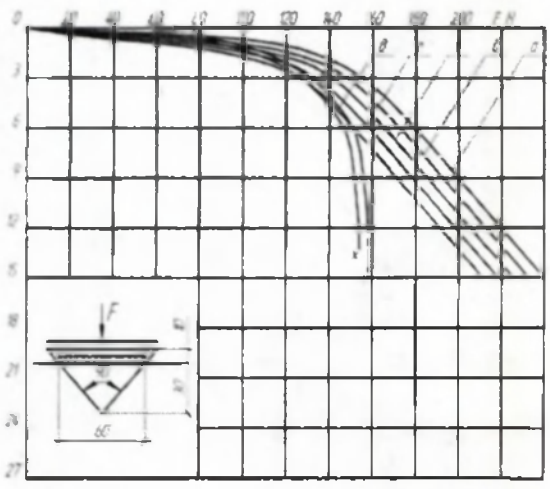


Рисунок 1.7 - графики «нагрузка - осадка» конических фундаментов с углами врезания 70^0

S, мм

а – при горизонтальных деформациях растяжения $\xi = 0$
б – при горизонтальных деформациях растяжения $\xi = 3*10^{-3}$
в – при горизонтальных деформациях растяжения $\xi = 6*10^{-3}$
г – при горизонтальных деформациях растяжения $\xi = 9*10^{-3}$
д – при горизонтальных деформациях растяжения $\xi = 12*10^{-3}$

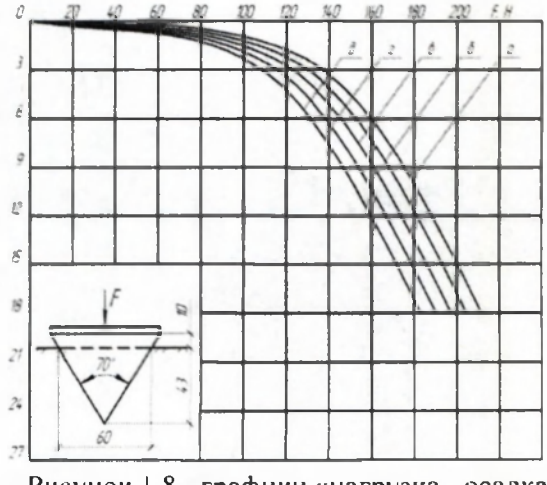


Рисунок 1.8 - графики «нагрузка - осадка» конических фундаментов с углами врезания 80^0

S,мм

а,е – при горизонтальных деформациях растяжения $\xi = 0$ для конического и столбчатого соответственно
б, ж – при горизонтальных деформациях растяжения $\xi = 3*10^{-3}$, для конического и столбчатого соответственно
в – при горизонтальных деформациях растяжения $\xi = 6*10^{-3}$
г – при горизонтальных деформациях растяжения $\xi = 9*10^{-3}$
д – при горизонтальных деформациях растяжения $\xi = 12*10^{-3}$

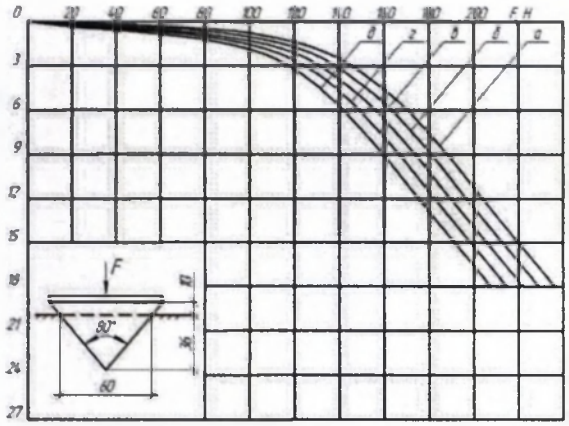


Рисунок 1.9 - графики «нагрузка - осадка» конических фундаментов с углами врезания 90^0

Такую сравнительную картину работы конических и столбчатых фундаментов можно наблюдать и на подрабатываемых основаниях с идентичным преимуществом конических фундаментов (рисунок 1.9). Также необходимо отметить, что предельная несущая способность конических фундаментов при данном принципе эксплуатации практически не достигается, так как по мере врезания фундамента увеличивается его несущая способность. Это объясняется тем, что по мере врезания фундамента в грунтовую толщу, увеличивается поверхностная площадь контакта с грунтом с одновременным уплотнением окружающего грунтового массива (рисунки 1.7; 1.8; 1.9).

Следует зафиксировать и обратную картину: увеличение несущей способности сопровождается равномерной врезкой фундамента в грунт.

Это обстоятельство благоприятно отражается на взаимодействии здания с подрабатываемой грунтовой толщей. Врезание конических фундаментов снижает нагрузки на надземные конструкции сооружений. Указанное обстоятельство необходимо учитывать при строительстве зданий на подрабатываемых территориях [40, 43, 44, 45, 138].

Эмпирическое выражение для определения осадок конических фундаментов, полученное в лабораторных условиях подработки, можно представить следующим образом:

$$S_u = S_0(1+D^*\varepsilon), \qquad (1.0)$$

где S_0 - осадка конического фундамента до подработки;

S_u - осадка конического фундамента после подработки;

D - эмпирический коэффициент:

- для конических фундаментов с разными углами врезания, равный 83,9;

ε - горизонтальная деформация растяжения, $0 < \varepsilon < 12^*10^{-3}$.

Формула (1.0) подтверждает структуру функционального выражения, найденного в результате расчета МКЭ (расхождение составляет порядка 7%).

ВЫВОДЫ

На основании проведенных исследований можно сделать следующие выводы:

1. Модельные испытания фундаментов с конической сердцевиной показали их радикальное преимущество по сравнению с традиционными формами фундаментостроения в условиях подрабатываемых территорий, которое объясняется совершенно принципиально новым механизмом их взаимодействия с грунтовым массивом.

2. В ходе экспериментов установлено, что предельная несущая способность практически у фундаментов конической формы не достигается, так как по мере вертикального врезания фундамента в грунтовую толщу увеличивается поверхностная площадь контакта с грунтовым массивом.

3. Наличие деформационного шва качения практически полностью ликвидирует влияние горизонтальных усилий на верхние конструкции зданий, возникающие при подработке.

Protection of the architecture under reconstruction and restoration of buildings and structures

Chekaeva Rakima Usmanovna, Chekaev Farid Mnirovich, Chekaev Mnir Gismetovich, Urtambayev Talgat Mazhitovich
ENU named after L.N. Gumilyov Astana, Kazakhstan

Reconstruction, restoration and protection of architectural monuments - the process is very complicated. The basis of it - a thorough and detailed study of the natural remains of ancient forms and constructions.

First of all, it is necessary to determine if any construction of the monument, its decorative elements in a dangerous condition. In this case, the work should be started with the elimination of accidents by installing temporary fixtures, fencing of dangerous places, and in some cases - temporary removal of damaged parts.

The next stage of work should be the implementation of major engineering works to strengthen the construction of the monument, designed for long term and carried out in accordance with a specially designed project. Only after being assured the stability of the monument to the constructive, it should actually go to its restoration.

Before starting work it is necessary that the manufacturer works with a representative of the project group workshop to get acquainted with the condition of the object and its surrounding area. Special attention should be paid to condition of building construction, the state of lighthouses, set in the ground deformation, and verified the absence of new strains that may emerge from the time of drafting. It also should be weighed carefully and justified the choice of building materials and above all the solutions.

The best way to prolong the life of the extant monuments - is to recreate in the restoration of old masonry mortar or plaster monument based on the analysis of ancient samples. But such a solution is now ready for the restorationof masonry will never get the same quality. But sometimes it fails, if the master a good command of their work. For example, in the village Deggaron Bukhara region, we surveyed the owner of one house, he made the restoration of mihmanhony - guest rooms, dahliza - hallway and bedrooms. Interior walls mihmanhony been fully implemented in ganchfloral ornament, doors, window bars were carved, wooden walnut. Cornice interiorand the western wall of the guest room nishoy was made in the form of stalactites - mukarnas. North-west corner of the basement guest suffered from age or poor quality construction and the walls of the house cracks. The house is completelydestroyed, and wanted to build on this site a new home.

But we persuaded him to a house, especially the guest room, he kept it. A year later, we saw that the owner of the house with her son with the jack very slowly over several days, this lifted the corner of the house and changed the old foundation of a new brick. Then he completely reconstructed solution, as prepared by his fatherand has made the restoration of the interior. Residential building and interiors were the work of his father - Bukhara mouth, he had previously helped him. Therefore, a beautiful monument - mihmanhona preserved [1].

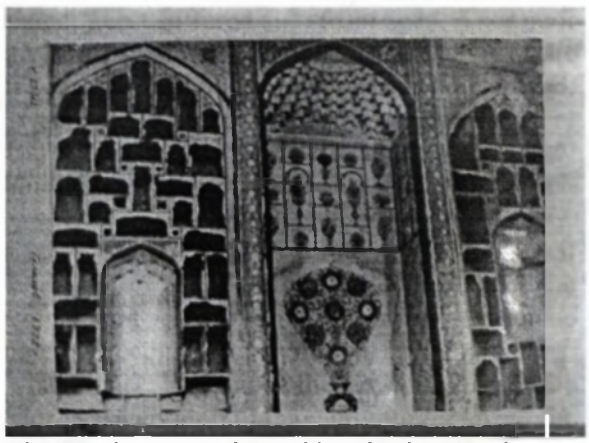


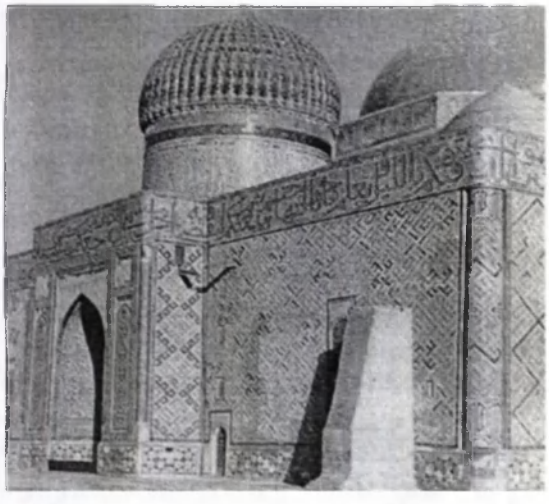
Fig. I In the center place with stalactites – mukarnas

Especially significant is the choice of materials used in the restoration of the surface layers of masonry. Good adhesion of new solutions to the core masonry is provided at a minimal shrinkage of new materials. This is achieved by applying athin, less shrinkage solutions. (Significantly increase the adhesion of solutions withits ancient masonry ¬ newest additions of polymeric materials, such as PVAemulsion, but

it may increase the phenomenon of shrinkage and drop vapor permeability of new solutions).

Durability of structures carried out after the restoration of the monument provides a rational use of materials with a responsible, durability and frost resistance, the technology works properly and carefully the implementation of all parts of input structures. Particular attention should be paid to the serial removal of water and the use of persistent enough to replace the destroyed structures. It should also be paidattention to the establishment of a normal microclimate in the building, the removalof surface water in the shade of the building and excessive vegetation on the normal operation of the facility. Therefore, it is necessary to hold a small heater in the spring in the massive stone unheated buildings in order to avoid moisture condensation drop-down stack of chilled water air.

The most serious damage to the ancient buildings are usually associated with a breach of its static equilibrium. Because of the differential settlement cracks appear in walls and vaults, the distortions of openings and the destruction ofbridges, the slopes of some or all of the walls of the building as a whole, etc. For example, the northern wall of the Mausoleum of Khoja Ahmed Yasawi, which gave a crack in the wall because of the settling of the foundation under the influence of waste water (sewage historic bathhouses were forced to flow along the north wall of the mausoleum because of the neglect of the local population, who paved a new pipeline and destroyed the ancient kubyry wastewater.



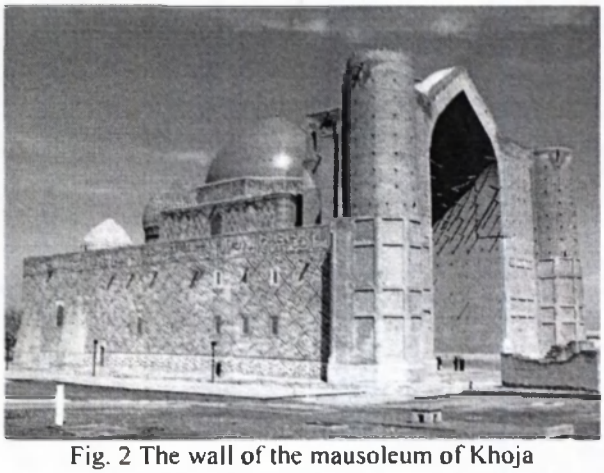


Fig. 2 The wall of the mausoleum of Khoja Ahmed Yasawi

Sometimes this is due to a failure at the time the choice of location for the construction and underreporting of negative properties of soils as a whole or a part thereof. For example, Sultan Baybars mosque complex in Cairo. During his reign, Sultan Baybars devoted much attention to the construction of mosques, mausoleums, irrigation, construction of roads and bridges. The complex of Sultan Baybars covers an area (120x120 m) and is currently located below the road at 1.50 -1.60 cm, since overgrown with cultural layer. Previously, he was not far fromthe Nile River (which is why there are many underground water), now living around the mosque building.

The architecture of the walls of the military-defensive nature, it can be seen on the battlements at the top of the wall, the same form of teeth we find in the architecture of Babylon and the Achaemenid Iran. The walls are built of limestone rectangular in shape, size 25h12h12sm. The courtyard of rectangular shape, the inner perimeter of the previously shady canopies - aivans with two rows of columns, where the congregation sat. On the eastern side of the courtyard is a large mosque with two large rooms with rows of columns three naves. On the north side of the great hall of the mosque destroyed in the south - is preserved [2].



Fig. 3 Mikhrab hall where Sultan Baybars prayed

Currently, there are maintenance and repair work involving the Egyptian and Kazakh architects and engineers and restorers. In 2004-2005, the department of "architect-ture" ENU. ENU has contributed greatly to the reconstruction of Sultan Baybars mosque complex. By tonnage drawings was executed renovation projectand the layout of this remarkable complex, which was transferred to Cairo.

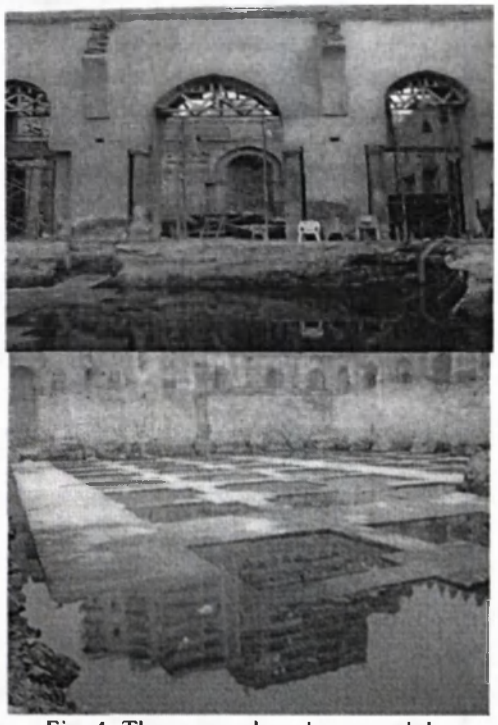


Fig. 4 The room where he prayed the Sultan Baybars. Restoration works

It took the advice of experts, doctors of technical sciences: A. Zhusupbekova, V.Popov, Professor Iwasaki (Japan). On the day of our arrival, the builders were engaged in pumping water from the galleries, it turned out that it was not necessarybecause the foundation will soon crumble. It was here that the groundwater, aspreviously Nile (Egyptian by Kem) flowing near the complex.





Fig. 5 restoration work. Professor Popov V.N. and doctoral Zhanara

Egyptian restorers have consulted an architect Chekaevoy R.U. prayer for the central hall, the hall with a mihrab, the restoration of galleries and their decor.

Popov V.N. explains doctoral Zhanara what to do in these cases suggests that the works are not professional. On
the flooded pit produced water pumping, but it is not carried out measures to prevent the admission of groundwater, which can lead to suffoglinnym processes, and subsequently to the uneven precipitation of the building of the mosque.

Sometimes it depends on the design of foundation failure that led to the destruction (calculation on clay, etc.), or inadequate, not meeting the estimated width of the building foundation. The strengthening of masonry foundations, broadening the area of the sole, liner, new foundations have already been sufficiently addressed inthe literature. However, the differential settlement of foundations is often due to deteriorating soil: a decrease in their load-carrying capacity as a result of soaking (subsidence of loess soils), organic decay of the bulk soil, rotting wood piles, leaching of small fractions of sandy soils changing condition of ground waters, or the device near the building of underground workings.



Fig. 6 A group of participants XVII International Geotechnical Conferenc e (ISSACE) in Alexandria, professors A.Zhusupbekov, V. Popov, R.Chekaeva, doctoral students: Zhanara and Serik (Kazakhstan), prof.E.Ivasaki, T. Tanaka, and T.Matsumoto and .Tohata (Japan), a representative of the Embassy Bahtuty-uly and Egyptian restorers in the mosque of Sultan Baybars complex in Cairo (2009)

For example, the Zemsk Hospital (1874) in Astana - located at the intersection of Dzhangildin, 40, and Pushkin (continued Republic Avenue). Previously, it was built on marshland, was built by order of one of the richest people, the Akmolinsk - Kubrin merchant for his nephew - a doctor, educated in Moscow. The hospital was designed for twenty-five seats. The building was 12 years old. Used for the construction of red brick, which is on the bulls brought from Atbasar, Akmola province. In the construction of the facility was used brick, wherein the size of a standard brick (120h250h65, 130h270h70). The structure of mortar masonry was part of the protein, which is an organic astringent. solution is preserved to this day, and is highly durable. Feature of the building are load-bearing walls as thick as one meter and the main facade of a beautiful decorative brickwork. In some places, the foundation has been repeatedly repaired. The thickness of the walls, a solid solution, a beautiful masonry - speak for what the object is suitable for use in subsequent years.

There are advanced methods of strengthening the foundations, the most widespread in recent years, is a chemical grouting base and strengthening the foundations and bases with rhizoid piles, which will be discussed in another article.

REFERENCES.

1.Pardaeva R.U. Folk architecture of Bukhara oasis (Unknown monuments XVI - XIX centuries.) Problems of history, theory and practice of Russian and Soviet architecture: Interuniversity thematic collection of works. L.: LISI, 1978.-p.15-31.

2.Chekaeva R. U. Arhitektura Sultan Baybars mosque complex in Cairo. Journal of ENU, Astana, № 1 (74) 2010. S. 233-238.

Change of properties loessial soil when flooding territories

R.A. Mangushev
Head of Geotechnical Department. Saint-Petersburg State Architectural and Civil Engineering University, Russia

R.A. Usmanov
Geotechnical Department. Saint-Petersburg State Architecture and Civil Engineering University, Russia

ABSTRACT: The results of years of research characteristics flooding and water logging areas in the Republic of Tajikistan, previously folded little moisture loess soils subsidence. Found that the water saturation of the soil contributes to the transition into the category of weak and high compressibility, a significant reduction in their strength and deformation parameters. The studies will improve the effectiveness of design and construction of buildings and structures in seismically active areas.

1 INTRODUCTION

In the Republic of Tajikistan loess soils cover about 70% of the total area of reclaimed areas and mainly distributed in the intermountain plains and low foothills, lie within the valleys of the Syr-Darya, Zarafshan, Vakhsh, Kafirnigan, Surkhandarya and other soils of most areas belong to the quaternary deposits and, if this loess soils are strongly subsidence and loess-like rocks are characterized by high subsiding to slightly subsiding, their thickness varies from 5 to 300 m and the thickness of subsident H_{sl} = 5-30 m, less than 30 m.

Many major cities and towns in the country built in the territories, composed loess soils and, therefore, construction of civil and industrial use, also carried out on them. However, the practice of building more and more often there are cases when the construction site can be represented by weak water-saturated loess soils with thickness of 4-25 m, which can be attributed to the prohibition of construction suitable for agriculture and development of arrays of ground for building previously unsuitable areas - flooded and waterlogged areas as well as the flooding of large areas under the influence of natural and anthropogenic factors.

Problems of intensive logging and extensive transition and local areas in the water-saturated condition in Tajikistan began in the early 70-ies. Tajikistan is an agrarian country and the development of agricultural production, mainly due to irrigated agriculture. A significant increase in the reclaimed areas (especially cotton plantations) required the construction of a large number of waterworks, reservoirs, irrigation systems and canals. As a result of uncontrolled irrigation, a number of other natural and anthropogenic factors, there was flooding and water saturation of loess soils.

2 FEATURES OF CHANGE OF PROPERTIES OF LOESSIAL SOIL WHEN FLOODING

Currently, the processes covered by the flooding in Northern, Central and Southern regions of Tajikistan, where the groundwater level is located at a depth of 0-5 m from the surface, below which lie the various types of water-saturated silty - clayey soils (loam, sandy loam, less often clay), thickness of 3-30 m or more. If in 1980 in the republic of the territories occupied by about 15% of the total area of loess formations, at the present time, the proportion exceeds 30% and a stable tendency to increase. Often the irrigated areas are located either within large cities and towns, or are located in close proximity to them, which contributes to the process of mutual influence and exacerbate the flooding of technological areas.

It should be noted that the conditions of flooding and inundation of loess rocks in the Republic of Tajikistan have their own regional characteristics. The presence of natural and artificial construction of numerous reservoirs and ponds for various purposes have a strong backwater and groundwater, along with natural and man-made factors, contribute to the rise of the groundwater level. Thus, the construction of the Nurek and Baipaza hydroelectric stations with similar reservoirs in the area of several hundred square kilometers, have contributed to the backwater of ground water and the Javan and Dangara valleys and led to flooding and water saturation of loess soils in these areas. In this backwater of groundwater is observed at a distance of several tens or even hundreds of kilometers from the location of the reservoirs.

As a result, flooding is a significant change in the physical and mechanical properties of soils, resulting in the previously solid little moisture loess soil goes into the category of weak and high compressibility. In Fig. 1 shows the graphs of some indicators of loess soils for different regions of the country with flooding and water saturation.

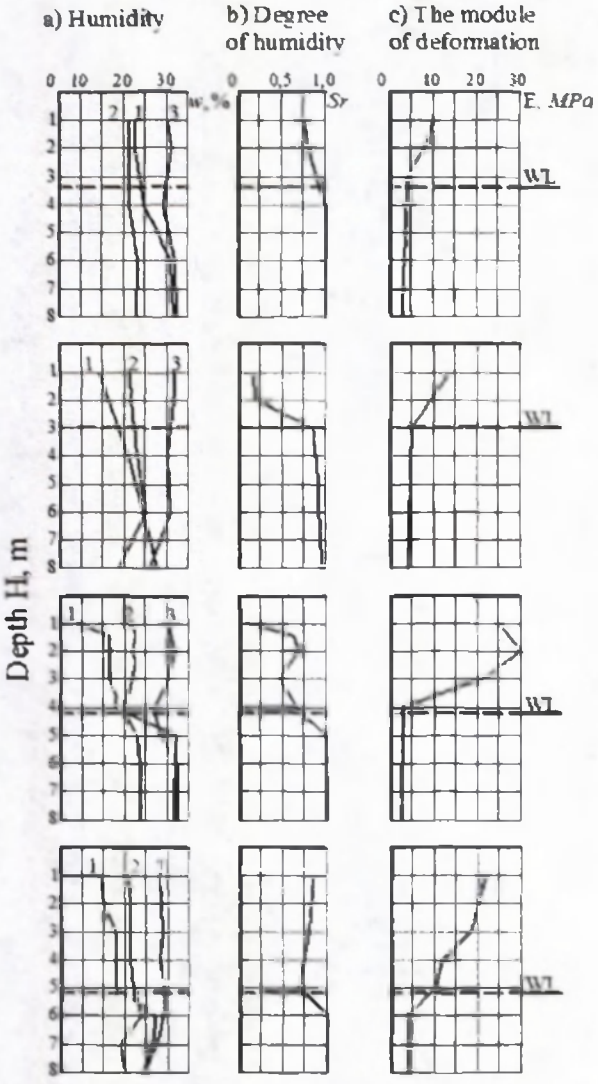


Fig. 1. Changing the humidity (a), degree of humidity (b) and module of deformation (c) of soils:
1- natural moisture content w; 2- border flow w_p; 3- humidity plastic limit w_l

Below the value of the groundwater level natural soil moisture w is close to the value of humidity at the boundary yield w_l, and above - the value of moisture on the plastic limit w_p. The degree of soil moisture above the groundwater level S_r in the range S_r = 0.5-0.8, and below - in conditions of full water saturation S_r = 0.95-1.0. The rise of the groundwater level has a significant influence on the variation of the modulus of deformation of loess soils, with the following groundwater level is a reduction of its value in 5-10 times, and usually is less than E < 5.0 MPa. Above the groundwater level, there is a reduction values of the modulus of deformation of soil in 3-5 times.

In table 1 summarizes the features of changes in subsidence and seismic characteristics in the flooding and water saturation of loess soils in different regions of the country. As a result of lower water saturation properties of ground subsidence groundwater level is completely eliminated. Besides the transition into the category of weak soils saturated leads to an increase in the estimated seismic stations in the construction of a 1-2 points and increase the purchase price of the foundations.

It is of interest especially water saturation thickness of loess soils in time, ie their rate of flooding. The analysis showed that the flooding, the rise of groundwater level to the surface or to a depth of 2-3 m below it, occurs within 6-12 years, with an average speed of 2.0-4.0 m / year.

In general, the analysis of materials engineering and geological surveys in the areas of different regions of the country shows that as a result of flooding and water saturation of the physical and mechanical properties of loess soils a significant change in the direction of their deterioration.

Design, construction and reliable operation of buildings and structures on these soils is very difficult, requires the use of effective methods for the device of the foundations. At the same time the development of artificial methods of preparing the grounds and foundations of the device is closely related to the study of specific changes in the strength and deformation characteristics of loess soil with water saturation. In order to determine the extent of their changes were generalized and systematized materials of numerous studies and research from almost all regions of Tajikistan, which are summarized in table 2.

By comparing test results of the compressibility of weak water-saturated loess soils was set very close convergence between laboratory (compression) and field (stamp) values of the modulus of deformation. The coefficient of the transition from laboratory to field values of the modulus of deformation varies from 0.83 to 1.35, with an average value of its 1.07. This indicates the possibility of using in the calculation of sediment foundation values of compression modulus of deformation of weak water-saturated loess soils.

Table 1. Changing the subsidence and seismic properties of loess soils in the water saturation

Name of territory	Location of the layer from the WL	Degree of humidity S_r	Flow rate I_l	Subsident thickness H_{sl}, m	Subsident S_{sl}, cm	Seismicity of the area, scores	
				to water saturation / after water saturation	to water saturation / after water saturation	to water saturation	after water saturation
1	2	3	4	5	6	7	8
Yavan city	above	0,56-0,78	0 – 0,5	>30	>50	7-8	9
	below	0,85-1,00	0,5-1,00	1,2-2,6	1,6-3,6		
Dangara city	above	0,65-0,74	0 – 0,5	>20	>50	7	8
	below	0,87-0,91	0,6-0,93	0,5-3,0	0,8-2,6		
Kulyab City	above	0,67-0,78	0 – 0,45	4 - 30	>50	8	9
	below	0,80- 1,0	0,5-1,0	2 – 2,7	1,1-3,0		
Vaksh city	above	0,12-0,55	0 – 0,5	10-12	<50	7	8
	below	0,80-0,92	0,8 – 0,9	1,0-4,0	2,8-9,3		
Somoni-yon city	above	0,63-0,74	0 – 0,48	18-20	<50	7-8	8-9
	below	0,82-0,90	0,6 – 1,0	1,2-4,0	1,3-5,3		

Table 2. Changing the physical and mechanical properties of loess soils during flooding subsiding

№	Natural characteristics of soil	Characteristics of soil after the water saturation
	Physical properties	
1	The density of solid soil particles. Located within the ρ_s = 2,6 - 2,70 t/m3	If flooding is unchanged.
2	The density of the soil. Make ρ = 1,3 - 1,65 t/m3, rarely more.	There is a significant increase in the values of density-tee to ρ = 1,9 - 2,1 t/m3, sometimes more.
3	The natural moisture. The values of humidity are within w = 4 - 10%, rarely more.	Is within w = 25 - 33%. Often, its values vary in the 2 - 5 times or more. In the pores of the soil is essential, but it increases the amount of free water.
4	The porosity of the soil. Characterized by high levels of n = 45 - 60%. The values of coeff. porosity are within e = 0,8 - 1,0 times or more.	There is a gradual climb from the bottom subsidence groundwater level upward sequences, soil porosity changes is insignificant (within 5 - 10%) and the thickness of the soil is practically retains its natural porosity.
5	The degree of soil moisture. Usually it is S_r = 0 - 0,5.	There is a significant increase in its value (S_r > 0,8 - 0,95 or more).
6	Flow Rate. Are in solid and semi-solid state (I_l = 0 - 0,25).	Varies considerably and is characterized by a ductile to soft-plastic fluid (I_l = 0,6 - 1,0 or more).
	Mechanical properties	
7	Compressibility. Characterized by low compressibility. Modulus of deformation Grun-comrade is in the range E = 15 - 25 MPa	Compressibility factor is increased by 2 - 5 times, and the modulus of deformation is reduced by 5 - 10 times, and often amounts to E < 5.0 MPa.
8	Resistance to shear. The angle of internal friction is a φ = 25 - 29°, and specific cohesion c = 30 - 55 kPa.	The value of the angle of internal friction is reduced to 30%, and specific adhesion an average of 2 - 5 times.
9	Water permeability of soils.	Characterized by a higher permeability compared with other types of soft ground.
10	Subsidence features. Primers majority belong to the properties of regions of type II with the magnitude of subsidence expected drawdown in natural pressure S_{sl} = 30 - 200 cm thick loess	After watering, the soil lying below the groundwater level completely lose sagging properties, and higher in some cases preserve their (mostly under additional pressure) and transformed into type I to subsidence.
11	Linear deformability (under static loading at $p \leq R_c$).	When loading is observed in all phases of the stress-strain state of the grounds.
12	Calculated sprotivlenie soils. In the natural state of their values are R > 200 kPa.	Soil flooding leads to a significant decrease in the values (according to the results of stamp testing die $R \leq$ 80 - 100 kPa).

3 CONCLUSIONS

1. The processes of flooding and flooding earlier little moisture loess soil subsidence cover almost all the irrigated areas of the country, take on the character patterns and a tendency to increase them. Typically, the irrigated areas are located within the major cities and towns, and therefore, urban development will be implemented through the development of the area represented by weak water-saturated loess soils. In turn, this fact contributes to mutual influence and exacerbate the flooding of the processes of technological areas.

2. In Tajikistan, the process of irrigation areas has its own regional characteristics and main causes of flooding are complex natural and anthropogenic factors, and the man-made factors are crucial, and they account for more than 70% of the total. Intensification of the impact of man-made factors contribute to widespread groundwater back pressure exerted by numerous natural and man-made reservoirs and ponds.

3. The features of the formation, distribution and modification of physical and mechanical properties of loess soil subsidence in different regions of the Republic of Tajikistan as a result of flooding. The basic factors of flooding, the nature and extent of changes in the basic properties of loess soils of construction depending on the location of the surface of the groundwater level. If flooding is observed rise of the groundwater level within 6-10 years at a rate of 2-4 m / year. In more than 60% of cases the groundwater level at depths 2-5 m and its level stabilizes within 2-4 years after the flooding.

4. As a result of flooding often occurs more than 80% water saturation subsiding strata (> 0.8 H_{sl}), which helps eliminate sagging properties of soils below the groundwater level and above - ground, in some cases retain them, basically, with the additional pressures and moving in 1 type of subsidence. In conducting research and designing of artificial methods of preparing the grounds and equipment foundations should take this into account.

5. As a result of raising the groundwater level and the water saturation significantly worse physical and mechanical properties of loess soils, they have become weak and high compressibility. For soils below the groundwater level is a decrease in the modulus of deformation 5-10 times internal friction angle of 25-30% and specific adhesion to a 3-5 times. Soils above the groundwater level, and change their properties: modulus of deformation is reduced in 2-4 times the angle of internal friction at 15-20% and specific cohesion of 1.5-2.5 times. In addition, flooding areas contributes to the calculated seismic construction sites in the 1-2 points, which also leads to an increase in the cost of preparing the grounds and equipment foundations.

Research has established the use of sludge in the calculation of the foundations of compressive deformation modulus of weak water-saturated loess soils.

Numerical analysis of a concrete face rockfill dam

B. Moussai, M. Abdellaoui
USTHB University, Algiers – Algeria

ABSTRACT: The performance of a concrete face rock fill dam depends mainly on the performance of its face concrete slab which provide the watertightness of the dam. The deformation of the dam embankment during construction and operation leads to concrete slab deformation. This deformation may cause major cracks in the concrete slab and as a result, the safety of the dam becomes a serious issue. The present paper deals with the deformation analysis of El – Agrem concrete face rockfill dam during reservoir filling using the finite element method.

1. INTRODUCTION

Owing to their economic advantage compared to other types of embankment dams, the construction of concrete face rock fill dams has known a considerable interest in many parts of the world during the last decades. The speed of construction, steep slopes, stabilizing effect of water load and resistance to seismic loading are some advantages of concrete face rock fill dams among other types of embankment dams. Furthermore, many engineers have argued that the concrete face rock fill dam is inherently safe against potential seismic damage (Sherard and Cooke 1987). This is because earthquake cannot cause pore water pressure build up and strength degradation of the free-draining compacted rockfill.

However, the problems we may encounter with concrete face rock fill dams are the vulnerability of perimetric joints, deformations, cracks and aging of the concrete face slab.

Generally, the deformation of face concrete slab during reservoir filling follows the deformation of dam embankment. This deformation should be compatible with the structural integrity of the concrete slab to minimize cracks and leakage.
The purpose of this study is to analyze the deformation of El – Agrem concrete face rockfill dam during reservoir filling using Plaxis 2010 finite element software.

2. DAM DESCREPTION

The El – Agrem concrete face rockfill dam is located 15km south - east of Jijel city (Algeria). The dam reservoir can store approximately 35 million cubic meters of water and provides drinking water to the surrounding region.

The dam is 64m high and 395m long with a crest width of 10 m. The embankment volume is 1.6×10^6 m^3 and consists of tow zones of granitic rockfill materials as shown in figure 1. Zone E1 comprises the majority of the embankment section with a maximum particle size of 500mm and compacted in 0.8m lifts. Zone E2 is a transition zone consists of smaller-size rock, provided between the concrete face slab and the rockfill embankment.

The rockfill is compacted to a high density in order to minimize deformations and concrete slab cracks and leakage. The upstream and downstream slopes of the dam were established at 1.7H:1V.

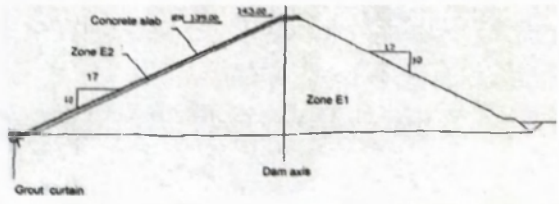


Fig. 1: Typical cross-section of El-Agrem concrete rockfill dam

The concrete slab on the upstream side, provides the watertightness of the dam above the ground together with the perimetric joints and the plinth. The concrete slab has a total area of 31000 m^2 with a variable thickness of 500mm at the foundation level and 350mm at the crest level.

The dam foundation consists of granite gneiss rock on the right bank and of marls on the left bank.

The dam embankment was almost completed in October 1993 (the embankment level reached was 140.5m) after that the construction activities were stopped for economic raisons. Construction activities resumed during the year 1999 and the embankment was raised to its final level 143m. The face slab was concreted during the year 2000, about 7 years after the end of embankment construction.

Reservoir filling was started in 17 February 2001 (about three months after the completion of the face slab in November 2000) and the water level reached 99.21m in 26 January 2002 and stabilized at this level until October 2002. From this date the water level continued to increase and reached the normal pool level of 139m in April 2003.

3. NUMERICAL ANALYSIS

The concrete slab is modelled as linear elastic with Young's modulus equals to 30000 MPa and Poisson ratio equals to 0.2. Rockfill materials are modelled with Mohr Coulomb model. Table 1 lists the parameters of the dam materials used in the numerical analysis.

Table 1: Parameters of the dam materials

Parameter	γ (kN/m³)	c (kPa)	ϕ°	ψ°	ν	E (MPa)
Zone E1	19.5	0	45	15	0.15	50
Zone E2	20	0	42	12	0.15	100

The numerical study was conducted on the maximum cross – section of the dam resting on rock foundation using Plaxis 2010 software. Figure 2 shows the finite element model having 350 elements and 2981 nodes. ψ°

The deformation of the dam foundation is considered negligible; therefore the model sets fixed displacements along the dam base in contact with the rock foundation. Furthermore, the dam is located in a wide valley (crest length / dam height equals to 6.1), thus three dimensional effect is negligible. 45°



Fig. 2 Two dimensional finite element mesh

4. RESULTS

Figure 3 shows the variation of the total displacement with respect to dam height for the concrete slab, the downstream face and along the dam axis at the end of reservoir filling (water level at 139m). This figure indicates that, the maximum displacement of the concrete slab is 0.18 m and takes place at a point about 44% of the dam height. The location of the maximum total displacement is in good agreement with the results obtained by Massiéra et al., 2006. Furthermore, the results obtained for different reservoir water levels show that the location of the maximum total displacement increases with increasing water level (figure 4).

The maximum crest settlement obtained at the end of reservoir filling (water level at 139 m) was 23mm (figure 5).

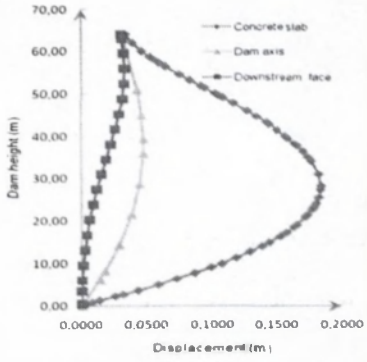


Fig. 3 Total displacement with respect to dam height at the end of reservoir filling

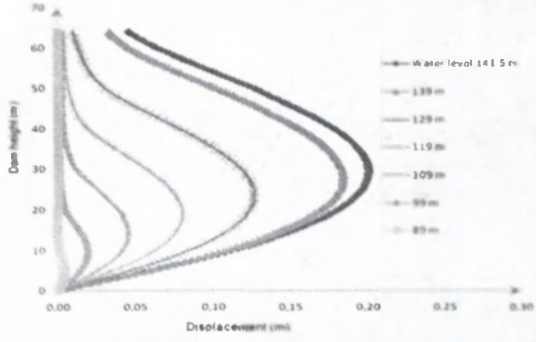


Fig. 4 Total displacement of the concrete slab for different reservoir water levels

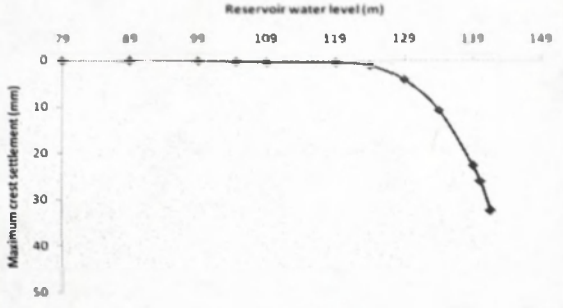


Fig. 5 Maximum crest settlement for different reservoir water levels

5. CONCLUSION

Since the reservoir filling in April 2003, the dam has performed well. The measured flow is less than 250 litre/min. The maximum crest settlement measured in – situ is about 35 mm. This value was obtained during the period from February 2001 which corresponds to the beginning of reservoir filling (that is more than 7 years after embankment construction and 3 months after concrete slab completion) to September 2004 (that is 17 months after the end of the first reservoir filling). The settlement obtained from numerical simulation at the end of reservoir filling (water level at 139m) is about 23mm (figure 4) which is lower than the settlement measured in situ. This may be due to the creep deformation of the rockfill materials which is not taken into account by the current computational model.

In order to obtain more realistic prediction of long term behaviour of a CFR dam, the numerical simulation should take into account the nonlinearity and the creep deformation of the rockfill materials.

REFERENCES

1. Cooke J. 1997. "The concrete face rockfill dam". Proc. 17 USCOLD Lect., San Diego (USA), 117-132.
2. ICOLD 2006 "Concrete Face Rockfill Dams, Concepts for design and construction" Committee on Materials For Fill Dams
3. Massiéra, M., Vautour, J., Coulibaly, Y., Hammamji, Y., Szostak-Chrzanowski, A. 2006. Prévisions des déformations et contraintes dans les barrages en enrochement avec masque amont béton. *Proceedings, The 2006 Annual General Conference of the Canadian Society for Civil Engineering.* Calgary, Alberta, Canada
4. PLAXIS, (2010), *Reference manual*, Web: http://www.plaxis.nl.com.
5. Sherard, J. L., and Cooke, J. B., 1987 "Concrete face rockfill dam: I. Asse to strong seismic excitation" and II. Design *Journal of Geotechnical Engineering*, ASCE, 121(2). 185 – 197

On Seismic Stability of Soil-Stone Structures

Salyamova K.D
Dynamics of Soils and Simulation of Complex Loading, Institute of Mechanics and Seismic Stability of Structures of the Academy of Sciences of the Republic of Uzbekistan, Tashkent, Uzbekistan.

Turdikulov X.X
Dynamics of Soils and Simulation of Complex Loading, Institute of Mechanics and Seismic Stability of Structures of the Academy of Sciences of the Republic of Uzbekistan, Tashkent, Uzbekistan.

ABSTRACT: Dams built of concrete in CIS countries are studied by the method of wave dynamics and in elastic statement. We are presenting here our own version of solution which takes into account wave character of dam motion. Let us consider in Cartesian system of coordinates an earth dam situated on rigid base. Dynamic influence on the dam is carried out through the movement of the base. Mathematical statement of the problem includes differential equations of motion. The equation of state of soil is taken in the form of elastic-plastic model proposed by S.S.Grigorian using generalized conditions of yielding by von Mises-Scheicher . To these equations we add an adequate initial and boundary conditions. The solution of this system is fulfilled with the method of finite differences according to Wilkins' scheme.

Construction, exploitation and projecting of major hydro-structures in seismic regions require continuous improvement of the methods of assessment of their seismic stability. This problem related to ground hydro-technical structures (dams; earth filled slopes, water reservoirs) is still an actual one, because a plenty of them are planned to be built in the nearest future and mostly in seismo-active zones. Design of strength and seismic stability of earth hydro-technical structures particularly the dams, demands a strict requirement, as their damage may lead to catastrophic aftermath.

An improved methods and algorithm of applied programs are given in the paper; they are based on modern numeric methods of solution of dynamic problems for earth hydrotechical structures with account of real geometry and nonlinear characteristics of the material of structure. Discussed problem is solved by the method of finite differences according to the scheme offered by Wilkins [1]. The reliability of the method is substantiated by the solution of test example. As an example the solution of dynamic problem for earth dam of Charvak hydro power plant with height 168 m is given here. Geometric and mechanical characteristics were given by Shear Holding "Hydroproject ".

The statement of the problem. The equations of motion for plane-deformed (bed section of the dam) structure in Cartesian system of coordinates have the following form

$$\rho\frac{dV_x}{dt}=\frac{\partial S_{xx}}{\partial x}+\frac{\partial P}{\partial x}+\frac{\partial \tau_{xy}}{\partial y},$$
$$\rho\frac{dV_y}{dt}=\frac{\partial S_{yy}}{\partial y}+\frac{\partial P}{\partial y}+\frac{\partial \tau_{xy}}{\partial x}-\rho g \qquad (1)$$

here ρ- is the density of soil, P- earth pressure; V_x, V_y -mass velocities, g- gravity; S_{xx}, S_{yy}, S_{zz}- components of the deviator of stresses .

Here complete stresses σ_{xx}, σ_{yy}, σ_{zz}- are relatively calculated from the following relations

$$\sigma_{xx}=S_{xx}-P,\ \sigma_{yy}=S_{yy}-P,\ \sigma_{zz}=S_{zz}-P, \quad (2)$$

here

$$P=P(\theta,\dot{\theta},I_s,\ldots);\ S_{ij}=S_{ij}(\varepsilon_{ij},\dot{\varepsilon}_{ij},I_s\ldots) \quad (3)$$

The equations of state for earth dam (3) are taken in concrete form depending on applied model of soil deformation.

The equation of continuity has the following form:

$$\frac{dP}{dt}=-K(dV/dt)/V, \quad (4)$$

The equations of state of soil in this case are taken in the form of S.S.Grigorian's elastic plastic model [2,3] :

$$dS_{xx}/dt+\lambda S_{xx}=2G(d\varepsilon_{xx}/dt-(dV/dt)/3V),$$
$$dS_{yy}/dt+\lambda S_{yy}=2G(d\varepsilon_{yy}/dt-(dV/dt)/3V), \quad (5)$$
$$dS_{zz}/dt+\lambda S_{zz}=2G(0-(dV/dt)/3V),$$
$$d\tau_{xy}/dt+\lambda\tau_{xy}=2Gd\varepsilon_{xy}/dt,$$

here $V=\rho_0/\rho$ - is a relative volume; ε_{xx}, ε_{yy}, ε_{xy} -components of deviator of deformations; G, K – modulus of shear and volume compression, respectively; λ -functional which is defined by using Mises-Schleihers condition:

$$2J_2 = S_{xx}^2 + S_{yy}^2 + S_{zz}^2 + 2\tau_{xy}^2 \le 2Y(P)/3$$

$$\lambda = (2GW - dJ_2/dt)/(2J_2), \qquad (6)$$

$$W = \Sigma S_{ij}(ds_{ij}/dt - dV/3Vdt) + \tau_{xy}d\varepsilon_{xy}/dt),$$

here $\lambda = 0 \quad J_2 < Y^2(P)/3, \lambda > 0 \quad J_2 = Y^2(P)/3.$

Here Y(P)- is a generalized condition of yielding, depending on pressure:

$$Y(P) = Y_0 + \mu P/(1 + \mu P/(Y_{Pl} - Y_0)), \qquad (7)$$

here Y_0- soil cohesion; μ- coefficient of friction; Y_{PL} -limit value of shear strength. With $Y_0 \to \infty$ in (6) and (7) coefficient λ equals to zero and discussed model transforms into an elastic one.

The connection of the tensor of velocities of deformation with these velocities of the particles is fulfilled by relations

$$\varepsilon_{xx} = \frac{\partial V_x}{\partial x}, \varepsilon_{yy} = \frac{\partial V_y}{\partial y}, \varepsilon_{xy} = (\frac{\partial V_x}{\partial y} + \frac{\partial V_y}{\partial x})/2 \quad (8)$$

The system of differential equations (1),(3) and relations (2), (5)-(8) is a closed one and with initial and boundary conditions it describes stress-strain state of discussed structure under dynamic loads. Initial conditions are taken as zero ones. Boundary conditions: – the crest and the slopes of the dam are considered free from stresses; and on the lower surface (basement) of the dam a seismic load is applied in the form of real velocigram of the earthquake, recorded in earth foundation of the structure by the Institute of Seismology of Uzbek Academy of Sciences together with NIC Hydroproject (Moscow) [4].

Numeric design of Charvak dam. Physical and mechanical characteristics of the material of soil of the dam, modulus of elasticity and Poisson's coefficients are: E=6,21 ГПа, ν=0,3 cores E=3,105 ГПа, ν=0,3; strength parameters of the slopes: Y_0=1 МПа, μ=0,4, $Y_{PL}=20Y_0$ and the core of the dam: Y_0=0,6 МПа, μ=0,4, $Y_{PL}=20Y_0$. On the borders of the core and the slopes of the dam the condition of complete cohesion is taken (the equality of displacements and velocities of the particles of the contact).

When solving the problem of stability of the slopes of earth dam with account of draw-down of waters reservoir the designers take into consideration the location of curve depression (the border between saturated and dry soil) .

According to the requirements of Normative Documents a design of structure (forces of gravitation, hydrostatic pressure of water) was carried out.

The problem of statics on definition of displacements, stresses and strains was studied with account of elastic-plasticity of the kernel of a dam .

With account of inelastic properties (elastic-plasticity) of soil, the distribution of stresses (Fig.1,2) along the dam bears almost symmetrical character and differs from elastic case. The greatest values of horizontal stresses are located on the foot of the center of kernel; vertical stresses – on near-kernel zone with 20-50% decrease

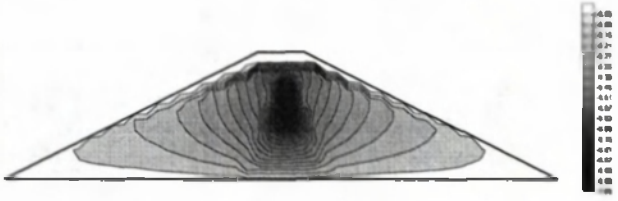


Fig.1. Lines of vertical displacements V(m) under gravitation forces in a dam.

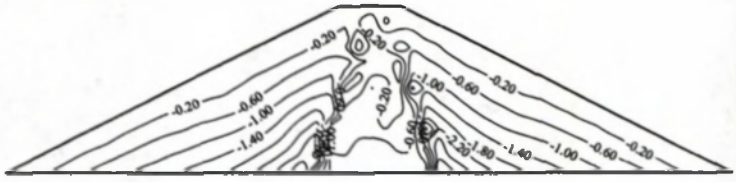
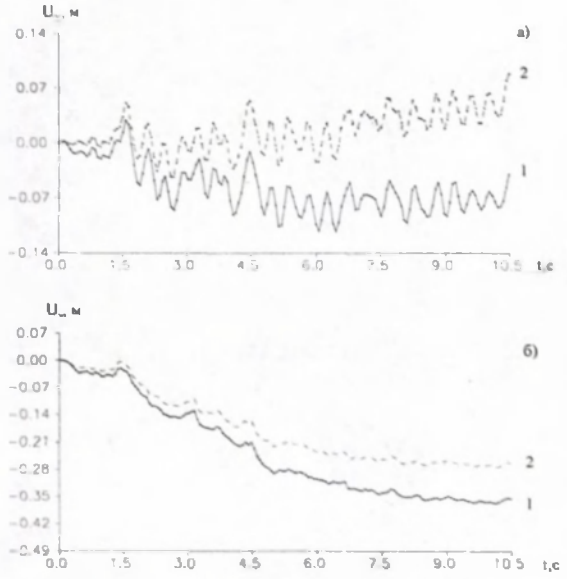


Fig.2. Lines of equal vertical stresses σ_{yy}(MPa) under gravitation forces in a dam.(elastic-plastic case).

An account of inelastic deformation of soil of dam kernel in analysis of results obtained leads to the discovery of sections of unevenness of stresses in a dam; this unevenness may lead to a damage of continuity of anti-filtration elements and transient zones, which provide the strength of a dam.

The density of stone loading $\rho^{к}_{сух}$=1950 kg/m^3 and $\rho^{п}_{сух}$=1710 kg/мм, the core of upper slope located higher than the curve of depression and lower for the zones in water saturated state : $\rho^{к}_{нас}$=2330 kg/m^3 and $\rho^{п}_{нас}$=2110 kg/m^3.The results of design under these conditions are given in (fig.3) (solid line 1-with account of curve depression, broken line -2 without curve depression) .

The change of horizontal displacements in time in near-crest and slope zones of the dam is shown in fig 1. From the beginning of the effect till 1,5 sec. the account of water saturation of soil does not lead to appearance of residual horizontal displacements, and after that approximately two times decrease of the these values is observed.



а) near-crest zone; б) slope zone.

Fig 3. Change of horizontal displacements in time in the dam.

The dependence of horizontal deformations in time in near-crest zone with account of curve depression is given in fig 4. From the beginning of the effect of load till 4,5 sec the account of water saturation does not depend on horizontal deformation, and after that it leads to increase of pre-compacting deformation.

In slope zone, as opposed to near-crest zone, the account of water saturation of soil does not depend on the behavior of the value of residual deformations.

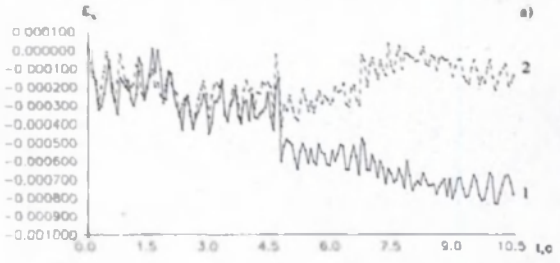


Fig.4 Change of horizontal deformations with time in near-crest zone of the dam.

The account of non-linear characteristics of soil (elastic plastic), asynchrony of seismic effect in dynamic design of earth structures permits to foresee stress-strain state of soil and to reveal the location of the zones of residual displacements, residual deformations which lead to compacting and loosening of soil.

REFERENCES

1.Wilkins M. L. Calculation of elastic-plastic flow // Methods Computat. Phys. – New York-London: Acad. Press, 1964. - V.3.- P. 211-263.

2.Grigorian S.S. On Pricipal Presentations of soil dynamics. // PMM. – 1960. – V.24. – № 6. – P.1057-1072.

3. Grigorian S.S. Some Problems of mathematical theory of deformation and destruction of solid rock. // PMM. 1967. V.31. № 4.-P.643-669.

4. Ivashchenko I.N., Nurtaev B. Modeling of the records of earthquakes for design of dams reliability.// Scientific woks Hydroproject number 150.-M.1988.-P.41-47.

Осадки фундаментов промышленных объектов Карагандинского металлургического комбината

А.В. Филатов

Карагандинский государственный индустриальный университет, г. Темиртау, Казахстан

А.С. Жакулин &. А.А. Жакулина, В. Нефедов

Карагандинский государственный технический университет, г. Караганда, Казахстан

АННОТАЦИЯ: В статье приведены результаты многолетних геодезических наблюдений за деформациями оснований крупных промышленных объектов Карагандинского металлургического комбината. Проводится сравнение фактических осадок сооружений с расчетными и предельно допустимыми по СНиП. Делается вывод о необходимости внесения поправок в общепризнанную формулу расчетов оснований по второй группе предельных состояний.

1 ВВЕДЕНИЕ

В течении более чем 40 лет за осадками крупных промышленных объектов АО «Миттал Стил Темиртау» (ранее Карагандинский металлургический комбинат) ведется геодезическое наблюдение. В период возведения фундаментов доменных печей № 1-4; коксовых батарей № 1-4; дымовых труб высотой 250 м были установлены репера (согласно требованиям проекта), которые вплоть до сегодняшнего дня фиксируют деформации основания сооружения.

Известно, что основная осадка происходит в период возведения сооружения и в течении первых нескольких лет его эксплуатации, причем в глинистых грунтах стабилизация осадки наступает значительно позднее, чем в песчаных грунтах. В связи с этим очень важно производить наблюдение за деформациями основания начиная с момента устройства фундамента, т.е. с самого начала передачи нагрузки на основание.

В центральной части Казахстана преобладают глинистые грунты (глины, суглинки) преимущественно твердой и полутвердой консистенции.

2 ФИЗИКО – МЕХАНИЧЕСКИЕ СВОЙСТВА ГРУНТОВ ОСНОВАНИЯ

Сводная ведомость осредненных физико-механических свойств грунтов крупных промышленных объектов АО «Миттал Стил Темиртау» приведена в табл. 1 по данным инженерно-геологических изысканий, выполняемых АО «КарагандаГИИЗ и К» с 1959 г. по настоящее время.

Таблица 1. Осредненные физико–механические свойства грунтов

Свойства грунта	Ед. изм	Объект					
		Дом. печь № 1-3	Кокс. батар. № 1-3	Дымовая труба			
				ТЭЦ H= 250 м	ТЭЦ H= 100 м	ТЭЦ -2	Аглофабрика
γ_0	кН/м^3	20,0	21,0	21,1	20,6	20,3	20,0
γ_s	кН/м^3	26,8	27,0	27,0	26,9	27,2	27,1
ω	%	12,5	14,2	18	19	17	16
J_l		0,01	0,1	0,03	0,01	0,01	0,05
J_p	%	27	26,0	31	28	30	25
e		0,52	0,76	0,49	0,66	0,52	0,61
φ	град.	21	24	21	22	19	21
c	МПа	0,08	0,06	0,06	0,08	0,06	0,08
E_0	МПа	19,5	14,1	15,0	16,9	17,2	18,0

3 ОСОБЕННОСТИ КОНСТРУКЦИИ ФУНДАМЕНТОВ

Фундаменты доменных печей №1 и №2 монолитные железобетонные, выполнены в виде сплошного массива, размерами в плане 27,0 х 27,0 м. Глубина заложения фундамента составляет 4,0 м. Армирование фундамента произведено сварными сетками из арматуры периодического профиля, класса А - II. В нижней зоне фундамента расположено три горизонтальные сетки с шагом арматуры 200 мм в обоих направлениях. В верхней зоне установлена одна сетка с шагом арматуры 400 мм. Согласно проекту принят бетон марки М200. Расчетная нагрузка на фундамент составляет 300 т/м^2. Бетонирование фундамента производилось в летний период, что соответствует требованиям проекта. Схема фундамента доменных печей приведена на рис. 1

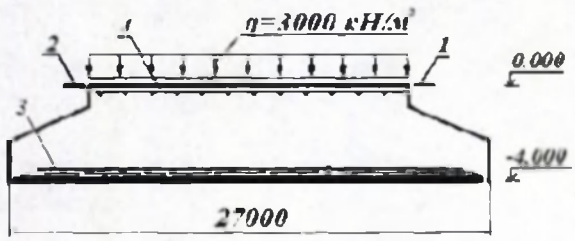


Рис. 1. Фундамент доменной печи. 1 – реперы Р-1, Р-3, 2 - реперы Р-2, Р-4, 3 – нижние арматурные сетки, 4 – верхняя арматурная сетка.

Фундаменты коксовых батарей № 1- 4 имеют коробчатое сечение и размеры в плане 15,0 х 80,0 м. Глубина заложения фундамента составляет 3,5 м. В теле каждого фундамента расположено 4 газохода и 1 вентиляционный желоб. Фундаменты армированы продольной и поперечной арматурой периодического профиля диаметром 20 мм, класса А - II. Расчетная нагрузка на фундамент составила 18,0 т/м^2. Схема фундамента коксовой батареи приведена на рис. 2.

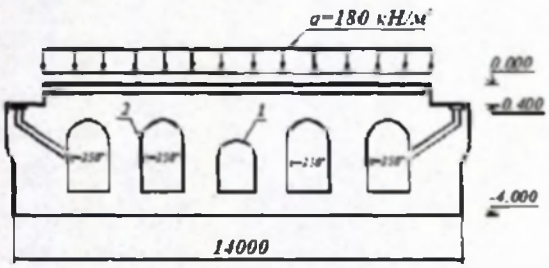


Рис. 2. Фундамент коксовых батарей. 1 – вентиляционный желоб, 2 – газоход.

Железобетонные дымовые трубы высотой 250 м входили в пусковые комплексы тепловых электростанций ТЭЦ-2, аглофабрик № 1 и № 2 АО «Миттал Стил Темиртау». Значительная высота обусловлена требованиями строительных норм «Охраны окружающей среды» и проектами оценки воздействия на окружающую среду (ОВОС).

Фундаменты дымовых труб ТЭЦ высотой 250 м и аглофабрик монолитные железобетонные. Подошва фундамента – круглая, диаметром 40,0 м, высотой 4,0 м. Для фундамента, согласно рабочим чертежам, выполненным проектной организацией РОТАП (г. Ростов-на-Дону), принят бетон марки М300, на сульфатостойком портландцементе. Грунтовых вод по материалам изысканий до глубины 30,0 м обнаружено не было. Показатель армирования фундамента составляет 66,8 кг/м^3. Расчетная нагрузка на основание от дымовых труб составляет примерно 21,1 т/м^2. Все исследуемые трубы расположены друг от друга на расстоянии 0,8 ÷ 1,2 км.

Конструкция фундамента железобетонной дымовой трубы показана на рис. 3.

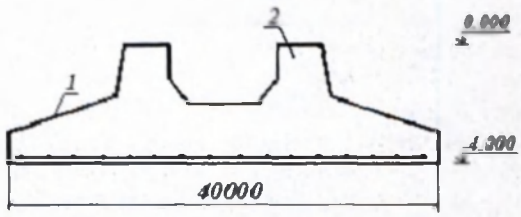


Рис. 3. Фундамент дымовой трубы Н=250 м. 1 – фундамент, 2 – монолитный железобетонный ствол.

4 РЕЗУЛЬТАТЫ НАБЛЮДЕНИЙ ЗА ОСАДКАМИ И ИХ АНАЛИЗ

В 1982 г. возникла необходимость полной замены доменной печи № 1, ее капремонт после 20 лет эксплуатации. В период демонтажа были зафиксированы упругие деформации основания, величина которых составила 12 мм. После возведения доменной печи и полной ее загрузки осадка стабилизировалась через 2 месяца. Подобная картина наблюдалась при реконструкции всех доменных печей Миттал Стил Темиртау. График изменения осадки доменных печей № 1-3 во времени показан на рис. 4.

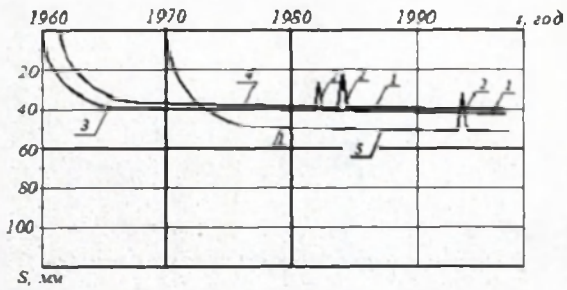


Рис. 4. Зависимость осадки фундаментов доменных печей № 1-3 во времени. 1-стабилизированная осадка, 2-упругие деформации, 3 - доменная печь № 1, 4 - доменная печь № 2, 5 - доменная печь № 3.

При полной замене коксовой батареи № 1-№ 3 в 1986 г. наблюдались упругие деформации основания, которые составили 9 мм, что является 1/5 от общей осадки батареи.

Графики зависимости осадки во времени коксовых батарей № 1-3 приведены на рис. 5.

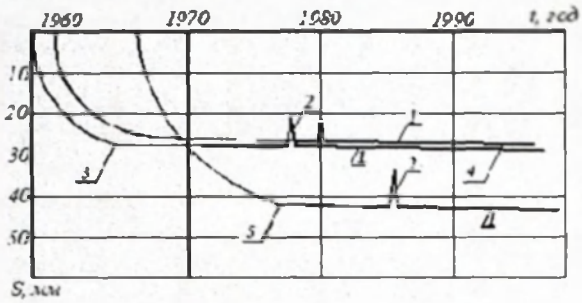


Рис. 5. Зависимость осадки фундаментов коксовых батарей. № 1-3 во времени. 1-стабилизированная осадка, 2-упругие деформации, 3 – коксовая батарея № 1, 4 – коксовая батарея № 2, 5 – коксовая батарея № 3.

Основание фундамента дымовой трубы ТЭЦ ПВС представлено красно-бурыми глинами твердой и полутвердой консистенции. Стабилизация осадки фундамента наступила через 5 лет после окончания работ по возведению монолитного железобетонного ствола. Графики зависимости осадки от времени железобетонных дымовых труб АО «Миттал Стил Темиртау» приведены на рис. 6.

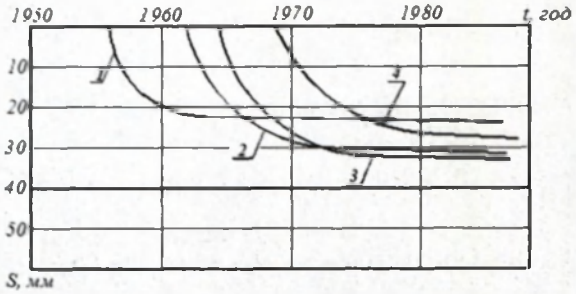


Рис. 6. Зависимость осадки дымовых труб Н=250 м и Н=100 м во времени. 1 - Дымовая труба ТЭЦ ПВС Н=100м, 2 - Дымовая труба ТЭЦ ПВС Н=250м, 3 - Дымовая труба ТЭЦ -2, 4 - Дымовая труба аглофабрики.

Было установлено, что деформации оснований фундаментов доменных печей, как и коксовых батарей наблюдались в течении 2-3 лет после их ввода в эксплуатацию, то фундаментов дымовых труб осадки затухали сразу же после завершения строительных и монтажных работ по возведению железобетонных стволов, устройства в них металлических стволов и выполнения обслуживающих площадок.

Представлял большой научный и практический интерес сопоставления результатов теории и практики полученным для данного региона, с грунтовыми условиями, характерными для центральной части Казахстана.

Для сравнения расчетных осадок фундаментов с фактическими и предельно допустимыми (по СНиП) значениями был произведен перерасчет осадки фундамента дымовой железобетонной трубы высотой 250 м, доменной печи №2 и коксовой батареи №3. Осадка определялась на расчетную нагрузку: для доменной печи 300 т/м^2; для дымовой трубы - 21,1 т/м^2 коксовой батареи – 18,0 т/м^2 на уровне верхнего обреза фундамента.

Осадки вычислялись методом элементарного послойного суммирования и методом эквивалентного слоя согласно СНиП РК 5.01-01-2002 «Основания зданий и сооружений» по формулам:

$$S = \beta \cdot \sum_{i=1}^{n} \frac{P_i \cdot h}{E_i} \qquad (1)$$

где s – осадка; P_i – среднее давление в середине элементарного слоя; h – толщина элементарного слоя; E_i – модуль деформации грунта; β – безразмерный коэффициент.

$$S = h_э \cdot m_{vm} \cdot \sigma_{zp} \qquad (2)$$

где $h_э$ – высота эквивалентной толщи грунта; m_{vm} – средний коэффициент относительной

сжимаемости; σ_{zp} – осадочное давление под подошвой фундамента.

Сравнение расчетных, фактических, а так же предельно допустимых по СНиП осадок показано в табл. 2.

Как видно из приведенных данных фактическая осадка фундаментов промышленных объектов в несколько раз меньше расчетных осадок.

Таблица 2. Сравнение расчетных, фактических и предельно допустимых по СНиП осадок

Объект	Осадка, мм			
	Фактическая	Расчетная		Предельная по СНиП
		Метод послойного суммирования	Метод эквивалентного слоя	
Доменная печь №1	45	156	210	400
Доменная печь №2	43	163	310	400
Доменная печь №3	55	178	200	400
Коксовая батарея №1	27	138	144	250
Коксовая батарея №2	26	120	132	250
Коксовая батарея №3	44	140	149	250
Дымовая труба аглофабрики	29	102	131	200
Дымовая труба ТЭЦ-2	34	92	103	200
Дымовая труба ТЭЦ ПВС Н=250 м	32	149	210	200
Дымовая труба ТЭЦ ПВС Н=100 м	23	83	90	200

Как видно из табл. 2, фактические осадки промышленных объектов во много раз меньше расчетных и предельных значений: для доменных печей в 6÷17; для коксовых батарей в 2,5÷7,0 раз, для дымовых труб в 2,5÷3,0 раза.

4 ВЫВОДЫ

Сопоставляя полученные результаты можно сделать вывод о необходимости проведения дополнительных исследований для накопления и систематизации новых данных и внесения поправок в общепризнанные формулы определения осадок фундаментов.

Корректировки и поправки основных расчетных формул позволят приблизить полученные данные о глубине распространения главных сжимающих напряжений, величине осадок, расчетных сопротивлений грунтов под подошвой фундаментов, получаемых теоретическим путем к практическим величинам, выявленных практикой строительства и многолетним наблюдением за деформациями эксплуатируемых зданий и сооружений.

Более точные (реальные) расчетные значения позволят сократить общую стоимость строительства, т.к. проектирование фундаментов зданий производится с большим запасом прочности, что влечет за собой лишние затраты труда и расходы на материалы. Вместе с тем, использование на практике модуля деформации грунта, полученного в приборе трехосного сжатия, позволит значительно сократить расходы и сроки проведения изыскательских работ.

ЛИТЕРАТУРА

1. Цытович Н.А. и др. Прогноз скорости осадок оснований сооружений – М.: Стройиздат, 1967.-239 с.
2. Цытович Н.А. Механика грунтов (краткий курс): Учебник для строительных вузов. 4-е изд., перераб и доп. – М.: Высшая школа, 1983.-288 с.
3. Чаповский Е.Г. Лабораторные работы по грунтоведению и механике грунтов. Изд. 4-е. М., «Недра», 1975, 304 с.
4. Булычев Н.С. Механика подземных сооружений в примерахи задачах: Учебное пособие для вузов.- М: Недра, 1989,270 с.
5. Вялов С. С. Реологические основы механики грунтов.- М.: Высшая школа,1978.-447 с.
6. Ухов С.Б. Механика грунтов, основания и фундаменты. – М.: Высшая школа, 2002.-566 с.
7. СНиП РК 5.01-01-2002 «Основания зданий и сооружений».

Numerical Solution for 3D Contaminant Trough Anisotropy Soil/Rock Media

Seyed Amirodin Sadrnejad, Mahsa, Memarianfard
Dept. of Civil Eng. K.N.Toosi University of Tech., Teheran, Iran

ABSTRACT: Estimating contamination transport as leaching potential requires calculation of drainage water volume and contamination concentration. A practical, quantitative contamination loss assessment tool can be developed that will enable technical service providers and other practitioners to estimate potential contamination loss and design best-management practices for land-applied waste management systems contamination in order to estimate and control contamination transport to soil and groundwater.
The objective of this paper is to describe governing equation of contamination transport mechanisms and factors essential to include in developing relatively simple and practical tools to quantify contamination loss, advection, diffusion and sorption in contamination transport into the groundwater at landfill sites.

1 INTRODUCTION

The relative success of attempts to model a process is a measure of how well it is understood. A first level of understanding produces a conceptual model and a higher level of understanding results in a quantitative model. Failure to understand dispersion in porous media at a level necessary for constructing reliable mathematical models has impeded progress in studying contaminant transport in ground water. Some of the dispersion observed by Slichter (1905), in field studies was probably a result of macroscopic dispersion.
Smith and Schwartz (1980), who conducted many numerical experiments of hypothetical aquifers, found that for most of the situations that they modeled the variance of the concentration distribution was highly irregular and did not approximate a Gaussian distribution within the lengths of the simulated flow paths.

Field evidence to corroborate these theoretical findings for porous media is sparse. Results from a field tracer test described by Sudicky and Cherry (1979) suggested that the concentration patterns were somewhat irregular near the source of the tracer but became approximately Gaussian farther downgradient. An analysis of the variance of the concentration distribution by Sudicky and Cherry (1979) indicated that the growth of the variance was nonlinear and the dispersivity increased with distance. Several other investigators (Molinari et a/., 1977; Lee et al, 1980; Pickens and Grisak, 1981a, 1981b) also noted an increase in dispersivity with distance from the tracer source, which indicates that dispersion was not Fickian within the distances in which the measurements were taken.

2 TRANSFER THEORY

Most attempts at quantifying contaminant transport have relied on a solution of some form of a well-known governing equation referred to as the advection-dispersion equation. Advection refers to the transport of contaminants at the same
speed as the average linear velocity of groundwater (u, v, w),

$$\frac{\partial Cs}{\partial t} = -\frac{\partial(uCs)}{\partial x} - \frac{\partial(vCs)}{\partial y} - \frac{\partial(wCs)}{\partial z} + \frac{\partial}{\partial x}\frac{\partial(kx.Cs)}{\partial x} + \frac{\partial}{\partial y}\frac{\partial(ky.Cs)}{\partial y} + \frac{\partial}{\partial z}\frac{\partial(kz.Cs)}{\partial z} - (k_{1s} + k_{2s})Cs + Es(x, y, z, t) + Qs(C1, C2, ..., Cq) \quad (1)$$

Where,

$$u = v = w = const \qquad k_{1s} + k_{2s} = \lambda$$

$$kx = Dx, \quad ky = Dy, \quad kz = Dz$$

$$E_S = \frac{M}{\theta}\delta(x - x')\delta(y - y')\delta(z - z')\delta(t - t') \quad (2)$$

Assuming:

$$S = K_d.C, \; Q = \rho_b.\frac{\partial S}{\partial t} = K_d\rho_b\frac{\partial C}{\partial t} \quad (3)$$

The substitution of the above assumption into main equation leads to:

$$R\frac{\partial Cs}{\partial t} = -\frac{u\partial(Cs)}{\partial x} - \frac{v\partial(Cs)}{\partial y} - \frac{w\partial(Cs)}{\partial z} + Dx\frac{\partial(Cs)}{\partial x^2} + Dy\frac{\partial(Cs)}{\partial y^2} + Dz\frac{\partial(Cs)}{\partial z^2} - \lambda Cs + \frac{M}{\theta}\delta(x-x')\delta(y-y')\delta(z-z')\delta(t-t') \quad (4)$$

Where, $R = 1 + K_d\rho_b\frac{\partial C}{\partial t}$, $M = \frac{Q\times C_0}{n\times V}$

Q $(\frac{m^3}{s})$ is the rate if inflow, C_0 $(\frac{mg}{litr})$ is contamination concentration, n is prosity, V (m^3) is volume. The above equation is a general form of advection, diffusion, decay, sorption& sink/source which is valid for contamination transfer in porous media.

Assuming, $\hat{C}_s \cong C_s$, $\frac{\partial C_s}{\partial t} = \dot{C}_s$ and applying weighted residual method:

$$\int w_i(\dot{\hat{C}}_s + \frac{u\partial(\hat{Cs})}{\partial x} + \frac{v\partial(\hat{Cs})}{\partial y} + \frac{w\partial(\hat{Cs})}{\partial z} - Dx\frac{\partial(\hat{Cs})}{\partial x^2} - Dy\frac{\partial(\hat{Cs})}{\partial y^2} - Dz\frac{\partial(\hat{Cs})}{\partial z^2} - \lambda\hat{Cs} + M)dV = 0 \quad (5)$$

$$\int W_i.(\dot{\hat{C}}_s + ADV_i\frac{\partial(\hat{Cs})}{\partial x_i} + DIFF_i\frac{\partial(\hat{Cs})}{\partial x_i^2} - \lambda\hat{Cs} + M)dV = 0 \quad (6)$$

, i = 1, 2, 3

Where, Dx, $DIFF_2$=Dy, $DIFF_3$=Dz, x_1=x, x_2=y, x_3= z = ADV_2=v, ADV_3=w, DIFF1 ADV_1=u,

In finite element framework, upon the use of shape function and the application of Galerkin method:

$$C_s \cong \hat{C}_s = \sum N_m \times C_m \quad (7)$$

$$\int N_i.(N_m\dot{C}_m + ADV_i \times N_m\frac{\partial(C_m)}{\partial x_i} + DIFF_i \times N_m\frac{\partial(C_m)}{\partial x_i^2} - N_m\lambda C_m + M)dV = 0 \quad (8)$$

Upon the use of weak form:

$$\int N_i\left[N_m\dot{C}_m + ADV_iN_m\frac{\partial C_m}{\partial x_i} + \lambda C_m - E\right]dV + \int\left[\sum_{i=1}^{3}K_i\frac{\partial N_i}{\partial x_i}N_m\frac{\partial C_m}{\partial x_i}\right]dV + \int\left[\sum_{i=1}^{3}K_iN_i.N_m\frac{\partial C_m}{\partial x_i}\right]n_i\,dS = 0 \quad (9)$$

The application of finite difference time marching is led to:

$$\dot{C}_s = \frac{\partial C_s}{\partial t} = \frac{C_s^t - C_s^{t-1}}{\Delta t} \quad (10)$$

In the simple form:

$$(ADV_{term}\Delta t + DIFF_{term}\Delta t + CONS_{term} + DECAY_{term}\Delta t)\times C_m = RES_{term}\times C_m^{t-1} + BOUNDRY_{term}\Delta t + N_iM \quad (11)$$

Also: $M_i = \sum_{j=1}^{6}\int_j N_{li}Qds = \sum_{j=1}^{6}M_{ij}$

$$SOUECE_{term} = M = \int N_iQds \Rightarrow M_i = \int N_{li}Qds \quad (12)$$

For a typical solid element having load of uper horizontal side, we can write:

$$A \approx ADV\ D \approx DIFF\ \lambda \approx DECA\ R \approx RES\ S \approx CONS\ M \approx SOUR$$

$$\begin{bmatrix} A_{11}+D_{11}+\lambda_{11}+S_{11} & A_{12}+D_{12}+\lambda_{12}+S_{12} & \cdots & A_{1n}+D_{1n}+\lambda_{1n}+S_{1n} \\ A_{21}+D_{21}+\lambda_{21}+C_{21} & A_{22}+D_{22}+\lambda_{22}+S_{22} & \cdots & A_{2n}+D_{2n}+\lambda_{2n}+S_{2n} \\ \vdots & & & \vdots \\ A_{n1}+D_{n1}+\lambda_{n1}+S_{n1} & A_{n1}+D_{n1}+\lambda_{n1}+S_{n1} & \cdots & A_{nn}+D_{nn}+\lambda_{nn}+S_{nn} \end{bmatrix}\begin{bmatrix} C_1 \\ C_2 \\ \vdots \\ C_n \end{bmatrix} = \begin{bmatrix} R+M \\ R+M \\ \vdots \\ R+M \end{bmatrix} \quad (13)$$

Therefore, the i^{th} equation for node i^{th} in element e is as follows:

$$(A^e_{i1}+D^e_{i1}+\lambda^e_{i1}+S^e_{i1})C^e_{i1}+(A^e_{i2}+D^e_{i2}+\lambda^e_{i2}+S^e_{i2})C^e_{i2}+\cdots+(A^e_{in}+D^e_{in}+\lambda^e_{in}+S^e_{in})C^e_{in} = R^e_i + M^e_i \quad (14)$$

The assemblage of equations in matrix form is as follows:

$$(A^G + B^G + \lambda^G + S^G)C_s^G = R^G + M^G \quad (15)$$

3 RESULTS

To verify the presented solution, a three dimensional cubic domain (200×200×600 mm) with a loading area as shown in Figure 3, meshed and solved by time. The corresponding parameters are given in Table 1.

To compare the model results with analytical, the contamination concentration contours in two *xy* and *xz* plans are presented as follows:

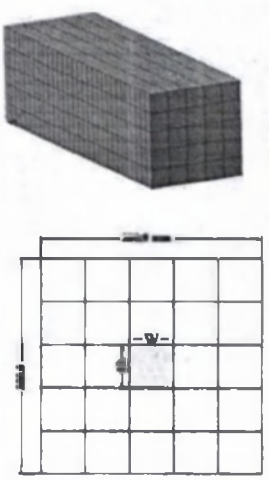


Fig. 1 Meshed domain and loading area at x=400 mm

Table 1. Parameters of the solved problem

u	v	w	Dx	Dy	Dz	λ	C_o
mm	mms^{-1}	mms^{-1}	mm^2s^{-1}	mm^2s^{-1}	mm^2s^{-1}	s^{-1}	mgl^{-1}
1	0	0	50	30	30	6e-4	12.5

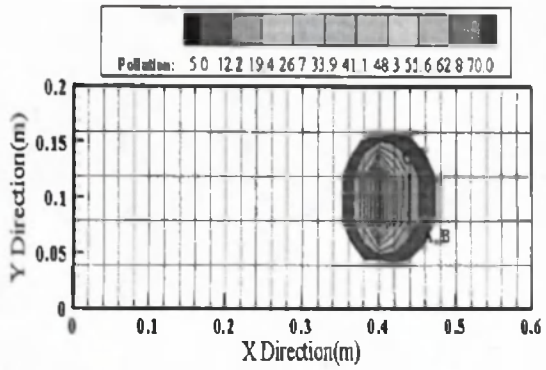


Fig. 2-a Model result in xy plane

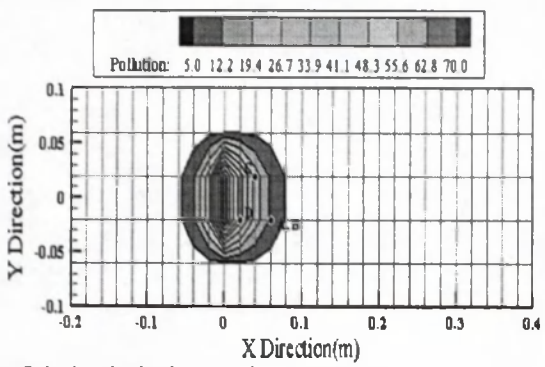


Fig. 2-b Analytical result in xy plane

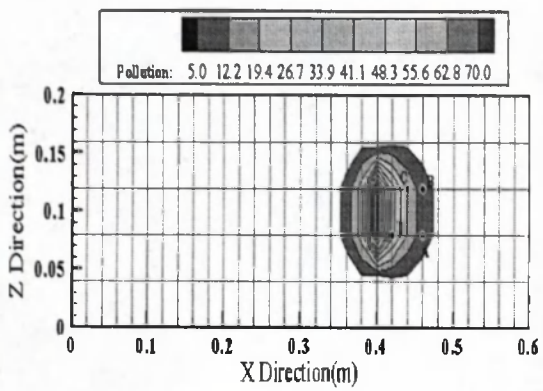


Fig. 3-a Model result in xz plane

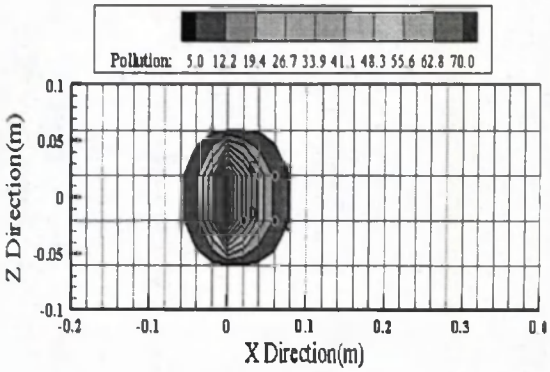


Fig. 3-b Analytical result in xz plane

For a better comparison the contour values on plane ABCD of model and analytical can be compared. These values are presented in Table 3.

Table 2 .A, B, C and D nodal values

Node. Tag	Node. No	Coordinates		
		X	Y	Z
A	1010	0. 46	0.08	0.08
B	1011	0. 46	0.08	0.12
C	999	0.44	0.12	0.12
D	978	0.42	0.08	0.08

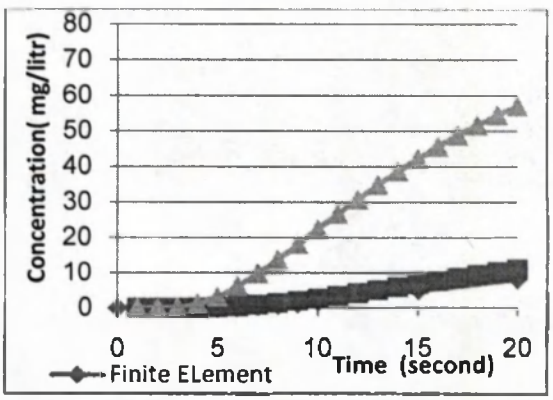


Fig. 4-a Time change variation of contamination concentration at 60 mm in x direction and 20 mm in y and z directions respect to loading area (nodes A and B)

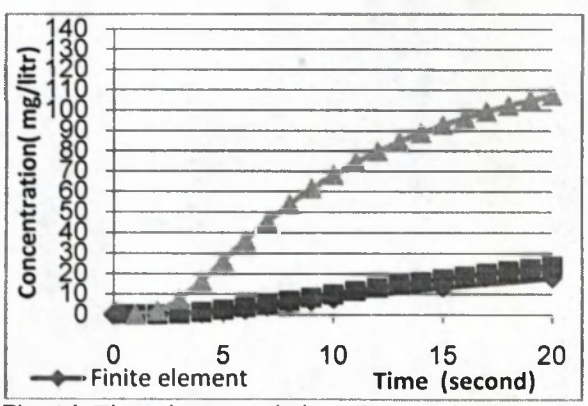


Fig. 4-b Time change variation of contamination concentration at 40 mm in x direction and 20 mm in y and z directions respect to loading area (nodes C)

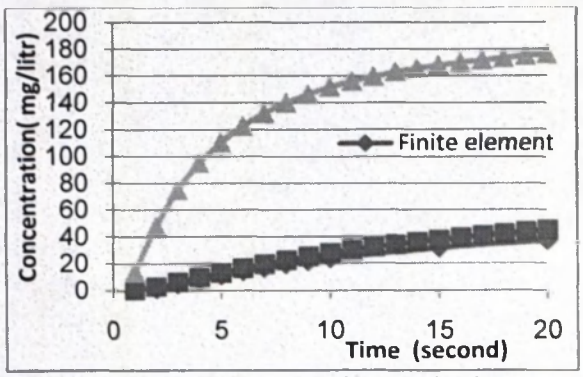


Fig. 4-c Time change variation of contamination concentration at 20 mm in x, y and z directions respect to loading area (nodes D)

Clearly, Domenico results are close to this finite element solution.

4 HETEROGENEITY VS. CONDUCTIVITY

A quantitative description of the degree of heterogeneity in geological formation is obtained by the study of the probability density function. A quantitative description of the trending heterogeneity can be obtained by giving the trend of the mean value of the probability distribution. A geological formation is isotropic at a point if the hydraulic conductivity K is independent of the direction of measurement at that point. With respect to a vertical plane through a horizontally bedded sedimentary formation, the principal directions in both directions in that vertical plane are the two directions corresponding with the maximum and the minimum conductivity. In this case the direction of maximum hydraulic conductivity will be the horizontal axis and the direction of minimum hydraulic conductivity will be the vertical axis. The principal directions are always perpendicular to each other.

In a three-dimensional porous medium, there are three principal directions that are also perpendicular to each other. In a sedimentary formation that consists of an alteration of sand and silty and/or clayey sand layers that are horizontally bedded the smallest hydraulic conductivity will always be measured in vertical direction. Generally, the hydraulic conductivity measured in all horizontal directions can be the same. If the whole distribution is considered then the equivalent horizontal conductivity is always infinitely large and the vertical conductivity is infinitely small. In Figure 5 the relation between the equivalent anisotropy of the layered formation is shown as $\sqrt{K_x} \sim \sqrt{K_z}$ and the standard deviation of the log-normal distribution for different central parts of the log-normal distribution taken into consideration.

For the case of anisotropy of not coinciding principal direction with the x, y, and z coordinate axes the generalized form of Darcy's law is employed as follows:

$$\begin{vmatrix} V_x \\ V_y \\ V_z \end{vmatrix} = \begin{bmatrix} K_{xx} & K_{xy} & K_{xz} \\ K_{yx} & K_{yy} & K_{yz} \\ K_{zx} & K_{zy} & K_{zz} \end{bmatrix} \begin{vmatrix} \frac{\partial h}{\partial x} \\ \frac{\partial h}{\partial y} \\ \frac{\partial h}{\partial z} \end{vmatrix} \qquad (16)$$

Now, since the hydraulic head h is a continuous function of x, y, and z, hydraulic gradient in an inclined direction of $l = \cos\theta_1$, $m = \cos\theta_2$, and $n = \cos\theta_3$ is written as follows:

$$\frac{\partial h}{\partial S} = \frac{\partial h}{\partial x} \cdot \frac{\partial x}{\partial S} + \frac{\partial h}{\partial y} \cdot \frac{\partial y}{\partial S} + \frac{\partial h}{\partial z} \cdot \frac{\partial z}{\partial S} \qquad (17)$$

Geometrically, $\partial x/\partial S = \cos\theta_1$, $\partial y/\partial S = \cos\theta_2$ and $\partial z/\partial S = \cos\theta_3$. These equations yields the following relation to find conductivity on an inclined orientation θ_1.

$$\frac{1}{K_\theta} = \frac{\cos^2\theta_1}{K_x} + \frac{\cos^2\theta_2}{K_y} + \frac{\cos^2\theta_3}{K_z} \qquad (18)$$

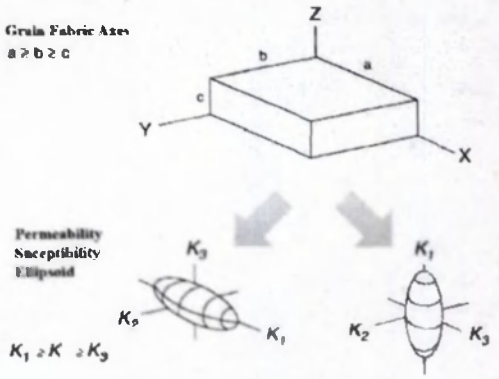


Fig. 5 Hydraulic conductivity ellipsoid

This means that knowing K_x, K_y, K_z through three simple permeability tests along major axes, the hydraulic conductivity ellipsoid is known on coordinate axes K_x, K_y, K_z.

5 SUMMARY AND DISCUSSION

The discussions of dispersion here focused on applications to continuous porous media; dispersion in fractured porous media is not be considered in here. The state of the art for quantifying dispersion in continuous porous media is summarized below.

Results from several studies suggest that dispersion is nonFickian near the source of the contaminant and therefore the standard form of the advection-dispersion-sorption equation does not apply. A modified form could be derived for analyzing non-Fickian transport for small times.

Gelhsaretal. (1979) presented such an equation for one-dimensional flow in a perfectly stratified aquifer. However, they caution that the approach that they used to derive the equation requires certain restrictions that may not be valid at small times. Other approaches that rely on the standard form of the advection-dispersion-sorption equation call for use of time-dependent dispersivities (Gill and Sankarasubramanian, 1972; Matheron and DeMarsily, 1980; Pickens and Grisak, 1981b).

The standard approach in analyzing dispersion involves the use of an average linear velocity and the use of a dispersion term to represent deviations of velocity from the average. The rationalization for this approach is based on the premise that a dispersion term is necessary because it will never be practical to define the velocity field in detail. Moreover, according to Dagan (1982) it is inappropriate to assume that local dispersion does not influence advection. Hence, several investigators (Gelhar et al., 1979; Gelhar and Axness 1981, Dagan, 1982) maintain that the key to a rational application of the advection-dispersion-sorption equation is to define the dispersivity in terms of various statistical properties of hydraulic conductivity.

Another approach, used by Schwartz (1977) and Smith and Schwartz (1980, 1981a, 1981b) among others, is based on attempts to represent the velocity field in detail by defining the hydraulic conductivity in a stochastic manner and in this way to simulate the effects of macroscopic dispersion directly. Smith and Schwartz (1980) concluded that for their simulations local dispersion was negligible because most dispersion observed in their modeled systems occurred at a macroscopic scale. Therefore, in subsequent studies (Smith and Schwartz, 1981a, 1981b) they used an advective model to simulate contaminant transport in a number of hypothetical systems characterized by different arrangements and shapes of heterogeneities. Results of their numerical experiments demonstrated that the solution of the contaminant transport model is quite sensitive to the structure of the heterogeneities within the porous material. Consequently, detailed information on the arrangement and shapes of the heterogeneities, knowledge of the values of hydraulic conductivity for the various units, and information on head gradients (or direct measurements of velocities) are essential for accurate prediction. Although they demonstrated that it is theoretically possible to predict contaminant transport given sufficient hydrogeologic data, they remained pessimistic regarding the practical limitations of obtaining the detailed information needed (Smith and Schwartz, 1981b). In addition they concluded that ". . . large uncertainties can be associated with transport predictions in heterogeneous media. These uncertainties must be dealt with in order to develop confidence in the application of mathematical models of site-specific problems. Unfortunately, the variety of possible sources of uncertainty and the difficulty in controlling their size suggest that progress will be slow." Similarly, Dagan (1982) concluded that "longitudinal dispersion can be represented asymptotically by a Fickian equation, with dispersivity much larger than pore-scale dispersivity," but given the uncertainties involved in defining the hydrogeologic system a stochastic approach is necessary and "the traditional approach of predicting solute concentrations by solving deterministic partial differential equations is highly questionable in the case of heterogeneous formations."

Although there has been considerable progress within the past 5 years in understanding the nature of macroscopic dispersion in porous media, to date, a credible, practical, and reliable model for analyzing contaminant transport near the source has not been identified. However, theoretical studies by several researchers suggest that for large times (or large travel distances) the dispersion component of the advection-dispersion-sorption equation can be represented by an expression analogous to Fick's second law of diffusion, and therefore the classical advection-dispersion-sorption equation will accurately simulate contaminant transport in porous media, provided that dispersivity can be quantified in a meaningful way.

Gelhar et al (1979), Gelhar and Axness (1981), and Dagan (1982) present formulas for defining dispersivity at large times in terms of statistical parameters. However, several investigators suggest that the length of time that must elapse before the advection-dispersion equation is applicable may be appreciable. Specifically, the travel distance of the contaminant must be on the order of 10s or 100s of meters from the source before the advection-dispersion equation is valid. Simulations of contaminant transport by Pickens and Grisak (1981b) suggest that the scale dependence of dispersivity at early times may have little effect on results for large times or travel distances. Hence, the use of an asymptotic dispersivity may be adequate for these conditions provided that sufficient geologic data are available to characterize the statistical parameters of the

hydraulic conductivity distribution (the variance and the correlation scales), as well as the orientation of the geologic units. More attention is needed in characterizing geologic systems in terms of these statistical parameters (e.g., see Smith, 1981; Neuman, 1982).

Moreover, field data needed to corroborate the theory itself are lacking. There is also a need for carefully designed field tracer tests to determine whether the theory is generally applicable and to serve as a basis for estimating the length of time before the Taylor limit is reached. Data from such tracer tests would allow an assessment of the reliability of recently derived expressions for dispersivity.

7 CONCLUSIONS

Accurate estimates of contamination transfer require methods to quantify 1) contamination adsorbed to eroding sediments, 2) soluble contamination in runoff water, 3) soluble contamination in leaching water, and 4) contamination losses related to the specific contamination sources.

The consensus is that dispersion in porous material is non-Fickian near the source of the contaminant, and therefore for small times or small distances from the source.However, the standard solution of the advection-dispersion-sorption equation in macro-scale upon the use of time-dependent dispersivities, and care in calibrationg the parameters by field data can obtain acceptable results in engineering.

Theoretical/numerical studies suggest that for many hydrogeologic settings, dispersion should become Fickian for large times or large distances (on the order of 10s to 100s of meters). In this case it is possible to express the dispersion parameter known as dispersivity in terms of statistical properties of the hydraulic conductivity distribution.

Carefully designed field tracer tests are needed to evaluate the applicability of the theory for large times and to refine the theory for small times.

Detailed hydrogeologic information is needed to predict dispersion for both small and large times. The unavailability of site-specific groundwater flow measurements to calibrate the model presents some limitations on the quality of the results.

6 REFERENCES

Dagan, G. (1982). Stochastic modeling of groundwater by unconditional and conditional probabilities, 2. *The solute transport, Water Resour,* Res. 18, 835-848.

Gelhar, L. W., and C. L. Axness (1981). Stochastic Analysis of Macro-Dispersion in Three-Dimensionally Heterogeneous Aquifers, Geo-physical Research Center, *Hydrology Research Program*, Rep. No. H8, *New Mexico Inst of Mining and Technology, Socorro, New Mexico, 140 pp.*

Gelhar, L. W., and C. L. Axness (1983). Three-dimensional stochastic analysis of macro-dispersion in aquifers, *Water Resour. Res.* 19.

Gelhar, L. W., A. L. Gutjahr, andR. L. Naff (1979). Stochastic analysis of macrodispersion in a stratified aquifer, *Water Resour. Res.* 15, 1387-1397.

Gill, W. N., and R. Sankarasubramanian (1972). Dispersion of non-uniformly distributed time-variable continuous sources in time-dependent flow, Proc. R. Soc. A327, 191-208.

Lee, D. R., J. A. Cherry, and J. F. Pickens (1980). Groundwater transport of a salt tracer through a sandy lakebed, *Limnol. Oceanogr.* 25, 45-61.

Matheron, G., and G, DeMarsily (1980). Is transport in porous media always diffusive? *Water Resour.* Res. 16, 901-917.

Molinari, J. P., B. G. Plaudecerf, and M, Launay (1977). Essais con-joints en laboratoire et sur le terrain en vue d'une approche simplifie de la prevision des propogations des substances miscibles dan les aquifers reels, in Proc. of the Symp. on Hydrodynamic Diffusion and Dispersion in Porous Media, Int. Assoc. for *Hydraulic Research, Pavia, Italy*, pp. 89-102.

Neuman, S. P. (1982) Statistical characterization of aquifer hetero-geneities: An overview, in Recent Trends in Hydrogeology, T. N. Narasimhan, ed., *Geol. Soc. Am. Spec. Pap.* 189, pp. 81-102.

Pickens, J. F., and G. E. Grisak (1981a). Scale-dependent dispersion in a stratified aquifer, *Water Resour.* Res. 17, 1191-1212.

Pickens, J. F., and G. E. Grisak (1981b). Modeling of scale-dependent dispersion in hydrogeologic systems, *Water Resour. Res.* 17, 1701-1711.

Sagar, B., 1982. Dispersion in three dimensions: approximate analytical solutions. *ASCE, hx nhvn Journal of Hydraulics Division 108* (HY1), 47–62.

Schwartz, F. W. (1977). Macroscopic dispersion in porous media: The controlling factors, *Water Resour. Res.* 13, 743-752.

Slichter, C. S. (1905). Field measurements of the rate of underground water, U.S. Geol. Surv. Water Supply Pap. 140, pp. 9-85.

Smith, L. (1981). Spatial variability of flow parameters in a stratified sand, /. Int. Assoc. Math. Geol. 13, 1-21.

Smith, L., and F. W. Schwartz (1980). Mass transport, 1, A stochastic analysis of macroscopic dispersion, Water Resour. Res. 16, 303-313.

Smith, L., and F. W. Schwartz (1981a). Mass transport, 2, Analysis of uncertainty in prediction, Water Resour. Res. 17, 351-369.

Smith, L., and F. W. Schwartz (1981b). Mass transport, 3, Role of hydraulic conductivity data in prediction, Water Resour. Res., 17, 1463-1479.

Sudicky, E. A., and J. A. Cherry (1979). Field observations of tracer dispersion under natural flow conditions in an unconfined sandy aquifer, Water Pollut. Res. Canada 14, 1-17.

Sudicky, E. A., and E. O. Frind (1982). Contaminant transport in fractured porous media: Analytical solutions for a system of parallel fractures, Water Resour. Res. 18, 1634-1642.

Инженерные проблемы сохранения памятников архитектуры

Абдурашидов К.С., Саидий С.А., Шадманова З.С., Рахманов Б.К.
Ташкентский архитектурно-строительный институт, Узбекистан

Большая часть территории нашей страны относится к высокоактивным сейсмическим районам, где расположены многие памятники архитектуры. В связи с этим изучение технического состояния и разработка конструктивных мероприятий по обеспечению их долговечности является актуальной задачей [1-2].

Анализ фактического состояния памятников архитектуры свидетельствует об увеличении памятников, получающих ежегодно значительные деформации и повреждения по различным причинам: сильные и слабые землетрясение, техногенные воздействия, поднятие уровня грунтовых вод, нарушение условий эксплуатации и др. Следовательно, сильно ухудшается техническое состояние многих архитектурных памятников.

Для решения этой проблемы сотрудниками кафедры «Строительная механика и сейсмостойкость сооружений» разработана комплексная научно-техническая программа «Инженерное обследование, оценка технического состояния, прогнозирование резерва несущей способности, разработка конструктивных мер по обеспечению устойчивости и сейсмостойкости архитектурных памятников Республики Узбекистан».

Объектами исследований является памятники архитектуры г. Шахрисабза, Самарканда, Бухары, Хивы и др. построенных в эпоху Темура и темуридов.

Анализ архивных материалов опубликованных работ показывает, что в период с 1880 по 1990 годы выполнены большие работы по изучению памятников архитектуры г. Шахрисабза. Но в них не выявлены комплексного подхода по сохранению памятников архитектуры, т.е. отсутствуют оценка напряженно-деформированного состояния конструкций, гидрогеологического состояния оснований, конкретных конструктивных мероприятий по восстановлению или усилению аварийных частей памятников, отсутствуют также расчеты на сейсмические воздействия, не проведены систематические инструментальные измерения по оценке их степени деформированности и т.д.

Для всестороннего изучению технического состояния, разработки комплекса мер по обеспечению устойчивости и долговечности памятников архитектуры рекомендуется выполнить следующее:

1. Детальное обследование с фиксацией повреждений и деформаций памятников архитектуры.
2. Изучение физико-механических характеристик строительных материалов и грунтов основания.
3. Геодезические наблюдения за осадками и кренами памятников архитектуры.
4. Выполнения расчетов на статические и сейсмические воздействия.
5. Инструментально-мониторинговые наблюдения по оценке технического состояния.
6. Разработка конструктивных мероприятий по обеспечению прочности, устойчивости и сейсмостойкости памятников архитектуры.

По данной рекомендации выполнена оценка технического состояния и конструктивные меры по сохранению дворца Оксарай в г. Шахрисабзе.

Детальное инженерное обследование дворца Оксарай.

Дворец построен в 1380-1404 годах. Он представлял собой обширный комплекс построек, сгруппированных в несколько дворов. На оси парадного двора было главное купольное здание. Двор обходило галерея, ведущая к основным помещениям.

В настоящее время от величественного дворца сохранились лишь два разобщенных пилона входного портала, соединенных некогда аркой. Пилоны фланкированы круглыми минаретами на граненом основании. Высота западного портала до разрушения достигала 74 м.

Западной пилон сохранился на высоту 38 м. Фасадная часть пилона представляет вертикальную плоскость.

Восточный пилон сохранился на высоту 35 м. Конструктивная кладка пилона в хорошем состоянии. Мраморные панели цокольной части утрачены полностью. Места панели заполнены кирпичной кладкой, выполненной в разное время и на различных растворах.

Южный дворовый фасад пилона имеет несколько ярусов по высоте.

Сохранился также пилон малой арки, а её фасадная стена является щипцовой стеной большого свода. Высота этого фрагмента составляет 22 м. Этот массив имеет отклонение от основного пилона на юго-восток и по верхнему обрезу кладки на 67 см. Трещина сквозная, доходящая до цокольной части. Массив, относящиеся к малому своду, оторвался от основного, и весь покрыт конструктивными трещинами. Сквозные трещины легко просматриваются на фасаде. С целью исследования динамики развития трещин и устойчивости состояния сохранившегося пилона малой арки установлены маяки [2].

Оценка физико-механических характеристик материалов.

Дворец построен из жженого кирпича почти квадратной формы. Размеры кирпича довольно устойчиво выдерживается в пределах всего дворца и составляет 22x28x(6-7) см, местами 25x25x5 см.

Результаты физико-механических испытаний показывают, что прочность кирпичей находится в пределах 80,6-115,0 кг/см^2. Марка раствора 20-60, коэффициент сцепления раствора с кирпичом равен 0,5-1,5 кг/см^2.

Грунты основания и их физико-механические свойства.

По результатам инженерно-геологических исследований территорий дворца установлено, что грунтами оснований памятника является насыпные грунты и подстилающие их лессовые суглинки и супеси. Насыпные грунты залегает непосредственно под фундаментами мощностью 2,0 - 2,3 м, лессовые грунты - нижнюю часть сжимаемой толщи.

В результате обработке полевых данных, полученных из двух шурфов, заложенных у оснований двух пилонов получены следующие данные: по западному пилону - плотность грунта 1,81 т/м^3; природная влажность 0,206; коэффициент пористости 0,784; показатель текучести 0,69; уголь внутреннего трения 26^0; удельное сцепления 0,0079 кг/см^2; коэффициент относительной просадочности 0,036; модуль деформации 43 кг/см^2. По восточному пилону - плотность грунта 1,73 т/м^3; природная влажность 0,226; коэффициент пористости 0,917; показатель текучести 0,63; уголь внутреннего трения 27^0; удельное сцепления 0,0069 кг/см^2; коэффициент относительной просадочности 0,036; модуль деформации 43 кг/см^2.

Определено расчетное сопротивление грунтов оснований: для западного пилона - 32,10 т/м^2, а для восточного - 31,94 т/м^2.

Уровень грунтовых вод меняется. Например, в 1998 году находился в пределах 305-3,10 м, а в 2001 году составило около 7,0 м.

Сейсмичность территории дворца равно 8 баллов.

Насыпные грунты по литологическому составу являются однородными. Представлены они, в основном, уплотненными суглинками. Грунты по степени уплотненности оказались разнородными. Особенно сильно отличаются грунты оснований восточного пилона. Здесь они являются менее уплотненными или являются наиболее рыхлого сложения.

По состоянию влажности грунты характеризуются высокой степенью увлажненности. Грунты, залегающие под фундаментами, находятся в зоне капиллярного увлажнения грунтовыми водами. Физико-механические свойства грунтов отличаются более высокой изменчивостью, показывающие большую их разнородность.

Таким образом, разнородность состава и разнородность деформационно-прочностных показателей грунтов является главной причиной, создающие неблагоприятные инженерно-геологические условия. С этой особенностью грунтов связаны большие неравномерные осадки зданий и сооружений и их другие деформационные характеристики.

Фундамент выполнен в основном из естественных камней. Нижняя часть выполнено из кладки галек и валунов на кирьевом растворе. Глубина заложения фундамента колеблется от 3,0 до 3,8 м. Верхняя цокольная часть фундамента состоит из кладки жженого кирпича на ганчевом растворе. На местах заложения шурфов она состоит из 9 рядов кирпича. Грунтами оснований являются насыпные грунты. Мощность насыпных грунтов ровна 4-5 м. Физико-механические свойства грунтов отличается более высокой изменчивостью.

Геодезические наблюдения за осадками и кренами.

Результаты высокоточных геодезических измерений осадок марок установленных по периметру комплекса показывают о нарушении стабильности восточного пилона в целом, деформированной части, в частности. Результаты измерений осадки, выполненных в 1991-1995 годах и двух циклов, проведенных, в июне-ноябре 2001 и третьего цикла выполненного в марте 2002 года показывают, что южная часть обоих пилонов осаживаются. Крайние точки деформированной части восточного пилона за последний восьмимесячный период дали осадки в пре-

делах 2-12 мм. Общая величина осадки за 1991-1995 годы составили 4-7 мм. Следует заметить, что в последнее время наблюдается значительное ускорение осадки, особенно поврежденной части восточного пилона. Следовательно, констатировать о стабильности дворца не приходится. Естественно, отклонение деформированной части восточного пилона продолжается. Допустимая нормативная величина крена должна быть не более +0,005H, где H - высота наблюдаемой точки, равно 22 м. Отсюда, допустимая величина крена 110 мм. Визуальное и инструментальное наблюдения, выполненные 11 марта 2002 года заложенных 6 октября 2001 года на высотах 6, 12, 15 метров маяков, показали, что они не имеют разрывов и сдвигов. Следует заметить, что крайняя южная точка деформированной части имеет отклонение от вертикальной линии, проведенной по крайней точке основания на 75 см. Такое отклонение было и раньше, т.е. до землетрясения 3 марта 2002 года. Измеренный в ноябре месяце 2001 г. крен этой точки составляет 48 мм. Таким образом, пока крен деформированной части находится в пределах допустимой.

Натурное исследование динамических характеристик.

Основной задачей инструментального наблюдения является получение динамических характеристик и оценка состояния степени деформированности конструкций. Они могут быть получены с помощью экспериментальных исследований колебаний отдельных пилонов в натурных условиях.

При экспериментальных исследованиях, выполненных в 1995, 1997, 1998, 2001, 2002, 2004, 2006 и 2008 годах микросейсмические колебания создавались движением и внезапным торможением загруженных грузовых автомобилей и тракторов.

В качестве измерительной аппаратуры использованы электродинамические сейсмографы типа ВЭГИК. Регистрация колебаний выполнялась осциллографом типа Н - 041 с зеркальным гальванометром ГВ-111 с частотой 5 Гц.

В результате проведенных экспериментальных работ получены записи колебаний пилонов по продольным и поперечным направлениям в виде осциллограмм. Анализ результатов записей показывает, что период поперечных колебаний деформированной части восточного пилона резко отличается от основного. Динамические характеристики восточного пилона показывает, что нарушена его монолитность. Следовательно, деформированная часть пилона работает независимо от основного.

Последствия землетрясения 3 марта 2002 года на дворец Оксарой.

Интенсивность этого (афганского) землетрясения в г. Шахрисабзе оценена 5-6 баллов.

В результате изучения последствий землетрясения выявлено следующее:

- на западной части аварийного массива появились мелкие трещины;
- на винтовой лестнице восточного пилона на разных высотах, особенно над «замками» арок появились новые трещины;
- появились новые трещины между минаретом и восточным пилонам;
- над «замками» винтовой лестницы западного пилона также появились новые трещины, увеличились поперечные и продольные размеры старых трещин на 3-4 см.

Эти обстоятельства подтверждает то, что архитектурные памятники чувствительны к сейсмическим воздействиям.

Усиление аварийного пилона дворца Оксарай.

Учитывая аварийное состояние, а также продолжающихся деформаций установленных сейсмометрическими, геодезическими и гидрогеологическими наблюдениями рекомендуется усилить (эскизный вариант) этого пилона в три этапа.

На период восстановительных работ надземной части аварийного пилона рекомендуется произвести опоясывания прокатной сталью с целью предотвращения от разрушения при усилении подземную часть и инъекцирование трещин надземной части пилона. Для этого тяжи укладываются по поверхности стен. Натяжение производится с помощью анкерных болтов. На углах и выступах будут установлены вертикальные уголки, обжимающие углы после натяжения поясов, которые производится посредством стяжных муфт одновременно по всему периметру. Устанавливается также ненапрягаемые связи в виде хомутов, анкеров, обвязок из арматуры и прокатной стали. Все элементы опоясывания соединяется болтами, что обеспечит сохранность архитектурных декоров.

Во втором этапе производится укрепления основания фундамента методом инъецирования.

После набора прочности и стабильности деформации основании производится усиление надземной части. При этом под большим давлением продуваются и промывают-

ся все трещины и заделываются специально подготовленными жидкими сильно сцепляющими материалами.

Только после полного завершения всех укрепительных работ, обеспечивающие устойчивость и долговечность деформированной части, следует снимать все внешнее металлические тяжи – конструкции укрепления.

ЛИТЕРАТУРА

Абдурашидов К.С. Ўзбекистондаги архитектура ёдгорликлари конструкцияларининг ҳолати ва келажаги // Архитектура и строительство Узбекистана. - 2001. - № 1. - С. 16-17.

Абдурашидов К.С. и др. Инженерные проблемы архитектурных памятников. – Ташкент: Фан, 2011. – 353 с.

К вопросу эксплуатации зданий и сооружений на основаниях, сложенных просадочными лессовыми грунтами и рекомендуемые противопросадочные мероприятия

Сапаров А.
«УзГАШКЛИТИ ДУК», Ташкент, Узбекистан

АННОТАЦИЯ. В работе приводятся причины деформации зданий и сооружений в процессе эксплуатации на основаниях сложенных просадочными лессовыми грунтами и мероприятия их устранения.

Большая часть городов Узбекистана располагается на территориях развития лессовых грунтов четвертичного возраста Ташкентского комплекса, в том числе на территории развития техногенных отложений. Оба вида отложений относятся к структурно-неустойчивым, и отличаются просадочными свойствами при их замачивании.

Недоучет особенностей геотехнической системы, особенно отрицательных свойств структурно-неустойчивых грунтов приводит к неблагоприятным последствиям просадочным явлениям, когда на территории их развития располагаются здания и сооружения различного вида и уровня ответственности.

Деформации толщи грунтов в виде опускания поверхности и образования просадочных трещин при их замачивании, достигают значительных значений, из-за чего в ряде случаев построенные на них здания и сооружения становятся непригодными для эксплуатации из-за их аварийного состояния.

Примеров строительства зданий и сооружений без соответствующей подготовки их оснований, т.е. без применения противопросадочных мер, особенно часто встречались в семидесятые годы XX века в городах Ташкенте, Чирчике и других городов Узбекистана.

Деформации земной поверхности возникают вследствие просадки грунтов от собственного веса и просадки от внешней нагрузки.

В соответствии с требованиями КМК 2.02.01-98 и КМК 2.01.09-97 проектирование зданий и сооружений для строительства на просадочных грунтах при возможности замачивания грунтов основания следует предусматривать одно из мероприятий, приведенных в п.3.12 КМК 2.02.01-98 [1]:

а) устранение просадочных свойств грунтов в пределах всей просадочной толщи;

б) прорезку просадочной толщи глубокими фундаментами, в том числе свайными и массивами из закрепленного грунта;

в)комплекс мероприятий, включающих частичное устранение просадочных свойств грунтов, водозащитные и конструктивные мероприятия.

В грунтовых условиях II типа наряду с устранением просадочных свойств грунтов или прорезкой просадочной толщи глубокими фундаментами должны предусматриваться водозащитные мероприятия, а также соответствующая компоновка генплана.

По территории Республики территориальными подразделениями ГУП «УзГАШКЛИТИ» обследованы более 200 зданий и сооружений, подверженных просадочным деформациям. Среди деформированных зданий наибольшее количество составляют жилые дома, производственные и административные здания, а также здания школ, больниц, кинотеатров, детских садов и прочие здания.

Причины деформаций указанного перечня зданий и сооружений кроется в основном в ошибках службы эксплуатации, встречаются и ошибки в проекте.

Из исследованного количества зданий и сооружений в 10% случаях фундаменты посажены на насыпные грунты, в остальных случаях - на просадочные лессовые грунты.

При этом за редким исключением противопросадочные мероприятия в соответствии с требованиями нормативных документов не были приняты. Как следствие произошли деформации зданий и сооружений в результате замачивания их оснований из-за утечек из водонесущих коммуникаций.

Многие здания и сооружения были построены без соответствующей подготовки их оснований, т.е. без применения противопросадочных мер, например по ул.Наккошлик и в других кварталах жилого

массива Чиланзар в городе Ташкенте, в годы после землетрясения 1966 года.

Замочка грунтов оснований указанных зданий произошла в результате многократных и длительных утечек из водонесущих коммуникаций как внутри помещений, так и извне, просачивания атмосферных, сточных и ирригационных вод через неуплотненную обратную засыпку пазух котлованов.

Из строек последних лет в качестве примера приведем девятиэтажный жилой дом в г.Ташкенте, который претерпел деформации из-за просадки его основания. Здание дома состоит из двух блоков- восточного и западного.

Участок жилого дома приурочен к поверхности четвертой надпойменной террасы р.Чирчик, сложенной пролювиальными отложениями Ташкентского комплекса (среднечетвертичного возраста), представленными макропористыми просадочными лессовыми породами, прикрытыми сверху насыпными грунтами мощностью до 5,2м.

Вскрытая мощность просадочных лессовых пород на данном участке составляет 18,5 м.

Подземные воды в пределах участка в 1994 году и в марте 2000 года были вскрыты на глубине от 17,3 до 18,5 м.

Величина ожидаемой просадки толщи лессовых пород по лабораторным данным составляла 21,4 см, т.е. по грунтовым условиям участок относится к II типу по просадочности.

В процессе подготовки основания здания слой насыпных грунтов был полностью удален и устроена грунтовая подушка толщиной 5 метров.

В результате обследований установлено, что фундаменты здания, сданного в эксплуатацию в 1995 году - железобетонная плита с глубиной заложения 2,5 м. Ниже подошвы фундамента устроена грунтовая подушка из утрамбованных до плотности 1,65-1,75 т/м3 суглинистых грунтов толщиной 5 метров в интервале глубин 2,5-7,5 м.

Как видим из вышеприведенного, плотность грунтов грунтовой подушки, также как и ее глубина, доведены до значений, отвечающих требованиям нормативных документов, в частности подпункта в) п.3.12 КМК 2.02.01-98.

Однако при проектировании нарушено требование того же п.3.12 КМК 2.02.01-98 о том, что в грунтовых условиях II типа наряду с устранением просадочных свойств грунтов или прорезкой просадочной толщи глубокими фундаментами должны предусматриваться водозащитные мероприятия.

Здесь вместо устранения просадочных свойств грунтов в пределах всей просадочной толщи или прорезки просадочной толщи глубокими фундаментами проектировщики ограничились принятием комплекса мероприятий, включающих частичное устранение просадочных свойств грунтов, водозащитные и конструктивные мероприятия. Как будет показано ниже, это не помогло.

Воду в подвале дома обнаружили вскоре после сдачи дома в эксплуатацию - во второй половине 1996 года. Чуть позже были обнаружены деформации здания.

По состоянию на 28 марта 2000 года, по данным геодезических измерений, просадочные деформации основания превысили 30 см, крен здания в среднем по восточному блоку здания составил 32,5см, что превышает предельно допустимые нормы более чем в два раза (при допуске в 13,5 см).

Разнонаправленный крен западного и восточного блоков дома отчетливо виден по осадочному шву, особенно в верхней его части.

В подвале дома постоянно находилась вода, высота столба которой доходила в отдельные дни до 1,2 м от пола подвала!!

В двух канализационных люках переднего фасада дома обнаружен подпор воды. Высота столба воды здесь достигала от 0,6 до 1,0 м. В канализационном люке, расположенном ниже по течению было сухо. Это указывает на то, что трасса канализации была забита на промежутке между верхним и нижним люками.

И на самом деле после того как трасса канализации была очищена, вода пошла через нижний люк и подпор воды в верхних люках исчез.

Выработки, пройденные вокруг здания, на расстоянии 1,5 - 2,0 м от стены дома в северной и южной частях второго блока вскрыли воду на глубине 2,0-2,5м.

Это указывает на то, что вода, вытекая из вышедших из строя подземных водонесущих коммуникаций, просачивалась через подвал дома и под подошву фундамента и располагалась над грунтовой подушкой, образуя верховодку.

По данным выработок, вскрывших основание фундаментов под грунтовой подушкой установлено, что толща просадочных лессовых грунтов начиная от

подошвы грунтовой подушки имеет повышенную, вплоть до состояния водонасыщения, влажность! И при этом на всю мощность просадочной толщи!!!

Это явление указывает на то, что львиная доля утечек из водонесущих коммуникаций уходила под грунтовую подушку, насыщая водой всю оставшуюся одиннадцатиметровую просадочную толщу!

Из вышеизложенного следует:

Причиной деформации послужило замачивание толщи просадочных лессовых грунтов основания под грунтовой подушкой водами, просочившимися в течение длительного времени из трассы канализации и других водонесущих коммуникаций, находящихся в доме и примыкающих к нему территорий!

Просачивание воды в основание происходило в обход грунтовой подушки, мощность которой составляла пять метров.

В результате замачивания повысилась влажность и плотность грунтов основания, но не настолько, чтобы они теряли свои просадочные свойства полностью. Величина «остаточной» просадки толщи грунтов под грунтовой подушкой составляет более 8,7 см.

Подобная картина наблюдалась под грунтовой подушкой семиэтажного административного здания в г.Ташкенте. Здесь фундаменты здания, сданного в эксплуатацию в 1975 году, заложены на глубине 7,0 м. Ниже подошвы фундамента устроена грунтовая подушка из утрамбованных до плотности 1,65-1,75 т/м^3 суглинистых грунтов толщиной 2 метра в интервале глубин 7,0-9,0 м, но это не могло предотвратить просачивание вод из водонесущих коммуникаций под подошву фундамента. Здесь просачивание воды в основание также происходило в обход грунтовой подушки.

Такая же картина наблюдалась под грунтовой подушкой здания школы №25 в г.Чирчике, т.е. просачивание воды в основание из водонесущих коммуникаций происходило в обход грунтовой подушки.

Вышеприведенные и другие примеры показывают, что просадочные деформации большинства зданий и сооружений происходили в основном из-за ошибок службы эксплуатации, вернее из-за незнания работников службы эксплуатации элементарных правил эксплуатации зданий и сооружений на территориях развития просадочных лессовых пород.

Анализ деформаций зданий и сооружений, расположенных на территории развития лессовых пород, отличающихся просадочными свойствами при их замачивании показывает на некоторые неувязки также и в требованиях нормативных документов, в частности КМК 2.02.01-98[1].

В нескольких пунктах КМК 2.02.01-98 (п.п. 2.67 ÷ 2.71. и п.п. 3.8, 3.12, 3.13) [1] приводятся требования по применению водозащитных и конструктивных мероприятий при проектировании оснований, сложенных просадочными грунтами, тем самым допускается частичное устранение просадочных свойств грунтов, водозащитные и конструктивные мероприятия.

Однако на приведенных выше примерах мы убедились, что принятие водозащитных мероприятий не могут служить надежной гарантией от увлажнения грунтов основания, в результате чего эти грунты дают просадку в любой момент в процессе эксплуатации зданий.

Что касается конструктивных мероприятий то в условиях высокого сейсмического риска эффект от жестких, осадкоустойчивых мер будет каким, это вопрос для отдельного обсуждения.

Ввиду вышеизложенного рекомендуется:

1) исключить подпункт в) п. 3.12 КМК 2.02.01-98, которое гласит: «п.3.12..... в) комплекс мероприятий, включающий частичное устранение просадочных свойств грунтов, водозащитные и конструктивные мероприятия (п.п.2,67-2,71 и требования КМК 2.09.09-97)»;

2) ограничить применение п.2в приложения 1 КМК 2.09.09-97 только для грунтовых условий I типа и зданий и сооружений II и III классов;

3) в ГУП «УзГАШКЛИТИ» организовать краткосрочные курсы подготовки и переподготовки для работников службы эксплуатации зданий и сооружений, занятых эксплуатацией зданий и сооружений на территориях развития просадочных лессовых грунтов;

4) разработать пособие или памятку для работников службы эксплуатации по эксплуатации зданий и сооружений на территориях развития просадочных лессовых грунтов.

5) осуществлять контроль качества подготовки оснований фундаментов, сооружения насыпей и обратных засыпок при строительстве зданий, сооружений и инженерных подземных коммуникаций в соответствии с указаниями [3].

ЛИТЕРАТУРА

1.КМК 2.02.01-98. «Основания зданий и сооружений». Госком-архитектстрой РУз., Ташкент, 1999.

2.КМК 2.01.09-97. «Здания и сооружения на просадочных и подрабатываемых территориях». Ташкент, 1998.

3.«Руководство по геологическому контролю за качеством сооружения оснований фундаментов, насыпей и обратных засыпок при строительстве зданий, сооружений и инженерных подземных коммуникаций на просадочных грунтах». Госкомархитектстрой РУз., Ташкент, 2009.

Роль техногенеза в изменении инженерно-геологических условий

Сапаров А.
«УзГАШКЛИТИ ДУК», Ташкент, Узбекистан

Сапарова М.А.
«Таш ГТУ», г.Ташкент, Республика Узбекистан

АННОТАЦИЯ. В статье анализируется роль антропогенных факторов в изменении инженерно-геологических условий. Продемонстрировано влияние инженерно- хозяйственной деятельности на режим подземных вод, на переформирование рельефа городской территории.

В связи с активной деятельностью человека, освоением им новых территорий в настоящее время необходимо уделять особое внимание процессам, влияющим на изменение инженерно- геологических условий территорий.

В условиях урбанизации городских территорий с образованием крупных мегаполисов эта проблема приобретает особо важное значение. Происходит подъём уровня подземных вод, изменение их химического состава и температурного режима, что в свою очередь влияет на физико-механические характеристики грунтов и эксплуатационную надёжность зданий и сооружений.

Наиболее быстрое изменение горных пород происходит в том случае, когда они являются многокомпонентными системами и когда соотношение между компонентами, составляющими горную породу, меняется достаточно быстро.

Это наиболее характерно для дисперсных грунтов, у которых особенно подвижны два компонента: вода и воздух, содержащиеся в порах.

В зависимости от того, полностью или частично будут заполнены поры водой (или газом), грунты будут представлять собой двух – или трёхкомпонентную систему, так как в порах их содержится вода и газ. В настоящее время следует говорить ещё и о четвёртом компоненте – живых организмах, в первую очередь микроорганизмах, присутствующих в породах и оказывающих большое влияние на некоторые свойсва пород, особенно техногенных насыпных грунтов.

Наиболее активно на изменение свойств грунтов влияет изменение режима и химического состава подземных вод. Здесь в равной степени могут оказаться опасными как понижение уровня подземных вод, так и их повышение. Общеизвестно, что в современном городе на территориях промышленных предприятий и жилых микрорайонов прокладываются всё новые подземные коммуникации (водопровод, канализация, теплотрассы, связь и т.п.), как правило, играющие также дренирующую роль. Иногда они способствуют осушению водонасыщенных горных пород. В результате исчезает взвешивающее влияние подземной воды, которое выражается формулой:

$$\gamma_{sb} = \gamma - 1 / 1 + e,$$

где e –коэффициент пористости грунта,

γ-удельный вес грунта,

γ_{sb}- удельный вес грунта во взвешенном состоянии

Плотность грунта практически повышается в 1,5-2 раза, основание претерпевает дополнительное уплотнение, сопровождающееся неравномерной осадкой сооружений.

Наряду с понижением уровня подземных вод, повышение уровня также оказывет активное влияние на состояние грунтов оснований зданий и сооружений.

Влажность грунтов жилых и особенно промышленных районов по истечению некоторого времени после постройки повышается. Это явление связано с уплотнением застройки, покрытием больших площадей асфальтом, озеленением, изменением естественного сложения грунтов при устройстве фундаментов и т.п.

Недостатки в организации поверхностного стока могут влиять на повышение влажности грунтов оснований застроенной территории. Этому способствует скопление воды в обратных засыпках эксплуатируемых зданий с нарушенными отмостками, временных траншеях, выемках и котлованах. Полив зелёных насаждений в городах и территориях промышленных предприятий так же отражается на повышении влажности грунтов основания.

Обычно на застроенной территории действует прямой водообмен: подземная вода - зона аэрации – атмосфера. Нарушение сложившегося динамического равновесия в водном балансе в связи с застройкой территории, как правило, приводит к накоплению влаги в зоне аэрации и в зоне подземных вод, вследствие чего происходит подъём уровня подземных вод.

В тех случаях, когда напластование грунтов не обладает хорошей водопроницаемостью, происходит подтопление территории, сопровождающееся деформациями зданий и сооружений. Подтоплению территории способствуют также утечки из водонесущих коммуникаций, инфильтрация утечек производственных и сточных вод, устройство водоёмов, плотин, запруд, каналов, накопителей и другие ирригационные мероприятия.

Даже при регламентированных утечках воды из водонесущих коммуникаций количество поступающей в грунт воды достигает значительных значений. Наибольшее количество воды поступает в грунты оснований из водопроводных и канализационных сетей: из нового водопровода 15-18%, из эксплуатируемого менее 50 лет – 18-30%, более 50 лет – 30-50%. Наиболее опасными для зданий является неравномерное или локальное замачивание лессовых грунтов, при котором возникают неодинаковые в различных сечениях здания деформации основания и конструктивных элементов (фото 1).

Повышение уровня подземных вод ведёт к разуплотнению грунтов в результате гидростатического взвешивания, изменению коэффициента пористости и коэффициента фильтрации. Модуль деформации непросадочных суглинков при повышении уровня подземных вод снижается в 1,5-2,0 раза. Особенно резко сказывается подтопление на свойствах просадочных грунтов: их влажность повышается в среднем в 2,5 раза, сцепление снижается в 3 раза, а угол внутреннего трения – в 1,5 раза. В результате грунты основания, обладавшие достаточно высокой несущей способностью и низкой деформативностью при естественной влажности, после повышения уровня подземных вод превращаются в слабые грунты



фото 1 (Фото А.Сапарова).

В просадочных грунтах уровень подземных вод, в зависимости от глубины залегания водоупора и свойств напластований, может повышаться не повсеместно, а в виде куполов. В таком случае в основании сооружений свойства грунтов будут уменьшаться локально, что повлечёт за собой неравномерные осадки зданий и сооружений.

Наряду с изменением физико-механических свойств грунтов, вызванных повышением уровня подземных вод разрушение конструктивных элементов может быть вызвано коррозией металлов, из которых они изготовлены.

Современные здания изготовлены, в основном, из железобетонных и бетонных элементов, поэтому наибольший интерес представляют вопросы взаимодействия с агрессивной средой бетона и железобетона и их долговечности.

В грунтах имеется значительное количество водорастворимых солей. В лёссовидных грунтах различают труднорастворимые (карбонаты-кальцит), среднерастворимые (сульфаты-гипс) и легкорастворимые (галоиды-галит, сульфаты) соли. Растворение солей в подземных водах существенно зависит от режима движения вод, их температуры и насыщенности уже растворимыми солями. Коррозия бетона и железобетона при взаимодействии с агрессивными водами происходит тем интенсивнее, чем больше содержится в воде хлоридов, сульфатов, агрессивной углекислоты и щелочей. Агрессивность подземных вод

предопределяется также и водородным показателем среды.

При повышении температуры в обычных условиях коррозия бетона и железобетона усиливается, так как более активно протекают химические и физические процессы, приводящие к разрушению материалов вследствие снижения их прочности при взаимодействии с компонентами агрессивной среды.

ВЛИЯНИЕ ИНЖЕНЕРНО-ХОЗЯЙСТВЕННОЙ ДЕЯТЕЛЬНОСТИ НА РЕЖИМ ПОДЗЕМНЫХ ВОД

Инженерно- хозяйственная деятельность весьма разнообразна и имеет специфическое воздействие на геологическую среду (подземное пространство). В зависимости от техногенных факторов можно выделить:

- взаимодействие подземных вод с гидрографической сетью города (арыков, каналов), которая не остаётся постоянной во времени;
- переформирование рельефа при перепланировке городской территории;
- ухудшение гидрогеологических условий после строительства крупных жилых массивов с большой плотностью зданий, вследствие резкого увеличения потерь воды из водопровода, теплотрасс, канализации, от поливов огородов, садов и зелёных зон;
- строительство и эксплуатация метрополитена;
- водозаборы, очистные сооружения, дренажи.

СВЯЗЬ ПОВЕРХНОСТНЫХ ВОДОТОКОВ С ПОДЗЕМНЫМИ ВОДАМИ

Вопрос о влиянии водотоков на подземные воды по территории г.Ташкента возник в семидесятые годы XX века. В 1970-73 годах Кечкурукской ГГП (2) была предпринята попытка установить связь поверхностных водотоков с подземными водами. На водотоках по территории города было проложено 11 створов по нормали к каналам или арыкам, в которых были оборудованы реечные посты. В течение трёх лет были организованы режимные наблюдения по скважинам, пробуренным в этих створах. . К сожалению только по четырём створам сохранились данные замеров по реечным постам. Все интересующие нас створы рассмотрим в направлении течения каналов с СВ на ЮЗ.

СТВОР I-I

Створ I-I располагается примерно в 900 м ниже Бурджарской ГЭС, на участке Национального парка. В состав створа входит 5 скважин. Створ проходит через каналы Анхор и Бурджар. По данным режимных наблюдений канал Анхор «подвешен» на 10-12 м относительно подземных вод. Взаимодействие поверхностного водотока Бурджар с подземными водами следующее. По мнению НПО Узбекгидрогеология канал с правого борта дренирует поток подземных вод, а левым бортом-подпитывает. По нашему мнению, поток подземных вод, ориентированный с СЗ на ЮВ, «проскакивает» под каналом с градиентом 0,006-0,009. Поскольку урез воды в канале в любое время года выше, чем подземные воды в непосредственной близости от канала, поверхностные воды круглогодично подпитывают подземные воды.

Вблизи канала Бурджар УПВ фиксировался на глубине 12-14 м, в водораздельной части – 13-18 м. С удалением от канала амплитуды годовых колебаний подземных вод увеличиваются с 0,6 до 2,0м. Наиболее низкое положение УПВ – в марте, наиболее высокое – в июле.

СТВОР II – II

Западнее озера Национального парка, вдоль проспекта Дружбы Народов, располагается створ II – II, состоящий из 7 скважин, который проходит через каналы Зах и Актепе.

Канал Зах подвешен на 20 м и может незначительно подпитывать воды только"дождеванием". Канал Актепе круглогодично подпитывает подземные воды. В летние месяцы (июль), когда наполнение канала максимальное, а уровни подземных вод занимают минимальное положение, за счёт больших градиентов ширина положения влияния канала наибольшая и подпитывание из канала максимальное. В весенние месяцы (апрель), когда подземные воды занимают наиболее высокое положение (при наиболее низком урезе канала), они подпирают фильтрационный поток из канала и подпитка из канала уменьшается.

Взаимодействие подземных вод с каналом Актепе на участке Актепинской ГЭС специалистами института Гидропроект оценивается следующим образом. Поток подземных вод имеет такое же направление как канал Актепе (почти с востока на запад). При

подходе к гидроузлу, на участке напорного бассейна ГЭС, отметка УПВ составляет 410-412 м . Перед напорным бассейном урез воды в канале в разрезе года колеблется от 428,5 до 429,3 м, следовательно, при глубине канала около 3 метров подземные воды залегают ниже дна канала на 13-16 м, т.е. канал Актепе "подвешен" и питает подземные воды "дождеванием" .

Всё описанное относилось к взаимодействию поверхностных водотоков и подземных вод в пределах IV надпойменной террасы.

На I и II террасах, в зоне влияния реки Чирчик и каналов Карасу и Салар, наблюдения за режимом подземных вод и их взаимодействием с поверхностными водотоками проводятся по скважинам института "Ташкент-Тадкикот" (ныне Ташкентский городской филиал ГУП УзГАШКЛИТИ) (с 1978 г.) и Центра гидроминеральных ресурсов (бывш. ГГП Узбекгидрогеология). По данным Центра гидроминеральных ресурсов (2) в полосе шириной 3,0-3,5 км фиксируется влияние режима реки Чирчик на режим подземных вод. В период весенне-летнего подъёма река питает подземные воды и амплитуды годовых колебаний УПВ составляют 3-5 м. С удалением от реки их величина уменьшается и на границе зоны влияния реки составляет 0,8-1,0 м.

По данным Ташкентского городского филиала ГУП УзГАШКЛИТИ вдоль улицы Новосергелийской годовые амплитуды колебания УПВ составляют 1,0-2,8 м. Вдоль Ташкентской кольцевой автодороги отмечаются наибольшие амплитуды колебаний, которые достигают 2,8-4,5 м. Севернее кольцевой автодороги амплитуды уменьшаются и составляют 0,9-2,2 м. По всем скважинам в долине реки минимальное положение УПВ фиксируется в марте – апреле, а максимальное – в июне – июле, повторяя режим реки Чирчик.

Влияние поверхностных водотоков Бозсу, Нижний Бозсу и Каракамыш неоднозначно. Рассматривая гидродинамическую обстановку вдоль канала Бозсу, следует отметить, что вниз по течению, канал Бозсу дренирует подземные воды с правого и левого берега вплоть до Аквапарка. Ниже по течению канала он подпитывает подземные воды (Саларская ГЭС, Бурджарская ГЭС). Амплитуды колебания УПВ вблизи канала Бозсу составляют 1,0-3,0 м.

Канал Нижний Бозсу на всём протяжении выполняет роль дрены, также как арыки, образующие его. Канал Нижний Бозсу глубоко врезаясь в русло, местами обнажает каменные лёссы нижнечетвертичного возраста.

Канал Каракамыш является дреной для северо-западной окраины города. Поверхностный сток канала формируется за счёт дренирования инфильтрационных поливных вод из-за пределов города, грунтовых и сточных вод.

В зоне влияния канала режим подземных вод довольно сложный, т.к. в пределах массивов Юнус-Абад и Каракамыш работают дренажи, которые накладывают отпечаток на режим подземных вод. В пределах Юнус-Абада и Каракамыша в долине канала Каракамыш, режим техногенный с максимумом в марте. При удалении от дренажных сооружений наблюдается до 10-12 циклов подъёма-снижения уровня. Годовые амплитуды изменения уровня чаще всего от 0,5 до 1,0м.

СТВОР III - III

Вниз по течению канал Бозсу, ниже Аквапарка, именуется канал Анхор. На канале Анхор в районе памятника «Матонат» заложен створ III - III из 5 скважин. По данным режимных наблюдений канал «подвешен» относительно УПВ на 8,8-10,0 м, ограниченно питает подземные воды «дождеванием». Годовые амплитуды колебаний УПВ составляют 0,6 м вблизи канала и до 2,0 метров при удалении от него. Несколько ниже по течению на канале Анхор располагается Бурджарская ГЭС, располагающая сетью режимных скважин, для решения собственных проблем. В верхнем бьефе гидроузла нами выбран створ из шести скважин, ориентированный нормально к каналу Анхор. В створе расположены 3 скважины глубиной по 5-7 м и 3 скважины глубиной от 24 до 29 м.

Бурением установлено, что под дном канала и его бортах залегают илы серовато-зелёного цвета мощностью 6-14 м. Мелкие скважины остановлены в илах. По этим скважинам в теле дамбы (левый и правый) зафиксированы уровни воды, фильтрующейся из канала. Это первый от поверхности, спорадически развитый водоносный горизонт, имеет инфильтрационное питание из канала. Вероятно, это локальное явление, связанное с присутствием илов в верхней части разреза. Водоносный горизонт, приурочен к среднечетвертичным суглинкам ($pQ_{II}ts$. Глубина до УПВ в период максимума 21,6 м– 19,8 м.

Таким образом, подземные воды располагаются на 18 метров ниже дна канала, канал «подвешен» и может незначительно питать подземные воды «дождеванием».

По данным института Гидропроект на участке Бурджарской ГЭС подземные воды располагаются на отметках 433,0 м (напорный бассейн) и 432,3 м (здание станции). Направление потока подземных вод с СВ на ЮЗ градиентом около 0,009. Выемка под напорные трубопроводы и здание станции искажает поток на этом участке, указывая на дренирующее воздействие сооружений ГЭС. Канал Анхор выше регулирующих щитов в верхнем бъефе, имеет из года в год зарегулированные отметки в пределах 454,2-452,6м, т.е. в течении года колебание уреза воды в канале Анхор составляет 1,6 м.

СТВОРЫ IV-IV и V-V

Наблюдениями в створах IV-IV и V-V в северо-восточной части города охарактеризовано взаимоотношение подземных вод с водотоками Бозсу и Салар. На участке створа V-V поток подземных вод подходит с северо-западного берега канала Бозсу под острым углом и с большими градиентами, которые сохраняются вниз по потоку вплоть до канала Салар, на расстоянии примерно 770м.

На этом участке градиенты потока подземных вод составляют в среднем 0,02. Это самый большой уклон поверхности подземных вод на всей территории города, который обусловлен малой мощностью водоносного горизонта (pQ_{II} ts), т.к. на этом участке на дневную поверхность выходят слабопроницаемые отложения N_2 - Q_I. Поток подземных вод дренируется правым бортом канала Бозсу, а левым бортом питает подземные воды. Канал Салар дренирует подземные воды.

ПЕРЕФОРМИРОВАНИЕ РЕЛЬЕФА ГОРОДСКОЙ ТЕРРИТОРИИ И РЕЖИМ ПОДЗЕМНЫХ ВОД

Интенсивность изменения рельефа в пределах города различна. К наиболее изменённым отнесена юго-западная часть города, где густота расчленения рельефа, начиная с 1966 года, снижена почти в 4 раза. Интенсивное изменение рельефа отмечено в северной, северо-восточной и западной частях города, где густота расчленения рельефа снижена примерно в 3 раза. Изменение рельефа в центральной части города, за период с 1966 года незначительное и связано с нивелированием ранее засыпанных оврагов и балок. Мощность техногенных грунтов достигает 15 м.

Практически не изменён рельеф в пределах долины р. Чирчик. Мощность техногенных отложений здесь локально достигает 2 м.

Подпор подземных вод в результате ликвидации (засыпки) отрицательных форм рельефа должен сниматься устройством дренажей в овражно-балочной сети. Дренаж должен быть корректно рассчитанным и выполненным точно по проекту. К сожалению это не всегда выполняется. Вероятно фильтрующий материал по грансоставу не соответсвует проектному, вследствие чего происходит суффозия грунта, либо кольматация фильтра.

При засыпке долины Джангох в 1985-86 годах выполнен дренаж. Его эффективность оценивается снижением уровня подземных вод по наблюдательной скважине на 6 м. Однако, начиная с 1989 года дренирующая способность сооружения снижается и в течение 1989-90 годов происходит подъём уровня на 5 м. Созданный подпор развивается вверх по долине. При этом по скважине, расположенной в верховье долины, отмечается подъём УПВ примерно на 1 м. Таким образом, дренаж проработал эффективно только 3 года.

Зона подтопления в долине Чорсу связана с ликвидацией эрозионного вреза с засыпкой его техногенным материалом. В верховьях долины построен стадион Пахтакор, позднее Телецентр, линии метрополитена со станциями Пахтакор и Навои, здание ГУМа и спортивно оздоровительный комплекс «Жар».

Зоны подтопления с глубиной до воды 4,5 месторождение формируются в долинах оврагов Чукур и Зах, которые освоены и по дну которых проложен закрытый горизонтальный дренаж.

В юго-западной части города в долине Чупаната, и в пределах 25 квартала Чиланзара сформировались зоны подтопления с медленным подъёмом УПВ. В нижней части долины канала Анхор существует зона подтопления, приуроченная к оврагам, погребённым под техногенные отложения. В шестидесятые годы XX века в этой зоне УПВ располагался на глубинах 22-25 месторождение, в настоящее время – на 8,6 м.

В юго-западной части, по границе с каналом Анхор, сформирована зона

техногенных отложений, вытянутая полосой 100-250 месторождение, а в районе Отчопар – до 1000 месторождение, протяжённостью более 6 км, от ул. Чупаната до Отчопар.

Останцы глубоких оврагов Бурджар, заполненные водой, при застройке массива Чиланзар были заполнены строительным мусором. По данным режимных наблюдений в результате строительных работ произошёл подъём уровня на 6,3 м.

Таким образом, во всех ликвидированных оврагах и балках развивается подпор подземных вод. В связи с таким положением дел необходима экспертиза проектов и осуществление жёсткого авторского надзора, особенно при укладке в дрену фильтрующего материала.

При планировке территории города происходит и обратный процесс – прорезка и срезание поверхности. Глубина или мощность срезаемой толщи достигает до 10м, что видно на фотографиях, снятых в районе Отчопар (фото 2-4).



Фото 2 (Фото А.Сапарова)



Фото 3 (Фото А.Сапарова)



Фото 4 (Фото А.Сапарова)

Роль остальных факторов, вызванных инженерно-хозяйственной деятельностью человека из-за ограниченного объема статьи считаем целесообразным рассмотреть в другой статье.

ЛИТЕРАТУРА:

1. Азизов У.А. Отчёт Хамзинской ГГП «Результаты эколого-гидрогеологических и инженерно-геологических исследований и картография г. Ташкента в пределах его перспективных границ» за 1992-97 гг.
2. «Анализ гидродинамической обстановки на гидроэлектростанциях Ташкентского каскада». Гидропроект, 1997 г. Фонды ОАО «Гидропроект».
3. Бородина Г.А. и др. Отчёт Кечкурукской гидрогеологической партии «Результаты гидрогеологических исследований по изучению режима подземных вод г. Ташкента» за 1970-73 года. Фонды «Ташкент-Тадкикот»

4.Изучение причин подтопления территории г. Ташкента и разработка мероприятий по их устранению за 1988 г., 1989-1990 г.г.. и 1990 г. Фонды «Ташкент-Тадкикот».

5.О т ч ё т по теме: «Создание и ведение мониторинга подземного пространства для прогноза аварийных деформационных явлений и подтоплений (режимные и гидротермические наблюдения)».2000г. Фонды «Ташкент-Тадкикот».

6.Худайбергенов А.М. «Инженерно- геологические условия северо-западной части Ташкентского геодинамического полигона в связи с сейсмическим микрорайонированием и районной планировкой строительства», 1977 г. Фонды «Ташкент-Тадкикот».

7.Чиркин О.М. и др. «Результаты геологической и инженерно-геологической съёмки масштаба 1:25000 на территории г. Ташкента (листы К-42-91-Г-в, К-42-91-В-г, К-42-103-Б-а)» Отчёт Чинабадской инженерно-геологической партии за 1966-67 года. Фонды «Ташкент-Тадкикот».

Исследование закономерностей распространения лессовых пород по долине реки Чирчик на базе современных информационных технологий

М.Ш.Шерматов, А.С.Хусамитдинов
«ИС АН РУз», Ташкент, Узбекистан

Б.Т.Курбанов, И.И.Усманходжаев
«УзГАШКЛИТИ» ДУК, Ташкент, Узбекистан

АННОТАЦИЯ: В статье приведены результаты проведенных в 2009-2011гг. инженерно-сейсмогеологических исследований с использованием фондовых и литературных материалов на базе применения современных ГИС-технологий, разработана цифровая «Схематическая карта прогноза просадочности лёссовых территорий долины реки Чирчик».

Современная методология прогноза землетрясений базируются на результатах исследований физики сейсмогенных процессов и феноменологии сопутствующих им аномальных проявлений природы. Акту непосредственного разрушения сейсмического очага предшествует этап подготовки от нескольких до десятка лет в зависимости от объема очага. В этот период под действием приложенных напряжений, зона будущего разрыва испытывает аномальные деформации. Магистральный разрыв происходит при достижении аномальных деформаций относительной величины 10^{-4}. Динамика деформаций в ходе подготовки землетрясения испытывает несколько этапов связанных с качественно различающимися фазами трещино-образования, которые обусловлены динамикой земной коры. В настоящее время установлены корреляционные зависимости между магнитудой землетрясения и длительностью предвестниковых аномалий геофизических и гидрогеологических параметров. Поскольку они являются вторичными эффектами аномальных деформаций, в виду их неоднозначной обусловленности от неоднородной структуры геологической среды, установление истинных зависимостей становится проблематичным. Инженерные геологические условия конкретной местности, оказывая воздействие на интенсивность сотрясения и изменяя интенсивность сотрясения до I= ± 2 баллов, играют важную роль при сейсмическом районировании территории, выработке рекомендаций по строительству промышленных и гражданских объектов.

Одним из основных факторов воздействия является распространение и просадочность лессовых пород. Оценка потенциальной сейсмической опасности, сейсмического районирования с учетом инженерно-геологических условий территории, закономерностей распро-странения и просадочности лессовых пород на современном уровне представляет собой сложную, многоплановую, требующую комплексного, научно обоснованного подхода проблему. В современных условиях реализацию такого сложного проекта в масштабах республики целесообразно проводить на базе современных информационно-коммуникационных технологий, включая геоинформационные (ГИС) технологий, GNSS –технологии и технологии использования материалов дистанционного зондирования. Реализация ГИС позволит решать в автоматизированном режиме комплекс задач, связанных оценкой потенциальной сейсмической опасности и с прогнозом землетрясений, принятием оптимальных решений с учетом инженерно-геологических условий анализируемой территории, с минимизацией ущерба от возможного землетрясения, в том числе:

- возможность оперативного получения полной информации о потенциальной сейсмической опасности любого района на территории республики;
- возможность совершенствования и автоматизации ведения банка данных о потенциальной сейсмической опасности территории с учетом инженерно-геологических условий;
- возможность разработки цифровых карт прогноза и сейсмического районирования;

• возможность оперативного предоставления потребителю запрашиваемой информации в удобном для него виде и др.

Успешная реализация ГИС возможна при грамотно спроектированной автоматизированной системе с учетом современных возможностей информационных систем, технической, технологической и кадровой обеспеченности, местных условий и реалий. Это позволит сэкономить бюджетные средства, трудозатраты на строительство промышленных и гражданских объектов, минимизировать ущерб от возможных негативных последствий землетрясений. На решение указанных проблем направлено данное исследование.

Распространение, генезис, вещественный состав и инженерно-геологические свойства лессовых пород региона изучены Г. А. Мавляновым и др [1], Вороновым [2], Х.А. Аскаровым [3], А.И. Исламовым [4], А.М. Худайбергеновым [5], М.Ш. Шерматовым [6], Э.В. Кадыровым [7], и многими другими.

Анализ результатов исследований вышеуказанных авторов, а также детальное изучение лессовых пород региона показывает, что они развиты довольно широко и представлены элювиальными, элювиально-делювиальными, делювиальными, делювиально-пролювиальными, аллювиально-пролювиальными, пролювиальными, аллювиальными и техногенными генетическими типами, различающимися между собой по возрасту, положению в рельефе, характеру распространения, мощности, вещественному составу, водно-физическим, деформационно-прочностным, просадочным и сейсмическим свойствам.

В их распространении существуют определенная вертикальная зональность и выделяются 3 зоны [6]:

Первая зона – зона сплошного распространения лессовых пород охватывает пространство от поймы рек Сырдарья, Чирчик и Келес до абсолютной отметки 1000-1100м., местами снижаясь до 750-800м. и поднимаясь местами до 1250м. Здесь возраста лессовых пород - голоценовый (сырдарьинский комплекс - Q_{IV}^{sd}), верхненеоплейстоценовый (мирзачульский комплекс – Q_{III}^{ml}), средненеоплейстоценовый (ташкентский комплекс - Q_{II}^{ts}) и нижненеоплейстоценовый (нанайский комплекс - Q_{II}^{n}). Голоцен и верхненеоплейстоцен представлен аллювиальными лессовидными суглинками и ими сложены I, II, III террассы Чирчика, Келеса, Сырдарьи и развиты преимущественно в пределах абсолютных отметок от 320 до 500-600м. и до 800-1250м. в долинах их притоков, мощность которых изменяется от 0,5-3м. (голоцен до 15-18м.) (верхненеоплейстоцен), залегают на галечниках и гравийно-галечниковых образованиях. Средненеоплейстоцен представлен пролювиальными, делювиально-пролювиальными лессами и лессовидными суглинками и приурочен к предгорным пролювиальным равнинам (соответствующим IV, V, VI террассам) и высокогорным частям региона. Максимальная мощность лессовой толщи доходит до 80-90м. Подстилаются галечником, конгломератами и каменными лессами. Нижненео-плейстоцен представлен лессовидными суглинками, каменными лессами. Они в основном ближе к горам обнажаются на дневной поверхности, а ближе к речным долинам уходят под отложения среднего неоплейстоцена. Только отдельные их выходы наблюдаются в районе ТашГРЭСа, Кадырьи.

Вторая зона характеризуется островным распространением лессовых пород, в геоморфологическом отношении соответствует высокопредгорной частям региона и охватывает начиная с абсолютной отметки 1000-1100м до 1800м. Здесь преимущественное распространение имеют делювиальные, делювиально-пролювиальные, элювиальные, элювиально-делювиальные генетические типы лессовых пород. Возраст их средненеоплейстоценовый, верхненеоплейстоценовый и голоценовый. Они подстилаются преимущественно на эоплейстоцене, верхнем плиоцене и местами других возрастных комплексов до четвертичных пород. Максимальная мощность (до 20-30 м даже до 80-90м) свойственна для делювиальных, делювиально-пролювиальных генети-ческих типов. Мощность элювиальных, элювиально-делювиальных лессовых пород не превышает 1-3м и 5-10 м. Характерной особенностью лессовых пород этой зоны является то, что почти 90% склоновых (оползневых) процессов региона приурочены именно к этим генетическим типам пород. Работы по этим частям исследований выполнены Р.А. Ниязовым [8], М.Ш. Шерматовым [9].

Третья зона - зона незначительного распространения лессовых пород занимает среднегорную и высокогорную части

территории, начиная с абсолютной отметки 1800-1850м. и выше. В основном возраст лессовых пород зоны голоценовый (сырдарьинский комплекс – Q_{IV}^{Sd}), редко верхненеоплейстоценовый (мирзачульскии комплекс –Q_{III}^{ml}), характеризуется распространением аллювиальных, элювиальных, делювиальных, элювиально-делювиальных (на склонах гор) генетических типов лессовых пород, небольшой мощности 0,25-5м. Такой характер распространения и формирования различных генетических и возрастных типов лессовых пород взаимосвязаны определенными фазами тектонических движений и циклами аккумуляции исходного лессового материала. Каждый цикл аккумуляции характеризуется формированием террассовых поверхностей (уровней) и образованиям палеопочвы. Древние палеопочвы, имеющие распространение в толще лессовых пород региона, рассматриваются в работах Ю.А. Скворцова, Я.М. Гусака, Я.М. Насырова, Ю.А. Скворцова Н.И. Кригера, М.Р. Москалева, М.Ш. Шерматова, Э.В. Кадырова, М.Ш. Шерматова, И.Н. Степанова, У. Абдуназарова, А.Е. Даданова, А.А Лазаренко, И.Н. Степанова, У.К. Абдуназарова, Н.Г. Мавлянова, В.Т. Трофимова, С.Д. Балыкова, Т.В. Андреева и др. Их гранулометрический, солевой, воловой, минералогический состав, водно-физические, просадочные и прочностные свойства были изучены М.Ш. Шерматовым [6], Н. Г. Мавлянновым [10].

На основе проведенных инженерно-сейсмогеологических исследований и использования фондовых и литературных материалов на базе применения современных ГИС-технологий нами разработана цифровая «Схематическая карта прогноза просадочности лёссовых территории долины реки Чирчик».

Процедура создания и обновления карт на основе ГИС-технологий существенно более проста по сравнению с традиционными методами. Нами были разработаны цифровые карты прогноза просадочности лёссовых территорий на основе материалов дистанционного зондирования и результатов геодезических измерений. На начальном этапе была разработана цифровая топооснова масштаба 1:500000. В дальнейшем на топооснову накладывается тематическая нагрузка. В качестве топоосновы служили топографические карты последних лет изданий.

Использование цифровых карт в электронном виде предоставляет более широкие возможности по сравнению с использованием карт, выведенных на бумажный носитель.

Карта была представлена в векторном формате, что представляет ряд удобств и дополнительных возможностей анализа и обработки картографической информации. Возможность послойного представления картографической информации создает ряд дополнительных удобств для анализа, позволяя включать или выключать из рассмотрения отдельные тематические слои. При увеличении картографического изображения, представленного в векторном формате, качество его зависит ос качества оцифровки.

Специальные средства ГИС позволяют проводить аналитическую обработку данных, а в более сложных случаях - моделирование реальных событий. При этом результаты работы модели могут быть представлены на экране монитора или выведены в виде твердой копии. В отдельных случаях в ГИС-проекте могут быть реализованы системы экспертной поддержки, способствующие поиску и выработке наиболее оптимальных управленческих решений.

Многие из упомянутых задач могут решаться и решались ранее без использования ГИС-средств. Использование ГИС позволяет с большой эффективностью и удобством для пользователя организовать в единый комплекс операции ввода и обновления исходной информации, ее переработки и отображения результатов, решать задачи так называемого пространственного анализа.

Применение ГИС-технологий дает возможность:

- существенно повысить оперативность всех этапов работы с пространственно-распределенными данными, начиная от ввода исходной информации, ее анализа и до выработки рекомендаций по принятию управленческих решений;
- использовать современные электронные средства геодезии и системы глобального позиционирования (GNSS), что позволит располагать оперативной информацией высокой степени точности.

Тематические, инструментальные и технологические компоненты ГИС могут формироваться при наличии должного картографического обеспечения и мониторинга состояния территорий, системы

распределенных баз данных с защищенной виртуальной корпоративной системой связи в региональной сети, с возможностью подключения к глобальной сети ИНТЕРНЕТ. Освоение технологии цифрового картографирования – главное и определяющее направление успешного создания широкопрофильной тематической ГИС.

Привлекательность ГИС состоит в представлении информации на картографическом фоне, что способствует повышению уровня восприятия, обработки и анализа информации при подготовке материалов для принятия управленческих решений, обеспечивает комплексное и наглядное представление информации с ее территориальной привязкой, позволяет наглядно отобразить динамику процессов и явлений, а также осуществить их моделирование. В то же время эффективное использование ГИС невозможно без использования научных разработок и подходов к решению поставленных проблем. Это, прежде всего, опыт разработки различных систем АСУ, использование разработок в области тематического геолого-сейсмологического картографиирования, методов создания оценочных и синтетических карт с использованием материалов дистанционного зондирования и современных компьютерных методов их обработки, разработки цифровых и электронных карт. [11-12].

Эффективность от использования ГИС не всегда очевидна, учитывая затраты на ее создание, и может быть выражена в следующих аспектах:

- снижение основных затрат от ведения и обновления БД, риска необоснованности принимаемых управленческих решений;
- применение вычислительных платформ и программного обеспечения, защищенных от несанкционированного доступа;
- одновременная обработка информации с большой территории в едином масштабе с высокой производительностью растровых и векторных операций, в том числе в реальном масштабе времени;
- возможное расширение от первоначально планируемой области применения до использования в других областях с расширением круга решаемых задач;
- многократное использование геоинформационной системы в интересах растущего круга пользователей, возможность ее использования в сети;
- повышение качества выходной продукции и производительности труда за счет использования высоких наукоемких технологий;
- повышение качества и оперативности принимаемых управленческих решений за счет более высокой объективности и качества используемой информации и др.
- На разработанной цифровой «Схематической карты прогноза просадочности лёссовых территории долины реки Чирчик» выделены следующие типы территории просадочности:
- очень сильнопросадочные с ожидаемой величиной просадки до 1,5;2);
- сильнопросадочные территории с ожидаемой величиной просадки до 1 м, местами и более 1 м;
- среднепросадочные с ожидаемой величиной просадки 0,5 до 1 м;
- слабопросадочные с ожидаемой величиной просадки от 0,15 до 0,5 м;
- очень слабопросадочные с ожидаемой величиной посадки от 0,005 до 0,15 м;
- непросадочные территории с величиной просадки менее 0,05 м.

На рис.1 представлена цифровая Схематической карте прогноза просадочности лёссовых территории долины реки Чирчик, разработанная в масштабе 1:500000. На рис.2 представлен фрагмент данной карты. Данная карта в дальнейшем будет использована при разработке ГИС современной геодинамики и оценки сейсмической опасности с разработкой основных процедур ГИС.



Рис.1. Схематическая карта прогноза просадочности лёссовых территории долины реки Чирчик



Рис.2. Фрагмент схематической карты прогноза просадочности лёссовых территории долины реки Чирчик

Реализация ГИС позволит решать в автоматизированном режиме комплекс задач, связанных оценкой потенциальной сейсмической опасности и с прогнозом землетрясений, принятием оптимальных решений с учетом инженерно-геологических условий анализируемой территории, с минимизацией ущерба от возможного землетрясения, в том числе:

- возможность оперативного получения полной информации о потенциальной сейсмической опасности любого района на территории республики;
- возможность совершенствования и автоматизации ведения банка данных о потенциальной сейсмической опасности территории с учетом инженерно-геологических условий;
- возможность разработки цифровых карт прогноза и сейсмического районирования;
- возможность оперативного предоставления потребителю запрашиваемой информации в удобном для него виде и др.

ЛИТЕРАТУРА

1. Мавлянов Г.А. Генетические типы лессов и лессовидных пород Центральной и Южной части Средней Азии и их инженерно-геологические свойства. Ташкент, 1958
2. Воронов Ф.И., Дмитриев В.Л. Просадочные явления в лессах Приташкентского района (по правобережью р. Чирчик). Ташкент, 1940.
3. Аскаров Х.А. О глубине залегания просадочных лессовых грунтов и методах оценки просадочности. Фонды Института сооружений, Ташкент. 1955
4. Исламов А.И. Изменение некторых физико-механических свойств лессовых пород после просадки. Узб. Геол. Журнал №2, 1963.
5. Худайберганов А.М. Инженерная геология городов правобережья р. Чирчик. Ташкент, «Фан», 1980,191 с.
6. Шерматов М.Ш. Инженерно-геологические свойства лессовых пород Чаткальской горной области. Изд-во «Фан», Ташкент, 1971.
7. Кадыров Э.В. Лессовые породы: происхождение и строительные свойства. Ташкент, 1979.
8. Ниязов Р.А. Оползни в лессовых породах. Ташкент, Фан, 1974.
9. Шерматов М.Ш. Экзогенные геологические процессы Срелнного Тянь-Шаня и главные факторы, определяющие их проявление и развитие. Узб. Геол. Журн. №3, 1987, с.45-50.
10. Мавлянов Н.Г. О формировании просадочностим лессовых пород Средней Азии./Инженерная геология лессовых пород/ тезисы Всесоюзного совещания. Т.1, Ростов-на-дону, 1989, с.20-21.
11. Курбанов Б.Т. Роль современных информационных систем в исследованиях окружающей среды. // Вестник НУУ, 2003. - №3. – с. 5-14.
12. Курбанов Б.Т., Самборский А.А. Роль и значение геоинформационного обеспечения при решении народнохозяйственных задач. Тезисы докладов Международного семинара «Новейшие геосистемы и технологии «TRIMBLE» для решения задач архитектуры, строительства и кадастра». Ташкент, 2004. с 10-14.

Разработка концепции схемы солеотводящих сетей бассейна реки Амударьи на базе интегрированных ГИС-технологий

Б.Т.Курбанов, А.Ш.Халматов
«УзГАШКЛИТИ» ДУК, Ташкент, Узбекистан

АННОТАЦИЯ. В статье анализируется актуальность и концептуальные основы разработки солеотводящих сетей бассейна р. Амударьи на базе интегрированных ГИС-технологий. Конкретизированы задачи, решение которых необходимо для достижения цели исследования.

В Республике Узбекистан площадь орошаемых земель составляет около 10%, давая более 90% сельскохозяйственной продукции. В последние годы острейшей проблемой для Республики Узбекистан стала усиливающаяся из года в год экологическая и демографическая нагрузка на землю. При сохраняющемся высоком приросте населения площадь орошаемых земель на душу населения неуклонно снижается и составляет на сегодня 0.17 га. Вместе с тем потенциал вовлечения в сельхозоборот новых орошаемых земель, пригодных для ведения сельского хозяйства, близок к исчерпанию. Наряду с указанным наблюдается постоянное снижение плодородия и возрастание загрязнения пахотных земель, снижение урожайности сельскохозяйственных культур. Одним из существенных факторов, ведущих к снижению урожайности, является вторичное засоление как следствие нерационального, недостаточно обоснованного с научной точки зрения использования водных ресурсов. При дефиците водных ресурсов, еще более обострившимся в новой геополитической обстановки в регионе, разработка схемы солеотводящих сетей и в первую очередь, его научно-технической основы, представляется актуальным, социально, экономически и экологически значимым для национальных интересов Узбекистана. Создание солеотводящих сетей призвано способствовать рациональному использованию водных ресурсов. устойчивому развитию сельского хозяйства в Республике Узбекистан в условиях дефицита водных ресурсов и ухудшения их качества.

Коллекторно-дренажные воды среднего и нижнего течения бассейна р. Амударьи не имеют единого стокоприемника и распластываются по всей площади бассейна. На этой территории по данным анализа материалов космических съемок сформировались и продолжают формироваться многочисленные локальные солеприемники. Они периодически высыхают, образовывая солончаковые поверхности. Такие образования в настоящее время занимают тысячи гектаров пастбищ и земель лесного фонда. Солончаки сами по себе не представляют интереса для кормопроизводства, в том числе не приносят пользы и диким животным. Эти накопленные экологические ущербы продолжают наращиваться, так как ежегодно с коллекторно-дренажными водами в местные солеприемники выносится до 10-15 миллионов тонн солей. Это только в среднем течении. Примерно такой же вынос солей наблюдается в нижнем течении. К тому же сброс коллекторно-дренажных вод в русло Акчадарьи приводит к расширению болотно-луговых угодий на территории Казахстана. Таким образом даже небольшая польза от отвода коллекторно-дренажных вод уходит за пределы страны.

Формируемый в среднем и нижнем течении р. Амударьи коллекторно-дренажный сток оценивается в кубокилометрах и он заслуживает внимания на предмет утилизации и устранения экологических ущербов. Целесообразность начала устранения наметившегося пробела очевидна. Причина, по которой проблема утилизации коллекторно-дренажных вод и устранения накопившихся экологических ущербов до сих пор не решается, заключается в отсутствии разработки научной концепции солеотведения в регионе и выявлении перспектив утилизации коллекторно-дренажных вод. Из этого положения формируется первоочередная цель по всей проблематике – разработать концепцию схемы солеотводящих сетей бассейна космических съемок. Эта цель достигается по территории Узбекистана.

Для достижения цели проекта планируется решение следующих задач:

- Уточнить объемы солеотведения с правобережных регионов Узбекистана в среднем и нижнем течении р. Амударьи;
- Оценка накопленного экологического

ущерба от засоления пастбищ и земель лесного фонда;

- Оценка текущего экологического ущерба от засоления речных вод в среднем и нижнем течении р. Амударьи;
- Сбор, обработка космических снимков среднего и высокого разрешения на анализируемую территорию;
- Разработка трехмерной модели местности на основе цифровых топокарт и космических снимков на анализируемую территорию;
- Выявление рациональных трасс солеотведения с Каршинского, Самаркандского, Навоийского и Бухарского оазисов и оазисов правобережья Каракалпакстана на основе анализа трехмерных цифровых моделей местности и ГИС-технологий;
- Оценка перспектив солеотведения в остаточные водоёмы Аральского моря-естественного солеприемника бассейна;
- Оценка эффективности охраны речных вод от засоления и загрязнения;
- Оценка перспектив утилизации маргинальных вод;
- Оценка перспектив солеустойчивого растениеводства, садоводства и лесозащиты на маргинальных водах;
- Обобщенная оценка социально-экологического солеотведения и утилизации маргинальных вод на правобережье р. Амударьи в пределах Узбекистана.

Методически и практически поставленная цель и намеченные задачи решаются традиционно на основе сбора и систематизации накопленной информации и проведения полевых изысканий.

Принципиальное отличие намеченной темы от аналогов заключается в том, что цель и задачи проекта впервые в республике решаются на базе интегрированных ГИС-технологий с применением методов трехмерного моделирования и использования материалов космических съемок высокого разрешения[1-3].

Как отмечалось выше, при дефиците водных ресурсов, еще более обострившимся в новой геополитической обстановки в регионе, разработка рациональной системы солеотведения, и в первую очередь, его научно-технической основы, представляется актуальным, социально, экономически и экологически значимым для национальных интересов Узбекистана. Разработка научнообоснованной основы солеотведения на базе современных интегрированных геоинформационных технологий, призвано способствовать рациональному использованию водных и земельных ресурсов. устойчивому развитию сельского хозяйства в Республике Узбекистан в условиях дефицита водных ресурсов и ухудшения их качества.

Анализ проводимых исследований показывает:

А). среднее течение Амударьи в среднем по водности год поступает около 30 млн тонн соли. Из них через территорию Узбекистана протекает около 20 млн тонн соли в год;

Б) со среднего течения Амударьи и средних и малых рек ее бассейна , а также Туркменистана в нижнем течении протекает около 20 млн тонн в год.

В). Солевой сток в Аральское море из Амударьи не фиксируется.

Лица, принимающие управленческие решения, получат инструмент, способствующий решению проблемы рационального солеотведения и устойчивого развития сельскохозяйственного сектора республики.

ЛИТЕРАТУРА

1.Kurbanov B.T., Lesnik T.Y. Water sources of the Republic of Uzbekistan: some problems. The Austria-Central Asia Centre for GISscience at the Kyrgyz State University of Construction, Transortation and Architecture and the Centre for Geoinformatics (Z_GIS), Salzburg University, Austria with support from the Eurasia-Pacific Uninet announce the Fourth Central Asia GIS Conference - GISCA'10 " Water: Life, Risk, Energy and Landuse" in May 27-28, 2010, Bishkek, Kyrgyzstan.

2.Курбанов Б., Лесник Ю., Магдиев Х. К вопросу оценки водообеспеченности территории Республики Узбекистан//Табиий ва иктисодий географик районлаштириш долзарб муаммолари (илмий-амалий конференция материаллари. Тошкент, 29-30 октябр 2004 йил). Тошкент,2004. с.203-205.

3.Курбанов Б.Т. Опыт использования материалов дистанционного зондирования Земли для сельскохозяйственного мониторинга. // Вестник НУУз, 2005, - №1. – с.103-107.

Применение современных информационных технологий при строительстве гидротехнических сооружений

Н.М.Джураев, А.С.Хусамитдинов, Ш.И.Ёдгоров
«ИС АН РУз», Ташкент, Узбекистан

Б.Т.Курбанов, Усманходжаев И.И.
«УзГАШКЛИТИ» ДУК, Ташкент, Узбекистан

АННОТАЦИЯ: В статье рассматриваются возможности применения современных интегрированных GIS- и GNSS технологий при разработке цифровых карт сейсмического микрорайонирования при проектировании и строительстве гидротехнических сооружений в зоне высокой сейсмичности.

Более 50 больших и малых водохранилищ, где могут произойти сильные, разрушительные землетрясения расположены в горной и предгорной зонах Узбекистана. Выбор оптимального места строительства гидротехнических сооружений (ГТС) – водохранилищ, с учетом природных условий, во многом определяет устойчивость сооружений и надёжность эксплуатации и геоэкологической безопасности. На практике проектирования ГТС – водохранилищ, как правило, выполняются много этапные исследования: технико-экономическое обоснование, технический проект и рабочий чертёжи. На ранней стадии проектирования выбираются наиболее вероятные варианты места расположения плотины в двух или трёх вариантах. Предварительная оценка сейсмической опасности основания водохранилища каждого варианта и их взаимное сравнение позволяет решить вопрос выбора наилучшего варианта расположения. На этом этапе, проведение исследований инженерно-геологических условий по оценке приращения сейсмической балльности от конкретных грунтовых условий помогает в оперативном порядке, предварительно, оценить каждый вариант выбранного створа политы. После выбора предпочтительного варианта, на стадии технического проекта, наряду с комплексными геолого-геофизическими исследованиями производятся инженерно-геологические исследования (ИГИ) по составлению инженерно-геологической основы (ИГО) сейсмического микрорайонирования (СМР). Работы по СМР завершаются составлением карты-схемы СМР, где указывается расчётный сейсмический балл для конкретных выделенных зон грунтовых условий и спектрально-частотный состав сейсмических колебаний вызываемых от реальных очаговых сейсмогенных геологических структур. Инженерно-геологические исследования для составления инженерно-геологической основы СМР в период проектирования, наряду с комплексными исследованиями, заключается в изучении состава, состояния и свойств грунтов основания и примыкающих к основанию участков, выявлении видов и характера проявления физико-геологических процессов и явлений. На основе изучения факторов формирования инженерно-геологических условий необходимо выделить участки, благоприятные и неблагоприятные, осложняющие условия строительства по инженерно-геологическим и сейсмическим свойствам грунтовых условий. Выделение и картирование этих участков с помощью GNSS систем позволит более точно и оперативно произвести инженерно-геологические исследовании. При этом важно особо отметить места, где могут произойти активизация процессов в момент землетрясения, даже при землетрясениях более слабых, чем расчетные. Опережение работ по составлению инженерно-геологической основы для СМР перед другим исследованием является обязательным с тем, чтобы к началу производства комплекса работ по СМР будут готовы оптимизация комплекса методов натурных наблюдений на площади ГТС. Инженерно-геологические исследования по составлению инженерно-геологической основы СМР для промышленно-гражданского строительства по территорию бывшего союза существенно развито и имеются ряд методические указаний (Рекомендации по сейсмическому микрорайонированию РСМ-73

(под редакцией Медведева С.В.). –Сб. «Влияние грунтов на интенсивность сейсмических колебаний» (Вопросы инженерной сейсмологии, вып. 15). Изд-во «Наука», 1973г., 6-34с.; Рекомендации по сейсмическому микрорайонированию при инженерных изысканиях для строительства, Москва, 1985г., с73 и эти вопросы частично рассмотрены в некоторых учебниках, как Сейсмическое микрорайонирование территории городов, населенных пунктов и больших строительных площадок / Заалишвили В.Б. [отв. Ред. А.В. Николаев]; Центр геофизических исследований Владикавказского НЦ РАН.- М.: Наука, 2009. –350с. (учебник для студентов горно-геологических и строительных специальностей, а также аспирантов, ученых и специалистов, занимающихся вопросами инженерной сейсмологии и сейсмостойкого строительства) и нормативных документах (Строительные нормы и правила СН и П II-7-81) и некоторые другие. Для СМР ГТС подобные рекомендации отсутствуют, а нормативный документ о необходимости проведения СМР территории ГТС указывается в ШНК 2.06.11-04 «Строительство в сейсмических районах. Гидротехническое сооружение» п.1.2. Госархитектстрой Республики Узбекистан, Ташкент, 2006г.

В Республике Узбекистан НИР по составлению инженерно-геологической основы СМР и оценке приращения сейсмической балльности от конкретных грунтовых условий для территории ГТС с применением GIS и GNSS технологий не проводлсь. Однако, подобные НИР без применении технологии GIS в Узбекистане и в частности Институте сейсмологи АН РУз имеются и коллектив института имеет определённый опыт в этом направления (Е.М. Бутовская, Г.А. Мавлянов, С.М. Касы-мовым, Н.М. Джураев, М.А. Туйчиева и др. Эти вопросы также рассматривались в ряде совещаний и семинаров (Ленинград, 1974, Симферополь, 1977, Ташкент, 1976, 1983, 1990, 2005 и др.). Учитывая уникальность, и высокую ответственность ГТС, расположенных в высокосейсмичной зоне, по сравнению с массовым промышленно-гражданским строительством, необходимость проведения подобных исследований с применением GIS и GNSS технологий (программно-технологический комплекс (ПТК) INTERGRAPH, ArcGIS и др.), очень высока. Особенности методики проведения СМР для ГТС- водохранилищ связана тем, что сооружения ГТС имеют большой зону влияния на геологическую среду в связи с чем и изменения геологической среды очень значительны по площади. Размеры сооружения соизмеримы с размерами сейсмических волн. Землетрясение большой силы приведет к несинхронным колебаниям отдельных частей – основания плотины и бортов примыкающих к ней, а также тело плотины, основание плотины и борта каньона в момент землетрясения будут испытывать напряженно-деформационные действия разного рода.

В качестве объектов исследований на базе применения GIS- и GNSS технологий применительно к настоящей работе, выбраны территории строительства следующих водохранилищ: Гиссаракского в Кашкадарьинской и Туполангского в Сурхандарьинской области, Чартакского и Чадакского водохранилищ в Наманганской области, расположенных в 8 и 9 балльной зоне сейсмичности. Для всех указанных водохранилищ в период проектирования проведены комплексные исследования и имеются материалы для составления цифровых карт-схем с использованием GIS технологий. В настоящее время из указанных водохранилищ полностью построены и эксплуатируются Чартакское и Гиссаракское водохранилища. Туполангское водохранилище находится на II стадии строительства и частично эксплуатируется, т.е. работает на неполной мощности. Чадакское водохранилище не было построено. С момента строительства этих водохранилищ прошло более 30 лет, и естественно, произошло изменение первоначальных инженерно-геологические условий. Однако, характер и степень изменения этих условий различны для каждого объекта исследования. Эти различия хорошо обнаруживается после проведения рекогносцировочных инженерно-геологических исследований на объектах с применением GNSS систем и составлением соответствующих цифровых карт-схем. В результате авторами планируется создание технологии комплексной оценки приращения сейсмической интенсивности землетрясений для конкретной площади ГТС- водохранилищ с использованием GIS и GNSS технологий, включая составление инженерно-геологической основы СМР. В процессе реализации проекта разрабатываются электронно-цифровые карты-схемы - инженерно-геологическая карта-схема

(как основы СМР) и карта-схема сейсмического микрорайонирования территорий водохранилищ.

Одной из основных целей использования ГИС-технологий при реализации указанного проекта является возможность с её помощью выработать наиболее рациональные, эффективные, оптимальные управленческие решения при возникновении чрезвычайной ситуации с угрозой для населения близлежащих территорий. Принимаемые управленческие решения могут быть оптимальными только в том случае, если они выработаны на базе достоверной информации и на основе использования научно-обоснованных методов. ГИС – это удобный инструмент в руках исследователя, способствующий процедуре более глубокого анализа ситуации в процессе обработки произведённого анализа и, в конечном счёте, нахождению наиболее эффективных и оптимальных управленческих решений. Функциональные возможности ГИС позволяют производить более детальный и глубокий анализ исходной информации, получить новые виды информационных продуктов, представленные в лаконичной картографической форме с дополнительными текстовыми пояснениями, таблицами, графиками, гистограммами и др. и выработать на основе их анализа более обоснованные управленческие решения. Представление информации в картографической форме упрощает процедуру анализа, позволяет просматривать различные варианты решения в более наглядной форме и даёт возможность выбора наиболее эффективных и оптимальных путей решения.

Уникальность, и высокая ответственность ГТС, расположенных в высокосейсмичной зоне, по сравнению с массовым промышленно-гражданским строительством, делает необходимым проведение исследований с применением с применением современных GIS и GNSS технологий и в первую очередь интегрированных ГИС и материалов дистанционного зондирования. . К настоящему времени творческой группой исполнителей проекта выполнен ряд исследований по составлению инженерно-геологической основы сейсмического микрорайонирования и сейсмическому микрорайонированию территории ряда (более 10) водохранилищ расположенных в 8 и 9 балльной сейсмичностью [1-4].

ЛИТЕРАТУРА

1. А.М. Худайбергенов, М.Ш Шерматов., М.А. Туйчиева, Н.М. Джураев. «Особенности формирования инженерно-геологических факторов сейсмического риска на урбанизированных территориях Ферганской долины на примере г. Наманган и его окрестностей». То же, как в п.44. Ташкент, 2009г. С. 128-131.
2. А.М. Худайбергенов, М.А. Туйчиева, Н.М. Джураев. Основные направления изменений геологи-ческой среды городских агломераций и актуальные задачи их изучения. Журнал Геология и минеральные ресурсы № 2 2010г, С. 55-60.
3. А.М. Худайбергенов Н.Г. Мавлянова М.А. Туйчиева, Н.М. Джураев, А.А. Каримов Закономерности развития геологических процессов в урбанизированных территориях и их влияние на устойчивость зданий и сооружений. Сб. Проблемы сейсмологии в Узбекистана №7 том II 2010 г, С. 250-254.
4. Хусомиддинов С.С., Курбанов Б.Т., Шерматов М.Ш., Хусомиддинов А.С. Оценка сейсмической опасности на основе современных информационных технологий. Геология и менеральные ресурсы Журнал 2010. №2

Оптимизация параметров свайных фундаментов под стены гражданских зданий

Мелиева Л.К.
«Кишлоккурилишлойиха» ,г. Ташкент, Республика Узбекистан
Усманходжаев И.И.
«УзГАШКЛИТИ» ДУК, г. Ташкент, Республика Узбекистан

АННОТАЦИЯ: В статье приводятся результаты работ по оптимальном ыболру параметров свайных фундаментов под стены зданий и сооружений.

Вопросам оптимального проектирования свайных фундаментов посвящены много работ, где излагаются методы определения оптимального шага свай, исходя из минимального объема свайного фундамента [1,2]. Однако в них имеются некоторые недостатки т.к:

- глубина погружения свай не превышает 7м.;
- грунт в пределах длины свай считается однородным;
- при определении несущей способности свай не учитывается глубина заложения ростверка.

Функциональная зависимость расчетных сопротивлений грунта аппроксимируется с погрешностью. С учетом перечисленных выше недостатков в данной работе предлагаются методика и алгоритм оптимального проектирования свайных фундаментов под стены гражданских зданий

Задачу оптимизации свайных фундаментов под стены можно сформулировать следующим образом.

Допустим, что заданы инженерно-геологическое условие строительной площадки, глубина заложения ростверка, характеристика материалов свай и ростверка, сейсмичность района строительства, отношение одного из экономических параметров на 1м^3 свай и ростверка, погонная нагрузка с учетом собственного веса грунта и ростверка по участкам лент фундаментов (рис1). При двухрядном расположении свай значение погонной нагрузки задается в два раза меньше.

Требуется минимизировать функцию Φ (объем материала) на 1пог.м. ленты фундамента

$$\Phi = \frac{F_c l_c}{L} + F_p Э \rightarrow min \qquad (1)$$

при ограничениях

$$N = gL \leq P_o \qquad (2)$$

$$P_o = m_1(\alpha_o + \alpha_1 x + \alpha_2 x^2) \qquad (3)$$

$$L_{min} \leq l_c \leq l_{max} \qquad (4)$$

$$d_{min} \leq d \leq d_{max} \qquad (5)$$

где : l – длина свай, м. равная

$$l_c = \left\{\sum_{i=1}^{n-1} h_1 + x - h_\phi\right\} \qquad (6)$$

где : F_p *и* F_c - соответственно площади ростверка свай, м^2

L- шаг свай, м;

$\alpha_0, \alpha_1, \alpha_2$ - коэффициенты т, т/м, и /тм^2 , аппроксимирующие несущей способности P_o одной сваи по грунту, значения которых определяются согласно табл. 1-3 [5] в зависимости от количества пройденных сваей слоев грунта ;

x - глубина заделки свай в толщу грунта, м.;

$\sum_{i=1}^{n-1} h_1$ - суммарная мощность слоев грнта, пройденных сваей до уровня отсчета x, м.;

$Э$ - отношение экономических параметров 1м^3 ростверка и свай ;

g - погонная нагрузка с учетом собственного веса грунта и ростверка, приходящегося на 1пог.м. длины ленты, т/м ;

L_{min} *и* l_{max} - соответственно минимальная и максимальная длины свай, м.;

d_{min} *и* d_{max} - то же, минимальный и максимальный диаметр свай, м.;

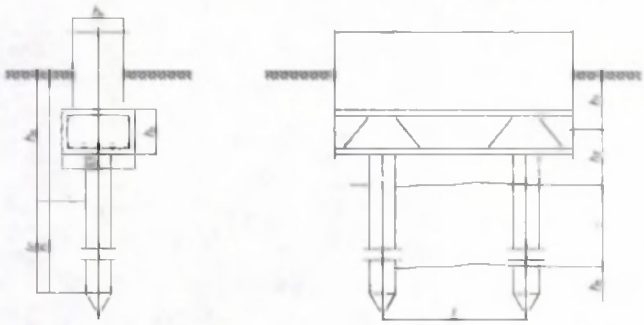
$m_1 = \frac{m}{kN}$ коэффициенты условий работы свай в грунте, принимаемый m=1;

kN - коэффициент надежности, принимаемый согласно [3]

Ограничение (2) требует, чтобы нагрузки, приходящиеся от веса стены и ростверка, не превышали несущей способности одной сваи, определяемой по формуле (3). Ограничения (4) и (5) соответственно требуют, чтобы длина и диаметр свай не выходили за предельные их значения.

Решение поставленной задачи считается законченным только тогда, когда

удовлетворяются ограничения (2-5) и достигается минимум функции цели (1).



К проектированию свайных фундаментов под стены приступаем, предварительно выбрав для данных грунтовых условий строительной площадки типовые размеры свай. При этом исходим из номенклатуры свай, изготовляемых в данном регионе и технической возможности строительных организаций по погружению свай.

Согласно [2], площадь ростверка F_p (1) линейно связана с расчетным пролетом L_p

$$F_p = C_1 L_p + в_p \delta$$

через постоянный коэффициент C_1, то есть

$$C_1 = \begin{cases} \dfrac{\sqrt{\dfrac{q\, в_p}{12\, A_0 R_{пр}}}}{\dfrac{2_q}{R_{пр}}} & \text{при } q \geq q_{гр} \quad (7) \\ & \text{при } q \geq q_{гр} \quad (8) \end{cases}$$

где L_p=*1,05 (L-d)* - расчетный пролет ростверка, м.;

A_0 -коэффициент, принимаемый равным 0,25м.;

$в_p$ - ширина ростверка, м.;

δ - расстояние от растянутой грани сечения до центра тяжести продольной арматуры ;

$R_{пр}$ - призменная прочность бетона ростверка,т/м^2.

Граничное значение погонной нагрузки $q_{гр}$ определим из условия равенства (7) и (8), как

$$q_{гр} = \frac{R_{пр}\, в_p}{48\, A_0}$$

Далее, заменив L_p = *1,05 (L - a)* и подставив (7) и (8) в функцию (1) получим

$$\Phi = \frac{F_s l_s}{l} + Э\left\{1{,}05 C_1 (L - d) + в_p \delta\right\} \quad (9)$$

При варьировании шагом L свай функции (9) достигаем минимума при $\frac{\delta \Phi}{\delta L} = 0$

Продифференцировав (9) по L, получим

$$\frac{\delta \Phi}{\delta L} = -\frac{F_c l_s}{L^2} + 1{,}05\, ЭС_1 = 0$$

или

$$F_c l_c = 1{,}05\, ЭС_1 L^2$$

откуда оптимальный шаг свай равен

$$L = \sqrt{\frac{F_c l_c}{1{,}05\, ЭС_1}} \quad (10)$$

Или соответствующая к нему длина свай

$$l_c = \frac{1{,}05\, ЭС_1 L^2}{F_c} \quad (11)$$

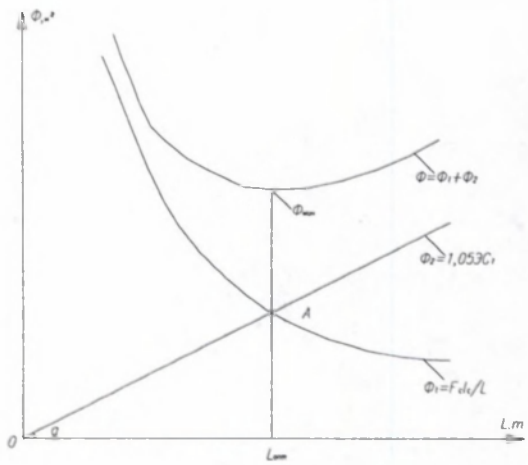


Рис. 2. Графики зависимостей Ф=f (L) расхода материалов фундаментов под стены.

Из выражения (10) следует, что оптимальным шагом L свай считается тот вариант, при котором достигается равенство между объемами одной сваи и 1пог.м. длины ростверка.

Далее для доказательства сказанного выше исследуем функцию от переменной L. Для этого вводим обозначению через

$$\Phi_1 = \frac{F_c\, l_s}{L} \text{ и } \Phi_2 = 1{,}05\, ЭС_1 L$$

Тогда функция (9) примет вид

$$\Phi = \Phi_1 + \Phi_2 \quad (12)$$

Исследование показало, что расход бетона свай Φ_1 изображается равносторонней гиперболой, а расход бетона ростверка Φ_2 прямой, проходящей через начало координат, причем тангенс угла наклона этой прямой относительно положительного направления оси абсцисс равен *1,05ЭС*$_1$. Оказывается, что минимум функции (12) суммарных затрат находится в точке пересечения линии Φ_1 и Φ_2. Полученный результат представлен на рис.2

Эти выводы можно сформулировать следующим образом : суммарные расходы Φ

минимальны для такого значения L, при котором расход материалов ростверка на 1пог.м. его длины равен расходу материалов, приходящемся на долю одной сваи.

Определим оптимальный шаг L свай. Для этого подставив (6) в (11) , получим зависимость в виде

$$x = \beta_1 L^2 - \beta \qquad (13)$$

где : $\beta_1 = \frac{1{,}05\,ЭС_1}{F_c}$ и $\beta = \sum_{i=1}^{n-1} h_1 - h_\phi$

а затем (3) в (2)

$$aL = a_0 + a_1 x + a_2 x^2 \qquad (14)$$

где : $a = gm_1$

Далее, подставив (13) в (14), получим многочлен в виде

$$AL^4 + BL^2 - CL + D = 0 \qquad (15)$$

где : $A = a_2\beta_1^2$; $B = a_2\beta_1 - 2a_2\beta\beta_1$;

$C - a$; $D - a_0 - a_1\beta + a_2\beta^2$

При однородном грунтовом слови значение $\beta = 0$.

Далее, решая (15) одним из численных методов, например, итерационным методом Ньютона

$$L_1 = L_0 = \frac{AL_0^4 + BL_0^2 - CL_0 + D}{4AL_0^3 + 2BL_0 - C} \qquad (16)$$

определим оптимальный шаг свай.

Процесс инерции (16) заканчивается только тогда, когда выполняется условие

$$/ L_1 - L_2 / \le \varepsilon_1$$

где : ε – заданная мера точности расчета.

При назначении первоначального шага L_0 исходим из следующих условий

$$L_0 = \begin{cases} \frac{c+\sqrt{c^2-4BD}}{2B} & \text{если } \sqrt{C^2 - 4B} > 0 \\ \frac{C}{2B} & \text{в противном случае} \end{cases}$$

В конечном итоге, определим L из (16), можно вычислить необходимую глубину заделки x свай из (13), общую длину свай из (6) и несущую способность P_0 одной сваи по грунту из (3). Высота ростверка определяется по формуле

$$h_p = C_1 L_p / b_p + \delta$$

Найденные значения L, l_c и h_p округляются до унифицированного их размера. Усилия и площади арматур в середине и на опоре ростверка вычисляются по соответствующим формулам 4.

Таким образом, нахождение оптимальных параметров (шага, длины, несущей способности и диаметра свай, а также высоты, усилий и площадей арматуры ростверка) свайных фундаментов под стены зданий и сооружений на висячих сваях осуществляется двумя этапами. На первом этапе при заданном диаметре свай находим шаг и длину свай, на втором – диаметр свай, для которого достигается минимум функции (9) на 1пог.м. длины ростверка.

В заключении можно сделать следующие выводы.

Порядок определения оптимальных параметров свайных фундаментов на сваях-стойках является частным случаем предлагаемого метода.

Оптимальным вариантом свайных фундаментов под стены является тот вариант, при котором расход материалов в ростверке на 1 пог. м. его длины равен расходу материалов, приходящемуся на долю одной сваи.

По разработанному алгоритму составлена программа создания пакетов прикладным программ фундаментов (ППП – фундамент), позволяющая определять оптимальные параметры (длину, шаг и диаметр свай, а также высоту, усилия и площади арматур ростверка) свайных фундаментов под стены гражданских зданий.

ЛИТЕРАТУРА:

1. Крутов В.Г. Номографический способ определения размеров свайных фундаментов под стены здания <Строительство и архитектура> № 6 1990
2. Борисов С.М., Козарь Н.А. Оптимальное проектирование фундаментов из коротких свай с монолитным ростверком для сельского строительство.<Основания, фундаментов и механика грунтов>, № 5, 1975.
3. КМК «Свайные фундаменты».
4. КМК «Бетонные и железобетонные конструкции».
5. Рахманов У. К., Ахмедов А.А. Методы аппроксимации несущей способности висячей сваи для оптимизации свайных фундаментов. Сб. научных трудов <Конструкции и инженерное оборудование гражданских зданий в Средней Азии> Тбилиси 1990.

Геоэкологические проблемы и инженерно-геологические условия южного Приаралья

Г.С. Дурдиева
Хорезмская академия Маъмуна, Узбекистан

Экологические проблемы связаны с изменениями исторически сложившегося геологического и гидрологического режима. В частности это подъём грунтовых вод и повышение в их составе концентрации солей, увеличение содержания влаги и соли в почве. Эти явления начали активно способствовать деформации конструкции и интенсивной эрозии стен и фундаментов памятников архитектуры.

Тревожащим фактором является то, что в конце концов обратные эффекты, возникшие в результате нарушения экологического баланса, начинают вредить место обитанию самого человека, в том числе и древним зданиям. Как результат в исторических городах начали возникать проблемы, связанные с деформациями памятников архитектуры, с интенсивным снижением из-за солевой агрессии прочности материалов цокольной части стен и фундаментов. Известно, что в процессе поднятия грунтовых вод возникает деформация поверхности земли. Это приводит к неравномерным осадкам гражданских и промышленных зданий, сооружений, а также исторических памятников архитектуры [3].

За последнее десятилетие возникли серьезные проблемы, связанные с сохранением всемирно известных шедевров архитектуры. В частности, засоленные грунтовые воды в силу своей агрессивности по отношению к строительным материалам в результате сложных физико-химических процессов начинают интенсивно эродировать подземные и надземные конструкции памятников, в результате чего часто происходит деформации, а в некоторых случаях и полное их разрушение. Как пример, можно принести катастрофическое разрушение некоторые глинобитных сооружение Каракалпакстана, сильные деформации у некоторых памятников комплекса «Ичан-Кальа» в г. Хиве (наклон минаретов комплекса Саиднияз Шоликарбая, мечете Джума, медресе Кутлуг Мурад-инака и др.)

Хива является одним из древнейших городов Центральной Азии. Одним из крупнейших в СНГ является Хивинский государственный историко-архитектурный музей заповедник Ичан-Кала (пл.26 га) [1].

Недавнее исследование, проведенное Институтом зоологии АН РУз, показало, что в Хиве из 56 строений в крепости Ичан-Кала термиты нанесли повреждения 31-му, а пяти строениям из них нанесен весьма серьезный ущерб (рис.1). Среди поврежденных строений - такие исторические памятники, как Куня Арк, Палвон Кари, Мечеть Джума, минареты Хорезм Шахов и мавзолей Пахлаван Махмуда.

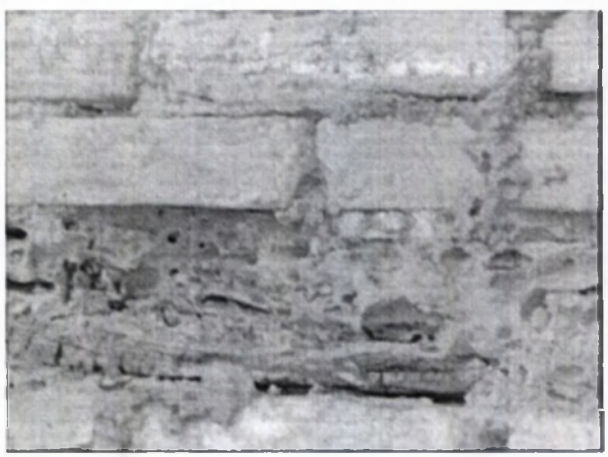


Рис. 1 Общий вид поврежденные деревянных конструкции памятников архитектуры в г. Хиве

Архитектурные памятники Хивы за период существования подвергались многократным природным воздействиям. В последнее время, все больше они подвергаются еще и техногенным воздействиям. Особенно это касается подземной части памятников. Поскольку сохранение архитектурных памятников во многом зависят от надежности их оснований и фундаментов, особую значимость приобретает сбор, изучение и анализ данных об изменении уровня грунтовых вод, влияния человеческой деятельности и других факторов, позволяющих достоверно оценить напряженно-деформированное состояние оснований и фундаментов памятников архитектуры во времени.

В 2003-2010 годах было предусмотрено проведение наземных сейсмических и электромагнитных исследований на территории

исторических памятников Ичан-Калы в г. Хиве. При этом, особое внимание было уделено изучению основания исторических памятников, где в настоящее время происходят деформационные процессы как в самих сооружениях, так и в их основаниях. Поэтому, в первую очередь полевые работы производились у оснований Джума мечети, Кутлуг Мурад-инак, Саидниязь-Шаликорбая. Следует отметить, что развитие деформационных процессов, в основном, связано с зонами переувлажнения. Задачей настоящего исследования являются обеспечение долговечности и эксплуатационных возможностей этих памятников.

В пределах территории медресе Кутлуг Мурад-инак зона переувлажнения приурочена к угловой восточной колонне (рис.2. а, б). Уровень грунтовых вод находится на глубине 3,5 метров. В отмеченной зоне вскрыты трубы ранее заложенной канализации (Средние века), по которой проходило движение сточных вод. Ширина переувлажненной зоны составила 2-3,5 м.



Рис. 2 Минарета медресе Кутлуг Мурад инака и Саидниязь-Шаликорбая. в г. Хиве

В ходе работе получены результаты сейсмических и электроразведочных исследований по отдельным площадям. При этом были выявлены и установлены переувлажненные зоны, отличающиеся особенностью. Достоверность этих исследований заключается в том, что установленные зоны деформирования вскрыты шурфами (рис. 4 а, б. горными выработками), изучены водно-физические и физико-механические свойства. Также как в предыдущем слое, переувлажненная зона, связанная с зоной деформирования, приурочена к основанию минарета мечети Саидниязь Шаликорбай. Уровень грунтовых вод (УГВ) в 2002 году поднялся на 70 см. (рис.3, 1-шурф). Высота минарета составляет 30,5 м, диаметр основания 5,3 м. Ствол минарета наклонен в юго-западную сторону. Приращение крена минарета, за прошедшие (12 г) с 1998 по 2010 гг произошло с 0,958 до 1,110, т.е. приращение составляет 1110-958=152 мм.



1-Шурф (2002 г)



2-Шурф (2009 г)

Рис. 3 Заложенные шурфы аварийного минарета комплекса Саидниязь Шаликорбая в г. Хиве

Здесь следует отметить, что при изучении поля влажности применялся метод многогоризонтного комплексного электрозондирования, который успешно применяется при решении подобных задач. Подобные установки также разрабатываются в фирме "Scintrex" Канады и МГУ России. Преимущество предложенной установки заключается в том, что использованная установка в условиях Ичан-Калы дала положительные результаты.

Результаты наблюдения уровня грунтовых вод на различных участках Ичан Калы и график его изменения в зависимости от времени приведен на рисунке 4.

На территории ансамбля подземные воды залегают в зависимости от рельефа и глубины залегания водоупора. УГВ залегает на глубине от 2 до 7 метров. Максимальный уровень грунтовых вод на территории Ичан-Калы наблюдается в феврале-марте месяцев (в период многоводья), а минимальный уровень грунтовых вод в июле месяце (в период маловодья).

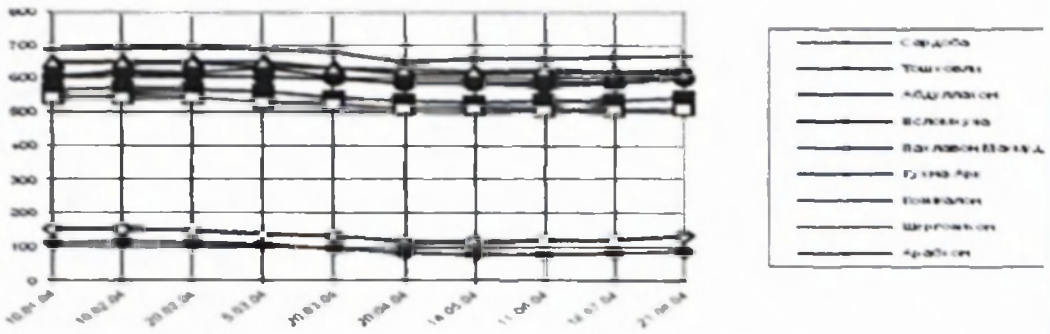


Рис. 4 Изменение уровня грунтовых вод во времени (2004 г).

В период многоводья максимальный уровень грунтовых вод составляет 1,5-6,5 м. т.е выше критический точки это приводит к подтоплению территории подземными водами.

В результате близкого залегания уровня грунтовых вод к поверхности земли, при многократном подъеме и опускании уровня грунтовых вод (годовые колебания уровня составляет 0,5-0,8 м) в верхних горизонтах зоны аэрации происходит увеличение засолённости грунтов, приводящий к его уплотнению, а в нижней части аэрации происходит (обратный процесс) расслоение грунтов, в связи с растворением и размывом легкорастворимых солей из толщи грунта.

Таким образом, резкий подъём УГВ приводит к подтоплению подземными водами территорий расположения комплексов памятников архитектуры Ичан-Калы в результате чего происходит развитие следующих нежелательных отрицательных процессов:

* увеличение влажности грунтов в зоне насыщения, приводит к снижению деформационных и прочностных свойств грунтов и частичного проявление дополнительной просадки грунтов в основании фундаментов зданий, приводящие к неравномерной деформации толщи грунтов оснований, который могут вызвать аварийную деформацию зданий;

* многократное повышение и опускание УГВ в зоне аэрации приводит к накоплению солей в ее верхних горизонтах, ухудшая эколого-мелиоративные условия территорий: уплотнение, снижение пористости и коэффициента фильтрации, затрудняющий инфильтрацию атмосферных осадков и поверхностного стока и накопление влаги под основанием фундаментов[2];

* при многократном подъеме и опускании УГВ в нижних горизонтах зоны аэрации происходит расслоение грунтов – растворение, размыв и вынос легкорастворимых солей из толщи грунтов, приводит к разрыхлению толщи грунта, способствующий проявлению деформаций верхней части толщи грунтов в основании фундаментов, которые увеличивает возможность проявления неравномерной аварийной деформации зданий.

Для недопущения выше перечисленных отрицательных нежелательных процессов нами рекомендуется следующее:

1. Подъем уровня подземных вод, временно и длительно развивающийся под влиянием природных и особенно, техногенных факторов, привел к обводнению и деформируемости основания памятников. Поэтому для недопущения скапливания вод атмосферных осадков и поверхностного стока на пониженных местах, улучшить систему водоотводов атмосферных и поверхностных вод и охватить сетью водоотводов всю территории комплекса Ичан-Калы.

2. Принять меры по улучшению работы существующих дренажных сооружений (очистка, капитальный ремонт и т.п.) в пределах комплекса Ичан-Калы.

СПИСОК ИСПОЛЬЗОВАННЫХ ИСТОЧНИКОВ

1. А. Манковская. В. Булатова «Памятники зодчества Хорезма». - Ташкент. 1978 г.
2. Рашидов Т.Р., Сирожиддинов З.С. Проблемы обеспечения сохранности памятников архитектуры. Узбекский журнал. «Проблемы механики». №5,2003 с.7-13.
3. Холмурадов Р.И, Хасанов А.З. Конструкции памятников архитектуры Самарканда. Самарканд, 2003. с.127.

Influence of soil structure on consolidation of soft clays using vertical geodrains

M.V. Shah
Applied Mechanics Department, L.D. College of Engineering, Ahmedabad, Gujarat, India
A.V. Shroff
Applied Mechanics Department, The M.S University of Baroda, Vadodara, Gujarat, India

ABSTRACT: Soft soil improvement using prefabricated vertical drain (PVD) through radial drainage is employed in the present investigation. Paper emphases on consolidation characteristics of soft soils through inward radial flow mainly affected by rate of dissipation and development of pore water pressure and the mechanics involved on soil structure using isochrones. Laboratory investigation is carried out by employing 254mm diameter hydraulically pressurized Oedometer along with pore pressure transducers and displacement transducers connected to data acquisition system interfaced with PC. Two vertical drains namely sand drain and sandwick of 'n' values 11.04, 16.93 and 21.71are used in present investigation. Experimental results are analyzed and compared with authors theory of consolidation through radial flow. Theory of consolidation proposed by authors introduces lump parameter 'λ' incorporating drain material effect, drain size, drain geometry, horizontal to vertical permeability ratio, non-homogeneity of soil, stress history and soil particle orientation (tortousity). Comparison of theoretical and experimental results indicate that authors lumped parameter theory fits appropriately and gives direct clue to field engineers for selection of appropriate vertical drain with respect to field conditions.

1 INTRODUCTION

Due to devastating Bhuj Earthquake (2001) long coastal belt of Gujarat state (INDIA) was suffered because of the higher sensitive nature of the coastal soft clays. Soil has lost its in-situ strength during seismic stresses because of change of metastable card house structure of illitic coastal soils. Strengthening of these soft soils by accelerating consolidation through radial drainage with the help of Prefabricated Vertical Geodrain will help to mitigate the danger of becoming soft clay quick. To accelerate the consolidation process and gain strength use of vertical sand filled holes known as sand drains and sandwicks (cylindrical geotextile bags filled with saturated sand)wells are used. The drain well permits the control over the water migrating in radial (horizontal) direction. This reduces the excess pore water pressure that is built up in the soil mass and reduces the drainage path thus increasing the rate of consolidation manifold. Due to provision of geodrains most of the settlement will occur during and not after construction. The advantages are threefold

- Expediting the rate of settlement.
- Consequently acceleration in the rate of gain in shear strength.
- Reduction in the lateral transmission of excess hydrostatic pressure.

2 SCOPE AND OBJECTIVE OF THE PAPER

The aim of the present work is to study consolidation due to radial drainage of Kaolinite clay using sand drains and sandwicks and study the effect of 'n' value (ratio of drain dia to sample dia) on consolidation parameters. The hydraulically pressurized Oedometer described by Rowe and Barden (1966) and further modified by Shroff and Shah (2006,2008) for pore pressure measurement during radial flow is employed in the present investigation.

- Paper presents experimental model of sand drains and sandwick reinforced soft soil mass to expedite the rate of consolidation due to radial drainage taking advantage of having more horizontal permeability than vertical.
- The effects of sand drains and sandwick of different 'n' values (ratio of drain diameter to sample diameter) on consolidation characteristics (coefficient of consolidation 'Cr' due to radial drainage) of Kaolinitic clay are undertaken to investigate the settlement and pore water pressure characteristics.
- The variation of ratio of zone of influence (r_e) to the diameter of drain has been varied to access the optimization of drain diameter for better performance with respect to increase of quick strength on the basis of settlement and pore pressure dissipation characteristics.

- To compare coefficient of horizontal permeability (Kr) for sand drains and sand wicks.
- To compare the degree of consolidation (Ur) for different 'n' values with author's solution from both settlement readings (SR) and pore pressure dissipation readings (PR).
- Comparison of theoretical isochrones and experimental isochrones obtained from pore pressure measurements at various radial distances using author's solution for the case of equal vertical strain.
- Study of soil structure effects on consolidation characteristics of soft clay mass using microstructure characterization (MIC) software.

The specific points kept in view while developing the system and analyzing the experimental data obtained during investigation are as under:

1. System adequacies and the compatibility of settlement measuring set up with recording system.
2. Interaction of radial flow with rate and magnitude of consolidation.
3. Orientation of particles and drainage path.
4. Tortuosity of the flow in radial and vertical path.
5. Soil structural changes along with changes in the soil skeleton, intermolecular water and permeability.

3 EXPERIMENTAL SET-UP

3.1 Modified Oedometer

The Oedometer of two different diameters 254mm and 152mm were used for testing the remolded samples. The cell body is machined from aluminum bronze sating which is resistant to corrosion. The base plate and top plate are bolted to the flanges while at the base 'o' ring is provided to make it water seal.

A uniform pressure is applied by means of conventional hydraulic pressure system on the convoluted rubber jack which transfers uniform pressure on the soil sample placed in the cell. To achieve equal strain condition a rigid top platen is inserted between the jack and the sample. The vertical settlement is measured at the center of the sample by means of brass hollow rod attached to the jack and passing out the cell cover to a suitable dial gauge. Pore pressures are measured at the three radial points located at 120 degree each with r/re distances as r/4, r/2 and 3r/4 respectively. (Refer fig. 1)

3.2 Drainage and Pore pressure measurement

Inward radial drainage was provided in our case. The drainage outlet is via the centre of the settlement hollow rod and a short length of flexible tube leading to valve at the edge of the cell cover. No vertical drainage is allowed and so the top of the sample is sealed with the jack alone or with a rigid impervious top platen between the sample and the jack. The important factor in all the above set-up is full control over drainage and uniform settlement measurement of the sample. For both the oedometer test diameter to height ratio was kept constant. The side friction was reduced by means of application of silicon grease on the walls of the cell.

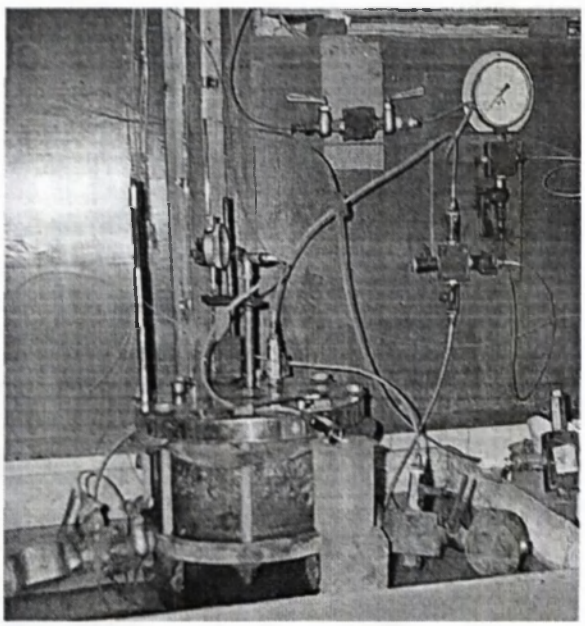


Fig.1 Complete test set-up of 254mm diameter of modified hydraulically pressurized Oedometer

3.3 Preparation of clay samples

The specific gravity of kaolin clay powder G = 2.592, liquid limit (L_L) = 67%, Plasticity index (P_I) = 33.43 and belonging to CH (clay of high plasticity) group according to I.S.Classification system. To ensure full maturation of the sample the clay was mixed to form slurry with twice the liquid limit using a de-aired distilled water. The shear strength is measured with the help of laboratory vane shear apparatus before and after the test.

3.4 Preparation and Installation of sand drains (SD)

The axial hole was formed with a thin walled mandrel, having area ratio of 0.8 to 1.6 attached with template and guide frame connection. The sand having specific gravity G=2.645, coefficient

of permeability k=8.50 x 10^{-3} cm/sec of well graded coarse type was used. The drain was filled with de-aired saturated sand with the aid of small diameter flexible tubing by siphoning action to cause nearly no smear. With least possible time gap a top rigid plate with a porous stone at the centre was placed.

3.5 Preparation and Installation of sand wicks (SW)

The sandwick consists of prepacked geotextile cylindrical bag (polypropylene) having diameter according different 'n' values selected. The polypropylene geotextile bag prepared before the test with height equal to that of sample.. In the present investigation n=11.04, 16.93 and 21.71 are used for detail study.

3.6 Testing Program

After installation of sample and fixing top platen along with dial gauge, displacement transducers, pore pressure transducers, bishop's apparatus are connected to their respective locations. Load increment is applied from constant pressure system to sample through water filed jacket, with closed position of the drainage valve at the top plate. Pressures are applied in the range of 20 kPa, 40 kPa, 80kPa, 160kPa and 320kPa with $\Delta p/p$ = 1.0.Each load increment is kept constant for about 96 hrs and secondary compression is also recorded. After completion of the test, the sample is taken for final moisture content measurement.

4 RESULTS AND ANALYSIS

4.1 Theoretical Review

Karl Terzaghi gave the general equation for consolidation due to radial flow.

$$\partial u/\partial t = Cvr\,[\partial^2 u/\partial r^2 + 1/r\;\partial u/\partial r] \quad \ldots\ldots\ldots\ldots(1)$$

Shroff & Shah (2006) proposed a new mathematical theory whose general solution directly gives a clue to design engineers for selection of most economical drain. This theoretical treatment incorporates non-homogeneity, time effects intrinsic to the soil skeleton along with physico-chemical changes, compressibility of pore fluid and solid, variation of compressibility and permeability during consolidation, type of the drain material, tortousity effect, k_h/k_v ratio under load variation, effect of 'n' value (drain diameter) and drainage path. The lump parameter (λ) incorporates above all factors.

The degree of consolidation (U_R) for different values of λ can be obtained using

$$U_R = \frac{e - e_0}{e_1 - e_0}$$

$$= \exp\left(\frac{\lambda}{2}\right)\left[\frac{Sinh\frac{\lambda}{2}R}{Sinh\frac{\lambda}{2}} + 2\pi\sum_{n=1}^{\infty}\frac{(-1)^n n Sin(n\pi R)}{\frac{\lambda}{4}+n^2\pi^2}\exp\left(\frac{\lambda}{4}+n^2\pi^2\right)T\right] +$$

$$\exp\left(\frac{\lambda}{2}\right)\left[\frac{Sinh\frac{\lambda}{2}(1-R)}{Sinh\frac{\lambda}{2}} - 2\pi\sum_{n=1}^{\infty}\frac{n Sin(n\pi R)}{\frac{\lambda}{4}+n^2\pi^2}\exp\left(\frac{\lambda}{4}+n^2\pi^2\right)T\right]$$

Isochrones for various positive and negative values of parameter λ ranging from +0.7 to -0.7 are obtained from which degree of consolidation at various radial points against time factor is possible. The value of average degree of consolidation is computed using Simpson's rule as explained in Taylor (1948) and Lambe-Whitman (1969).

4.2 Plots and Discussion

Comparative plots of settlement analysis(SM) and pore pressure analysis (PM) at lower stress of 40kPa and higher engineering stress of 160kPa are presented 'n' values 11.04, 16.93 and 21.71 respectively. For sand drain and sandwick notation SD and SW are used.

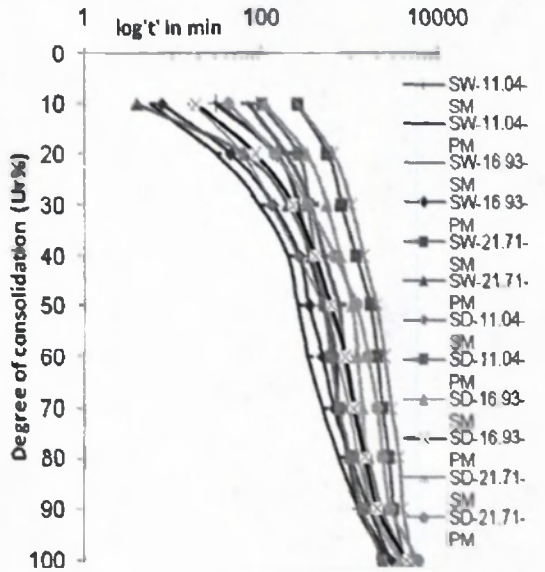


Fig.2 Comparison of degree of consolidation vs.log't' for 'n' values of SD and SW at 40kPa

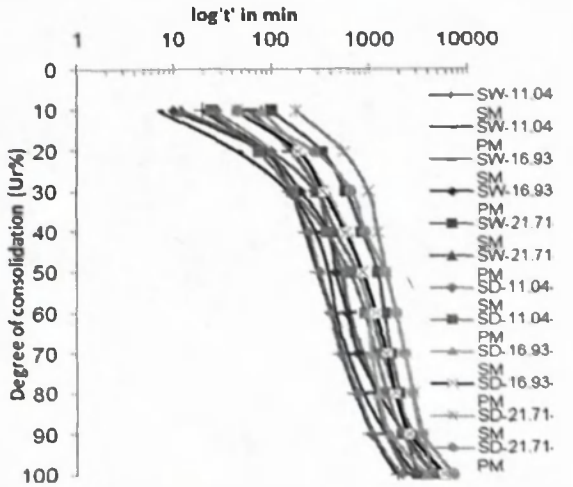


Fig.3 Comparison of degree of consolidation vs.log't' for 'n' values of SD and SW at 160kPa

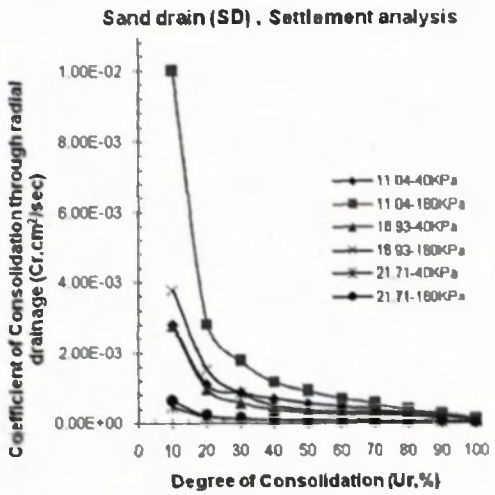


Fig.4 Comparison of Cr vs. Ur for SD for all 'n' values

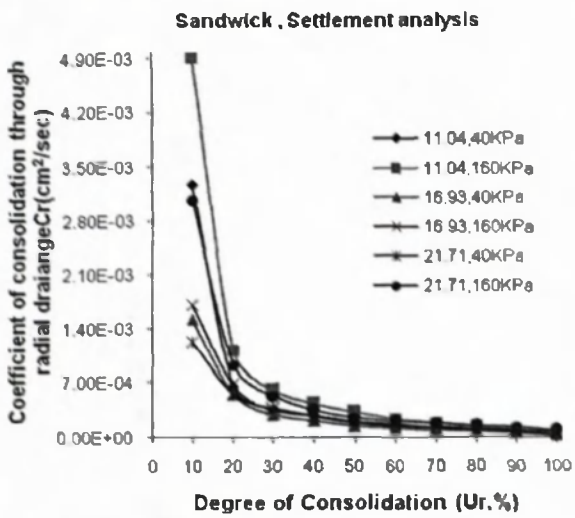


Fig.5 Comparison of Cr vs. Ur for SW for all 'n' values

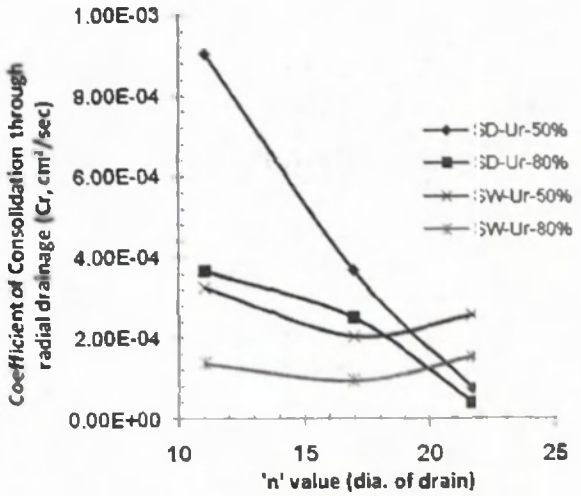


Fig.6 Comparison of Cr vs. 'n' value for Ur-50% and Ur-80% at 40kPa

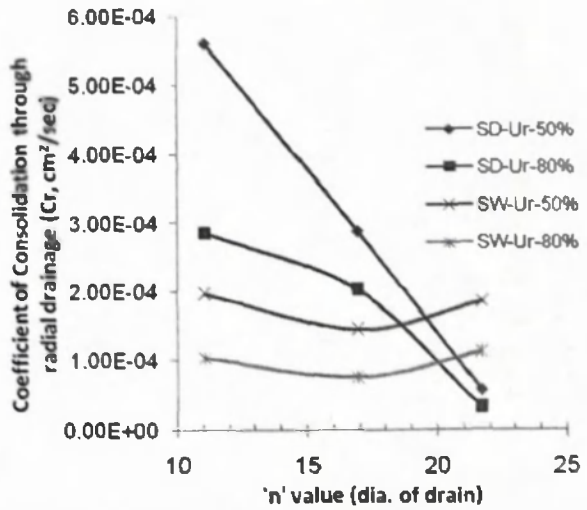


Fig.7 Comparison of Cr vs. 'n' value for Ur-50% and Ur-80% at 160kPa based on SM

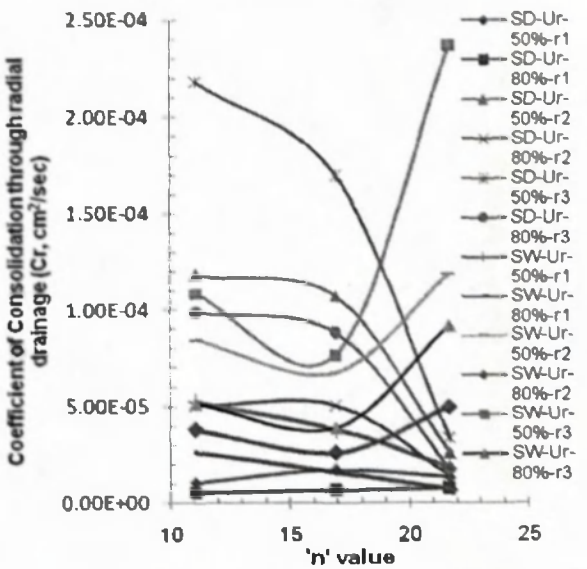


Fig.8 Comparison of Cr vs. 'n' value for Ur-50% and Ur-80% at 160kPa based on PM

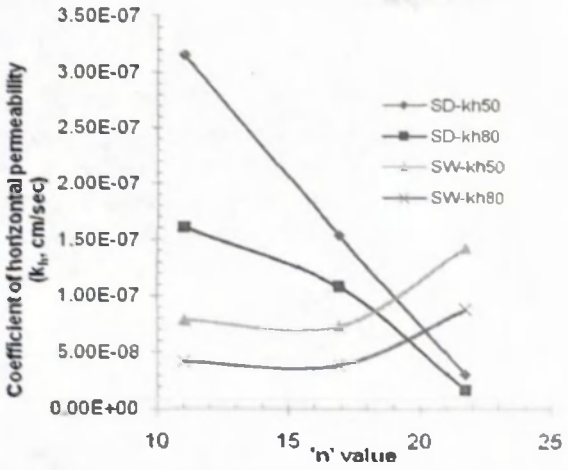


Fig.9 Comparison of k_h vs. 'n' value for Ur-50% at 160kPa based on SM

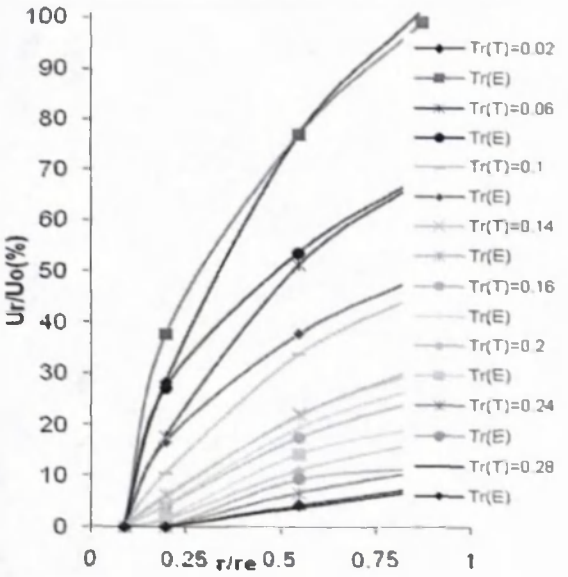


Fig.10 Comparison of theoretical and experimental isochrones for SD at 160kPa

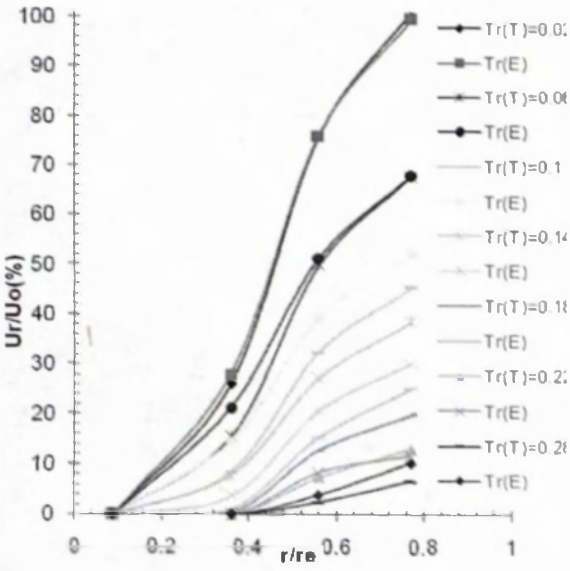


Fig.11 Comparison of theoretical and experimental isochrones for SW at 160kPa

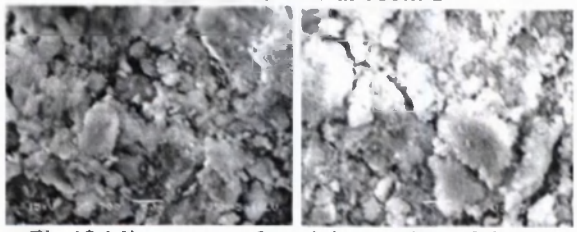


Fig.12 Microscopy of sand drain (SD) at X2700

Discussion:

- From settlement and pore pressure measurement (refer fig.2 &3) considerations it infers that for 50% and 80% consolidation, SW shows more rate of compressibility thus showing more rate of dissipation of pore water pressure compare to SD for all pressures and for all 'n' values. For any load intensity and drain material, the time deformation curve with respect to pore pressure dissipation remain towards the vertical axis compare to curve of settlement, that is time require for 50% or 80% consolidation is less compare to settlement curve which also reflects in isochrones curves. This is because of direction of flow from the void space is radial which allows early dissipation compare to particle reorientation achieving same degree of consolidation.
- Rate of drainage of a radial points nearer to drainage being faster the time taken for particular % of consolidation is less in compare to radial points farther away, it also reflects this observation in settlement measurements to some extent showing more compressibility gradient towards central drain. It seems from the micrograph of several drains the pore space in terms of nanomeaurement is larger compare to other drains. This reflects the efficiency of SW with respect to micro structure opening even under light and heavy constructional loading.(refer fig.12)
- During pore pressure measurements for middle radial point r_2 it concludes that n=11.04 for 50% consolidation shows 405% and 583% higher C_r value compare to n=16.93 and 21.71 for any drain material under light loading and 483% and 580% under constructional loading. Similarly for 80% consolidation shows 227% and 239% higher C_r value compare to n=16.93 and 21.71 for any drain material under light loading and 290% and 298% under constructional loading. (refer fig. 4,5,6,7 &8)
- n=16.93 is found to be more efficient then n=21.71 under both light and constructional loadings. n=16.93 shows averagely 92% higher

C_r value under light loading while 60% higher under constructional loading compare to n=21.71 but 61% lower compare to n=11.04 under light loading and 56% lower under constructional loading.

- Amongst the various 'n' values the n equal to 11.04 provides optimum specific surface area to the saturated surrounding soil structure for a given diameter of influence zone of soil mass. Because of this gradient of radial flow during consolidation can help producing low level of structural resistance to compression in this case compare to other 'n' value of 16.93 and 21.71. The load component during higher level of loads can help structural breakdown or pushing the particles at a more rate leading to final consolidated mass at 320kPa. It is reflected in micro porosity, degree of orientation and tortousity measurements.
- From settlement analysis it concludes that n=11.04 for 50% consolidation shows 278% and 289% higher k_h value compare to n=16.93 and 21.71 for any drain material under light loading and 735% and 3025% under constructional loading. Similarly for 80% consolidation shows 190% and 200% higher k_h value compare to n=16.93 and 21.71 for any drain material under light loading and 442% and 1862% under constructional loading as shown in fig.9. From pore pressure analysis n=16.93 shows averagely 63% and 411% higher k_h value under light loading and constructional loading compare to n=21.71 but 45% and 73% lower compare to n=11.04 under light loading and constructional loading for 50% consolidation under any drain material
- Gain in shear strength was observed for all three 'n' values for any drain material after consolidation, but highest gain was observed in case of 'n' equal to 11.04 for any drain material. Average post shear strength increased to 150kPa from pre shear strength of 15kPa.
- With reference to isochrones (refer fig.10 &11) for various T_r values reveals that sequence of consolidation for CJ of n=11.04 at any radius of influence seems to be efficient compare to all other drains. Comparing isochrones of all three 'n' values it is concluded that n=11.04 is more effective compare to n=16.93 and n=21.71, while n=16.93 is more superior compare to n=21.71 for all drain materials. Trajectory of isochrones for n=11.04 lies above the n=16.93 and n=21.71 for both light and constructional loading. Also trajectory of isochrones for n=16.93 lies above n=21.71 for all drain materials and loadings. The micro pore structures of the SW drain and other drains are quite distinct that is initial micro porosity of SW is less compare to other drains which reflects in isochrones characteristics.
- As 'λ' value increases, drain diameter ('n' value) decreases. Experimental results almost match with theoretical results with λ=-0.15 particularly for SWfor n=11.04, λ = -0.14 for n=16.93 and λ = -0.12 for n=21.71 proves to be efficient while for SD, λ= -0.1, -0.07, -0.02 fits respectively. From theoretical considerations n=11.04 proves to be efficient amongst other 'n' values.

5 CONCLUSIONS

i. Theoretical solution of author's non-linear equal strain theory of consolidation by radial flow fits very well with experimental results for various soil conditions. Various factors affecting rate of consolidation like drain material, drain size, drain shape, ratio of horizontal permeability to vertical permeability, physico-chemical factors are well considered in authors theory and its effect are reflected because of typicality of pore pressure dissipation phenomena.

ii. It is concluded that sandwick drain of 'n' equal 11.04 is most efficacious in dissipating pore water pressure at shortest time along with higher gain in shear strength of consolidated mass. Author's theory of consolidation based on pore water dissipation (isochrones) yields better comparative results more easily applicable to fields by design engineers. Also trajectory of curves for various degrees of consolidation acts as a readymade tool for selection of optimum drain w.r.t material, shape and size. The appropriate value of lumped parameter (λ) will directly give the clue to design engineer regarding the selection of prefabricated vertical geodrain with respect to field conditions.

ACKNOWKEDGEMENTS

The authors are highly thankful to the Prof.(Dr) Ambika Misra, Dean, Faculty of Technology & Engineering, Prof. (Dr) I.I. Pandya Head, AMD, Prof. (Dr) D.L.Shah, P.G.Incharge, AMD, The Maharaja Sayajirao University of Baroda, Vadodara and Prof. M.N.Patel, Dean, L.D.College of Engineering and Prof.(Dr) R.K.Gajjar,Head, AMD,LDCE, Ahmedabad, India for providing all necessary research facilities.

Проблемы сохранения памятников архитектуры Узбекистана и их реабилитация на основе композиционных материалов

А.А. Ашрабов, А.А. Ишанходжаев,
ТАДИ, г. Ташкент, Узбекистан.

Реабилитация памятников архитектуры Узбекистана имеет большое градостроительное значение и обычно ведется на уникальных, представляющих историческую ценность, объектах. Под реабилитацией в первую очередь подразумевается их восстановление и усиление и нередко ее совмещают с инженерно-консервационными мероприятиями. Часто возникает необходимость одновременного восстановления основного ядра памятника и позднейших дополнений к нему, имеющих определенную мемориальную ценность или способствующих сохранности самого памятника. Разработка проектных материалов по реабилитации памятников архитектуры начинается с подготовки предварительной документации, которая обобщает результаты ознакомления с памятником и состоянием его конструкций, намечает программу натурных исследований (шурфы, зондажи, обмеры). Одновременно производится историко-архивное исследование и составляется историческая справка. По полученным данным разрабатывается проект реабилитации.

Для реабилитационных работ характерна определенная специфичность и ограниченные возможности в области применения механизации, сборных элементов, прогрессивных конструкций и материалов. Основными проблемами сохранения объектов культурного наследия являются: высокая степень амортизации памятников архитектуры с их возможной утратой; устаревшие технологии работ по восстановлению и усилению несущих элементов; несоответствующие техническим требованиям условия содержания и эксплуатации; несовершенство практики проведения экспертизы их технического состояния.

Среди позитивно зарекомендовавших себя основных методов оценки состояния памятников архитектуры следует отметить: натурные обследования, включая фотофиксацию; экспертную оценку по результатам визуальных наблюдений; зондаж и инструментальные замеры; лабораторные, библиографические и архивные. Очевидно, что наиболее полные и точные результаты мониторинга технического состояния памятников архитектуры возможны при использовании всех перечисленных методов. Однако в силу их высокой затратности во многих случаях это не осуществимо. Поэтому обычно используются методы натурных обследований и экспертной оценки.

Как известно, территория Узбекистана расположена в чрезвычайных природных условиях, для которых характерны: высокая сейсмичность (7 и более баллов по шкале MSK); оползни; пылевые штормы; зоны пустынь; резко континентальный сухой и жаркий климат; осадка и пучение грунтов; засоленные и высоко минерализованные почвы, подземные воды и т.п. Отрицательное влияние природных явлений ухудшается тем, что основные материалы исторических зданий – кирпич и гипс – очень к ним чувствительны. Большинство памятников расположены на антропогенных почвах, а увлажнение грунта оснований резко уменьшает их прочность и увеличивает их осадку.

За последние годы процесс деградации архитектурных памятников значительно усилился. Под воздействием быстро ухудшающейся окружающейся среды в материалах несущих конструкций памятников архитектуры происходит постепенное накопление повреждений, что влечет за собой их ускоренную деградацию и «старение». Это ведет к образованию и большому раскрытию трещин, снижению несущей способности или разрушению конструкций. Типичными и наглядными примерами служат
повреждения медресе на площади Регистан в Самарканде, где процессы образования трещин (шириной в несколько см), деформирования и неравномерной осадки настолько существенны, что гипсовые марки, установленные в марте 1993г., были повреждены уже до ноября того же года, рис. 1 [1]. Ситуация ухудшается тем, что каких либо систематических исследований поведения большинства архитектурных памятников не выполнено, а данные об их истинном техническом состоянии отсутствуют. Это влияет на принятие адекватных решений по их реабилитации.

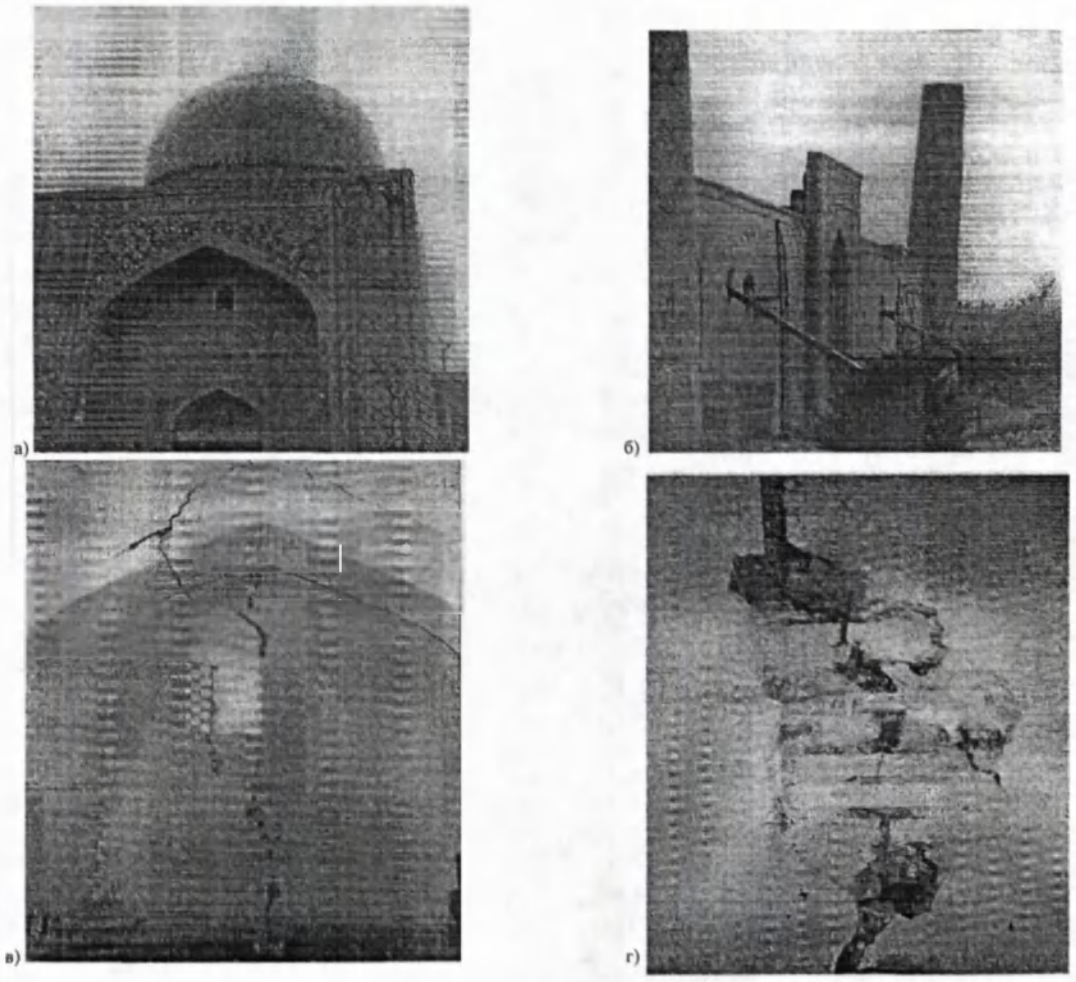


Рис.1. Повреждения медресе Тиллякарн и Улугбека: а) разрушения ке-рамики фасада; б) наклон минаретов; в) трещины в стенах подвала; г) разрушенные гипсовые марки

Среди главных причин и аспектов устранения повреждений природного и техногенного характера нужно отметить следующие:

- рост сейсмической активности и землетрясения различной интенсивности, которые приводят к накоплению напряжений в несущих элементах; недостаточное восстановление, развитие осадок и повреждений сделали их весьма уязвимыми даже для слабых землетрясений; такие воздействия могут ожидаться с высокой вероятностью в следующие годы и могут вызвать непоправимое повреждение конструктивной системы или вызвать е разрушение; необходимо дополнительно усилить каменную кладку и конструкции фундаментов, остановить дальнейшие деформации, принять меры для уменьшения давления под фундаментов, обеспечивая однородное давление под всем зданием; необходим с определением фактических динамических характеристик конструкций и оснований;

- тенденции к повышению уровня грунтовых вод по всей территории Узбекистана, а не только на территории расположения мемориалов; высокий уровень засоленности почв и загрязнений воздуха; необходим систематический и детальный осмотр условий расположения фундаментов, оснований и уровня грунтовых вод, оценка влажности строительных материалов; необходимы постоянный контроль прочностных и деформативных свойств конструкционных материалов и оценка солевой коррозии в каменной кладке; необходимо улучшение систем дренажа и защиты фундаментов при атмосферных осадках, введение защитных зон (например, мощение по периметру здания), устранение утечек и расстройств в инженерно – технических сетях;

нужны ремонт старых систем понижения уровня грунтовых вод и материалы стойкие к резким перепадам температурно – влажностных условий;

- отсутствие систематического контроля за техническим состоянием несущих элементов архитектурных памятников; необходима программа, определяющих технические, организационные и финансовые условия и методы реабилитации и эксплуатации памятников.

Традиционные методы восстановления и усиления поврежденных элементов являются весьма недолговечными и не всегда эффективными, а именно: они недостаточно надежны и существенно увеличивают собственный вес усиляемых элементов, вызывая вторичные повреждения; они требуют специального оборудования при реставрации; стальные элементы усиления искажают архитектурный облик объекта и легко подвергаются коррозии; они трудоемки в изготовлении, особенно для элементов с характерными сложными сечениями неправильной формы. Такая ситуация побуждает оперативно разрабатывать новые, рациональные решения по поддержанию и восстановлению работоспособности основных несущих конструкций архитектурных памятников.

Для преодоления указанных недостатков в последние годы ведется активный поиск альтернативных решений по усилению существующих архитектурных памятников, в том числе обращаясь к опыту усиления и продления в ряде развитых стран широкие исследования показали, что на сегодняшний день наиболее эффективными и перспективными материалами для усиления несущих конструкций из различных материалов являются тканевые полимерные волокнистые материалы (ПВМ). Они выполнены из тонких волокон высокой прочности (нитей или пряжи), работающих в составе матрицы из полимерных (эпоксидных) смол и свободны от отмеченных недостатков. Матрица имеет две главные функции – она позволяет перераспределять нагрузку между смежными волокнами и защищает волокна от экологических воздействий. Волокна пропитаны полимерной смолой, которая окружает и связывает волокна и действует как защитное покрытие для волокна. От традиционных материалов они отличаются комбинацией уникальных особенностей: легкость и высокие прочность, долговечность, коррозионная и химическая стойкость, антимагнитность и диэлектрические свойства, низкий коэффициент теплового расширения, долговечность, способность быстро и легко закрепляться на конструкциях с различной геометрией поверхности и сечений, низкая трудоемкость использования и малые эксплуатационные расходы. Усиление из ПВМ уже широко используется для увеличения несущей способности, жесткости и сейсмостойкости несущих конструкций зданий и сооружений.

Волокна ПВМ разделяются на три основных вида: углепластиковые, стеклопластиковые и арамидопластиковые. Для достижения максимальной эффективности их использования армирующие волокна вводятся в состав матрицы с определенной ориентацией и при различном процентом содержании. Волокна могут быть ориентированы в одном (вдоль поперек или под различными углами) или обоих направлениях в составе волокнистых тканей (непрерывных или в виде отдельных листов или лент). Двунаправленные ткани составлены из волокон, ориентируемых под углом 0^0 и 90^0 . Практика использования различных ПВМ показала, что наиболее эффективными для усиления конструкций являются тканевые полимерные материалы на основе углепластиков (УПВМ) [2]. На рис. 2 показаны образцы таких полимерных композиционных материалов.

Использование ПВМ в качестве внешнего усиления открывает новые перспективы для улучшения работы конструкций памятников. Оно может использоваться увеличения несущей способности балок, кладки стен, фундаментов и т. д. Их использование повышает эффективность работы сжатых элементов, обеспечивая прочную обойму и пластичность деформирования ядра сечения. Легкость проведения строительных работ и минимальные изменения в поперечном сечении конструкции после применения внешнего усиления – основные преимущества в использовании ПВМ в конструкциях архитектурных памятников.

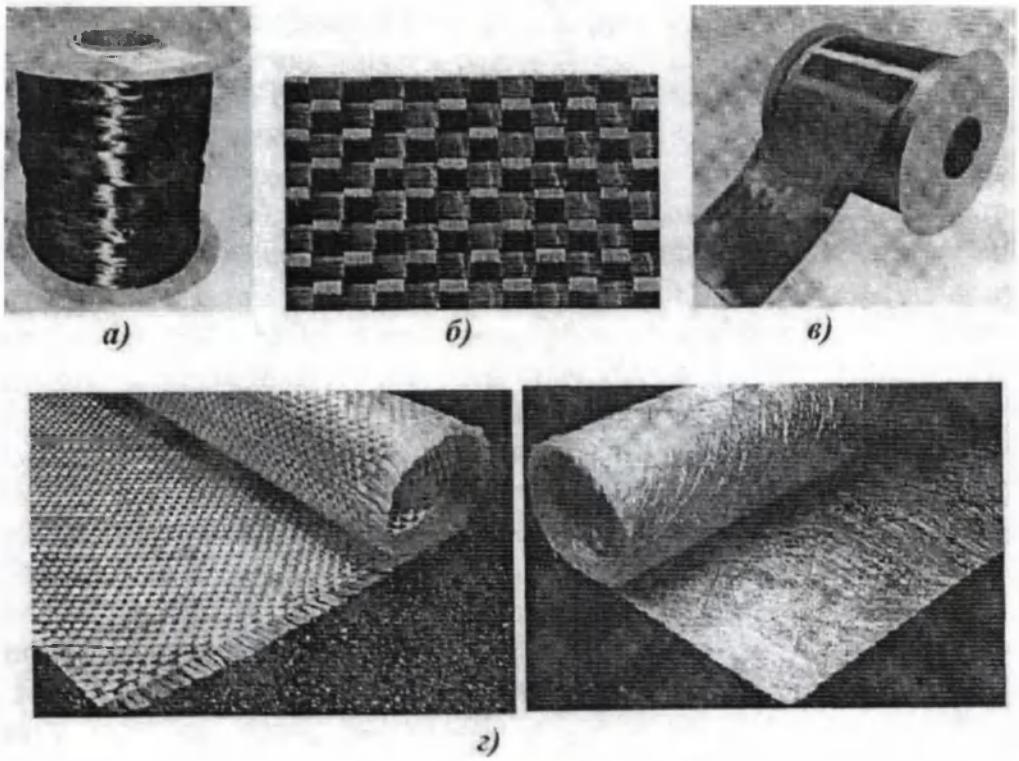


Рис. 2. Образцы материалов на основе стеклопластикового и углепластикового волокна: жгуты (*а*), тканевые листы и ленты (*б,в*); тканевые рулоны из стекловолокна (*г*).



Рис. 3. Диаграммы деформирования для углепластиков (УПВМ), стеклопластиков (СПВМ), арамидопластиков (АПВМ) и стали

Дальнейшие наиболее эффективные потенциальные возможности использования ПВМ находятся в области ремонта, усиления и восстановления существующих конструкций в качестве внешнего армирования в виде листов или оберток на несущих элементах, обеспечивая их прочность даже после интенсивных запроектных силовых воздействий.

Указанные волокна разделяются на углеродные, стекляные и арамидные. Угле и стеклопластики в шесть раз прочнее и пять раз легче чем сталь. Стекловолокна могут быть разделены на два типа: тип I (обозначаемые E, A, C, E-CR) с модулем упругости 70 ГПа и прочностью в диапазоне 1000...2000 МПа; тип 2 (обозначаемые R, S и AR) с модулем 85 ГПа и прочностью в пределах 2000...3000 МПа. Углепластиковые волокна диаметром (4...10 μм) имеют плотность порядка 1900 кг/м^3. Типичные значения модуля упругости волокна могут изменяться в пределах 230...300 ГПа, а прочность в пределах 3000...5000 МПа. Арамидопластики из ароматических полиамидных волокон характеризуются высокой прочностью до 3000 МПа, модулем

упругости в пределах 60-120 ГПа и очень низкой плотностью – около 1400 кг/м^3. Различают два типа арамидных волокон: Kevlar 29 – с модулем упругости 60-70 ГПа и Kevlar 49 – с модулем в два раза выше. Однонаправленные арамидные волокна имеют высокую прочность в пределах 1200-1400 МПа. Эпоксидные связующие смолы представляют класс термоактивных связующих клеев и предназначены для прочного приклеивания ПВМ к поверхности конструкции и полной передачи напряжений по всей толщине слоя связующего. Такая матрица имеет две главные функции: она позволяет перераспределять нагрузку между смежными волокнами; защищает волокна от экологических воздействий.

В настоящее время в ТАДИ проводятся широкие исследования специальных железобетонных образцов и балок, усиленных внешним армированием из углепластиковых тканевых материалов (УПВМ), проведена оценка несущей способности и жесткости сечений с трещинами. Результаты эксперимента показали, что несущая способность увеличивалась соответственно на 12 – 60 % по сравнению с контрольными образцами и балками. Разработанная новая технология усиления конструкций полосами УПВМ может быть эффективно использована для значительного увеличения несущей способности элементов при реабилитации памятников архитектуры Узбекистана.

ЛИТЕРАТУРА

1. Sh. A. Khakimov, A. A. Ashrabov. Natural and climatic factors determininig the state of monuments and of their restoration and conservation. Proceedings of Uzbek-German workshop "Historic Monuments in Seismic Regions", Weimar, 1995, pp. 21-29.
2. А. А. Ашрабов, Ч. С. Раупов. К исследованию железобетонных элементов с трещинами, усиленных полимерными волокнистыми материалами. Сб. трудов Российской академии архитектуры и строительных наук (РААСН), т. 2. – М. 2011, с. 42-49.
3. А. А. Ашрабов, Д. Джайяпракаш. Прочность железобетонных элементов, усиленных внешним армированием на углепластиковой основе. Вестник ТАДИ, №2, 2011, с. 18-24.

Реологические свойства антропогенных грунтов в основании сооружений

Расулов Х.З.
Архитектурно-строительный институт, Ташкент, Узбекистан
Нарбаев С.М.
Архитектурно-строительный институт, Ташкент, Узбекистан

АННОТАЦИЯ. Доклад посвящен вопросам оценки реологических свойств антропогенных грунтов, залегающих на территории древних городов. Отмечается, что длительная деформация антропогенных грунтов происходит за счет изменения величины связности грунта под действием касательных сдвигающих напряжений. Даются формулы для определения величины деформации грунтов под ленточных, квадратных и прямоугольных фундаментов.

ABSTRACT. The report is devoted to the matters of grading reologic characteristics anthropogenic soils in the basis in ancient towns. It is mentioned that prolonged deformation of anthropogenic soils happens because of corrections sire change of the soil under the influence of tangent moving pressure. Formulas for determining the sire of soil's deformation under stripe, square and rectangle basis are given.

Одним из основных условий обеспечения устойчивости любого сооружения заключается в том, что осадка зданий, возникающая в процессе эксплутации должна быть меньше допустимой величины для подобных объектов. Однако, соблюдение этого условия не всегда удается по ряду причин, одной из которых - длительное изменение прочностных характеристик грунта в связи с ползучей его способностью.

Ниже излагается, метод оценки длительной деформации антропогенных грунтов, широко распростаненных в основании древних городов.

Скорость деформации $e_p(t)$ грунта во времени от внешней нагрузки (p_x) по Н.Н.Маслову представляется следующим виде [1]:

$$de_p(t) = \frac{p_x}{\eta_0 - (\eta_0 - \eta_6)\cdot e^{-\mu}} dt \qquad (1)$$

где p_x - расчетное давление у подошвы фундамента, вычисляемое по зависимости:

$$p_x = p_{ш} - H\gamma \qquad (2)$$

здесь $p_{ш}$ - средное значение давления от веса сооружения (с учетом веса фундамента);

H - глубина заложения фундамента;

γ - осредненная плотность грунта и материала фундамента.

η_0, η_6 - соответственно начальное и конечное значения коэффициента вязкости; μ - коэффициент, определяемые экспериментальным путем в зависимости от свойства грунта [2].

Интегрирование (1) в пределах от начала строительства $(t = 0)$ до определенного времени (t) приводит к решению:

$$e_p(t) = p_x\left[\frac{1}{\eta_0} + \frac{1}{\mu\eta_0}\ln\frac{\eta_0 - (\eta_0 - \eta_6)e^{-\mu}}{\eta_6}\right] \qquad (3)$$

Выражение (3) позволяет определить относительную деформацию (осадку) основания во времени. Коэффициент вязкости грунта в выражении принят изменяющимся во времени $\eta = f(t)$, и постоянной по глубине (z), т.е $[\eta_t = f(z) = const]$. Давление p_x также принято постоянным по глубине $[p_x = f(z) = const]$.

Деформация основания (осадки сооружения) во времени в рассматриваемых условиях представляется:

$$s_t = p_x\left[\frac{1}{\eta_0} + \frac{1}{\mu\eta_0}\ln\frac{\eta_0 - (\eta_0 - \eta_6)\cdot e^{-\mu}}{\eta_6}\right]\cdot d \qquad (4)$$

где d – мощность сжимаемой толщи.

На основании принятых выше допущений (о постоянстве коэффициента вязкости и давления по глубине) формула 4 может быть использована для случаев неглубокой сжимаемой толщи и при достаточной ширины подошвы фундамента. В противном случае давление $[p_z = f(z) \neq const]$ следует рассматривать изменяющимся по глубине толщи, что может

быть достигнуто путем интегрирования выражения (4) в пределах от подошвы фундамента (0) до низа сжимаемой толщи (d), т.е:

$$s_t = \int_0^d p_z \left[\frac{1}{\eta_0} + \frac{1}{\mu\eta_0} \ln \frac{\eta_0 - (\eta_0 - \eta_б)\cdot e^{-\mu t}}{\eta_б} \right] \cdot dz \quad (5)$$

Для решения этого уравнения должен быть известен характер изменения давления p_z по глубине толщи z. По данному вопросу бытуют различные предложения. Среди них представилось более целесообразным использовать предложения Бринг Ханзена для конкретных разновидностей фундаментов [3]:

Интегрирование уравнения (5) в пределах $0-d$ с учетом предложений Ханзена дает возможность определить осадку сооружения (s_t) во времени t в следующем виде:

а) для ленточных фундаментов:

$$s_t = p_z b \left[\frac{1}{\eta_0} + \frac{1}{\mu\eta_0} \ln \frac{\eta_0 - (\eta_0 - \eta_б)\cdot e^{-\mu t}}{\eta_б} \right] \cdot \ln \frac{b+d}{b}; \quad (6)$$

б) для квадратных фундаментов:

$$s_t = p_z \frac{b\cdot d}{b+d} \left[\frac{t}{\eta_0} + \frac{1}{\mu\eta_0} \ln \frac{\eta_0 - (\eta_0 - \eta_б)\cdot e^{-\mu t}}{\eta_б} \right]; \quad (7)$$

в) для прямоугольных фундаментов:

$$S_t = p_z \frac{b\cdot d}{a-b} \left[\frac{t}{\eta_0} + \frac{1}{\mu\eta_0} \ln \frac{\eta_0 - (\eta_0 - \eta_б)\cdot e^{-\mu t}}{\eta_б} \right] \cdot \ln\left(\frac{b+d}{a+d} \cdot \frac{a}{b}\right) \cdot \quad (8)$$

где: $b\cdot a$ - размеры подошвы фундамента.

Формулы (6)-(8) в принятых условиях позволяют определить осадку сооружения в любой момент в процессе его эксплуатации. Один из основных приимуществ их заключается решение вопроса на базе коэффициента вязкости грунта , определяемого в лабораторных условиях несложным путем, минуя предварительного исследования физико-механических показателей грунта.

ЛИТЕРАТУРА

1. Маслов Н.Н. Основы инженерной геологии и механики грунтов. –М.: Стройиздат,1987. -320 с.
2. Расулов Х.З. Прогноз деформации сооружений в результате пластического течения грунтов оснований при землетрясениях. // Труды 1-го Центрально –Азиатского геотехнического симпозиума. –Астана,2000. –С.266-270.
3. Brinch Hansen. Hauptprobleme der Bodenmechanic. – Berlin, 1960, -93 p.

Оползневые явления в откосах в результате разжижения грунтов

Расулов Х.З.
Архитектурно-строительный институт, Ташкент, Узбекистан

Садыков А.Х.
Архитектурно-строительный институт, Ташкент, Узбекистан

ABSTRACT. This work is dedicate to appearing of landslide in moistening natural rocks and slopes during Earthquakes. It's mentioned the landslides in moisture rocks often become the result of soils dilute in the process of shake. The formula for estimating the depth of active cone depending on parameters which is given as well.

АННОТАЦИЯ. Доклад посвящается исследованиям процесса возникновения оползни в увлажненных откосах при воздействии на них сильных сотрясений. Отмечается, что явление разжижения грунта в соответствующих условиях может послужить причиной возникновения оползни в сильно водонасыщенных грунтах. Исследуется распространение оползневой толщи в зависимости от влияющих на процесс внешних и внутренних факторов.

Анализ оползневых явлений, имевших место в увлажненных природных склонах и откосах во время землетрясений показывает, что этот процесс нередко происходит в результате разжижения грунтов при сотрясениях. Известно, что разжижение грунта возникает в результате взвешивающего воздействия избыточного давления (динамического напора h_z) в пределах активной, уплотняющейся зоны [1]. Природа динамического напора h_z весьма сложна, которая зависит от многих внутренних (гранулометрический и минералогический составы, пористость, связность, скорость уплотнения, фильтрационная способность) и внешних (внешняя нагрузка, интенсивность и характер динамического воздействия и т.п.) факторов.

Исследованию динамического напора (h_z) в водонасыщенных песчаных грунтах посвящен целый ряд работ [2,3,4,] в которых раскрыто условие возникновения h_z исходя из механизма разрушения структуры грунта при воздействии на него динамической нагрузки. Вопрос о динамическом напоре в водонасыщенных лессовых грунтах рассмотрен Х.З.Расуловым [1] Формула для определения величины h_z, возникающего на любой глубине толщи грунта с мощностью (H) в момент времени (t) после приложения динамической нагрузки, им представлена в виде:

$$h_{z,t} = \frac{v_0^2}{2K_\phi} L^2 .t, \qquad (1)$$

где K_ϕ- коэффициент фильтрации грунта;

L – активная (переходящая в динамически возбужденное состояние) зона;

v_0 - коэффициент динамического уплотнения, свидетельствующий скорость уплотнения конкретного грунта при определенном динамическом режиме, определяемый опытным путем по виброкомпрессионной кривой зависимости изменения пористости грунта (n) от расчетного ускорения колебаний $a_{расч}$, т.е: $a_{расч} = f(n)$ в виде:

$$v_0 = \frac{dn}{dt}. \qquad (2)$$

Формула (1) позволяет определить на горизонте z в пределах активной зоны L величину динамического напора h_z в любой момент времени t в пределах от 0 до t_{max} (отвечающего полному разжижению грунта).

Для наиболее худшего случая, когда грунт в составе склона или откоса залегает в весьма рыхлом и полностью водонасыщенном состоянии условие полного разжижения определяется равенством:

$$h_z = L \qquad (3)$$

В соответствии с этим величина времени t_{max} требуемой для перехода в полностью разжиженное состояние грунт в пределах L определяется в виде:

$$t_{max} = \frac{2K_\phi}{v_0^2 . L} \qquad (4)$$

При решении задач, связанных с оползневым явлением в результате разжижения грунтовых масс при сейсмическом воздействии на склоны или откосы приобретает особое значение установление на тот или иной момент времени (соответствующей длительности

сейсмического воздействия) величины активной зоны в пределах которой произойдет процесс смещения грунтовой массы.

Можно предположить, что в любой момент времени (t) воздействия землетрясений на толщу склона мощностью H нижнюю границу активной, разжиженной зоны может быт определена из условии

$$S_{сейс}=S_{\sigma,w} \qquad (5)$$

где $S_{сейм}$- сейсмическое напряжение, возникающее в грунте при воздействии на него ускорением a_c ;

$S_{\sigma,w}$ - прочность (сопротивляемость сдвигу) грунта.

Сейсмическое напряжение $S_{сейс}$ представляется в виде:

$$S_{сейм} = \frac{\gamma_w}{g} . T . v_{волн} . a_c \qquad (6)$$

где γ_w – плотность грунта;

T – период колебания;

$v_{волн}$ - скорость волны.

Сопротивляемость грунтов сдвигу, отвечающая заданному состоянию плотности – влажности грунта, в общем случае может быть найдена из известного выражения:

$$S_{\sigma,w} =(\sigma + \gamma_w z)tg\varphi_{w+c_v} \qquad (7)$$

где σ - динамическое напряжение от веса грунта и пригрузки откоса;

z – рассматриваемый горизонт в пределах активной зоны;

φ_w – угол внутреннего трения грунта;

c_v – общее сцепление грунта.

Подставив выражения (6) и (7) в условие равновесия (5), находим глубину z, выражаемому в данном случае активную зону L :

$$L = \frac{S_{сейс} -(\sigma tg\varphi_w+c_v)}{\gamma_w\, tg\varphi_w} \qquad (8)$$

Полученное таким образом выражение (8) позволяет в каждом частном случае определить величину активной зоны L в момент воздействия сейсмической силы на склон или откос в условиях $a^{\beta}_{кр} < a_{расч}$ Где $a_{расч.}$- расчетное и $a^{\beta}_{кр}$- критическое ускорения колебаний [1]). При этом основным фактором, определяющим величину активной зоны, является сейсмическое напряжение $S_{сейс.}$, воспринимаемое грунтовой толщей при воздействии сейсмического ускорения интенсивностью a_c или его активно действующей частью $a_{расч.}$ Кроме напряжения $S_{сейс.}$ в значении активной зоны немаловажное влияние оказывают нормальные напряжения (σ) от веса пригрузочного слоя откоса и сцепление между частицами грунта (c_v).

Следует отметить, что величина активной зоны L, определяемая с помощью выражения (8), отвечает начальному моменту воздействия сейсмической нагрузки на толщу, т.е. условию $a^{\beta}_{кр} = a_c$. На основании проведенных анализов можно утверждать, что в условиях сотрясений в связи с ослаблением прочности грунта отмечается постепенное увеличение величины активной зоны.

В данном процессе величина активной зоны L должна определяться уже с учетом изменения прочностных характеристик грунта в виде:

$$L_t = \frac{S_{сейс} -(\sigma - \gamma_w h_{zt})tg\varphi_w+c_{v,t})}{\gamma_w\, tg\varphi_w} \qquad (9)$$

Формула (9) является важной с точки зрения установления величины сползающей толщи с учетом длительности воздействия землетрясения.

Экспериментальная проверка зависимости (9) дает хорошую сходимость. Зная величину сползающей зоны, можно принять конкретные меры во избежание неблагоприятных последствий.

ЛИТЕРАТУРА

1. Расулов Х.З. Сейсмостойкость лессовых оснований зданий и сооружений. –Т. «Узбекистан», 1977. 161 с.
2. Маслов Н.Н. Условия устойчивости водонасыщенных песков. –М., Госэнергоиздат, 1959. -161 с.
3. Иванов П.Л. Уплотнение несвязных грунтов взрывами. –М. Гостройиздат, 1967
4. Гришин П.А. Исследование потери устойчивости песков в затопленных откосах земляных сооружений при динамических воздействиях.–В сб.: Вопросы механики грунтов. Вып.28, ЛИСИ, 1968

Сейсмопросадочная деформация лессовых грунтов

Расулов Р.Х.
ГУП «УЗГАШЛИТИ», Ташкент, Узбекистан

Набиев Э.
Архитектурно-строительный институт, Ташкент, Узбекистан

АННОТАЦИЯ. Доклад посвящается освящению результатов полевых исследований деформации лессовых грунтов под воздействием вибромеханизма. Дается оценка степени сейсмопросадки грунта в этих условиях.

ABSTRACT. The lecture dedicated to questions the research of settling deformations of loess soils in the field conditions at the influence of vibration load from movements of pack road-roller. Gives to method and findings of experiment received by different vibrations of soils

Одним из надежных методов, обеспечивающих прочность и устойчивость оснований и бесперебойной эксплуатации сооружений, назначением величины расчетного давления на основание и расчета ограничения величины средней осадки и разности осадок соседних фундаментов, послужило бы соблюдение условия, когда $a_{пр} > a_c$ (где $a_{пр}, a_c$ - соответственно величины порогового и сейсмического ускорений колебания частиц грунта) во всех точках основания [1 – 4].

Условия, когда $a_{пр} > a_c$ можно достигнуть за счет увеличения прочностных характеристик грунтов. Одним из способов повышения прочностных характеристик грунтов является их уплотнение.

В настоящее время уплотнение ведется одним из известных методов: с помощью катков, тяжелых трамбовок, виброуплотнением и т.п. [5 – 7]. Исходя из условий задачи наибольший интерес для наших исследований (повышение прочностных характеристик грунта по мере заглубления фундамента и т.д.) представляло виброуплотнение катками. Виброуплотнение катками широко применяется в практике гидротехнического и дорожного строительства [4 – 6].

Виброуплотнение катками наиболее экономичен и эффективен, особенно для уплотнения насыпных грунтов, залегающих вокруг фундамента. Это обеспечивает создание соответствующей прочности грунтов основания в боковых зонах фундамента и способствует ликвидации явлений сейсмопросадок повышая значение $a_{пр}$ в рассматриваемых зонах.

Для осуществления полевых исследований специально подготавливались экспериментальные площадки с тремя опытными участками одинаковых размеров 13 х 6,5 м [5]. Эти участки сложены идентичными лессовыми суглинками.

Участки подготавливались опыту в течение 40-45 дней. В целях определения возникающей в период вибрации деформации грунта, в различной дальности и глубине от дорожки передвижения виброкатка, были установлены специальные репера в количестве 45 шт. С целью создания различной влажности в идентичных грунтовых условиях производилось замачивание толщи. Для замочки грунтов по середине второго и третьего участков выкапывались траншеи размерами 8 х 0,4 х 1,4 и 8 х 0,4 х 1,0 м. Траншеи заполнялись мелким щебнем размером 5-20мм. Затем осуществлялась непрерывная замочка участков с помощью водопроводного шланга в течение 12 – 15 дней.

После прекращения замочки в течение 30 суток отбирались пробы грунта для определения их физико-механических показателей. В результате этих работ мы располагали тремя идентичными участками, отличающимися между собой только влажностью. Влажность грунтов на участках соответствовала: участок №1 – 13-14%, участок №2 – 19-20%, участок №3 – 16-17%.

С целью изолирования влажности каждого участка в период их замочки между ними оставлялась защитная зона шириной 6 м. На различных глубинах от поверхности грунта (0,5; 1,5; 3,0 м) были установлены сейсмоприемники (ОСП, ВЭГИК, С-5-С) для регистрации колебаний почвы от работы виброкатка.

Точка наблюдения, откуда снимались показания реперов (где записывались показания вибродатчиков) при вибрации площадки находились на расстояние 70 м от среднего участка. Показания датчиков записывались с помощью осциллографов типа Н-041.

Затем приступили ко второму этапу опыта, связанного с изучением виброуплотняемости грунтов. На каждом участке в нескольких местах с интервалом через 1,5 – 2,0 м производилось виброуплотнение. Виброкаток перемещался вдоль каждого участка по прямой линии. При этом можно было создать различные вибрации и длительности колебания грунта путем регулирования режима работы катка.

После осуществления вибрации заново отбирались образцы грунтов для определения показателей физико-механических свойств с интервалом через 1,5 – 2,0 м производилось виброуплотнение. Виброкаток перемещался вдоль каждого участка по прямой линии. При этом можно было создать различные вибрации и длительности колебания грунта путем регулирования режима работы катка.

После осуществления вибрации заново отбирались образцы грунтов для определения показателей физико-механических свойств. Обработка результатов опытов произведена по осциллографическим записям вибраций грунта. По данным записей основные опыты проведены в условиях вибрации с частотой 12-25 Гц и ускорением колебаний грунта до 10 000 мм/с^2 и более.

На опытных участках осуществлено более 30 различных исследований с вибрацией грунта. Обратимся к данным табл.1, где сведены показания опытов изменения плотности-влажности грунтов при вибрации с различной длительностью и интенсивностью. В качестве интенсивности динамического режима в данном случае принят соответствующий режим виброкатка, отвечающий максимальному и минимальному положениям.

Как видно из данных таблицы влажность грунта повышается по глубине толщи. Это по-видимому объясняется условием замочки опытных участков. Изменение плотности грунтов вследствие нарушения их структуры и деформации уменьшается по глубине толщи, что является вполне закономерным. Однако, на поверхностных горизонтах толщи, куда передаются интенсивные колебания наблюдается резкое изменение плотности грунта. Более сильная деформация грунта имеет место при работе виброкатка на максимальном режиме.

Опыты, проведенные в полевых условиях с вибрацией толщи, показали повышение деформации грунта с увеличением длительности колебания. Наблюдается линейная зависимость между повышением плотности грунта от длительности колебании, которая по количеству падает с глубиной толщи.

В экспериментальных исследованиях нами было уделено особое внимание на дальнейшее поведение грунтов после осуществления вибрации. Произведены наблюдения и измерения показателей грунтов в течение 2-х месяцев. Результаты наблюдения сведены в табл.2.

Также проведены опыты, характеризующие повышение плотности грунта, подверженного динамическим воздействиям с различными колебаниями.

Как следует из результатов опытов, более интенсивное возрастание плотности отмечается у предварительно вибрированных грунтов с большой частотой, что является важным показателем для назначения мероприятий по уплотнению грунта.

Таблица 1

Изменение плотности-влажности грунтов при различной вибрации

Глу-бина	f=12,5Гц, t=30с			f=23Гц, t=30 с		
	W	γ_d	γ_d^l	W	γ_d	γ_d^l
0,1	11,0	1,66	1,42	12	1,68	1,42
	15,4	1,70	1,47	14,1	1,70	1,47
	15,7	1,68	1,46	16,6	1,68	1,46
0,5	15,0	1,60	1,43	15,6	1,64	1,43
	17,5	1,59	1,48	16,0	1,59	1,48
	18,6	1,58	1,47	18,6	1,58	1,47
1,5	16,5	1,50	1,45	16,0	1,51	1,45
	20,4	1,49	1,49	19,5	1,51	1,49
	20,5	1,48	1,46	21,5	1,50	1,46

Продолжение табл. 1

f=12.5Гц, t=90с			f=23Гц, t=90с		
W	γ_d	γ_d^l	W	γ_d	γ_d^l
12,9	1,70	1,42	10,5	1,66	1,42
15,6	1,72	1,47	10,6	1,65	1,47
14,0	1,70	1,46	11,5	1,68	1,46
15,5	1,65	1,43	14,0	1,59	1,43
18,8	1,62	1,48	15,0	1,60	1,48
18,8	1,61	1,47	15,0	1,63	1,47
16,0	1,52	1,45	14,0	1,50	1,45
19,0	1,51	1,49	16,7	1,51	1,49
20,0	1,50	1,46	17,7	1,52	1,46

Примечание: γ_d^l - плотность сухого грунта до вибрации; γ_d - плотность сухого грунта после вибрации; t- длительность вибрации; f-частота вибрации.

Повышение плотности грунта во времени сопровождается увеличением его прочностных показателей (угла внутреннего трения и сцепления). Причем это увеличение протекает более интенсивно в течение первой недели после вибрации. Отмечается возрастание угла внутреннего трения в зависимости от длительности вибрации.

Таблица 2

Изменение прочностных показателей грунтов после осуществления вибрации.

Время	Глубина отбора пробы H = 0,4-0,5 м							
	Частота вибрации f=12,5-14Гц Длительность вибрации t=30с				Частота вибрации f=12,5-14Гц Длительность вибрации t=90с			
	W,%	γ, т/м³	φ, град	c,МПа	W,%	γ, т/м³	φ, град	c,МПа
До вибрации	17,1	1,48	25	0,046	16,1	1,43	25	0,049
Через 3 суток	18,0	1,60	26,5	0,030	17,5	1,66	29	0,035
Через 50 суток	16,6	1,62	27	0,059	15,1	1,67	30	0,060

Так, при вибрации, продолжительностью 30 суток возрастание угла внутреннего трения составляет 2 град., в течение 50 суток – 3 град, а в течение 90 суток эта величина составляет 5 град.

Аналогично, но в более выраженном виде это обстоятельство характерно и для сцепления грунта. Повышение сцепления грунта с течением времени является результатом приобретения грунтом новой прочности и уплотнения под влиянием собственного веса.

ЛИТЕРАТУРА

1.Иванов П.Л. Влияние пригрузки на разжижение песчаных водонасыщенных оснований – Гидротехническое строительство, 1986, №6

2.Кригер Н.И. и др. Вибрационная (сейсмическая просадка). – Инженерные изыскания в строительстве. Реф.сб.-М.,1986, вып.8

3.Маслов Н.Н. Вопросы сейсмической устойчивости затопленных песчаных оснований сооружений. – Труды 4 Международного конгресса по механике грунтов и фундаментостроению,Лондон,1967

4. Расулов Х.З. Сейсмостойкость грунтовых оснований.– Ташкент, «Узбекистан»,1984

5.Расулов Х.З., Хакимов Г.А. Полевой опыт уплотняемости лессовых грутов в естественных условиях с помощью вибромашин. Сборник научных трудов ТашПИ,Ташкент,1987

6.Расулов Х.З., Хакимов Г.А., Частоедов Ю.Н. Просадочные деформации лессовых грунтов при динамических воздействиях. -Материалы 6 Всесоюзного съезда по теоретической и прикладной механике.Ташкент,1986

7.Хакимов Г.А. Процесс изменения прочностных характеристик рыхлых лессовых грунтов при увлажнении.- Материалы республиканской научно-практической конференции молодых ученых и специалистов, Ташкент,1987

Глубина разжижаемой зоны в основании зданий при землетрясении

Ташходжаев А.У.
Ташкентский архитектурно-строительный институт, Ташкент, Узбекистан

АННОТАЦИЯ. В докладе излагаются результаты исследований по вопросу определения глубины разжижаемой зоны в основании зданий при сильных землетрясениях. Отмечается, что начальная глубина разжижаемой зоны не является постоянной величиной, а увеличивается в зависимости от длительности колебания. Даются формулы определения начальной и последующей любому моменту времени глубин разжижаемых зон.

ABSTRACT. In the report considers results of investigation at the question determination at the depth of dilution zone in the basis the buildings at the strong earthquake. Mentions, first at a depth of dilution zone iz not constant sizes, it rises dependence at the duration vibrations. Propose formula of determination at the first and next moment a time depth of dilution zone.

Основными факторами, определяющими разжижаемой зоны в основаниях сооружений, являются сейсмическое напряжение $S_{сейс}$, воспринимаемое грунтовой толщей при воздействии ускорения интенсивностью a_i или его активно действующая часть $a_{расч}$, прочностные характеристики грунта (φ_w, C_w), нормальное напряжение от веса здания σ, и плотность грунта γ_w.

Для изучения роли этих показателей на образование разжижаемой зоны в толще основания были осуществлены лабораторные исследования. В качестве примера на рис. 1-4 иллюстрированы графики, где получили отражения зависимость разжижаемой зоны от интенсивности динамического воздействия (α_c), внешней пригрузки (p), общего сцепления (связности C_w) и плотности (пористости n) грунта.

В процессе разжижения грунта существенную роль принадлежит интенсивности динамического воздействия, выражаемой, в нашем случае, ускорением колебательного движения. Очевидно, чем больше величина ускорения, тем быстрее возникает активная зона и интенсивно распространяется вглубь толще. Этот неоспариваемый факт усматривается из рис. 1, где приводится зависимость вида $L = f(\alpha_c)$ для исследованных лессовых грунтов № 3 и №7, характеризующихся осредненными физико-механическими и прочностными показателями.

Как видно из графика повышение ускорения колебаний в исследованных грунтах приводит интенсивному заглублению разжиженной зоны по глубине толщи, что

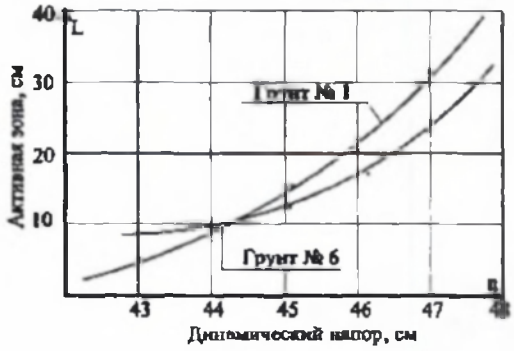


Рис.1. Зависимость вида Z=f(α) для исследованных грунтов

является весьма важным для нашего анализа.

Роль пригрузки (p) по грунту в возникновение зоны разжижения следует из рис. 2, который демонстрирует наличие обратной зависимости между ними.

Одновременно рис. 2 со всей очевидностью свидетельст-вует о заметном влиянии пригрузки образца, не только на возникновение, но и дальнейшее распространение активной зоны, что необходимо учесть при разработке мероприятий против разжижения откоса и образования оползни в склоне.

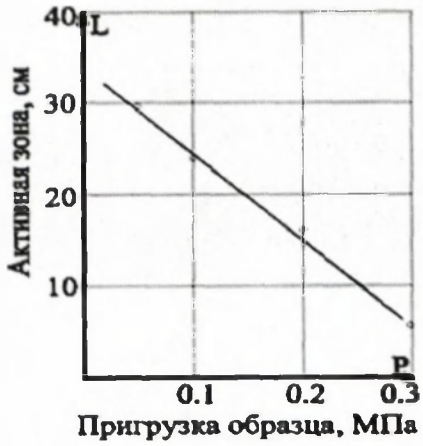


Рис.2. Зависимость активной зоны от пригрузки образца

Общее сцепление c_w, выражающее прочность грунта во всех случаях оказывает благоприятную роль в обеспечении динамической устойчивости грунта (рис.3). Однако его значение различное для разных грунтов. Например, если толща сложена пластичными лессами ($\varphi = 0$, c_c=0), из известного условия следует: $\tau_c = c_w$.

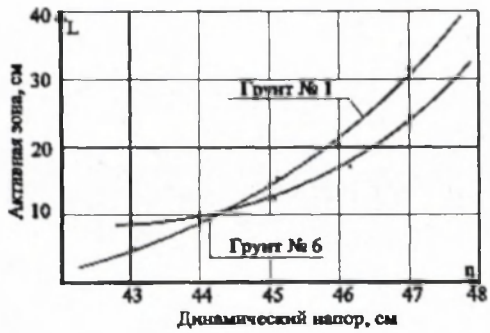


Рис.3. Характер изменения активной зоны L зависимости от связности лёссовидного грунта

Исследования на грунтах с различным состоянием плотности показали, что последний фактор также имеет значение в возникновение разжижения в условиях колебаний (рис.4). Увеличение плотности грунта, или уменьшение его пористости всегда вызывает большую интенсивность динамической нагрузки, способной нарушать структуры грунта. С повышением плотности грунта зона распространения разжижения заметно уменьшается.

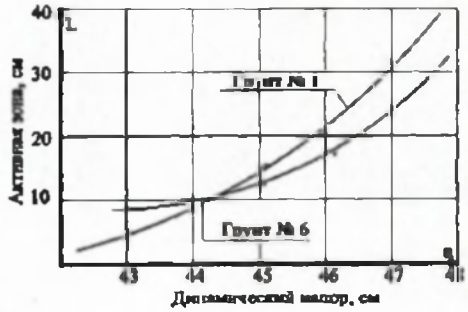


Рис.4. График зависимости активной зоны от пористости грунта

Разжижаемая зона, соответствующая к начальному моменту возникновения условий $a_c = a_{кр}$ не остается неизменной, а возрастает по мере увеличения значения динамического напора h_z, возникающего в пределе активной зоны. В свете этого обстоятельства представлял интерес изучить влияние h_z на изменение разжиженной зоны в процессе сотрясения. Один из результатов таких опытов представлен на рис. 5 в виде зависимости $L_t = f(h_z)$. Следующий из этой зависимости вывод о том, что увеличение активной зоны L_t в условиях колебаний происходит в результате падения прочности грунта (за счет уменьшения c_w и $\sigma_{дин}$).

Это обстоятельство было впервые обнаружено П.Л.Ивановым при исследовании разжижаемости песка («послойное разжижение») [4], а затем этот вопрос детально рассматривался Х.З.Расуловым [5].

Известно, что ослабление прочности

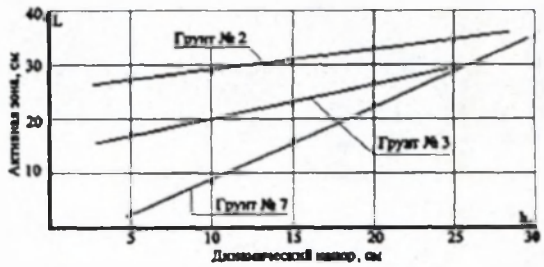


Рис.5. График вида $Z = f(\alpha)$ для обычных лёссов

грунта в процессе сотрясений является следствием взвешивающего воздействия динамического напора h_z.

Графики вида $L_t=f(h_z)$ отображают закономерность увеличения активной зона L_t по мере возрастания динамического напора h_z на определенной глубине z. Как усматривается из графика на рис.5, любое увеличение динамического напора внутри толщи приводит к соответствующему возрастанию величины разжижаемой зоны, что является весьма важным для оценки устойчивости склона в целом.

В данном случае определяющим окажется длительность сейсмического воздействия на склон или откос, чем дольше она продолжается, тем больше заглубляется разжижаемая зона в толще грунта. В связи с этим можно заметить, что определение разжижаемой зоны при всех прочих условиях должно производится с учетом длительности возникновения землетрясений.

ЛИТЕРАТУРА

1. Расулов Х.З. Сейсмостойкость грунтовых оснований. –Ташкент: Изд-во «Узбекистан», 1984. -192 с.
2. Хакимов Г.А. Исследование структурной прочности увлажненных лессовых грунтов при сейсмических воздействиях: Дисс… канд. Геол.-минер.наук. – Ташкент,1991.-183 с.
3. Частоедов Ю.П. Количественная оценка динамической структуры водонасыщенных песков: Дисс…канд. Геол.-минер.наук. –М.: ПНИИС.,1989. -176 с.
4. Иванов П.Л. Уплотнение малосвязных грунтов взрывами. –М.: Стройиздат. 1983. – 218 с.
5. Расулов Х.З. Сейсмостойкость лессовых оснований зданий и сооружений. –Ташкент: Изд-во «Узбекистан», 1977. -163 с.

Исследование устойчивого уклона искусственных откосов при интенсивных колебаниях

Казаков.Э.
Ташкентский архитектурно-строительный институт, Ташкент, Узбекистан

АННОТАЦИЯ. Доклад посвящен вопросам устойчивости искусственных откосов в сейсмических районах. Исхода из условий равновесия грунта под воздействием сдвигающих сейсмических и сопротивляющихся сил получена формула для определения угла сейсмоустойчивого откоса. Отмечается, что эта формула представляет интерес проектировщиков и строителей, связанных с возведением откосов в сейсмоопасных районах.

ABSTRACT . The report is dedicated to the issues of artificial slopes durability in seismic regions. As the result of soils' balance under the influence of moving and opposing powers the formula for determining the angle of seismic durable slope is provided as well. It is noted that this formula represents the interest of project makers and builders dealing with constructing the slopes in seismically dangerous regions.

Одним из факторов, влияющих на устойчивость уклона откоса ($tg\alpha$) в сейсмических районах, является динамическое воздействие (a_c) и его составляющие: частота (f) и амплитуда (А) [А].

Осуществлены исследования с различными грунтами при неизменных прочностных показателях (φ, c) грунта и высоты откоса (H). Изменяющимся параметром явилось динамическое воздействие, в качестве чего служило ускорение колебательного движения (a_c). Заданное ускорение достигалось путем изменения одного из составляющих: частоты или амплитуды. Главным объектом наблюдения в этих исследованиях явился устойчивый уклон откоса при колебании с заданным ускорением. Этот уклон зафиксировался по началу осадки репера или подъема уровни воды в пьезометре, установленных в толщи откоса. Величина колебательного движения, соответствующего началу изменения в показаниях репера или пьезометра принималась за предельное воздействие (критическое ускорение) для принятого в опытах условия. Считалось, что при ускорениях, ниже этого значения грунт в теле откоса будет устойчивым.

На табл.1 приведены зависимости устойчивого уклона откосов, сложенных пылеватыми лессовыми грунтами от интенсивности динамического воздействия.

Табл.1

Зависимость устойчивого наклона откосов от ускорения колебания

Грунт	Ускорение колебания, мм /с^2						
	500	1000	1500	2000	2500	3000	3500
№2	0,6	0,31	0,22	0,17	0,13	0,11	0,08
№7	-	0,46	0,34	0,26	0,13	0,05	-

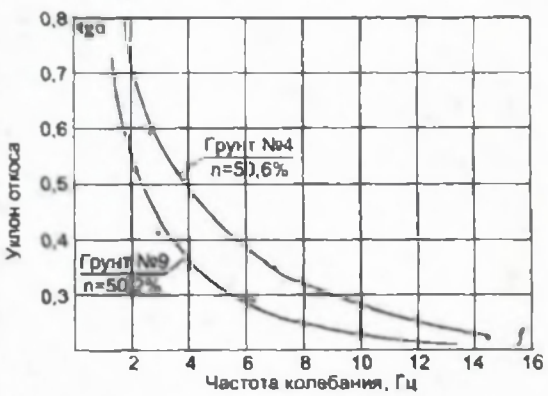


Рис. 1. Влияние частоты колебания на уклон откоса

Один из результатов исследований, проведенных для выяснения роли частоты колебания в значении наклона откоса, иллюстрирован на рис.1.

Действующее на откос ускорение в опытах достигалось за счет изменения частоты, сохраняя при этом постоянной амплитуды колебаний.

Как усматривается из рис.1 при ускорении 2880 мм/с^2 с частотами до 4-6 Гц откос характеризуется достаточно пологим, а

дальнейшее увеличение частоты приводит к повышению наклона. Наблюдается резкое возрастание наклона откоса при частотах 16-17Гц. Очевидно, что данное значение частоты находится близко к собственной частоты колебания водонасыщенных лессов (18 - 20 Гц) [2]. Наблюдающиеся при этих частотах резонансные явления оказывают сильное разрушающее воздействие на структуру грунта.

Вместе с тем роль амплитуды колебания в устойчивости наклона оказывается заметно меньшим. Однако, применительно к землетрясениям, амплитуда которых характеризуется большой разбросанностью, данный вопрос требует специального рассмотрения.

В процессе колебания изменяется

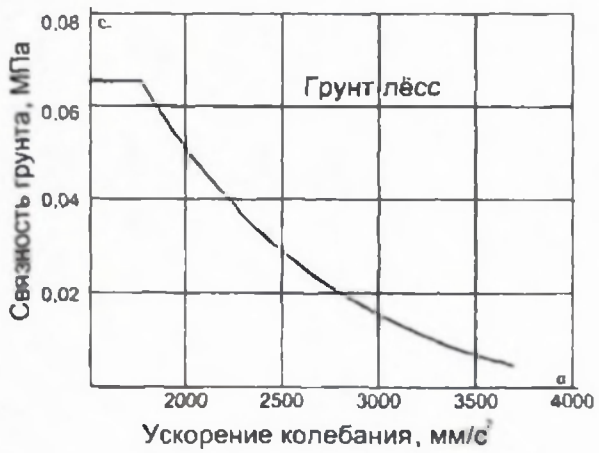


Рис. 2. Зависимость $C_ж=f(a_c)$

прочность грунта в результате ослабления в этих условиях сцепления (пластичной связности). Данный процесс приобретает прогрессивный характер при условии $a_c > a_{кр}$ (рис.2).

Из рисунка следует, что ослабление связности грунта начинается не сначала колебания, а по истечение некоторой времени после приложения нагрузки.

Связанный с критическим ускорением $a_{кр}$ этот отрезок времени различен для разных грунтов в зависимости от прочности связей. Например, для лессов средней плотности начало ослабления связности соответствовало 40-50 с, в то же время в более плотных грунтах оно равнялось 60-90 с. Следует отметить, что начало ослабления связности колеблющегося грунта наряду с прочностью структурных связей, зависело и от ускорения, в частности от частоты колебания.

Вместе с тем проведенные на водонасыщенных лессах исследования показали, что колебание грунта в условиях $a_c < a_{кр}$ сопутствовало со следующими процессами:

а) постепенное ослабление внутренних связей грунта;

б) возникновение динамического напора (порового давления), в процессе уплотнения нарушенных структур частиц грунта;

в) ослабление прочности грунта в результате нарушения связности частиц и взвешивающего воздействия динамического

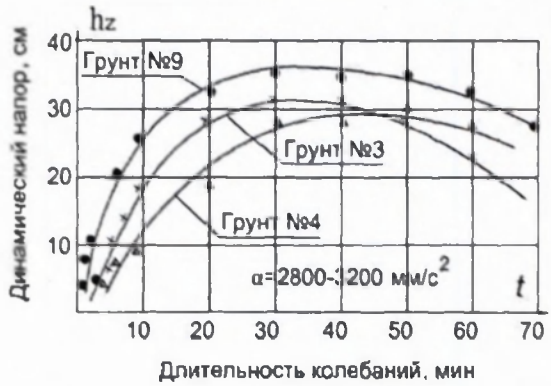


Рис. 3. Зависимость $h_z=f(t)$

напора.

Происходящий в рассматриваемых условиях данный процесс вынуждает рассмотреть динамический напор не только разжижающим грунт, но и снижающим устойчивого уклона откоса при сотрясении.

Известны многочисленные работы по исследованию динамического напора h_z [3 – 5]. Ими установлены, что h_z наряду с свойством и составом грунта (гранулометрический состав, плотности грунта, шероховатости поверхности частиц, сил связности и т.п.) зависит от внешней силы и интенсивности динамического воздействия также.

На рис.3 иллюстрирована зависимость вида $h_z=f(t)$ для исследованных откосов, подвергавшихся колебанию с ускорением 2800 - 3200 мм/с^2. Следующий из рисунка характер изменения динамического напора во времени свойствен всем исследованным грунтам. Если в песчаных грунтах возрастание h_z протекает быстро, а в связных грунтах этот процесс сравнительно замедляется. Здесь, очевидно, имеет место влияние связности грунта.

Роль динамического напора в устойчивом уклоне откоса усматривается из табл.2, где грунты подвергались ускорению колебаний 2800 мм/с^2.

Таблица 2

Зависимость устойчивого уклона откоса от динамического напора

Грунт	Динамический напор, см				
	10	20	30	40	60
№3	-	-	0,58	0,36	0,25
№5	0,43	0,30	0,19	0,10	0,06
№7	0,52	0,21	0,08	-	-
№8	-	0,50	0,30	0,21	0,19

Рис. 4 демонстрирует устойчивый уклон откосов, состоящих из разных грунтов.



Рис. 4. Зависимость $tg\alpha = f(h_z)$ для разных грунтов

В итоге можно заключить, что снижение устойчивости откосов из водонасыщенных грунтов (лессов) в результате взвешивающего воздействия динамического напора может объяснить многие случая аварий, происходящие во время сильных землетрясений.

ЛИТЕРАТУРА

1.Маслов Н.Н. Условия устойчивости водонасыщенных песков.- М.:"Энергия",1961.-328 с.

2.Расулов Х.З. Сейсмостойкость лессовых оснований зданий и сооружений. -Ташкент: Изд-во "Узбекистан",1977. -163 с.

3.Иванов П.Л.Разжижение песков. - М.:"Энергия", 1969. - 181 с

4.Шкицкий Ю.П. Некоторые вопросы оценки гидродинамической устойчивости несвязного водонасыщенного грунта дорожных насыпей. // Труды МАДИ,1973. Вып.62. - С.36-39.

5.Муасэлян А.А. Динамические характеристики лессовых грунтов. //В кн. Динамика оснований, фундаментов и подземных сооружений. - Ташкент: Изд-во «Фан»,1977. -С.212-215.

Несущая способность оснований зданий при сильных землетрясениях

Расулов Х.З., Бабаджанов М.Б.
Ташкентский архитектурно-строительный институт, Ташкент, Узбекистан

АННОТАЦИЯ. Доклад посвящен освящению проведенных авторами исследований по изучению несущей способности оснований сооружений с учетом сейсмических воздействий. Практическое использование результатов исследований показывается в конкретном примере.

ABSTRACT.The report covers the formula proposed by the authors for determining the capacity of erections' basis with a view of seismic influences. The concrete is done as an example of formula's practical usage

Оценка несущей способности оснований в сейсмических районах является одной из сложных задач геомеханики, которая зависит не только от величины внешней нагрузки, но и многочисленных других факторов, таких как: состояния плотности-влажности,прочности-деформируемости грунта, глубины заложения и площади подошвы фундамента и мн. др. Задача осложняется еще и тем, что в данном случае необходимо учитывать весьма трудоемкие процессы, связанные с воздействием землетрясения.

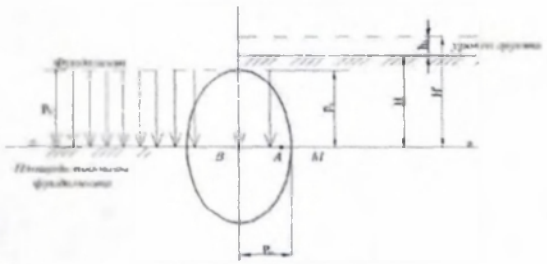


Рис 1. Расчетная схема действия нагрузки

Теоретическое решение таких задач основано на базе составления весьма сложных дифференциальных уравнений с многими неизвестными. В связи с этим в практике расчета ползуются различными эмпирическими коэффициентами для упрощения задач [1]. Такой подход безусловно связан с известными недостатками.

Ниже излагается предлагаемый авторами метод оценки несущей способности оснований с учетом влияния сейсмики.

Обратимся к рис.1. Рассмотрим работу грунта, расположенного на уровне глубины заложения ленточного фундамента. Известно, что наиболее трудные условия работы грунта на данном уровне имеет место на боковых поверхностях фундамента [2]. На этих местах, в основном, наблюдается выпор грунта из под подошвы фундамента.

Изображенный на рисунке фундамент заглублен на глубину H по плоскости a-a. Проанализируем работу грунта в точке M, расположенной вне фундамента. Известно, что фундамент воспринимая нагрузку от сооружения, оказывает давление (p_o) на точку M. В свою очередь грунт в рассматриваемой точке сопротивляется этому давлению своей прочностью, характеризующейся углом трения и сцеплением (φ *ва* c).

Заменяем сцепления грунта воображаемой толщиной h_ϕ, выражаемой силами трения, в виде [3]:

$$h_\phi = \frac{c}{\gamma_w tg\varphi} \quad , \qquad (1)$$

где γ_w - средняя плотность грунта; φ- угол трения грунта.

В этом случае глубина заложения точки M возрастает на $H' = H + h_\phi$. Воздествующему в точке M давлению p_m' сопротивляется давление грунта собственным весом p_{zp} по высоте H. В свою очередь давление p_m, возникающее от силы p_m' в статических условиях выражается

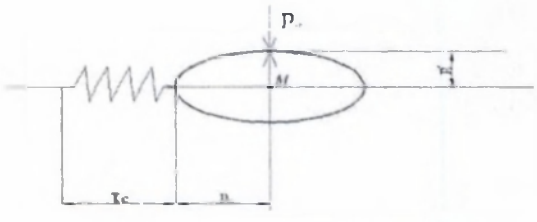


Рис 2. Условная работа грунта в точке А

давлением p_o в точке A, действующим в

горизотальном направлении по горизонту *а-а* (рис. 2).

Величину активного давления p_m, вызывающего сдвиг грунта, находящегося в предельном состоянии можно выразить по известной формуле [4] :

$$p_m = p_o tg^2(45 - \frac{\varphi}{2}) \qquad (2)$$

Учет влияния сейсмики в виде сейсмического горизонтального напряжения может быт осуществлен с помощью выражения [5]:

$$\tau_c = \frac{\gamma_w}{g} H \cdot a_c \qquad (3)$$

где: γ_w – плотность грунта; g – ускорение свободного падения; a_c-ускорение сейсмических колебаний.

Это обстоятельство позволяет выразить активное давление в процессе колебаний p_M^c, в виде:

$$p_m^c = p_m + \tau_c \qquad (4)$$

Или подставив значения p_M и τ_c, имеем:

$$p_m^c = p_o tg^2(45 - \frac{\varphi}{2}) + \gamma_w H k_c, \qquad (5)$$

где k_c - коэффициент сейсмичности.

Как отмечалось выше, выпор грунта из под подошвы фундамента под воздействием силы p_M погащается весом грунта ($p_{гр}$) толщиной (H'), выше горизонта *а - а*, т.е:

$$p_{гр} = \gamma_w H' = \gamma_w (H + h_\phi) \qquad (6)$$

В рассматриваемых условиях равновесие грунта в точке М представляется:

$$p_M^c = p_{гр} \qquad (7)$$

или:

$$p_o tg^2(45 - \frac{\varphi}{2}) + \gamma_w H k_c = \gamma_w (H + h_\phi) \qquad (8)$$

Нагрузка у подошвы фундамента p_0, соответствующая предельному состоянию считается безопасной для данного случая $p_{без}$. Ее значение расчитывается по формуле:

$$p_{без} = [\gamma_w H(1 - k_c) + \gamma_w h_\phi] \cdot tg^2(45^0 + \frac{\varphi}{2}) \qquad (9)$$

или, имея ввиде равенства (1) получим окончательно:

$$p_{без} = [\gamma_w H(1 - k_c) + \frac{c}{tg\varphi}] \cdot tg^2(45^2 + \frac{\varphi}{2}) \qquad (10)$$

В случаях, если $k_c = 0$, из выражения (10) вытекает известная формула Паукера-Маслова.

Пример. Требуется определить несущую способность основания под заглубленным на *Н* = 2м фундаментом. Плотность грунта $\gamma = 1{,}05$ *т*/м^3, угол внутреннего трения грунта $\varphi = 18^0$ ($tg\varphi = 0{,}32$), силы сцепления грунта c = 1,2 *т*/м^2. Сила сейсмичности k_c=0,3.

Решение:

$$[1.05 \cdot 2 \cdot (1 - 0{,}3) + \frac{1{,}2}{0{,}32}]tg^2(45^0 + \frac{18}{2}) = (1{,}47 + 3{,}75)tg^2 54^0 = 9{,}92$$

$$p_{без} = 9{,}92 т/м^2 = 0{,}99 кг/см^2$$

Несущая способность основания в отсутствии сейсмического воздействия (k_c=0) определялась величиной - 11,12 т/м^2 (1,12 кг/см^2), что свидетельствует снижение величины $p_{без}$ при 8 балльном землетрясении на 8,9% .

ЛИТЕРАТУРА

1. КМК 2.02.01-98. Основания зданий и сооружений. Издание официальное. –Ташкент,1996. -48с
2. Маслов Н.Н.Основы инженерной геологии и механики грунтов. – М.:"Высшая школа",1982. -571 с.
3. Цытович Н.А. Механика грунтов (Краткий курс). – М.,1983. -288 с.
4. Ухов С.Б., Семенов В.В. и др. Механика грунтов, основания и фундаменты. –М.:Изд-во АСВ,1994. - 524 с.
5. Расулов Х.З. Сейсмостойкость грунтовых оснований. –Ташкент: Изд-во "Узбекистан",1984. - 192 с.

Dilution of water-sated lousier soil at seismic influences

H.Z Rasulov

Department of Civil and Structural Engineering, The Architectural and Civil Engineering Institute, Tashkent, Uzbekistan

ABSTRACT. The report is dedicated to the question of breaching the steadiness of aqueous less structure soils and its changes into the dilution condition at the seismic influences. Basic conditions of physic - mechanical theory about the dynamical branches of aqueous less structure are provided into the basis the change of resistibility displacements at the intensive vibration is given. The formula for determination of quantities of dynamical pressure and connectedness soils taking into account duration of dynamical influence.

АННОТАЦИЯ. Доклад посвящен вопросам исследования нарушения прочности водонасыщенных лессовых грунтов и их разжижении при сейсмических на них воздействиях. На базе физико-механической теории о динамическом нарушении прочности структуры лесса объясняется изменение сопротивляемости грунта сдвигу при интенсивных вибрациях. Предлагается формула для количественного определения динамического напора и силы связности грунта в условиях динамического воздействия.

Infringement of stability of the water-sated less thickness and transition in a diluted status at seismic influence occurs not far in all cases and to a different degree of intensity. It is possible to believe, that the significant role thus is played with intensity of the most seismic influence. On the other hand, important value has also a natural status of density-humidity soils.

The degree of infringement of structure water-sated less soils and transition in a diluted status at fluctuation, and from here their dynamic mode is defined by influence only some part of the seismic loading enclosed to them. It is estimated by the size of the maximal seismic acceleration peculiar to fluctuation arising at it a_c.

Having designated actively operating part of acceleration of fluctuations through (a_a) we can write down:

$$a_a = a_c - a_{kr} \qquad (1)$$

Where a_{kr} -size of critical acceleration as some limited acceleration which is absorbed inside of soil thickness by forces of resistance operating in it and first of all as has shown the analysis, forces of coupling (c_w) and internal friction (φ_w) [1].

Provided that the size of critical acceleration can be considered as some acceleration at which the structure of the water-sated loess is not broken.

Hence, at all values of seismic accelerations it is less (a_{kr}) resistance to shift of the water-sated loess ground (τ) It is defined on expression:

$$\tau = \sigma_{din} tg\varphi_w + c_w \qquad (2)$$

where (σ_{din}) - dynamic normal pressure from weight of the ground laying above considered horizon and weight of constructions; (φ_w) - a corner internal friction at humidity «w»; C_w - the general coupling of a ground at humidity «w».

Obviously, the higher the size of critical acceleration (a_{kr}) the smaller on size the acceleration α_a, defining the dynamic mode of soil thickness.

Critical acceleration is functionally connected with solid characteristics of soils. In particular, N.N.Maslov described this dependence in the form of [2]:

$$a_{kr} = \mu'(\sigma_{din} tg\varphi + c_w), \qquad (3)$$

where μ' - some parameter connected with property and a condition soil, and also a character of a dynamic mode.

According to the expression (3) the size of (a_{kr}) seismic conditions can change due to partial, or full decrease in those or other parameters, such as a normal pressure (σ), a corner of internal friction (φ_w) and the general coupling (c_w).

It results, with other things being equal according to expression (1), to increase in time of value of an active part of acceleration a_a.

Thus, disclosing of the nature of infringement of structure lassie water-sated soils is reduced to revealing parameters of resistance changing in dynamic conditions to their shift,(φ_w, c_w).

Resistances to shift - these basic solid parameters of resistance soils to external forces, are variables depending on pressure and conditions in points of contact of the particles, resisting to shift.

The question on resistance to shift is the most complex in case of coherent soils, differing from

inconsistent (sand, etc.) that particles of these soils are connected among themselves plastic and partially rigid (cement - crystal) by connections, thus resistance to their shift (durability) basically will be defined by their connectivity (forces of coupling).

The analysis of numerous natural cases of loss of stability with transition in diluted condition similar soils at strong earthquakes and the given experimental researches have allowed Rasulov H.Z. to develop the physical theory about dynamic infringement of structure water-sated less soils [l]. In a basis of these theory possible variants of change in dynamic conditions of parameters of resistance coherent soils to shift in a following kind are put:

1. At ($\alpha_c < \alpha_{kr}$) the ground keeps the structure and change of resistance to shift it is defined {detennined} by the account only the inertial forces caused by fluctuations of system of the bases-constructions, that is characteristic to cases of concussion dense soils at influence concerning weak earthquakes.

2. At ($\alpha_c > \alpha_{kr}$) the structure of a soil collapses also resistance to shift it is defined in view of the variable intense condition of environment, and also parameters of durability of a soil changing in these conditions, that is characteristic to cases of fluctuations of weak soils at influence of intensive seismic loadings.

It is known, that owing to repeated and repeated action of seismic loading in a soil there is an effect of temporary unloading and at loadings which leads to short-term and periodic change of the intense condition, which in final result is connected with a change of resistance to shift.

This change with reference to dense and dry soils can affect first of all on change of forces of internal friction operating in a soil. The last can be observed and in plastic soils also due to change of the density connected with unloading and possible{probable} increase in humidity of soils, that, naturally, conducts to downturn of sizes of true corners of internal friction φ_w and connectivity

c_w breeds and, as consequence - to falling their resistance to shift, or on the contrary.

The increase (or reduction) resistibility to shift of a ground in the above-named conditions should contact two factors:

1) factor - with increase (or downturn) forces of internal friction operating in a soil with reference to a new condition of its loads at constant value of a true corner of internal friction of the soil ad equating to its initial condition on density-humidity;

2) factor - with additional condensation a ground under influence of loading and corresponding increase (or decrease) sizes: φ_w, c_w

Forces of internal friction in considered conditions increase in a ground (or decrease) practically simultaneously after the appendix to a ground of additional loading (is conditional-instant reaction).

Experience shows, that all coherent soils differ ability at unloading to keep to some extent the density reached at preceded higher loading. It is distinctly shown in experiences on a compression, spent in consecutive cycles of loading and unloading. Finally the branch of unloading usually lays down below a branch of loads, and thus at the same loadings density of breed, - was in the beginning under higher loading and then tested some unloading, happens in all cases of higher. However in different breeds character of display of this process appears far unequal.

From here the conclusion follows, that the size of an increment or easing of resistance to shift of coherent soils at the same values of change of loading $\pm\Delta_p$ turns out considerably below in conditions of unloading $(-\Delta_p)$ in comparison with size in conditions loading $(+\Delta_p)$. However the effect loading too is less essential in view of short duration of action of seismic loading.

This circumstance enables at the decision of the questions connected with clay soils, to ignore in increase (or downturn) resistance to shift of value of change of density-humidity of a soil under loading and to carry it only due to the loading (concept about critical acceleration).

The circumstance specified above causes, at an estimation of prospective influence on a degree of stability of coherent soils of additional inertial loading $\pm\Delta_p$ to use already expression:

$$\tau_c = (\sigma \pm \Delta\sigma) tg\varphi_w + c_w \qquad (4)$$

Passing to the second to item{point} we shall note, that the seismic influences enclosed to humidified coherent soils, are perceived first of all by internal communications{connections}
operating{working} in them (c_w) - While internal forces are not overcome by operating{working} shifting seismic pressure {voltage}, the coherent soil will behave as a kwazisolid body possessing only elastic forces of coupling.

Under forces of coupling in this, as well as others, cases meant resistance of structural connection to any moving particles connected by them, irrespective of size of external pressure.

At excess of the seismic power influence expressed in the form of acceleration (a_c) of critical value (defined with the account of change of pressure inside of the shaking environment owing to changeability of external loading), peculiar to data " to a soil and caused by its structural durability, these communications{connections} can appear broken. The opportunity and a degree of infringement of communications {connections} of a soil are caused by this or that intensity of an operating{a working} active part of acceleration (a_w) and with reference to the water-sated{water-saturated} losses duration (t) fluctuations.

Conditions and character of infringement of these connections can be explained to the following:

During earthquake on soil thickness take place various seismic longitudinal both cross-section deep and superficial waves which, extending in firm, liquid and gaseous phases, cause pressure compression-stretching and shift. Thus alongside with elastic deformations on occasion observe destruction of structure and irreversible deformations of a ground.

It is considered, that at action of shifting seismic loading destruction of structural connections (both viscoplastic, and rigid) will simultaneously go. However thus special value is given to connectivity (c_w) a soil and to change of its durability caused

Water environments on a surface of the particles giving to them corresponding friability. Presence of water environments on particles, as is known, is connected with the electric charges acting on surfaces of particles.

One of substantive provisions of the theory starts with change during concussions of durability of connections soil, this or that water environment depending on thickness. It is supposed, that the last occurs due to change of thickness of the water environments, accompanied by infringement of orientation of molecules in colloid-seen environments of a ground and transition to the connected water in free in these conditions. Finally it leads to infringement of structure of a ground and an opportunity of its condensation. However noted process becomes complicated occurrence in these conditions of hydro dynamical effect at condensation of the broken connections of particles.

In conditions of full water-saturation of thickness condensation of particles can occur only in case of outflow from thickness of some superfluous for a new condition of its density of volume of the water filling times in a ground that can lead to formation of a filtration stream, to the certain gradient of a pressure (I). Last is supported arising at concussion in soil thicknesses by superfluous pressure (dynamic pressures), increasing on depth (z) and in time (t).

Thus, in conditions of easing of connectivity and an opportunity of condensation in soil thickness it appears operating antipreausure, weighing particles of a ground. This circumstance promotes the most intensive easing of connectivity of the ground, remained not broken {disturbed} on this or that reason. Easies or completely contacts between particles that leads to braking of purchase of new internal connection disappear. All weight of the ground, deprived connections can get properties of a liquid that is observed on occasion in experiments of dilution.

In summary it is possible to believe, that in conditions of concussions in a coherent ground there are rather complex phenomena which to be a subject to complex consideration at their quantitative forecast. Generally afore-mentioned is connected with falling durability soils during vibration. From here there was a necessity of the account of decrease {reduction} in durability (resistance to shift) such soils with reference to some set time defined by duration of possible seismic influence under which action can develop process of easing of connectivity (c_w) and progressive increase dynamic pressure (h).

It enables to present size of resistibility of the water-sated less soils to shift in seismic conditions in the form of:

$$\tau_c = \left[(\sigma \pm \Delta\sigma) - \gamma_w h_t\right] g\varphi_w + c_{w,t} \quad (5)$$

Where φ_w- density of water; h_t -the dynamic pressure arising at opportunities of condensation of the particles deprived to connectivity and increasing on depth (z) in time (t); $C_{w,t}$-the coupling (connectivity) ad equating to the moment of time t.

According to expression (5) decrease in resistance to shift dilution of the water-sated losses at seismic influences speaks easing in time of connectivity (c_w) and strained conditions (σ soil at a constant true corner of internal friction (φ_w)

For deflnition of change of a dynamic pressure (h) depending on duration of fluctuation (t) dependence of a kind is offered

$$h(z,t) = \frac{v_o}{k_f}\left(H_z - \frac{z^2}{2}\right)\left(e^{-\mu} - e^{\lambda}\right) \quad (6)$$

And for coupling (connectivity) in these conditions:

$$c_w(t) = c_w(k) + [c_w(n) - c_w(k)]e^{-\mu} \quad (7)$$

In expressions (6) and (7): V_o-speed of condensation of the soil, defined experiment in the form of $\frac{dn}{dt}$

n- soil porosity; k_f- coefficient of filtrations: H-thickness of a layer; z - depth of considered horizon; μ - parameters of a soil defined by practical consideration; $c_w(n)$, $c_w(k)$ initial and final values of connectivity of a soil.

LITERATURE

1. *Rasulov H.Z. Seismic stability of the soil bases, Tashkent, «Uzbekistan» 1984*
2. *Maslov N.N. Condition of stability of the water-sated sand, M, "Energy", 1959.*

Длительная деформация медресе Амир Тура в г. Хиве

Нарбаев С.М.
Архитектурно-строительный институт, Ташкент, Узбекистан

Аннотация. Доклад посвящен освящению результатов исследований длительной деформации медресы Амир Тура в г.Хиве. Анализируются физико-механические и прочностные показатели антропогенных грунтов, залегающих в основании медресы. Отмечается, что длительная деформация памятника происходит в результате изменения связности грунта с течением времени, что подтверждается экспериментальными исследованиями.

Abstract. The given report is dedicated to the research of prolonged deformation of Amir Tura's mosque in Hiva. Physic-mechanic and durable index of antropoghen soils which lie in the basis of mosque are analyzed. It is mentioned that prolonged deformation of the monument occurs as the result of soil's correction change with the time flow which is proved by experimental research.

Медресе Амир Тура построена в 1870 г. на мощной толщи слабых грунтах антропогенного происхождения на северной части Ичан Калы в г. Хивс. Толщина антропогенных грунтов в основании здания 9,5 м. В настоящее время практически все стены и перекрытия здания покрыты трещинами различных размеров результате неравномерной осадки фундамента [1]. По данным специалистов, обследовавщих деформации, оседание мадресы продолжалось в течение многих десятилетий. Характер расширяющихся с низа к верху трещин (3-4 см) в стенах главного входного портала и в несущих стенах северного фасада указывают помимо осадок и на некоторую наклонность их в фасадную сторону здания.

Антропогенные грунты в основании здания характеризуются следующими показателями: плотность скелета - $2{,}66\text{-}2{,}72\cdot10^4$ Н/м^3, природная плотность – $1{,}26\text{-}2{,}0\cdot10^4$ Н/м^3, плотность сухого грунта – $1{,}23\text{-}1{,}62\cdot10^4$ Н/м^3, природная влажность – 1,0÷18,0%, пористость - 32,2-54,1%, коэффициент пористости – 0,475-1,179.

Грунты по степени пластичности находятся между песков и супесей (5,1-13,3%). Несущая способность их низкая. В водонасыщенном состоянии под $0{,}3\cdot10^5$ Па нагрузкой они показали угол внутреннего трения - 25^0-30^0, коэффициент трения - 0,470-0,630, силы сцепления - $0{,}04\text{-}0{,}23\cdot10^4$ Па и коэффициента относительной просадочности - $0{,}14\text{-}1{,}80\cdot10^4$ Па.

Антропогенные грунты содержат различные (органические и неорганические) включений (30%), которые представлены в виде сжженного кирпича, металла, керамики, корни деревьев и различных остатков жизнидеятельности человека. Горизонт подземных вод - 5,0–6,0 м.

Они обладают просадочными свойствами. Под начальным просадочным давлением 0,2 МПа относительная просадочность 0,0049.

Следует отметить, что просадочная способность сохраняется даже в случаях полного водонасыщения их. В целом вся площадка застройки по просадочному свойству относится к 2-му типу просадочности. Опыты показали, что просадка от собственного веса грунта проявляется начиная с 3 м. глубины. Они весьма пористые (коэффициент пористости $e = 0{,}894$), обладают незначительным модулем общей деформации ($2{,}25\cdot10^5$ Па) и коэффициентом сжимаемости 0,048 см^2/кг (под нагрузкой $p = 2\cdot10^5$ *Па*).

Давление на грунт от здания – $1{,}5\cdot10^5$ Па. Опыты показали, что под таким давлением антропогенные грунты, взятые на пробу способны проявлять длительную деформацию. Следует отметить, что постоянное увлажнение грунта основания здания различными путями (мадрасе расположена внутри жилого квартала) длительное время они сохраняют свое пластичное свойство в пределе текучести. Это обстоятельство, повидимому способствовало длительному неравномерную деформацию грунта основания.

По материалам архива "Главного управления по охране и реконструкции исторических памятников" Министерства Культуры Республики изучение деформации памятников Ичан-Калы, в частности Медресы Амир Тура, началось в 50-десятые годы прошлого столетия. Произведенные в те годы измерения трещин у фасада и на северо-западных стенах медресы показали 0,5-1,0 см

величин. Установленные в дальнейшем репера свидетельствовали о медленно продолжающихся деформаций стен здания.

Сопоставление данных исследований последних лет с предидушими показаниями указало на повышение влажности грунта на 0,14 (22%) и природной плотности на 0,07 (3,9%) [2]. В тоже время угол внутреннего трения грунта практически не изменялся, а сцепление уменьшилось на $0,7 \cdot 10^5$ Па (44 %).

Показание марок, установленных на стенах медресы и медленное расширение трещин свидетельствовали о продолжающейся деформации сооружения (рис.1). Изменение скорости деформации во времени можно усмотреть из рис.2.

Анализ результатов исследований показал, что длительная деформация грунта в основном связана с ослеблением во времени связности c_w (рис.1-3).

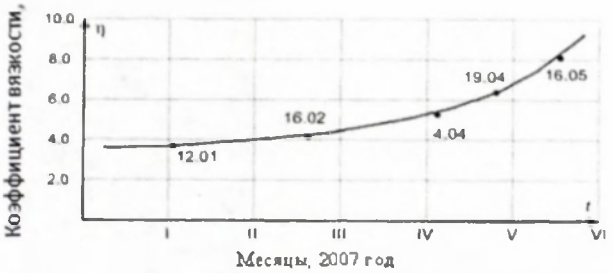


Рис.1. Изменение деформации грунта во времени в основании медресы Амир Тура

Как следует из гафиков, что коэф. вязкости грунта за короткий период времени (6 месяцев) увеличился в 5 раз, что подтвердило зависмости длительности протекания деформации от изменения величины связности грунта.

Оценка длительной деформации основания медресы. Исходные данные: Фундамент здания – ленточный с шириной подошвы B=1,43 м. Расчетное давление на основание $1,5.10^5$Па. Природная плотность грунта $\gamma_w = 1.86 \cdot 10^4$ Н/м^3. Значения коэф. вязкости грунта: $\eta_w = 10.8 \cdot 10^{13}$ Па·с;

Рис.2. Скорость деформации грунта в основании медресы Амир Тура

$\eta_0 = 12,93 \cdot 10^{13}$ Пас ; $\eta_{200} = 11,9 \cdot 10^{13}$ Па·с.

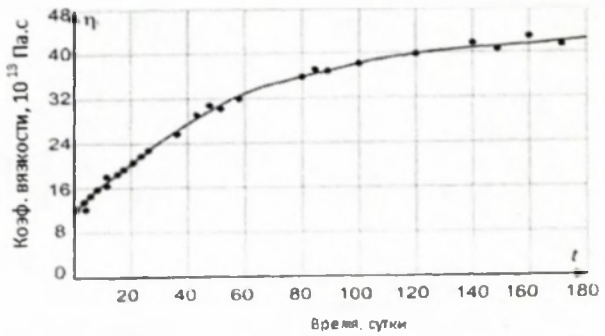
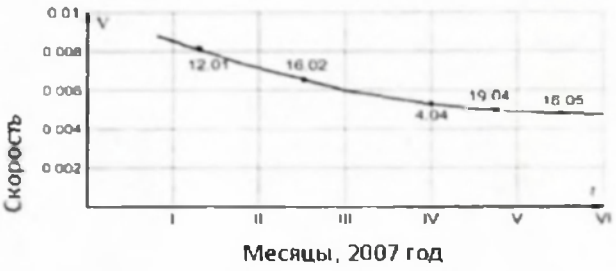


Рис.3. Изменение коэф. вязкости во времени



(w_T=26.7%; w_0=27.9%; w_p=8.6: φ_w=25^0; c_w=0,08·10^5 Па).

Решение:

1. Определим величины коэф. μ [3].

$$\mu = \frac{1}{0,1} \ln \frac{(129,3-10,8)\cdot 10^{13}}{(129,3-11,9)\cdot 10^{13}} = 0.023 \text{ сут}^{-1}$$

2. В соответствии с условием $p_{(D)} = 0,2p_p$ толщина сжимаемой толщи равняется $D = 9,2$ м.

3. Отсюда величина осадки здания за 100 лет [4]:

$$S_{100} = 1,5 \cdot 10^5 \cdot 1,43 \left[\frac{100}{12 \cdot 9,3 \cdot 10^{13}} + \frac{1}{0,23 \cdot 12 \cdot 9,3 \cdot 10^{13}} \right.$$

$$\left. \ln \frac{12 \cdot 9,3 \cdot 10^{13} - (12 \cdot 9,3 \cdot 10^{13} - 10,8 \cdot 10^{13}) \cdot e^{-0,23 \cdot 100}}{12 \cdot 9,3 \cdot 10^{13}} \right] \cdot \ln \frac{1,43+9,2}{1,43} = 12,79$$

см.

Оценка реологического свойства грунта в основании здания.

Исходные данные: $P_p = 1,5.10^5$ Па; $B = 1,48м$; $\varphi_w = 16^0 30'$; $c_v = 0,9.10^5$ Па; $\gamma_w = 1,86 \cdot 10^4$ Н/м^3; глубина заложения фундамента $H = 0,8м$.

Решение:

1. Определяем безопасную нагрузку на основание $p_{0,6}$ [5]. Для этого находим коэффициентов M_H ва M_c в зависимости от угла трения φ [6]: $M_H = 2,6$ ва $M_c = 5,1$.

2. Расчет $p_{0,6}$ произведем по формуле:

$$p_{pб} = M_H \cdot H \cdot \gamma_w + M_C \cdot c_v = 1{,}26 \cdot 10^5 \text{ Па}$$

3. Основываясь на условии $p_{pб} \succ p_p$ ($1{,}26 \cdot 10^5$Па < $1{,}5 \cdot 10^5$Па), определяем возможность длительной деформации грунта в основании здания. Для этого выполняем нижеследующие расчеты:

5. Определяем порог ползучести η_{lim} грунта [3]:

$$\tau_{lim} = p_z \cdot tg\varphi_w + c_w + c_c = 1{,}5 \cdot 10^5 \cdot 0{,}29 + 0{,}45 \cdot 10^5 + 0{,}05 \cdot 10^5 = 0{,}93 \cdot 10^5 Па$$

здесь:

$$c_v = c_w + c_c = 0{,}5 \cdot 10^5 Па$$

($c_w = 0{,}45 \cdot 10^5 Па$; $c_c = 0{,}05 \cdot 10^5$ $Па$).

Подставив эти значения в формулу $\tau_{lim} = p_n tg\varphi_w + c_c$ получим:

$\tau_{lim} = 1{,}5.10^5.0{,}29 + 0{,}05.10^5 = 0{,}83.10^5$ Па

6. Максимальная величина сдвигающего напряжения определяется по выражению:

$$\tau_{max\,max} = \frac{2p_0}{\pi} = \frac{3.0.10^5}{3.14} = 0{,}95.10^5 \text{ Па}$$

7. $0{,}95 \cdot 10^5$Па > $0{,}83 \cdot 10^5$ Па и $\tau_{max\,max} \succ \tau_{lim}$ условия свидетельствуют о наличии пластов, обладающих длительной деформацией грунта в основании здания.

8. На рис. 4 изображен произведенный расчет коэф. сдвига τ_{dc} для 50 точек в основании медресы.

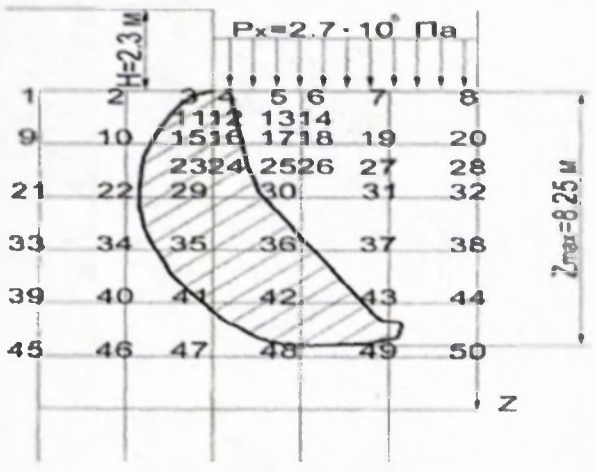


Рис.4. Распространение деформации сдвига в основании

В этих условиях возникает необходимость определения глубины распространения зоны (z_{max}) пластической деформации грунта ($k_{dc} \prec 1$) в основании сооружения [5]:

$$z = \frac{1}{\gamma_w tg\varphi_w}\left\{\frac{p_z}{\pi}\sin\alpha \cdot \sin 2(45^0 + \frac{\varphi_w}{2}) - \left[\frac{p_z}{\pi}(\alpha + \sin\alpha)\cos 2(45^0 + \frac{\varphi_w}{2}) + \right.\right.$$

$$\left.\left. + \gamma_w (H + h_c)\right]tg\varphi_w - c_c\right\} \qquad (1)$$

Продифференцировав по α получим z' в следующем виде:

$$z' = \frac{1}{\gamma_w tg\varphi_w} \cdot \frac{p_z}{\pi}\left[\cos\alpha \sin 2(45^0 + \frac{\varphi_w}{2}) - \cos\alpha \cos 2(45^0 + \frac{\varphi_w}{2})tg\varphi_w - tg\varphi_w\right] \qquad (2)$$

Максимальное значение z_{max} достигается при условии равенства нулю величин в квадратной скобке:

$$\cos\alpha_{z_{max}} = \frac{tg\varphi_w}{\sin 2(45^0 + \frac{\varphi_w}{2}) - \cos 2(45^0 + \frac{\varphi_w}{2})tg\varphi_w} \qquad (3)$$

Определив из этого выражения угол видимости $\alpha_{z_{max}}$ для любого значения угла внутреннего трения грунта по выражению (2) можем расчитать глубину распространения зоны с максимальными сдвиговыми деформациями в виде: (z_{max}) в виде:

$$z_{max} = \frac{1}{\gamma_w tg\varphi_w}\left\{\frac{p_z}{\pi}\sin\alpha_{z_{max}} \cdot \sin 2(45^0 + \frac{\varphi_w}{2}) - \left[\frac{p_z}{\pi}(\alpha_{z_{max}} + \sin\alpha_{z_{max}})\cos 2(45^0 + \frac{\varphi_w}{2}) + \right.\right.$$

$$\left.\left. + \gamma_w (H + h_c)\right]tg\varphi_w - c_c\right\} \qquad (4)$$

Представим выражения (3) в следующем виде:

$$\cos\alpha_{z_{max}} = \frac{tg\varphi_w}{\cos\varphi_w + \sin\varphi_w \cdot tg\varphi_w} = 0{,}27 \qquad (5)$$

Отсюда можем определить величины угла $\alpha_{z_{max}}$ равной $88^0 24'$ или 1.54 радиан.

Фиктивная высота (h_c), обуславливающая сцепления грунта равняется :

$$h_c = \frac{c_c}{\gamma_w tg\varphi_w} = 9{,}43 \text{ м}$$

Подставив все найденные значения в формулу (4) определим максимальную глубину распространения зоны, в пределах которой развивается сдвиговая деформация грунта. Эта зона равняется $z_{max} = 9{,}45$ м.

ЛИТЕРАТУРА

1. Длительная деформация слабых грунтов в основании исторических памятников Узбекистана. Отчет о научно-исследовательской работе. – Ташкент, ТАСИ, 2000. -45 с.
2. Архивные материалы Главного управления охраны и реконструкции исторических памятников при Министерстве культуры и спорта республики.
3. Маслов Н.Н. Длительная устойчивость и деформация смещения подпорных сооружений. -М.: Энергия,1968.-159 с.
4. Расулов Х.З. Прогноз деформации сооружений в результате пластического течения грунтов оснований при землетрясениях // Труды 1-го Центрально – Азиатского геотехнического симпозиума. –Астана, 2000. –С.266.
5. Маслов Н.Н. Основы инженерной геологии и механики грунтов. -М.: Высшая школа, 1982. -551 с.
6. Расулов Х.З. Сейсмостойкость грунтовых оснований. – Ташкент: Узбекистан,1984. -192 с.

Comparison of Geotechnical Freezing Characteristics between Korea and Kazakhstan Soils

E.C. Shin & B.H. Ryu
Department of Civil & Environmental Engineering, University of Incheon, Republic of Korea

A.Zh. Zhussupbekov & Zh.A. Shakhmov
Department of Civil Engineering, L.N. Gumilyov Eurasian National University, Astana, Kazakhstan

ABSTRACT. The integrity of roadbed is an important element to resist the sustained load transmitted by the traffic load on the road surface. In the seasonal freezing climate both Korea and Kazakhstan can be significantly influenced to the integrity of roadbed. The soil specimens obtained from both countries are used for subgrade in the highway construction. The proper determination of magnitude of frost heave and heaving pressure by the influence of the cold freezing temperature during the winter season are necessary for design and construction highway.

1 INTRODUCTION

The integrity of roadbed is an important element to resist the sustained load transmitted by the traffic load on the road surface. In the seasonal freezing climate both Korea and Kazakhstan can be significantly influenced to the integrity of roadbed. The soil specimens obtained from both countries are used for subgrade in the highway construction. The proper determination of magnitude of frost heave and heaving pressure by the influence of the cold freezing temperature during the winter season are necessary for design and construction highway. The laboratory model tests were conducted for the specimens obtained from Astana, Kazakhstan and Korea to determine the freezing pressure and the magnitude of frost heaving.

Shin and Park (2012) studied the soil freezing characteristics and temperature distribution in ground LNG storage tanks with consideration of several variables include soil type and heterogeneity, variation of soil temperature with time and depth, rate of freezing and availability of water.

Choi al. (2011) reported the rapid reduction of shear strength of railway roadbed soil. The strength reduction rate is not significant for the soil which is contained 25% of passing #200 sieve due to the freezing-thawing cycles.

The characteristics of frost heaving in the field is not easy to estimate because several factors are influenced as described previously including soil properties. Many researches were tried to propose the laboratory test procedure for the measurement of the frost heaving accurately since 1960's (Grim, 1952; Hoekstra, 1966; Lawectal, 1969).

However, TRRL(Transport and Road Research Laboratory) method in England (Jones, 1981), US. Army Corps of Engineer's method (American Society for Testing and Materials D 5918-96, 2006), the method proposed by Japanese Geotechnical Society (2003) are currently being used for estimation of frost heave ratio (ε) and frost heave rate (U_h). The frost heave ratio (ε) can be expressed in Eq.(1) as follows,

$$\varepsilon(\%) = \frac{H_f}{H_1} \tag{1}$$

Where, H_f is the total amount of frost heaving after completed freezing, and H_1, is the original height of soil specimen prior to freezing. The frost heave rate (U_h) can also be expressed in Eq.(2) as follows,

$$U_h(mm/h) = \frac{\Delta H}{\Delta t} \tag{2}$$

where, ΔH is the total amount of frost heave; and Δt is the elapsed time in hour.

Table 1. (a) Frost heaving criteria by different methods

TRRL (U.K.)			JGS (Japan)	
judgment	Frost heave ratio(%)	Frost heave rate (mm/hr)	judgment	Frost heave rate(mm /hr)
Negligible frost susceptibility(NFS)	Less than 12	Less than 0.375	low	Less than 0.1
Possible Frost Susceptibility(PFS)	Over 12	Over 0.375	medium	0.1-0.3
			high	Over 0.3

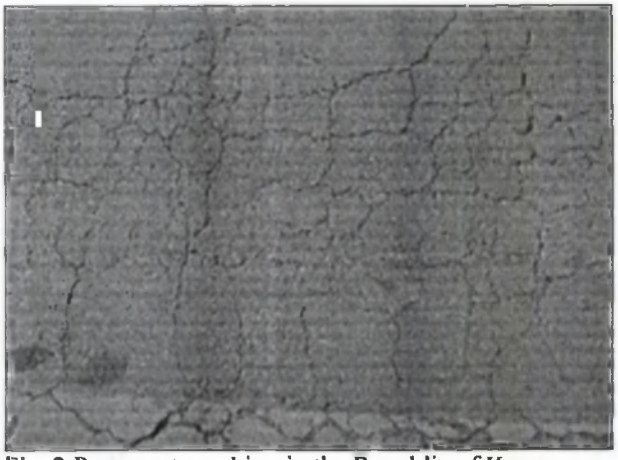
Table 1. (b) Frost heaving criteria by CRREL(U.S.) methods

CRREL (U.S.)	
judgment	Frost heave rate (mm/hr)
negligible	Less than 0.021
Very low	0.021-0.042
low	0.042-0.083
Medium	0.083-0.167
high	0.167-0.333
very high	Over 0.333

Current judgment criteria of frost heave is tabulated in Table 1. The amount of frost heave and the heaving pressure were experimentally studied previous by Taber (1929), Miller et al. (1960), Kinoshita and Ono (1963),Shin and Park (2003). Hoekstra et al. (1965), Yong and Oster (1971), Penner (1974), Domashuk (1982), Akagawa, S (1983), and Akagawa et al. (1985) were also studied regarding on the frost heave characteristics related to the specimen site, uplight forces of structural foundation through the field and laboratory tests. Shin et al. (2012) conducted by using a large scale laboratory test in the freezing chamber sited in 3.2m(L) x 3.2m(B) x 2.4 m(H) to determine the change of plastic modulus caused by the cycle of frost heave and thawing for the paved roadbed. Pavement becomes distorted during winter causing increased roughness and cracking of the pavement surface as shown in Figures 1and 2.



Fig. 1 Pavement cracking in the Astana (Kazakhstan)


Fig. 2 Pavement cracking in the Republic of Korea

The results of laboratory freezing test indicate that the Korea soil were much susceptible to the freezing temperature than that of Kazakhstan soil.

The magnitude of frost heaving of Korea soil is about 25% higher than that of Kazakhstan. Also, the magnitude of freezing pressure of Korea soil is approximately 2 times higher than that of Kazakhstan. The percentage of number #200 passing in sieve analysis and Atterberg limits(LL,

PL) are greatly contributed to the freezing heaving of soil.

2 SOIL PROPERTIES AND FREEZING TEST

The special mold which can eliminate the side friction between soil and wall was used in the laboratory freezing test. Prior to the laboratory freezing test, geotechnical properties of the soils were determined throw the basic tests. The geotechnical properties of both Kazakhstan soil and Korea soil are presented in Table 2.

The specimen is remolded and prepared in mold which is appropriate for freezing chamber. Four molds were fixed in the freezing chamber and putted them into the freezing apparatus. However, all soil specimen molds were saturated in the water barrel. Only after saturation, they were putted in the freezing apparatus.

Table 2. Geotechnical properties of soil specimens

Description	Kazakhstan	Korea	SP	SM
Specific gravity (G_s kN/m^3)	2.62	2.63	2,63	2,67
Natural water content (w_n,%)	21	N.P	N.P	N.P
Particle size passed #200 (%)	52	66	19,6	1,9
Liquid limit (LL, %)	27.01	50.50	N.P	N.P
Plastic limit (PL, %)	17.75	31.94	N.P	N.P
Maximum dry unit weight (γ_{dmax}, kN/m^3)	1.79	1.27	1,92	1,93
Optimum water content (w_{opt}, %)	15.9	32.25	11,5	12,4
USCS	CL	OH	SP	SM

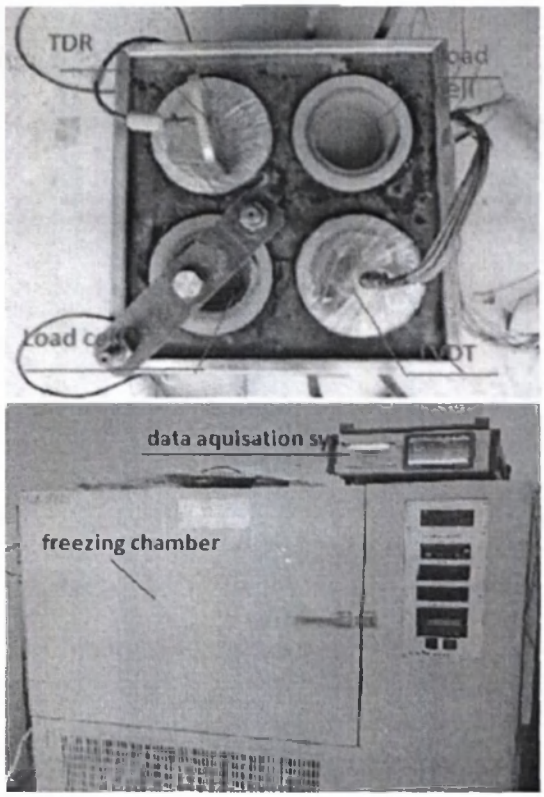


Fig. 3 General view of the freezing equipments.

General view of freezing chamber filled in with soil and freezing equipment is presented in Figure 3. The grain size distribution curves of the soils are presented in Figure 4.

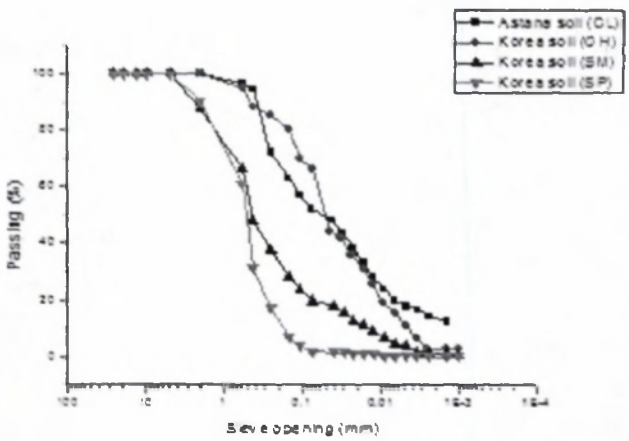


Fig. 4 Grain size distribution curves of Kazakhstan and Korea soils.

The first 24 hours is a conditioning period. Both the top and bottom plates are kept the temperature at 3 ^{0}C. The first freeze starts at the beginning of the second 24-hours period. First recording the initial dial gage or transducer readings; take a reading for each device if both are being used. The

temperature of the top plate was lowered and hold it up at -3 ^{0}C. The temperature of the bottom plate was kept at 3 ^{0}C for 8 hours. The temperature of the top plate (T_t) was lowered at -12 ^{0}C after 8 hours have passed, and the bottom plate (T_b) was kept at 0 ^{0}C. These temperatures were kept for 16 hours. The temperature of the water for opening system of testing is kept 4 °C + 0.5.

The first thawing process starts at the beginning of the third 24-hours period (ASTM, 2004). The top plate temperature and hold it up at 12 ^{0}C. The bottom plate temperature were also raised and hold it up at 3 ^{0}C for 16 hours. During the next 8hours, keeping both the top and bottom plate temperatures at 3 ^{0}C. The second freeze starts at the beginning of the fourth 24-hours period. This procedure is the same as that used in the first freeze. Also boundary temperature conditions are presented in Table 3.

Table 3. Boundary temperature conditions

Day	Elapsed Time (t), h	Top Plate Temperature (T_t), °C	Bottom Plate Temperature (T_b), °C
1	0	3	3
2	24	-3	3
	32	-12	0
3	48	12	3
	64	3	3
4	72	-3	3
	80	-12	0
5	96	12	3
	112 to120	3	3

The second thawing process starts at the beginning of the fifth 24-hours period. This procedure is the same as that used for the first thawing process.

During freezing-thawing test, all temperature sensors and displacement transducers are recorded at least every half an hour throughout the first 8-hour of freezing and after then at 1-hour intervals.

At the end of the second thawing period (120 hours after the beginning of the test), recorded that dial gage reading. The circulating liquid turning off to the temperature control plates. The dial gage and the displacement transducer assembles are removed with the surcharge weights and the top temperature control plate assembly. The insulation of around the soil specimen makes a loose condition to allow access to the temperature sensors from the side of the specimen by pulling them gently away from the acrylic rings. The specimen assembly and the base plate are removed completely from the temperature control chamber.

3 LABORATORY FREEZING TEST RESULTS AND DISCUSSION

The laboratory freezing tests were performed for understanding frost susceptibility of the soil and predetermination possible frost action to the structure. The frost penetration into the specimen results of the freezing test are presented in Figure 5.

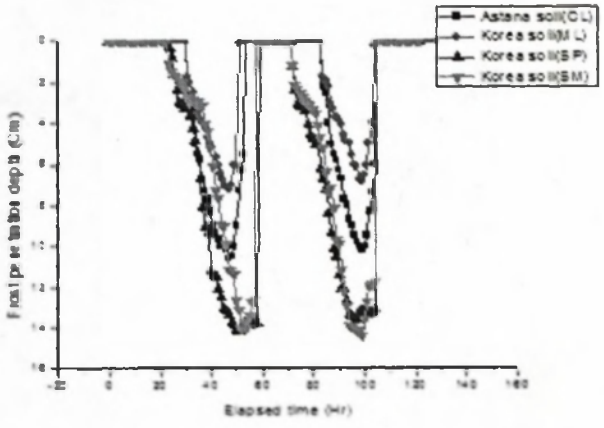


Fig. 5 Results of frost penetration depth of the Kazakhstan (Astana) and Korea soils

There are some curves which show frost penetration depth of the Kazakhstan and Korea soil. The frost penetration of Kazakhstan soil is about 3 cm more deeper that of Korea soil. The horizontal numbers show the time in hour and the vertical numbers show depth penetration in cm. Frost penetration of Kazakhstan soil is more than 10 cm. The rate at which soil frozen or frost penetration is depend on its thermal properties, moisture content, and the ambient air temperature. Probably the most important is the amount of water to be frozen, since it requires 144 heat units (Btu) for freezing each pound of water and by comparison only about 0.20 heat units to change the temperature of a pound of dry soil by 1°F. The density, conductivity of the soil particles and water content of the soil are all influenced by thermal conductivity of soil. Because clay particles have a higher insulation value than those of silt or sand particles and since clay soils normally keep more moisture than silt and sand, the depth of frost penetration is usually greater in silt and sand (light-textured soils) than in clays and silty clays (heavy-textured soils). Even the water content of Kazakhstan soil is less than Korea soil the frost penetration depth of

Kazakhstan soil is greater than that of Korea soil. But the particle size of Kazakhstan soil is less passed through #200 sieve than that of Korea soil.

There are other factors that have influence to the depth of freezing. The insulating effect of snow deserves special attention. It has been shown that each foot of undisturbed snow reduces the depth of soil freezing by approximately to the same amount. Air temperature is probably the most significant than meteorological factors such as sunshine, precipitation, and wind velocity,

Using of "degree-days of freezing" as a guide for calculating frost depth for a given area illustrates the strong influence of air temperature to soil temperature. A degree-day of freezing results when the mean outside air temperature for one day is 1 ^{0}C degree below 32°C. For example, if the average air temperature for a given day is 31°C this is one degree-day of freezing. The "freezing index" is simply the total number of degree-days of freezing for a given winter.

Using of the freezing index to predict the depth of frost penetration must be used with caution since based only on air temperature and does not take into consideration other factors such as soil type, snow cover and local climatic differences. Freezing on a concrete platform are defined by heat exchange conditions on a ground surface, its structure and a condition. Depth of freezing depends on basically on following four characteristics: average annual temperatures of soil, annual amplitudes of temperatures on a surface, structure and humidity of a ground. The decision of private problems for cases of freezing at continuously occurring phase transitions, and also taking into account process of migration of a moisture show that movement downwards borders of section of phases in many cases can occur under the law like $d_f = \alpha\sqrt{t}$, where $\alpha>0$ is constant which determine speed of freezing and depend on temperature and moisture, t - is time (Karlov, 2007).

There are curves which present temperature of the every soil layer. Sensors are putted every 1 cm in sample which height is 20 cm. It means that 19 sensors putted to the soil during the preparation to the freezing test.

The sensor which putted on the top of the soil sample have the maximum low temperature -4 ^{0}C. The sensor which putted in the toe of the soil sample have the high temperature +4 ^{0}C on the chamber lowest temperature -12 ^{0}C. Also there is changing the temperature penetration among two circumstances of the freezing during the test.

At freezing a ground the water filling a pore between particles, turning to ice, extends and deforms a ground which freezing together with a base body, heaving it up. Such phenomenon in freezing through soil carries the name frosty heaving, and soil are called heaving soil.

It is visible that in a case of deepening the base below possible depth of freezing lateral surfaces of the base will influence τ – force tangents heaving. The total size of tangents of forces heaving for strong heaving soil can exceed weight of a two-stored building, i.e. even to lift a building upwards.

In a case of deepening the base above possible depth of freezing lateral surfaces of the base will influence both τ – force tangents heaving, and σ - normal forces heaving. The total size of tangents and normal forces heaving for strong heaving soil is that can exceed weight even a five-floor building.

Thus, at depth definition installing the base in freezing through heaving soil, it is necessary to aspire to decrease in negative influence of forces heaving, deepening the bases below settlement depth of freezing in the given area. The constructive decision on removal of tangents of forces heaving by the device not frozen a plastering of lateral surfaces of the base is in certain cases admissible.

Heaving are subjected to dusty sand, loams and clay – soft plastic and fluid.

The scheme of a low arrangement of level of ground waters concerning depth freezing that at a finding soil in a firm and semifirm condition allows not to consider practically heaving.

At such low humidity (a firm and semifirm condition) heaving makes about 1% from freezing through thickness that is considered insignificant and calculation isn't accepted. However at designing it is necessary to consider that humidity, in the course of building could change, for example as a result removal of a grassy cover or infringement of a natural drain of water.

Heave amount of the soil also is the main determination of frost susceptibility of the soil. The heave amounts of Kazakhstan soil and Korea soils are illustrated in Figure 6.

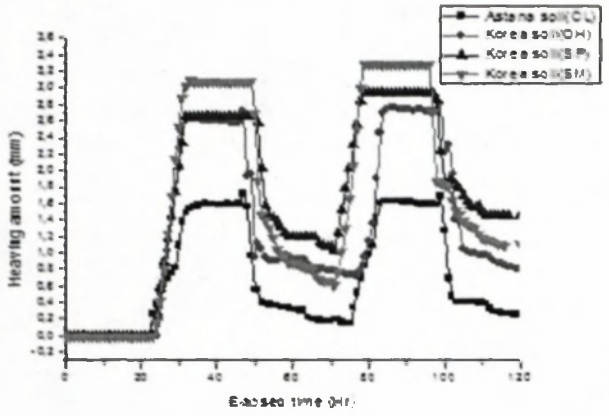


Fig. 6 The frost heaving amount of the Kazakhstan (Astana) and Korea soils

The heave amount of Korea soil is 5 times higher than that of Kazakhstan soil. The reason of this difference is the sieve analysis of Korea soil is finer than Kazakhstan soil. Also the initial moisture content and unfrozen water content of the soil are different but the condition of the freezing is the same situation.

The freezing pressure during testing Kazakhstan and Korea soils is presented in Figure 7. Obviously Korea soils show more heaving pressure than Kazakhstan clay soil.

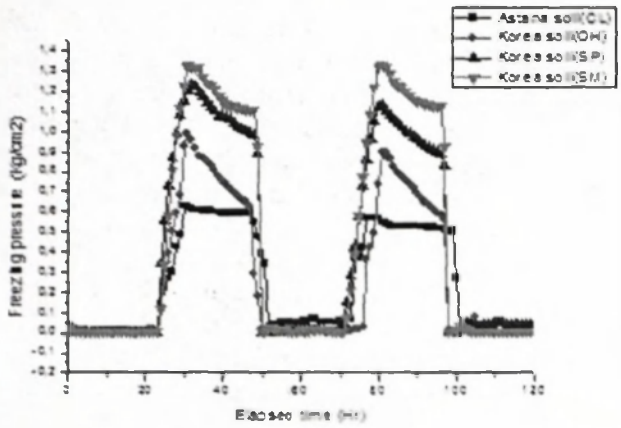


Fig. 7 The freezing pressure curves of Kazakhstan (Astana) and Korea soils

The heaving of the frozen soil more clearly should be understandable by the ice formation of the soil during freezing process. Ice formation is the main process which causing the heaving process during freezing of the soil. By the Beskow theory of ice formation the soil particles are enveloped by water films in which the water pressure is considerably higher than the pressure of water in the middle of pores in the soil. Due to the high pressure, the freezing point of the water in the water films is lower than that of the "free water" inside the pores (Williams, 1962). When the temperature of the soil goes down, the first ice crystals are formed in the center of the pores. The molecules of the outer water films also start to join with the ice crystal by decreasing temperature. The water films have a tendency to return to their original thickness in places where the ice crystal has penetrated the film and therefore the film pushes the ice crystal further away from the soil particles. However, some water molecules frozen to the crystal will also be pushed further, that is the reason why the ice crystal will grow by the water molecules stolen from the water films (Keinonen, 1960). Figure 8 shows the ice formation process in the soil during freezing process.

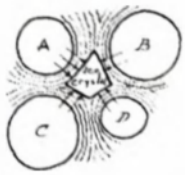


Fig. 8 The forces created during the growth of the ice crystal tend to push the crystal farther from the soil particles. Because of these forces the soil particles A, B, C and D move away from each other.

During cold winter months, frost penetrates pavement materials and subgrade soils. While progressing in the pavement structure, frost causes interstitial water to expand and can also cause segregation ice to form in unbound granular materials. Notwithstanding the fact that the latter phenomenon is generally considered insignificant in pavement granular materials, it causes the loosen materials. Frost heaving of pavement surfaces reaching 10 to 15 mm are systematically being observed on experimental test sites before the front reaches the subgrade soil. When the frost front reaches frost susceptible subgrade soils, water is sucked toward the frozen fringe where ice lenses are formed. Frost heaving of the pavement surface resulting from these phenomena can reach and even exceed 150 mm for climatic conditions prevailing in cold regions like as Kazakhstan. If the magnitude of the frost heaving were uniform, it would not be damaging for pavements. However, the frost action is generally uneven because of the variability of subgrade soil characteristics and because of the embankment geometry. Differential frost heaving is therefore a major factor affecting winter roughness of roads built in cold regions.

The climatic conditions of Kazakhstan is more colder than the temperature of Korea and sharply continental. Coldest temperature in winter can reach -43 ^{0}C and +45 ^{0}C in summer season in Kazakhstan. Average temperature of January — from -19°C to -4°C, average temperature of July — from +19°C to +26°C in Kazakhstan. By this climatic conditions the frost penetration can reach 2.5-2.7 meters, frost heaving and pressure high and getting peak in March. This climatic condition is more severe influence to the pavement system than that of Korea and also frost heave more than Korea soil. The problem with frost heave results mainly from the fact that the phenomenon is rarely uniform.

Differential frost heaving can be attributed to four major causes. The first cause, described by Peterson and Krantz (1998), is associated with the instability of the one-dimensional freezing process. The one-dimensional frost heave has the propensity to evolve into multidimensional differential frost heave as a function of soil properties and environmental conditions. The other causes of differential heaving are the variability in the frost susceptibility characteristics of the subgrade soil (including moisture availability), the variability of the thermal regime and the topography of the surface or the geometric characteristics of the earth structure (Guy Dore & Hannele K. Zubeck, 2009).

Two conditions must exist for the occurrence of problems related with differential frost heaving by Guy Dore and Hannele K.Zubeck. First, frost heave has to be significant. Frost heaving becomes more important with increasing frost depth, frost susceptibility of subgrade soil, and moisture availability. Second, frost heaving has to be uneven. Spatial variability of soil characteristics is the major factor contributing to the unevenness of frost heaving. If only one of these conditions is present in the field, differential frost heaving should not be a major problem. It should be possible to reliably predict poor winter performance of the pavement by applying the proposed model during preliminary studies of a road construction project,. It should be possible to modify pavement design or construction practices in order to mitigate the inconvenience caused by differential heaving. If variability seems to be the dominant problem, subgrade homogenization techniques can be used to reduce the differential effects of frost heaving. Moreover, if frost heaving is expected to be the dominant problem frost penetration could be reduced by increasing the thickness of a granular subbase or by placing an insulation layer in the pavement structure. In the longer term, increasing construction costs associated with these techniques would probably be compensated by a significant reduction in maintenance costs. They would also improve the winter and the long-term ride quality of the road, resulting in reduced vehicle maintenance and operation costs.

Another important differential heaving problem affecting pavement structures is the result of the important variations of thermal regime along the transversal section of the pavement. Mainly snow accumulation on the pavement sides impedes heat extraction at that location. As a result, frost penetration at the center of the pavement is much greater than at the edge of the pavement. Frost heaving being proportional to frost penetration, a transverse differential heaving is initiated in the pavement. The movement can be assimilated to a bending imposed to the pavement transverse section. It is likely to generate excessive tensile stresses and initial longitudinal or meandering cracks. Road users are not directly affected by the phenomena, but the resulting cracks can be highly detrimental to the structural performance of the pavement because they intercept running water at the surface, which then infiltrates the pavement structure.

4 CONCLUDING REMARKS

Laboratory freezing tests were conducted for the soil specimens obtained from Kazakhstan and Korea to understand the freezing characteristics of soils. The fine particles which passed the sieve number #200 for Korea soil is much greater than that of Kazakhstan soil, and the water content of Korea soil is also much lower than that of Kazakhstan soil. Therefore, the heaving amount of Korea soil is about 25% higher than the magnitude of Kazakhstan soil. Frost heaving and thawing are the major causes of creating damages on the pavement of road. It should be avoid this damages and reduce the influence of the extreme climatic conditions for transportation geotechnics. There are several ways to prevent the damageable influence of the frost heaving in Kazakhstan condition. The frost heaving susceptible soil is replaced by granular soil. The drainage system must be developed to dissipate the all the water sources from the road. Finally, the design and construction manual should be developed with consideration of frost penetration depth, asphalt binding material, freezing index, types and

thickness of anti-freezing layer, height of embankment for road.

ACKNOWLEDGMENT

The part of laboratory works described in this paper was done at the University of Incheon under consulting of Professor E.C. Shin (University of Incheon, Republic Korea). The authors wish to express gratitude to him, graduate student Mr.Myung Jin Cho.

REFERENCES

Dore, G., Zubeck, K., Hannele, G. (2009): Cold Regions Pavement Engineering, 88-92.

Fukuda, M., Kinosita, S. (1985): Field frost heave prediction related to ice segregation processes during soil freezing, *Annals of Glaciology 6*, 87.

Hoekstra, P. (1966): "Moisture Movement in Soils Under Temperature Gradients with the Cold Side Temperature Below Freezing", *Water Resources Res*, Vol 2, pp 241-250.

Karlov, V.D. (2007): Ground and foundations on seasonal-freezing heaving soil, 81-82 (in Russian).

Keinonen, L. (1960): New theory to explain the ice formation, pp. 2-3.

Michalowski L.R., Ming Zhu .(2005): "Frost heave modeling using porosity rate function", *International Journal for Numerical and Analytical Methods in Geomechanics*, USA.

Penner, E. (1960): Ground freezing and Frost Heaving, 1-2.

Shin, E.C. and Park, J.J. (2012): "Soil freezing characteristics and temperature distribution in in-ground LNG storage tank", *International Journal of Offshore and Polar Engineering,Vol.22. No.1*, 53-62.

Standard Test Methods for Frost Heave and Thaw Weakening Susceptibility of Soils,(2004): *ASTM D 5918-06*, Copyright ASTM International, pp. 401-408.

Williams, P.J. (1962): Climatic factors controlling the distribution of certain frozen ground phenomena, 1-4.

Vulnerability Assessment and Seismic Rehabilitation of Stone Masonry Buildings Using Pipe Bracing System

Mussa Mahmoudi
Assistant Professor, Civil Engineering Department,Shahid Rajaee Teacher Training University, Tehran, Iran

Farshid Ebadi
M.S. in Structural Engineering, Shahid Rajaee Teacher Training University, Tehran, Iran

ABSTRACT: It is estimated that a lot of stone masonry buildings are seismic vulnerable in the world and need to be rehabilitated. There are a few techniques for seismic upgrading of the stone masonry buildings. This paper introduces the pipe bracing system for rehabilitation of stone masonry buildings to resist severe earthquakes safely. Pipe bracing system includes precast steel pipes buried into the ground (about five meters) and connected to the floors at each level. The lateral load due to earthquakes will be transferred by this system from story levels to the ground. Pipe bracing systems behave as cantilever beam. The advantages of this system are; there is no need severe destruction in the buildings for rehabilitation purposes, the time period of the construction will be decreased, and also it will be economic in cost. In order to do the performance assessment of the system, some model (short masonry buildings) was selected and their seismic vulnerability was assessed by the FEMA273 instruction. The effect of soil-structure interaction was considered. It was controlled, the system's stiffness, strength and ductility demands by nonlinear static pushover analysis. The results indicate that this system will be able to strengthen the vulnerable stone masonry buildings and increase ductility and stiffness capacity.

Keywords: Stone masonry buildings, Rehabilitation, Pipe bracing system, Seismic evaluation

1. INTRODUCTION

The past earthquakes have showed that many of the unreinforced masonry buildings in the world are seismically vulnerable. Mahmoudi and his colleagues (2005-a) evaluated, seismic vulnerability of the 125 URM buildings in Mazandaran province (north of Iran). They concluded that 69 percent of the buildings will be collapsed during a severe earthquake and should be considered for retrofitting.

Codes for new construction cannot be used for seismic rehabilitation of existing buildings. Therefore set of guidelines for seismic rehabilitation of buildings was developed by the Federal Emergency Management Agency. In Iran, the first instruction for seismic rehabilitation was initially developed in (2005-b). This instruction is applicable for all kind of the structures, such as steel structures, concrete structures and unreinforced masonry buildings. The separated instruction for unreinforced masonry buildings was developed in (2007-a).

Different retrofitting techniques are available for rehabilitation of the unreinforced masonry buildings which increase the strength, ductility and stiffness capacities of the buildings. Although a variety of technical solutions have been implemented for seismic retrofitting, there exists little information or technical guidelines with which an engineer can judge the relative merits of these methods. Furthermore, no reliable analytical techniques are available to evaluate the seismic resistance of retrofitted masonry structures (2004). This paper introduces the pipe bracing systems for rehabilitation of URM buildings and evaluates its performance during severe earthquakes.

2. REHABILITATION METHODS

2.1 Surface treatment

Surface treatment is a common method, which has largely developed through experience. Surface treatment incorporates different techniques such as ferrocement, reinforced plaster, and shotcrete (Fig. 1). By nature this treatment covers the masonry exterior and affects the architectural or historical appearance of the structure (2004).

2.2 Grout and epoxy injection

Grout injection is a popular strengthening technique, as it does not alter the aesthetic and architectural features of the existing buildings. The main purpose of injections is to restore the original integrity of the retrofitted wall and to fill the voids and cracks, which are present in the masonry due to physical and chemical deterioration and/or mechanical actions (2004).

2.3 External reinforcement

A steel plates or tubes can be used as external reinforcement for existing URM buildings. Steel system is attached directly to the existing diaphragm.

2.4 R.C. tie columns

Confined masonry with R.C. weak frame, represents one of the most widely used masonry construction system in Asia and Latin America. In Europe, Eurocode 8 (EC 8) recommends the usage of such confined system for masonry constructions. In China, they used such confinement in new masonry buildings as well as it is used as retrofitting for existing URM buildings (Fig. 2). However, it is not easy to construct such confinement in existing masonry buildings (2004).

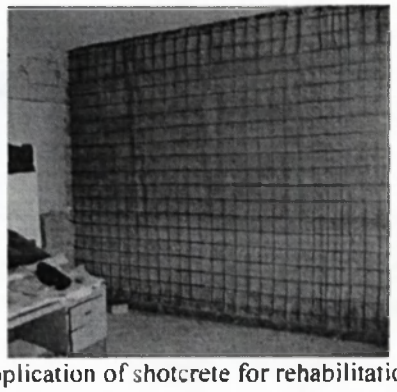


Fig. 1: application of shotcrete for rehabilitation

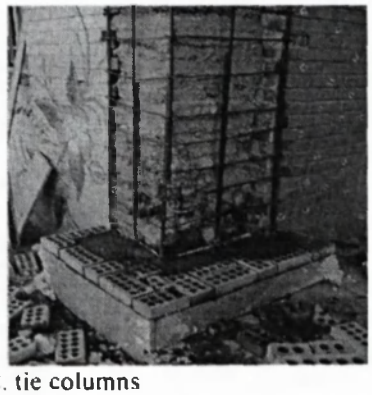


Fig. 2: R.C. tie columns

2.5 Shear wall

For many years, inner reinforced concrete (RC) shear walls have been widely used as lateral load resisting systems for earthquake loading. It can be used for rehabilitation of unreinforced masonry buildings.

2.6 External annexed system

External moment frame, bracing frame systems can be used for rehabilitation of masonry buildings as external annexed systems. Figs. 3 and 4 show masonry buildings rehabilitated by external moment frame and bracing frame systems, respectively.

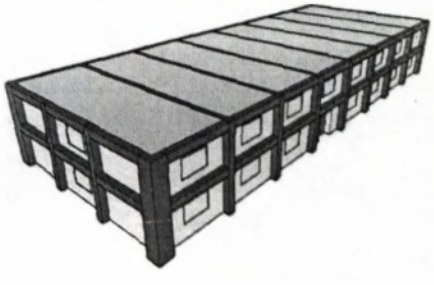


Fig. 3: moment framed system



Fig. 4: bracing framed system

3. PIPE BRACING SYSTEM

This paper introduces a new technology for rehabilitation of SM buildings named pipe bracing system. Pipe bracing system includes some precast steel pipes located vertically and buried into the ground (about five meters) and connected to the floors at each level (Fig. 5). The lateral load due to earthquakes will be transferred by this system from story levels to the ground. Pipe bracing systems behave as cantilever beam. The advantages of this system are; there is no need severe destruction in the buildings for rehabilitation purposes, the time period of the construction will be decreased, and also it will be economic in cost. The length of pipes buried in the soil depends on the soil characteristics. It can be decreased by a rigid floor or tie beams at the ground level (2007-b).

3.1 The layout of pipes

In this method, at least two pipes will be installed in the plan, symmetrically (Fig. 6). The number of pipes depends on the number of stories and the area of the building.

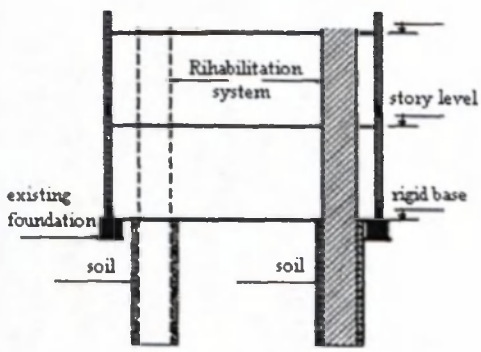


Fig. 5: Pipe bracing system

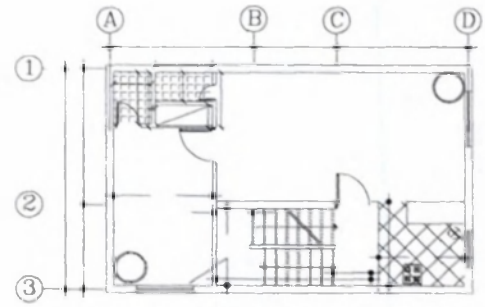


Fig. 6: layout of the pipes in the plan

3.2 Connections

The details of connections are very important in this method. The pipe and floor connection should be able to transfer seismic load from building to system. Fig. 7 shows the connection of pipes and floors by steel profiles or reinforced concrete members.

3.3 Floors

The floors in this system must be rigid. Because the floors should be able to transfer seismic load to the pipes without damage. The floors can be rigid by rods located X shaped (Fig. 8) or by a layer of reinforced concrete.

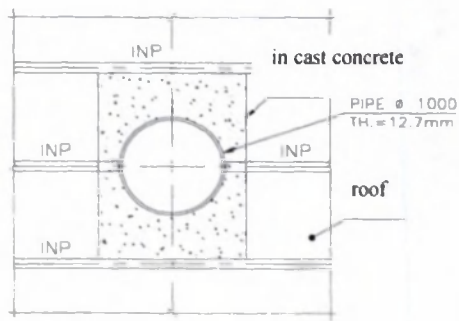


Fig. 7: Details of roof and pipes



Fig. 8: rigidifying the roofs by rods or concrete

4. MODEL

In order to investigate the effectiveness of the proposed system, a vulnerable SM buildings was selected and rehabilitated by pipe bracing system. This is a two story building with educational usage. The diaphragm was from joist and the bearing walls have 35 cm thickness. The building is regular in plan and height according to FEMA 273 (1997). The building is located in very high level of relative seismic hazard with design base acceleration of 0.35g. The soil type is II. The building area is 792 m^2. Fig 9 shows the building plan and the wall numbers.

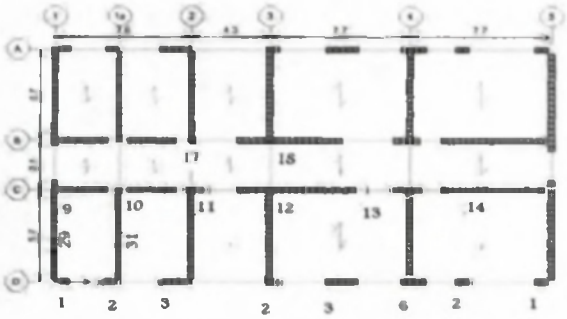


Fig. 9: The plan of the building

5. SEISMIC VULNERABILITY ASSESMENT OF ORIGINAL BUILDING

At first, the building was seismically evaluated by the provisions of FEMA 273 (1997) and using nonlinear static analysis (pushover analysis). Pushover analysis has been known as an acceptable method for seismic assessment of the buildings and its result is more reliable. In pushover analysis, the buildings systems are subjected to a set of lateral static forces in a fixed distribution that increase progressively as individual elements of the system deform beyond their proportional limits.

5.1 Target displacement

Using pushover analysis procedure, system is pushed to an expected target displacement, δ_t, as given by equation 1,

$$\delta_t = C_0 C_1 C_2 C_3 S_a \frac{T_e^2}{4\pi^2} g \qquad (1)$$

where C_0 relates the roof displacement to the spectral displacement, C_1 relates the inelastic displacement to the elastic displacement for short period buildings, C_2 accounts for a pinching of the hysteresis loop, C_3 accounts for P-Δ effects for negative post-yield stiffnesses, S_a is the spectral acceleration at the fundamental period of the building, T_e.

5.2 Lateral load patterns

For both two- and three-dimensional analysis, at least two vertical distributions of lateral load shall be considered. The first pattern, often termed the uniform pattern, shall be based on lateral forces proportional to the total mass at each floor level. The second pattern, termed the modal pattern depends on the modal shapes. In this paper, uniform pattern and triangular pattern was selected.

5.3 Plastic hinges definition

In nonlinear static analysis, deformation-controlled wall and pier components shall be assumed to deflect to nonlinear lateral drifts as given in Fig. 10. Variables d and e, representing nonlinear deformation capacities for primary and secondary components, are expressed in terms of story drift ratio percentages (Table 1). This table also shows the acceptance criteria for each performance levels. IO means Immediate Occupancy; LS represents Life Safety and CP means Collapse Prevention (2007).

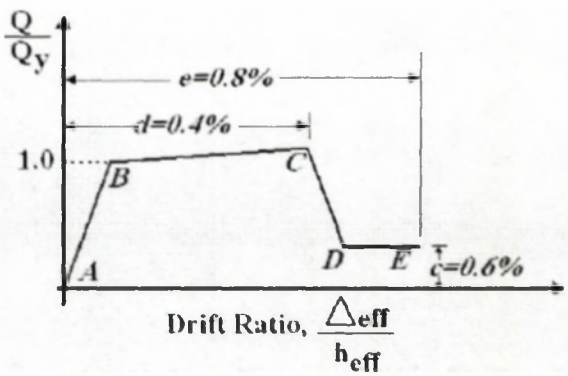


Fig. 10: Load-deflection curve for wall and pier components

Table 1: Simplified Force-Deflection Relations for URM Walls and Piers

Limiting Behavioral Mode				Primary			Secondary	
	c %	d %	e %	IO %	LS %	CP %	LS %	CP %
Bed-Joint Sliding	0.6	0.4	0.8	0.1	0.3	0.4	0.6	0.8
Rocking	0.6	$0.4h_{eff}/L$	$0.8h_{eff}/L$	0.1	$0.3h_{eff}/L$	$0.4h_{eff}/L$	$0.6h_{eff}/L$	$0.8h_{eff}/L$

5.4 Vulnerability assessment results

Table 2 shows the building target displacements. The building has to be pushed up to these target displacements. The non-linear analysis results usually were shown with capacity curve, in which the horizontal axis shows the building roof displacement and the vertical axis represents base shear. Fig. 11 shows the structural capacity curves up to target displacement. The analysis indicates that the building is vulnerable for life safety (LS) performance. For example the wall types 3 and 6 in the building do not have enough strength to remain safe during the design earthquake.

Table 2: Buildings target displacements

Rectangular pattern X direct (m)	Uniform pattern X direct (m)	Rectangular pattern Y direct (m)	Uniform pattern Y direct (m)
0.008	0.0077	0.0073	0.007

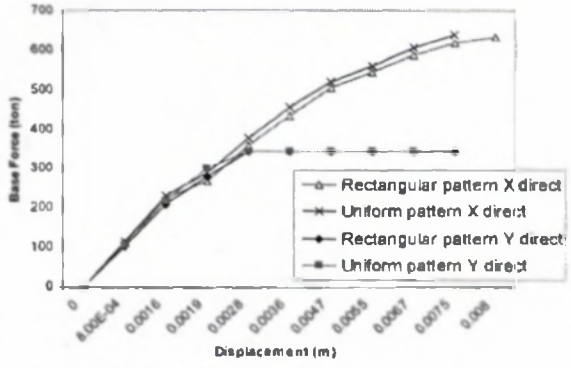


Fig. 11: Capacity curve for original building

6. SEISMIC VULNERABILITY ASSESMENT OF REHABILITATED BUILDING

The vulnerable building is rehabilitated by pipe bracing system. Various layouts were applied as the rehabilitation system. Table 3 shows the number of pipes, their diameters and thicknesses of the systems. The rehabilitated building is evaluated by pushover analysis the same as the original building for life safety (LS) performance. The pipes and soil were modeled according to FEMA 273 (1997) provisions. Soil-structure interaction (SSI) may modify the seismic demand on a building. A rational method of modeling SSI was used in this research.

Table 3: Buildings target displacements

case number	Tube number	Tube diameter (m)	Tube thickness (cm)
1	Two	2	2
2	Four	1.2	1.5
3	Four	1.4	1
4	Four	2	1

Table 4 shows the target displacements of X direction (vulnerable direction) for the building in the four cases. The vulnerability of the building was seismically evaluated. Fig. 12 shows the global response curve (capacity curve) up to target displacement for cases number 3 (triangle pattern) and 4 (uniform pattern). The result indicates that there was no vulnerability in all cases. Therefore the pipe bracing system can promote the stiffness, strength and ductility of the unreinforced masonry buildings. The result shows that the third case (Four pipes with 2m in diameter and 1cm in thickness) is the most optimum case.

Resistivity profiles and foundation structure of Central Tower, Bayon in Angkor

K. Nakagawa
Graduate School of Science, Osaka City University, Osaka, Japan

I. Shimoda. S. Yamada, R. Kanau & Y. Ogawa
Faculty of Science and Engineering, Waseda University, Tokyo. Japan

Y. (Yasuda) Ohta
Graduate School of Technolog}', Kyoto University, Kyoto. Japan, at present, Tokyo gas Co.. Ltd, Tokyo, Japan

M. Fukuda
Taisei Geotech Co. Ltd
, Kumamoto. Japan

A. Jomori & T. Takahashi
Neo Science, Osaka. Japan

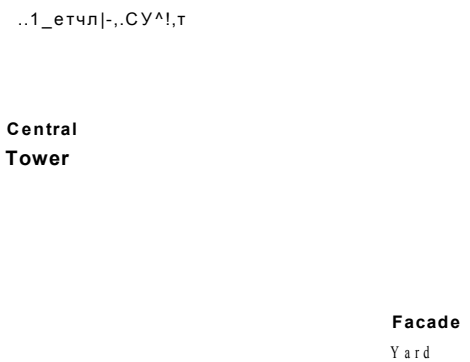
Y. Iwasaki
Geo-Research Institute, Osaka, Japan

ABSTRACT: Electric exploration surveys were conducted to study the foundation structure of the Central Tower at third terrace and ground condition of facade yard. Bayon, Angkor Thom in Cambodia. Four poles type measurements called Wenner's and Eltran's techniques were adopted at the all sites. Three different unit spacing was adapted for the electrodes as, 0.25m. 1 Om. and 4m. Magnitude of the resistivity obtained ranges common values from 10 to 1000 ohm meter. Comparing with geotechnical boring for the foundation mound, the high resistivity pails were found to correspond to latcritc blocks in the foundation mound.
In the facade yard, hand augur samplings were carried out at several points. The sampled soil consists from filled ground of various soils and natural ground of stiff silty clays. The results of electric surv ey at the facade were estimated as rather shallow pond structure by comparing the sampled soil and the distribution of the resistivity.

I INTRODUCTION

Bayon, which is shown in Fig. 1, is the centra! temple in the Angkor Thom, where JSA (Japanese Government Team for Safeguarding Angkor) has been engaged in the conservation work. Electrical resistivity and electromagnetic surveys were conducted (Sugimoto et al., 2007). Electric survey was recognized as one of the useful tools to study ground condition in Angkor.

Three boreholes of one vertical and two oblique borings were performed from the third ten-ace in 2011 to examine the geotechnical conditions of the ground. The vertical drilling shows the cores of the laterite blocks with thickness of six meter beneath flagstones that were laid on the terrace surface The two other oblique borings did not reach any laterite blocks. Accordingly, electrical prospecting was planned to estimate the underground structure, especially, distribution of the laterite blocks. Additional survey was also conducted at pond area in the facade yard.



- Fig. I General Plan and Section of Bayon

2.1 *Basic principle*

Resistivity is one of the inherent physical

properties in materials. Ground material has the characteristic resistivity. Four poles type measurement techniques called Wenner's and Eltran's techniques were adopted at the all measurement sites. Electrode array pattern of those techniques is shown in Fig. 1. The Wenner's technique is adequate to extract the characteristic continuity of the underground structure. Contrastively, the Eltran's technique is adequate to extract discontinuous structure. The resistivity profiles were analyzed by inversion in terms of the finite element method.

The minimum interval of the electrodes, that is, unit spacing is a quarter of a meter. The shorter spacing is commonly used to evaluate the detail structure near the surface.

Both Wenner' and Eltran's techniques were used alternately by the switching box for the measurement.

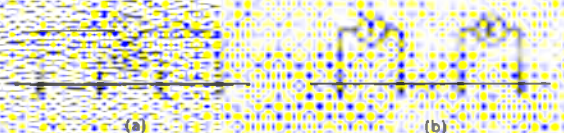


Fig.2 Electrode array of four poles technique
(a) Wenner's technique (b) Eltran's technique
Symbol: I in a circle: two current electrodes, E in a circle: two potential electrodes

2.2 *Measurement*

In this area, ground material consists of the Holocene silty, clay, compacted sandy soil, laterite block and sandstone block. In order to evaluate the geotechnical underground structure, four and three measurement lines were planned on the top terrace of the central tower and the ground of facade yard, respectively. The locations of these survey lines are shown in Fig. 3 and Fig. 4.

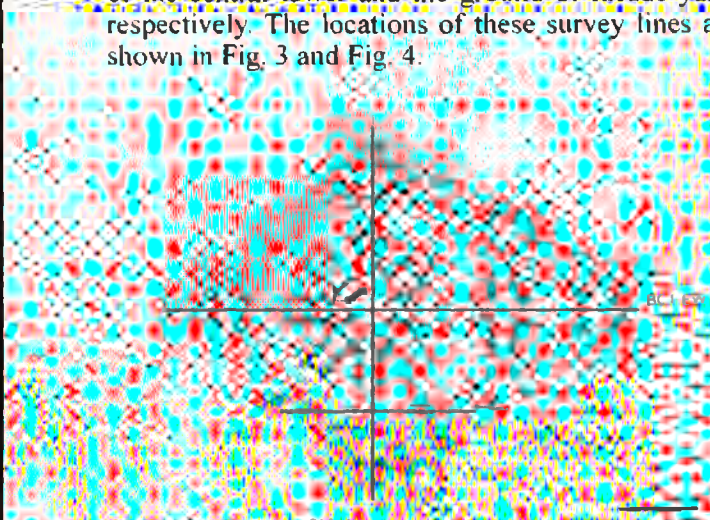


Fig. 3 Electric survey lines in the site of the central Tower at the top third terrace

Length of the measurement lines are listed in Table 1. The length of measurement cable is 100m and the number of electrodes is twenty.

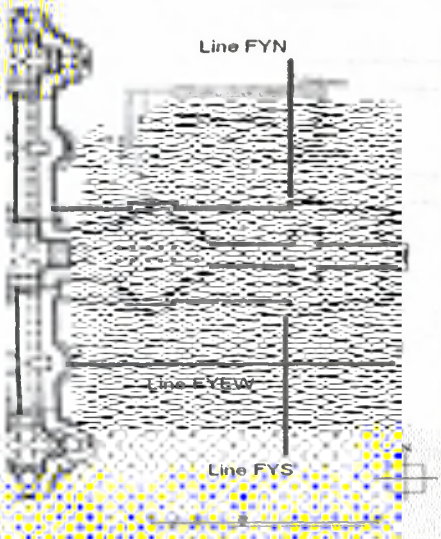


Fig. 4 Measurement lines in the site of Facade Yard of the Bayon Temple

Conventional peg type of steel rod (6mm in diameter and 40cm in length) was used for electrodes in the ground of façade. However, for the top terrace of Bayon where the surface was covered by stone, aluminum foil electrodes with conductive paste were used. Conductive paste was made by wheat flour with saline water. This electrode setting was useful to decrease the contact resistance between electrode and stone.

Three different unit spacing of the electrodes were adapted as 0.25, 1, and 4 meters. Resolution of the resistivity profile depends on the electrode spacing. Accordingly, for limited number of electrodes, the narrower unit spacing has the higher resolution picture of the underground structure. On the other hand, the wider unit spacing has the broader and deeper picture of it.

Table 1 Length of the measurement lines

Name of the line	length (m)
Line TR WE	28.5
Line TR SENW	17.0
Line CTEW	65.0
Line CTSN	52.0
Line FYN	39.0
Line FYS	39.0
Line FYEW	70.0

3 RESULTS OF ELECTRIC SURVEYS

The resistivity profiles were analyzed after field survey by inversion in terms of the finite element method.

In this paper, the results are shown for different

unit spacing respectively.

3.1 *Line TR WE Southern Side on Top Terrace*

The measurement line was set at the southern side corner of the top terrace with a direction from west to east with about 30m as shown in Fig. 3. This line crosses the Line TRSENW at southeast of the central Tower. The results is shown in Fig.5



Fig. 5 Resistivity profile of the Line TR WE
(unit spacing: 1.0m)

3.2 *Line TR SENW South-Eastern*

The line TR SENW is extended from the center to south southeast on the top terrace with direction from the east to the west with results as shown in Fig.6..

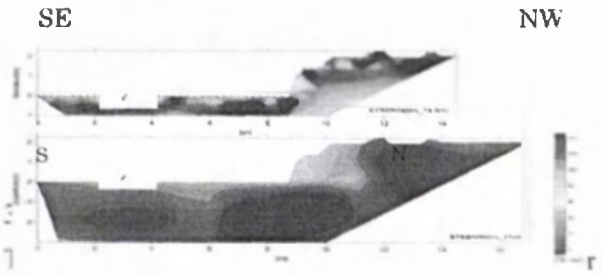


Fig. 6 Resistivity profile of the Line TR SENW.
(upper):unit spacing. 0.25m; (lower): unit spacing. 1.0m

3.3 *Line BCT EW*

This line has the longest length of 65 meters. The resistivity profiles obtained are shown in Fig. 7.

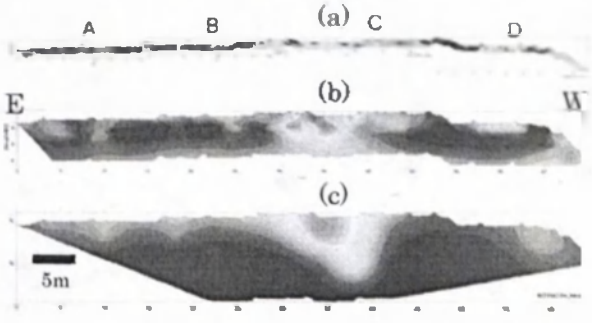


Fig. 7 Resistivity profile of the Line BCTEW
Unit spacing: (a). 0.25m, (b) 1.0m, (c) 4m

3.4 *Line CTSN SN-line through center*

The line CTSN also runs through the center of the Tower with direction from the south to the north and crosses with the CTEW at the center of the Tower. The length of the line is 52 meters. Those profiles are shown in Fig. 8.

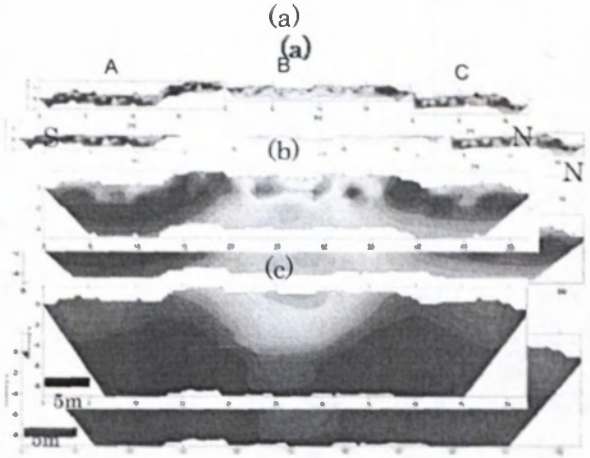


Fig. 8 Resistivity profile of the Line CTSN
Unit spacing (a) 0.25m;, (b), 1.0m, (c) 4m

3.5 *Line FYN, FYS and FYEW in the facade yard*

The northern and southern lines, FYN and FYS were set to N-S direction at both sides of the approach to the temple in the façade yard. An E-W line, FYEW is parallel to the approach to the temple. Those profiles of the lines are shown in Fig.9.

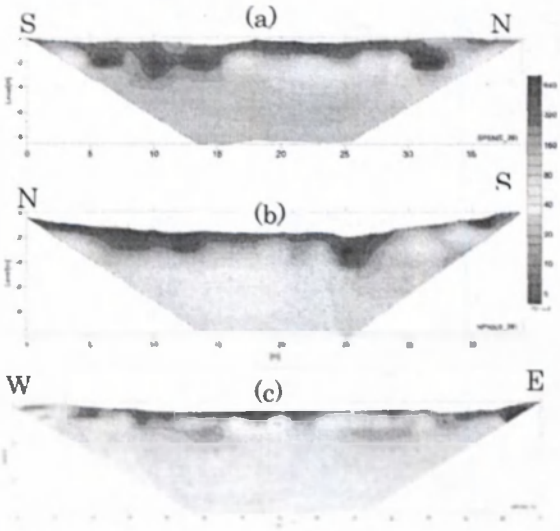


Fig. 9 Resistivity profile of the Lines FSN (a), FYS and FYEW (c)

4 DISCUSSIONS

4.1 *Foundation of Central Tower*

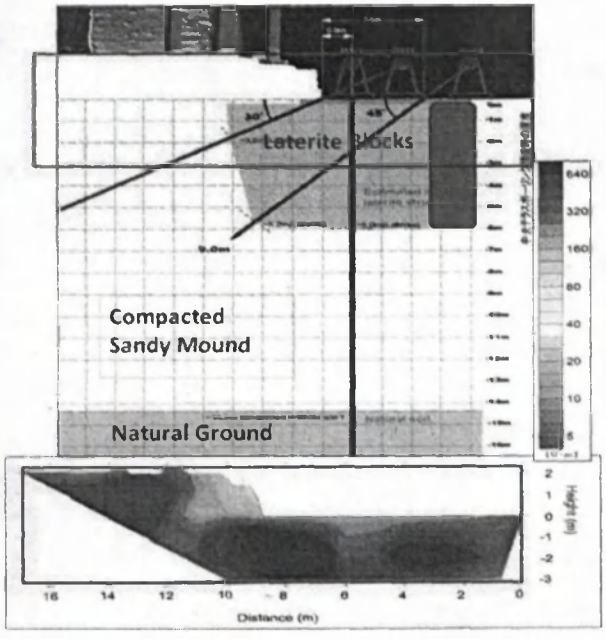


Fig. 10 South South-East Cross section obtained from the drilling data and the corresponding resistivity profile (TR SENW) analyzed from the unit spacing of 1.0 m

The results of three boings from the south east side of the central tower to the center of the tower on the top third terrace (Fig.2 and Fig.3) are schematically shown in Fig.10.

Laterite blocks, which were usually found under the surface stone pavement with one or two layers, were found with extraordinary thickness of more than 5m down to 6m from the surface of top terrace identified by a vertical boring in October, 2010.

Two additional inclined boring were further carried out to sound inner structures of the foundation mound.

The Central Tower was built upon a compacted sandy mound of about 14m in thickness. The foundation of the tower is sandstone blocks directly laid upon the manmade fill. The boring results revealed the existence of laterite blocks outside of the tower structure itself.

Comparison between the electric survey and the boring section, rather high resistivity zone of more than 600 ohm-m corresponds to the laterite blocks. Fig.11 shows north-south cross section of the foundation of the central Tower with resistivity profile along BCTSN line. Shallow zone beneath the northern part shows high resistivity.

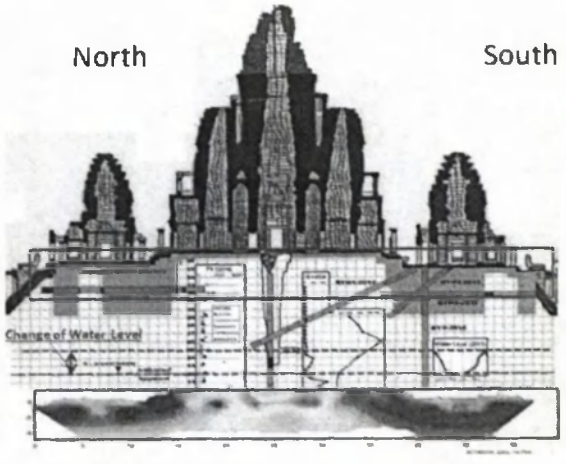


Fig.11 North-South Cross section with resistivity profile along survey line BCTSN

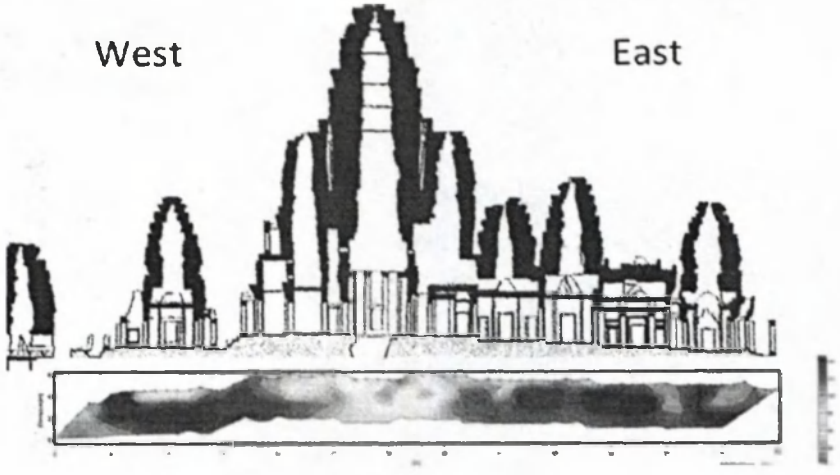


Fig.12
West-East Cross section with resistivity profile along survey line BCTEW

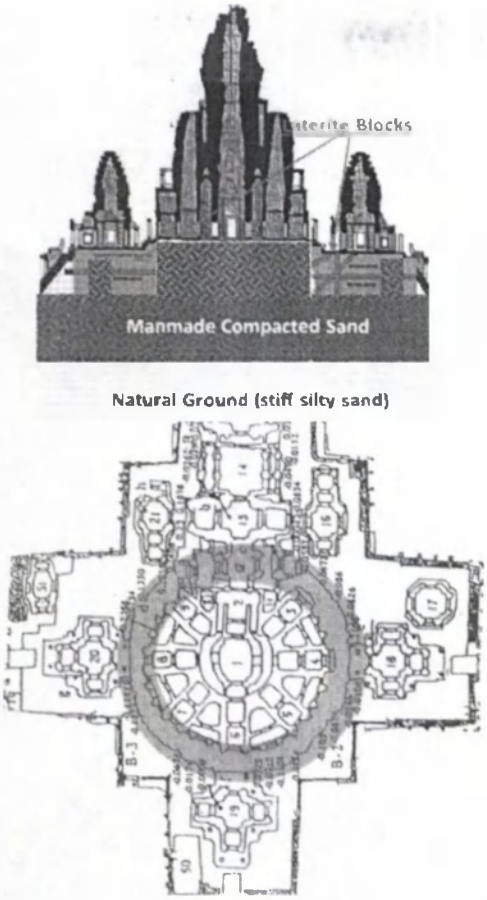


Fig.13 Expected basic structure of foundation mound under the central Tower, Bayon Temple

In March, 2012, an additional horizontal boring was carried out from the north side of the foundation mound into the center of the foundation mound. The result is shown in Fig.11, which shows similar situation of the existence of the laterite blocks as in Fig.10. The corresponding resistivity also shows rather high electric resistivity zone.

Fig.12 shows west-east cross section of resistivity profile. The common characteristics of the resistivity profile of north-south and west-east sections are low resistivity zone at the center of the tower and high resistivity zone at the outer side of the foundation of the central tower.

Fig.13 is an expected structure of the foundation mound of the central tower of the Bayon temple based upon geotechnical boring and electric surveys at present. The main part of the mound is a well compacted manmade sand ground with thickness of about 14m from the natural ground. A large number of laterite blocks are expected in a cylindrical shape surrounding the fringe of the foundation of the tower.

4.2 *Eastern Side of Façade Area*

In façade area, hand augur samplings were carried out to compare the resistivity values obtained by the electric survey. The results of sampled soils showed loose surface soils and natural stiff silty clays. Fig.14 shows the sampled points and vertical profiles at each point.

The textures of surface soils change from sand to

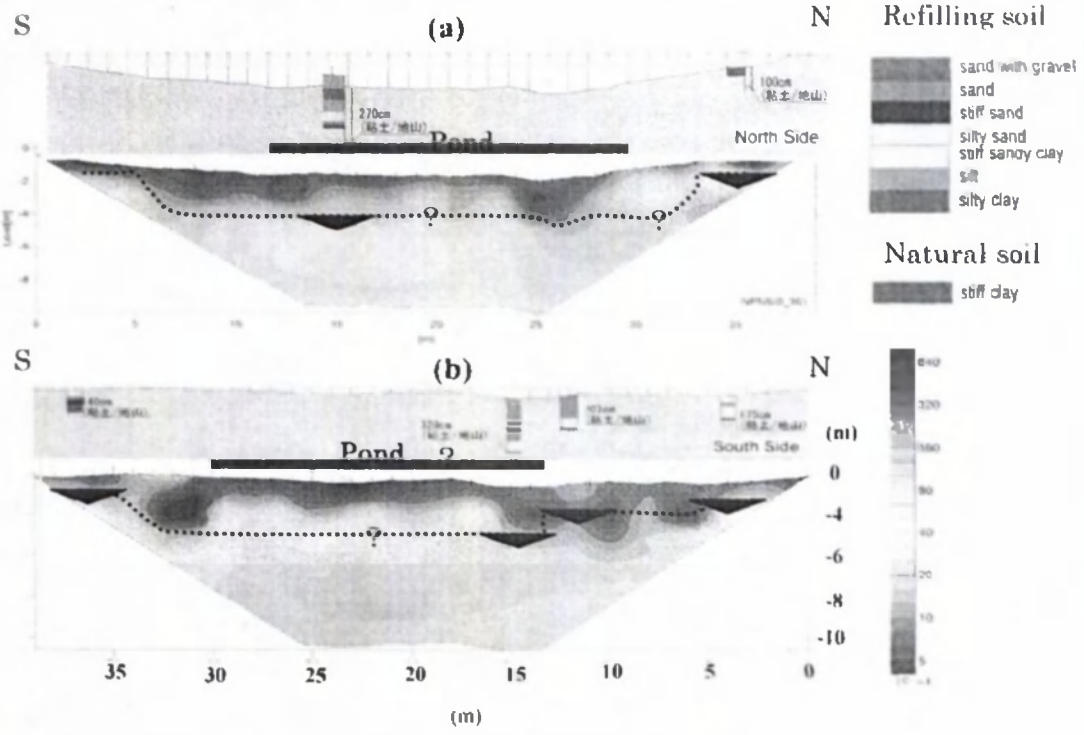


Fig. 14 The resistivity profile and the soil column section at the Façade Yard
(a) Line FYN, (b)Line FYS, and (c) Line FYEW

silty clay and the corresponding resistivity is rather high values.

On the contrary, the natural ground of stiff clay shows lower resistivity than 300 ohm-m. Fig.13 shows a possible boundary of natural ground of stiff clay and loose filled soils.

CONCLUSIONS

The electric survey that was carried out at Bayon, Angkor Thom was interpreted with a comparison with boring data as well as hand augur samplings.

1. Laterite blocks that were identified by boring under the foundation mound for the central tower, Bayon, correspond to high resistivity zone of about 600 ohm-m.
2. It is very likely that the laterite blocks were used in a cylindrical shape under the peripheral of the foundation of the tower.
3. In façade zone, natural stiff clay corresponds well to low resistivity of less than about 300 ohm-m.
4. The estimated upper boundary of still clay of natural ground was about 4-5meters from the present ground surface, which may corresponds to the bottom of ancient ponds.
5. Electric survey, when combined with some ground proof, could make to add and improve some useful interpretation of the underground structure in addition to the basic geotechnical data provided by boring.

REFERENCE

Sugimoto et al.(2008)"Geophysical Prospecting Survey at the Bayon Complex," Annual Technical Report on the Survey of AngkorMonument, 2008, Safeguarding of Bayon Temple of Angkor Thom, JASA, published by JSA, Tokyo, pp.96-107

Разрешено в печать 9 сентября 2012 года.
Заказ №1378. Тираж 85 экз. Формат А4.

Отпечатано в типографии СамГАСИ.
Адрес: г. Самарканд, ул. Лолазор, 70.

20.000 ceşeli.